# DESIGN AND SYNTHESIS OF A HYALURONAN OLIGOSACCHARIDE AND ANALOGUES AS POTENTIAL INHIBITORS OF CD44-HYALURONAN BINDING

By

Xiaowei Lu

A DISSERTATION

Submitted to
Michigan State University
in partial fulfillment of the requirements
for the degree of

DOCTOR OF PHILOSOPHY

Chemistry

2012

## ABSTRACT

DESIGN AND SYNTHESIS OF A HYALURONAN OLIGOSACCHARIDE AND ANALOGUES AS POTENTIAL INHIBITORS OF CD44-HYALURONAN BINDING

By

Xiaowei Lu

Hyaluronan (HA) is a non-sulfated negatively charged linear polysaccharide, which is composed of 2,000-25,000 repeating units of disaccharides: [-D-glucuronic acid-*β*-1→3-*N*-acetyl-D-glucosamine-*β*-1→4-]. Tumor microenvironment contains different type of cells and ECM. HA and HA binding proteins are the major components of extraceullular matrix (ECM). CD44 is the primary receptor for HA. CD44, a single chain transmembrane protein, is composed of four parts: the *N*-terminal hyaluronan binding domain (HABD), the stem domain, the transmembrane domain and the C-terminal cytoplasmic-tail domain. Multivalent HA-CD44 interactions induce signaling pathways that promote tumor cell invasiveness, proliferation, survival and multidrug resistance (MDR). Multivalent HA-CD44 interactions are required for formation of constitutive signaling complexes. Replacement of the multivalent interactions with monovalent interactions by the treatment with hyaluronan oligosaccharide (sHA) causes disassembly of constitutive signaling complexes and attenuated signaling pathway. These finally lead to the inhibition of tumor cell proliferation and MDR.

In this dissertation, the chemical synthesis of a hyaluronan decasaccharide ($HA_{10}$) using the pre-activation based chemoselective glycosylation strategy is described. Assembly of large oligosaccharides is generally challenging due to the increased difficulties in both glycosylation and deprotection. Indeed, the same building blocks

previously employed for hyaluronan hexasaccharide ($HA_6$) synthesis failed to yield the desired $HA_{10}$. After extensive experimentation, the $HA_{10}$ backbone was successfully constructed with an overall yield of 37% from disaccharide building blocks. The trichloroacetyl group was used as the nitrogen protective group for the glucosamine units and the addition of trimethylsilyl triflate (TMSOTf) was found to be crucial to suppress the formation of trichloromethyl oxazoline side-product and enable high glycosylation yield. For deprotections, the combination of a mild basic condition and the monitoring methodology using $^1$H-NMR allowed the removal of all base-labile protective groups, which facilitated the generation of the fully deprotected $HA_{10}$.

Based on the co-crystal structure of CD44 HABD and hyaluronan octasaccharides ($HA_8$), hyaluronan pentasaccharide ($HA_5$) analogues were designed and synthesized. Due to synthetic difficulties, the initial design of **Library A** was abolished. By rotating S-C4 bond, new analogues, **Library B** and **Library C,** were generated. Eleven compounds in **Library B** and **Library C** were synthesized by a cutting edge method, and screened by inhibitory Enzyme-linked immunosorbent assay (ELISA). Finally, it was found that the aromatic group in analogue **56** contributes to the binding of **56** to CD44. And this interaction overcomes the loss of favorable enthalpy caused by the loss of H-bonds from COOH of glucronic acid 7 (GluUA7) and primary OH of *N*-Acetylglucosamine 8 (GlcNAc8). Although the binding affinity of **56** is only comparable to $HA_6$ and less than $HA_8$, this provides a new direction towards further design of novel HA inhibitors.

# DEDICATION

I dedicate this dissertation to my husband, Liping Liu, for his remarkable patience, unwavering love and support over the course of my research. I dedicate this dissertation to my parents, Yueyue Dong and Zhiwei Lu, for their sacrifices and support. Finally, I dedicated this dissertation to my grandparents, Jixiang Lu and Longying Chen, who are in heaven.

ACKNOWLEDGEMENTS

I would like to thank all of those people who helped make this dissertation possible.

First, I wish to thank my advisor, Professor Xuefei Huang, for all his guidance, encouragement, support, and patience. His sincere interests in science, aggressiveness, personality and dedication have been a great influence on me. My advisor is a great teacher who knows that real growth comes through pain. I appreciated my advisor for challenging me and believing that I am able to go through it. By going through those challenges, I have learned a lot and gained immense confidence. My parents brought me to this world and provided me with good educations. Professor Huang taught me how to be a professional scientist and how to thrive in the real world.

Also, I would like to thank my committee members Professor Gregory Baker, Professor Gary Blanchard and Professor John McCracken for their input, valuable discussions and accessibility.

I am very thankful to the Department of Chemistry at Michigan State University, especially Professor Gary Blanchard, associate Chair for education, for been a strong support to me throughout my graduate school career.

I give many thanks to Dr. Daniel Holmes and Mr. Kermit Johnson for the help on NMR, Dr. Daniel Jones and Ms. Lijun Chen for the help on mass spectrometer. I would like to thank all the staffs in department of chemistry for their hard work and dedication. Finally, I would like to thank all my lab mates for all the help over the years.

TABLE OF CONTENTS

LIST OF TABLES……viii

LIST OF FIGURES ……ix

LIST OF ABBREVIATIONS ……xix

LIST OF SCHEMES ……xxviii

CHAPTER 1 **Functions of CD44-Hyaluronan Interactions in Inflammation and Malignancy**……1
1.1. CD 44, a major receptor for HA ……1
1.1.1. HA ……1
1.1.2. CD 44……2
1.1.3. CD44-HA interactions……3
1.2. Functions of CD44 and HA interactions in the immune system ……4
1.2.1. Pro-inflammatory role ……4
1.2.2. Anti-inflammatory role ……6
1.2.2.1. HA uptake……6
1.2.2.2. AICD……6
1.3. Functions of CD44 and HA interactions in cancer ……7
1.3.1. Tumor microenvironment ……7
1.3.2. Tumor initiation and progression ……7
1.3.2.1. HA in invasion……7
1.3.2.2. CD44 in extravagation of tumor cells during metastasis……8
1.3.2.3. CD44 reduces Fas-mediated killing of tumor cells……8
1.3.2.4. EMT……8
1.3.2.5. Cancer stem cell……8
1.3.3. MDR ……9
1.3.4. Signaling pathway ……10
1.3.5. Perturbation of HA-CD44 with sHA……11
References ……13

CHAPTER 2 **Syntheses of HA Oligosaccharides** ……22
2.1. Enzymatic synthesis ……22
2.2. Chemical synthesis ……25
2.2.1. The first method with glucose building blocks……26
2.2.1.1. Synthesis by Vliegenthart's group……26
2.2.1.2. Synthesis by Petillo's group……29
2.2.1.3. Interactive one-pot synthesis by Huang's group……31
2.2.2. The second method with glucuronic acid building blocks……37
2.2.2.1. Synthesis by Jacquinet's group……37
2.2.2.2. Synthesis by van der Marel's group……39
2.2.2.3. Synthesis by Huang's group……44
References ……45

CHAPTER 3 **Chemical Synthesis of $HA_{10}$**.....49
3.1. Introduction ..... 48
3.2. Results and Discussion .....49
3.3. Conclusion .....59
3.4. Experimental Section .....61
Appendix A (NMR Spectra).....85
References .....139

CHAPTER 4 **Design and Synthesis of $HA_5$ Analogues as Potential Inhibitors of CD44-HA binding** .....143
4.1. Introduction .....143
4.2. Results and Discussion .....148
4.2.1. $HA_2$ Library.....148
4.2.1.1. The Design and Synthesis of $HA_2$ Library.....148
4.2.1.2. The ELISA.....150
4.2.1.3. Results and Discussion.....153
4.2.2. $HA_5$ Library.....155
4.2.2.1. The Design.....155
4.2.2.2. The Syntheses.....156
4.2.2.3. Results and Discussion.....170
4.3. Conclusion ..... 173
4.4. Experimental Section ..... 175
Appendix B (NMR Spectra) .....204
References .....271

LIST OF TABLES

**Table 2.1.** One-pot synthesis .....34

**Table 3.1.** The effects of additives on glycosylation product distribution .....56

LIST OF FIGURES

**Figure 1.1.** CD44 pre-mRNA .....2

**Figure 1.2.** CD44s and CD44v1-10 .....3

**Figure 1.3.** Co-crystal of CD44 HABD and $HA_8$ .....4

**Figure 1.4.** H-Bonds between CD44 HABD and $HA_8$.....5

**Figure 1.5.** Leukocyte recruitment .....6

**Figure 1.6.** CD44-HA signaling pathway .....10

**Figure 1.7.** Perturbation of HA-CD44 interaction.....11

**Figure 2.1.** Scheme of catalyst generation and dual-enzyme reactor. A, mutagenesis was used to transform the dual-action HAS into two single-action catalysts, GlcNAc-transferase (*GN-T*) and GlcUA-transferase (*GA-T*). *B*, a starting acceptor was combined with the UDP-GlcNAc precursor and circulated through the GlcNAc-transferase reactor (*white circle*, GlcNAc; *black circle*, GlcUA). After coupling, UDP-GlcUA precursor was added to the mixture and circulated through the GlcUA-transferase reactor. This stepwise synthesis can be repeated as desired (*dashed line*) until the target oligosaccharide size is reached.....24

**Figure 2.2.** Compounds **1**, **2**, **3** and **4**.....28

**Figure 2.3.** Compounds **12**, **13**, **14**, **15**, **16**, **17**, **18**, **19**, **20** and **21**.....29

**Figure 2.4.** Compounds **22**, **23** and **24**.....30

**Figure 2.5.** Compounds **32**, **33**, **34**, **35** and **36**.....33

**Figure 2.6.** Compounds **41**, **42**, **43** and **44**.....35

**Figure 2.7.** Compounds **45**, **46**, **47** and **48**.....35

**Figure 2.8.** Compounds **49**, **50**, **51** and **52**.....37

**Figure 2.9.** Compounds **53**, **54** and **55**.....39

**Figure 2.10.** Compounds **63**, **64** and **65**.....40

**Figure 2.11.** Compounds **71**, **72** and **73**.....41

**Figure 2.12.** Compounds **81**, **82** and **83**.....44

**Figure 3.1.** Compound **4**.....51

**Figure 3.2.** Compounds **25**, **26**, **27** and **28**.....57

**Figure 3.3.** $^{1}$H-NMR of compound **9** (500 MHz, $D_2O$)..... 86

**Figure 3.4.** $^{1}$H-NMR of compound **10** (500 MHz, $CDCl_3$) ..... 87

**Figure 3.5.** $^{13}$C-NMR of compound **10** (125 MHz, $CDCl_3$).....88

**Figure 3.6.** $^{1}$H–$^{1}$H gCOSY of compound **10** (500 MHz, $CDCl_3$)..... 89

**Figure 3.7.** $^{1}$H–$^{13}$C gHMQC of compound **10** (500 MHz, $CDCl_3$) ..... 90

**Figure 3.8.** $^{1}$H–$^{13}$C gHMQC (without $^{1}$H decoupling) of compound **10** (500 MHz, $CDCl_3$)..... 91

**Figure 3.9.** $^{1}$H–$^{13}$C gHMBC of compound **10** (500 MHz, $CDCl_3$) .....92

**Figure 3.10.** $^{1}$H-NMR of compound **19** (500 MHz, $CDCl_3$) .....93

**Figure 3.11.** $^{13}$C-NMR of compound **19** (125 MHz, $CDCl_3$) .....94

**Figure 3.12.** $^{1}$H–$^{1}$H gCOSY of compound **19** (500 MHz, $CDCl_3$).....95

**Figure 3.13.** $^{1}$H–$^{13}$C gHMQC of compound **19** (500 MHz, $CDCl_3$).....96

**Figure 3.14.** $^{1}$H–$^{13}$C gHMQC (without $^{1}$H decoupling) of compound **19** (500 MHz, $CDCl_3$).....97

**Figure 3.15.** $^{1}$H–$^{13}$C gHMBC of compound **19** (500 MHz, $CDCl_3$) .....98

**Figure 3.16.** $^{1}$H-NMR of compound **11** (500 MHz, $CDCl_3$) .....99

**Figure 3.17.** $^{13}$C-NMR of compound **11** (125 MHz $CDCl_3$) .....100

**Figure 3.18.** $^{1}H–^{1}H$ gCOSY of compound **11** (500 MHz, $CDCl_3$) .....101

**Figure 3.19.** $^{1}H–^{13}C$ gHMQC of compound **11** (500 MHz, $CDCl_3$) .....102

**Figure 3.20.** $^{1}H–^{13}C$ gHMQC (without $^{1}H$ decoupling) of compound **11** (500 MHz, $CDCl_3$).....103

**Figure 3.21.** $^{1}H–^{13}C$ gHMBC of compound **11** (500 MHz, $CDCl_3$) .....104

**Figure 3.22.** $^{1}H$-NMR of compound **12** (500 MHz, $CDCl_3$) .....105

**Figure 3.23.** $^{13}C$-NMR of compound **12** (125 MHz, $CDCl_3$) .....106

**Figure 3.24.** $^{1}H–^{1}H$ gCOSY of compound **12** (500 MHz, $CDCl_3$) .....107

**Figure 3.25.** $^{1}H–^{13}C$ gHMQC of compound **12** (500 MHz, $CDCl_3$) .....108

**Figure 3.26.** $^{1}H–^{13}C$ gHMQC (without $^{1}H$ decoupling) of compound **12** (500 MHz, $CDCl_3$).....109

**Figure 3.27.** $^{1}H–^{13}C$ gHMBC of compound **12** (500 MHz, $CDCl_3$) .....110

**Figure 3.28.** $^{1}H$-NMR of compound **13** (500 MHz, $CDCl_3$) .....111

**Figure 3.29.** $^{13}C$-NMR of compound **13** (125 MHz, $CDCl_3$) .....112

**Figure 3.30.** $^{1}H–^{1}H$ gCOSY of compound **13** (500 MHz, $CDCl_3$) .....113

**Figure 3.31.** $^{1}H–^{13}C$ gHMQC of compound **13** (500 MHz, $CDCl_3$).....114

**Figure 3.32.** $^{1}H–^{13}C$ gHMQC (without $^{1}H$ decoupling) of compound **13** (500 MHz, $CDCl_3$).....115

**Figure 3.33.** $^{1}H–^{13}C$ gHMBC of compound **13** (500 MHz, $CDCl_3$) .....116

**Figure 3.34.** $^{1}$H-NMR of compound **25** (500 MHz, $CDCl_3$) .....117

**Figure 3.35.** $^{13}$C-NMR of compound **25** (125 MHz, $CDCl_3$).....118

**Figure 3.36.** $^{1}$H–$^{1}$H gCOSY of compound **25** (500 MHz, $CDCl_3$) .....119

**Figure 3.37.** $^{1}$H–$^{13}$C gHMQC of compound **25** (500 MHz, $CDCl_3$) .....120

**Figure 3.38.** $^{1}$H–$^{13}$C gHMQC (without $^{1}$H decoupling) of compound **25** (500 MHz, $CDCl_3$).....121

**Figure 3.39.** $^{1}$H–$^{13}$C gHMBC of compound **25** (500 MHz, $CDCl_3$).....122

**Figure 3.40.** $^{1}$H-NMR of compound **26** (500 MHz, $CDCl_3$).....123

**Figure 3.41.** $^{13}$C-NMR of compound **26** (125 MHz, $CDCl_3$).....124

**Figure 3.42.** $^{1}$H–$^{1}$H gCOSY of compound **26** (500 MHz, $CDCl_3$) .....125

**Figure 3.43.** $^{1}$H–$^{13}$C gHMQC of compound **26** (500 MHz, $CDCl_3$) .....126

**Figure 3.44.** $^{1}$H–$^{13}$C gHMQC (without $^{1}$H decoupling) of compound **26** (500 MHz, $CDCl_3$).....127

**Figure 3.45.** $^{1}$H–$^{13}$C gHMBC of compound **26** (500 MHz, $CDCl_3$) .....128

**Figure 3.46.** $^{1}$H-NMR of compound **27** (500 MHz, $CDCl_3$) .....129

**Figure 3.47.** $^{13}$C-NMR of compound **27** (125 MHz, $CDCl_3$).....130

**Figure 3.48.** $^{1}$H–$^{1}$H gCOSY of compound **27** (500 MHz, $CDCl_3$) .....131

**Figure 3.49.** $^{1}$H–$^{13}$C gHMQC of compound **27** (500 MHz, $CDCl_3$) .....132

**Figure 3.50.** $^{1}$H-NMR of compound **28** (500 MHz, $CDCl_3$) .....133

**Figure 3.51.** $^{13}$C-NMR of compound **28** (125 MHz, $CDCl_3$) .....134

**Figure 3.52.** $^{1}$H–$^{1}$H gCOSY of compound **28** (500 MHz, $CDCl_3$) .....135

**Figure 3.53.** $^{1}$H–$^{13}$C gHMQC of compound **28** (500 MHz, $CDCl_3$) .....136

**Figure 3.54.** $^{1}$H–$^{13}$C gHMQC (without $^{1}$H decoupling) of compound **28** (500 MHz, $CDCl_3$).....137

**Figure 3.55.** $^{1}$H–$^{13}$C gHMBC of compound **28** (500 MHz, $CDCl_3$) .....138

**Figure 4.1.** Inhibitors reported by Takahashi's group.....144

**Figure 4.2.** H-bonds in CD44-$HA_8$ co-crystal structure.....145

**Figure 4.3.** Ligands of Galectin-3.....147

**Figure 4.4.** Co-crystal structure of galectin-3 and analogue **2**.....147

**Figure 4.5.** MAG Ligands.....148

**Figure 4.6.** The hydrophobic pocket in CD44-$HA_8$ co-crystal structure.....148

**Figure 4.7.** Docking results of $HA_2$ library .....149

**Figure 4.8.** $HA_8$ inhibition curve .....152

**Figure 4.9.** Inhibition ELISA of compounds **10** ~ **16**.....154

**Figure 4.10.** Alternative Inhibition ELISA of compound **10**, Linker **1** and **2**.....155

**Figure 4.11.** Compound **10**, Linker **1** and **2**..... .....155

**Figure 4.12.** $HA_5$ backbone.....156

**Figure 4.13.** Visualization of the amide linked hydrophobic groups in CD44 HABD..156

**Figure 4.14.** $HA_5$ analogues a) Library A; b) Library B; c) Library C .....164

**Figure 4.15.** Library B .....165

**Figure 4.16.** Library C .....165

**Figure 4.17.** Visualizations of compounds **49** and **50** in CD44 HABD.....166

**Figure 4.18.** Visualizations of compounds **51** - **56** in CD44 HABD.....166

**Figure 4.19.** Visualizations of compounds **56** - **59** in CD44 HABD.....167

**Figure 4.20.** Inhibition ELISA of sHA and analogues .....171

**Figure 4.21.** sHA and analogues.....172

**Figure 4.22** Inhibition curve of compound 56, $HA_6$ and $HA_8$.....172

**Figure 4.23.** $^{1}$H-NMR of compound **10** (500 MHz, $CDCl_3$).....205

**Figure 4.24.** $^{1}$H-NMR of compound **11** (500 MHz, $CDCl_3$).....206

**Figure 4.25.** $^{1}$H-NMR of compound **12** (500 MHz, $CDCl_3$).....207

**Figure 4.26.** $^{1}$H-NMR of compound **13** (500 MHz, $CDCl_3$).....208

**Figure 4.27.** $^{1}$H-NMR of compound **14** (500 MHz, $CDCl_3$).....209

**Figure 4.28.** $^{1}$H-NMR of compound **15** (500 MHz, $CDCl_3$).....210

**Figure 4.29.** $^{1}$H-NMR of compound **16** (500 MHz, $CDCl_3$).....211

**Figure 4.30.** $^{1}$H-NMR of NMR of compound **38** (500 MHz, $CDCl_3$) .....212

**Figure 4.31.** $^{13}$C-NMR of compound **38** (125 MHz $CDCl_3$) .....213

**Figure 4.32.** $^{1}$H–$^{1}$H gCOSY of compound **38** (500 MHz, $CDCl_3$) .....214

**Figure 4.33.** $^{1}$H–$^{13}$C gHMQC of compound **38** (500 MHz, $CDCl_3$).....215

**Figure 4.34.** $^{1}H–^{13}C$ gHMQC (without $^{1}H$ decoupling) of compound **38** (500 MHz, $CDCl_3$).....216

**Figure 4.35.** $^{1}H–^{13}C$ gHMBC of compound **38** (500 MHz, $CDCl_3$).....217

**Figure 4.36.** $^{1}H$-NMR of compound **40** (500 MHz, $CDCl_3$).....218

**Figure 4.37.** $^{1}H–^{1}H$ gCOSY of compound **40** (500 MHz, $CDCl_3$).....219

**Figure 4.38.** $^{1}H–^{13}C$ gHMQC (without $^{1}H$ decoupling) of compound **40** (500 MHz, $CDCl_3$).....220

**Figure 4.39.** $^{1}H–^{13}C$ gHMBC of compound **40** (500 MHz, $CDCl_3$) .....221

**Figure 4.40.** $^{1}H$-NMR of compound **72** (500 MHz, $CDCl_3$).....222

**Figure 4.41.** $^{13}C$-NMR of compound **72** (125 MHz, $CDCl_3$) .....223

**Figure 4.42.** $^{1}H–^{1}H$ gCOSY of compound **72** (500 MHz, $CDCl_3$) .....224

**Figure 4.43.** $^{1}H–^{13}C$ gHMQC (without $^{1}H$ decoupling) of compound **72** (500 MHz, $CDCl_3$).....225

**Figure 4.44.** $^{1}H$-NMR of compound **73** (500 MHz, $CDCl_3$) .....226

**Figure 4.45.** $^{13}C$-NMR of compound **73** (125 MHz, $CDCl_3$).....227

**Figure 4.46.** $^{1}H–^{1}H$ gCOSY of compound **73** (500 MHz, $CDCl_3$) .....228

**Figure 4.47.** $^{1}H–^{13}C$ gHMQC (without $^{1}H$ decoupling) of compound **73** (500 MHz, $CDCl_3$).....229

**Figure 4.48.** $^{1}H$-NMR of compound **61** (500 MHz, $CDCl_3$) .....230

**Figure 4.49.** $^{13}$C-NMR of compound **61** (125 MHz, $CDCl_3$) .....231

**Figure 4.50.** $^{1}$H–$^{1}$H gCOSY of compound **61** (500 MHz, $CDCl_3$).....232

**Figure 4.51.** $^{1}$H–$^{13}$C gHMQC of compound **61** (500 MHz, $CDCl_3$) .....233

**Figure 4.52.** $^{1}$H–$^{13}$C gHMQC (without $^{1}$H decoupling) of compound **61** (500 MHz, $CDCl_3$).....234

**Figure 4.53.** $^{1}$H–$^{13}$C gHMBC of compound **61** (500 MHz, $CDCl_3$) .....235

**Figure 4.54.** $^{1}$H-NMR of compound **62** (500 MHz, $CDCl_3$) .....236

**Figure 4.55.** $^{13}$C-NMR of compound **62** (125 MHz, $CDCl_3$) .....237

**Figure 4.56.** $^{1}$H–$^{1}$H gCOSY of compound **62** (500 MHz, $CDCl_3$).....238

**Figure 4.57.** $^{1}$H–$^{13}$C gHMQC (without $^{1}$H decoupling) of compound **62** (500 MHz, $CDCl_3$).....239

**Figure 4.58.** $^{1}$H–$^{13}$C gHMBC of compound **62** (500 MHz, $CDCl_3$) .....240

**Figure 4.59.** $^{1}$H-NMR of compound **63** (500 MHz, $CDCl_3$) .....241

**Figure 4.60.** $^{13}$C-NMR of compound **63** (125 MHz, $CDCl_3$) .....242

**Figure 4.61.** $^{1}$H–$^{1}$H gCOSY of compound **63** (500 MHz, $CDCl_3$) .....243

**Figure 4.62.** $^{1}$H–$^{13}$C gHMQC of compound **63** (500 MHz, $CDCl_3$) .....244

**Figure 4.63.** $^{1}$H–$^{13}$C gHMQC (without $^{1}$H decoupling) of compound **63** (500 MHz, $CDCl_3$).....245

**Figure 4.64.** $^{1}$H-NMR of compound **64** (500 MHz, $CDCl_3$) .....246

**Figure 4.65.** $^{13}$C-NMR of compound **64** (125 MHz, $CDCl_3$).....247

**Figure 4.66.** $^{1}$H–$^{1}$H gCOSY of compound **64** (500 MHz, $CDCl_3$).....248

**Figure 4.67.** $^{1}$H–$^{13}$C gHMQC (without $^{1}$H decoupling) of compound **64** (500 MHz, $CDCl_3$).....249

**Figure 4.68.** $^{1}$H-NMR of compound **49** (600 MHz, $D_2O$) .....250

**Figure 4.69.** $^{1}$H–$^{1}$H gCOSY of compound **49** (600 MHz, $D_2O$) .....251

**Figure 4.70.** $^{1}$H-NMR of compound **50** (600 MHz, $D_2O$) .....252

**Figure 4.71.** $^{1}$H–$^{1}$H gCOSY of compound **50** (600 MHz, $D_2O$).....253

**Figure 4.72.** $^{1}$H-NMR of compound **51** (600 MHz, $D_2O$) .....254

**Figure 4.73.** $^{1}$H–$^{1}$H gCOSY of compound **51** (600 MHz, $D_2O$).....255

**Figure 4.74.** $^{1}$H-NMR of compound **52** (600 MHz, $D_2O$) .....256

**Figure 4.75.** $^{1}$H–$^{1}$H gCOSY of compound **52** (600 MHz, $D_2O$) .....257

**Figure 4.76.** $^{1}$H-NMR of compound **53** (600 MHz, $D_2O$).....258

**Figure 4.77.** $^{1}$H–$^{1}$H gCOSY of compound **53** (600 MHz, $D_2O$) .....259

**Figure 4.78.** $^{1}$H-NMR of compound **54** (600 MHz, $D_2O$) .....260

**Figure 4.79.** $^{1}$H–$^{1}$H gCOSY of compound **54** (600 MHz, $D_2O$) .....261

**Figure 4.80.** $^{1}$H-NMR of compound **55** (600 MHz, $D_2O$) .....262

**Figure 4.81.** $^{1}$H–$^{1}$H gCOSY of compound **55** (600 MHz, $D_2O$).....263

**Figure 4.82.** $^{1}$H-NMR of compound **56** (600 MHz, $D_2O$) .....264

**Figure 4.83.** $^{1}$H–$^{1}$H gCOSY of compound **56** (600 MHz, $D_2O$) .....265

**Figure 4.84.** $^{1}$H-NMR of compound **57** (600 MHz, $D_2O$) .....266

**Figure 4.85.** $^{1}$H–$^{1}$H gCOSY of compound **57** (600 MHz, $D_2O$).....267

**Figure 4.86.** $^{1}$H-NMR of compound **58** (600 MHz, $D_2O$) .....268

**Figure 4.87.** $^{1}$H-NMR of compound **59** (600 MHz, $D_2O$) .....269

**Figure 4.88.** $^{1}$H-NMR of compound **67** (600 MHz, $D_2O$).....270

LIST OF ABBREVIATIONS

Acetic acid (AcOH)

Acetic anhydride ($Ac_2O$)

Acetonitrile (MeCN)

Acetyl (Ac)

Activation-induced cell death (AICD)

Adipic dihydrazide (ADH)

Alanine (Ala)

Allyl (All)

Allyloxycarbonyl (Alloc)

Ammonium acetate ($NH_4OAc$)

Arginine (Arg, R)

Avidin conjugated horseradish peroxidase (Avidin-HRP)

Azobisisobutyronitrile azobisisobutylonitrile (AIBN)

Benzoyl (Bz)

Benzoyl chloride (BzCl)

Benzyl (Bn)

[Bis(acetoxy)iodo]benzene (BAIB)

Boron trifluoride etherate ($BF_3{\cdot}Et_2O$)

Bovine serum albumin (BSA)

Breast cancer resistance protein (BCRP)

Calcium carbonate ($CaSO_4$)

Camphorsulfonic acid (CSA)

Catalytic amount (Cat.)

Ceric ammonium nitrate (CAN)

Chloroform ($CHCl_3$)

Concentrated (conc.)

Copper sulfate ($CuSO_4$)

Correlation spectroscopy (COSY)

Cysteine (Cys)

Cytotoxic T lymphocytes (CTL)

Degree celsius ($^{\circ}C$)

Dichloromethane (DCM)

Deuterated chloroform ($CDCl_3$)

Deuterated methanol ($CD_3OD$)

Deuterated water ($D_2O$)

1,8-Diazabicyclo[5.4.0]undec-7-ene (DBU)

2,3-Dichloro-5,6-dicyano-1, 4-benzoquinone (DDQ)

Diethyl ether ($Et_2O$)

4-Dimethylaminopyridine (DMAP)

Dimethylformamide (DMF)

Dimethyl(methy1-thio)sulfonium triflate (DMTST)

Dimethyl sulfoxide (DMSO)

Di-*tert*-butylsilylidene (DTBS)

Doublet (d)

Electrospray ionization mass spectrometry (ESI-MS)

Epidermal growth factor receptor (EGFR)

Epithelial-mesenchymal transition (EMT)

Equivalent (eq.)

Erizin-radixin-moiesin (ERM)

Ethanol (EtOH)

Ethyl acetate (EA)

1-Ethyl-3-(3-dimethyl-aminopropyl)carbodiimide hydrochloride (EDCI)

Extraceullular matrix (ECM)

Enzyme-linked immunosorbent assay (ELISA)

Galactose (Gal)

Glucronic acid (GlcUA)

Glycosaminoglycan (GAG)

Gram (g)

Grb2-associated binder (Gab)

Growth factor receptor-bound protein (Grb)

Guanine nucleotide exchange factor (Vav)

Glucose (Glc)

Glucuronic acid (GlcUA)

Hepatocyte growth factor (HGF)

Heteronuclear multiple bond coherence (HMBC)

Heteronuclear multiple quantum coherence (HMQC)

High performance liquid chromatography (HPLC)

Hour (hr)

Human epidermal growth factor receptor 2 (ErbB2)

Hyaluronan (HA)

Hyaluronan binding domain (HABD)

Hyaluronan decasaccharide ($HA_{10}$)

Hyaluronan disaccharide ($HA_2$)

Hyaluronan heptasaccharide ($HA_7$)

Hyaluronan hexasaccharide ($HA_6$)

Hyaluronan-mediated motility receptor (RHAMM)

Hyaluronan octasaccharides ($HA_8$)

Hyaluronan oligosaccharide (sHA)

Hyaluronan pentasaccharide ($HA_5$)

Hyaluronic acid receptor for endocytosis (HARE)

Hyaluronan synthases (HAS)

Hyaluronan tetrasaccharide ($HA_4$)

Hyaluronan trisaccharide ($HA_3$)

Hydrazine hydrate ($NH_2NH_2{\cdot}H_2O$)

Hydrazine acetate ($NH_2NH_2{\cdot}HOAc$)

Hydrochloric acid (HCl)

Hydrogen bond (H-Bond)

Hydrogen fluoride (HF)

Hydrogen peroxide ($H_2O_2$)

Hydroxyl (OH)

Isoleucine (Ile)

Levulinoyl (Lev)

Lymphatic vessel endothelial hyaluronan receptor (LYVE)

Molecular sieve (MS)

Megahertz (MHz)

Methanol (MeOH)

Methyl (Me)

Methyl amine ($MeNH_2$)

Methoxyphenyl (MP)

Microliter (µl)

Milligram (mg)

Millimolar (mmol)

Mitogen-activated protein kinases (MAPK)

Multiplet (m)

Multidrug resistance (MDR)

Multidrug resistance-associated protein (MRP)

Myelin associated glycoprotein (MAG)

*N*-Acetylglucosamine (GlcNAc)

*N*-hydroxysuccinimide (NHS)

*N*-iodosuccinimide (NIS)

*N*, *N'*-Dicyclohexylcarbodiimide (DCC)

Nuclear magnetic resonance (NMR)

Palladium hydroxide ($Pd(OH)_2$)

Palladium on activated carbon (Pd/C)

P-glycoprotein (P-gp)

*p*-Methoxybenzyl (PMB)

*p*-toluoyl (Tol)

Phenyl (Ph)

Phenyl diazomethane ($PhCHN_2$)

Phthalimido (Phth)

Phosphate buffered saline (PBS)

PBS solution with Tween 20 (PBST)

Phosphatidylinositol 3-kinase (PI3K)

Potassium bicarbonate ($KHCO_3$)

Potassium carbonate ($K_2CO_3$)

Potassium iodide (KI)

Protein kinase B (AKT)

Proteoglycan (PG)

Proto-oncogene tyrosine-protein kinase (Src)

*p*-Toluenesulfenyl chloride (*p*-TolSCl)

*p*-Toluenesulfenyl triflate (*p*-TolSOTf)

*p*-Toluenesulfonic acid (*p*-TsOH)

Pyridine (Py)

Pyridinum chlorochromate (PCC)

Pyridinium dichromate (PDC)

Ras homolog gene family, member A (RhoA)

Ras-related C3 botulinum toxin substrate 1 (Rac1)

Receptor tyrosine kinase (RTK)

RNA triphosphatase (RTPase)

Room temperature (r.t.)

Quantitatively convert (quant.)

Serine (Ser)

Serum-derived HA-binding protein (SHAP)

Sialic acid (Sia)

Silver triflate (AgOTf)

Silver carbonate ($Ag_2CO_3$)

Singlet (s)

Size-exclusion column (G-15)

Sodium acetate (NaOAc)

Sodium bicarbonate ($NaHCO_3$)

Sodium carbonate ($Na_2CO_3$)

Sodium chlorite ($NaClO_2$)

Sodium hydride (NaH)

Sodium hydroxide (NaOH)

Sodium hypochlorite (NaClO)

Sodium methoxide (NaOMe)

Sodium sulfate ($Na_2SO_4$)

Sodium thiosulfate ($Na_2S_2O_3$)

Structure–activity relationship (SAR)

*n*-Butanol (*n*-BuOH)

*t*-Butanol (*t*-BuOH)

Tetrabutylammonium hydroxide (TBAOH)

Tetrabutylammonium thioacetate (TBASAc)

*tert*-butyl diphenyl silyl (TBDPS)

*tert*-butyl diphenylchlorosilane (TBDPSCl)

2, 2, 6, 6-Tetramethylpiperidin-1-oxyl (TEMPO)

Tetrahydrofuran (THF)

3,3′,5,5′-Tetramethylbenzidine (TMB)

Thin layer chromatography (TLC)

Thioacetic acid (HSAc)

Threonine (Thr)

TNF-α-stimulated protein 6 (TSG-6)

TNF receptor superfamily, member 6 (Fas)

Toll-like receptors (TLR)

Tosyl (Ts)

tributyltin hydride ($Bu_3SnH$)

Trichloroethoxycarbonyl (Troc)

Triethylamine (TEA)

Triethylamine tris-hydrofluoride ($TEA^{\cdot}$ 3HF)

Triflic acid (TfOH)

Trifluoromethanesulfonic anhydride ($Tf_2O$)

Trimethylsilyl triflate (TMSOTf)

Triphenylphosphine oxide ($Ph_2SO$)

tri-*tert-butyl* pyrimidine (TTBP)

Triplet (t)

Trichloroacetyl (TCA)

Triethyl phosphite (TEP)

Triethylsilane ($Et_3SiH$)

Trifluoroacetic acid (TFA)

tri-*tert*-butyl silyl (TBS)

Tyrosine (Tyr, Y)

Uridine diphosphate (UDP)

Uridine triphosphate (UTP)

Very late antigen (VLA)

Zinc (Zn)

LIST OF SCHEMES

**Scheme 2.1.** Enzymatic synthesis of HA with regeneration of sugar nucleotides.....23

**Scheme 2.2.** Transglycosylation reaction by testicular hyaluronidase.....23

**Scheme 2.3.** HA synthesis with oxazoline building block.....25

**Scheme 2.4.** Two general strategies for sHA assembly.....25

**Scheme 2.5.** Synthesis by Vliegenthart's group.....27

**Scheme 2.6.** Deprotections of compound **12** and **13**.....28

**Scheme 2.7.** Synthesis by Petillo's group.....31

**Scheme 2.8.** Interactive one-pot synthesis .....32

**Scheme 2.9.** Synthesis of $HA_2$ building blocks.....33

**Scheme 2.10.** Deprotection of compound **44**.....37

**Scheme 2.11.** Synthesis by Jacquinet's group.....38

**Scheme 2.12.** Synthesis of compound **70**.....40

**Scheme 2.13.** Synthesis of compound **80**.....41

**Scheme 2.14.** Synthesis of compound **86** and **87**.....43

**Scheme 3.1.** Previous synthesis on $HA_6$ 3.....51

**Scheme 3.2.** Previous synthesis on $HA_{10}$.....52

**Scheme 3.3.** Retrosynthetic scheme towards $HA_{10}$ **9**.....53

**Scheme 3.4.** Synthesis of monosaccharide building blocks **14** and **15**.....53

**Scheme 3.5.** Assembly of $HA_2$ building blocks.....54

**Scheme 3.6.** Oxazoline formation.....55

**Scheme 3.7.** Deprotection.....59

**Scheme 4.1.** Synthesis of Biotin-HA.....150

**Scheme 4.2.** Retrosynthetic scheme of compound **1**.....151

**Scheme 4.3.** Retrosynthetic scheme of compound **17**.....157

**Scheme 4.4.** Synthesis of compound **23**.....158

**Scheme 4.5.** Synthesis towards $HA_5$ with STol donor.....159

**Scheme 4.6.** Synthesis towards $HA_5$ with Br donor.....160

**Scheme 4.7.** Synthesis towards $HA_5$ with trichloroacetimidate donor.....161

**Scheme 4.8.** Synthesis route towards $HA_5$ thioglycoside.....162

**Scheme 4.9.** Synthesis toward $HA_2$ thioglycoside .....163

**Scheme 4.10.** Synthesis of library B.....168

**Scheme 4.11.** Synthesis of library C.....169

**Scheme 4.12.** Deprotection of compound **57**.....170

**Scheme 4.13.** Deprotection Preparation of monosaccharide 35, 36, 37, 38, 15 and 23.....184

# CHAPTER 1

## Functions of CD44-HA Interactions in Inflammation and Malignancy

### 1.1. CD 44, a major receptor for HA

#### 1.1.1. HA

HA is a non-sulfated negatively charged linear polysaccharide, which is composed of 2,000-25,000 repeating units of disaccharides: [-D-glucuronic acid-*β*-1→3-*N*-acetyl-D-glucosamine-*β*-1→4-]. The molecular weight is around $10^6$- $10^7$ Da and the polymer length is 2-25 μm[1]. Unlike other glucosaminoglycan, HA is not linked to core proteins. HA is synthesized by three hyaluronan synthases (HAS) (HAS1, HAS2 and HAS3) on the plasma membrane and the chains are extruded into the extracellular space[2-5].

HA is a major component of ECM. HA is tethered to cell surface by either cell-surface receptors such as CD44 or HAS. This HA 'coat' can incorporate proteoglycan (PG) and other HA binding proteins, such as TNF-α-stimulated protein 6 (TSG-6) and link protein[6-7].

There are multiple HA binding proteins, also called hyaladherins: lymphatic vessel endothelial hyaluronan receptor 1 (LYVE1) is mainly restricted to lymphatic vessel and lymph node[8]; hyaluronic acid receptor for endocytosis (HARE) clears HA from circulation[9]; toll-like receptors (TLRs) and TSG-6 are related to the immune system[8, 10]; CD44 is related to the immune system atherosclerosis and cancer[11-12];

hyaluronan-mediated motility receptor (RHAMM) is important to wound healing and cancer[13].

### 1.1.2. CD 44

**Figure 1.1.** CD44 pre-mRNA. Adapted with permission from Ref 14. **Copyright 2003 Nature Publishing Group**. For interpretation of the references to color in this and all other figures, the reader is referred to the electronic version of this dissertation.

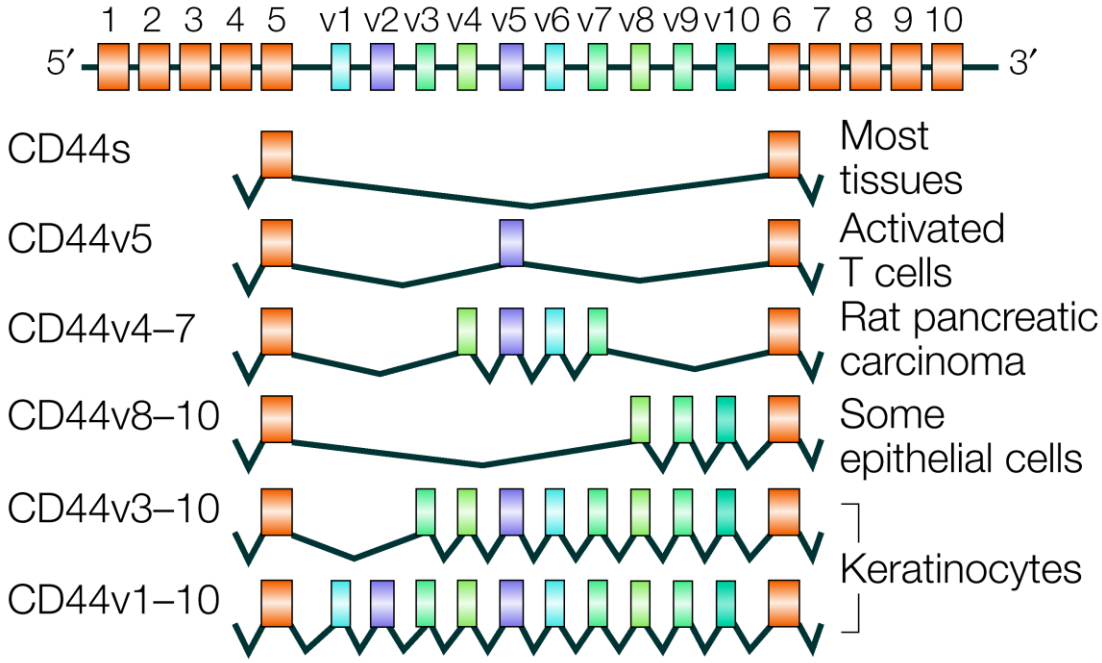


CD44 is the primary receptor for HA. CD44 is a single chain transmembrane protein. The CD44 pre-mRNA is encoded by 20 exons (**Figure 1.1**) [14]. The first five non-variable exons encode the *N*-terminal HABD. In this region, 90 amino acids (32-123), which are conserved in many hyaladherins, are named 'link module'[15] (**Figure 1.2**[14]). Between HABD and the transmembrane domain is the stem domain. In the standard isoform CD44s, this region is composed of 46 amino acids. By alternative splicing, this domain can be enlarged by different combination of variant exons (V1-V10) to generate

different isoforms of CD44[16-17]. The transmembrane domain is composed of 13 hydrophobic amino acids and a cysteine. This domain participates in CD44 condensation[18] and CD44-lipid rafts interaction[19-20]. The *C*-terminal cytoplasmic-tail domain plays a crucial role in signaling.

**Figure 1.2.** CD44s and CD44v1-10. Adapted with permission from Ref 14. **Copyright 2003 Nature Publishing Group**.

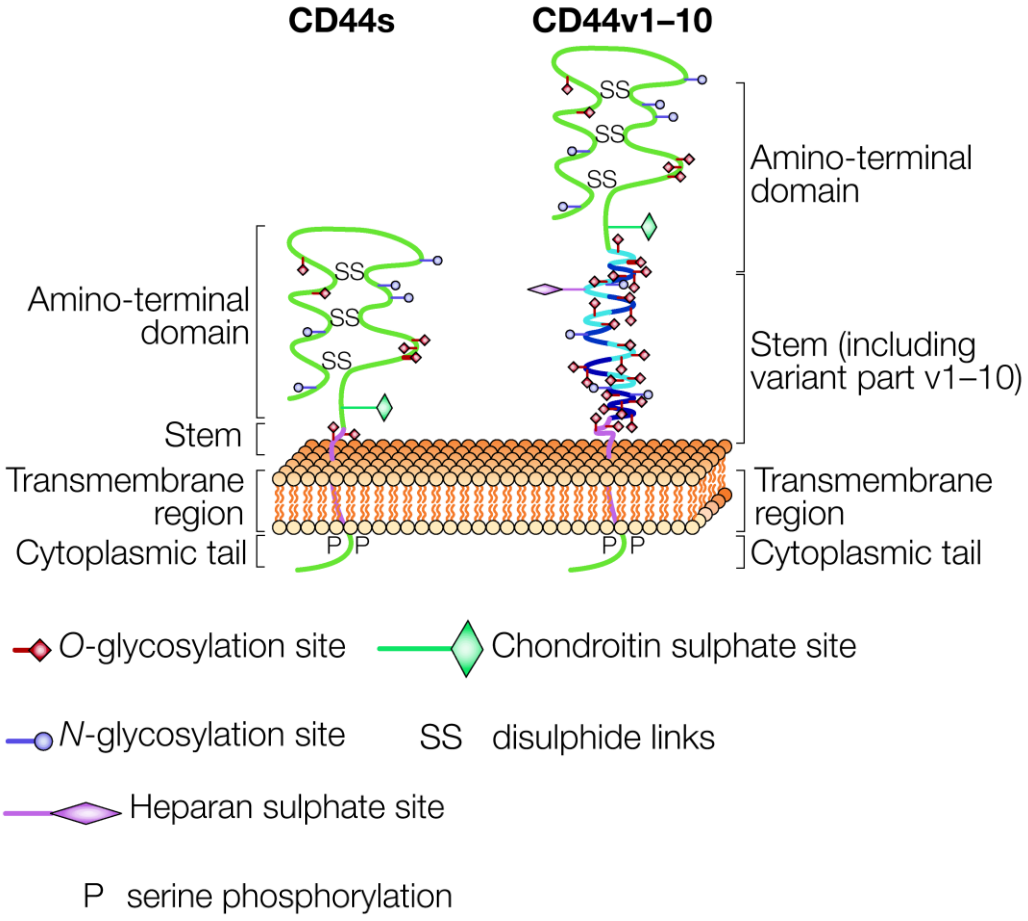


### 1.1.3. CD44-HA interactions

In 2007, Jackson's group reported the co-crystal structure of murine CD44 HABD and $HA_8$ (**Figure 1.3**)[21]. $HA_8$ binds to a shallow groove and the interactions are dominated by H-Bonds and hydrophobic interactions. The hydrophobic interactions are

from sugar rings from GlcNAc4 to GlcUA7 and the methyl group in GlcNAc6. The H-Bonds are from GlcUA5 to GlcNAc8 as summarized in **Figure 1.4**. In addition, two conformers are identified. These two forms differed in the orientation of arginine 45 (Arg45) which move closer to $HA_8$.

**Figure 1.3.** Co-crystal of CD44 HABD and $HA_8$. Adapted with permission from Ref 21. **Copyright 2008 Nature Publishing Group**.

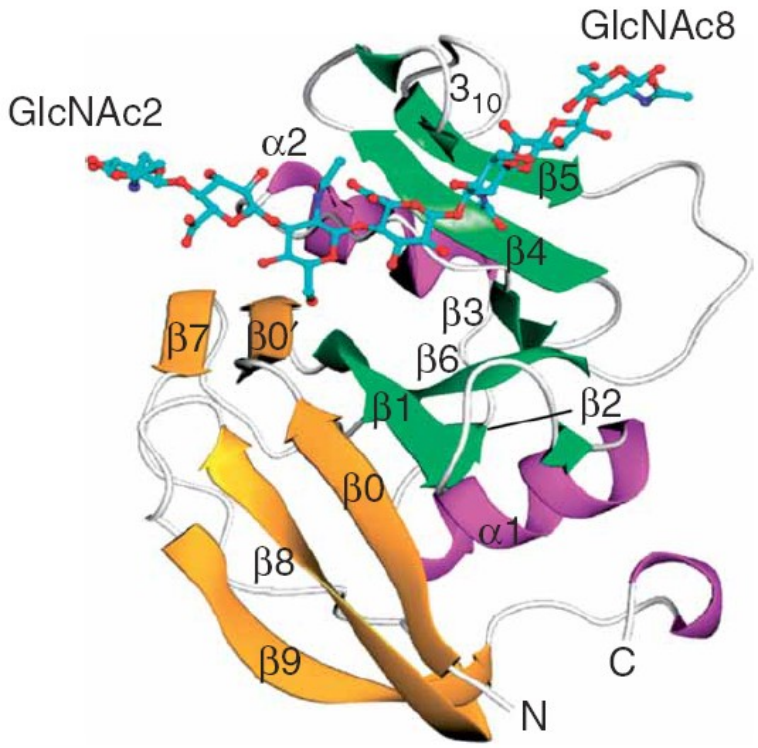


### 1.2. Functions of CD44 and HA interactions in the immune system

#### 1.2.1. Pro-inflammatory role

Leukocytes are recruited to inflammatory site in four steps (**Figure 1.5**)[22]. First,

leukocytes in the blood stream are tethered to endothelial cells through binding with cell adhesion molecules. Second, tethering and rolling reduce the velocity and allow further interactions with endothelial cells, which leads to adhesion. Third, adhesion is followed by the arrest step. Finally leukocytes move outward through intact vessel walls into surrounding body tissue, which is also called diapedesis (**Figure 1.5**). CD44-HA interactions and selectins-ligands interactions contribute to the initial tethering and rolling steps leading to integrin-mediated adhesion[23].

**Figure 1.4.** H-Bonds between CD44 HABD and $HA_8$

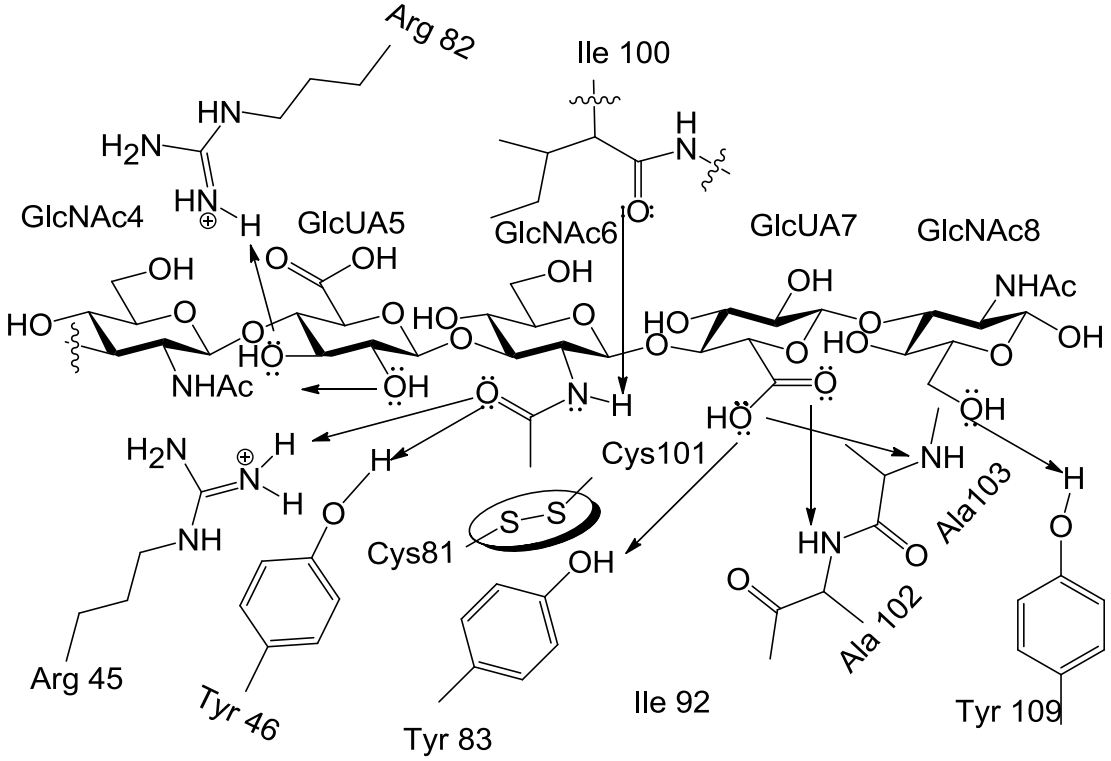


Siegelman's group reported that T cell rolling is CD44 and HA dependent[23-25]. In inflammation sites, endothelial cell surface CD44 binds HA, and present HA to T cell

surface CD44. This CD44-HA-CD44 'sandwich' interaction leads to rolling[26-27]. CD44 also participates in T cell adhesion. This process is mediated by integrin very late antigen 4 (VLA-4) and CD44 cytoplasmic domain[28-29].

Neutrophil recruitment is reduced in CD44 null mice[30-31]. Reduced recruitment of macrophages is observed in CD44 null macrophages[32-33]. However, how CD44 and HA involved in neutrophil and macrophage recruitments is not very clear[23, 34].

**Figure 1.5.** Leukocyte recruitment. Adapted with permission from Ref 22. **Copyright 2002 Elsevier**.

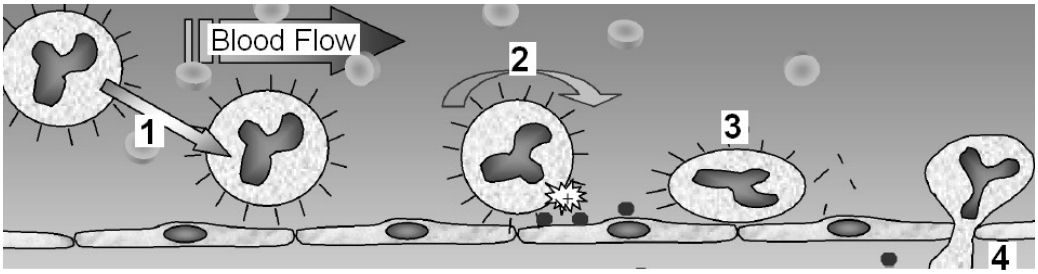


### 1.2.2. Anti-inflammatory role

#### 1.2.2.1. HA uptake

Successful repair after inflammation requires removal of the ECM break down products. During inflammation, accumulated HA fragments have proinflammatory functions[10]. CD44 positive macrophages play important roles in HA fragment clearance and maintain HA homeostasis[35-37]. Since HA fragments up-regulate TLR-2 and 4 responses, HA uptake can down-regulate TLR-2 and 4 signaling and reduce

inflammatory response[38-39].

#### 1.2.2.2. AICD

Stimulation from T cell receptors to already expanded T cell without appropriate co-stimulation could lead to T cell death, named activation-induced cell death (AICD)[40]. AICD removes activated T cells to maintain immune homeostasis. High MW HA-CD44 binding enhances AICD in T cells[23, 41-42]. This CD44-mediated AICD is TNF receptor superfamily member 6 (Fas)-independent[43].

### 1.3. Functions of CD44 and HA interactions in cancer

#### 1.3.1. Tumor microenvironment

The tumor microenvironment contains different type of cells, including vascular cells, fibroblasts, immune cells and ECM[44]. HA and HA binding proteins are the major components of ECM[45-46]. HA provides a favorable environment for cell proliferation and migration. HA binding proteins regulate HA functions[47-48]. serum-derived HA-binding protein (SHAP), TSG-6 and versican contribute to the formation of HA meshwork. CD44, LYVE-1 and RHAMM are the cell surface receptor for anchoring[49-51]. In addition, tumor cell and other types of cells communicate with each other to adjust the components in tumor microenvironment for tumor cell proliferation, migration, invasion, and metastasis[52-53].

### 1.3.2. Tumor initiation and progression

#### 1.3.2.1. HA in invasion

HA promotes tumor cell migration and invasion from three aspects. Cancer-associated fibroblasts amplify the synthesis of HA and proteoglycans, and the expanded ECM leads to increased viscoelasticity and malleability which support the cancer cell shape change and tissue penetration[54]. HA is involved in the protease production and presentation. Finally, HA participates in the induction of cytoskeleton rearrangements[1, 6].

#### 1.3.2.2. CD44 in tumor cells extravagation during metastasis

Metastatic process is similar to leukocyte recruitment. Tumor cells must tether and adhere to endothelial cells of the blood vessel wall and then transmigrate to the tissue. HA-CD44 interaction leads to the amplification of integrin-mediated adhesion to the vessel wall[55-57].

#### 1.3.2.3. CD44 reduces Fas-mediated killing of tumor cells

Although cytotoxic T lymphocytes (CTL)-mediated cytotoxicity plays a major role in tumor rejection, tumors often protect themselves against CTL recognition and attack. CD44-HA interactions reduce both Fas expression and Fas-mediated apoptosis, leading to less susceptibility to CTL-mediated cytotoxicity[55, 58].

#### 1.3.2.4. Epithelial-mesenchymal transition (EMT)

EMT is the transition of cells which involves decreased intercellular junctions, escaped apoptosis and enhanced invasiveness which CD44-HA interaction is important for EMT. Disruption of HA-CD44 interaction can block the EMT induction from HGF treatment and overexpresion of beta-catenine[1, 53].

#### 1.3.2.5. Cancer stem cell

Cancer stem cells are stem cells within tumors. Very small number of cancer stem cells can rapidly regenerate a fully grown tumor when implanted in an animal host[59-61]. CD44 is the common marker for cancer stem cell isolation. It was reported that CD44 has important functions in leukemia stem cells, brain tumor stem cells, pancreatic cancer stem cells and breast cancer stem cells[59, 62-65]. However, nothing is known about the role of HA-CD44 in cancer stem cells[66].

### 1.3.3. MDR

Four ways could generate MDR: the reduced uptake of drugs from the tissue barriers; enhanced repair systems; increased anti-apoptosis; and finally, enhanced drug efflux[67-69].

HA and CD44 promote MDR in many cancer cell types[66, 70-72]. The possible mechanisms are: decreased tissue barrier and enhanced drug penetration[73-75];

enhanced cell survival signaling pathways[76]; and finally, enhanced drug efflux by regulating the expression and membrane stabilization of dug transporters, including P-glycoprotein, multidrug resistance-associated protein 2 (MRP2) and BCRP[70, 77].

P-gp is a well characterized ATP-binding cassette transporter (ABC-transporter) in MDR subfamily. P-gp is in close vicinity to CD44 in lipid rafts[78]. Perturbation of HA-CD44 interaction induces internalization of P-gp and CD44 into the cell. In addition, expression of CD44 and P-gp are co-regulated[79-80].

### 1.3.4. Signaling pathway

Multivalent HA-CD44 interactions induce direct and indirect interactions with RTK receptor tyrosine kinases (RTKs) including human epidermal growth factor receptor 2 (ErbB2) and epidermal growth factor receptor (EGFR), and non-receptor kinases of proto-oncogene tyrosine-protein kinase (Src) family or Ras family GTPases (**Figure 1.6**) [1, 13, 81]. Adaptor proteins such as guanine nucleotide exchange factor 2 (Vav2), growth factor receptor-bound protein 2 (Grb2), and Grb2-associated binder 1 (Gab-1) mediate the formation of above complex and mediate the interaction of CD44 with upstream effectors such as Ras homolog gene family member A (RhoA), Ras-related C3 botulinum toxin substrate 1 (Rac1) and Ras, which eventually influence down stream mitogen-activated protein kinases (MAPK) and phosphatidylinositol 3-kinase (PI3K)/ protein kinase B (AKT) signaling pathways[82]. The above signaling pathways promote

tumor cell invasiveness, proliferation, survival and MDR[13, 83].

In addition, CD44 can influence cellular events including tumor cell proliferation and motility by cross-linking to actin cytoskeleton through ankyrin or ERM family[13-14, 84].

**Figure 1.6. CD44-HA signaling pathway**

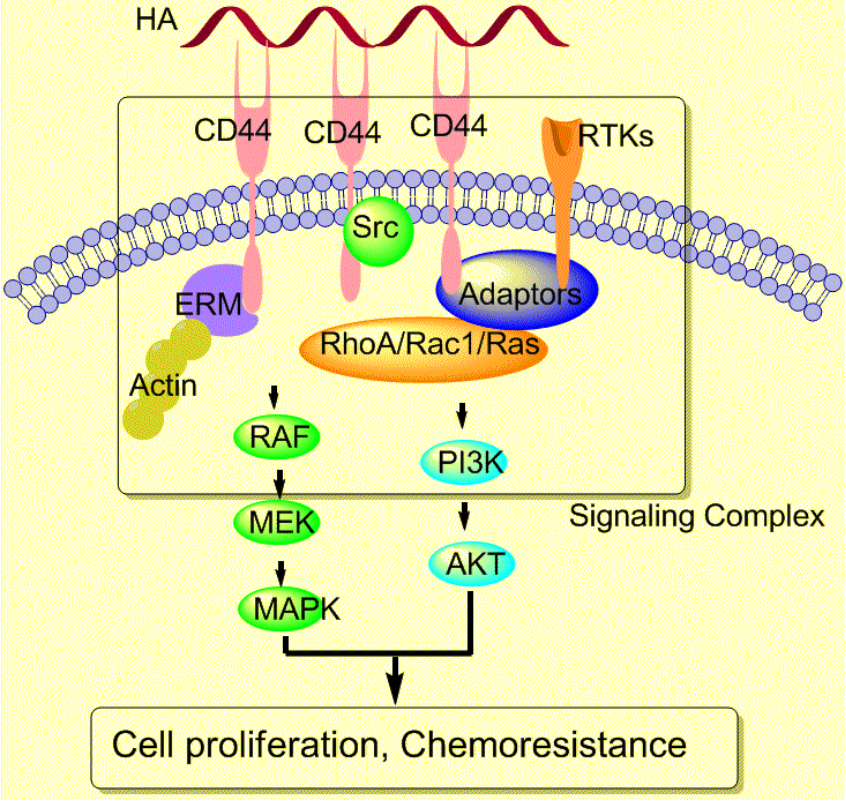


### 1.3.5. Perturbation of HA-CD44 with HA oligomers (sHA)

Multivalent HA-CD44 interaction is required for formation of constitutive signaling complexes containing CD44, RTKs, Src, adaptor proteins, erizin-radixin-moiesin (ERM) and other signaling components (**Figure 1.7a**)[76, 85-86]. Replacement of the multivalent interactions with monovalent interaction by the treatment with sHA causes disassembly

of constitutive signaling complexes and attenuated signaling pathway (**Figure 1.7b**)[83]. These finally lead to the inhibition of cell proliferation and MDR[87].

**Figure 1.7.** Perturbation of HA-CD44 interaction by. Adapted with permission from Ref 1. **Copyright 2004 Nature Publishing Group**.

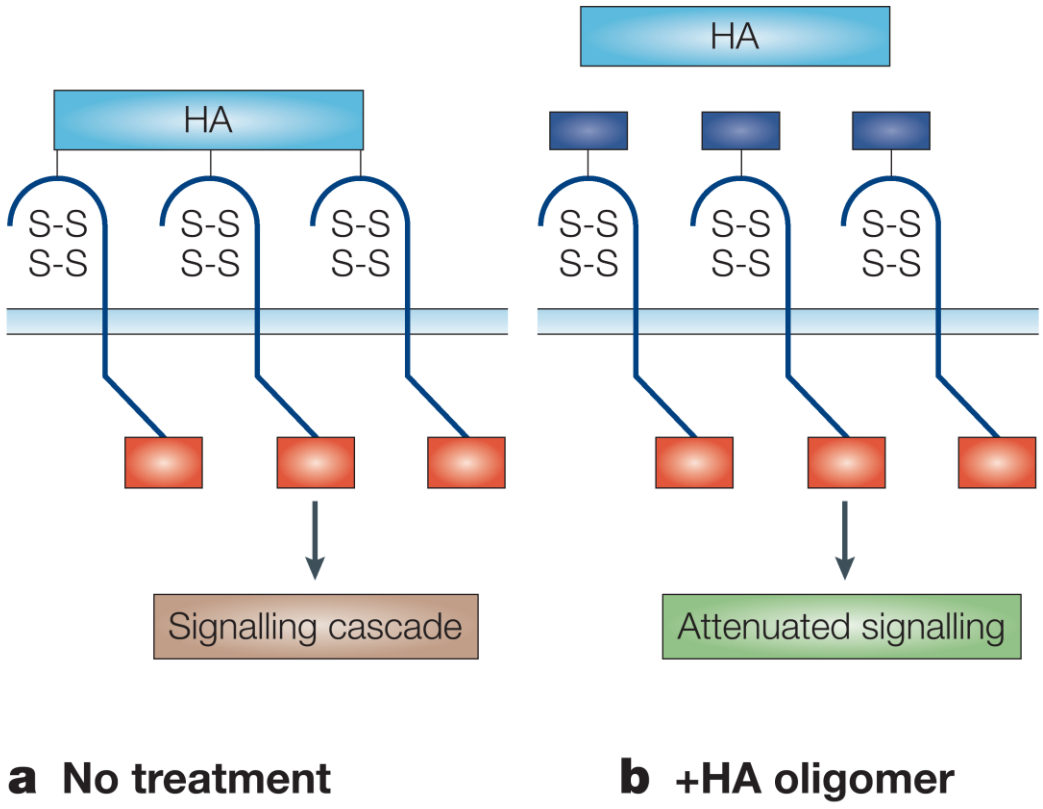

## References

## References


1. Toole, B. P., Hyaluronan: From extracellular glue to pericellular cue. *Nat Rev Cancer* **2004,** *4* (7), 528-539.

2. Weigel, P. H.; Hascall, V. C.; Tammi, M., Hyaluronan synthases. *J Biol Chem* **1997,** *272* (22), 13997-14000.

3. Tammi, M. I.; Day, A. J.; Turley, E. A., Hyaluronan and homeostasis: A balancing act. *J Biol Chem* **2002,** *277* (7), 4581-4584.

4. Watanabe, K.; Yamaguchi, Y., Molecular identification of a putative human hyaluronan synthase. *J Biol Chem* **1996,** *271* (38), 22945-22948.

5. Prehm, P., Release of hyaluronate from eukaryotic cells. *Biochem J* **1990,** *267* (1), 185-189.

6. Toole, B. P., Hyaluronan in morphogenesis. *Semin Cell Dev Biol* **2001,** *12* (2), 79-87.

7. Toole, B. P., Hyaluronan in morphogenesis and tissue remodelling. *Science of hyaluronan today* **1998**.

8. Jackson, D. G., Immunological functions of hyaluronan and its receptors in the lymphatics. *Immunol Rev* **2009,** *230* (1), 216-231.

9. Pandey, M. S.; Harris, E. N.; Weigel, J. A.; Weigel, P. H., The cytoplasmic domain of the hyaluronan receptor for endocytosis (HARE) contains multiple endocytic motifs targeting coated Pit-mediated internalization. *J Biol Chem* **2008,** *283* (31), 21453-21461.

10. Jiang, D.; Liang, J.; Noble, P. W., Hyaluronan in tissue injury and repair. *Annu Rev Cell Dev Biol* **2007,** *23*, 435-461.

11. Johnson, P.; Ruffell, B., CD44 and its role in inflammation and inflammatory diseases. *Inflammation Allergy Drug Targets* **2009,** *8* (3), 208-220.

12. Toole, B. P.; Wight, T. N.; Tammi, M. I., Hyaluronan-cell interactions in cancer and vascular disease. *J Biol Chem* **2002,** *277* (7), 4593-4596.

13. Toole, B. P., Hyaluronan-CD44 Interactions in cancer: Paradoxes and possibilities. *Clin Cancer Res* **2009,** *15* (24), 7462-7468.

14. Ponta, H.; Sherman, L.; Herrlich, P. A., CD44: From adhesion molecules to signalling regulators. *Nat Rev Mol Cell Biol* **2003,** *4* (1), 33-45.

15. Sherman, L.; Sleeman, J.; Herrlich, P.; Ponta, H., Hyaluronate receptors: Key players in growth, differentiation, migration and tumor progression. *Curr Opin Cell Biol* **1994,** *6* (5), 726-733.

16. Konig, H.; Ponta, H.; Herrlich, P., Coupling of signal transduction to alternative pre-mRNA splicing by a composite splice regulator. *EMBO J* **1998,** *17* (10), 2904-2913.

17. Weg-Remers, S.; Ponta, H.; Herrlich, P.; Konig, H., Regulation of alternative pre-mRNA splicing by the ERK MAP-kinase pathway. *EMBO J* **2001,** *20* (15), 4194-4203.

18. Liu, D.; Sy, M.-S., Phorbol myristate acetate stimulates the dimerization of CD44 involving a cysteine in the transmembrane domain. *J Immunol* **1997,** *159* (6), 2702-2711.

19. Neame, S. J.; Uff, C. R.; Sheikh, H.; Wheatley, S. C.; Isacke, C. M., CD44 exhibits a cell type dependent interaction with Triton X-100 insoluble, lipid rich, plasma membrane domains. *J Cell Sci* **1995,** *108* (9), 3127-3135.

20. Perschl, A.; Lesley, J.; English, N.; Hyman, R.; Trowbridge, I. S., Transmembrane domain of CD44 is required for its detergent insolubility in fibroblasts. *J Cell Sci* **1995,** *108* (3), 1033-1041.

21. Banerji, S.; Wright, A. J.; Noble, M.; Mahoney, D. J.; Campbell, I. D.; Day, A. J.; Jackson, D. G., Structures of the CD44-hyaluronan complex provide insight into a fundamental carbohydrate-protein interaction. *Nat Struct Mol Biol* **2007,** *14* (3), 234-239.

22. Kubes, P., Introduction: The complexities of leukocyte recruitment. *Semin Immunol* **2002,** *14* (2), 65-72.

23. Ruffell, B.; Johnson, P., Hyaluronan induces cell death in activated T cells through CD44. *J Immunol* **2008,** *181* (10), 7044-7054.

24. DeGrendele, H. C.; Estess, P.; Picker, L. J.; Siegelman, M. H., CD44 and its ligand hyaluronate mediate rolling under physiologic flow: A novel lymphocyte-endothelial cell primary adhesion pathway. *J Exp Med* **1996,** *183* (3), 1119-1130.

25. Clark, R. A.; Alon, R.; Springer, T. A., CD44 and hyaluronan-dependent rolling interactions of lymphocytes on tonsillar stroma. *J Cell Biol* **1996,** *134* (4), 1075-1087.

26. Mohamadzadeh, M.; Degrendele, H.; Arizpe, H.; Estess, P.; Siegelman, M., Proinflammatory stimuli regulate endothelial hyaluronan expression and CD44/HA-dependent primary adhesion. *J Clin Invest* **1998,** *101* (1), 97-108.

27. Nandi, A.; Estess, P.; Siegelman, M. H., Hyaluronan anchoring and regulation on the surface of vascular endothelial cells is mediated through the functionally active form of CD44. *J Biol Chem* **2000,** *275* (20), 14939-14948.

28. Nandi, A.; Estess, P.; Siegelman, M., Bimolecular complex between rolling and firm adhesion receptors required for cell arrest: CD44 association with VLA-4 in T cell extravasation. *Immunity* **2004,** *20* (4), 455-465.

29. Bonder, C. S.; Clark, S. R.; Norman, M. U.; Johnson, P.; Kubes, P., Use of CD44 by CD4+ Th1 and Th2 lymphocytes to roll and adhere. *Blood* **2006,** *107* (12), 4798-4806.

30. Khan, A. I.; Kerfoot, S. M.; Heit, B.; Liu, L.; Andonegui, G.; Ruffell, B.; Johnson, P.; Kubes, P., Role of CD44 and hyaluronan in neutrophil recruitment. *J Immunol* **2004,** *173* (12), 7594-7601.

31. McDonald, B.; McAvoy, E. F.; Lam, F.; Gill, V.; de la Motte, C.; Savani, R. C.; Kubes, P., Interaction of CD44 and hyaluronan is the dominant mechanism for neutrophil sequestration in inflamed liver sinusoids. *J Exp Med* **2008,** *205* (4), 915-927.

32. Cuff, C. A.; Kothapalli, D.; Azonobi, I.; Chun, S.; Zhang, Y.; Belkin, R.; Yeh, C.; Secreto, A.; Assoian, R. K.; Rader, D. J.; Pure, E., The adhesion receptor CD44 promotes atherosclerosis by mediating inflammatory cell recruitment and vascular cell activation. *J Clin Invest* **2001,** *108* (7), 1031-1040.

33. Hollingsworth, J. W.; Li, Z.; Brass, D. M.; Garantziotis, S.; Timberlake, S. H.; Kim, A.; Hossain, I.; Savani, R. C.; Schwartz, D. A., CD44 regulates macrophage recruitment to the lung in lipopolysaccharide-induced airway disease. *Am J Respir Cell Mol Biol* **2007,** *37* (2), 248-253.

34. Johnson, P.; Maiti, A.; Brown, K. L.; Li, R., A role for the cell adhesion molecule CD44 and sulfation in leukocyte-endothelial cell adhesion during an inflammatory response? *Biochem Pharmacol* **2000,** *59* (5), 455-465.

35. Teder, P.; Vandivier, R. W.; Jiang, D.; Liang, J.; Cohn, L.; Pure, E.; Henson, P. M.; Noble, P. W., Resolution of lung inflammation by CD44. *Science* **2002,** *296* (5565), 155-158.

36. Underhill, C. B.; Nguyen, H. A.; Shizari, M.; Culty, M., CD44 positive macrophages take up hyaluronan during lung development. *Dev Biol* **1993,** *155* (2), 324-336.

37. Culty, M.; Nguyen, H. A.; Underhill, C. B., The hyaluronan receptor (CD44) participates in the uptake and degradation of hyaluronan. *J Cell Biol* **1992,** *116* (4), 1055-1062.

38. Liang, J.; Jiang, D.; Griffith, J.; Yu, S.; Fan, J.; Zhao, X.; Bucala, R.; Noble, P. W., CD44 is a negative regulator of acute pulmonary inflammation and lipopolysaccharide-TLR signaling in mouse macrophages. *J Immunol* **2007,** *178* (4), 2469-2475.

39. Kawana, H.; Karaki, H.; Higashi, M.; Miyazaki, M.; Hilberg, F.; Kitagawa, M.; Harigaya, K., CD44 suppresses TLR-mediated inflammation. *J Immunol* **2008,** *180* (6), 4235-4245.

40. Krammer, P. H.; Arnold, R.; Lavrik, I. N., Life and death in peripheral T cells. *Nat Rev Immunol* **2007,** *7* (7), 532-542.

41. Chen, D.; McKallip, R. J.; Zeytun, A.; Do, Y.; Lombard, C.; Robertson, J. L.; Mak, T. W.; Nagarkatti, P. S.; Nagarkatti, M., CD44-deficient mice exhibit enhanced hepatitis after concanavalin a injection: Evidence for involvement of CD44 in activation-induced cell death. *J Immunol* **2001,** *166* (10), 5889-5897.

42. McKallip, R. J.; Do, Y.; Fisher, M. T.; Robertson, J. L.; Nagarkatti, P. S.; Nagarkatti, M., Role of CD44 in activation-induced cell death: CD44-deficient mice exhibit enhanced T cell response to conventional and superantigens. *Int Immunol* **2002,** *14* (9), 1015-1026.

43. Do, Y.; Rafi-Janajreh, A. Q.; McKallip, R. J.; Nagarkatti, P. S.; Nagarkatti, M., Combined deficiency in CD44 and Fas leads to exacerbation of lymphoproliferative and autoimmune disease. *Int Immunol* **2003,** *15* (11), 1327-1340.

44. Bhowmick, N. A.; Neilson, E. G.; Moses, H. L., Stromal fibroblasts in cancer initiation and progression. *Nature* **2004,** *432* (7015), 332-337.

45. McDonald, J. A.; Camenisch, T. D., Hyaluronan: Genetic insights into the complex biology of a simple polysaccharide. *Glycoconjugate J* **2003,** *19* (4/5), 331-339.

46. Laurent, T. C.; Fraser, J. R. E., Hyaluronan. *Faseb J* **1992,** *6* (7), 2397-2404.

47. Itano, N.; Zhuo, L.; Kimata, K., Impact of the hyaluronan-rich tumor microenvironment on cancer initiation and progression. *Cancer Sci* **2008,** *99* (9), 1720-1725.

48. Day, A. J.; de la Motte, C. A., Hyaluronan cross-linking: A protective mechanism in inflammation? *Trends Immunol* **2005,** *26* (12), 637-643.

49. Misra, S.; Heldin, P.; Hascall, V. C.; Karamanos, N. K.; Skandalis, S. S.; Markwald, R. R.; Ghatak, S., Hyaluronan-CD44 interactions as potential targets for cancer therapy. *Febs J* **2011,** *278* (9), 1429-1443.

50. Day, A. J.; Prestwich, G. D., Hyaluronan-binding proteins: Tying up the giant. *J Biol Chem* **2002,** *277* (7), 4585-4588.

51. Matsumoto, K.; Shionyu, M.; Go, M.; Shimizu, K.; Shinomura, T.; Kimata, K.; Watanabe, H., Distinct interaction of versican/PG-M with hyaluronan and link protein. *J Biol Chem* **2003,** *278* (42), 41205-41212.

52. Coussens, L. M.; Werb, Z., Inflammatory cells and cancer: Think different! *J Exp Med* **2001,** *193* (6), F23-F26.

53. Zhuo, L.; Kimata, K., Cumulus oophorus extracellular matrix: Its construction and regulation. *Cell Struct Funct* **2001,** *26* (4), 189-196.

54. Skandalis, S. S.; Kletsas, D.; Kyriakopoulou, D.; Stavropoulos, M.; Theocharis, D. A., The greatly increased amounts of accumulated versican and decorin with specific post-translational modifications may be closely associated with the malignant phenotype of pancreatic cancer. *Biochim Biophys Acta, Gen Subj* **2006,** *1760* (8), 1217-1225.

55. Yasuda, M.; Nakano, K.; Yasumoto, K.; Tanaka, Y., CD44: Functional relevance to inflammation and malignancy. *Histol Histopathol* **2002,** *17* (3), 945-950.

56. Fujisaki, T.; Tanaka, Y.; Fujii, K.; Mine, S.; Saito, K.; Yamada, S.; Yamashita, U.; Irimura, T.; Eto, S., CD44 stimulation induces integrin-mediated adhesion of colon cancer cell lines to endothelial cells by up-regulation of integrins and c-met and activation of integrins. *Cancer Res* **1999,** *59* (17), 4427-4434.

57. Kobayashi, T.; Okamoto, K.; Kobata, T.; Hasumuna, T.; Nishioka, K., Apomodulation as a novel therapeutic concept for the regulation of apoptosis in rheumatoid synoviocytes. *Curr Opin Rheumatol* **1999,** *11* (3), 188-193.

58. Yasuda, M.; Tanaka, Y.; Fujii, K.; Yasumoto, K., CD44 stimulation down-regulates Fas expression and Fas-mediated apoptosis of lung cancer cells. *Int Immunol* **2001,** *13* (10), 1309-1319.

59. Dalerba, P.; Cho, R. W.; Clarke, M. F., Cancer stem cells: Models and concepts. *Annu Rev Med* **2007,** *58*, 267-284.

60. Hill, R. P.; Perris, R., "Destemming" cancer stem cells. *J Natl Cancer Inst* **2007,** *99* (19), 1435-1440.

61. Vescovi, A. L.; Galli, R.; Reynolds, B. A., Brain tumor stem cells. *Nat Rev Cancer* **2006,** *6* (6), 425-436.

62. Al-Hajj, M.; Wicha, M. S.; Benito-Hernandez, A.; Morrison, S. J.; Clarke, M. F., Prospective identification of tumorigenic breast cancer cells. *Proc Natl Acad Sci* **2003,** *100* (7), 3983-3988.

63. Li, C.; Heidt, D. G.; Dalerba, P.; Burant, C. F.; Zhang, L.; Adsay, V.; Wicha, M.; Clarke, M. F.; Simeone, D. M., Identification of pancreatic cancer stem cells. *Cancer Res* **2007,** *67* (3), 1030-1037.

64. Prince, M. E.; Sivanandan, R.; Kaczorowski, A.; Wolf, G. T.; Kaplan, M. J.; Dalerba, P.; Weissman, I. L.; Clarke, M. F.; Ailles, L. E., Identification of a subpopulation of cells with cancer stem cell properties in head and neck squamous cell carcinoma. *Proc Natl Acad Sci* **2007,** *104* (3), 973-978.

65. Jin, L.; Hope, K. J.; Zhai, Q.; Smadja-Joffe, F.; Dick, J. E., Targeting of CD44 eradicates human acute myeloid leukemic stem cells. *Nat Med* **2006,** *12* (10), 1167-1174.

66. Toole, B. P.; Slomiany, M. G., Hyaluronan: A constitutive regulator of chemoresistance and malignancy in cancer cells. *Semin Cancer Biol* **2008,** *18* (4), 244-250.

67. Gottesman, M. M.; Fojo, T.; Bates, S. E., Multidrug resistance in cancer: Role of ATP-dependent transporters. *Nat Rev Cancer* **2002,** *2* (1), 48-58.

68. Cheng, J. Q.; Lindsley, C. W.; Cheng, G. Z.; Yang, H.; Nicosia, S. V., The Akt/PKB pathway: Molecular target for cancer drug discovery. *Oncogene* **2005,** *24* (50), 7482-7492.

69. Li, Z.-W.; Dalton William, S., Tumor microenvironment and drug resistance in hematologic malignancies. *Blood Rev* **2006,** *20* (6), 333-342.

70. Misra, S.; Ghatak, S.; Toole, B. P., Regulation of MDR1 expression and drug resistance by a positive feedback loop involving hyaluronan, phosphoinositide 3-kinase, and ErbB2. *J Biol Chem* **2005,** *280* (21), 20310-20315.

71. Wang Steven, J.; Bourguignon Lilly, Y. W., Hyaluronan-CD44 promotes phospholipase C-mediated $Ca^{2+}$ signaling and cisplatin resistance in head and neck cancer. *Arch Otolaryngol Head Neck Surg* **2006,** *132* (1), 19-24.

72. Wang Steven, J.; Bourguignon Lilly, Y. W., Hyaluronan and the interaction between CD44 and epidermal growth factor receptor in oncogenic signaling and chemotherapy resistance in head and neck cancer. *Arch Otolaryngol Head Neck Surg* **2006,** *132* (7), 771-778.

73. Kerbel, R. S.; St Croix, B.; Florenes, V. A.; Rak, J., Induction and reversal of cell adhesion-dependent multicellular drug resistance in solid breast tumors. *Hum Cell* **1996,** *9* (4), 257-264.

74. Baumgartner, G.; Gomar-Hoss, C.; Sakr, L.; Ulsperger, E.; Wogritsch, C., The impact of extracellular matrix on the chemoresistance of solid tumors - experimental and clinical results of hyaluronidase as additive to cytostatic chemotherapy. *Cancer Lett* **1998,** *131* (1), 85-99.

75. Desoize, B.; Jardillier, J., Multicellular resistance: A paradigm for clinical resistance? *Crit Rev Oncol Hematol* **2000,** *36* (2-3), 193-207.

76. Ghatak, S.; Misra, S.; Toole, B. P., Hyaluronan oligosaccharides inhibit anchorage-independent growth of tumor cells by suppressing the phosphoinositide 3-Kinase/Akt cell survival pathway. *J Biol Chem* **2002,** *277* (41), 38013-38020.

77. Ohashi, R.; Takahashi, F.; Cui, R.; Yoshioka, M.; Gu, T.; Sasaki, S.; Tominaga, S.; Nishio, K.; Tanabe, K. K.; Takahashi, K., Interaction between CD44 and hyaluronate induces chemoresistance in non-small cell lung cancer cell. *Cancer Lett* **2007,** *252* (2), 225-234.

78. Bacso, Z.; Nagy, H.; Goda, K.; Bene, L.; Fenyvesi, F.; Matko, J.; Szabo, G., Raft and cytoskeleton associations of an ABC transporter: P-glycoprotein. *Cytometry, Part A* **2004,** *61A* (2), 105-116.

79. Miletti-Gonzalez, K. E.; Chen, S.; Muthukumaran, N.; Saglimbeni, G. N.; Wu, X.; Yang, J.; Apolito, K.; Shih, W. J.; Hait, W. N.; Rodriguez-Rodriguez, L., The CD44 receptor interacts with P-Glycoprotein to promote cell migration and invasion in cancer. *Cancer Res* **2005,** *65* (15), 6660-6667.

80. Toole, B. P.; Slomiany, M. G., Hyaluronan, CD44 and emmprin: Partners in cancer cell chemoresistance. *Drug Resist Updates* **2008,** *11* (3), 110-121.

81. Turley, E. A.; Noble, P. W.; Bourguignon, L. Y. W., Signaling properties of hyaluronan receptors. *J Biol Chem* **2002,** *277* (7), 4589-4592.

82. Bourguignon, L. Y. W., Hyaluronan-mediated CD44 activation of RhoGTPase signaling and cytoskeleton function promotes tumor progression. *Semin Cancer Biol* **2008,** *18* (4), 251-259.

83. Toole, B. P.; Ghatak, S.; Misra, S., Hyaluronan oligosaccharides as a potential anticancer therapeutic. *Curr Pharm Biotechnol* **2008,** *9* (4), 249-252.

84. Stamenkovic, I.; Yu, Q., CD44 meets merlin and ezrin: Their interplay mediates the pro-tumor activity of CD44 and tumor-suppressing effect of merlin. *Hyaluronan Cancer Biol* **2009**, 71-87.

85. Ghatak, S.; Misra, S.; Toole, B. P., Hyaluronan constitutively regulates ErbB2 phosphorylation and signaling complex formation in carcinoma cells. *J Biol Chem* **2005,** *280* (10), 8875-8883.

86. Alaniz, L.; Garcia, M. G.; Gallo-Rodriguez, C.; Agusti, R.; Sterin-Speziale, N.; Hajos, S. E.; Alvarez, E., Hyaluronan oligosaccharides induce cell death through PI3-K/Akt pathway independently of NF-κB transcription factor. *Glycobiology* **2006,** *16* (5), 359-367.

87. Misra, S.; Ghatak, S.; Zoltan-Jones, A.; Toole, B. P., Regulation of multidrug resistance in cancer cells by hyaluronan. *J Biol Chem* **2003,** *278* (28), 25285-25288.

# CHAPTER 2

# Syntheses of sHA

## 2.1. Enzymatic syntheses

sHA can be assembled via either chemoenzymatic or chemical synthesis. Earlier chemoenzymatic approaches utilized the biosynthetic pathways through HAS and associated accessory enzymes (**Scheme 2.1**)[1] or a transglycosylation reaction catalyzed by hyaluronidases (**Scheme 2.2**)[2]. Recently, oxazolidine containing building blocks, which are transition state analogues for hyaluronidases, have been polymerized to yield HA (**Scheme 2.3**)[3-5]. In order to control the length of HA from enzymatic reactions, a HA synthase was converted by mutagenesis into two single-action glycosyltransferases (GlcUA transferase and GlcNAc transferase) (**Figure 2.1**)[6]. The alternating stepwise usage of these two novel enzymes led to the construction of a series of monodisperse synthetic sHA. Despite these successes, the inherent substrate specificities of enzymes limit the structural diversity of sHA analogues that can be generated. Chemical syntheses can complement the chemoenzymatic approaches to create greater varities of sHA structures, facilitating the structure–activity relationship (SAR) studies.

**Scheme 2.1.** Enzymatic synthesis of HA with regeneration of sugar nucleotides

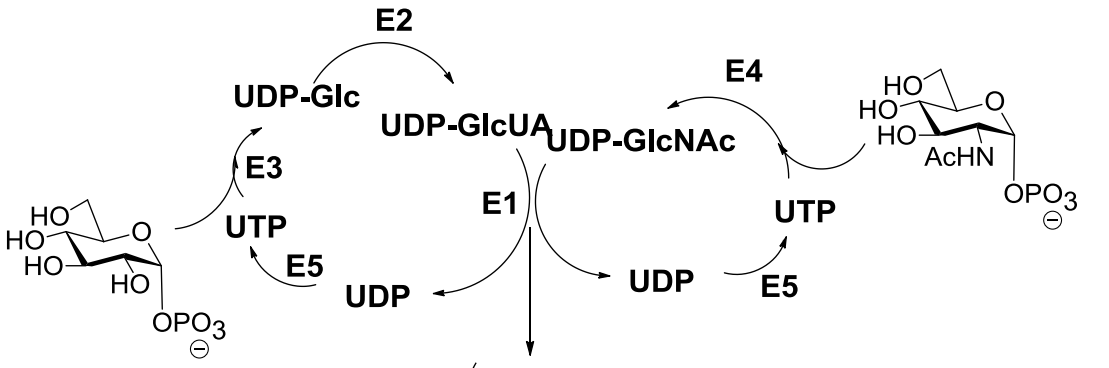


**Scheme 2.2.** Transglycosylation reaction by testicular hyaluronidase

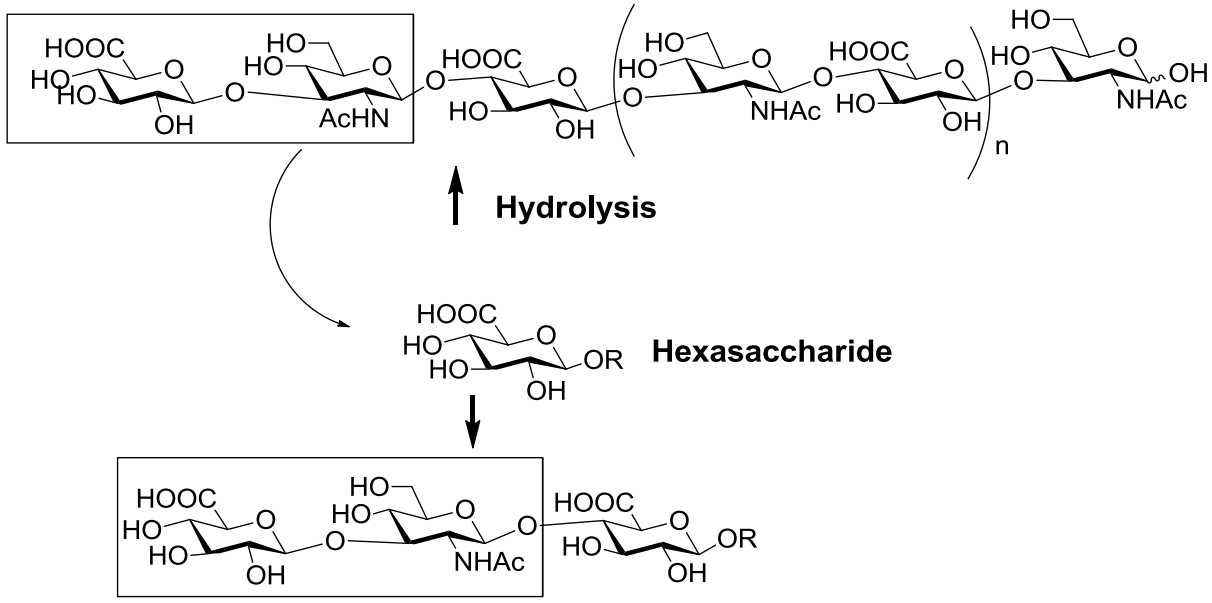

**Figure 2.1.** Scheme of catalyst generation and dual-enzyme reactor. A, mutagenesis was used to transform the dual-action HAS into two single-action catalysts, GlcNAc-transferase (*GN-T*) and GlcUA-transferase (*GA-T*). *B*, a starting acceptor was combined with the UDP-GlcNAc precursor and circulated through the GlcNAc-transferase reactor (*white circle*, GlcNAc; *black circle*, GlcUA). After coupling, UDP-GlcUA precursor was added to the mixture and circulated through the GlcUA-transferase reactor. This stepwise synthesis can be repeated as desired (*dashed line*) until the target oligosaccharide size is reached. Adapted with permission from Ref 6.
**Copyright 2003 American Society for Biochemistry and Molecular Biology**

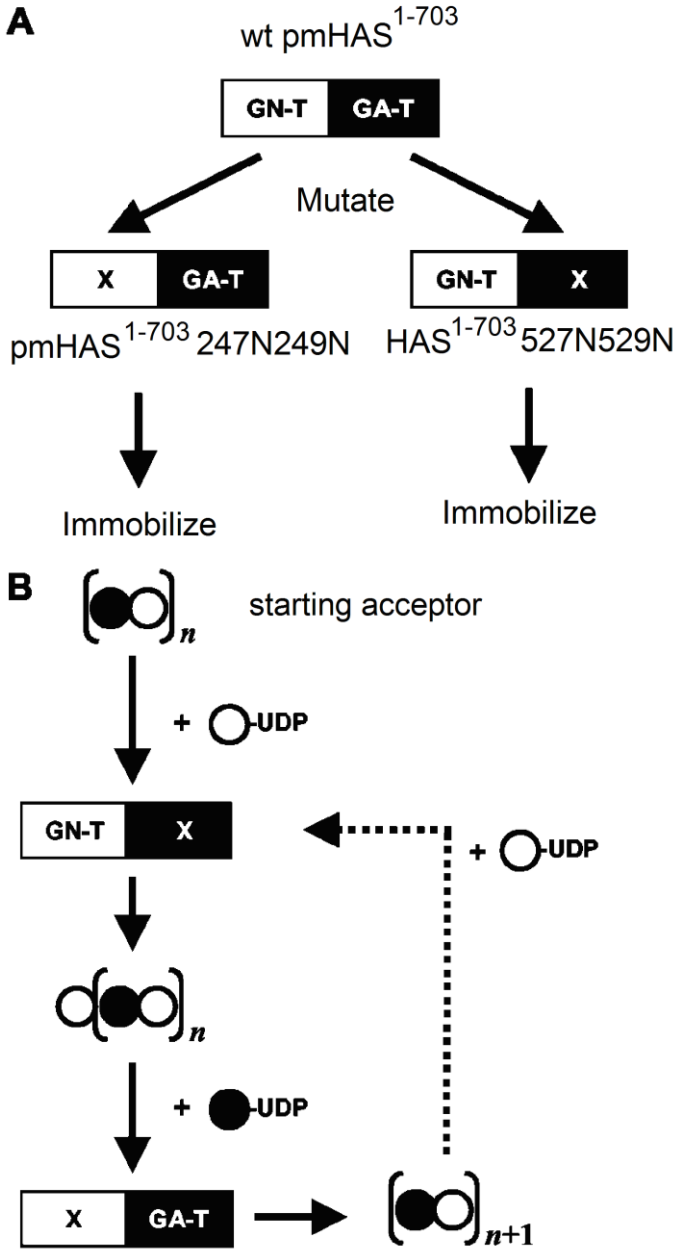

**Scheme 2.3.** HA synthesis with oxazoline building block

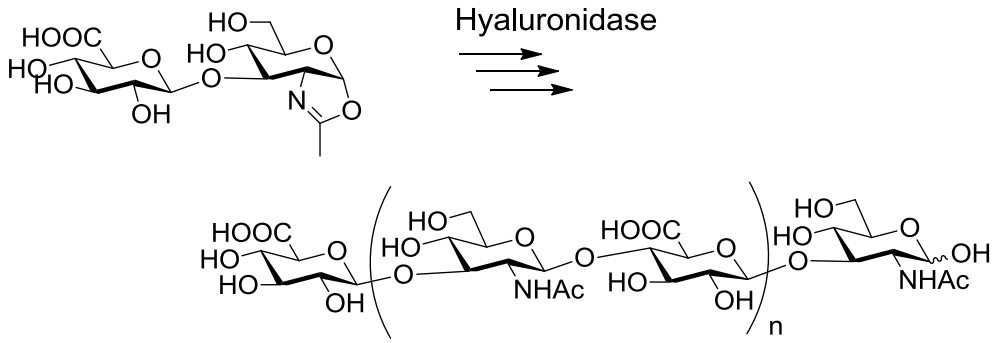


## 2.2. Chemical synthesis

**Scheme 2.4.** Two general strategies for sHA assembly

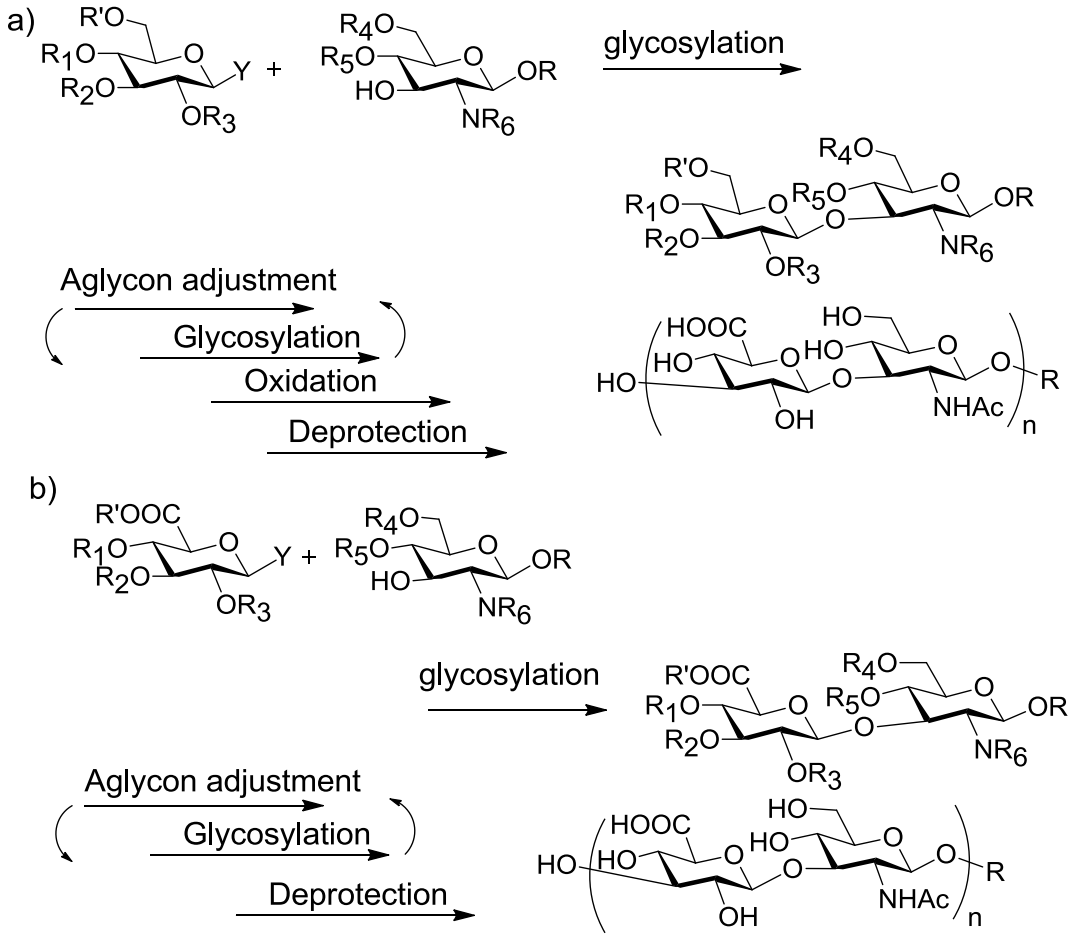


There are three central factors need to be taken into consideration in designing a synthetic

route for sHA: 1) the stereocontrolled construction of the oligosaccharide backbone; 2) introduction of GlcUA; and 3) installation of acetamido groups. Two general strategies for sHA assembly are typically adapted depending upon the order of transformations (**Scheme 2.4**)[7]. In the first method, more reactive glucose is used as building blocks with post glycosylation conversion to GlcUA via oxidation (**Scheme 2.4a**)[8-14], while the second method utilizes GlcUA directly as the glycosyl donor (**Scheme 2.4b**)[15]. Currently, both approaches have been successfully applied in preparation of sHA.

### 2.2.1. The first method with glucose building blocks

#### 2.2.1.1. Synthesis by Vliegenthart's group

For the first approach, a selectively removable protective group must be installed on the 6- hydroxyl (OH) group of glucose to allow for later oxidation state adjustment. As an example, Vliegenthart and coworkers have reported the chemical synthesis of tetrasaccharide **1** with GlcUA at reducing end (**Scheme 2.5**)[11]. The desired 1,2-*trans* linkages were controlled by the presence of participating neighboring groups, i.e. *N*-phthalimido (Phth) on glucosamines **2** and **3** and Tol on glucoside **4**. The Lev moiety was installed on 6-*O* of glucoside **4** as a selectively removable protective group. Following glycosylation of **4** by donor **2**, adjustment of the aglycon group at the reducing end by removal of the anomeric methoxyphenyl (MP) group and imidation of the resulting hemiacetal yielded disaccharide donor **6** (**Scheme 2.5a**). Reaction of **4** with **3** and subsequent deprotection gave disaccharide acceptor **8**, which was followed by

glycosylation by donor **6** and isopropylidene removal producing tetrasaccharide core **9** (**Scheme 2.5b**). Acetylation and selective cleavage of the two levulinoyl (Lev) groups by hydrazine acetate ($NH_2NH_2$.HOAc) yielded diol **10**, which was oxidized to the corresponding di-carboxylic acid **11** by tandem Swern and sodium chlorite ($NaClO_2$) oxidations. Treatment of **11** by methyl amine ($MeNH_2$) and subsequent *N*-acetylation produced the target tetrasaccharide **1**.

**Scheme 2.5.** Synthesis by Vliegenthart's group

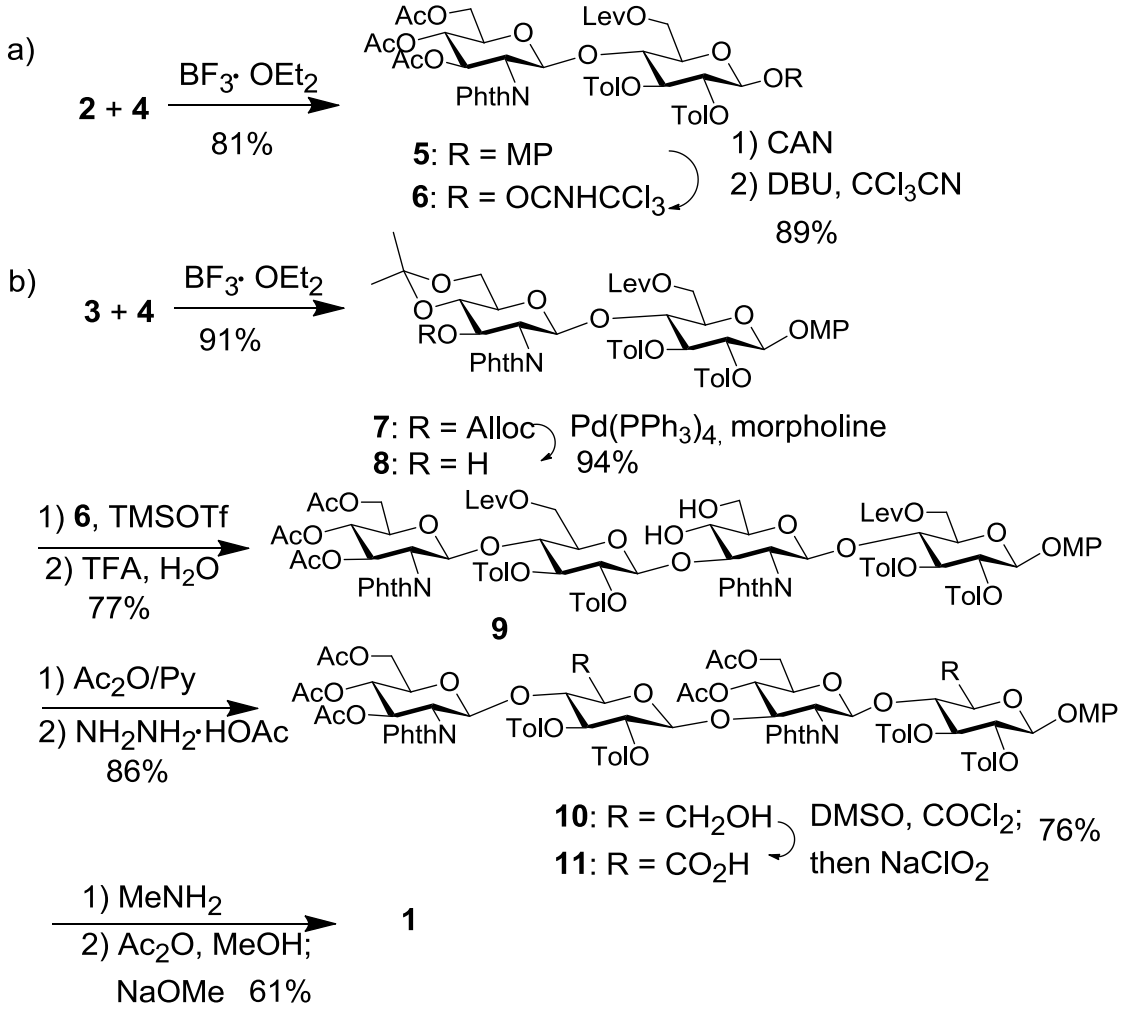

**Figure 2.2.** Compounds **1**, **2**, **3** and **4**

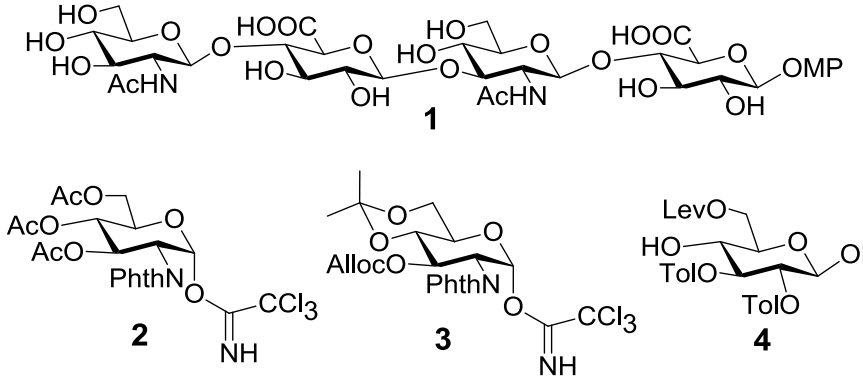


**Scheme 2.6.** Deprotections of compounds **12** and **13**

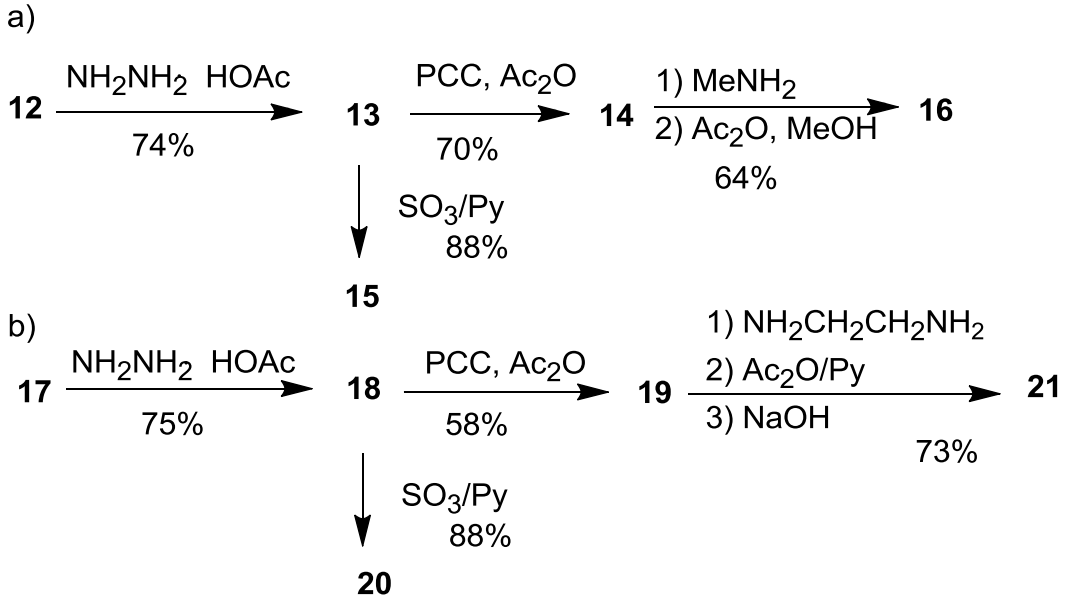


This strategy has been expanded to synthesize pentasaccharide **12** and hexasaccharide **17** with glucosamine at the reducing end[10]. However, after delevulinoylation of **12** with $NH_2NH_2 \cdot HOAc$, oxidation of the diol **13** by the tandem Swern and $NaClO_2$ oxidations did not give satisfactory results. Instead, the usage of pyridinum chlorochromate (PCC) and acetic anhydride ($Ac_2O$) was necessary producing the desired diacid **14** in good yield (**Scheme 2.6a**). Following the same oxidation method with PCC, the conversion of triol **18** to triacid **19** was achieved (**Scheme 2.6b**).

Dephthaloylation/ deacylation of triacid **19** using $MeNH_2$ in ethanol gave a complex mixture. Ultimately, the removal of *N*-phthaloyl moieties was carried out with treatment of ethylenediamine in *n*-butanol (*n*-BuOH) followed by *N*-acetylation to afford the fully deprotected hexasaccharide **21**. Besides oxidation, the free OH groups in **13** and **18** can be sulfated generating analogues **15** and **20**, which will be difficult to obtain through the chemoenzymatic approach, thus highlighting the advantage of chemical synthesis approach.

**Figure 2.3.** Compounds **12**, **13**, **14**, **15**, **16**, **17**, **18**, **19**, **20** and **21**

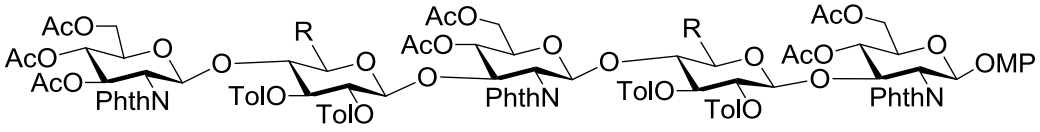

**12**: R = $CH_2OLev$

**13**: R = $CH_2OH$

**14**: R = $CO_2H$

**15**: R = $CH_2OSO_3^-\ Na^+$

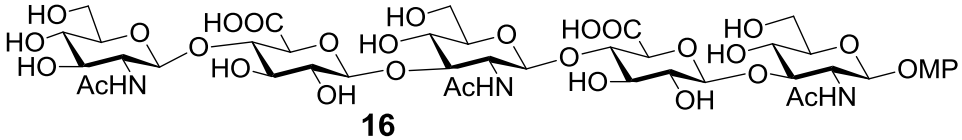

**16**

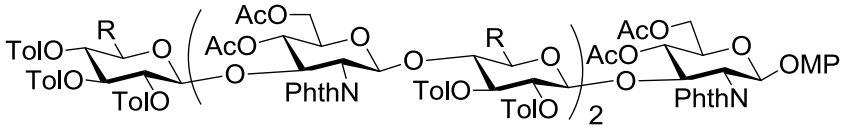

**17**: R = $CH_2OLev$

**18**: R = $CH_2OH$

**19**: R = $CO_2H$

**20**: R = $CH_2OSO_3^-\ Na^+$

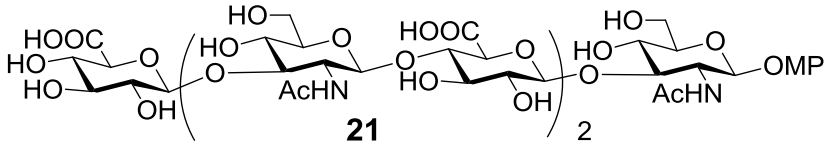

**21**

### 2.2.1.2. Synthesis by Petillo's group

Petillo and coworkers have reported syntheses of hyaluronan trisaccharide ($HA_3$) with the combination of the sulfoxide and trichloroacetimidate glycosylation methodologies (**Scheme 2.7**)[9]. Glycosylation of acceptor **22** by glycosyl sulfoxide **23** produced disaccharide **25**. The protective groups on **25** were adjusted leading to acceptor **26** with a PMB group masking the 6-OH of the glucose unit. Troc was employed as the 1,2-*trans* directing *N*-protective group for glucosamine trichloroacetimidate donor **24**, which glycosylated alcohol **26** yielding trisaccharide core **27**. Conversion of the *N*-trichloroethoxycarbonyl (Troc) and azido into acetamido moieties gave trisaccharide **28**. The *p*-methoxybenzyl (PMB) group was selectively removed by ceric ammonium nitrate (CAN) exposing the 6-OH group of the glucose, which was directly converted to carboxylic acid by a 2, 2, 6, 6-Tetramethylpiperidin-1-oxyl (TEMPO) mediated sodium hypochlorite (NaClO) oxidation in a modest 57% yield. Subsequent deacetylation and hydrogenolysis produced trisaccharide **31**.

**Figure 2.4.** Compounds **22**, **23** and **24**

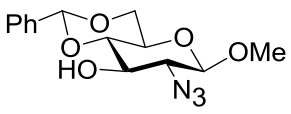


**22**

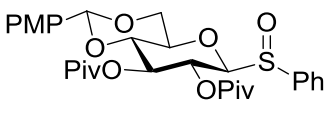


**23**

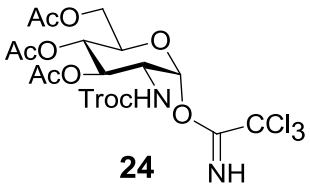


**24**

**Scheme 2.7.** Synthesis by Petillo's group

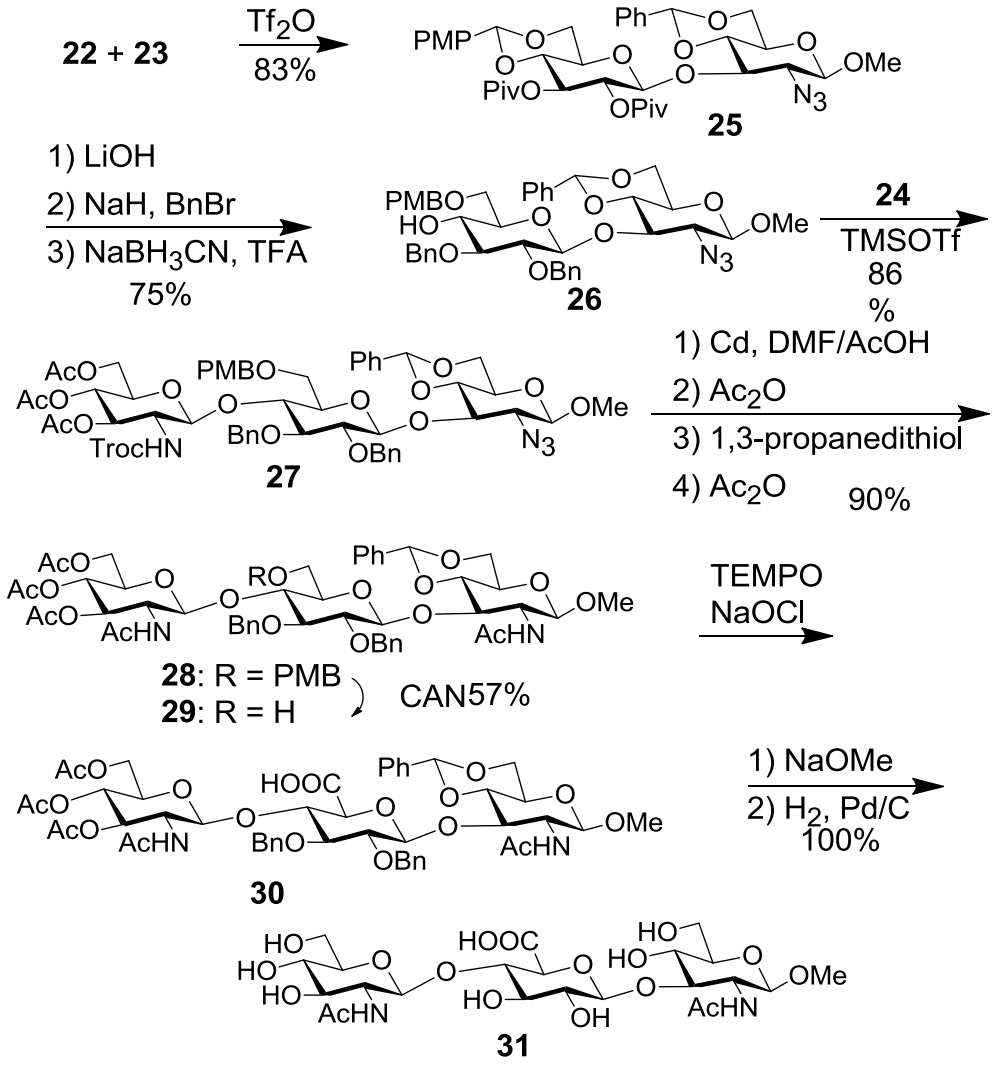


### 2.2.1.3. Interative one-pot synthesis by Huang's group

As described above, traditional oligosaccharide synthesis required multiple modifications of aglycons, adjustments of protective groups on advanced oligosaccharide intermediates as well as purification of these intermediates. Our group developed a novel iterative one-pot oligosaccharide assembly strategy[16], in which a thioglycosyl donor is pre-activated by a thiophilic promoter in the absence of an acceptor,

generating a reactive intermediate. Upon addition of a thioglycosyl acceptor to the reaction, the free OH group of the acceptor will attack on the reactive intermediate leading to a disaccharide. With its anomeric thioacetal moiety, the disaccharide can be subjected to another round of pre-activation and nucleophilic substitution extending the oligosaccharide chain. Multiple glycosylations can be sequentially carried out in the same flask without intermediate separations, thus greatly facilitating glyco-assembly (**Scheme 2.8**). Furthermore, because donor activation and glycosylation are carried out in two distinct steps, anomeric reactivities of thioglycosyl donor and acceptor do not need to be differentiated[17], granting greater flexibilities in selecting of protective groups to achieve high yields in glycosylation.

**Scheme 2.8.** Interactive one-pot synthesis

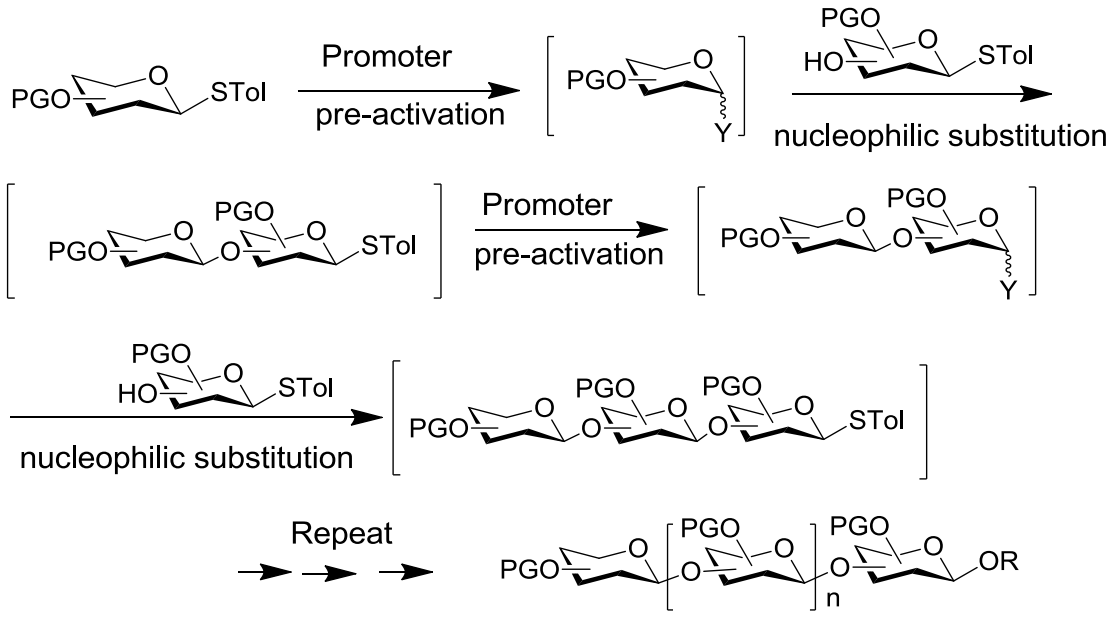


The one-pot method was successfully applied to the $HA_6$ synthesis, which was described below. Donor **32** was pre-activated by the promoter *p*-toluenesulfenyl triflate

(*p*-TolSOTf), formed *in situ* through reaction of silver triflate (AgOTf) with *p*-TolSCl (**Scheme 2.9a**). Subsequent addition of acceptor **35** and a sterically hindered non-nucleophilic base *tri-tert-butyl* pyrimidine (TTBP) to the reaction formed disaccharide **37**, which was deprotected to give disaccharide **38**. Disaccharide acceptor **40** with a methoxy group at the reducing end was prepared by reacting **32** with acceptor **36**, followed by removal of tri-*tert*-butyl silyl (TBS) (**Scheme 2.9b**).

**Scheme 2.9.** Synthesis of disaccharide building blocks

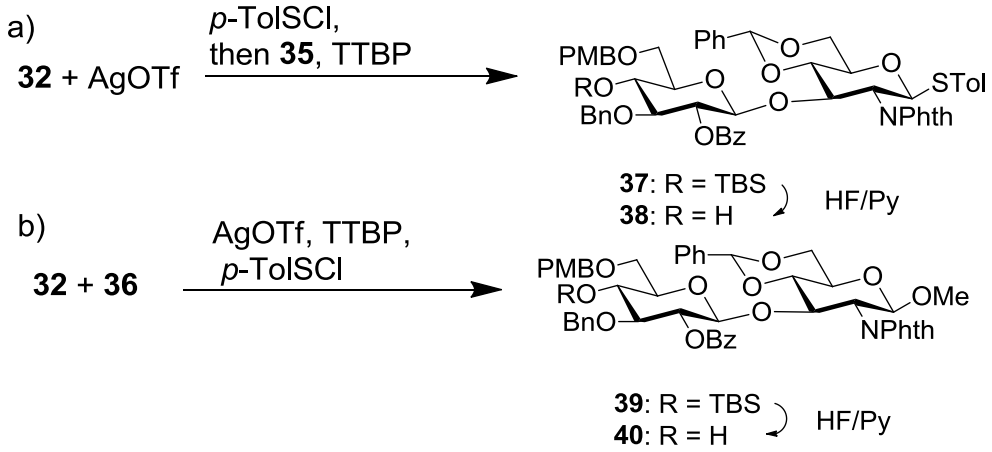


**Figure 2.5.** Compounds **32**, **33**, **34**, **35** and **36**

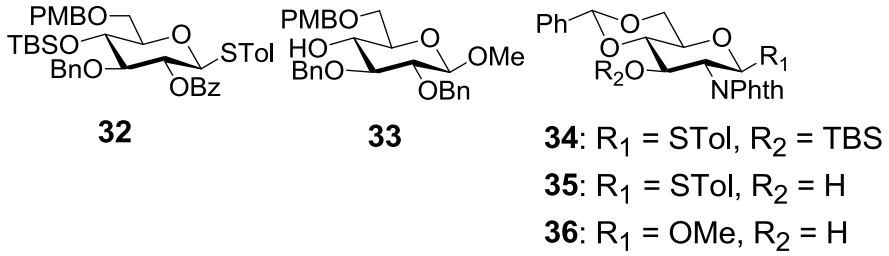


**32** **33**

**34**: $R_1$ = STol, $R_2$ = TBS
**35**: $R_1$ = STol, $R_2$ = H
**36**: $R_1$ = OMe, $R_2$ = H

With all necessary building blocks in hand, one pot syntheses were performed. Pre-activation of donor **32** by *p*-TolSOTf was followed by addition of acceptor **35** and TTBP. Upon completion of the reaction, addition of acceptor **40**, TTBP and promoter

*p*-TolSOTf to the same reaction flask produced tetrasaccharide core **41** in excellent overall yield in just 3 hrs (**Table 2.1**, entry 1), which was the only compound needed purification in this three component one-pot synthesis. sHA core sequences containing odd number of monosaccharide units can also be synthesized. Two pentasaccharide **42** and **43** with different sequences were constructed through three and four component one-pot reactions in excellent yields (**Table 2.1**, entries 2, 3). A hexasaccharide **44** was easily accessed as well in high yield following the pre-activation protocol (**Table 2.1**, entry 4).

**Table 2.1.** One-pot synthesis

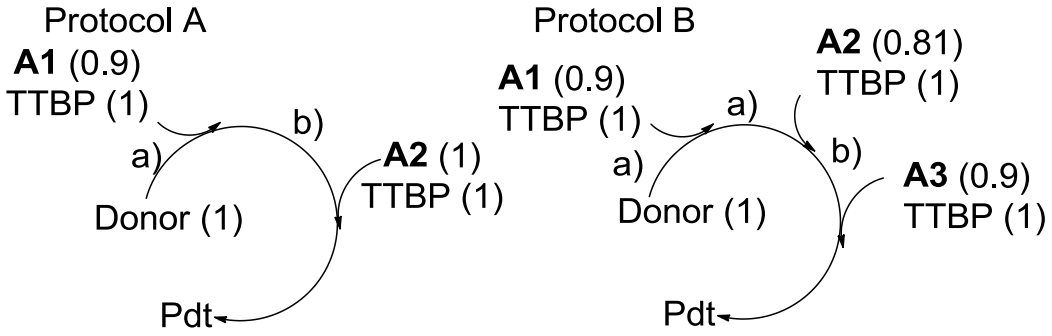


Reagents and conditions: a) AgOTf, *p*-TolSCl, - 65 $^{o}$C, 10 min; then acceptor, TTBP, 90 min to 0 $^{o}$C; 15 min, 0 $^{o}$C; b) acceptor, TTBP, AgOTf, *p*-TolSCl, - 65 $^{o}$C - 0 $^{o}$C in 90 min.

| Entry | Protocol | Donor | Acceptor 1 (A1) | Acceptor 2 (A2) | Acceptor 3 (A3) | Product | Yield |
|---|---|---|---|---|---|---|---|
| 1 | A | **32** | **35** | **40** | | **41** | 64 - 75% |
| 2 | A | **34** | **38** | **40** | | **42** | 65% |
| 3 | B | **32** | **35** | **38** | **33** | **43** | 55% |
| 4 | B | **33** | **35** | **38** | **40** | **44** | 54 - 60% |

**Figure 2.6.** Compounds **41**, **42**, **43** and **44**

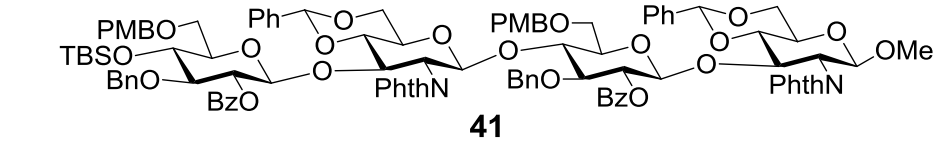

**41**

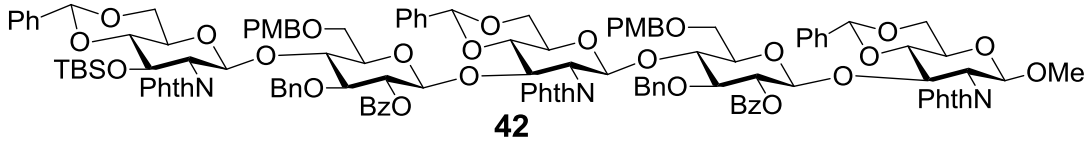

**42**

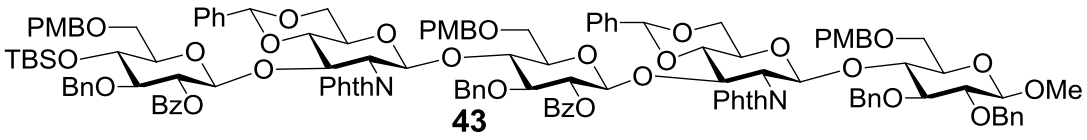

**43**

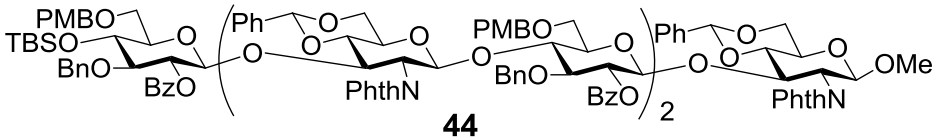

**44**

**Figure 2.7.** Compounds **45**, **46**, **47** and **48**

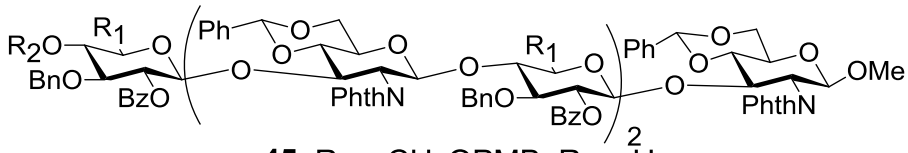

**45**: $R_1 = CH_2OPMB$, $R_2 = H$

**46**: $R_1 = CH_2OH$, $R_2 = TBS$

**47**: $R_1 = CO_2Bn$, $R_2 = TBS$

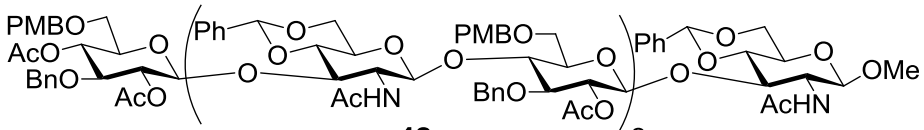

**48**

After the establishment of sHA core, the next stages were deprotections and oxidation state adjustments. Initial efforts of removing the three PMB groups from hexasaccharides **45** and **48** failed using either CAN or 2, 3-Dichloro-5, 6-dicyano-1, 4-benzoquinone (DDQ), although similar reactions have been reported such as CAN oxidation of trisaccharide **28** (**Scheme 2.10**)[9]. After repeated trials, it was found that the presence of TBS moiety was beneficial for deprotection of PMB, as CAN oxidation of hexasaccharide **44** yielding triol **46** in good yield (**Scheme 2.10**). Conversion of **47** into

tricarboxylic acids turned out to be challenging. Several methods such as TEMPO/NaClO, NaClO/$NaClO_2$ catalyzed by TEMPO, TEMPO/[bis(acetoxy)iodo]benzene (BAIB), and Dess-Martin oxidation followed by $NaClO_2$ did not give the desired product presumably due to the need to oxidize multiple OH groups in the same molecule. Instead, multiple partially oxidized products were often obtained from these reactions. Finally, it was discovered that a convenient 2 step one-pot protocol using TEMPO/NaClO followed by treatment of $NaClO_2$ afforded the desired tri-carboxylic acid, which was isolated as benzyl ester **47** by subsequent treatment with phenyl diazomethane ($PhCHN_2$) in high yield and good purity (**Scheme 2.10**)[18]. This protocol was also found to be compatible with a variety of sensitive functional groups, such as allyl, thioacetal, PMB and isopropylidene. Final deprotections of sHA **47** was carried out smoothly by the reaction sequence of desilylation, hydrogenation, saponification and *N*-acetylation to produce the sHA hexasaccharide **49**. This procedure for deprotection and oxidation state adjustment has also been extended to generate tetrasaccharide **50** and pentasaccharide **51** and **52**.

**Scheme 2.10.** Deprotection of compound **44**

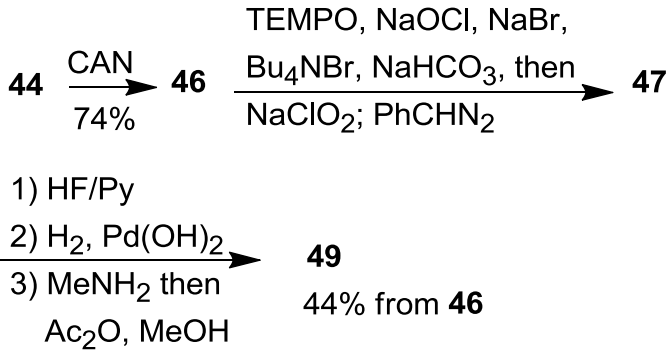

**Figure 2.8.** Compounds **49**, **50**, **51** and **52**

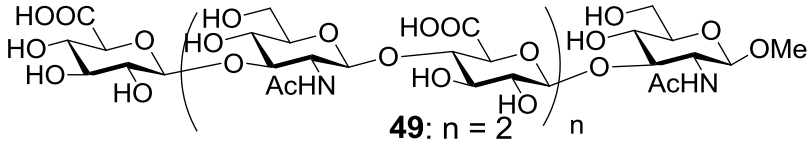


**49**: n = 2

**50**: n = 1

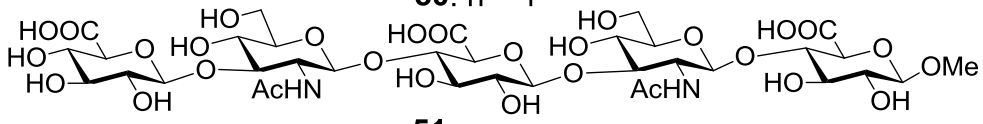


**51**

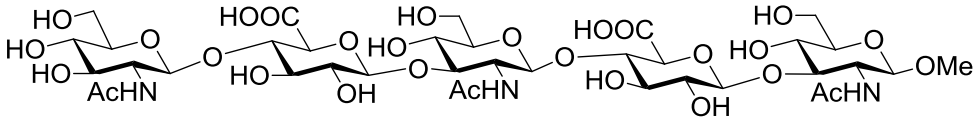


**52**

### 2.2.2. The second method with GlcUA building blocks

As an alternative to glucosyl donors, GlcUA building blocks can be directly utilized for sHA assembly. Due to the presence of electron withdrawing carboxylic acid on the pyranose ring, GlcUA building blocks are known to be less reactive than glucoside both as glycosyl donors and acceptors.

#### 2.2.2.1. Synthesis by Jacquinet's group

Jacquinet and coworkers developed a nice strategy using the reactive GlcUA trichloroacetimidate donors[15]. Trichloroacetyl (TCA) was employed as the *N*-protective group of glucosamine, which can be readily converted into the corresponding acetamides under the neutral tributyltin hydride ($Bu_3SnH$) reduction condition without going through amine intermediates.

**Scheme 2.11.** Synthesis by Jacquinet's group

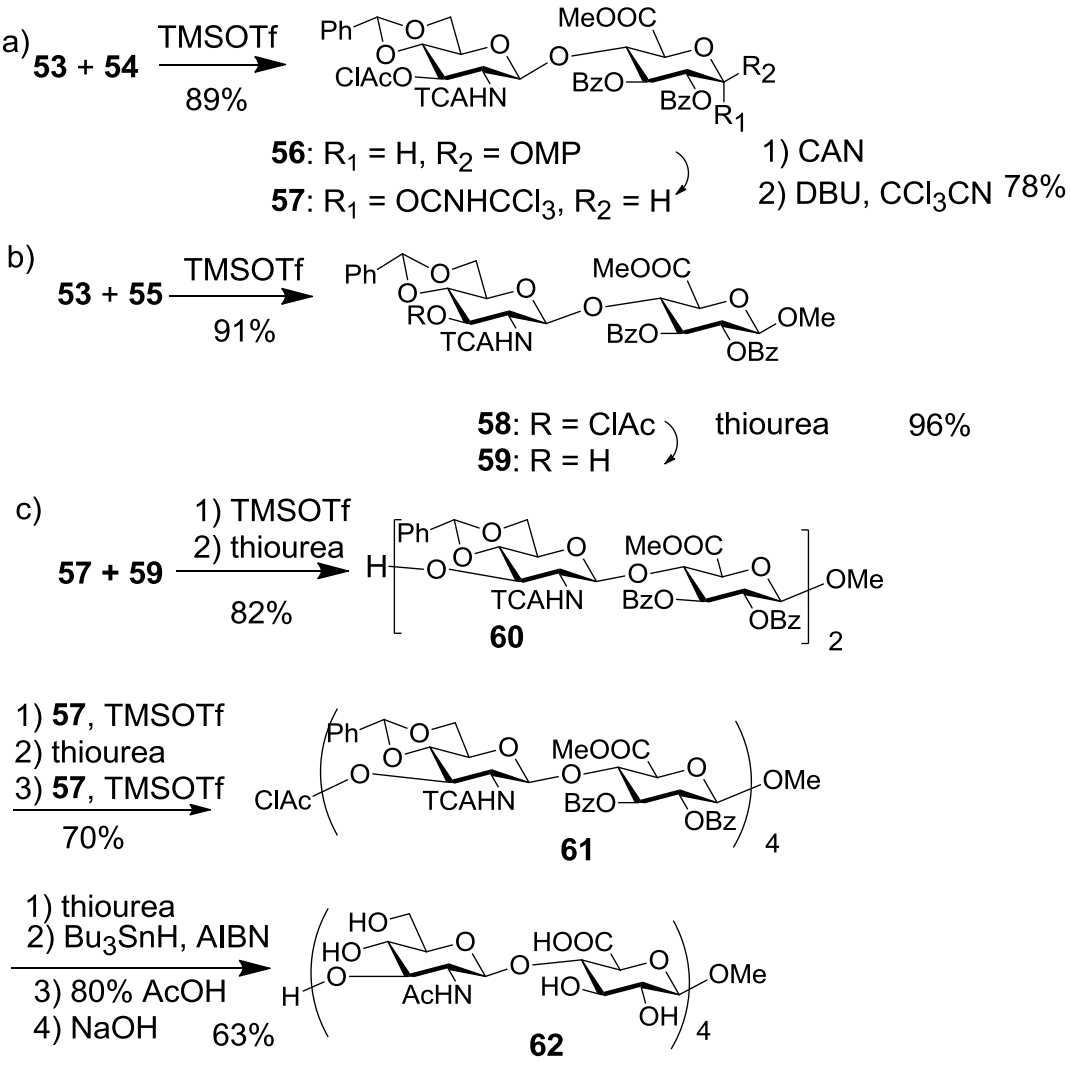


The two key disaccharides **56**, **58** in Jacquinet synthesis were prepared from the coupling of glycosyl donor **53** with acceptors **54** and **55** respectively (**Scheme 2.11a, b**). Disaccharide **56** was transformed into trichloroacetimidate donor **57** over 2 steps, while disaccharide **58** was subjected to dechloroacetylation to afford acceptor **59**. Coupling of **59** with **57** followed by dechloroacetylation gave tetrasaccharide acceptor **60** (**Scheme 2.11**). Repetition of glycosylation by **57**, deprotection of the chloroacetyl group and glycosylation afforded octasaccharide **61**. Subsequent deprotections were performed in

the following order: removal of the chloroacetyl group by thiourea, transformation of NH-TCA into NHAc via $Bu_3SnH$ reduction, debenzylidene and saponification to provide sHA octasaccharide **62** (**Scheme 2.11c**).

**Figure 2.9.** Compounds **53**, **54** and **55**

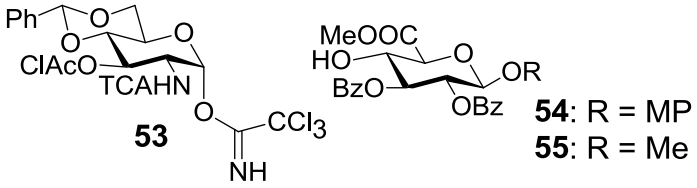


**53**

**54**: R = MP
**55**: R = Me

### 2.2.2.2. Synthesis by van der Marel's group

Van der Marel and co-workers synthesized HA pentasaccharide by chemoselective strategies based on their previous finding that 1-hydroxysugar donors can be condensed with 1-thioglycosides acceptor using Gin's activator system for dehydative glycosylations[19-23]. Triphenylphosphine oxide ($Ph_2SO$)/ trifluoromethanesulfonic anhydride ($Tf_2O$)/TTBP mediated condensation of donor **63** and acceptor **65** yield thiodisaccharide **66**, which was condensed with acceptor glucuronide **64** under the same condition provide trisaccharide **67** (**Scheme 2.12**). Donor **66** was condensed with acceptor **68** yielding HA pentasaccharide **69**. The yield for glycosidic bond formation was moderate, because the acid instability of benzylidene acetal required careful tuning of the amount of TTBP. Too little TTBP gave cleavage of benzylidene groups, whereas orthoester/oxazoline formation would be observed with excess of TTBP. After acid cleavage of the benzylidene group, saponification or the ester

and NHTCA groups and *N*-acetylation, **70** was obtained in good 48% yield.

**Figure 2.10.** Compounds **63**, **64** and **65**

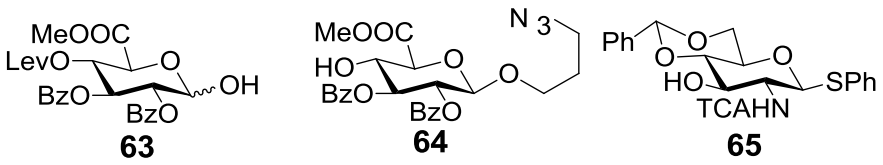


**Scheme 2.12.** Synthesis of compound **70**

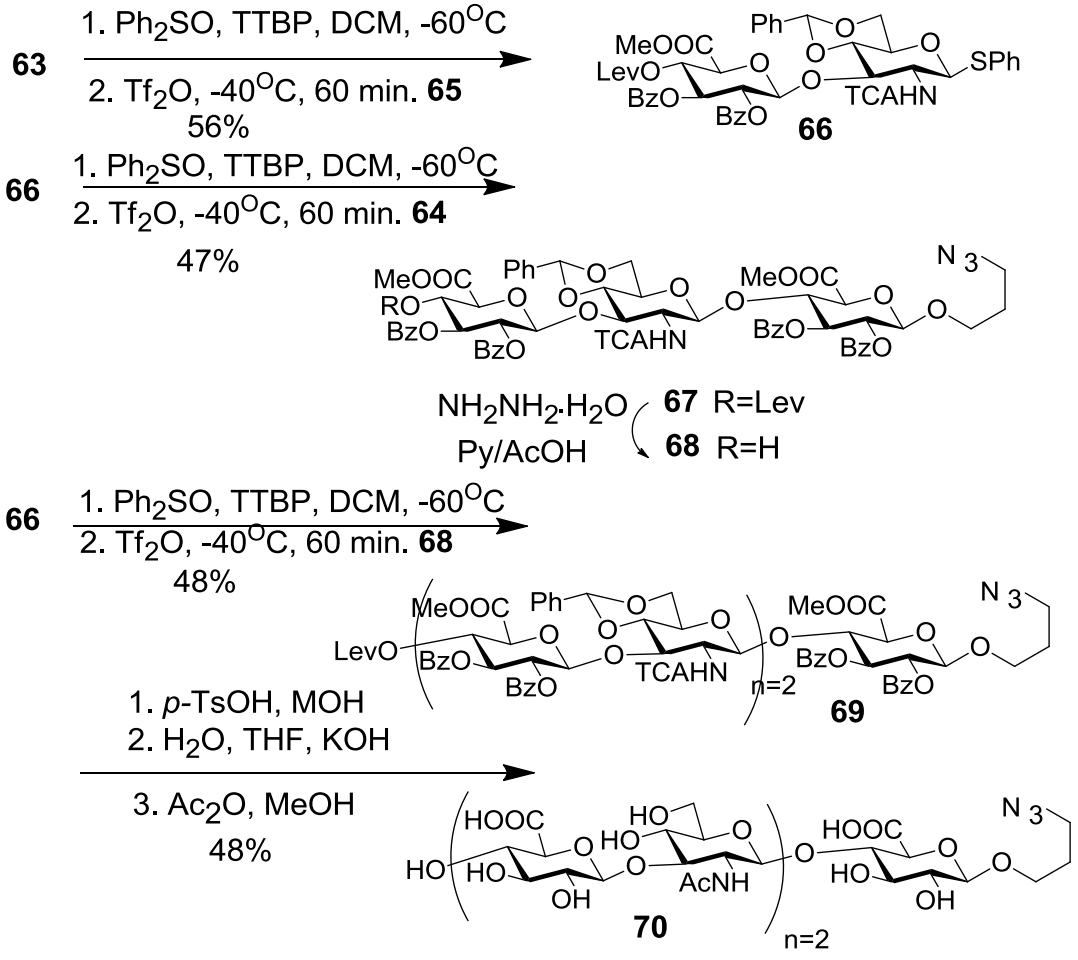

**Figure 2.11.** Compounds **71**, **72** and **73**

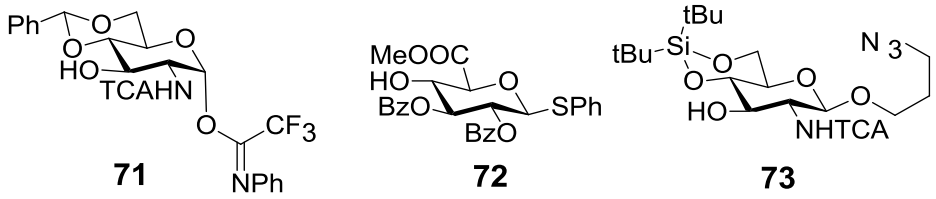


**Scheme 2.13.** Synthesis of compound **80**

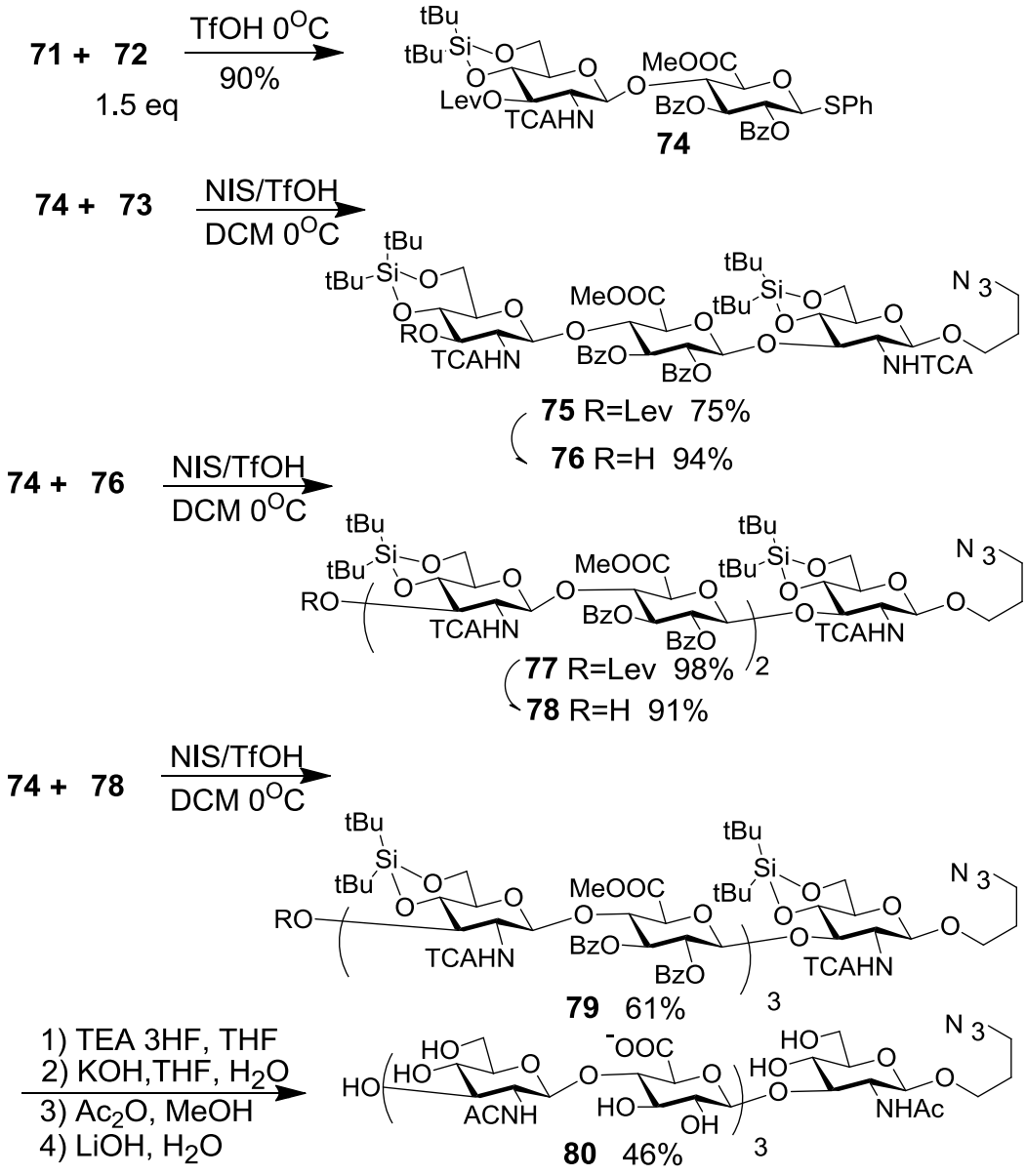


This strategy has been expanded to synthesize heptasaccharide **80** through

chemoselective strategies with glucuronate ester thioglycoside and trifluoro-*N*-phenylimidate glucosamine building blocks (**Scheme 2.13**). More acid stable di-*tert*-butylsilylidene (DTBS) groups were used to replace benzylidene groups[24]. Imidate donor **71** was condensed with acceptor **72** using a catalytic amount of TfOH to yield disaccharide **74** in 90% yield. Under *N*-iodosuccinimide (NIS)/TfOH condition, disaccharide **74** and acceptor **73** were condensed to give trisaccharide **75** in 75% yield. In the same condition, disaccharide **74** and trisaccharide **76** were condensed to give pentasaccharide **77** in 98% yield. Disaccharide **74** and pentasaccharide **78** were condensed to give heptasaccharide **79** in 61% yield. The deprotection was similar to their previous pentasaccharide synthesis, except triethylamine tris-hydrofluoride (TEA·3HF) was used for DTBS removal. Fully deprotected heptasaccharide **80** was produced in a very good 46% yield. Compared to their previous pentasaccharide synthesis, the yields for glycosidic bond formation was significantly improved.

The HA heptasaccharide synthesis was adapted to the syntheses of HA tetrasaccharide analogues with 4-methylumbelliferyl group at the reducing end, with 4-OH at the non-reducing glucuronate either removed or methylated[25]. Imidate donor **82** or **83** condensed with acceptor **81** using a catalytic amount of TfOH to yield disaccharide **84** or **85** in good yield (**Scheme 2.14.**). Global deprotection was more difficult than previous heptasaccharide synthesis due to the co-existence of 4-methylumbelliferyl group and two NHTCA groups. To remove TCA groups, pervious strong basic condition

had to be replaced with reductive dehalogenation with zinc (Zn)/ acetic acid (AcOH). Since monochloroacetamide were obtained as the major product, KI was used to transfer monochloroacetamide to monoiodideacetamide, which was transferred to acetamide group by dehalogenation. The overall yields for deprotections were good.

**Scheme 2.14.** Synthesis of compounds **86** and **87**

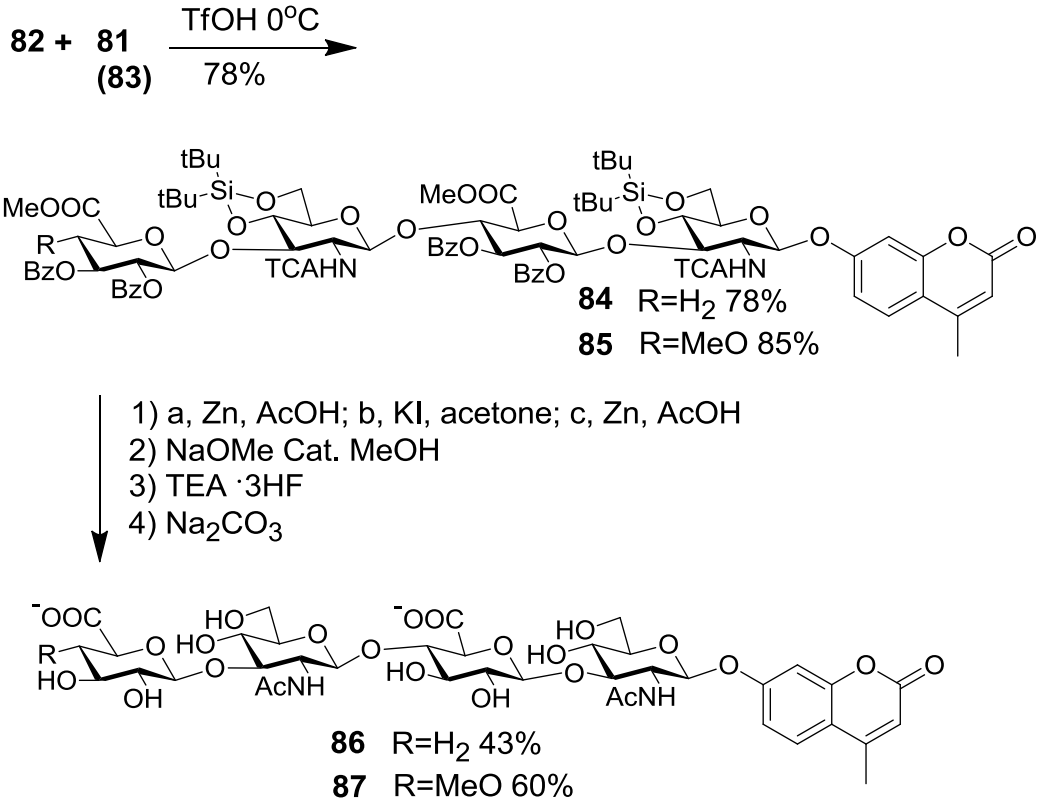

**Figure 2.12.** Compounds **81**, **82** and **83**

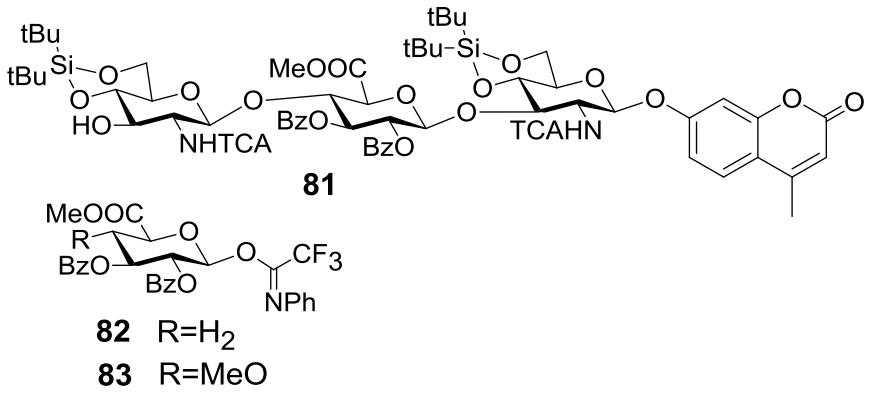


### 2.2.2.3.. Synthesis by Huang's group

We reported the first chemical synthesis of a fully deprotected $HA_{10}$, which is elaborated in **chapter 3**[26].

## References

## References


1. De Luca, C.; Lansing, M.; Martini, I.; Crescenzi, F.; Shen, G.-J.; O'Regan, M.; Wong, C.-H., Enzymic synthesis of hyaluronic acid with regeneration of sugar nucleotides. *J Am Chem Soc* **1995,** *117* (21), 5869-5870.

2. Saitoh, H.; Takagaki, K.; Majima, M.; Nakamura, T.; Matsuki, A.; Kasai, M.; Narita, H.; Endo, M., Enzymic reconstruction of glycosaminoglycan oligosaccharide chains using the transglycosylation reaction of bovine testicular hyaluronidase. *J Biol Chem* **1995,** *270* (8), 3741-3747.

3. Kobayashi, S.; Ohmae, M.; Ochiai, H.; Fujikawa, S., A hyaluronidase supercatalyst for the enzymatic polymerization to synthesize glycosaminoglycans. *Chem-Eur J* **2006,** *12* (23), 5962-5971.

4. Ochiai, H.; Ohmae, M.; Mori, T.; Kobayashi, S., Bottom-up synthesis of hyaluronan and its derivatives via enzymatic polymerization: Direct incorporation of an amido functional group. *Biomacromolecules* **2005,** *6* (2), 1068-1084.

5. Kobayashi, S.; Morii, H.; Itoh, R.; Kimura, S.; Ohmae, M., Enzymatic polymerization to artificial hyaluronan: A novel method to synthesize a glycosaminoglycan using a transition state analogue monomer. *J Am Chem Soc* **2001,** *123* (47), 11825-11826.

6. DeAngelis, P. L.; Oatman, L. C.; Gay, D. F., Rapid chemoenzymatic synthesis of monodisperse hyaluronan oligosaccharides with immobilized enzyme reactors. *J Biol Chem* **2003,** *278* (37), 35199-35203.

7. Karst, N. A.; Linhardt, R. J., Recent chemical and enzymatic approaches to the synthesis of glycosaminoglycan oligosaccharides. *Curr Med Chem* **2003,** *10* (19), 1993-2031.

8. Codee, J. D. C.; van den Bos, L. J.; Litjens, R. E. J. N.; Overkleeft, H. S.; Van Boom, J. H.; van der Marel, G. A., Sequential one-pot glycosylations using 1-hydroxyl and 1-thiodonors. *Org Lett* **2003,** *5* (11), 1947-1950.

9. Yeung, B. K. S.; Hill, D. C.; Janicka, M.; Petillo, P. A., Synthesis of two hyaluronan trisaccharides. *Org Lett* **2000,** *2* (9), 1279-1282.

10. Halkes, K. M.; Slaghek, T. M.; Hypponen, T. K.; Kruiskamp, P. H.; Ogawa, T.; Kamerling, J. P.; Vliegenthart, J. F. G., Synthesis of hyaluronic-acid-related oligosaccharides and analogs, as their 4-methoxyphenyl glycosides, having

*N*-acetyl-*β*-D-glucosamine at the reducing end. *Carbohydrate Res* **1998,** *309* (2), 161-174.

11. Slaghek, T. M.; Hypponen, T. K.; Ogawa, T.; Kamerling, J. P.; Vliegenthart, J. F. G., Synthesis of hyaluronic acid related di- and tetrasaccharides having a glucuronic acid at the reducing end. *Tetrahedron Asymmetry* **1994,** *5* (11), 2291-2301.

12. Slaghek, T. M.; Nakahara, Y.; Ogawa, T.; Kamerling, J. P.; Vliegenthart, J. F. G., Synthesis of hyaluronic acid-related di-, tri-, and tetrasaccharides having an *N*-acetylglucosamine residue at the reducing end. *Carbohydrate Res* **1994,** *255*, 61-85.

13. Slaghek, T. M.; Hyppoenen, T. K.; Ogawa, T.; Kamerling, J. P.; Vliegenthart, F. G., Synthesis of a tetrasaccharide fragment of hyaluronic acid having a glucuronic acid at the reducing end. *Tetrahedron Lett* **1993,** *34* (49), 7939-7942.

14. Slaghek, T.; Nakahara, Y.; Ogawa, T., Stereocontrolled synthesis of hyaluronan tetrasaccharide. *Tetrahedron Lett* **1992,** *33* (34), 4971-4974.

15. Blatter, G.; Jacquinet, J.-C., 2-Deoxy-2-trichloroacetamido-D-glucopyranose derivatives in syntheses of hyaluronic acid-related tetra-, hexa-, and octa-saccharides having a methyl *β*-D-glucopyranosiduronic acid at the reducing end. *Carbohydrate Res* **1996,** *288*, 109-125.

16. Huang, X.; Huang, L.; Wang, H.; Ye, X.-S., Iterative one-pot synthesis of oligosaccharides. *Angew Chem, Int Ed* **2004,** *43* (39), 5221-5224.

17. Zhang, Z.; Ollmann, I. R.; Ye, X.-S.; Wischnat, R.; Baasov, T.; Wong, C.-H., Programmable one-pot oligosaccharide synthesis. *J Am Chem Soc* **1999,** *121* (4), 734-753.

18. Huang, L.; Teumelsan, N.; Huang, X., A facile method for oxidation of primary alcohols to carboxylic acids and its application in glycosaminoglycan syntheses. *Chem-Eur J* **2006,** *12* (20), 5246-5252.

19. Dinkelaar, J.; Codee, J. D. C.; Van den Bos, L. J.; Overkleeft, H. S.; Van der Marel, G. A., Synthesis of hyaluronic acid oligomers using $Ph_2SO/Tf_2O$-mediated glycosylations. *J Org Chem* **2007,** *72* (15), 5737-5742.

20. Codee, J. D. C.; Stubba, B.; Schiattarella, M.; Overkleeft, H. S.; Van Boeckel, C. A. A.; Van Boom, J. H.; Van der Marel, G. A., A modular strategy toward the synthesis of

heparin-like oligosaccharides using monomeric building blocks in a sequential glycosylation strategy. *J Am Chem Soc* **2005,** *127* (11), 3767-3773.

21. Garcia, B. A.; Poole, J. L.; Gin, D. Y., Direct glycosylations with 1-hydroxy glycosyl donors using trifluoromethanesulfonic anhydride and diphenyl sulfoxide. *J Am Chem Soc* **1997,** *119* (32), 7597-7598.

22. Codee, J. D. C.; Litjens, R. E. J. N.; den Heeten, R.; Overkleeft, H. S.; van Boom, J. H.; van der Marel, G. A., $Ph_2O/Tf_2O$: A powerful promotor system in chemoselective glycosylations using thio glycosides. *Org Lett* **2003,** *5* (9), 1519-1522.

23. Crich, D.; Smith, M., 1-Benzenesulfinyl piperidine/trifluoromethanesulfonic anhydride: A potent combination of shelf-stable reagents for the low-temperature conversion of thioglycosides to glycosyl triflates and for the formation of diverse glycosidic linkages. *J Am Chem Soc* **2001,** *123* (37), 9015-9020.

24. Dinkelaar, J.; Gold, H.; Overkleeft, H. S.; Codee, J. D. C.; van der Marel, G. A., Synthesis of hyaluronic acid oligomers using chemoselective and one-pot strategies. *J Org Chem* **2009,** *74* (11), 4208-4216.

25. Gold, H.; Munneke, S.; Dinkelaar, J.; Overkleeft, H. S.; Aerts, J. M. F. G.; Codee, J. D. C.; van der Marel, G. A., A practical synthesis of capped 4-methylumbelliferyl hyaluronan disaccharides and tetrasaccharides as potential hyaluronidase substrates. *Carbohydrate Res* **2011,** *346* (12), 1467-1478.

26. Lu, X.; Kamat, M. N.; Huang, L.; Huang, X., Chemical synthesis of a hyaluronic acid decasaccharide. *J Org Chem* **2009,** *74* (20), 7608-7617.

# CHAPTER 3

## Chemical Synthesis of a $HA_{10}$

### 3.1. Introduction:

HA is the major ligand of CD44. Evidence is accumulating suggesting that the size of HA fragments recognized by CD44 provides a physiologically important switch between its adhesion and signaling functions[1]. Binding of HA polymers to CD44 usually leads to cell adhesion[2-3] rather than activation. In contrast, recognition of HA fragments instead of the polymer leads to CD44 signaling, which is involved in diseases such as cancer and inflammation[4-7]. CD44 requires at least a $HA_6$ sequence for binding. and only a $HA_{10}$ or higher can effectively compete with polymeric HA[8]. Therefore, access to synthetic HA with variable length and sequence can greatly facilitate the establishment of its SAR [9].

HA can be synthesized via either enzymatic or chemical methods. Although impressive enzymatic synthesis has been achieved, the inherent substrate specificities of enzymes limit the structural diversity of HA analogs that can be generated. Chemical synthesis can thus complement the enzymatic approaches to create greater varieties of HA structures.

The longest sHA chemically assembled to date are an $HA_8$[10]. Previously, our group has developed a synthetic strategy to acquire sHA ranging from di- to hexa-saccharides[11]. With the fascinating biological activities of longer sHA, we became interested in pursuing their chemical synthesis, which is not a trivial extension of shorter

oligomers as elongation of the sugar sequences but can create significant new challenges in both glycosylation and deprotection. Herein, we report our results on overcoming the obstacles for chemical synthesis of an $HA_{10}$.

**3.2. Results and Discussion:**

The design of a successful route to HA oligosaccharides must take into account three factors: 1) stereochemical control in glycosylation; 2) introduction of the GlcUA; and 3) protective groups for the glucosamine nitrogen moieties. In our previous $HA_6$ synthesis, we used two key building blocks **1** and **2**, which led to high yield of hexasaccharide **3** in one pot (**Scheme 3.1**)[11]. The Bz and Phth groups were crucial to facilitate the formation of 1,2-*trans* glycosidic linkages. Due to its high inherent reactivities[12], glucoside building block **1** was utilized as a GlcUA surrogate[11]. The PMB groups in **3** masking the glucoside 6-O-position were selectively removed by DDQ oxidation and the resulting triol was successfully oxidized and deprotected producing $HA_6$. Following the success of $HA_6$ synthesis, our initial attempt towards $HA_{10}$ hinged upon the usage of monosaccharides **1** and **2**, from which decasaccharide **4** was assembled. However, removal of the five PMB groups in **4** turned out to be very problematic (**Scheme 3.2a**). The previously employed DDQ oxidation[11] decomposed the oligosaccharide. CAN oxidation[13] or the combination of *p*-tolyl sulfonamide and triflic acid (TfOH)[14] also failed to lead to the desired penta-ol. To circumvent this problem, the 6-OH group liberation and oxidation state adjustment were performed on disaccharide **6** (**Scheme 3.2b**). DDQ mediated PMB removal followed by primary OH oxidation and

benzyl ester formation produced disaccharide **7** containing the GlcUA moiety. Condensations of the resulting disaccharides afforded decasaccharide **8** with the GlcUA already installed, which set the stage for deprotection. Although it has been shown previously that Phth groups could be deprotected in molecules containing carboxylic esters[11, 15-16], despite repeated trials and screening of a variety of reagents and reaction conditions, the conditions required to remove all five Phth groups in disaccharide **7** turned out to be incompatible with the five carboxylic ester moieties present and *vice versa*. This prompted us to abandon the Phth group and utilize the TCA group[10, 17] as an alternative protective group for nitrogen.

Based on these considerations, a new retrosynthetic route towards decasaccharide **9** was designed (**Scheme 3.3**). The fully protected decasaccharide **10** would be assembled from disaccharides **11**, **12** and **13**, which in turn would be derived from monosaccharide building blocks **1**, **14** and **15**.

**Scheme 3.1.** Previous synthesis on $HA_6$ **3**

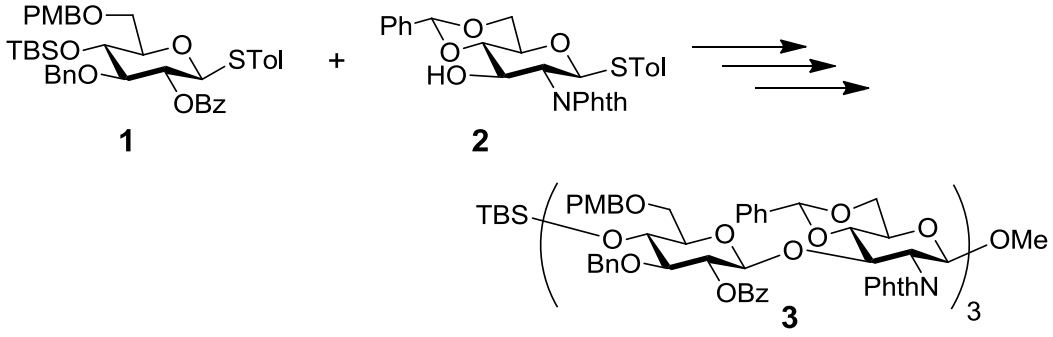

**Figure 3.1.** Compound **4**

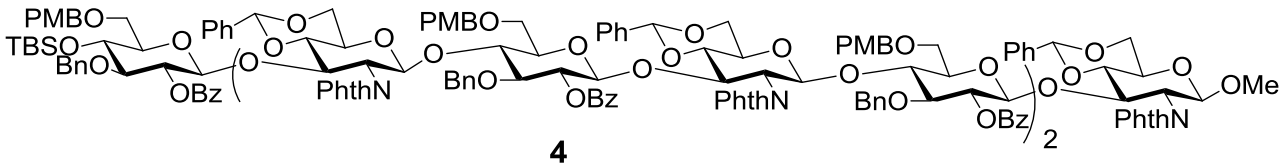


**4**

**Scheme 3.2.** Previous synthesis on $HA_{10}$

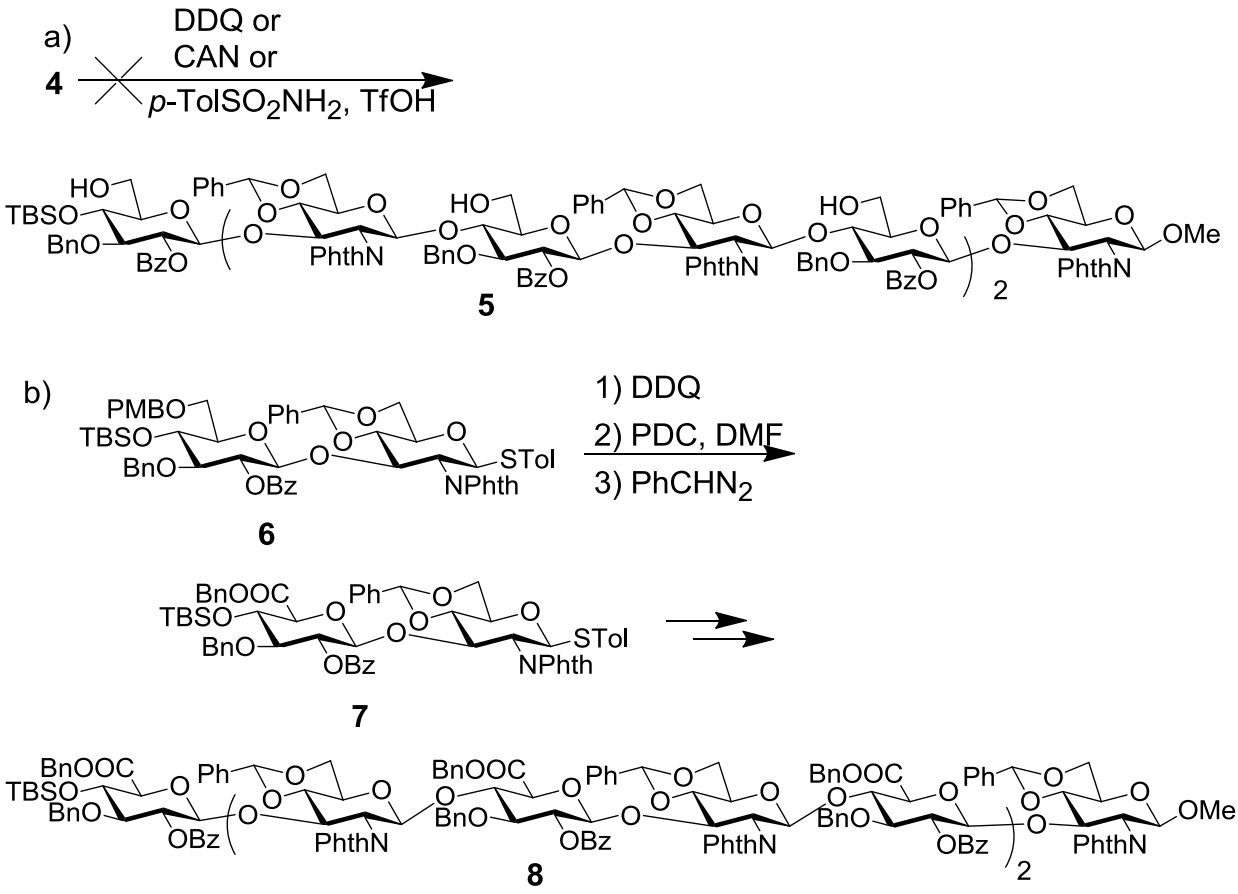


Glucoside donor **1** was prepared according to a literature procedure[11] and the syntheses of glucosamine building blocks **14** and **15** were outlined in **Scheme 3.4**. Peracetylated *N*-TCA-glucosamine **16**[10] was transformed into the corresponding 1-*β*-*p*-tolyl thioglycoside **17** and the 1-*β*-methoxy derivative **18.** Compound **17** was then

deacetylated and protected with a benzylidene group to afford **14,** whereas compound **18** was protected by benzylidene to give **15**.

**Scheme 3.3.** Retrosynthetic scheme towards $HA_{10}$ **9**

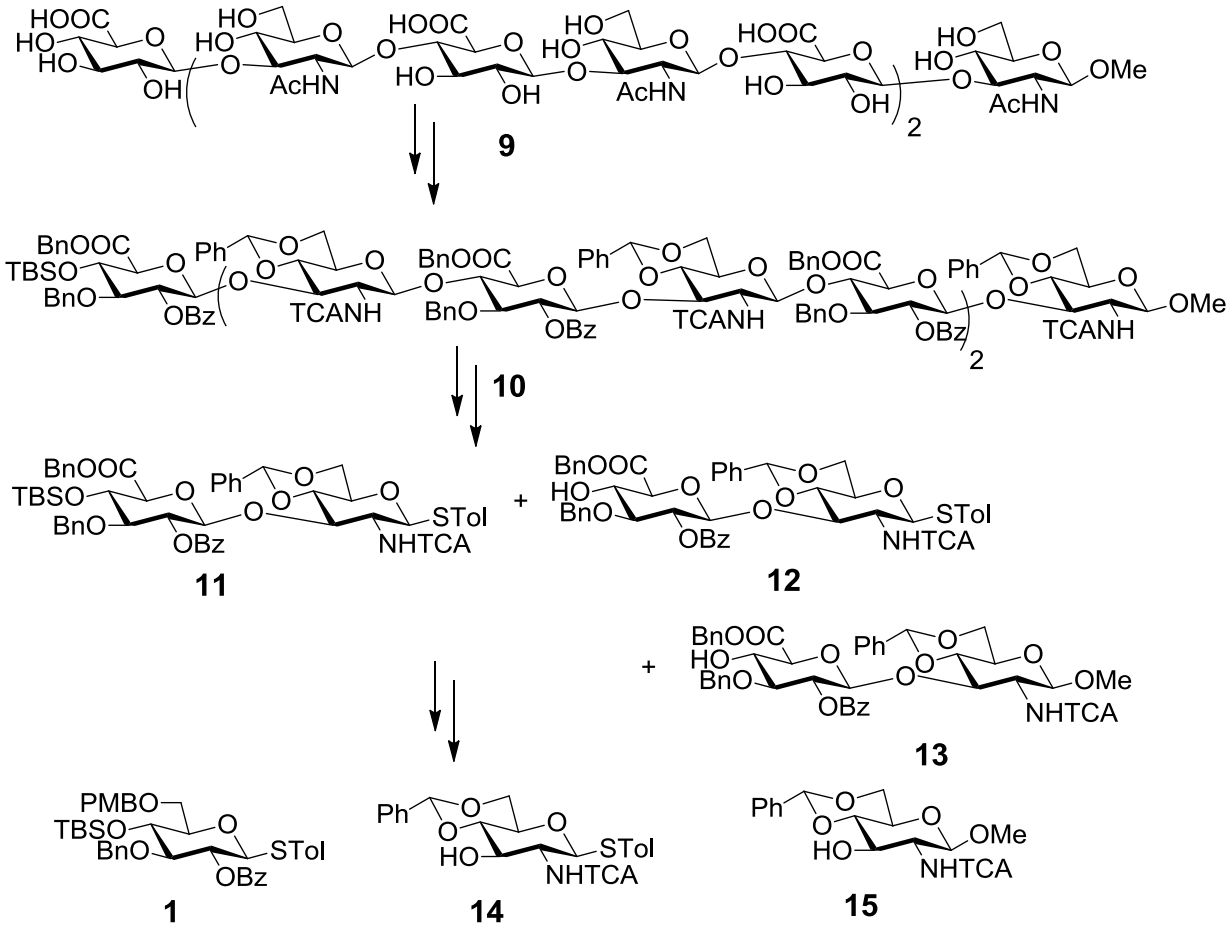


**Scheme 3.4.** Synthesis of monosaccharide building blocks **14** and **15**

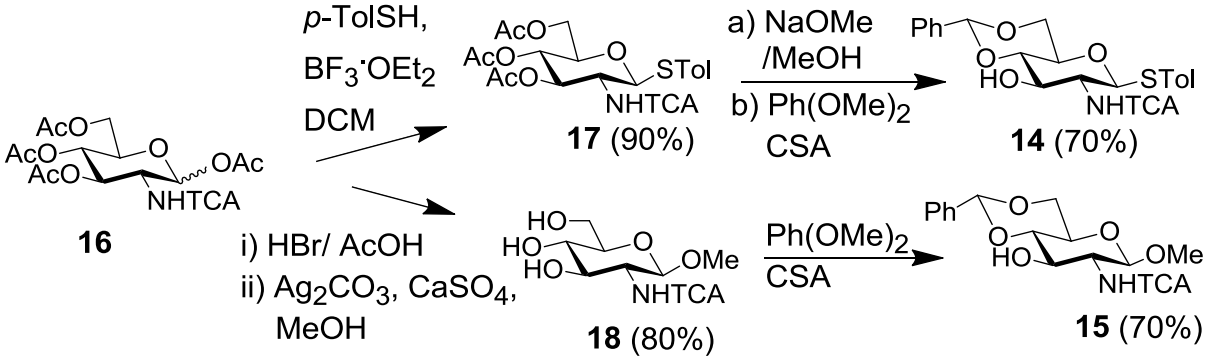

**Scheme 3.5.** Assembly of $HA_2$ building blocks

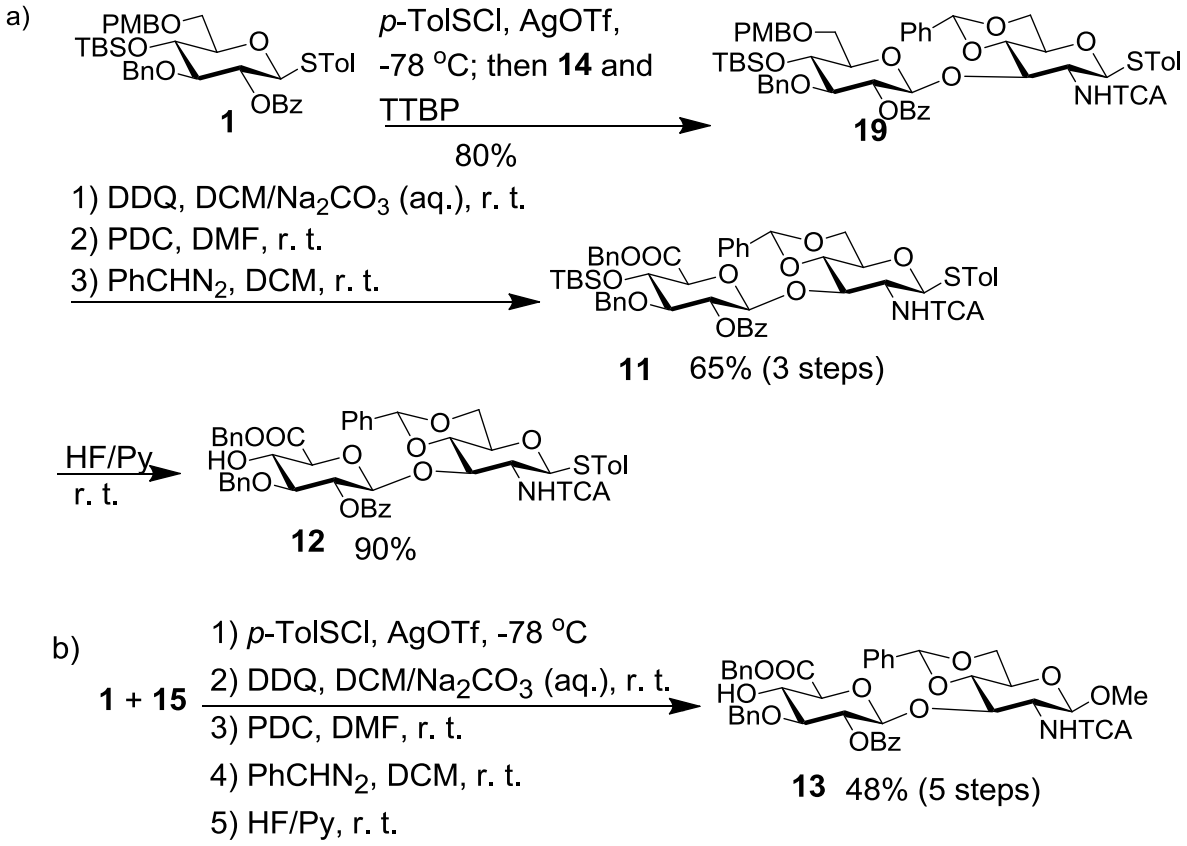


With the monosaccharides in hand, disaccharide synthesis was performed. Pre-activation of glucoside donor **1** by the reagent combination of AgOTf and *p*-Toluenesulfenyl chloride (*p*-TolSCl)[11, 18] at – 78 °C was performed followed by the addition of acceptor **14** and a bulky base TTBP[19] leading to disaccharide **19** in 80% yield. The primary OH group in **19** was liberated by treatment with DDQ and oxidized by PDC in DMF to afford its carboxylic acid derivative, which was protected as a benzyl ester (disaccharide **11**) in 65% yield for the 3 steps. Subsequent removal of the TBS group led to the disaccharide acceptor **12** bearing a free secondary OH group (**Scheme 3.5a**). Disaccharide **13** was constructed through a similar sequence from **1** and **15** in an overall

yield of 48% for the 5 steps (**Scheme 3.5b**).

Following the same glycosylation protocol as used in the preparation of disaccharide **19**, coupling of disaccharide donor **11** with acceptor **12** was attempted (**Scheme 3.7a**). However, no desired tetrasaccharide was obtained with full recovery of acceptor **12**. Oxazoline derivative **20** ($^{3}J_{H1\text{-}H2}$ = 8.0 Hz[20-21]) was isolated from the reaction in quantitative yield with the possible mechanism for its formation depicted in **Scheme 3.6b**. Neighboring group participation by the TCA group through attachment of its carbonyl oxygen to the oxacarbenium ion forms the oxazolinium ion intermediate **22**, which can react with an acceptor to afford the expected 1,2-*trans*-glycoside **23** (pathway a, **Scheme 3.6b**). Alternatively, deprotonation of the oxazolinium ion produces the stable trichloro-oxazoline **24** (pathway b).

**Scheme 3.6.** Oxazoline formation

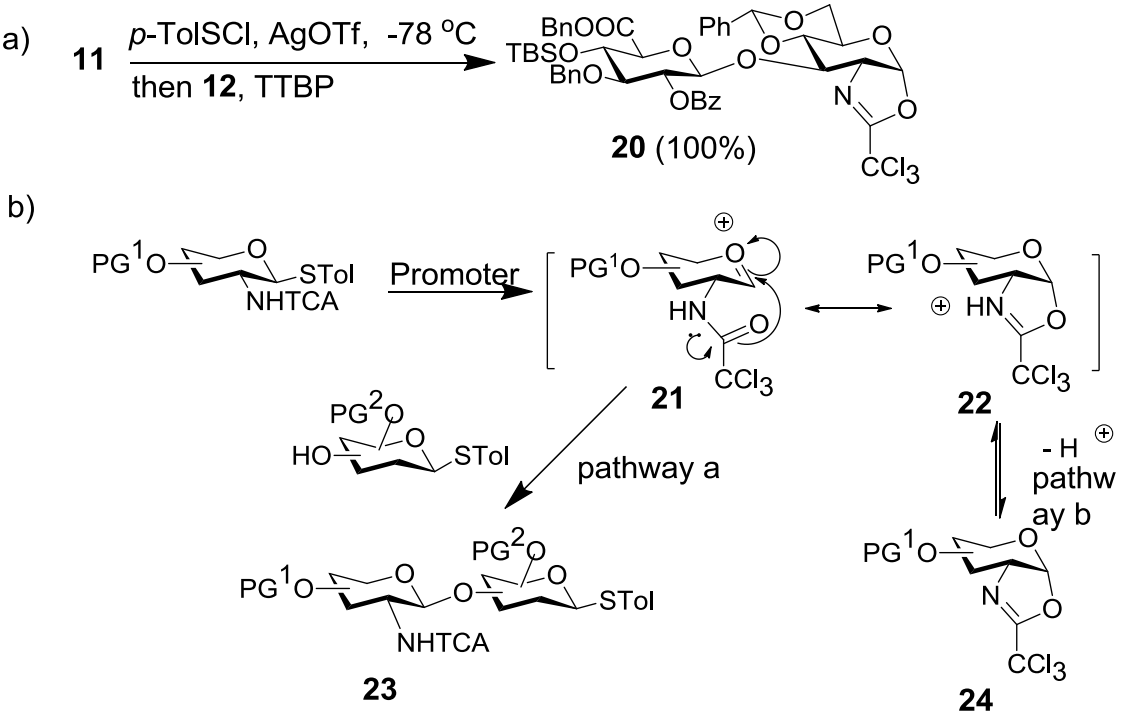

**Table 3.1.** The effects of additives on glycosylation product distribution

| Entries | Reaction conditions | Donor **11** + acceptor **12** | Donor **25** + acceptor **13** | Donor **25** + acceptor **28** |
|---|---|---|---|---|
| 1 | $1^{st}$ Generation<br>TTBP was added after donor was activated | **20** (100%) | **-** | - |
| 2 | $2^{nd}$ Generation<br>No TTBP was added after donor was activated | **25** (55%) + **20** (40%) | **26** (40%) + **27** (50%) | **10** (10%) + **27** (85%) |
| 3 | $3^{rd}$ Generation<br>TfOH was added after donor was activated | **25** (55%) | **26** (60%) | **10** (40%) |
| 4 | $4^{th}$ Generation<br>TMSOTf was added after donor was activated | **25** (82%) | **26** (71%) | **10** (77%) |

Following this mechanism, the failure of glycosylation could be attributed to the addition of TTBP[17], which is used to scavenge the TfOH accumulated upon productive glycosylation. Therefore, a $2^{nd}$ generation glycosylation protocol was adopted by omitting TTBP from the reaction. Following this protocol, **11** (1 eq.) was condensed with **12** (1 eq.) to produce tetrasaccharide **25** in 55% yield with 40% oxazoline by-product **20** (**Table 3.1**, entry 2). The next condensation of tetrasaccharide donor **25** (1 eq.) with disaccharide acceptor **13** gave hexasaccharide **26** in 40% yield and oxazoline **27** (50% yield). Subsequent cleavage of TBS group in **26** gave the hexasaccharide acceptor **28** in 90% yield. Disappointingly, the final coupling of **25** (1.25 eq.) and **28** (1 eq.) only gave decasaccharide **10** in 10% yield, with the majority of **25** converted to oxazoline **27** (85%

yield, **Table 3.1**, entry 2). The substantial increase of the amounts of oxazoline side products is presumably because with the increasing sizes of the glycosyl donor and acceptor, the compounds become less reactive towards glycosylation (**Scheme 3.6b**, pathway a), which in turn favors the competing reaction of oxazoline formation even in the absence of base (**Scheme 3.6b**, pathway b).

**Figure 3.2.** Compound **25**, **26**, **27** and **28**

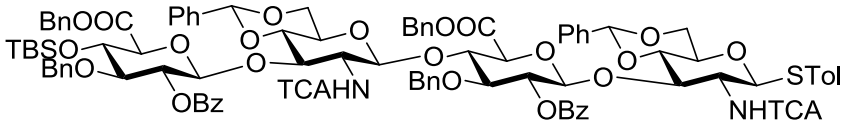


**25**

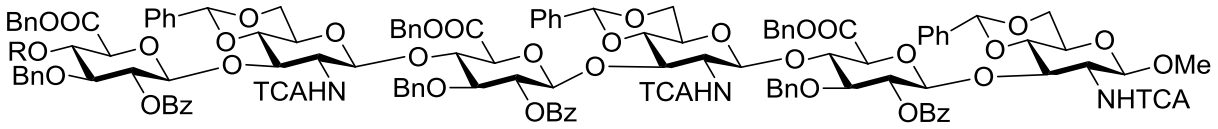


**26**: R = TBS
**28**: R = H

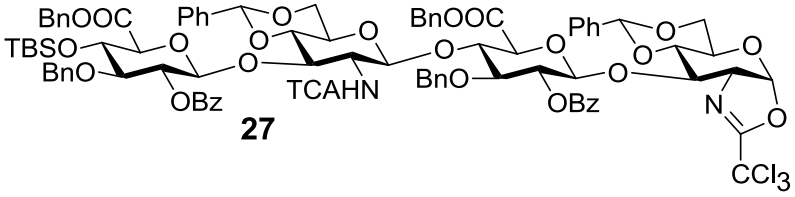


**27**

In order to suppress the amount of oxazoline, exogenous TfOH (~ 0.4 eq.) was introduced to the reaction mixture after the donor activation to shift the equilibrium from oxazoline **24** to the oxazolinium ion **22** (**Scheme 3.6b**). Following this 3$^{rd}$ generation procedure, although the reaction of **11** and **12** was not affected, the yields for **25** with **13** and **28** were enhanced to 60% and 40% respectively (**Table 3.1**, entry 3). The acid sensitive benzylidene moieties were found to be stable under this condition. To further improve on the glycosylation, Lewis acid TMSOTf was examined as an alternative to

TfOH. Based on this protocol, significant enhancements were observed for all three reactions (**Table 3.1**, entry 4), with the yield of decasaccharide **10** reaching 77%, which enabled us to acquire over 200 mg of this decasaccharide. These results suggest that the addition of TMSOTf successfully suppressed the formation of trichloro-oxazoline by-products.

Deprotection of large complex oligosaccharides could be very challenging due to the presence of multiple protective groups, as observed in our attempts on decasaccharides **4** and **8**. To deprotect decasaccharide **10**, its TBS group was removed first by HF in Py to give **29** in 79% yield. This was followed by a mild basic condition (20 eq. of KOH added in 10 portions to a solution of **29** over 2 days[22]) in order to cleave all ten carboxylic esters and five trichloroacetamides (**Scheme 3.7**). Harsh basic conditions should be avoided to prevent epimerization of the GlcUA. The progress of the hydrolysis turned out to be difficult to monitor by TLC for two reasons. First, the liberated amino groups gave no ninhydrin test presumably due to steric hindrance. Secondly, the compounds with free carboxylic acid and amino groups became zwitterionic, which streaked on TLC. MS analysis of the crude reaction mixture did not yield much information resulting from signal suppression by the presence of salts. NMR analysis of the reaction mixture turned out to be most informative. The cluster of peaks around 8.0 ppm in $^{1}$H-NMR assigned to the *ortho*-hydrogens of Bz groups, merged into a doublet like pattern over time signifying the cleavage of benzoyl esters to benzoate salt. Another characteristic of the NMR is that the set of four doublets around 7.0 ppm

representing the amide protons of trichloroacetamide groups in **29**, became smaller and eventually disappeared as the reaction proceeded. The rate of trichloroacetamide cleavage was much slower compared with that of the benzoates. When the crude NMR spectra did not show much change after week 5, the reaction was stopped. The reaction mixture was *N*-acetylated followed by hydrogenation and size exclusion chromatography to produce the fully deprotected HA decasaccharide **9** in 35% yield from **29**. NMR analysis indicated all the glycosyl linkages were *beta*, confirming no epimerizations occurred despite the prolonged reaction time.

**Scheme 3.7.** Deprotection

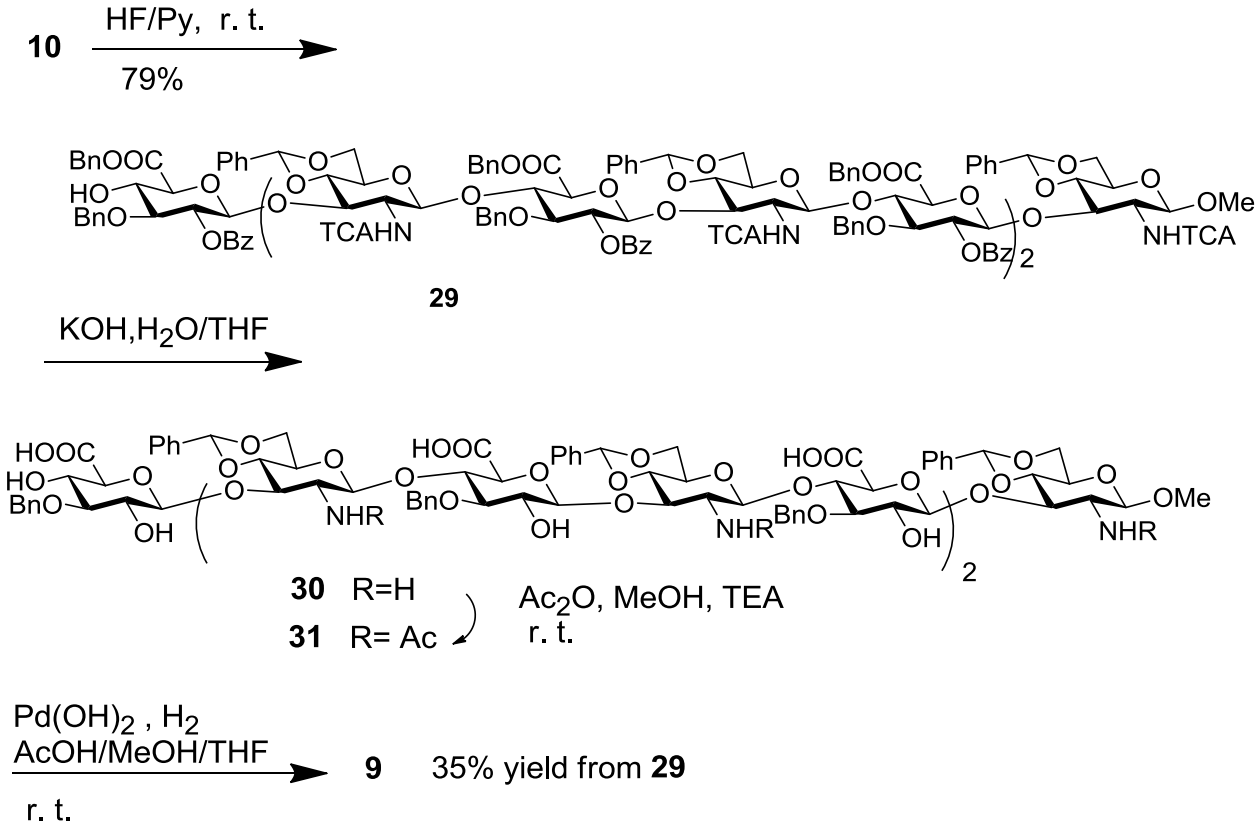

### 3.3. Conclusions

We reported the first chemical synthesis of a fully deprotected $HA_{10}$. Our pre-activation based thioglycoside strategy with *p*-TolSCl/AgOTf as the promoter was successfully applied for efficient construction of the decasaccharide backbones. However, considerable difficulties were encountered in deprotection, with the selection of nitrogen protective group turned out to be crucial. While removal of all five Phth was found to be incompatible with the carboxylic esters present in the decasaccharide, TCA could be removed together with the esters under a mild basic condition. The TCA associated oxazoline formation side reaction during glycosylation was suppressed by addition of TMSOTf to the reaction mixture. Our experience highlights the challenges associated with assembly of large oligosaccharides, as the conditions employed for synthesis of shorter counterparts may not be directly translatable and each synthesis needs individual optimization and development. We believe our strategy on the HA decasaccharide assembly can open up possibilities to chemical synthesis of longer sHA and facilitate the structure-activity relationship studies of this important class of molecules.

### 3.4. Experimental Section:

**General procedure for deprotection of PMB group:** PMB-protected compound (1 mmol) and DDQ (1.3 eq.) were dissolved in a solvent mixture of dichloromethane (DCM) and a saturated aqueous solution of sodium bicarbonate ($NaHCO_3$) (v/v 19:1), which was kept in dark. The reaction mixture is stirred for 2 hrs from 0 °C to room temperature (r.t.). Then a $2^{nd}$ portion of DDQ (0.5 eq.) was added to the reaction mixture, and a $3^{rd}$ portion of DDQ (0.5 eq.) could be added 15 min after the addition of the $2^{nd}$ portion to further push the reaction to completion. When most starting material disappeared, the reaction mixture was diluted with DCM and washed repeatedly with a saturated aqueous solution of $NaHCO_3$ until the organic layer become colorless. The organic layer was concentrated, and the resultant residue was purified by silica gel chromatography to give the desired compound.

**General procedure for oxidation of alcohols to carboxylic acids:** After a mixture of alcohol (1 mmol) and MS-4Å (5 g) in anhydrous dimethylformamide (DMF) was stirred at r.t. for 2 hrs, a solution of pyridinium dichromate (PDC) (6 mmol) in DMF was added dropwise to the reaction. The reaction mixture was stirred at r.t. until thin layer chromatography (TLC) indicated completion of the reaction, which typically required overnight. The reaction was diluted with ethyl acetate (EA) and filtrated to remove the insoluble PDC. The filtrate was washed with brine to remove DMF. The crude product was then purified by silica gel chromatography with EA/DCM/methanol (MeOH) solvent systems.

**General procedure for benzyl ester formation:** The carboxylic acid containing compound was dissolved in DCM (5 ml) and treated with $PhCHN_2$ solution in diethyl ether ($Et_2O$) (~2 eq.) for 2–3 hrs until the disappearance of all the starting material. The crude product was purified by silica gel chromatography.

**General procedure for removal of TBS groups:** The TBS-protected compound (0.5 mmol) was dissolved in pyridine (Py) (4 ml) in a plastic flask followed by the addition of 65–70% hydrogen fluoride (HF)/Py solution (2 ml) at 0 °C. The solution was stirred for 24 hrs until TLC indicated completion of the reaction. The reaction mixture was diluted with EA (50 ml) and washed with 10% aqueous copper sulfate ($CuSO_4$) solution (20 ml). The aqueous phase was extracted with EA (30 ml) twice and the combined organic layers were washed with a saturated aqueous solution of $NaHCO_3$ to remove HF. The crude product was purified by silica gel chromatography.

***p*-Tolyl 4,6-*O*-benzylidene-2-deoxy-2-trichloroacetamido-*β*-D-glucopyranoside (14):** After D-glucosamine hydrochloride (10.8 g, 50.0 mmol) and sodium methoxide (NaOMe) (50.0 ml, 1M NaOMe/MeOH, 50.0 mmol) in MeOH were stirred at r.t. under $N_2$ protection for 45 min, trichloroacetyl chloride (5.61 ml, 50.0 mmol) and triethylamine (TEA) (6.95 ml, 50.0 mmol) were added. After overnight when electrospray ionization mass spectrometry (ESI-MS) indicated that D-glucosamine hydrochloride completely disappeared, MeOH was removed by a rotary evaporator and the flask was placed under high vacuum for 2 hrs. $Ac_2O$ and Py (150 ml, v/v 1:2) were then added and the reaction mixture was stirred for 2 days. The mixture was

concentrated, and the resulting residue was diluted with EA and washed with a saturated aqueous solution of $NaHCO_3$, 10% HCl, $H_2O$, and brine. The organic phase was dried over $Na_2SO_4$, filtered, and concentrated. After recrystallization, 1,3,4,6-tetra-*O*-acetyl-2-deoxy-2-trichloroacetamido-D-glucopyranoside (**16**) was obtained as a white solid (16.3 g, 33.0 mmol, 66% for 2 steps). Boron trifluoride etherate ($BF_3{\cdot}Et_2O$) (7.75 ml, 89 mmol) was added to a solution of **16** (4.93 g, 10 mmol) and *p*-toluenethiol (1.99 g, 16.0 mmol) in dry DCM (200 ml). The reaction mixture was stirred at r.t. under $N_2$ protection overnight, diluted with DCM (300 ml), washed with saturated $NaHCO_3$, dried over $Na_2SO_4$, filtered, and concentrated. Recrystallization afforded *p*-tolyl 3,4,6-tri-*O*-acetyl-2-deoxy-2-trichloroacetamido-1-thio-*β*-D-glucopyranoside (**17**) as a white solid (5.01 g, 9.00 mmol, 90%). **17** (5.01 g, 9.00 mmol) was dissolved in mixed solvent of DCM/MeOH (v/v 1:1, 200 ml). NaOMe (2.70 ml, 1M in MeOH, 2.70 mmol) was added, and the mixture was stirred at r.t. under $N_2$ protection for 2 hrs, neutralized with Amberlite IR-120, concentrated and dried under vacuum. Benzaldehyde dimethyl acetal (1.52 ml, 10.8 mmol) was added to a solution of resulting residue and camphorsulfonic acid (CSA) (0.750 g, 4.05 mmol) in anhydrous toluene (200 ml). The reaction mixture was stirred under $N_2$ protection at 80 °C for 1 hr. When TLC showed around 70% conversion of starting material to product, the reaction flask was placed on a high vacuum rotary evaporator to further push the reaction to completion. When toluene was completely removed by the high vacuum rotary evaporator, the reaction mixture was neutralized with TEA in DCM. The mixture was diluted with DCM (300 ml) and washed

with saturated $NaHCO_3$, dried over $Na_2SO_4$, filtered, and concentrated. Recrystallization afforded **14** as a white solid (3.27 g, 6.30 mmol, 70% for 2 steps).

**Methyl 4,6-*O*-benzylidene-2-deoxy-2-trichloroacetamido-*β*-D-glucopyranoside (15):** Compound **16** (4.93 g, 10 mmol) was dissolved in HBr in AcOH (30.0 ml, 33% wt., 174 mmol). After 6 hrs, the mixture was diluted with DCM (240 ml) and poured onto crushed ice in saturated $NaHCO_3$ (600 ml). The organic phase was separated and washed again with saturated $NaHCO_3$ until the pH reached 7, which was then dried over sodium sulfate ($Na_2SO_4$), filtered, and concentrated. The resulting crude residue was mixed with silver carbonate ($Ag_2CO_3$) (2.76 g, 10.0 mmol), calcium carbonate ($CaSO_4$) (2.72 g, 20.0 mmol) and anhydrous MeOH (100 ml). The mixture was stirred at r.t. under $N_2$ protection for 1 day until TLC showed one major product, on which all three acetyl groups has already been cleaved because of the basic reaction condition. The mixture was concentrated and purified by silica gel chromatography with DCM/MeOH system. Methyl 2-deoxy-2-trichloroacetamido-*β*-D-glucopyranoside (**18**) was afforded (2.70 g, 8.00 mmol, 80% for 2 steps). Compound **18** (2.70 g, 8.00 mmol) was mixed with CSA (0.84 g, 3.60 mmol), benzaldehyde dimethyl acetal (1.35 ml, 9.60 mmol) in anhydrous toluene (200 ml). The reaction mixture was stirred under $N_2$ protection at 80 °C for 1 hr. When TLC showed around 70% conversion of starting material to product, the reaction flask was placed on a high vacuum rotary evaporator to further push the reaction to completion. When toluene was completely removed by the high vacuum rotary evaporator, the reaction mixture was neutralized with TEA in DCM.

The mixture was diluted with DCM (300 ml) and washed with saturated $NaHCO_3$, dried over $Na_2SO_4$, filtered, and concentrated. Recrystallization afforded **15** as a white solid (2.39 g, 5.6 mmol, 70%). $[\alpha]_D^{20}$ -29.3 $^{o}$ (*c* 0.5, DCM); $^{1}$H NMR (500 MHz, $CDCl_3$): δ = 3.46-3.59 (m, 6 H, -$OCH_3$, H-2, H-4, H-5), 3.80-3.84 (m, 1 H, H-6), 4.38-4.42 (m, 2 H, H-3, H-6), 4.87 (d, 1 H, *J* = 8.0 Hz, H-1), 5.57 (s, 1 H, C*H*Ph), 6.93 (d, 1 H, *J* = 7.0 Hz, NH), 7.38-7.51 (m, 5 H, $CH_{arom}$); $^{13}$C NMR (125 MHz, $CDCl_3$): δ = 57.8 (-$OCH_3$), 59.8 (C-2), 66,4 (C-5), 68,8 (C-6), 69.8 (C-3), 81.8 (C-4), 92.5 ($CCl_3$), 101,2 (C-1), 102,2 (*C*HPh), 126.5 -129.6 ($C_{arom}$), 137.12 ($C_q$ $C_{arom}$), 162.6 (C=O TCA); HRMS $[M + Na]^+$: m/z: calcd for $C_{16}H_{18}Cl_3NNaO_6$ 448.0097, found 448.0088.

***p*-Tolyl *O*-(2-*O*-benzoyl-3-*O*-benzyl-4-*O*-*tert*-butyldimethylsilyl-6-*O*-*p*-methoxybenzyl-*β*- D-glucopyranosyl)-(1→3)-4,6-*O*-benzylidene-2-deoxy-1-thio-2-trichloroacetamido-*β*-D- glucopyranoside (19):** The mixture of donor **1** (715 mg, 1 mmol) and freshly activated molecular sieve (MS)-4Å (800 mg) in $Et_2O$ (20.0 ml) was stirred in a dry ice–isopropanol bath for 1 hr, followed by the addition of AgOTf (771 mg, 3.00 mmol) in $Et_2O$ (10.0 ml). After 5 min, orange colored *p*-TolSCl (157 µl, 1.00 mmol) was added via a micro-syringe. Since the reaction temperature was lower than the freezing point of *p*-TolSCl, *p*-TolSCl was added directly into the reaction mixture to prevent it from freezing on the flask wall. The characteristic yellow color of *p*-TolSCl in the reaction solution dissipated rapidly within a few seconds indicating depletion of *p*-TolSCl. The temperature at which pre-activation was performed was not crucial as long as it did not exceed -50 °C. After the donor was completely consumed according to

TLC analysis (about 5 min at −78 °C), a solution of acceptor **14** (467 mg, 0.900 mmol) and TTBP (248 mg, 1.00 mmol) in a mixture solvent of DCM and MeCN (v/v 19:1, 3.00 ml) was then added dropwise within 10 min to the reaction mixture (MeCN was necessary as acceptors **14** were not freely soluble in DCM). The reaction mixture was warmed to −10 °C under stirring in 2 hrs. TEA (0.500 ml) was then added and the mixture was diluted with DCM (100 ml) and filtered over celite. The celite was further washed with DCM until no organic compounds were observed in the filtrate by TLC. All DCM solutions were combined and washed twice with a saturated aqueous solution of $NaHCO_3$ (100 ml) and twice with $H_2O$ (100 ml). The organic layer was concentrated and the crude product was purified by silica gel chromatography. Compound **19** (800 mg, 0.720 mmol, 80%) was afforded as white solid. $[\alpha]_D^{20}$ +22.2 ° (*c* 0.5, DCM); $^1$H NMR (500 MHz, $CDCl_3$): δ = -0.08 (s, 3 H, Si*CH*$_3$), -0.05 (s, 3 H, Si*CH*$_3$), 0.79 (s, 9 H, SiC(*CH*$_3$)$_3$), 2.35 (s, 3 H, PhC*H*$_3$), 3.35-3.43 (m, 3 H, H-5', H-6', H-2), 3.49 (ddd, 1 H, *J* = 4.5 Hz, 5.0 Hz, 9.0 Hz, H-5), 3.56-3.68 (m, 4 H, H-3', H-4', H-6, H-6'), 3.72 (t, 1 H, *J* = 9.0 Hz, H-4), 3.80 (s, 3 H, $CH_3$ PMB), 4.27 (dd, 1 H, *J* = 5.0 Hz, 10.5 Hz, H-6), 4.34 (d, 1 H, *J* = 12.0 Hz, C*H*$_2$PMP), 4.54 (d, 1 H, *J* = 11.0 Hz, C*H*$_2$Ph), 4.58 (d, 1 H, *J* = 11.0 Hz, C*H*$_2$Ph), 4.63 (d, 1 H, *J* = 12.0 Hz, C*H*$_2$PMP), 4.66 (t, 1 H, *J* = 9.0 Hz, H-3 ) ,4.93 (d, 1 H, *J* = 8.0 Hz, H-1'), 5.20 (t, 1 H, *J* = 8.0 Hz, H-2'), 5.32 (s, 1 H, C*H*Ph), 5.44 (d, 1 H, *J* = 10.5 Hz, H-1), 6.89 (d, 1 H, *J* = 8.5 Hz, NH), 7.04-7.11 (m, 7 H, $CH_{arom}$), 7.20-7.42 (m, 14 H, $CH_{arom}$), 7.82-7.84 (m, 2 H, $CH_{arom}$ Bz); $^{13}$C NMR (125 MHz, $CDCl_3$): δ = -4.5

(Si*C*$H_3$), -3.6(Si*C*$H_3$), 18.1 (Si*C*$(CH_3)_3$), 21.4 (Ph*C*$H_3$), 26.0 (x3, SiC(*C*$H_3)_3$), 55.5 (PhO*C*$H_3$), 57.6 (C-5'), 68.7 (C-6), 69.1 (C-6'), 70.9 (C-5), 71.7 (C-4'), 73.3, (*C*$H_2$PMP), 74.4 (C-2'), 75.0 (*C*$H_2$Ph), 76.0 (C-3), 77.4 (C-2), 78.8 (C-4), 83.5 (C-3'), 85.4 (C-1), 92.5 ($CCl_3$), 98.0 (C-1'), 101.3 (*C*HPh), 114.0 ($C_{arom}$-2 *Ph*O$CH_3$), 126.4-130.2 ($CH_{arom}$), 133.3, 133.8 (x2), 137.3, 137.9, 139.0 ($C_q$ SPh$CH_3$, $C_q$ CHPh, $C_q$ Bn, $C_q$ Bz, $C_{arom}$-4 *Ph*O$CH_3$), 159.6 ($C_{arom}$-1 *Ph*O$CH_3$), 161.7, 165.3 (C=O TCA, C=O Bz); HRMS [M + Na]$^+$: m/z: calcd for $C_{56}H_{64}Cl_3NNaO_{12}SSi$ 1130.2882, found 1130.2845.

***p*-Tolyl *O*-(benzyl 2-*O*-benzoyl-3-*O*-benzyl-4-*O*-*tert*-butyldimethylsilyl-*β*-D-glucopyranosyluronate)-(1→3)-4,6-*O*-benzylidene-2-deoxy-1-thio-2-trichloroacetamido-*β*-D-glucopyranoside (11): 19** was converted to **11** in 3 steps (65% for 3 steps) following the general procedures for deprotection of PMB, oxidation of alcohol to carboxylic acid and benzyl ester formation**.** $[\alpha]_D^{20}$ +10.2 $^o$ (*c* 0.5, DCM); $^1$H NMR (500 MHz, $CDCl_3$): δ = -0.16 (s, 3 H, Si*CH*$_3$), -0.13 (s, 3 H, Si*CH*$_3$), 0.74 (s, 9 H, SiC(*CH*$_3)_3$), 2.36 (s, 3 H, PhC*H*$_3$), 3.30 (ddd, 1 H, *J* = 7.5 Hz, 9.0 Hz, 10.5 Hz, H-2), 3.49-3.55 (m, 2 H, H-3', H-5), 3.65-3.70 (m, 2 H, H-6, H-4), 3.83 (d, *J* = 6.5 Hz, H-5'), 4.13 (t, *J* = 6.5 Hz, H-4'), 4.32 (dd, 1 H, *J* = 5.0 Hz, 10.0 Hz, H-6), 4.54 (t, 1 H, *J* = 9.0 Hz, H-3) ,4.59 (d, 1 H, *J* = 11.5 Hz, -C*H*$_2$Ph ), 4.65 (d, 1 H, *J* = 11.5 Hz, -C*H*$_2$Ph), 5.03 (d, 1 H, *J* = 7.0 Hz, H-1'), 5.13 (d, 1 H, *J* = 10.5 Hz, -COOC*H*$_2$Ph ), 5.17 (d, 1 H, *J* = 10.5 Hz, -COOC*H*$_2$Ph ), 5.18 (dd, 1 H, *J* = 6.0 Hz, 7.0 Hz, H-2'), 5.29 (d, 1 H, *J* = 10.5 Hz, H-1), 5.32 (s, 1 H, C*H*Ph), 6.96 (d, 1 H, *J* = 7.5 Hz, NH), 7.10-7.18 (m, 7 H, $CH_{arom}$), 7.26-7.38 (m, 14 H, $CH_{arom}$),

7.51-7.54 (m, 1 H, $CH_{arom}$), 7.88-7.89 (m, 2 H, $CH_{arom}$ Bz); $^{13}C$ NMR (125 MHz, $CDCl_3$): δ = -5.0 (Si*C*$H_3$), -4.3 (Si*C*$H_3$), 18.0 (Si*C*$(CH_3)_3$), 21.4 (Ph*C*$H_3$), 25.9 (x3, SiC(*C*$H_3)_3$), 57.5 (C-2), 67.4 (COO*C*$H_2$Ph), 68.8 (C-6), 70.8 (C-5), 71.4 (C-4'), 73.7 (O*C*$H_2$Ph), 74.4 (C-2'), 76.5 (C-3), 77.6 (C-5'), 80.2 (C-4), 81.3 (C-3'), 84.6 (C-1), 92.2 ($CCl_3$), 99.0 (C-1'), 101.8 (*C*HPh), 126.5-130.2 ($CH_{arom}$), 133.5, 134.2, 135.3, 137.3, 137.9, 139.2 ($C_q$ STol, $C_q$ CHPh, $C_q$ OBn, $C_q$ Bz, $C_q$ COOBn), 161.8, 165.4, 168.6 (C=O TCA, C=O COOBn, C=O Bz); HRMS $[M + Na]^+$ calcd for $C_{55}H_{60}Cl_3NNaO_{12}SSi$ 1114.2563, found 1114.2560.

***p*-Tolyl *O*-(benzyl 2-*O*-benzoyl-3-*O*-benzyl-*β*-D-glucopyranosyluronate)-(1→3)- 4,6-*O*-benzylidene-2-deoxy-1-thio-2-trichloroacetamido-*β*-D-glucopyranoside (12): 11** was converted to **12** following the general procedure for TBS removal (90%). $[\alpha]_D^{20}$ +5.5 $^{o}$ (*c* 1.0, DCM); $^1H$ NMR (500 MHz, $CDCl_3$): δ = 2.36 (s, 3 H, PhC*H*$_3$), 3.02 (s, 1 H, OH), 3.30 (ddd, 1 H, *J* = 7.0 Hz, 9.0 Hz, 10.5 Hz,H-2), 3.52 (ddd, 1 H, *J* = 4.0 Hz, 4.5 Hz, 9.0 Hz, H-5), 3.55-3.60 (m, 3 H, H-3', H-5', H-6), 3.70 (t, 1 H, *J* = 9.0 Hz, H-4), 4.03 (t, 1 H, *J* = 9.0 Hz, H-4'), 4.27 (dd, 1 H, *J* = 4.0 Hz, 10.0 Hz, H-6), 4.59 (t, 1 H, *J* = 9.0 Hz, H-3 ) ,4.62 (d, 1H, *J* = 11.5 Hz, -C*H*$_2$Ph ), 4.72 (d, 1 H, *J* = 11.5 Hz, -C*H*$_2$Ph ), 4.86 (d, 1 H, *J* = 8.0 Hz, H-1'), 5.15 (d, 1 H, *J* = 11.5 Hz, -COOC*H*$_2$Ph ), 5.17 (t, 1 H, *J* = 8.0 Hz, H-2'), 5.26 (d, 1 H, *J* = 11.5 Hz, -COOC*H*$_2$Ph ), 5.32 (s, 1 H, C*H*Ph), 5.37 (d, 1 H, *J* = 10.5 Hz, H-1), 7.05 (d, 1 H, *J* = 7.0 Hz, NH), 7.08-7.18 (m, 7 H, $CH_{arom}$), 7.30-7.45 (m, 14 H, $CH_{arom}$), 7.54-7.57 (m, 1 H, $CH_{arom}$), 7.92-7.94 (m, 2 H, $CH_{arom}$

Bz); $^{13}$C NMR (125 MHz, $CDCl_3$): δ = 21.4 (Ph*C*$H_3$), 57.4 (C-2), 68.1 (COO*C*$H_2$Ph), 68.7 (C-6), 70.7 (C-5), 72.2 (C-4'), 73.2 (C-2'), 74.0 (O*C*$H_2$Ph), 74.7 (C-3), 76.9 (C-5'), 80.1 (C-4), 81.0 (C-3'), 84.4 (C-1), 92.1 ($CCl_3$), 99.6 (C-1'), 101.4 (*C*HPh), 126.3-130.2 ($CH_{arom}$), 133.6, 134.1, 134.8, 137.3, 137.8, 139.2 ($C_q$ STol, $C_q$ CHPh, $C_q$ OBn, $C_q$ Bz, $C_q$ COOBn), 161.8, 165.3, 169.3 (C=O TCA, C=O COOBn, C=O Bz); HRMS $[M + Na]^+$: m/z: calcd for $C_{49}H_{46}Cl_3NNaO_{12}S$ 1000.1699, found 1000.1706.

**Methyl *O*-(benzyl 2-*O*-benzoyl-3-*O*-benzyl-*β*-D-glucopyranosyluronate) -(1→3)-4,6-*O*-benzylidene-2-deoxy-2-trichloroacetamido-*β*-D-glucopyranoside (13):** The mixture of donor **1** (715 mg, 1.00 mmol), acceptor **15** (427 mg, 1.00 mmol) and freshly activated MS-4Å (800 mg) in a mixture solvent of DCM and MeCN (v/v 40:1, 20.0 ml) was stirred for 1 hr at -78 °C, followed by the addition of AgOTf (771 mg, 3.00 mmol) in $Et_2O$ (10 ml). After 5 min, *p*-TolSCl (157 µl, 1.00 mmol) was added via a syringe to activate the donor. The yellow color of the reaction disappears quickly and TLC analysis showed the donor was completely consumed. A solution of TTBP (248 mg, 1.00 mmol) in DCM (1.00 ml) was then added dropwise to the reaction mixture. The reaction mixture was warmed to −10 °C under stirring in 2 hrs, followed by the same workup and purification procedures described above for the synthesis of compound **19**. The resulting disaccharide was subjected to deprotection of PMB, oxidation of alcohol to carboxylic acid, benzyl ester formation and TBS removal reactions following the general procedures to afford compound **13** (426 mg, 0.480 mmol, 48% for 5 steps) as a white solid. $[\alpha]_D^{20}$

+8.2 $^{o}$ (*c* 0.5, DCM); $^{1}$H NMR (500 MHz, $CDCl_3$): δ = 3.00 (d, 1 H, *J* = 2.5 Hz, OH), 3.30 (ddd, 1 H, *J* = 7.0 Hz, 8.0 Hz, 9.5 Hz, H-2), 3.48-3.50 (m, 4 H, -$OCH_3$, H-5), 3.57-3.60 (m, 3 H, H-3', H-5', H-6), 3.76 (t, 1 H, *J* = 9.0 Hz, H-4), 4.03 (ddd, 1 H, *J* = 2.5 Hz, 9.0 Hz, 9.0 Hz, H-4'), 4.26 (dd, 1 H, *J* = 5.0 Hz, 10.5 Hz, H-6), 4.59 (dd, 1 H, *J* = 9.0 Hz, 9.5 Hz, H-3 ) ,4.63 (d, 1 H, *J* = 11.5 Hz, -C*H*$_2$Ph ), 4.73 (d, 1 H, *J* = 11.5 Hz, -C*H*$_2$Ph ), 4.88 (d, 1 H, *J* = 7.5 Hz, H-1'), 4.99 (d, 1 H, *J* = 8.0 Hz, H-1), 5.14 (d, 1 H, *J* = 12.0 Hz, -COOC*H*$_2$Ph ), 5.20 (dd, 1 H, *J* = 7.5 Hz, 9.5 Hz, H-2'), 5.26 (d, 1 H, *J* = 12.0 Hz, -COOC*H*$_2$Ph ), 5.36 (s, 1 H, C*H*Ph), 7.05 (d, 1 H, *J* = 7.0 Hz, NH), 7.08-7.09 (m, 3 H, $CH_{arom}$), 7.27-7.40 (m, 14 H, $CH_{arom}$), 7.54-7.57 (m, 1 H, $CH_{arom}$), 7.92-7.94 (m, 2 H, $CH_{arom}$ Bz); $^{13}$C NMR (125 MHz, $CDCl_3$): δ = 57.8 (-$OCH_3$) 59.3 (C-2), 66.3 (C-5), 68.0 (COO*C*$H_2$Ph), 68.8 (C-6), 72.3 (C-4'), 73.2 (C-2'), 74.0 (C-5'), 74.7 (O*C*$H_2$Ph), 76.2 (C-3), 80.3 (C-4), 81.1 (C-3'), 92.1 ($CCl_3$), 99.7 (C-1), 100.0 (C-1'), 101.4 (*C*HPh), 126.2-130.2 ($CH_{arom}$), 133.5, 134.9, 137.4, 138.0 ($C_q$ CHPh, $C_q$ OBn, $C_q$ Bz, $C_q$ COOBn), 162.3, 165.3, 169.3 (C=O TCA, C=O COOBn, C=O Bz); HRMS $[M + Na]^+$: m/z: calcd for $C_{43}H_{42}Cl_3NNaO_{13}$ 908.1619, found 908.1616.

**2-Trichloromethyl *O*-(benzyl 2-*O*-benzoyl-3-*O*-benzyl-4-*O*-*tert*-butyldimethylsilyl-*β*-D- glucopyranosyluronate)-(1→3)-4,6-*O*-benzylidene-1,2-dideoxy-*α*-D-glucopyrano-[2,1-*d*]-2-oxazoline (20):** $[\alpha]_D^{20}$ +54.1 $^{o}$ (*c* 1.0, DCM); $^{1}$H NMR (500 MHz, $CDCl_3$): δ = -0.06 (s, 3 H, Si*CH*$_3$), -0.05 (s, 3 H, Si*CH*$_3$), 0.81 (s, 9 H, SiC(*CH*$_3$)$_3$), 3.53 (dd, 1 H, *J* = 5.0 Hz, 10.0 Hz, H-6), 3.61 (t, 1 H, *J* = 10.0 Hz, H-5), 3.68 (t, 1 H, *J* = 7.5 Hz, H-3'), 3.91 (dd, 1 H, *J* = 7.5 Hz, 10.0 Hz, H-4), 4.01 (d, 1 H, *J* = 8.0 Hz,

H-5') ,4.15-4.18 (m, 2 H, H-3, H-4'), 4.22 (dd, 1 H, *J* = 5.0 Hz, 8.0 Hz, H-2), 4.34 (dd, 1 H, *J* = 5.0 Hz, 10.0 Hz, H-6), 4.66 (d, 1 H, *J* = 12.5 Hz, C*H*$_2$Ph ), 4.69 (d, 1 H, *J* = 12.5 Hz, C*H*$_2$Ph ), 5.02 (d, 1 H, *J* =7.5 Hz, H-1'), 5.11 (d, 1 H, *J* = 12.0 Hz, COO*C*H$_2$Ph), 5.15 (d, 1 H, *J* = 12.0 Hz, COO*C*H$_2$Ph), 5.38 (t, 1 H, *J* = 7.5 Hz, H-2'), 5.39 (s, 1 H, C*H*Ph), 6.08 (d, 1 H, *J* = 8.0 Hz, H-1), 7.13-7.17 (m, 4 H, CH$_{arom}$), 7.31-7.43 (m, 13 H, CH$_{arom}$), 7.53-7.70 (m, 1 H, CH$_{arom}$), 8.00-8.10 (m, 2 H, CH$_{arom}$ Bz); $^{13}$C NMR (125 MHz, $CDCl_3$): δ = -4.9 (Si*C*H$_3$), -4.0 (Si*C*H$_3$), 18.1 (Si*C*(CH$_3$)$_3$), 26.1 (x3, SiC(*C*H$_3$)$_3$), 63.4 (C-5), 67.5 (COO*C*H$_2$Ph), 68.7 (C-6), 69.0 (C-2), 72.1 (C-4'), 74.1 (C-2'), 74.6 (O*C*H$_2$Ph), 77.4 (C-5'), 78.7 (C-4), 80.3 (C-3), 82.3 (C-3'), 101.1 (C-1'), 101.5 (*C*HPh), 105.3 (C-1), 110.0 ($CCl_3$), 125.5-128.7 (CH$_{arom}$), 133.5, 135.2, 137.1, 137.8 (C$_q$ CHPh, C$_q$ OBn, C$_q$ Bz, C$_q$ COOBn), 162.5, 165.5, 168.2 (C=N, C=O COOBn, C=O Bz); HRMS $[M + Na]^+$: m/z: calcd for $C_{48}H_{52}Cl_3NNaO_{12}Si$ 990.2222, found 990.2231.

***p*-Tolyl *O*-(benzyl 2-*O*-benzoyl-3-*O*-benzyl-4-*O*-*tert*-butyldimethylsilyl-*β*-D-glucopyranosyluronate)-(1→3)-*O*-(4,6-*O*-benzylidene-2-deoxy-2-trichloroacetamido-*β*-D-glucopyranosyl)-(1→4)-*O*-(benzyl 2-*O*-benzoyl-3-*O*-benzyl-*β*-D-glucopyranosyluronate) -(1→3)-4,6-*O*-benzylidene-2-deoxy-1-thio-2-trichloroacetamido-*β*-D-glucopyranoside (25):** The mixture of donor **11** (37.0 mg, 33.9 μmol) and freshly activated MS-4Å (300 mg) in $Et_2O$ (2.00 ml) was stirred for 1 hr at -78 °C, followed by the addition of AgOTf (26.0 mg, 102 μmol) in $Et_2O$ (1.00 ml). After 5 min, *p*-TolSCl (5.30 μl, 33.9 μmol) was added via a micro-syringe to activate the donor. The characteristic yellow color of *p*-TolSCl in the reaction solution dissipated rapidly

within a few seconds indicating depletion of *p*-TolSCl and TLC analysis showed the donor was completely consumed. A solution of acceptor **12** (30.0 mg, 30.5 μmol) in a mixture solvent of DCM and acetonitrile (MeCN) (v/v 19:1, 0.700 ml) was then added dropwise to the reaction mixture. After 5 min, TMSOTf (2 μl, 11.0 μmol) was added via micro-syringe. The reaction mixture was warmed to −10 °C under stirring in 2 hrs followed by the same workup and purification procedures described above for the synthesis of compound **19**. Compound **25** (54.0 mg, 27.8 μmol, 82%) was afforded as white solid. $[\alpha]_D^{20}$ +2.9 ° (*c* 0.5, DCM); $^1$H NMR (500 MHz, $CDCl_3$): δ = -0.14 (s, 3 H, Si*CH*$_3$), -0.11 (s, 3 H, Si*CH*$_3$), 0.78 (s, 9 H, SiC(*CH*$_3$)$_3$), 2.31 (s, 3 H, PhC*H*$_3$), 3.09 (ddd, 1 H, *J* = 5.0 Hz, 5.0 Hz, 10.0 Hz, H-5''), 3.17-3.22 (m, 1 H, H-6''), 3.44-3.50 (m, 2 H, H-2, H-5), 3.53 (dd, 1 H, *J* = 9.5 Hz, 10.0 Hz, H-3), 3.55 (t, 1 H, *J* = 7.0 Hz, H-3'''), 3.58-3.61 (m, 2 H, H-4'', H-6), 3.64 (t, 1 H, *J* = 8.0 Hz, H-3'), 3.72 (t, 1 H, *J* = 9.0 Hz, H-2''), 3.81 (dd, 1 H, *J* = 9.0 Hz, 9.5 Hz H-4), 3.86 (d, 1 H, *J* = 7.0 Hz, H-5'''), 3.87 (d, 1 H, *J* = 8.0 Hz, H-5'), 4.02 (dd, 1 H, *J* = 5.0 Hz, 10.5 Hz, H-6''), 4.17 (t, 1 H, *J* = 7.0 Hz, H-4'''), 4.20 (t, 1 H, *J* = 8.0 Hz, H-4' ), 4.29 (dd, 1 H, *J* = 5.0 Hz, 10.5 Hz, H-6 ), 4.41 (t, 1 H, *J* = 9.0 Hz, H-3'' ), 4.53 (d, 1 H, *J* = 11.5 Hz, -C*H*$_2$Ph ), 4.61 (d, 1 H, *J* = 9.0 Hz, H-1''), 4.61 (d, 1 H, *J* = 11.5 Hz, -C*H*$_2$Ph ), 4.68 (d, 1 H, *J* = 11.5 Hz, -C*H*$_2$Ph ), 4.74 (d, 1 H, *J* = 11.5 Hz, -C*H*$_2$Ph ), 4.97 (d, 1 H, *J* = 10.0 Hz, -COOC*H*$_2$Ph ), 5.00 (s, 1 H, C*H*Ph ), 5.00 (d, 1 H, *J* = 7.0 Hz, H-1'''), 5.06 (t, 1 H, *J* = 8.0 Hz, H-2'), 5.12 (d, 1 H, *J* = 7.5 Hz, H-1), 5.12 (d, 1 H, *J* = 10.0 Hz, -COOC*H*$_2$Ph), 5.16 (d, 1 H, *J* = 10.0 Hz, -COOC*H*$_2$Ph), 5.17 (d, 1 H, *J* = 8.0

Hz, H-1' ), 5.19 (d, 1 H, *J* = 11.5 Hz, -COOC*H*$_2$Ph ), 5.20 (t, 1 H, *J* = 7.0 Hz, H-2'''), 5.32 (s, 1 H, C*H*Ph), 6.49 (d, 1 H, *J* = 9.0 Hz, NH), 7.08 (d, 1 H, *J* = 7.5 Hz, NH''), 7.10-7.20 (m, 13 H, $CH_{arom}$), 7.26-7.42 (m, 25 H, $CH_{arom}$), 7.53-7.58 (m, 2 H, $CH_{arom}$), 7.89-7.91 (m, 2 H, $CH_{arom}$ Bz), 7.95-7.97 (m, 2 H, $CH_{arom}$ Bz); $^{13}$C NMR (125 MHz, $CDCl_3$): δ = -5.0 (Si*C*$H_3$), -4.2 (Si*C*$H_3$), 18.1 (Si*C*$(CH_3)_3$), 21.4 (Ph*C*$H_3$), 26.0 (x3, SiC(*C*$H_3)_3$), 56.8 (C-2), 57.6 (C-2''), 66.4 (C-5''), 67.4 (COO*C*$H_2$Ph ), 68.4 (COO*C*$H_2$Ph ),68.0 (C-6), 68.0 (C-6''), 70.8 (C-5), 71.4 (C-4'''), 73.7 (O*C*$H_2$Ph), 74.6 (O*C*$H_2$Ph), 74.6 (C-2'''), 75.0 (C-2'), 75.0 (C-5'), 75.8 (C-4), 77.0 (C-3''), 77.3 (C-4'), 77.8 (C-5'''), 78.5 (C-3'), 79.8 (C-4''), 80.2 (C-3), 81.4 (C-3'''), 85.6 (C-1), 92.4 ($CCl_3$), 92.7 ($CCl_3$), 99.3 (*C*HPh), 100.0, 100.0 (C-1'', C-1'''), 101.0 (*C*HPh), 101.7 (C-1'), 126.2-130.1 ($CH_{arom}$), 133.5, 133.5, 134.1, 135.4, 135.4, 137.4, 137.4, 138.0, 138.4, 138.4 ($C_q$ STol, $C_q$ CHPh x2, $C_q$ OBn x2, $C_q$ Bz x2, $C_q$ COOBn x2), 161.7, 165.0, 165.3, 165.7, 168.5, 169.1 (C=O TCA x2, C=O COOBn x2, C=O Bz x2); HRMS $[M + H]^+$: m/z: calcd for $C_{97}H_{99}Cl_6N_2O_{24}SSi$ 1949.4191, found 1949.4142.

**Methyl *O*-(benzyl 2-*O*-benzoyl-3-*O*-benzyl-4-*O*-*tert*-butyldimethylsilyl-*β*-D-glucopyranosyluronate)-(1→3)-*O*-(4,6-*O*-benzylidene-2-deoxy-2-trichloroacetamido-*β*-D-glucopyranosyl)-(1→4)-*O*-(benzyl 2-*O*-benzoyl-3-*O*-benzyl-*β*-D-glucopyranosyluronate)-(1→3)-*O*-(4,6-*O*-benzylidene-2-deoxy-2-trichloroacetamido-*β*-D-glucopyranosyl)-(1→4)-*O*-(benzyl 2-*O*-benzoyl-3-*O*-benzyl-*β*-D-glucopyranosyluronate)-(1→3)-4,6-*O*-benzylidene-2-deoxy-2-trichloroacetamido-*β*-D-glucopyranoside (26):** After a mixture of donor **25** (33.4 mg, 17.1 μmol), acceptor **13**

(15.2 mg, 17.1 μmol) and MS-AW-300 (200 mg) in a mixture solvent of DCM and MeCN (v/v 19:1, 2.00 ml) was stirred at -78 °C for 1 hr, AgOTf (13.0 mg, 51.4 μmol) in $Et_2O$ (0.7 00 ml) was added. When the temperature of the reaction mixture reduced to -78 °C, *p*-TolSCl (17.1 μmol, 2.46 μl) was added via a micro-syringe. After 5 min when the yellowish color disappears, TMSOTf (0.750 μl, 4.13 μmol) was added via micro-syringe. The reaction mixture was warmed to −10 °C under stirring in 2 hrs, followed by the same workup and purification procedures described above for the synthesis of compound **19**. Compound **26** (33.0 mg, 12.0 μmol, 71%) was afforded as white solid. $[\alpha]_D^{20}$ -1.7 $^{o}$ (*c* 0.5, DCM); $^{1}$H NMR (500 MHz, $CDCl_3$): δ = -0.14 (s, 3 H, Si*CH*$_3$), -0.10 (s, 3 H, Si*CH*$_3$), 0.78 (s, 9 H, SiC(*CH*$_3$)$_3$), 3.00 (dd, 1 H, *J* = 4.5 Hz, 9.5 Hz, H-6$^{a/c/e}$), 3.13 (ddd, 1 H, *J* = 4.5 Hz, 5.0 Hz, 9.5 Hz, H-5$^{a/c/e}$), 3.15 (dd, 1 H, *J* = 4.5 Hz, 9.5 Hz, H-6$^{a/c/e}$), 3.18-3.23 (m, 1 H, H-5 $^{a/c/e}$), 3.42-3.48 (m, 3 H, H-5$^{a/c/e}$, H-6$^{a/c/e}$, H-2$^{a/c/e}$), 3.50 (s, 3 H, $OCH_3$), 3.52-3.61 (m, 3 H, H-3$^{a/c/e}$, H-3$^{b/d/f}$ x2), 3.61-3.70 (m, 3 H, H-3$^{a/c/e}$, H-3$^{b/d/f}$ , H-4$^{a/c/e}$), 3.72-3.78 (m, 2 H, H-2$^{a/c/e}$ x2), 3.81 (dd, 1 H, *J* = 9.0 Hz, 9.5 Hz, H-4$^{a/c}$), 3.81 (dd, 1 H, *J* = 9.0 Hz, 9.5 Hz, H-4$^{a/c}$), 3.85 (d, 1 H, *J* = 6.5 Hz, H-5$^{b/d/f}$), 3.86 (d, 1 H, *J* = 8.5 Hz, H-5$^{b/d/f}$), 3.90 (d, 1 H, *J* = 8.5 Hz, H-5$^{b/d/f}$), 4.02 (dd, 1 H, *J* = 4.5 Hz, 10.0 Hz, H-6$^{a/c/e}$), 4.04 (dd, 1 H, *J* = 4.5 Hz, 10.5 Hz, H-6$^{a/c/e}$), 4.17 (t, 1 H, *J* = 6.5 Hz, H-4$^{b/d/f}$), 4.19 (t, 1 H, *J* = 8.5 Hz, H-4$^{b/d/f}$), 4.25 (t, 1 H, *J* = 8.5 Hz, H-4$^{b/d/f}$), 4.29 (dd, 1 H, *J* = 5.5 Hz, 10.5 Hz, H-6$^{a/c/e}$), 4.47 (dd, 1 H, *J* = 9.0 Hz, 9.5 Hz, H-3$^{a/c/e}$), 4.52 (d, 1 H, *J* = 8.0 Hz, H-1$^{c/e}$), 4.56 (d, 1 H, *J* = 11.5 Hz, -C*H*$_2$Ph ), 4.57 (d, 1 H, *J* = 12.0 Hz, -C*H*$_2$Ph ), 4.62 (d,

1 H, *J* = 11.5 Hz, -C*H*$_2$Ph ), 4.68 (d, 1 H, *J* = 12.0 Hz, -C*H*$_2$Ph ), 4.72 (d, 1 H, *J* = 8.0 Hz, H-1$^{c/e}$), 4.75 (d, 1 H, *J* = 11.5 Hz, -C*H*$_2$Ph ), 4.78 (d, 1 H, *J* = 11.5 Hz, -C*H*$_2$Ph ), 4.84 (d, 1 H, *J* = 8.5 Hz, H-1$^{a}$),4.94 (d, 1 H, *J* = 6.0 Hz, H-1$^{b/d/f}$), 4.97 (d, 1 H, *J* = 6.5 Hz, H-1$^{b/d/f}$), 4.99 (d, 1 H, *J* = 7.0 Hz, H-1$^{b/d/f}$), 5.01 (d, 1 H, *J* = 12.0 Hz, -COOC*H*$_2$Ph), 5.04 (d, 1 H, *J* = 12.0 Hz, -COOC*H*$_2$Ph), 5.07 (dd, 1 H, *J* = 6.0 Hz, 8.0 Hz, H-2$^{b/d/f}$), 5.11 (d, 1 H, *J* = 12.0 Hz, -COOC*H*$_2$Ph ), 5.12 (dd, 1 H, *J* = 6.5 Hz, 8.5 Hz, H-2$^{b/d/f}$), 5.14 (s, 1 H, C*H*Ph), 5.18 (d, 1 H, *J* = 12.0 Hz, -COOC*H*$_2$Ph), 5.19 (s, 1 H, C*H*Ph), 5.20 (d, 1 H, *J* = 12.0 Hz, -COOC*H*$_2$Ph), 5.21 (d, 1 H, *J* = 12.0 Hz, -COOC*H*$_2$Ph), 5.21 (dd, 1 H, *J* = 6.0 Hz, 7.0 Hz, H-2$^{b/d/f}$), 5.32 (s, 1 H, C*H*Ph), 6.48 (d, 1 H, *J* = 8.5 Hz, NH), 6.60 (d, 1 H, *J* = 8.5 Hz, NH), 6.99 (d, 1 H, *J* = 8.0 Hz, NH), 7.13-7.60 (m, 54 H, $CH_{arom}$), 7.89-7.98 (m, 6 H, $CH_{arom}$ Bz); $^{13}$C NMR (125 MHz, $CDCl_3$): δ = -5.0 (Si*C*$H_3$), -4.2 (Si*C*$H_3$), 18.1 (Si*C*(C$_3$)$_3$), 26.0 (x3, SiC(*C*$H_3$)$_3$), 57.2 (C-2$^{a/c/e}$), 57.5 (C-2$^{a/c/e}$), 57.7 ($OCH_3$), 58.8 (C-2$^{a/c/e}$), 66.3, 66.4, 66.4 (C-5$^{a/c/e}$, C-6$^{a/c/e}$, C-5$^{a/c/e}$), 67.4 (COO*C*$H_2$Ph ), 68.0 (COO*C*$H_2$Ph ), 68.1 (COO*C*$H_2$Ph ), 68.3, 68.6, 68.7 (C-6$^{a/c/e}$, C-6$^{a/c/e}$, C-5$^{a/c/e}$), 71.4 (C-4$^{f}$), 73.7 (O*C*$H_2$Ph), 74.3 (C-2$^{b/d/f}$), 74.7 (O*C*$H_2$Ph), 74.7 (O*C*$H_2$Ph), 74.7 (x2, C-5$^{b/d/f}$ x2), 75.0 (C-2$^{b/d/f}$), 75.1 (C-2$^{b/d/f}$), 76.0 (C-3$^{a/c/e}$), 76.8 (C-4$^{a/c/e}$), 77.0 (C-4$^{a/c/e}$), 77.5 (C-4$^{b/d}$), 77.6 (C-4$^{b/d}$), 77.8 (C-5$^{b/d/f}$), 78.8 (C-3$^{b/d/f}$), 79.0 (C-3$^{b/d/f}$), 80.0 (x2, C-3$^{a/c/e}$ x2), 82.2 (C-4$^{a/c/e}$), 81.5 (C-3$^{b/d/f}$), 92.4 ($CCl_3$), 92.6 ($CCl_3$), 92.7 ($CCl_3$), 99.3 (C-1$^{b/d/f}$), 99.9 (C-1$^{b/d/f}$), 100.0 (C-1$^{c/e}$), 100.1 (C-1$^{c/e}$), 100.3 (C-1$^{b/d/f}$), 100.8 (C-1$^{a}$), 100.9 (*C*HPh), 101.1 (*C*HPh), 101.7 (*C*HPh), 126.3-130.4 ($CH_{arom}$), 133.4, 133.5, 133.6, 135.0 (x2),

135.4, 137.4, 137.5, 137.5, 137.9, 138.3, 138.5 ($C_q$ CHPh x3, $C_q$ OBn x3, $C_q$ Bz x3, $C_q$ COOBn x3), 161.6, 162.0, 162.3, 165.3, 165.6, 165.6, 168.6, 169.0, 169.1 (C=O TCA x3, C=O COOBn x3, C=O Bz x3); HRMS $[M + Na]^+$: m/z: calcd for $C_{133}H_{132}Cl_9N_3NaO_{37}Si$ 2734.5383, found 2734.5469.

**2-Trichloromethyl *O*-(benzyl 2-*O*-benzoyl-3-*O*-benzyl-4-*O*-*tert*-butyldimethylsilyl- *β*-D-glucopyranosyluronate)-(1→3)-*O*-(4,6-*O*-benzylidene-2-deoxy-2-trichloroacetamido-*β*-D-glucopyranosyl)-(1→4)-*O*-(benzyl 2-*O*-benzoyl -3-*O*-benzyl-*β*-D-glucopyranosyl- uronate)-(1→3)-4,6-*O*-benzylidene-1,2-dideoxy -*α*-D-glucopyrano-[2,1-*d*]-2-oxazoline (27):** $[\alpha]_D^{20}$ +19.3 ° (*c* 0.5, DCM); $^1$H NMR (500 MHz, $CDCl_3$): δ = -0.15 (s, 3 H, Si*CH*$_3$), -0.12 (s, 3 H, Si*CH*$_3$), 0.77 (s, 9 H, SiC(*CH*$_3$)$_3$), 3.02 (ddd, 1 H, *J* = 4.5 Hz, 5.0 Hz, 9.5 Hz, H-5''), 3.26-3.31 (m, 1 H, H-6''), 3.44-3.48 (m, 2 H, H-6, H-5), 3.55 (t, 1 H, *J* = 7.0 Hz, H-3'''), 3.63 (t, 1 H, *J* = 9.5 Hz, H-4''), 3.73-3.68 (m, 2 H, H-3', H-2''), 3.82-3.91 (m, 4 H, H-3, H-4, H-5', H-5'''), 4.04 (dd, 1 H, *J* = 5.0 Hz, 11.0 Hz, H-6''), 4.13-4.23 (m, 4 H, H-2, H-3'', H-4', H-4'''), 4.28-4.29 (m, 1 H, H-6), 4.55 (d, 1 H, *J* = 8.0 Hz, H-1''), 4.57 (d, 1 H, *J* = 11.5 Hz, -C*H*$_2$Ph), 4.60 (d, 1 H, *J* = 11.5 Hz, -C*H*$_2$Ph ), 4.67 (d, 1 H, *J* = 11.5 Hz, -C*H*$_2$Ph ), 4.77 (d, 1 H, *J* = 11.5 Hz, -C*H*$_2$Ph ), 4.89 (d, 1 H, *J* = 7.5 Hz, H-1'''), 4.95 (d, 1 H, *J* = 12.0 Hz, -COOC*H*$_2$Ph), 5.02 (d, 1 H, *J* = 7.0 Hz, H-1'), 5.15 (d, 1 H, *J* = 12.0 Hz, -COOC*H*$_2$Ph ), 5.17 (s, 1 H, C*H*Ph), 5.19 (d, 1 H, *J* = 12.0 Hz, -COOC*H*$_2$Ph), 5.20 (d, 1 H, *J* = 12.0 Hz, -COOC*H*$_2$Ph ), 5.20 (t, 1 H, *J* = 7.0 Hz, H-2' ), 5.24 (dd, 1 H, *J* = 7.5 Hz, 8.5 Hz, H-2'''), 5.34 (s, 1 H, C*H*Ph), 6.09 (d, 1 H, *J* = 7.5 Hz, H-1), 6.58 (d, 1 H, *J* = 8.5 Hz, NH''), 7.10-7.18 (m, 10 H, $CH_{arom}$),

7.29-7.45 (m, 22 H, $CH_{arom}$), 7.59-7.52 (m, 2 H, $CH_{arom}$), 7.95-8.00 (m, 4 H, $CH_{arom}$ Bz); $^{13}C$ NMR (125 MHz, $CDCl_3$): δ = -5.0 (Si*C*$H_3$), -4.2 (Si*C*$H_3$), 18.1 (Si*C*$(CH_3)_3$), 26.0 (x3, SiC(*C*$H_3)_3$), 57.6 (C-2''), 63.4 (C-5), 66.4 (C-5''), 67.4 (COO*C*$H_2$Ph ), 67.8 (COO*C*$H_2$Ph ), 68.6 (C-6), 68.6 (C-6''), 68.9 (C-2), 71.4 (C-4'''), 73.1 (C-2'''), 73.7 (O*C*$H_2$Ph), 74.7 (C-2'), 74.8 (O*C*$H_2$Ph), 75.2 (C-5), 76.7 (C-4''), 77.1 (C-3''), 77.8 (C-5'''), 78.5 (C-4), 79.9 (C-3'), 80.1 (C-4'), 80.2 (C-3), 81.4 (C-3'''), 92.6 ($CCl_3$, TCA), 99.2 (C-1'), 99.4 (C-1''), 101.0 (C-1'''), 101.3 (*C*HPh), 101.7 (*C*HPh), 110.0 (N=C-*C*$Cl_3$), 105.2 (C-1), 126.2-130.1 ($CH_{arom}$), 133.4x2, 135.1, 135.4, 137.1, 137.4, 138.0, 138.2 ($C_q$ CHPh x2, $C_q$ OBn x2, $C_q$ Bz x2, $C_q$ COOBn x2), 161.8, 162.5, 165.3, 165.4, 168.2, 168.5 (C=N-$CCl_3$, C=O TCA, C=O COOBn x2, C=O Bz x2); HRMS $[M + Na]^+$: m/z: calcd for $C_{90}H_{90}Cl_6N_2NaO_{24}Si$ 1843.3682, found 1843.3724.

**Methyl *O*-(benzyl 2-*O*-benzoyl-3-*O*-benzyl-*β*-D-glucopyranosyluronate)-(1→3)-*O*- (4,6-*O*-benzylidene-2-deoxy-2-trichloroacetamido-*β*-D-glucopyranosyl)-(1→4)-*O*-(benzyl 2-*O*-benzoyl-3-*O*-benzyl-*β*-D-glucopyranosyluronate)-(1→3)-*O*-(4,6-*O*-benzylidene-2- deoxy-2-trichloroacetamido-*β*-D-glucopyranosyl)-(1→4)-*O*-(benzyl 2-*O*-benzoyl-3-*O*- benzyl-*β*-D-glucopyranosyluronate)-(1→3)-4,6-*O*-benzylidene-2-deoxy-2-trichloroacetamido-*β*-D-glucopyranoside (28):** **26** was converted to **28** following the general procedure for TBS removal as described before (90%). $[\alpha]_D^{20}$ -3.0 $^o$ (*c* 0.5, DCM); $^1H$ NMR (500 MHz, $CDCl_3$): δ = 3.00 (ddd, 1 H, *J* = 5.0 Hz, 5.0 Hz, 10.0 Hz, H-5$^{a/c/e}$), 3.07 (s, 1 H, OH), 3.12-3.20 (m, 3 H, H-6$^{a/c/e}$ x3),

3.43-3.48 (m, 3 H, H-5$^{a/c/e}$x2, H-2$^{a/c/e}$), 3.50 (s, 3 H, $OCH_3$), 3.61 (t, 2 H, *J* = 9.0 Hz, H-3$^{a/c/e}$ x2), 3.63-3.70 (m, 3 H, H-3 $^{b/d/f}$ x2, H-4$^{a/c/e}$), 3.72-3.79 (m, 2 H, H-2$^{a/c/e}$ x2), 3.82 (dd, 1 H, *J* = 8.5 Hz, 9.0 Hz, H-4$^{a/c/e}$), 3.82 (dd, 1 H, *J* = 8.5 Hz, 9.5 Hz, H-4$^{a/c/e}$), 3.87 (d, 1 H, *J* = 8.5 Hz, H-5$^{b/_d}$), 3.90 (d, 1 H, *J* = 8.0 Hz, H-5$^{b/d}$), 4.02 (dd, 1 H, *J* = 4.5 Hz, 9.5 Hz, H-6$^{a/c/e}$), 4.05 (dd, 1 H, *J* = 4.5 Hz, 11.0 Hz, H-6$^{a/c/e}$), 4.08-4.18 (m, 3H, H-3$^{b/d/f}$, H-4$^{b/d/f}$ x2), 4.19 (dd, 1 H, *J* = 8.0 Hz, 8.5 Hz, H-4$^{b/d/f}$), 4.25 (d, 1 H, *J* = 8.5 Hz, H-5$^{b/d/f}$), 4.29 (dd, 1 H, *J* = 5.5 Hz, 10.5 Hz, H-6$^{a/c/e}$), 4.48 (dd, 1 H, *J* = 9.0 Hz, 9.5 Hz, H-3$^{a/c/e}$), 4.52 (d, 1 H, *J* = 8.0 Hz, H-1$^{c/e}$), 4.56 (d, 1 H, *J* = 12.0 Hz, -C*H*$_2$Ph ), 4.57 (d, 1 H, *J* = 12.0 Hz, -C*H*$_2$Ph ), 4.66 (d, 1 H, *J* = 11.5 Hz, -C*H*$_2$Ph ), 4.75 (d, 1 H, *J* = 7.5 Hz, H-1$^{c/e}$), 4.75 (d, 1 H, *J* = 11.5 Hz, -C*H*$_2$Ph ), 4.76 (d, 1 H, *J* = 12.0 Hz, -C*H*$_2$Ph ), 4.79 (d, 1 H, *J* = 12.0 Hz, -C*H*$_2$Ph ), 4.85 (d, 1 H, *J* = 8.0 Hz, H-1$^{a}$), 4.85 (d, 1 H, *J* = 7.5 Hz, H-1$^{b/d/f}$), 4.94-4.98 (m, 2 H, H-1$^{b/d/f}$ x2), 5.02 (d, 1 H, *J* = 11.5 Hz, -COOC*H*$_2$Ph), 5.04 (d, 1 H, *J* = 12.0 Hz, -COOC*H*$_2$Ph), 5.06 (dd, 1 H, *J* = 8.0 Hz, 8.5 Hz, H-2$^{b/d/f}$), 5.10 (d, 1 H, *J* = 12.0 Hz, -COOC*H*$_2$Ph ), 5.13 (s, 1 H, C*H*Ph), 5.16 (d, 1 H, *J* = 12.0 Hz, -COOC*H*$_2$Ph), 5.16 (d, 1 H, *J* = 12.0 Hz, -COOC*H*$_2$Ph), 5.17 (dd, 1 H, *J* = 7.5 Hz, 8.5 Hz, H-2$^{b/d/f}$), 5.19 (dd, 1 H, *J* = 6.5 Hz, 8.0 Hz, H-2$^{b/d/f}$), 5.21 (s, 1 H, C*H*Ph ), 5.25 (d, 1 H, *J* = 11.5 Hz, -COOC*H*$_2$Ph), 5.32 (s, 1 H, C*H*Ph), 6.45 (d, 1H, *J* = 8.5 Hz, NH), 6.63 (d, 1 H, *J* = 9.0 Hz, NH), 7.02 (d, 1 H, *J* = 7.5 Hz, NH), 7.13-7.61 (m, 54 H, $CH_{arom}$), 7.90-8.04 (m, 6 H, $CH_{arom}$ Bz); $^{13}$C NMR (125 MHz, $CDCl_3$): δ = 57.1 (C-2$^{a/c/e}$), 57.5 (C-2$^{a/c/e}$), 57.7 ($OCH_3$), 58.8 (C-2$^{a/c/e}$), 66.3, 66.4 (C-5$^{a/c/e,}$ C-6$^{a/c/e}$), 66.4 (COO*C*$H_2$Ph ), 68.0

(COO*C*$H_2$Ph ), 68.1 (COO*C*$H_2$Ph ), 68.1, 68.3, 68.5, 68.7 (C-$6^{a/c/e}$ x2, C-$5^{a/c/e}$ x2), 72.0 (C-$4^{f}$), 73.6 (C-$2^{b/d/f}$), 74.2 (C-$2^{b/d/f}$), 74.3 (C-$5^{b/d}$), 74.6 (O*C*$H_2$Ph), 74.8 (O*C*$H_2$Ph), 74.7 (O*C*$H_2$Ph), 74.9 (C-$5^{b/d}$), 75.2 (C-$2^{b/d/f}$), 76.0 (C-$3^{f}$), 76.9 (C-$4^{a/c/e}$), 77.2 (C-$4^{b/d}$), 77.4 (C-$4^{b/d}$), 77.6 (C-$5^{f}$), 78.8 (C-$3^{a/c/e}$), 79.0 (C-$3^{a/c/e}$), 80.1, 80.1, 80.1 x2 (C-$3^{b/d/f}$ x2, C-$4^{a/c/e}$ x2), 81.1 (C-$3^{a/c/e}$), 92.4 ($CCl_3$), 92.6 ($CCl_3$), 92.7 ($CCl_3$), 99.8 (C-$1^{b/d/f}$), 99.9 (C-$1^{b/d/f}$), 100.0 (C-$1^{c/e}$), 100.0 (C-$1^{c/e}$), 100.4 (C-$1^{b/d/f)}$, 100.8 (C-$^{1a}$), 100.9 (*C*HPh), 101.1 (*C*HPh), 101.4 (*C*HPh), 126.1-130.3 ($CH_{arom}$), 133.5, 133.6, 133.6, 134.9, 135.0, 135.1, 137.4, 137.5 x2, 138.0, 138.3, 138.5 ($C_q$ CHPh x3, $C_q$ OBn x3, $C_q$ Bz x3, $C_q$ COOBn x3), 161.7, 162.0, 162.4, 165.1, 165.6, 165.7, 169.0, 169.3, 169.3 (C=O TCA x3, C=O COOBn x3, C=O Bz x3); HRMS $[M + Na]^+$: m/z: calcd for $C_{127}H_{118}Cl_9N_3NaO_{37}$ 2620.4513, found 2620.4595.

**Methyl *O*-(benzyl 2-*O*-benzoyl-3-*O*-benzyl-4-*O*-*tert*-butyldimethylsilyl-*β*-D-glucopyranosyluronate)-(1→3)-*O*-(4,6-*O*-benzylidene-2-deoxy-2-trichloroacetamido-*β*-D -glucopyranosyl)-(1→4)-*O*-(benzyl 2-*O*-benzoyl-3-*O*-benzyl-*β*-D-glucopyranosyluronate) -(1→3)-*O*-(4,6-*O*-benzylidene-2-deoxy-2-trichloroacetamido-*β*-D-glucopyranosyl)-(1→4)-*O*-(benzyl 2-*O*-benzoyl-3-*O*-benzyl-*β*-D-glucopyranosyluronate)-(1→3)-*O*-(4,6-*O*- benzylidene-2-deoxy-2-trichloroacetamido-*β*-D-glucopyranosyl)-(1→4)-*O*-(benzyl 2-*O*- benzoyl-3-*O*-benzyl -*β*-D-glucopyranosyluronate)-(1→3)-*O*-(4,6-*O*-benzylidene-2-deoxy-2-trichloroacetamido-*β*-D-glucopyranosyl)-(1→4)-*O*-(benzyl 2-*O*-benzoyl-3-*O*-benzyl -*β*-D-**

**glucopyranosyluronate)-(1→3)-4,6-*O*-benzylidene-2-deoxy-2-trichloroacetamido-*β*-D-glucopyranoside (10):** After a mixture of donor **25** (33.4 mg, 17.1 μmol), acceptor **28** (25.0 mg, 9.62 μmol) and MS-AW-300 (200 mg) in a mixture solvent of DCM and MeCN (v/v 19:1, 2.00 ml) was stirred at -78 °C for 1 hr, AgOTf (51.4 mg, 20.0 μmol) in $Et_2O$ (0.7 00 ml) was added. When the temperature of the reaction mixture reduces to -78 °C, *p*-TolSCl (17.1 μmol, 2.50 μl) was added via a micro-syringe. After 5 min, when the yellowish color disappeared, TMSOTf (1.25 μl, 6.90 μmol) was added via micro-syringe. The reaction mixture was warmed to −10 °C under stirring in 2 hrs, followed by the same workup and purification procedures described above for the synthesis of compound **19**. Compound **10** (32.6 mg, 7.37 μmol, 76.6%) was afforded as white solid. $[\alpha]_D^{20}$ -2.7 ° (*c* 0.5, DCM); $^1$H NMR (500 MHz, $CDCl_3$): δ = $^1$H NMR (500 MHz, $CDCl_3$): δ = -0.14 (s, 3 H, Si*CH*$_3$), -0.10 (s, 3 H, Si*CH*$_3$), 0.79 (s, 9 H, SiC(*CH*$_3$)$_3$), 3.01 (dd, 1 H, *J* = 5.0 Hz, 9.0 Hz, H-5 $^{a/c/e/g/i}$), 3.03 (dd, 1 H, *J* = 5.0 Hz, 9.0 Hz, H-5 $^{a/c/e/g/i}$), 3.05 (dd, 1 H, *J* = 5.0 Hz, 9.0 Hz, H-5 $^{a/c/e/g/i}$), 3.12-3.22 (m, 5 H, H-5 $^{a/c/e/g/i}$, H-6 $^{a/c/e/g/i}$ x4), 3.42-3.48 (m, 3 H, H-2 $^{a/c/e/g/i}$, H-5 $^{a/c/e/g/i}$, H-6$^{a/c/e/g/i}$), 3.50 (s, 3 H, $OCH_3$), 3.53 (dd, 1 H, *J* = 7.0 Hz, 7.5 Hz), 3.55 (dd, 1 H, *J* = 6.0 Hz, 7.0 Hz), 3.56 (dd, 1 H, *J* = 5.5 Hz, 6.0 Hz), 3.60 (dd, 2 H, *J* = 8.5 Hz, 10.0 Hz), 3.66 (dd, 1 H, *J* = 6.5 Hz, 8.5 Hz), 3.67 (t, 2 H, *J* = 8.0 Hz), 3.68 (dd, 2 H, *J* = 8.5 Hz, 9.0 Hz) (H-4 $^{a/c/e/g/i}$, H-3 $^{a/c/e/g/i}$ x4, H-3 $^{b/d/f/h/j}$ x5), 3.72-3.78 (m, 4 H, H-2 $^{a/c/e/g/i}$ x4), 3.80 (dd, 2 H, *J* = 9.0 Hz, 9.5 Hz, H-4$^{b/d/f/h/j}$ x2), 3.81 (dd, 2 H, *J* = 9.0 Hz, 9.5 Hz, H-4$^{b/d/f/h/j}$ x2), 3.85 (d, 1 H, *J* = 6.5 Hz, H-5$^{b/d/f/h/j}$), 3.86 (d, 1 H, *J* = 7.0 Hz,

H-5$^{b/d/f/h/j}$), 3.88 (d, 2 H, *J* = 9.0 Hz, H-5$^{b/d/f/h/j}$ x2), 3.90 (d, 1 H, *J* = 8.5 Hz, H-5$^{b/d/f/h/j}$), 4.01-4.06 (m, 4 H, H-6 $^{a/c/e/g/i}$ x4), 4.14 (t, 1 H, *J* = 7.0 Hz, H-4$^{b/d/f/h/j}$), 4.16 (t, 1 H, *J* = 7.0 Hz, H-4$^{b/d/f/h/j}$), 4.18 (t, 1 H, *J* = 8.5 Hz, H-4$^{b/d/f/h/j}$), 4.24 (dd, 1 H, *J* = 8.5 Hz, 9.0 Hz, H-4$^{b/d/f/h/j}$), 4.25 (dd, 1 H, *J* = 8.5 Hz, 9.0 Hz, H-4$^{b/d/f/h/j}$), 4.28 (dd, 1 H, *J* = 5.0 Hz, 10.5 Hz, H-6 $^{a/c/e/g/i}$), 4.48 (dd, 1 H, *J* = 9.0 Hz, 9.5 Hz, H-3 $^{a/c/e/g/i}$), 4.53 (d, 1 H, *J* = 8.0 Hz, H-1 $^{a/c/e/g/i}$), 4.56 (d, 1 H, *J* = 11.5 Hz, -C*H*$_2$Ph ), 4.56 (d, 1 H, *J* = 11.5 Hz, -C*H*$_2$Ph ), 4.56 (d, 1 H, *J* = 8.5 Hz, H-1 $^{a/c/e/g/i}$), 4.57 (d, 1 H, *J* = 11.5 Hz, -C*H*$_2$Ph ), 4.62 (d, 1 H, *J* = 11.5 Hz, -C*H*$_2$Ph ), 4.63 (d, 1 H, *J* = 8.0 Hz, H-1 $^{a/c/e/g/i}$), 4.63 (d, 1 H, *J* = 11.5 Hz, -C*H*$_2$Ph ), 4.69 (d, 1 H, *J* = 11.5 Hz, -C*H*$_2$Ph), 4.75 (d, 1 H, *J* = 8.0 Hz, H-1 $^{a/c/e/g/i}$), 4.76 (d, 1 H, *J* = 11.5 Hz, -C*H*$_2$Ph ), 4.79 (d, 1 H, *J* = 11.5 Hz, -C*H*$_2$Ph x3 ), 4.83 (d, 1 H, *J* = 8.0 Hz, H-1 $^{a/c/e/g/i}$), 4.91 (t, 2 H, *J* = 6.0 Hz, H-2$^{b/d/f/h/j}$ x2), 4.95 (d, 1 H, *J* = 6.0 Hz, H-1$^{b/d/f/h/j}$), 4.96 (d, 1 H, *J* = 6.0 Hz, H-1$^{b/d/f/h/j}$), 5.00 (d, 1 H, *J* = 7.0 Hz, H-1$^{b/d/f/h/j}$), 4.98 (d, 1 H, *J* = 11.0 Hz, -COOC*H*$_2$Ph), 5.00 (d, 1 H, *J* = 12.0 Hz, -COOC*H*$_2$Ph), 5.02 (d, 1 H, *J* = 11.5 Hz, -COOC*H*$_2$Ph x2), 5.06 (d, 1 H, *J* = 8.0 Hz, H-1$^{b/d/f/h/j}$), 5.06 (d, 1 H, *J* = 8.0 Hz, H-1$^{b/d/f/h/j}$), 5.06 (d, 1 H, *J* = 12.0 Hz, -COOC*H*$_2$Ph), 5.09 (dd, 1 H, *J* = 8.0 Hz, 9.0 Hz, H-2$^{b/d/f/h/j}$), 5.12 (d, 1 H, *J* = 11.5 Hz, -COOC*H*$_2$Ph ), 5.13 (s, 3 H, C*H*Ph x3), 5.15 (d, 1 H, *J* = 11.5 Hz, -COOC*H*$_2$Ph), 5.15 (dd, 1 H, *J* = 8.0 Hz, 9.0 Hz, H-2$^{b/d/f/h/j}$), 5.19 (d, 1 H, *J* = 12.0 Hz, -COOC*H*$_2$Ph ), 5.19 (s, 1 H, C*H*Ph ), 5.20 (d, 1 H, *J* = 11.0 Hz, -COOC*H*$_2$Ph ), 5.21 (d, 1 H, *J* = 12.0 Hz, -COOC*H*$_2$Ph ), 5.21 (dd, 1 H, *J* = 7.0 Hz, 8.5 Hz, H-2$^{b/d/f/h/j}$), 5.31 (s, 1H, C*H*Ph), 6.50 (d, 1 H, *J* = 9.0 Hz, NH), 6.55 (d, 2 H, *J* = 8.0 Hz, NH x2), 6.64 (d, 1 H, *J* = 9.0 Hz, NH), 7.02 (d, 1 H, *J* = 7.5 Hz, NH), 7.10-7.58 (m, 90

H, $CH_{arom}$), 7.90-7.95 (m, 10 H, $CH_{arom}$ Bz); $^{13}C$ NMR (125 MHz, $CDCl_3$): δ = -5.0 (Si*C*$H_3$), -4.2 (Si*C*$H_3$), 18.1 (Si*C*($C_3$)$_3$), 26.0 (x3, SiC(*C*$H_3$)$_3$), 57.1, 57.1 (x2) (C-$2^{a/c/e/g/i}$ x3), 57.8 (C-$2^{a/c/e/g/i}$), 57.8 ($OCH_3$), 58.7 (C-$2^{a/c/e/g/i}$), 66.4, 66.3 (x2), 66.3 (x2) (C-$5^{a/c/e/g/i}$ x5), 67.4 (COO*C*$H_2$Ph ), 68.1 (x5, COO*C*$H_2$Ph x4, C-$6^{a/c/e/g/i}$), 68.4 (x2, C-$6^{a/c/e/g/i}$ x2), 68.6 (C-$6^{a/c/e/g/i}$), 68.7 (C-$6^{a/c/e/g/i}$), 71.4 (C-$4^{j}$), `73.7 (O*C*$H_2$Ph), 74.3 (C-$2^{b/d/f/h/j}$), 74.6 (C-$2^{b/d/f/h/j}$), 74.7 (O*C*$H_2$Ph), 74.8 (x7), 74.9 (O*C*$H_2$Ph x3, C-$5^{b/d/f/h/j}$ x5), 75.0 (C-$2^{b/d/f/h/j}$), 75.0 (C-$2^{b/d/f/h/j}$), 75.2 (C-$2^{b/d/f/h/j}$), 76.0 (C-$3^{a/c/e/g/i}$), 77.8, 77.6, 77.4 (x2) (C-$4^{b/d/f/h}$ x4), 77.1 (x3), 76.9 (C-$4^{a/c/e/g/i}$ x4), 81.4, 83.3, 80.1 (x4), 79.0, 79.0 (x2), 78.8 (C-$3^{b/d/f/h/j}$ x5, C-$3^{a/c/e/g/i}$ x4, C-$4^{a/c/e/g/i}$), 92.4, 92.6, 92.7, 92.8 (x2) ($CCl_3$ x5), 99.3 (C-$1^{b/d/f/h/j}$), 100.0 (C-$1^{a/c/e/g/i}$), 100.0 (C-$1^{a/c/e/g/i}$), 100.2 (C-$1^{b/d/f/h/j}$), 100.3 (C-$1^{a/c/e/g/i}$ x2), 100.3 (C-$1^{b/d/f/h/j}$ x3), 100.8 (C-$1^{a/c/e/g/i}$), 100.9 (*C*HPh), 100.9 (*C*HPh x2), 101.1 (*C*HPh), 101.7 (*C*HPh), 126.2-130.2 ($CH_{arom}$), 133.5, 133.5 (x2), 133.5, 133.6, 135.0 (x2), 135.0 (x2), 135.4, 137.4, 137.5 (x2), 137.5, 137.5, 138.0, 138.3, 138.5 (x2), 138.5 ($C_q$ CHPh x5, $C_q$ OBn x5, $C_q$ Bz x5, $C_q$ COOBn x5), 161.6, 161.9 (x2), 162.0, 162.3, 165.3, 165.6, 165.6, 165.7, 165.6, 168.6, 169.1 (x2), 169.3, 169.4 (C=O TCA x5, C=O COOBn x5, C=O Bz x5); MALDI $[M + Na]^+$: m/z: calcd for $C_{217}H_{208}Cl_{15}N_5NaO_{61}Si$ 4442.85, found 4443.15.

**Methyl *O*-(*β*-D-glucopyranosyluronic acid)-(1→3)-*O*-(2-*N*-acetyl-2-deoxy-*β*-D-glucopyranosyl)-(1→4)-*O*-(*β*-D-glucopyranosyluronic acid)-(1→3)-*O*-(2-*N*-acetyl-2-deoxy-*β*-D-glucopyranosyl)-(1→4)-*O*-(*β*-D-glucopyranosyluronic acid)-(1→3)-*O*-(2-*N*- acetyl-2-deoxy-*β*-D-glucopyranosyl)-(1→4)-*O*-(*β*-D-glucopyranosyluronic**

**acid)-(1→3)-*O*-(2-*N*-acetyl-2-deoxy-*β*-D-glucopyranosyl)-(1→4)-*O*-(*β*-D-glucopyransyluronic acid)-(1→3)-2-*N*-acetyl-2-deoxy-*β*-D-glucopyranoside (9): 10** was converted to **29** following the general procedure for TBS removal as described before (79%). Compound **29** (44.0 mg, 10.0 μmol) was dissolved in THF (2 ml). 0.2 M KOH aqueous solution (1.00 ml, 200 μmol) was added in 10 portions during 2 days. The reaction mixture was stirred at r.t. during which the ratio of $H_2O$ to THF was gradually increased for a better solubility of the reaction mixture. Reaction was checked by comparisons of the crude $^1H$ NMR spectra which was taken by the end of each week. Reaction was stopped by the neutralization with 0.2 M AcOH in $H_2O$ by the end of the fifth week when peaks around 7.0 ppm in 1H-NMR of the crude NMR indicating NHTCA groups disappeared and peaks around 8.0 peaks for ortho-hydrogens on benzoyl groups changed from several equally height peaks into two main peaks. The solvent was completely removed by high vacuum rotary evaporator, and the crude residue was dissolved in anhydrous MeOH (3.00 ml) and cooled to 0°C. TEA (7.0 μl, 50 μmol) and acetic anhydride ($Ac_2O$) (118 μl, 1.25 mmol) were added, and the reaction mixture was stirred for two days under $N_2$ protection at r.t.. The reaction was stopped when TLC (AcOH/ DCM/ MeOH solvent systems) show one main product forms. The reaction mixture was concentrated and purified by silica gel chromatography (AcOH/ DCM/ MeOH solvent systems) to yield a mixture mainly composed of **31**. $Pd(OH)_2$ (50.0 mg) was added to a solution of the **31** in THF (0.5 ml), MeOH (0.7 ml) and AcOH (0.5 ml). The reaction flask was evacuated using a water aspirator and filled with hydrogen. This

process was repeated three times and the reaction mixture was stirred under hydrogen atmosphere for 3 days. The solution was filtered and concentrated, and the crude product was purified by Sephadex G-15 size exclusion chromatography to give the desired product **9** (6.60 mg, 3.50 μmol, 35% from **29** for 3 steps). $[\alpha]_D^{20}$ -27 ° (*c* 0.05, $H_2O$); $^1H$ NMR (500 MHz, $D_2O$): δ = 1.90-1.92 (m, 15 H, NHCO*CH*$_3$ x5), 3.20-3.26 (m, 5 H), 3.35-3.43 (m, 15 H), 3.45-3.48 (m, 5 H), 3.56-3.66 (m, 20 H), 3.70-3.82 (m, 10 H), 4.34 (d, 2 H, *J* = 8.5 Hz, anomeric H x2), 4.36 (d, 4 H, *J* = 7.0 Hz, anomeric H x4), 4.44 (d, 2 H, *J* = 8.5 Hz, anomeric H x2), 4.45 (d, 2 H, *J* = 7.5 Hz, anomeric H x2); HRMS $[M-3H]^{3-}$: m/z: calcd for $C_{71}H_{106}N_5O_{56}$ 641.5200, found 641.5198.

Appendix A

**NMR Data**

**Figure 3.3.** $^{1}$H-NMR of compound **9** (500 MHz, $D_2O$)

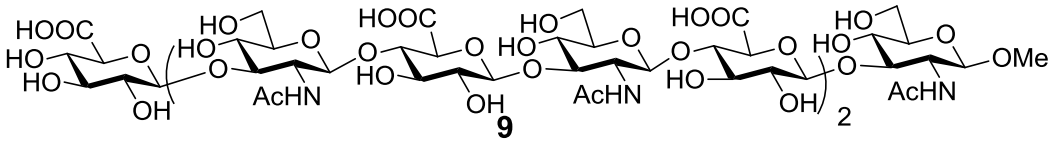


**9**

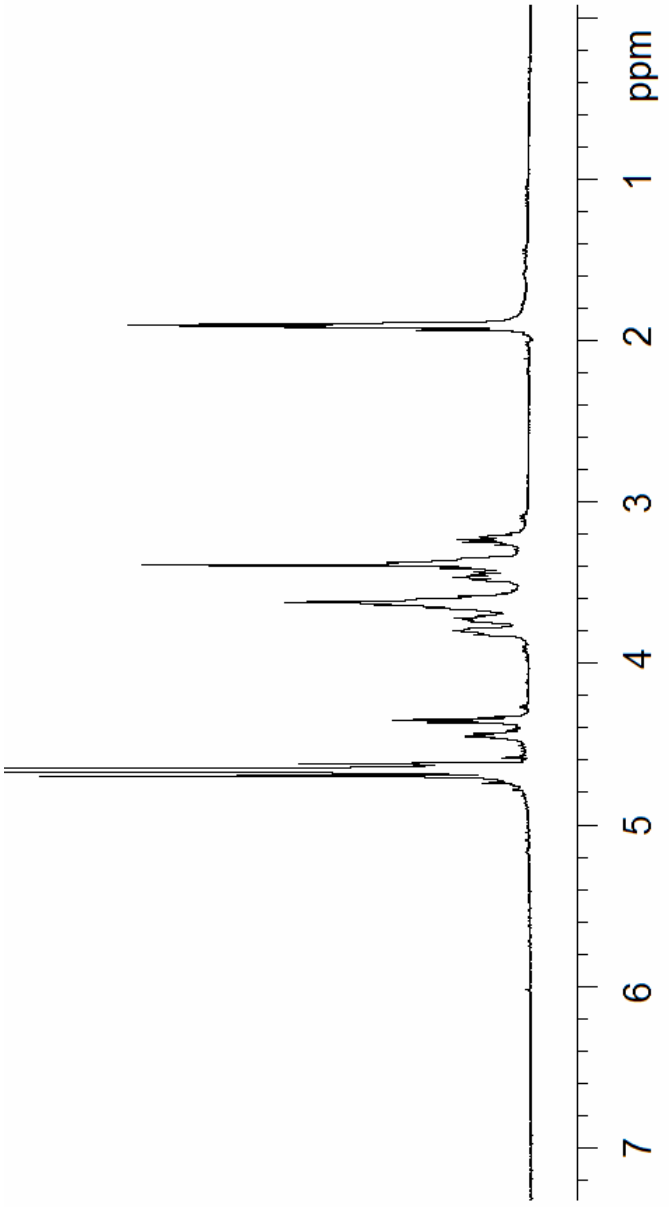

**Figure 3.4.** $^{1}$H-NMR of compound **10** (500 MHz, $CDCl_3$)

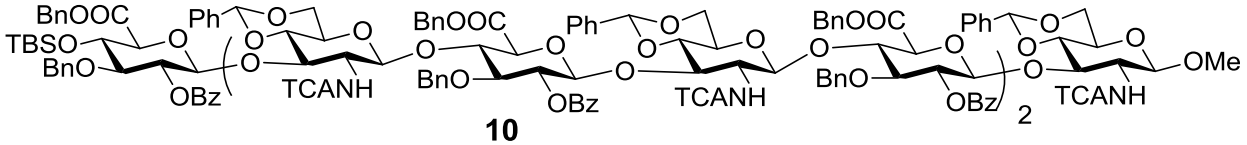


**10**

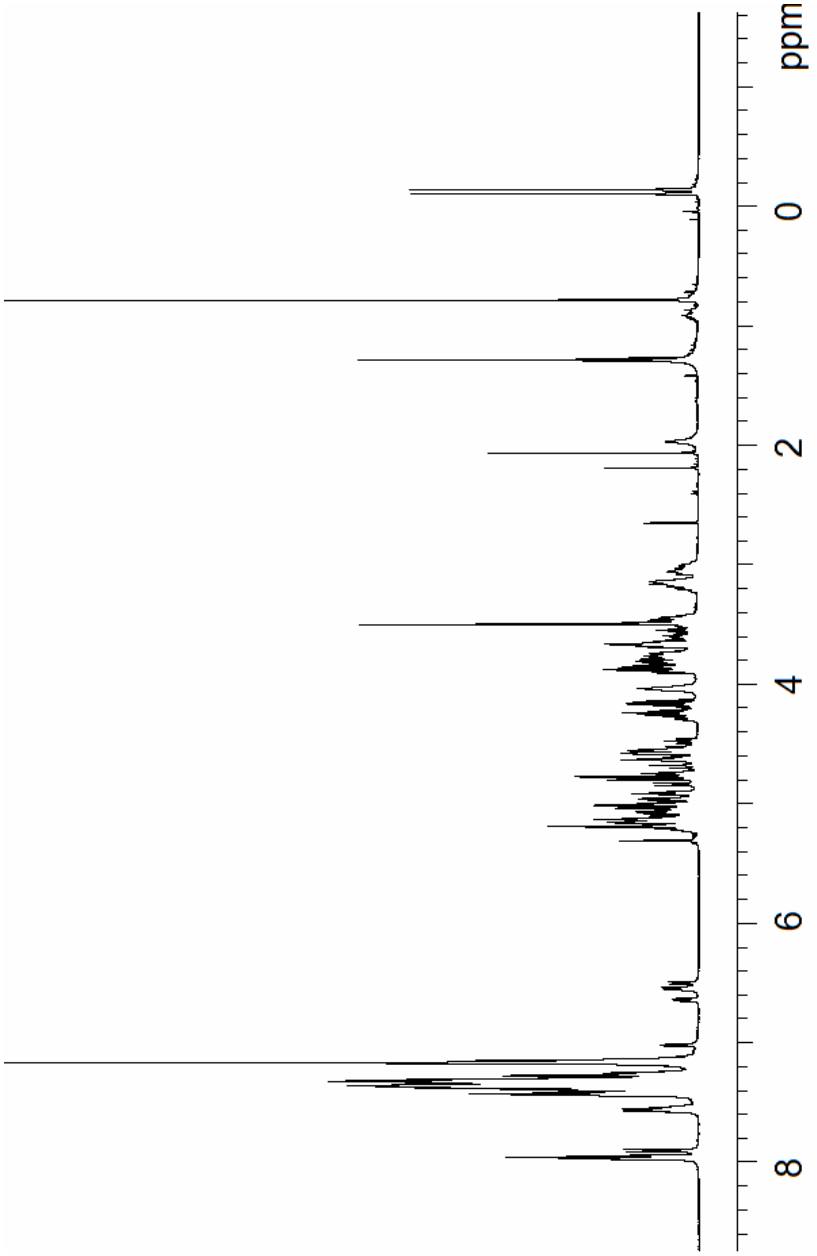

**Figure 3.5.** $^{13}$C-NMR of compound **10** (125 MHz, $CDCl_3$)

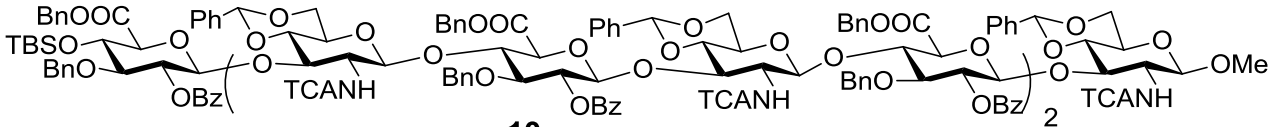


**10**

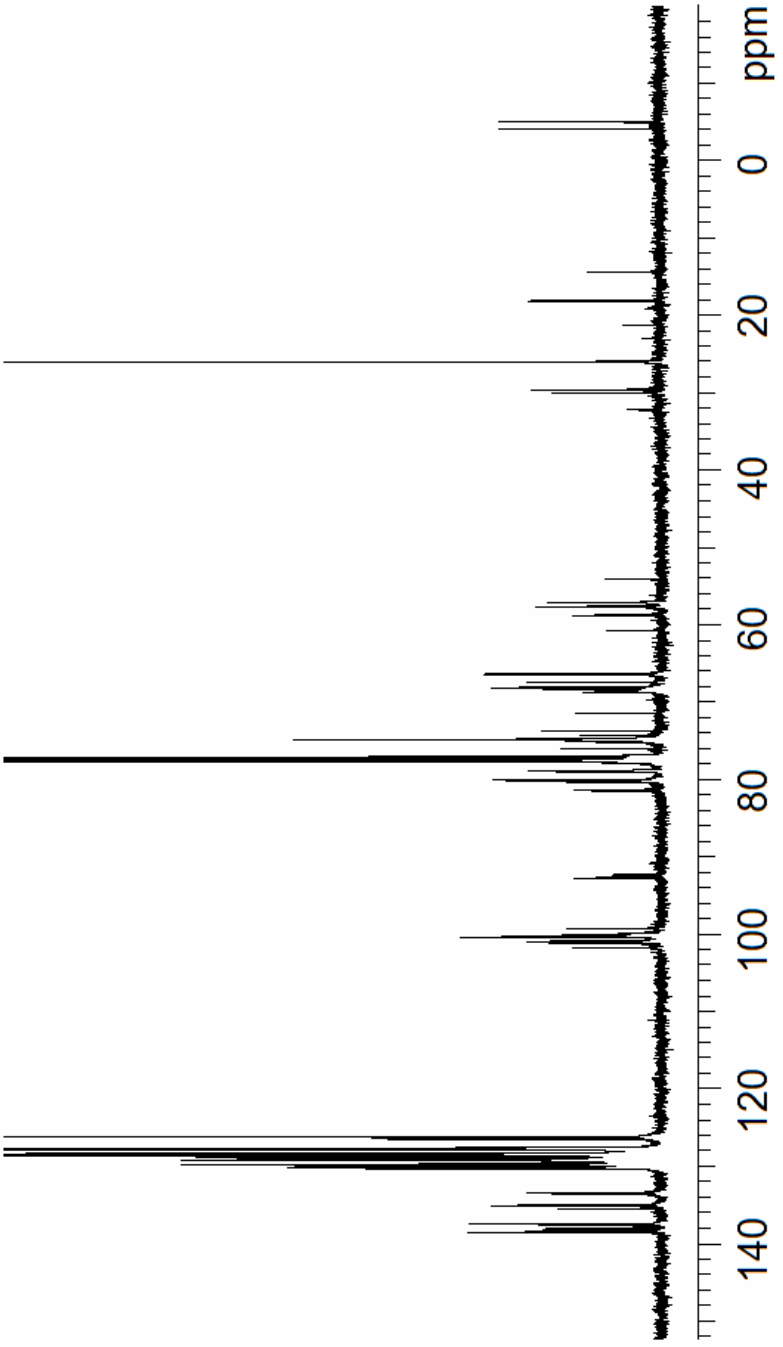

**Figure 3.6.** $^{1}H–^{1}H$ gCOSY of compound **10** (500 MHz, $CDCl_3$)

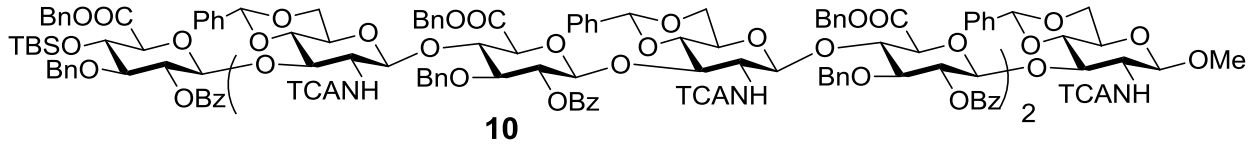


**10**

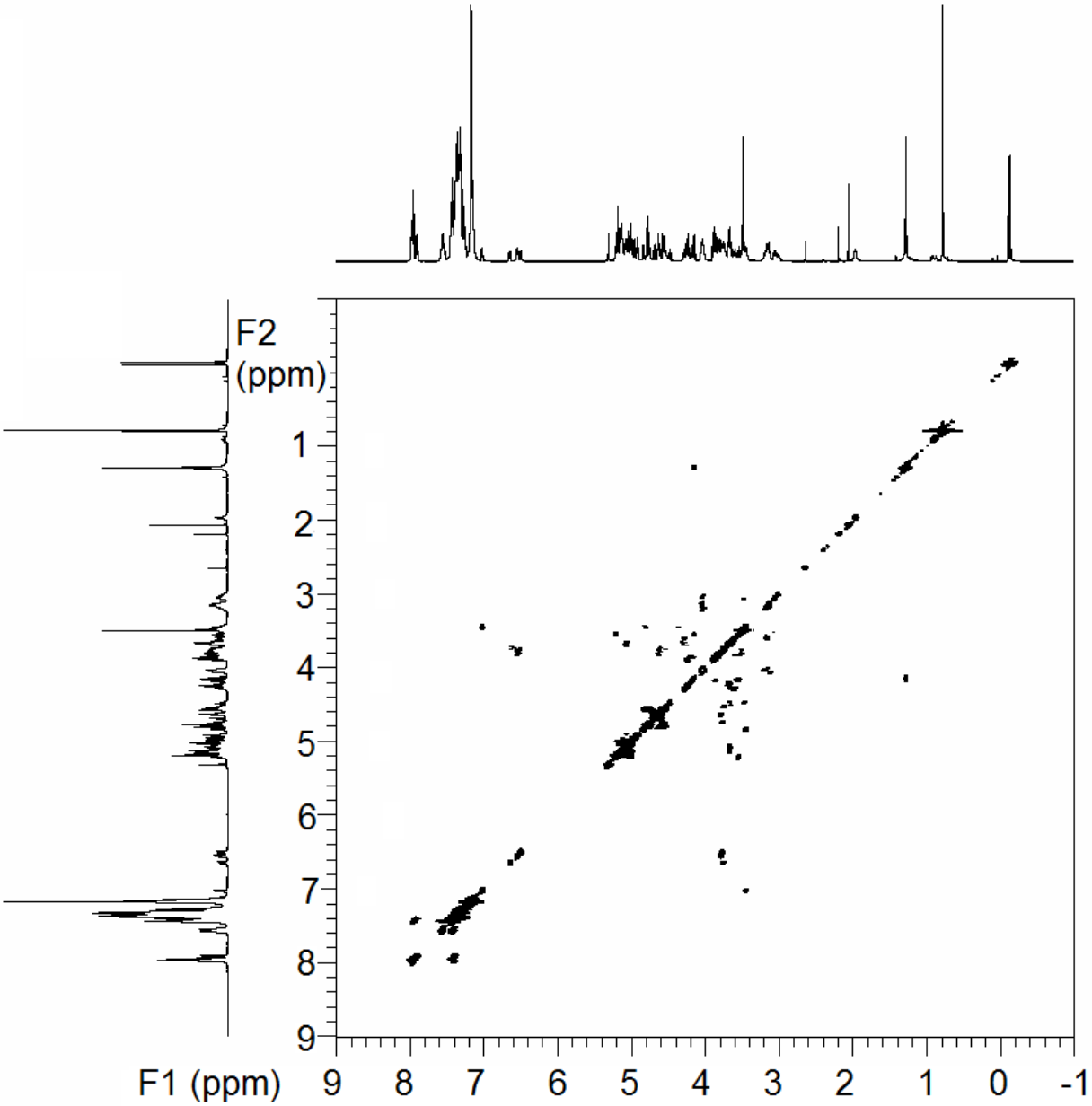

**Figure 3.7.** $^{1}H–^{13}C$ gHMQC of compound **10** (500 MHz, $CDCl_3$)

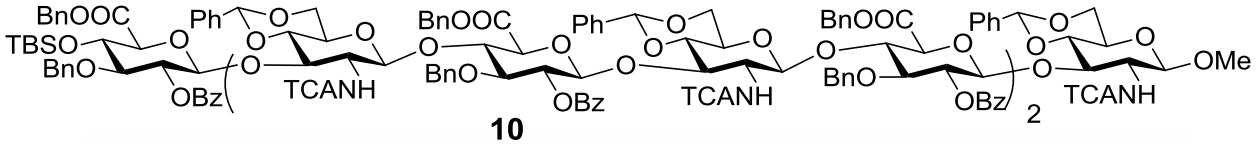


**10**

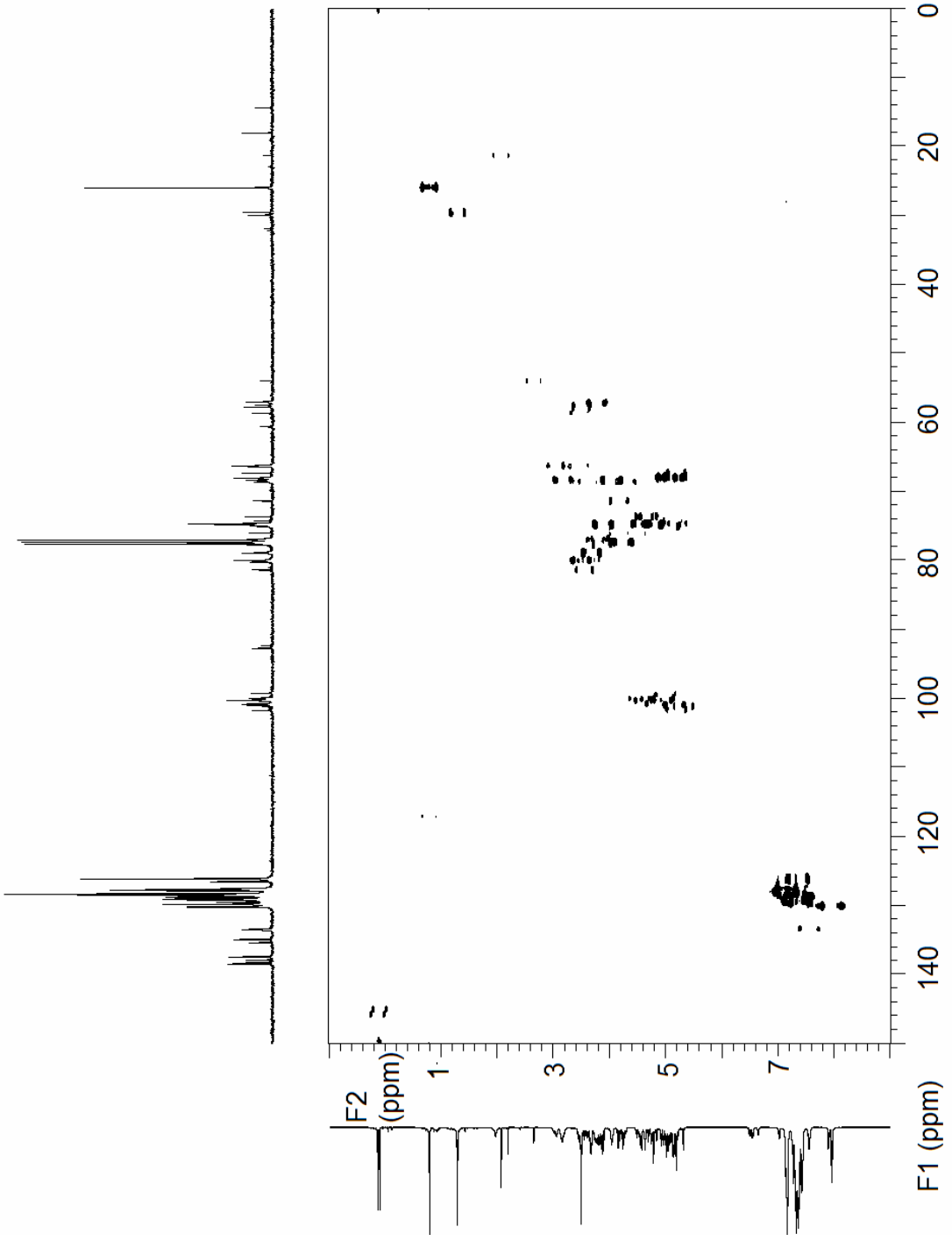

**Figure 3.8.** $^{1}H$–$^{13}C$ gHMQC (without $^{1}H$ decoupling) of compound **10** (500 MHz, $CDCl_3$)

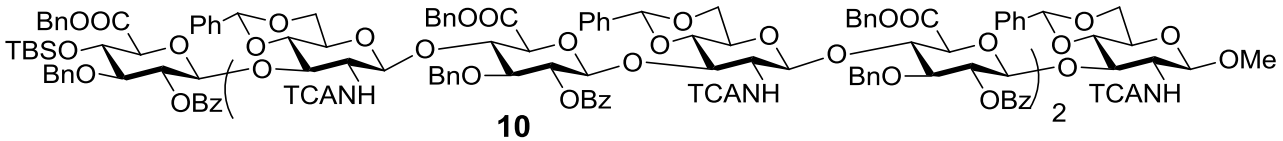


**10**

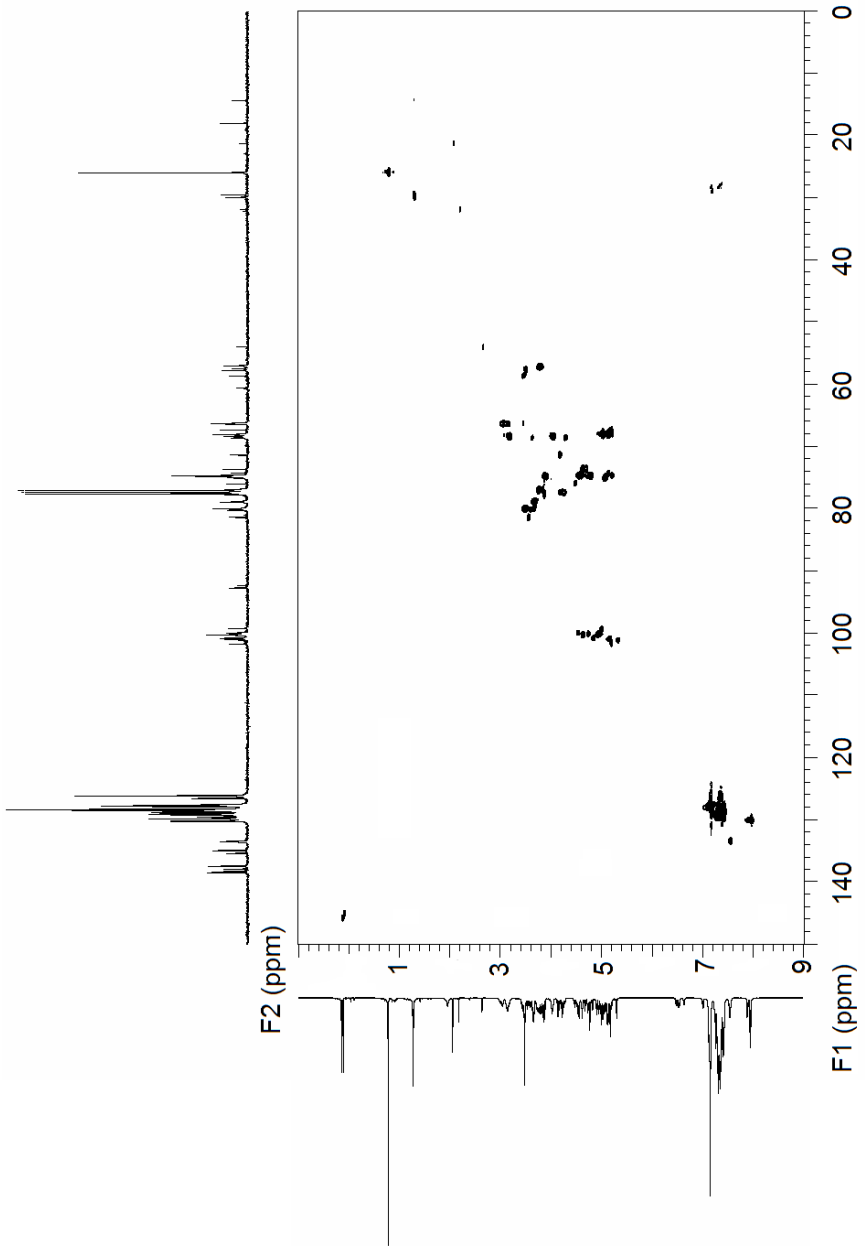

**Figure 3.9.** $^{1}H–^{13}C$ gHMBC of compound **10** (500 MHz, $CDCl_3$)

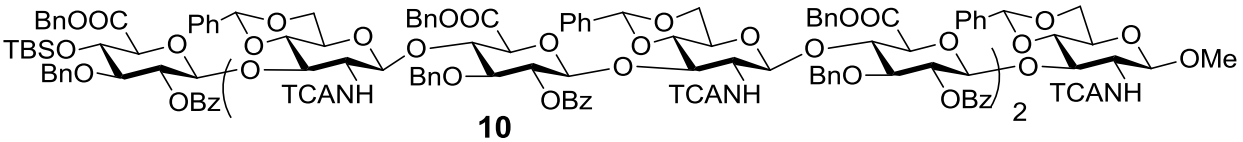


**10**

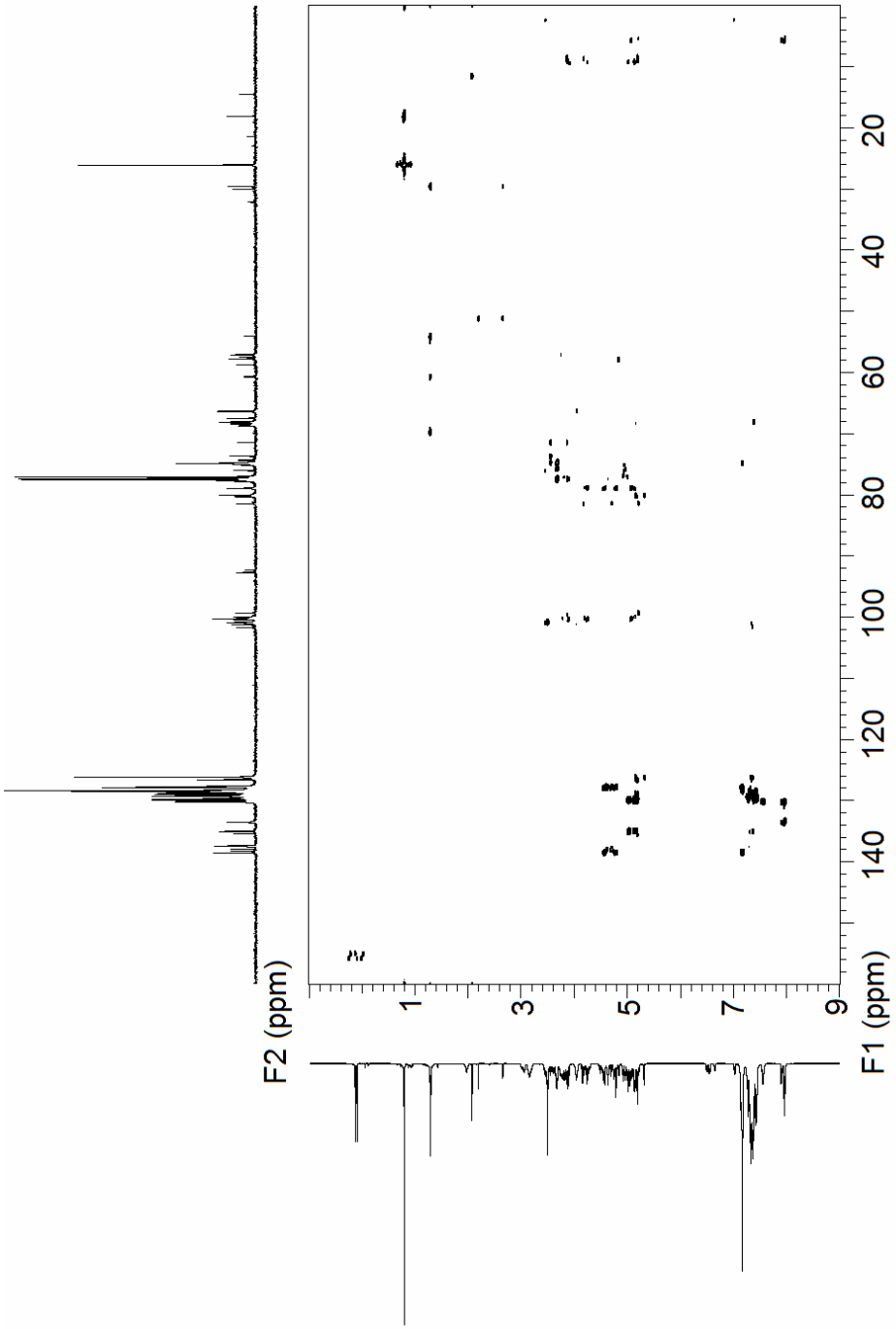

**Figure 3.10.** $^{1}$H-NMR of compound **19** (500 MHz, $CDCl_3$)

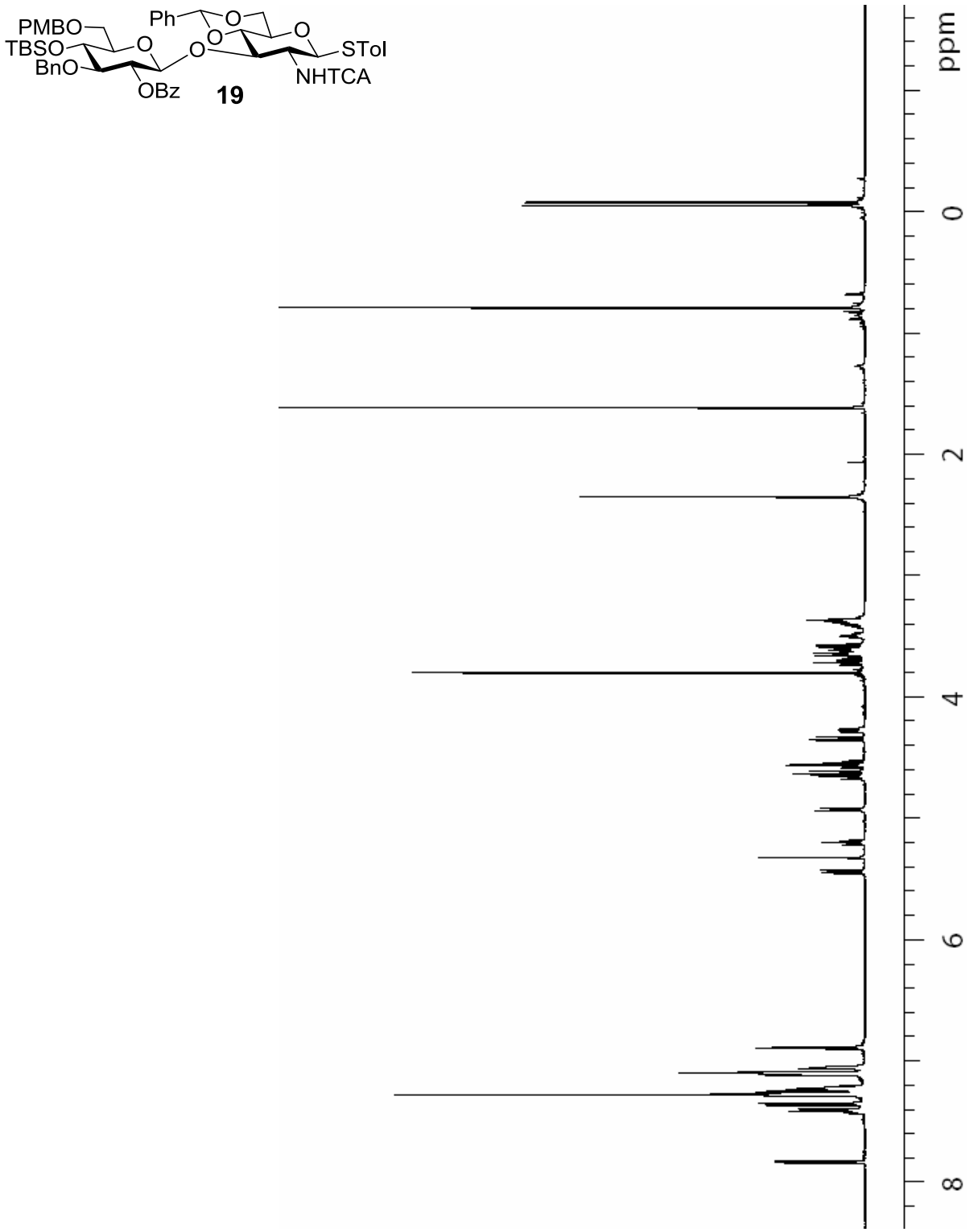

**Figure 3.11.** $^{13}$C-NMR of compound **19** (125 MHz, $CDCl_3$)

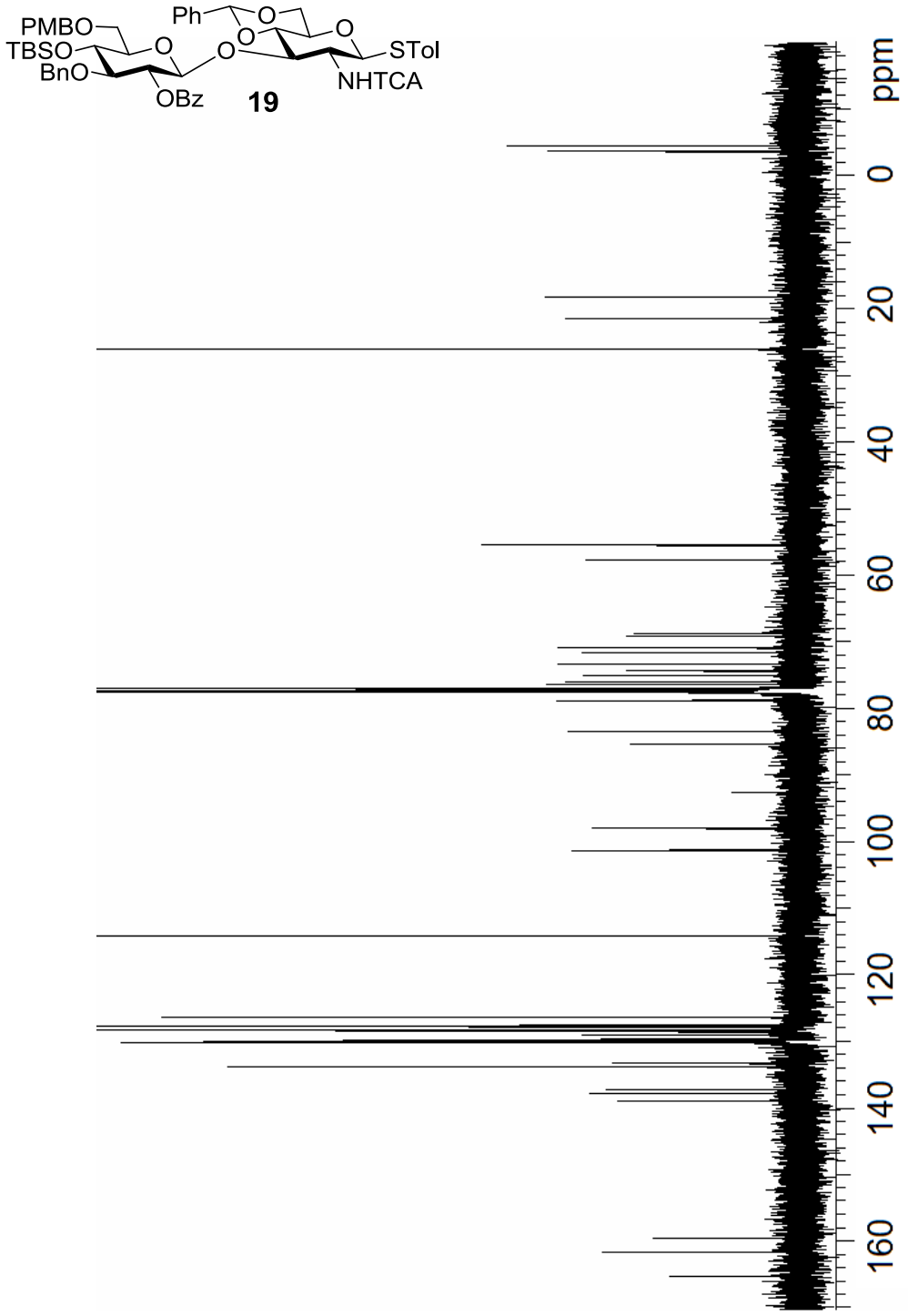

**Figure 3.12.** $^{1}H–^{1}H$ gCOSY of compound **19** (500 MHz, $CDCl_3$)

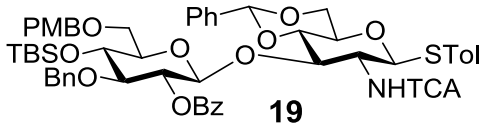


**19**

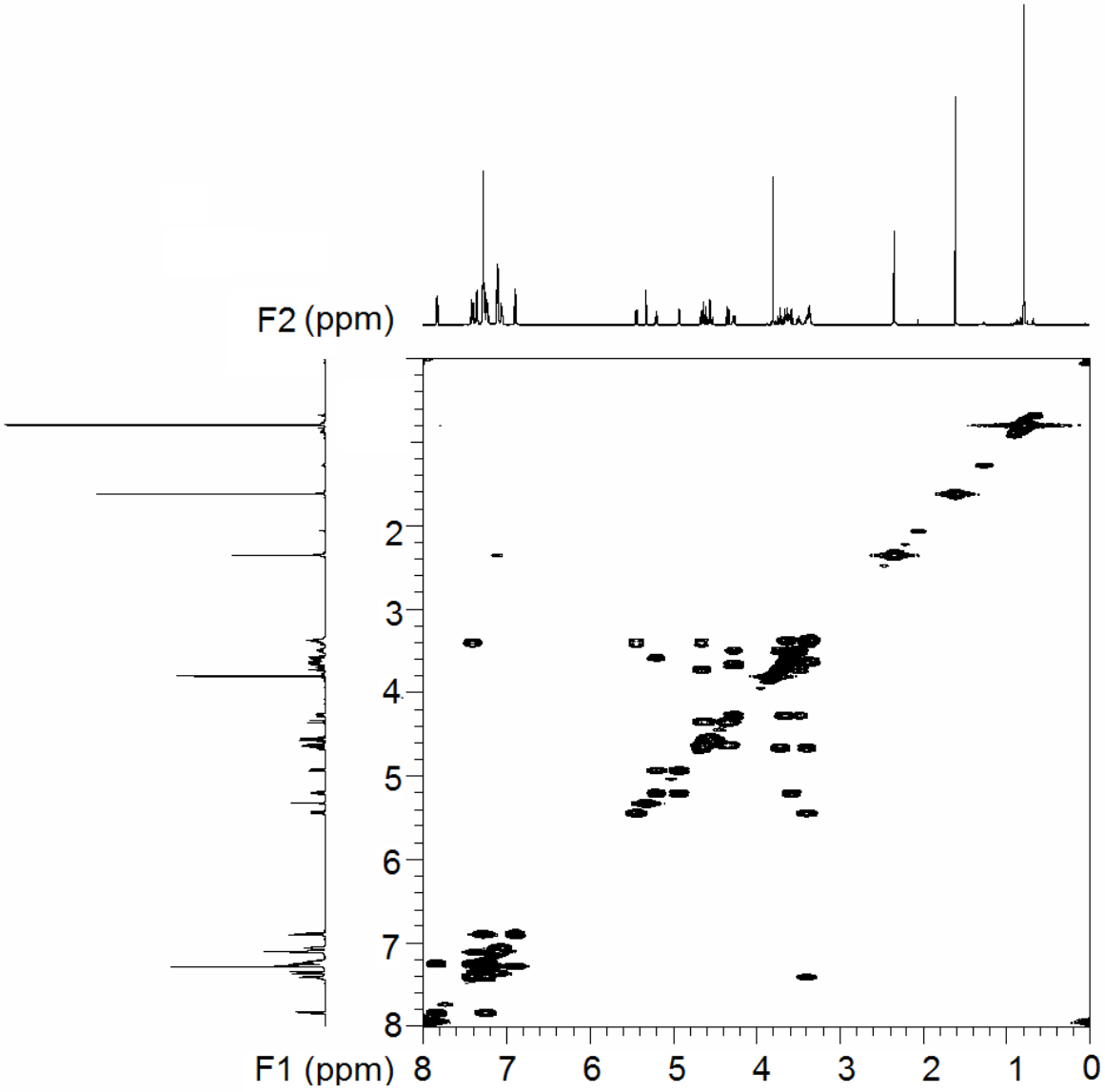

**Figure 3.13.** $^{1}H–^{13}C$ gHMQC of compound **19** (500 MHz, $CDCl_3$)

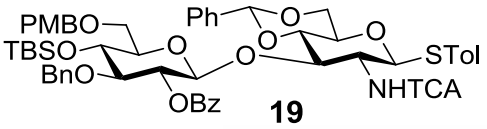


**19**

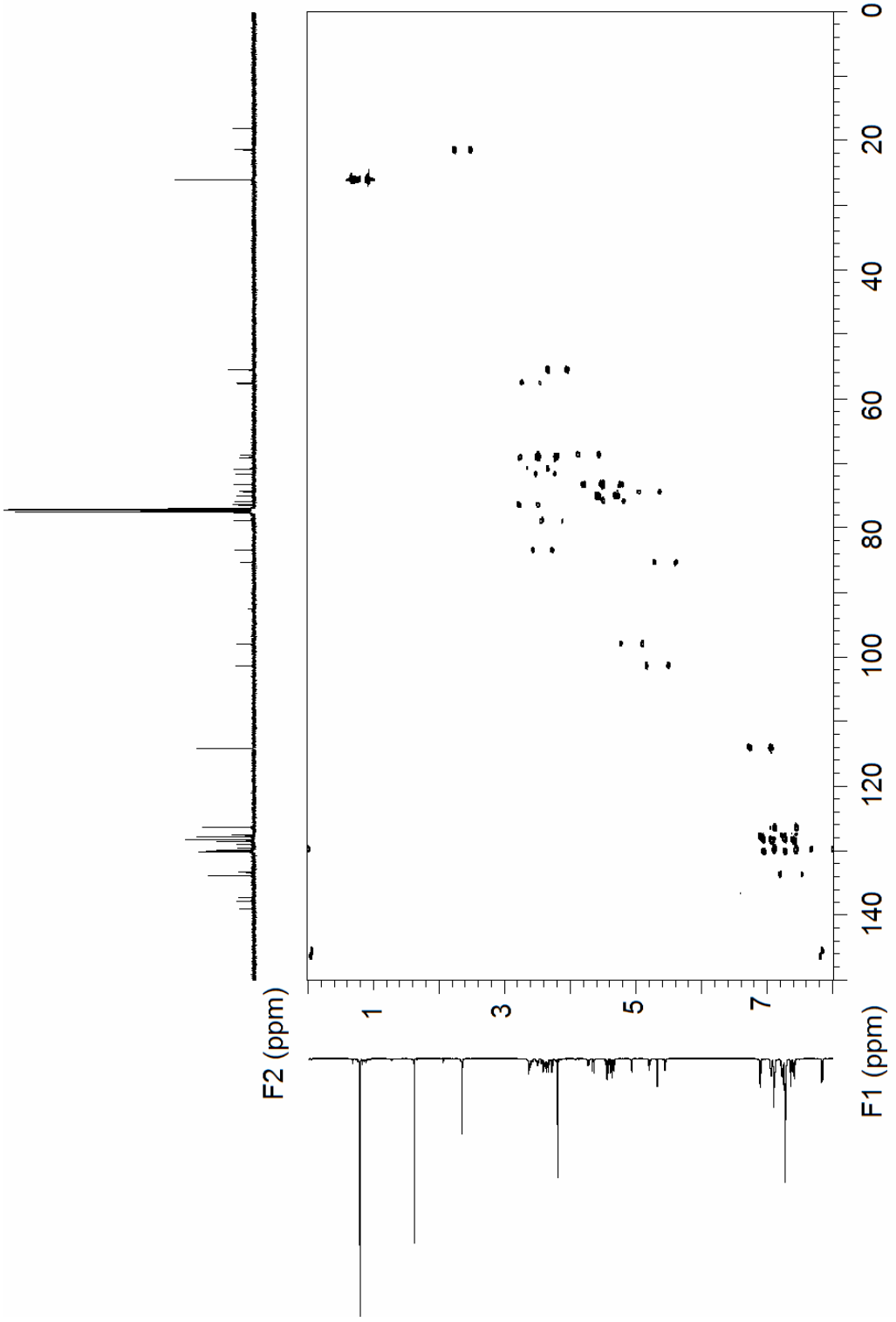

**Figure 3.14.** $^{1}H–^{13}C$ gHMQC (without $^{1}H$ decoupling) of compound **19** (500 MHz,$CDCl_3$)

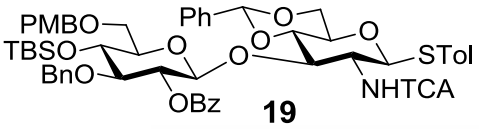


**19**

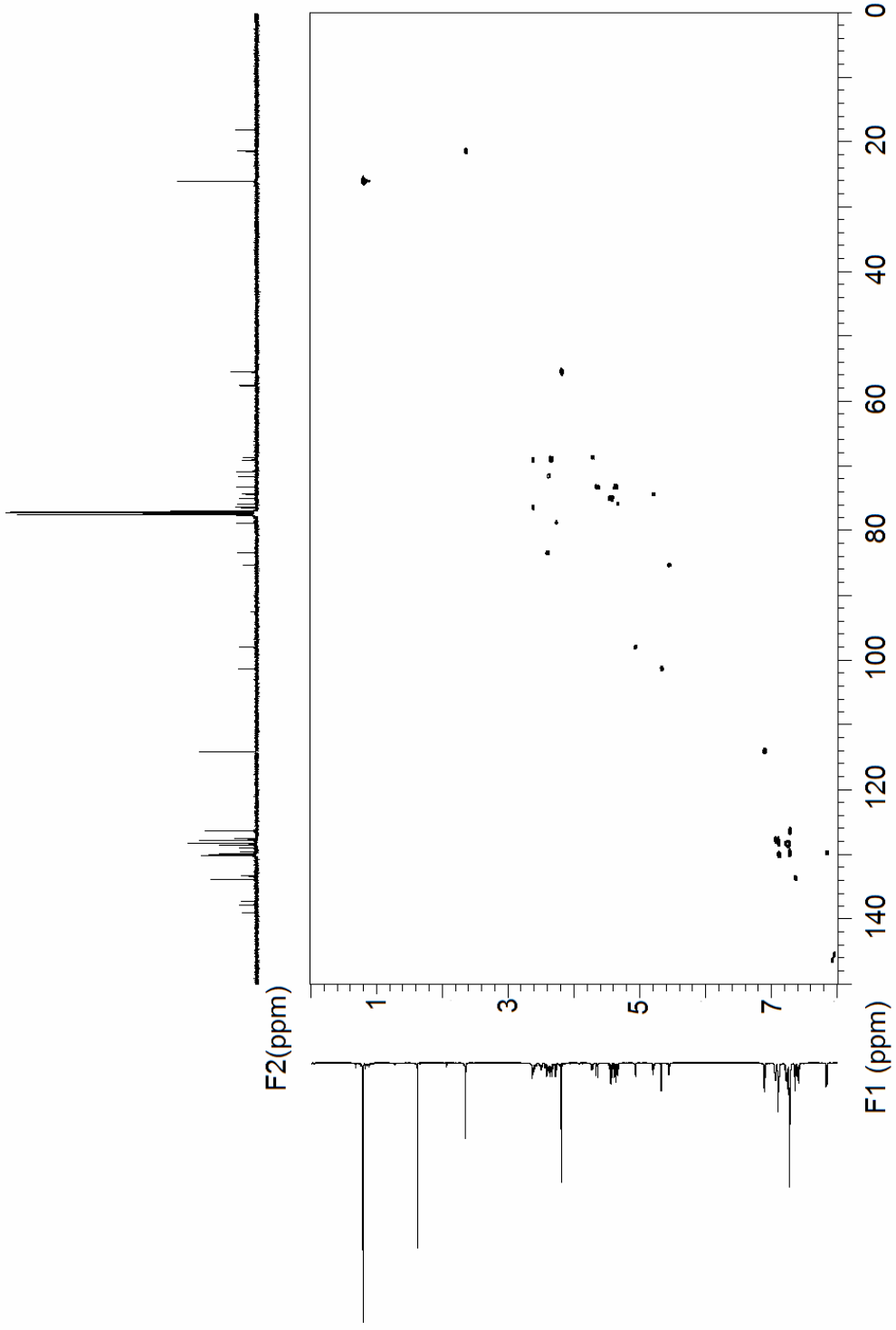

**Figure 3.15.** $^{1}H–^{13}C$ gHMBC of compound **19** (500 MHz, $CDCl_3$)

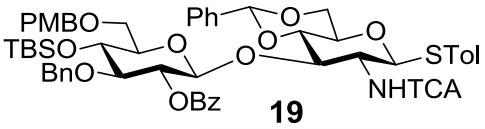


**19**

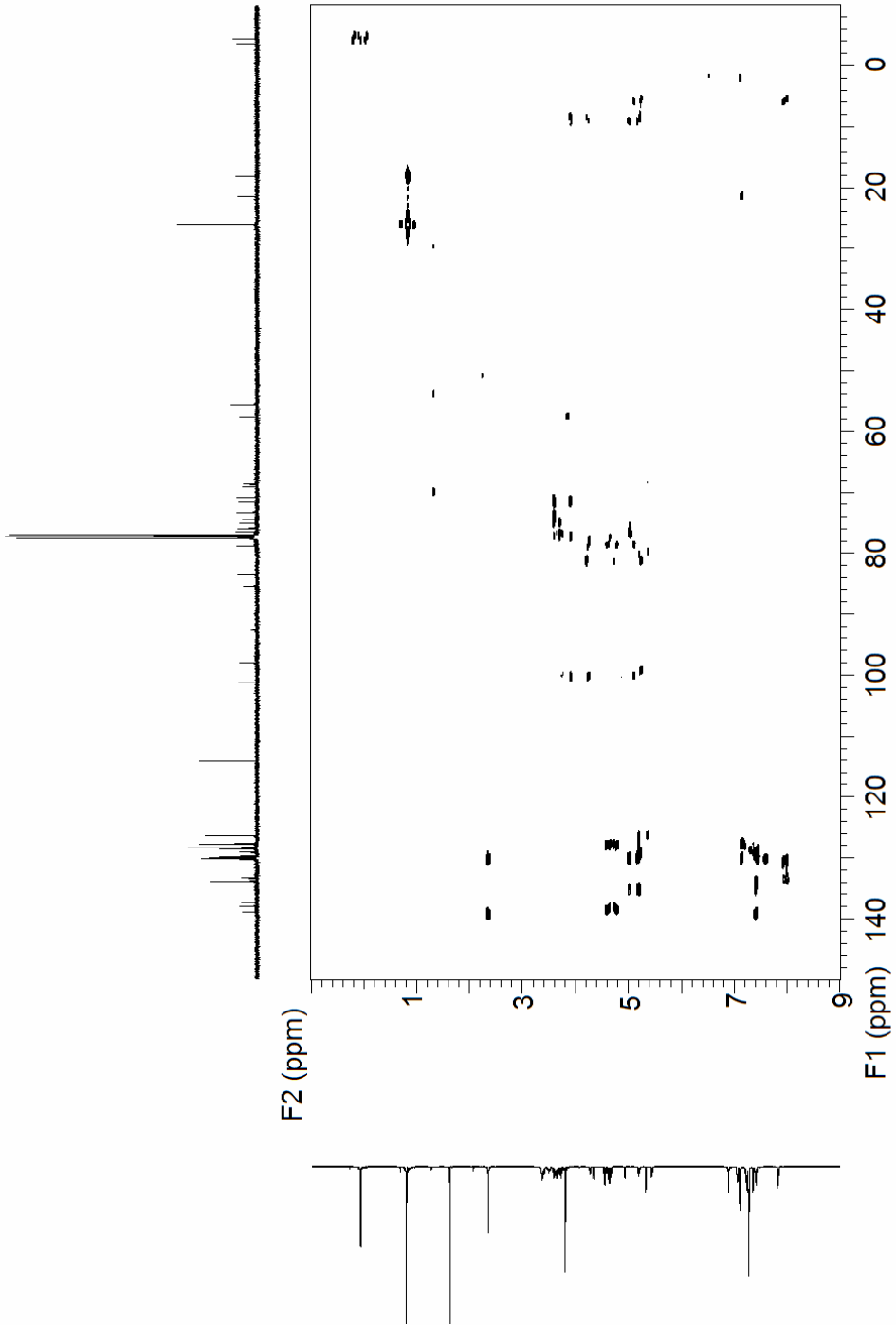

**Figure 3.16.** $^{1}$H-NMR of compound **11** (500 MHz, $CDCl_3$)

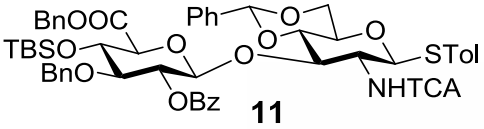


**11**

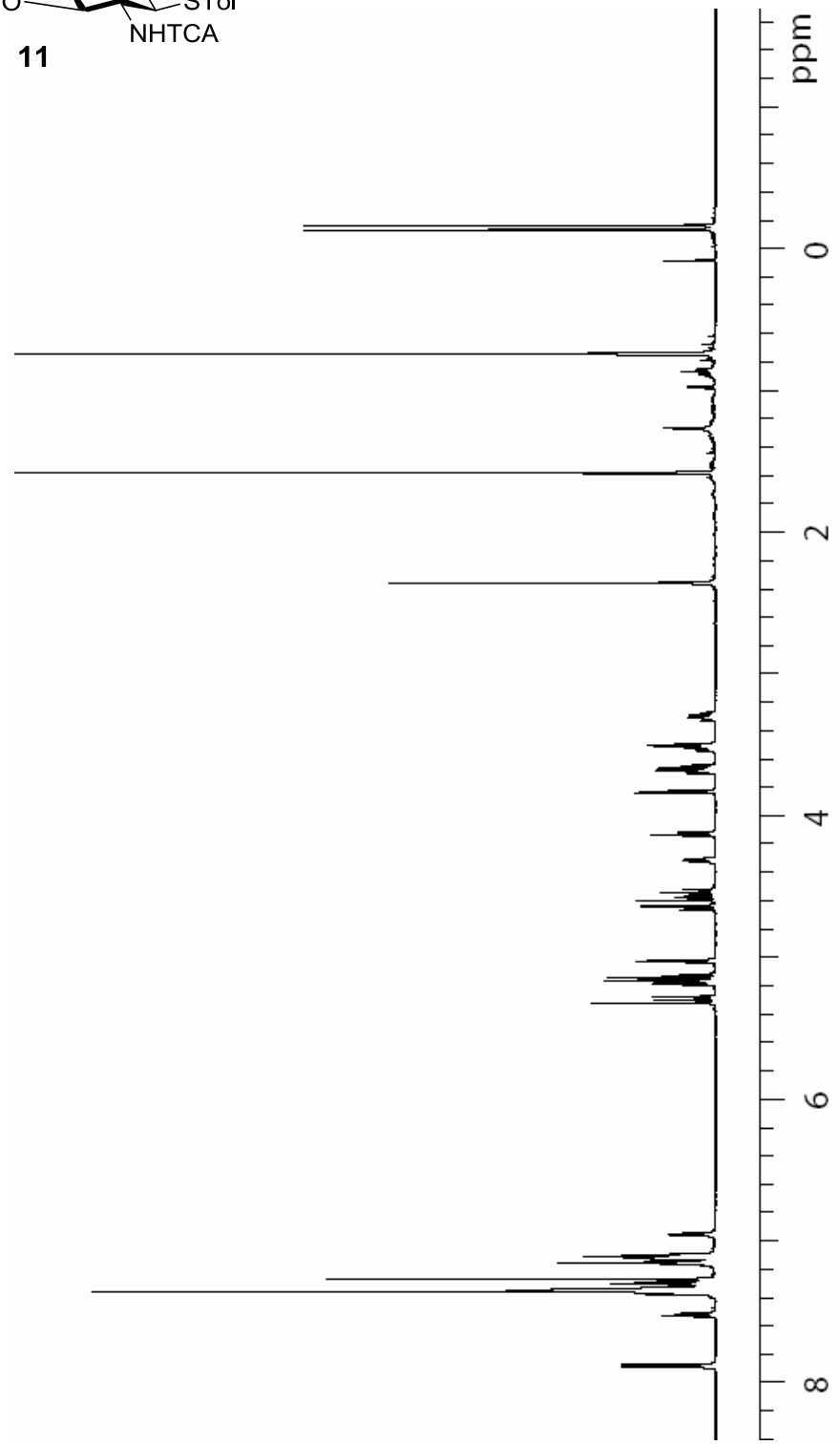

**Figure 3.17.** $^{13}$C-NMR of compound **11** (125 MHz $CDCl_3$)

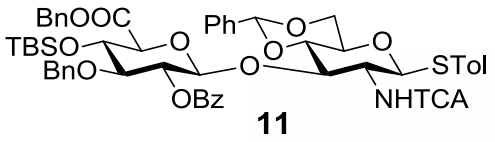


**11**

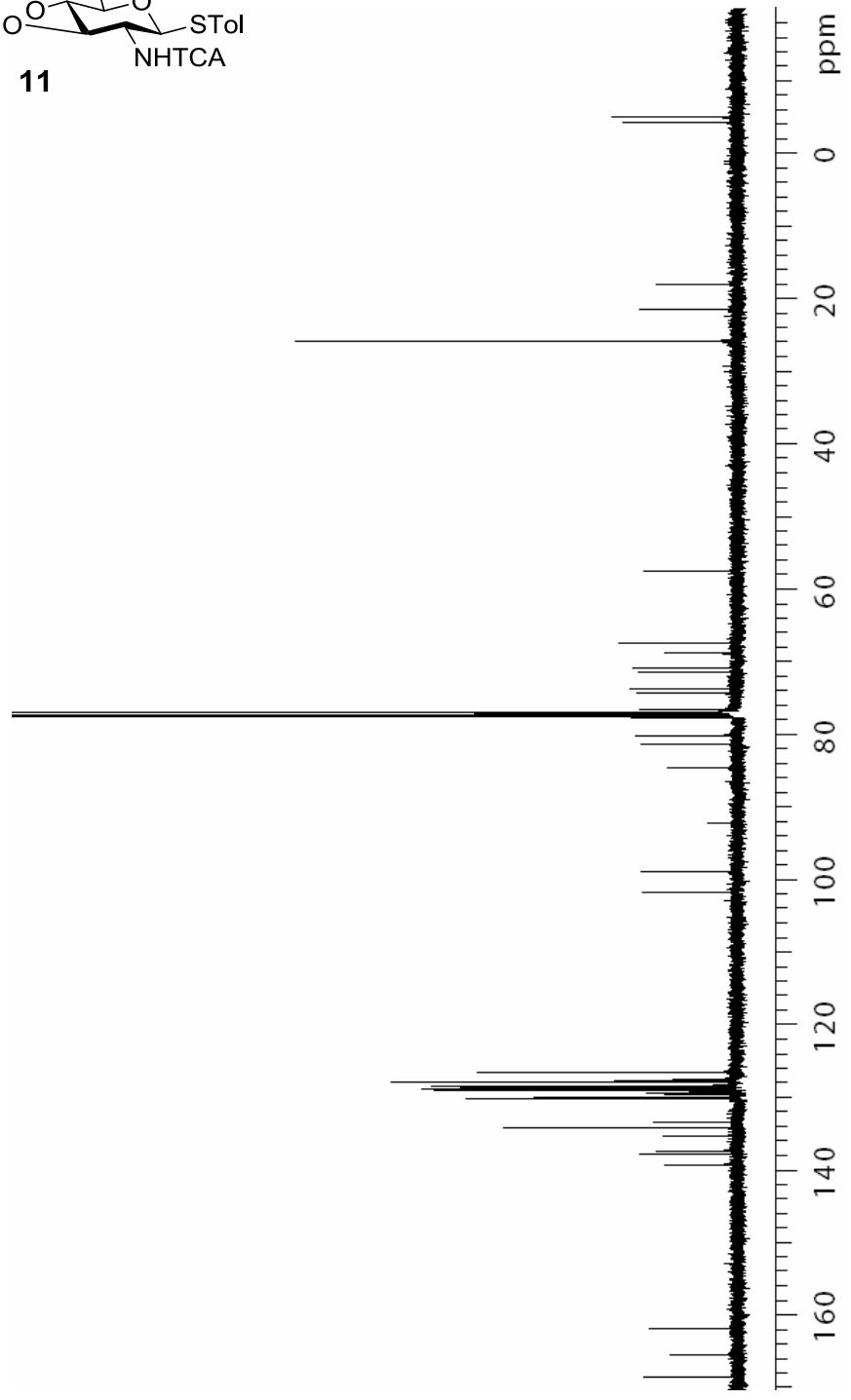

**Figure 3.18.** $^{1}H–^{1}H$ gCOSY of compound **11** (500 MHz, $CDCl_3$)

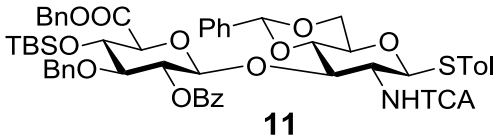


**11**

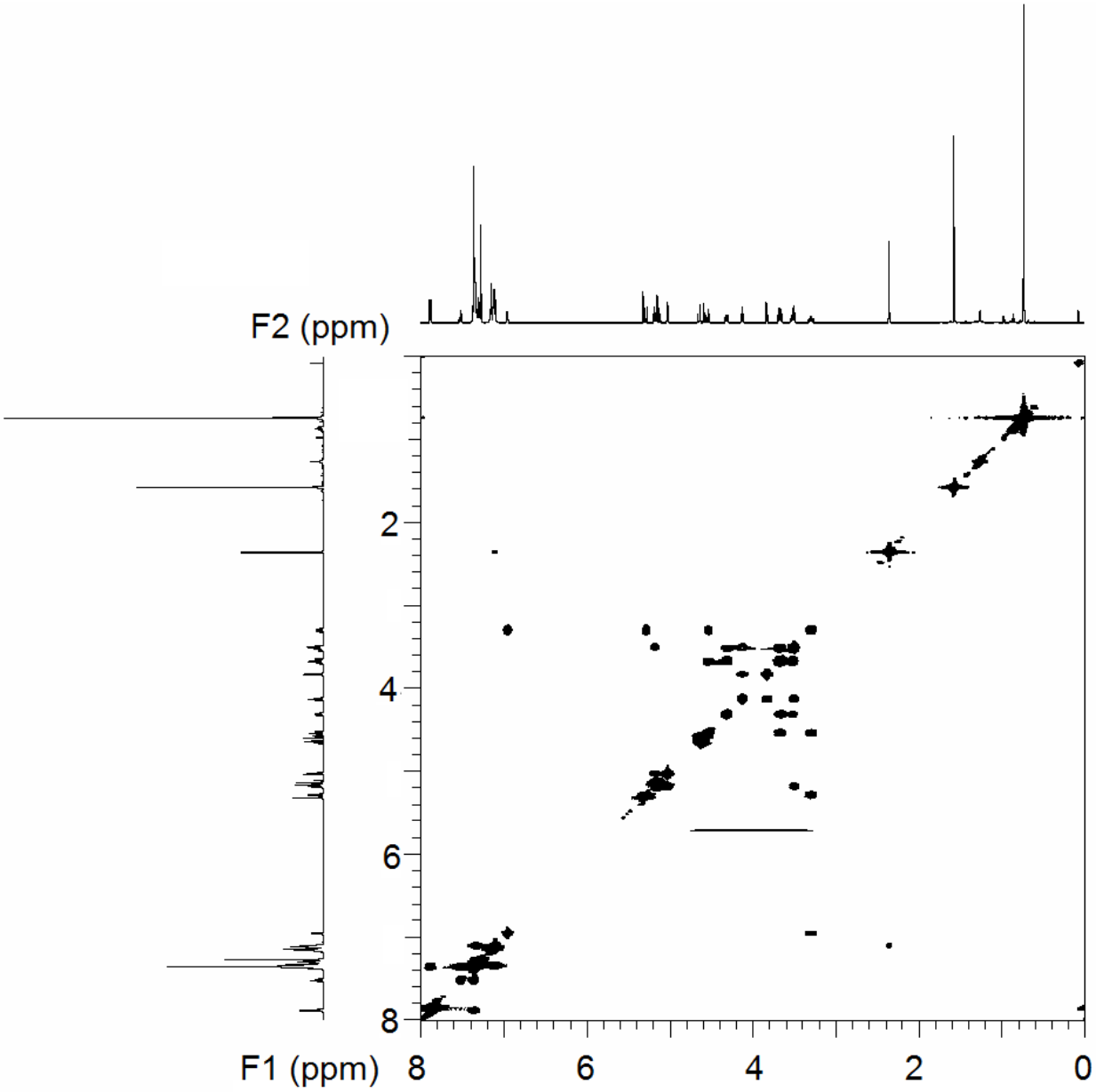

**Figure 3.19.** $^{1}H–^{13}C$ gHMQC of compound **11** (500 MHz, $CDCl_3$)

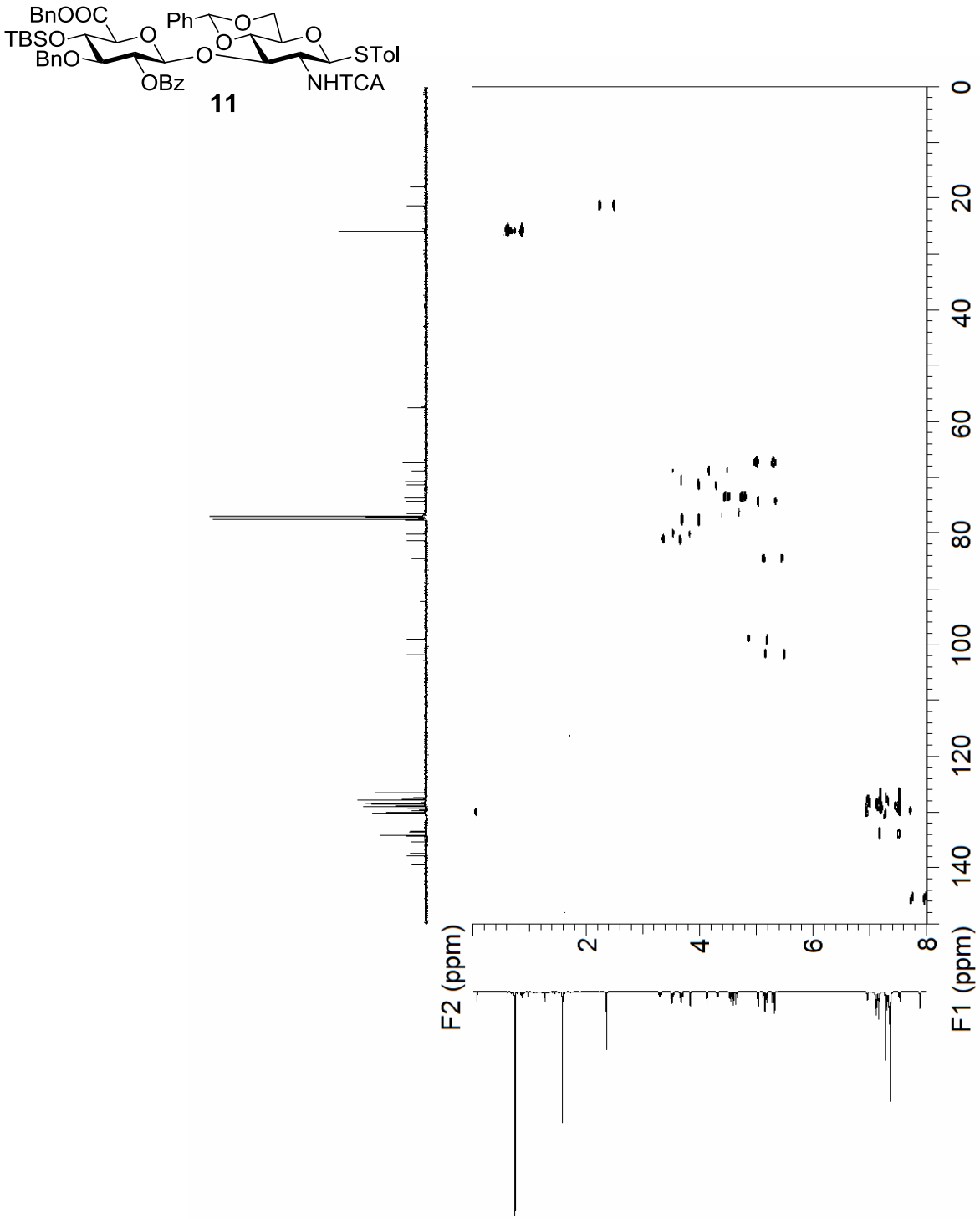

**Figure 3.20.** $^{1}H$–$^{13}C$ gHMQC (without $^{1}H$ decoupling) of compound **11** (500 MHz,$CDCl_3$)

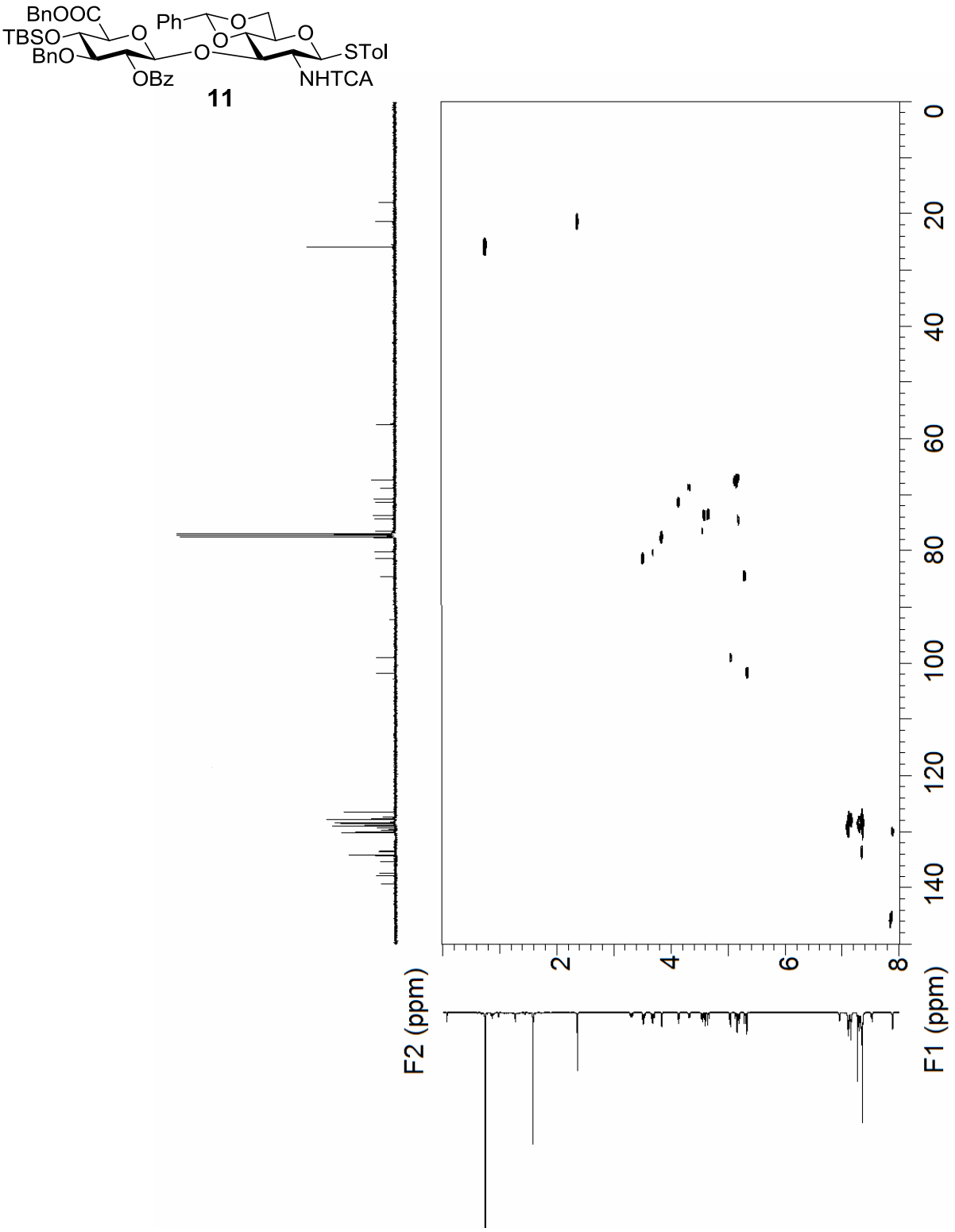

**Figure 3.21.** $^{1}H–^{13}C$ gHMBC of compound **11** (500 MHz, $CDCl_3$)

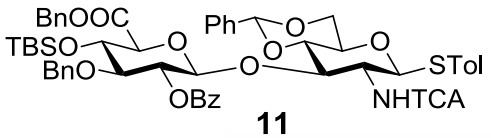


**11**

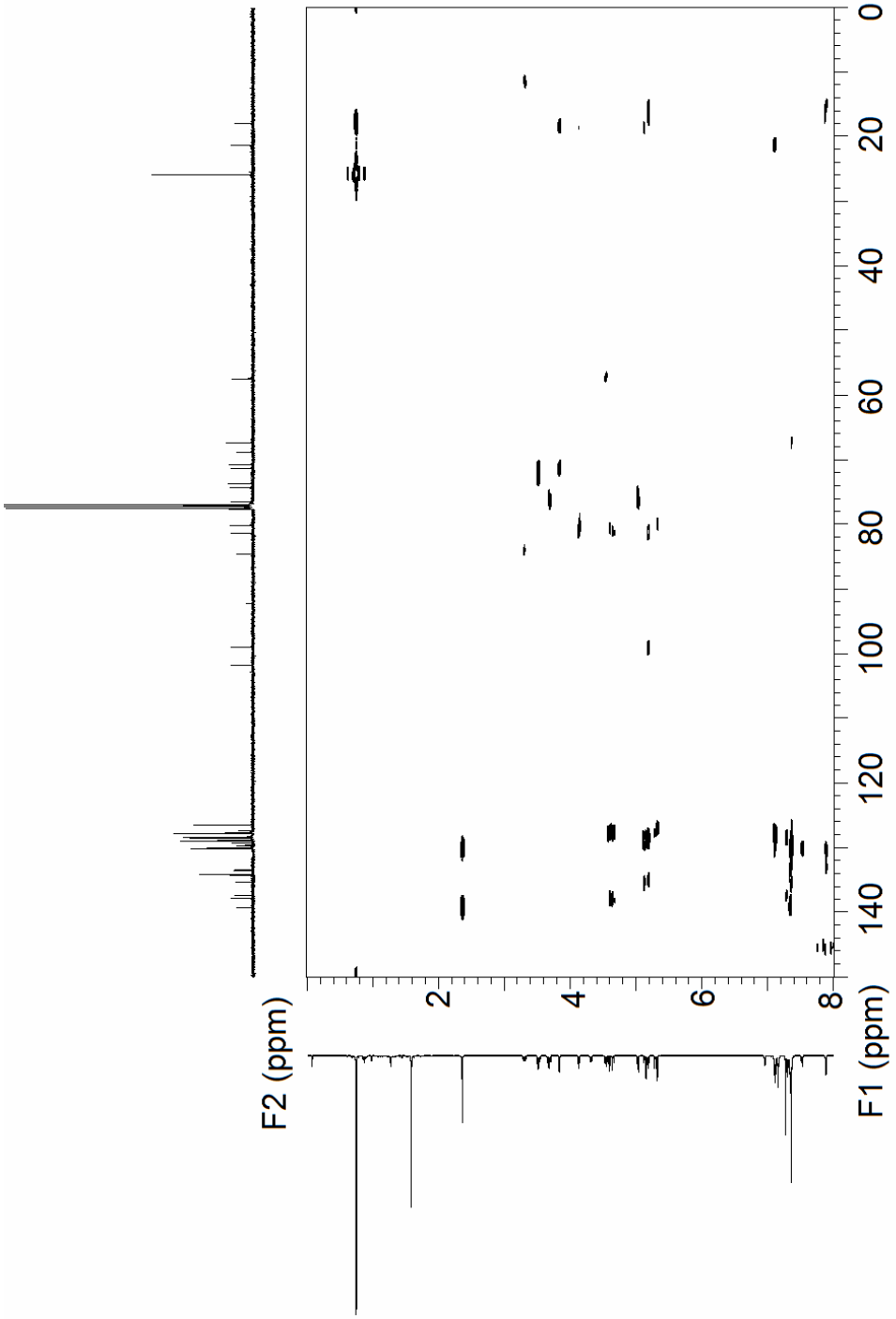

**Figure 3.22.** $^{1}$H-NMR of compound **12** (500 MHz, $CDCl_3$)

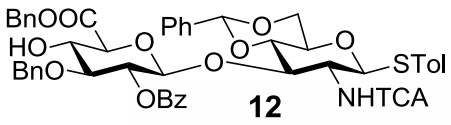


**12**

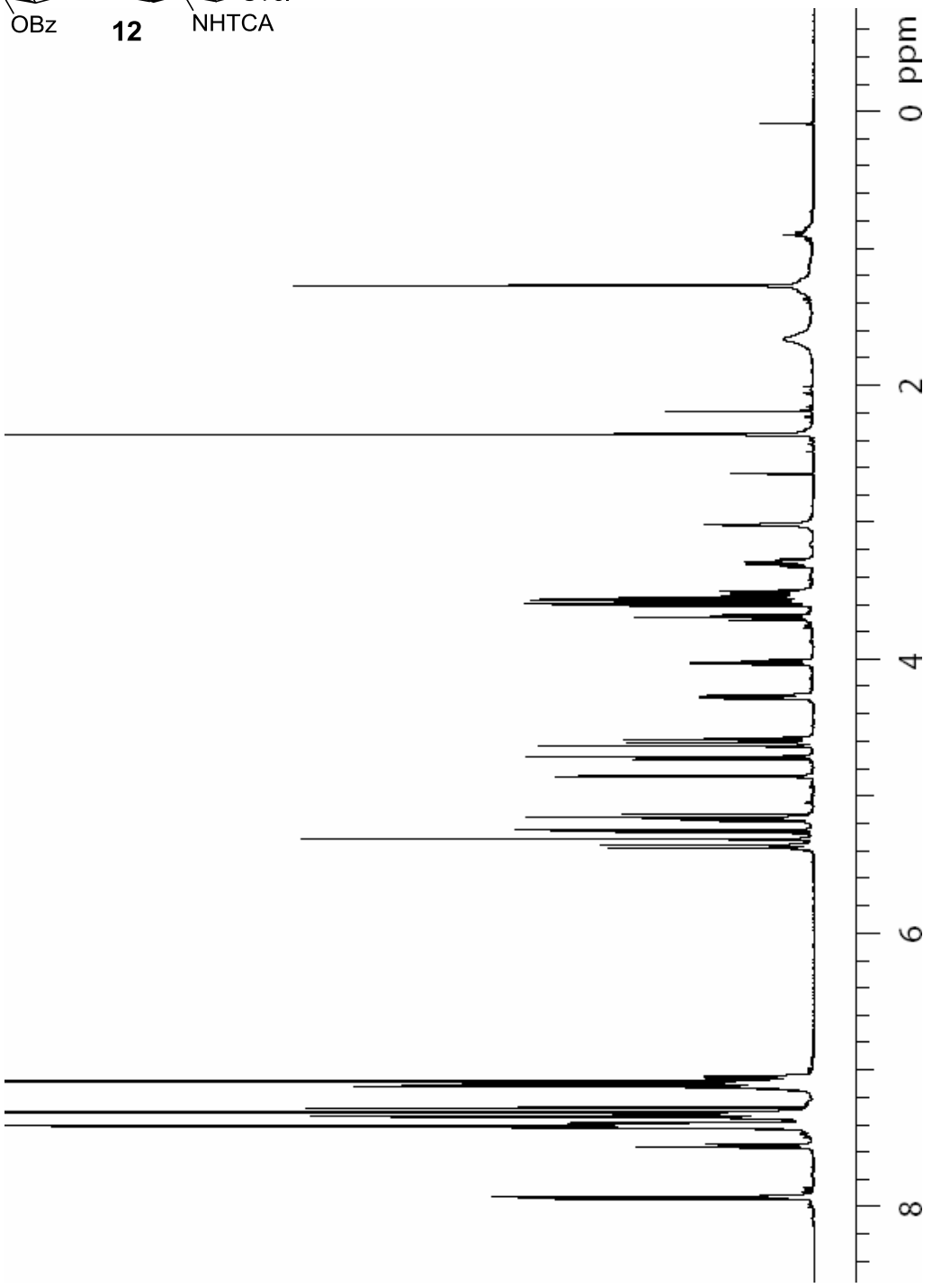

**Figure 3.23.** $^{13}$C-NMR of compound **12** (125 MHz, $CDCl_3$)

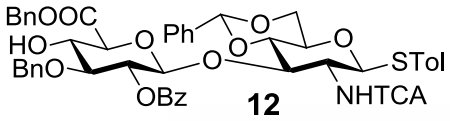


**12**

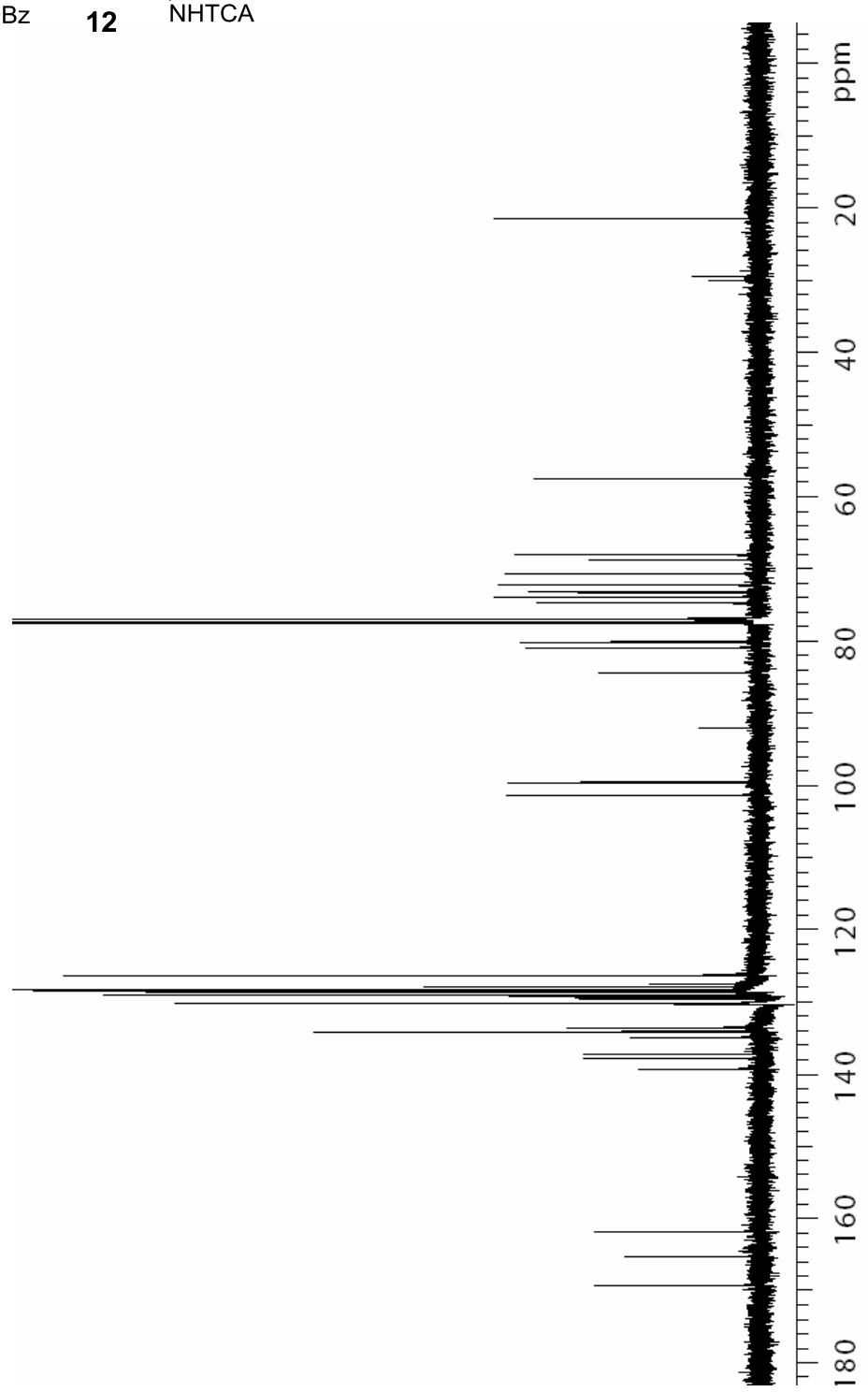

**Figure 3.24.** $^{1}H–^{1}H$ gCOSY of compound **12** (500 MHz, $CDCl_3$)

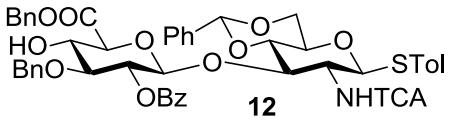


**12**

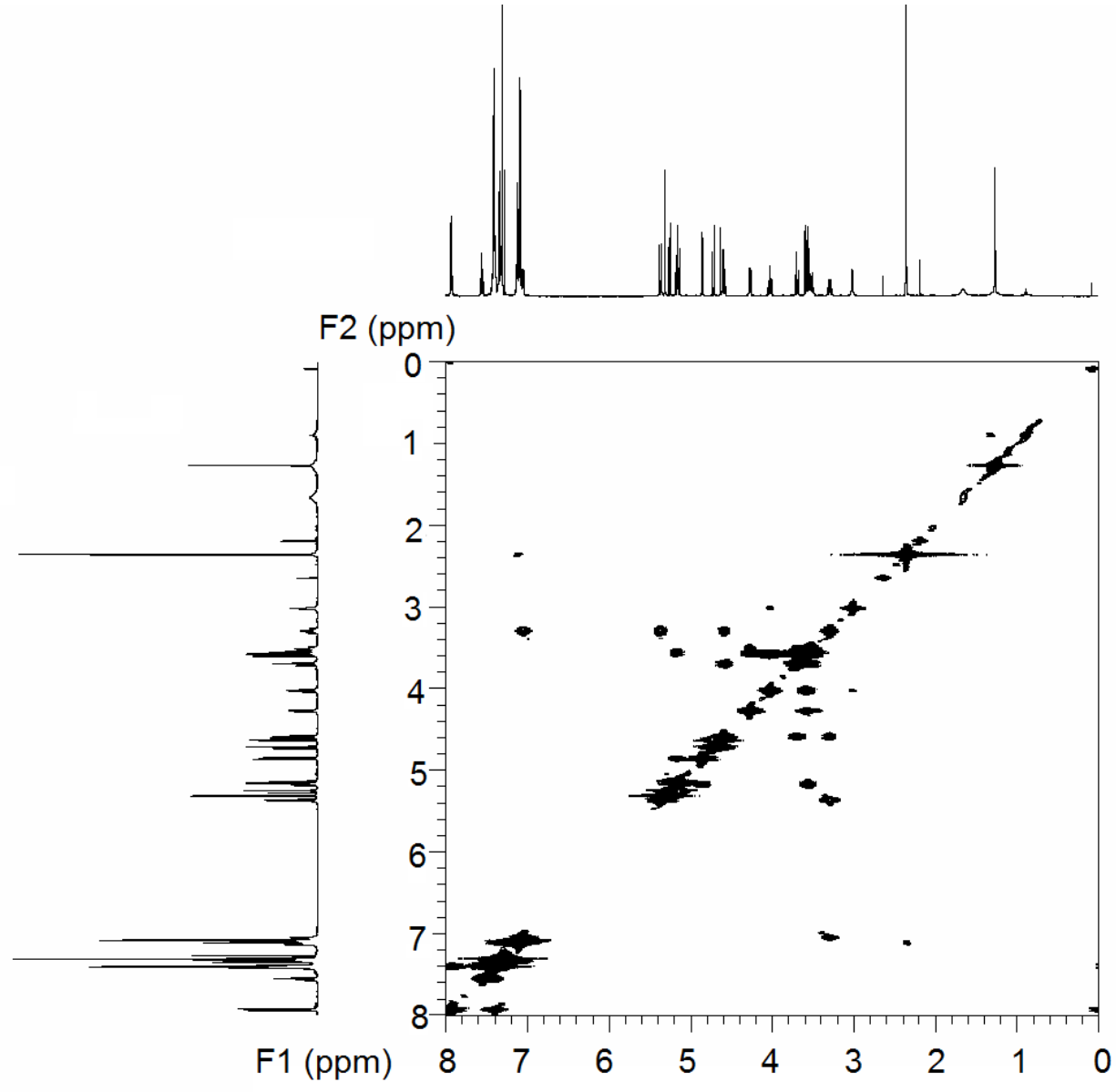

**Figure 3.25.** $^{1}H–^{13}C$ gHMQC of compound **12** (500 MHz, $CDCl_3$)

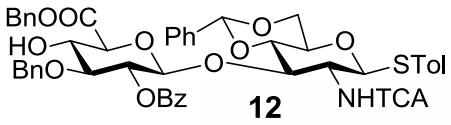


**12**

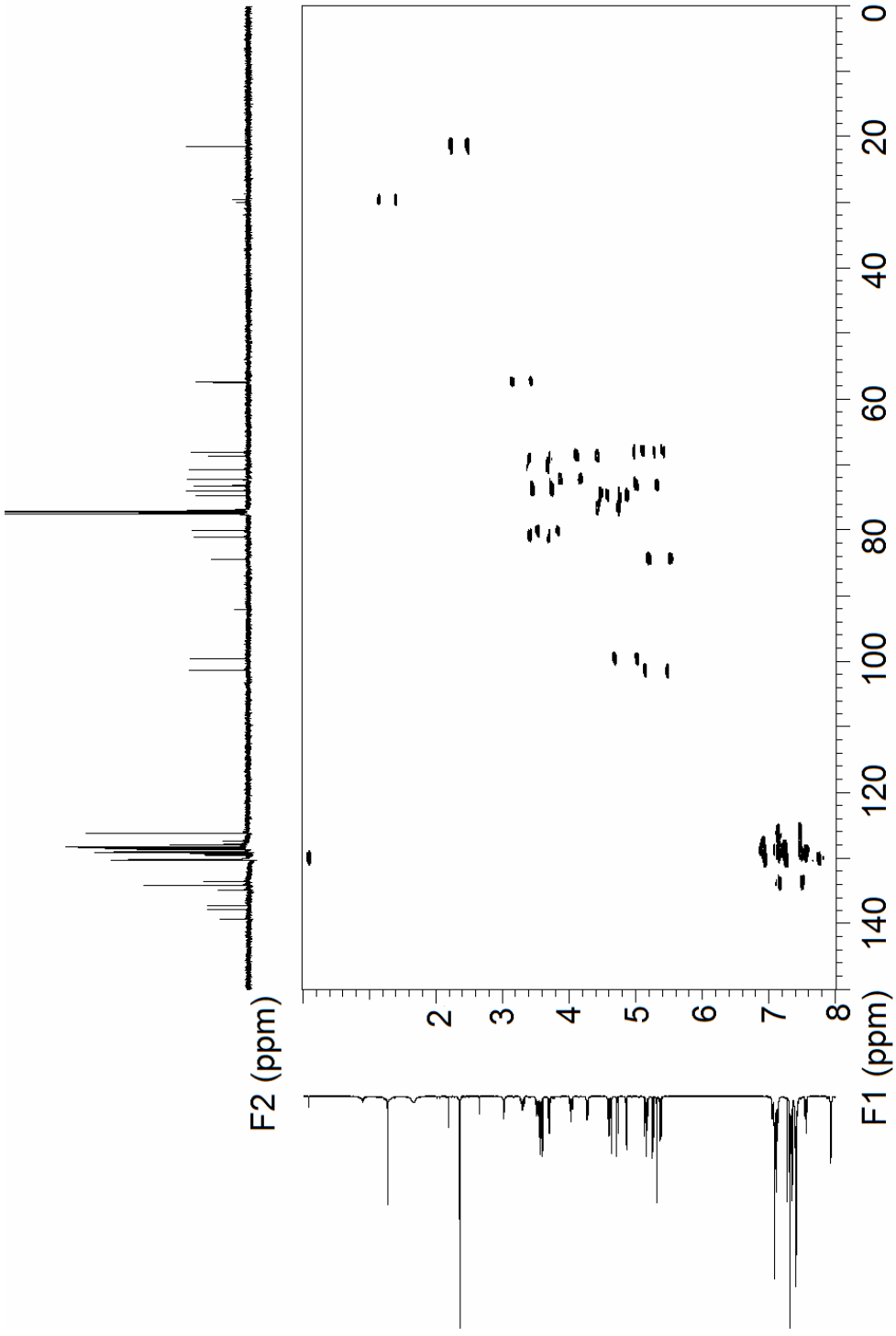

**Figure 3.26.** $^{1}H–^{13}C$ gHMQC (without $^{1}H$ decoupling) of compound **12** (500 MHz,$CDCl_3$)

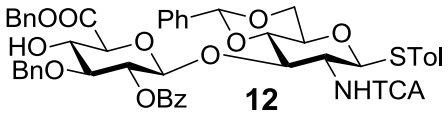


**12**

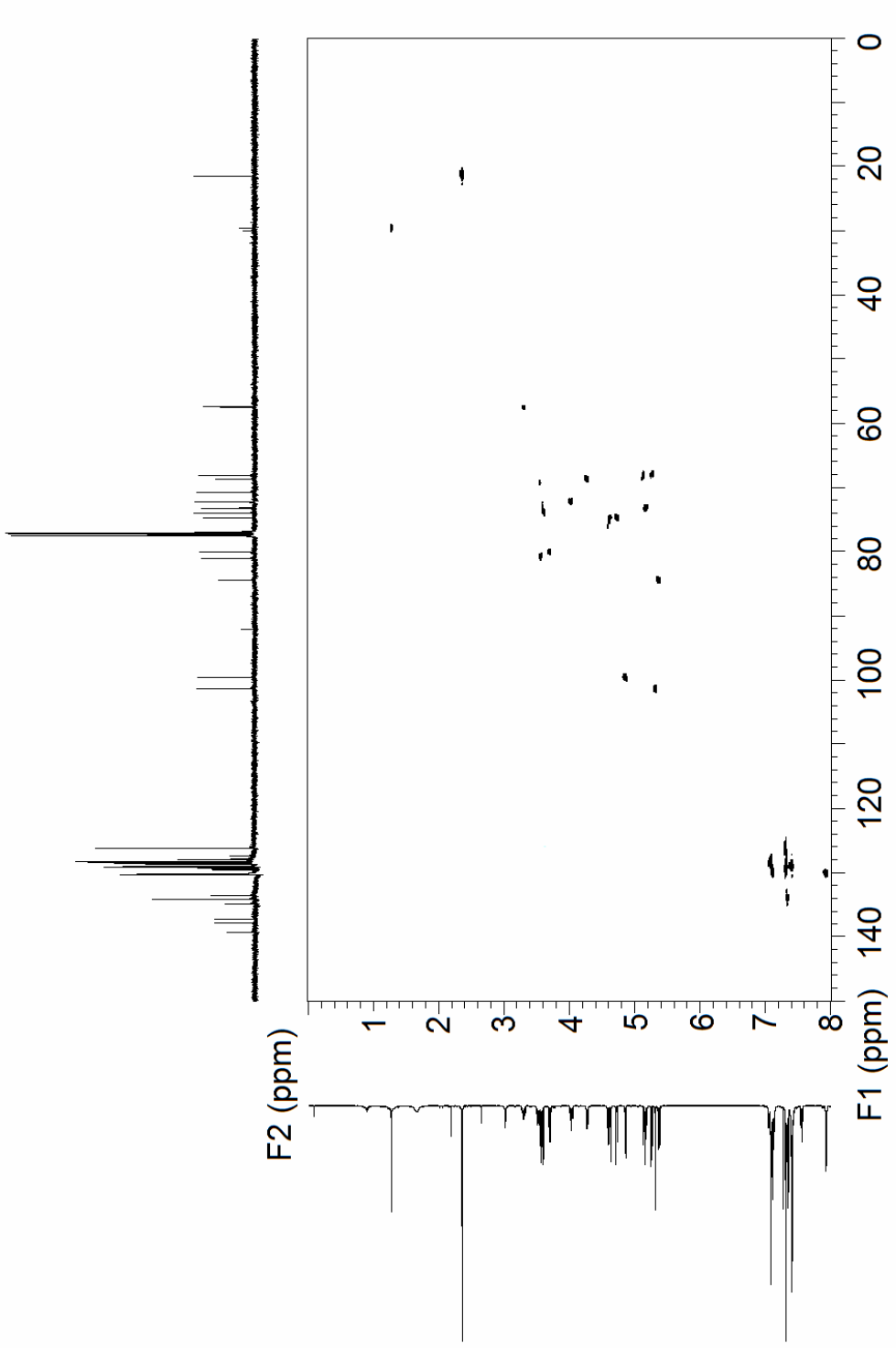

**Figure 3.27.** $^{1}H–^{13}C$ gHMBC of compound **12** (500 MHz, $CDCl_3$)

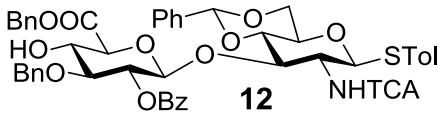


**12**

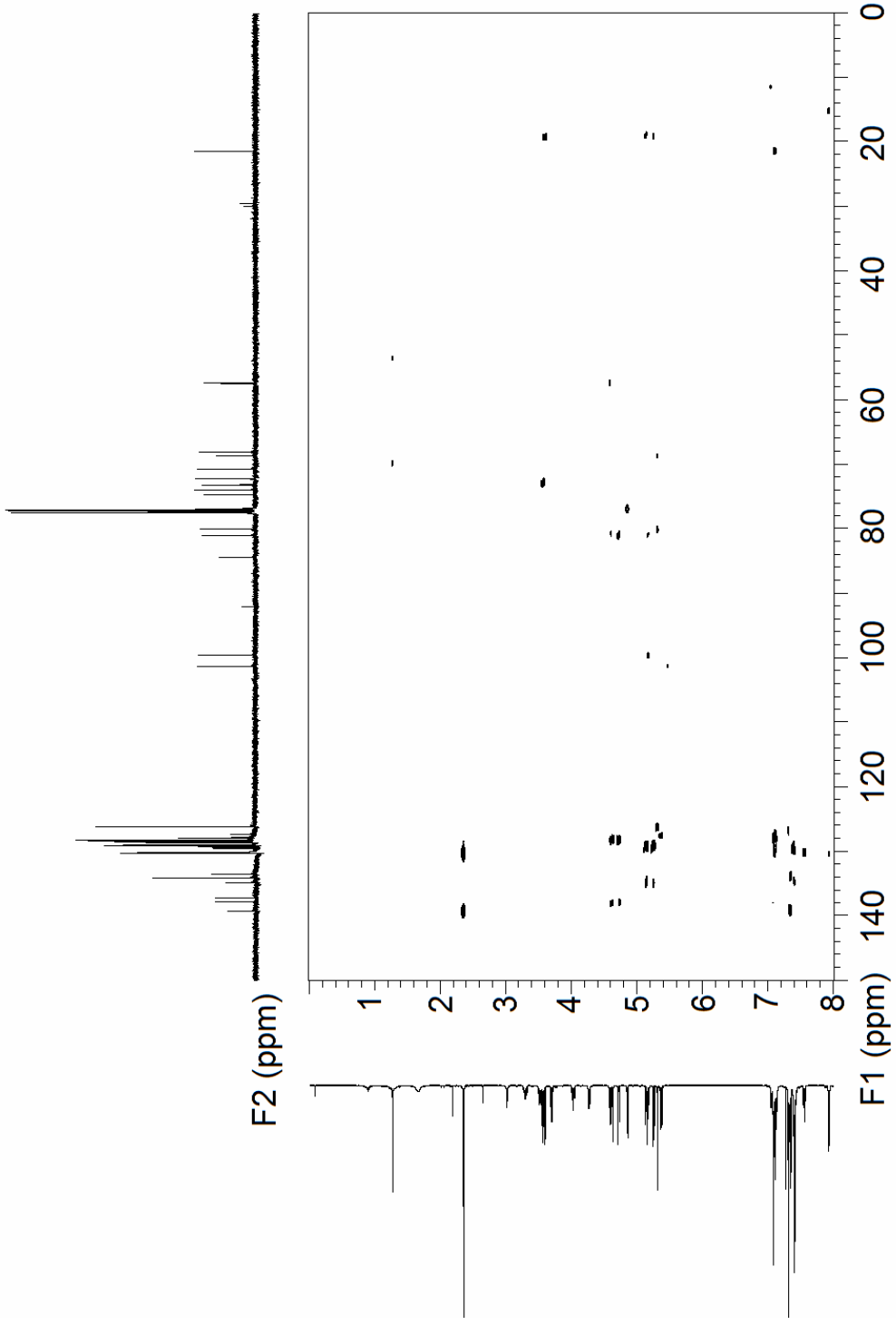

**Figure 3.28.** $^{1}$H-NMR of compound **13** (500 MHz, $CDCl_3$)

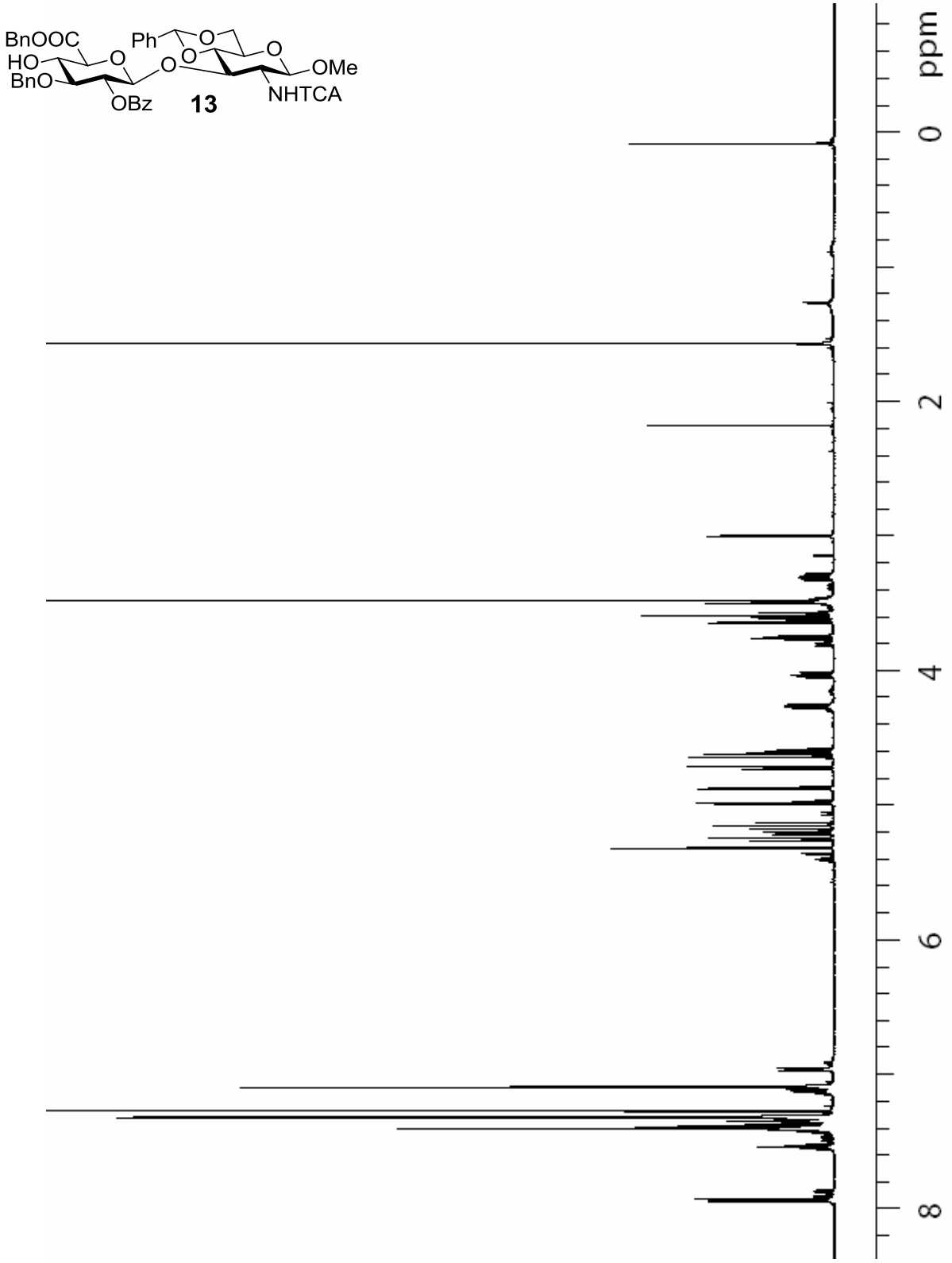

**Figure 3.29.** $^{13}$C-NMR of compound **13** (125 MHz, $CDCl_3$)

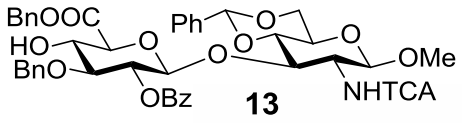


**13**

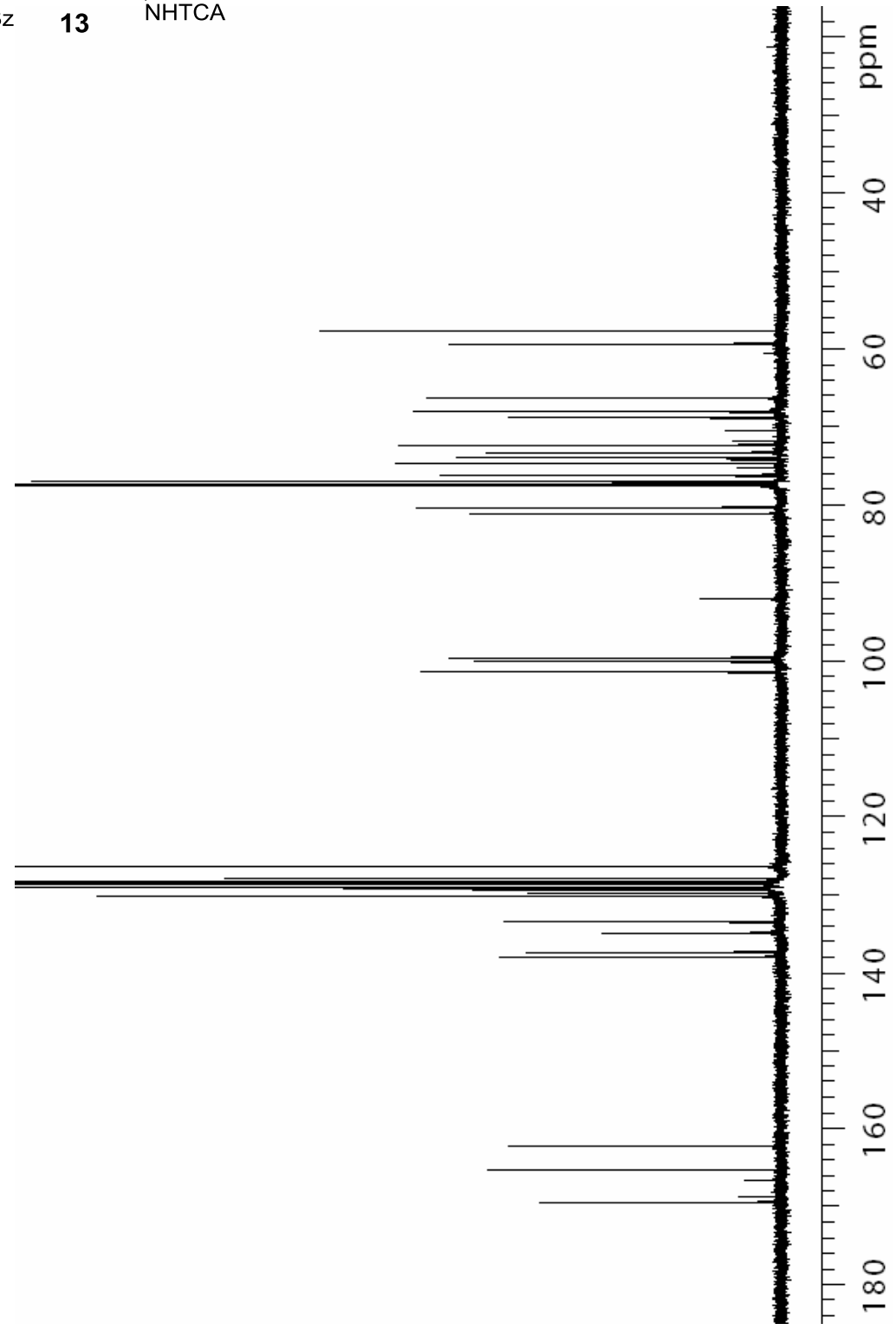

**Figure 3.30.** $^{1}H–^{1}H$ gCOSY of compound **13** (500 MHz, $CDCl_3$)

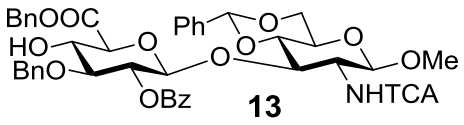


**13**

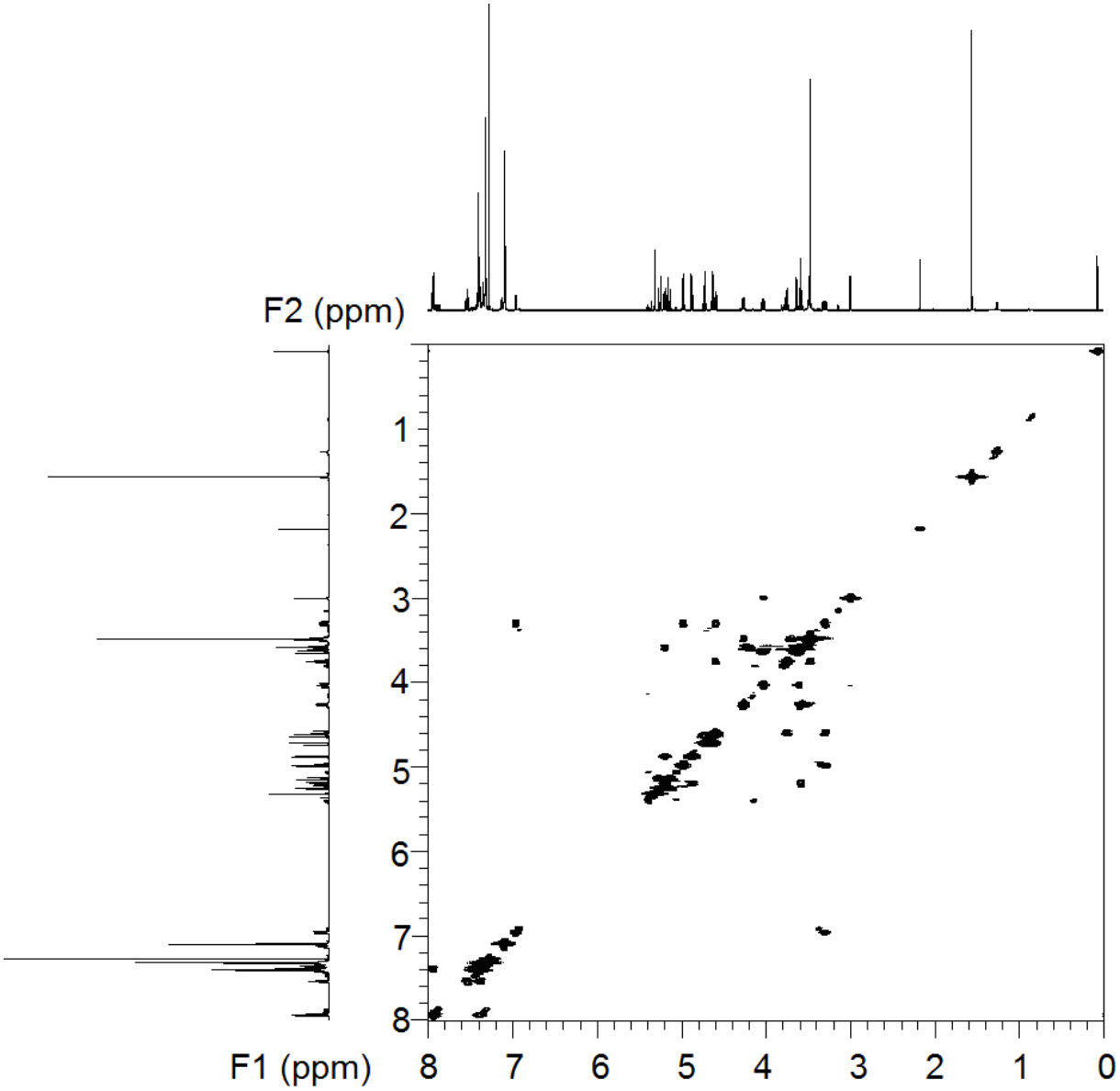

**Figure 3.31.** $^{1}H–^{13}C$ gHMQC of compound **13** (500 MHz, $CDCl_3$)

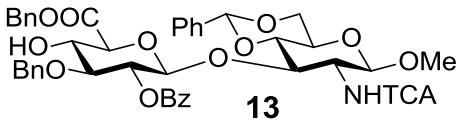


**13**

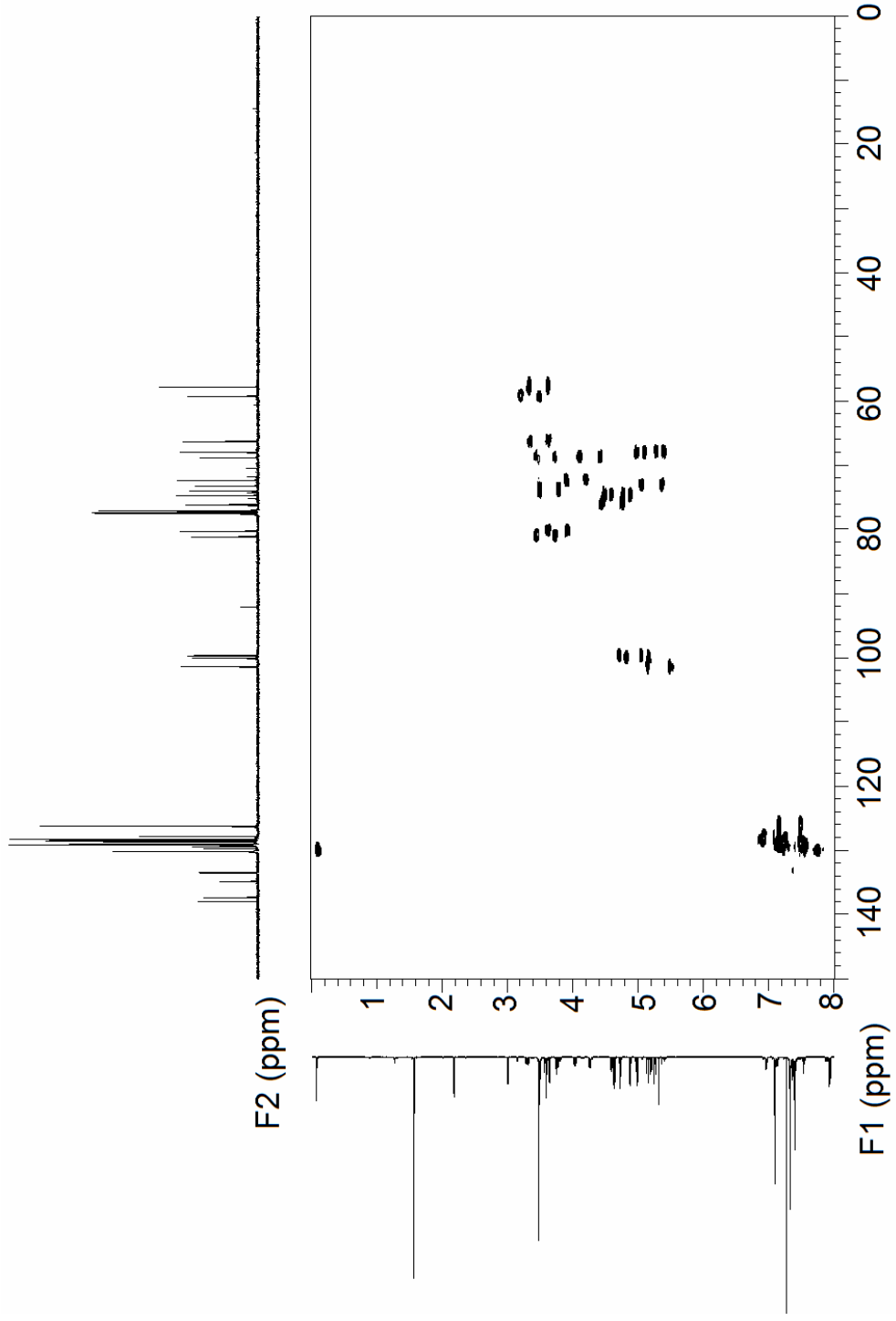

**Figure 3.32.** $^{1}H–^{13}C$ gHMQC (without $^{1}H$ decoupling) of compound **13** (500 MHz,$CDCl_3$)

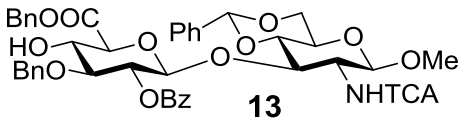


**13**

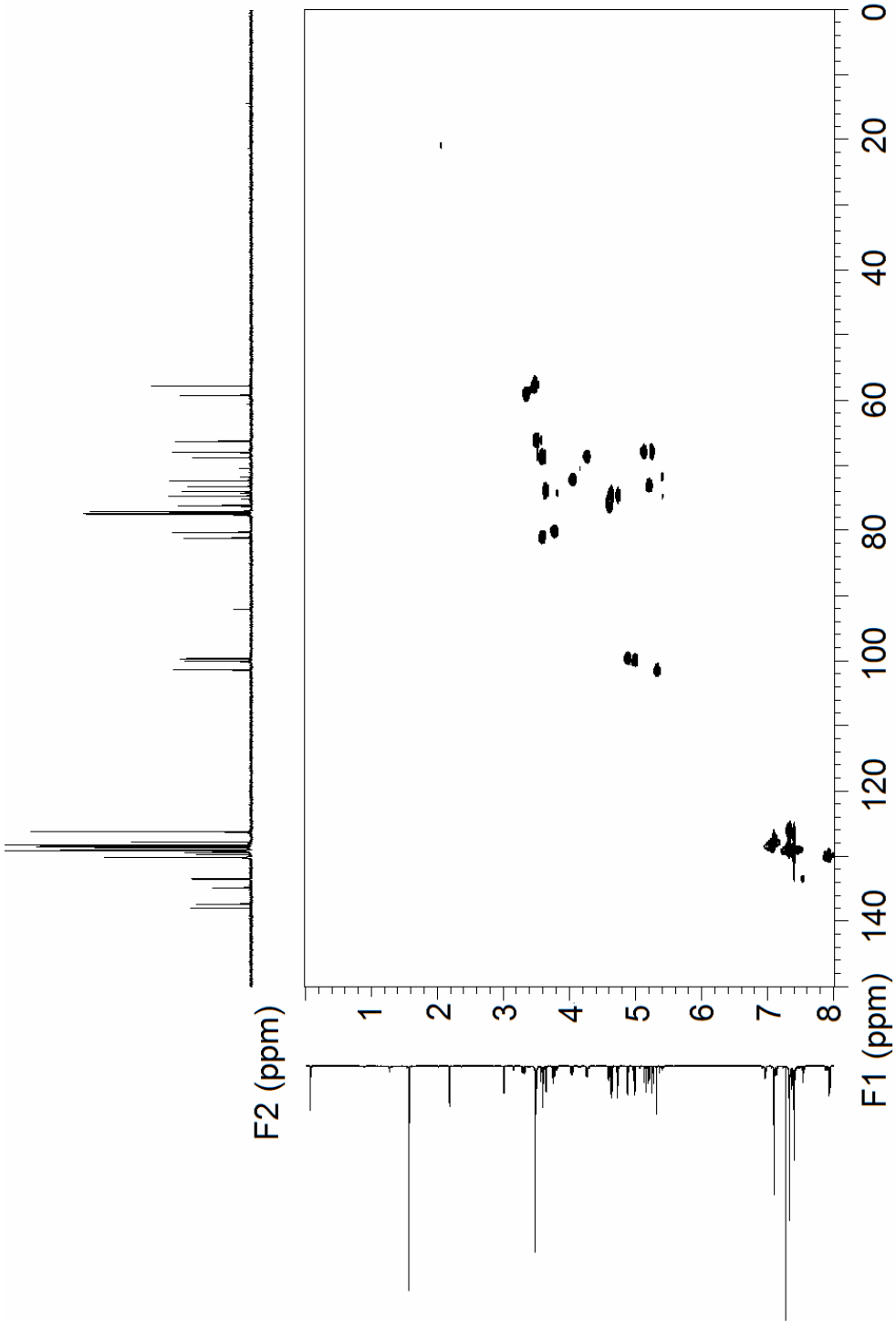

**Figure 3.33.** $^{1}H–^{13}C$ gHMBC of compound **13** (500 MHz, $CDCl_3$)

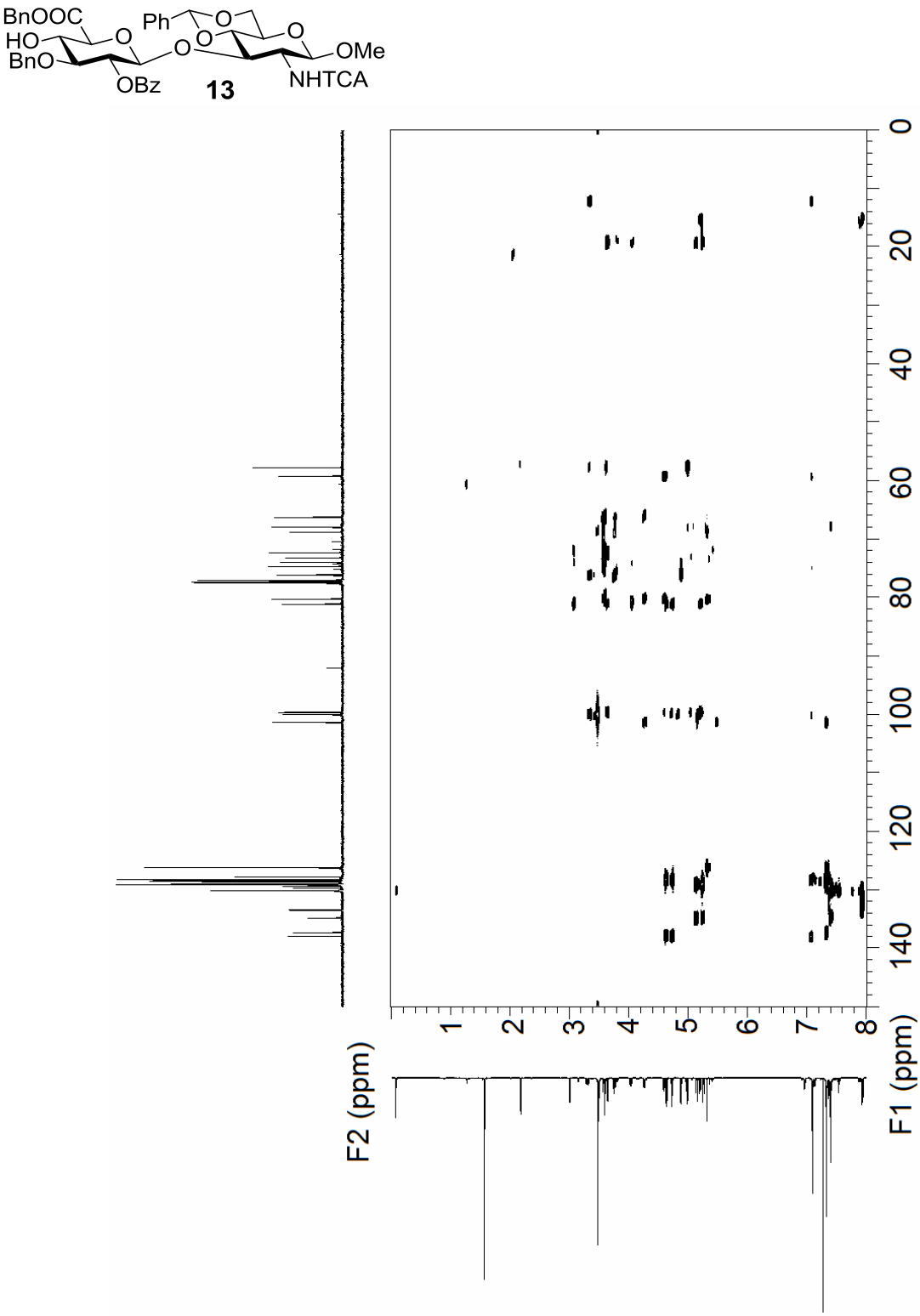

**Figure 3.34.** $^{1}$H-NMR of compound **25** (500 MHz, $CDCl_3$)

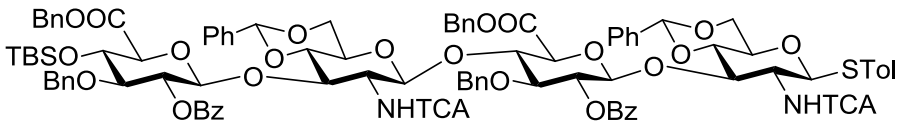


**25**

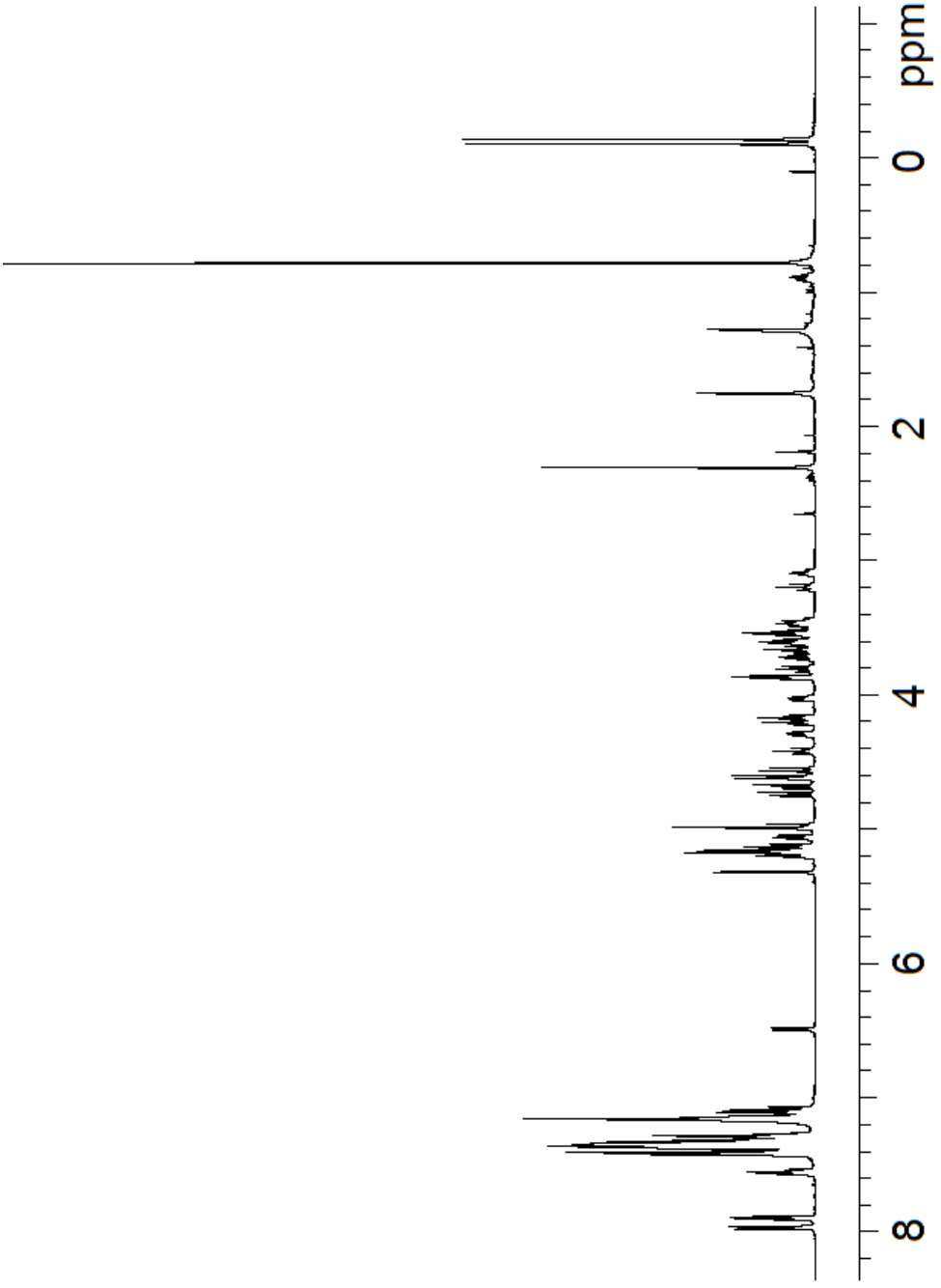

**Figure 3.35.** $^{13}$C-NMR of compound **25** (125 MHz, $CDCl_3$)

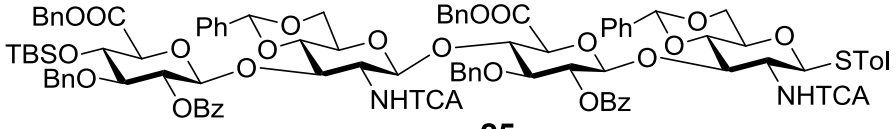


**25**

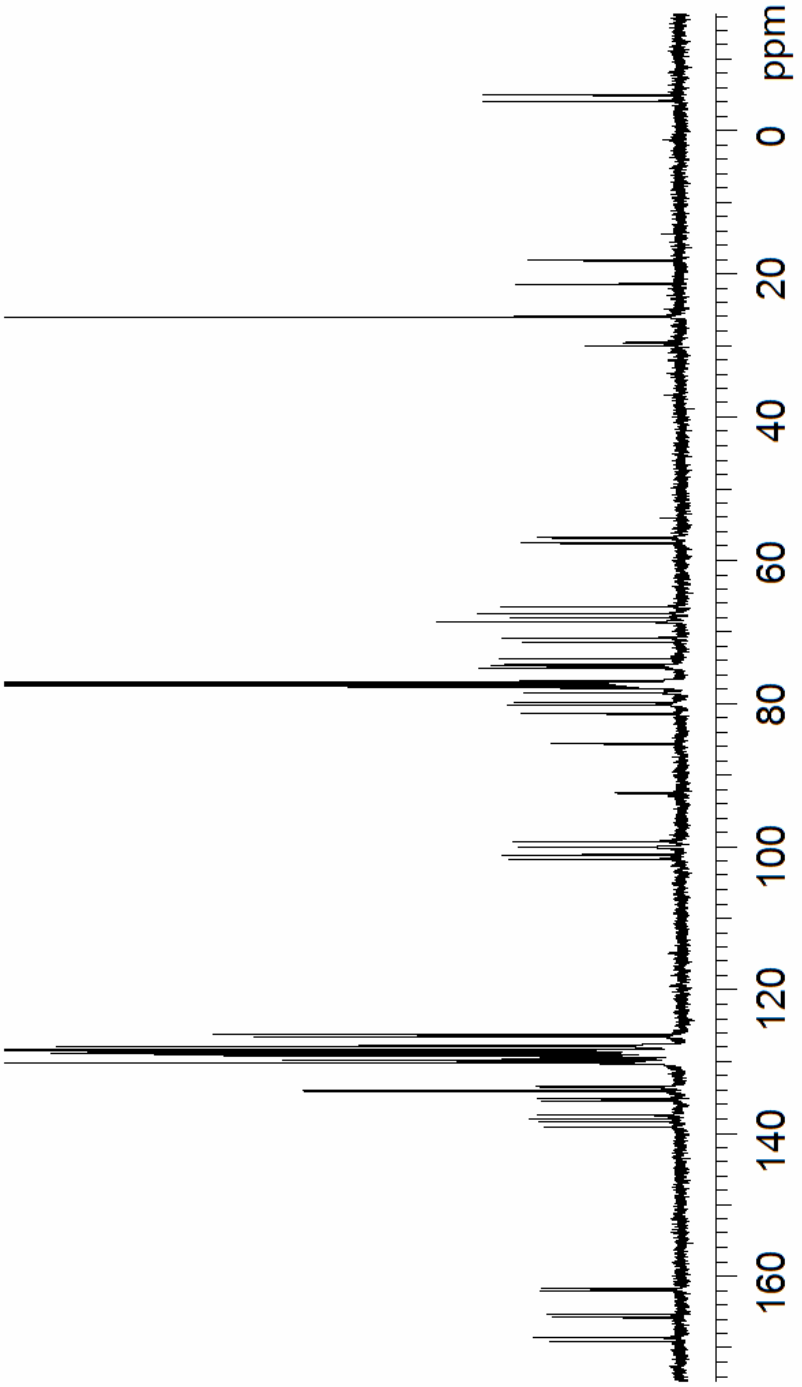

**Figure 3.36.** $^{1}H–^{1}H$ gCOSY of compound **25** (500 MHz, $CDCl_3$)

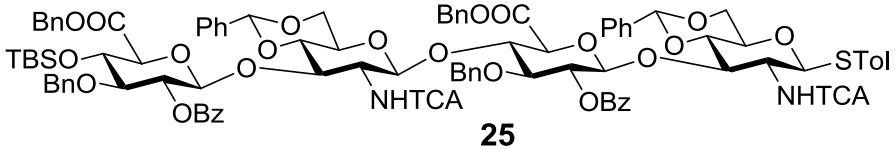


**25**

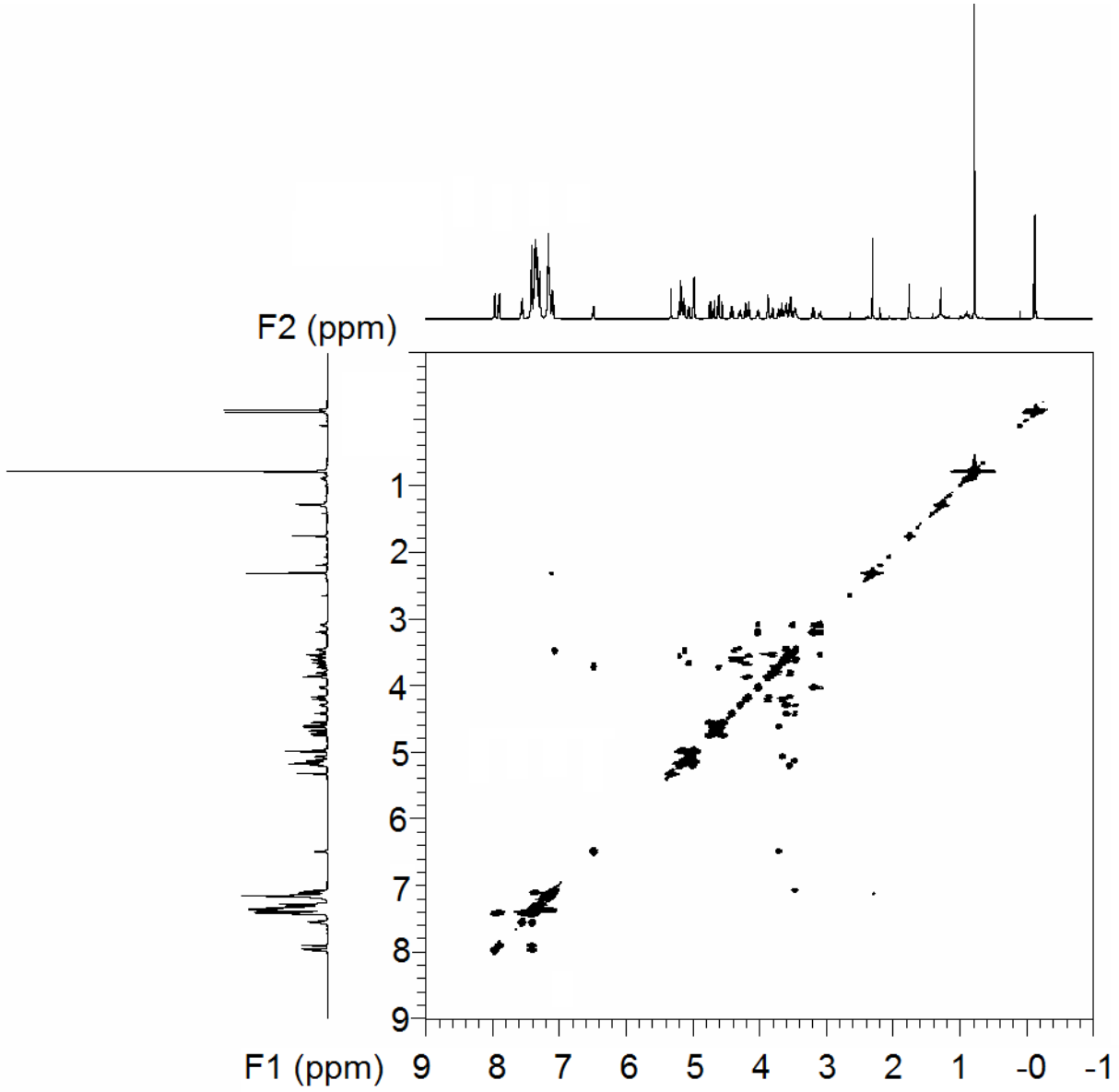

**Figure 3.37.** $^{1}H$–$^{13}C$ gHMQC of compound **25** (500 MHz, $CDCl_3$)

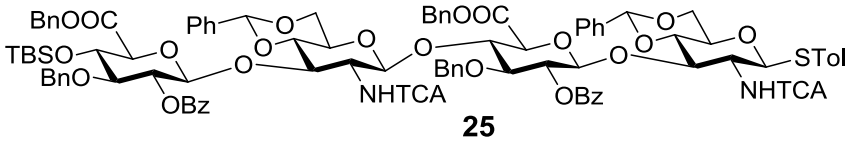


**25**

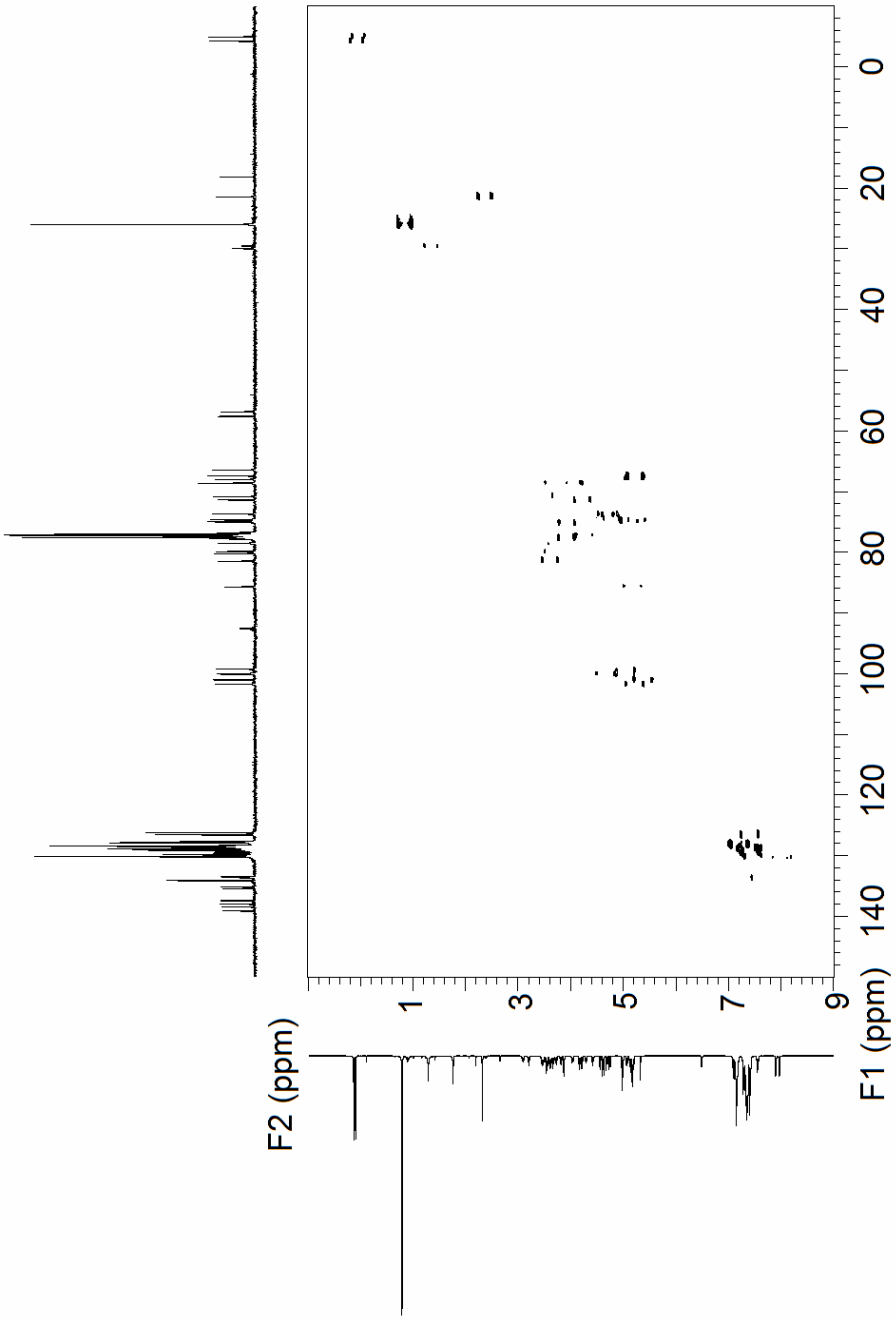

**Figure 3.38.** $^{1}H–^{13}C$ gHMQC (without $^{1}H$ decoupling) of compound **25** (500 MHz,$CDCl_3$)

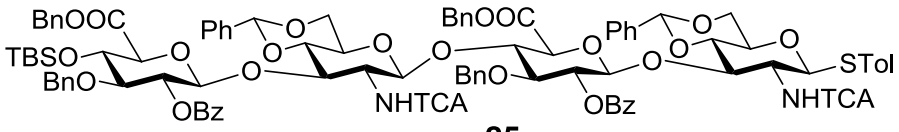


**25**

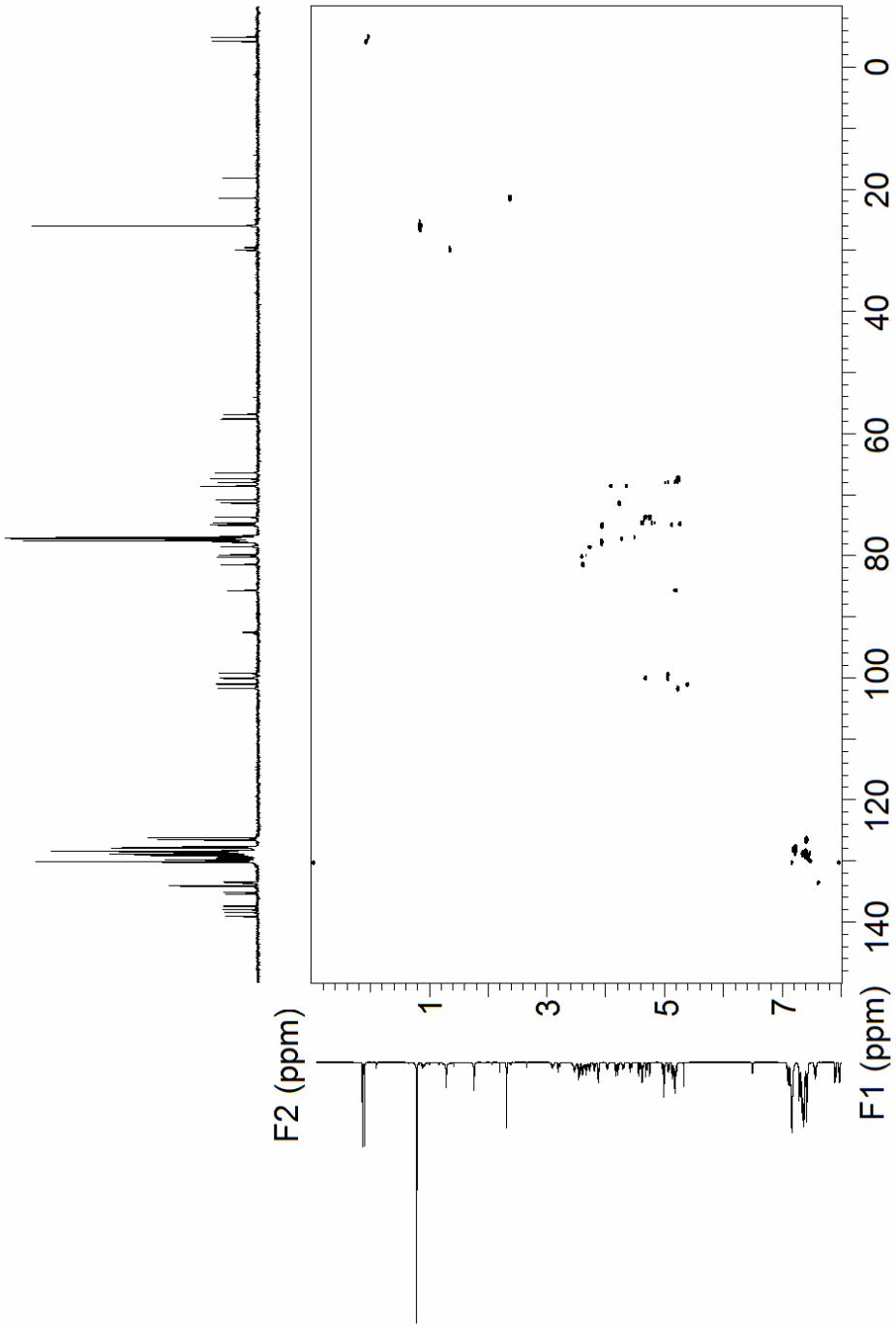

**Figure 3.39.** $^{1}H–^{13}C$ gHMBC of compound **25** (500 MHz, $CDCl_3$)

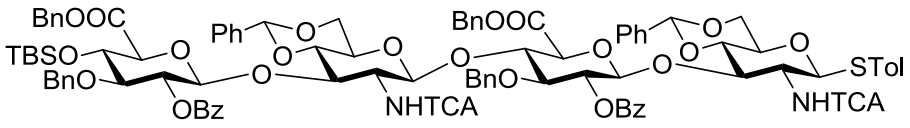


**25**

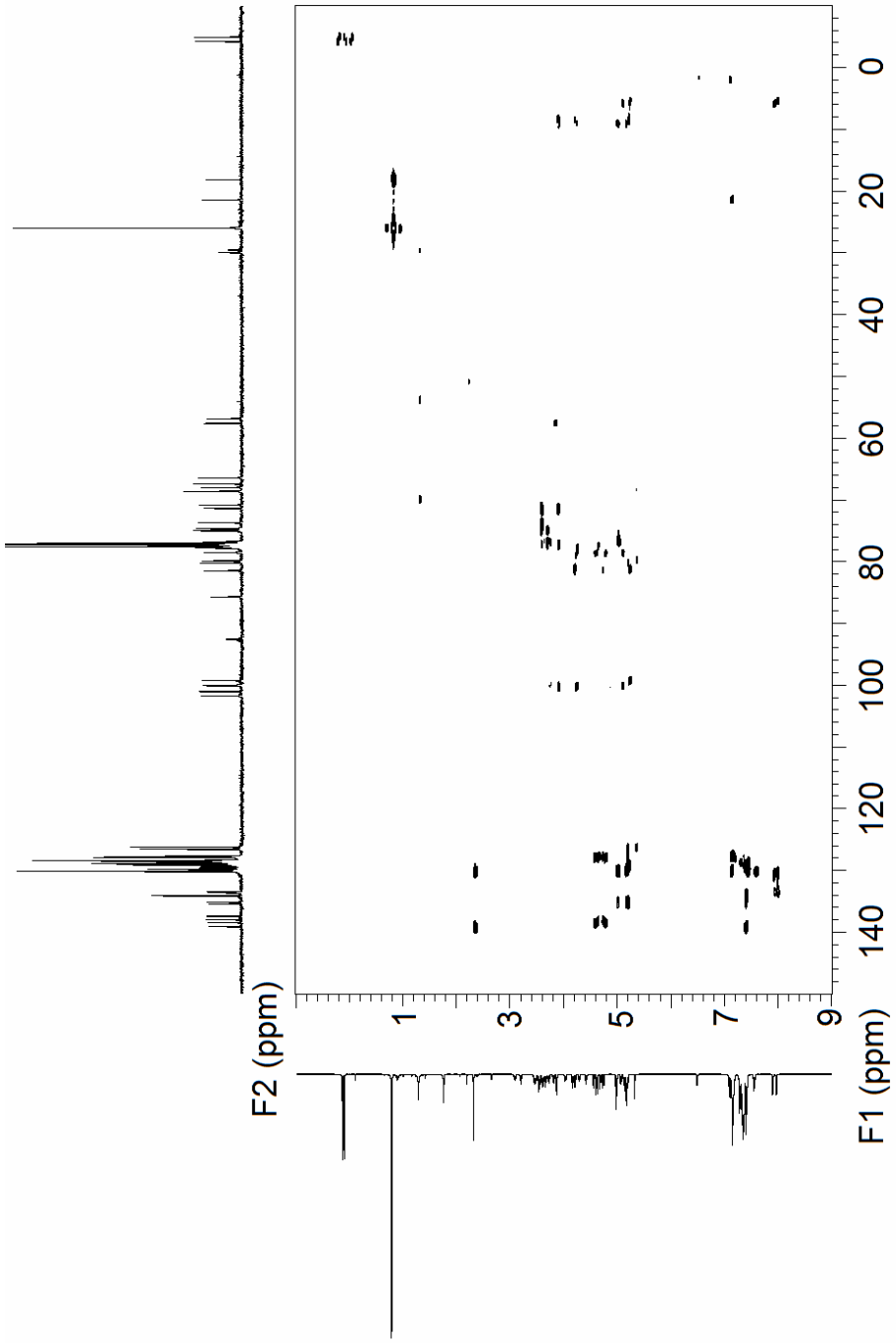

**Figure 3.40.** $^{1}$H-NMR of compound **26** (500 MHz, $CDCl_3$)

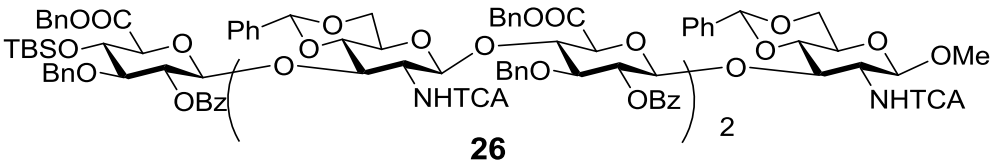


**26**

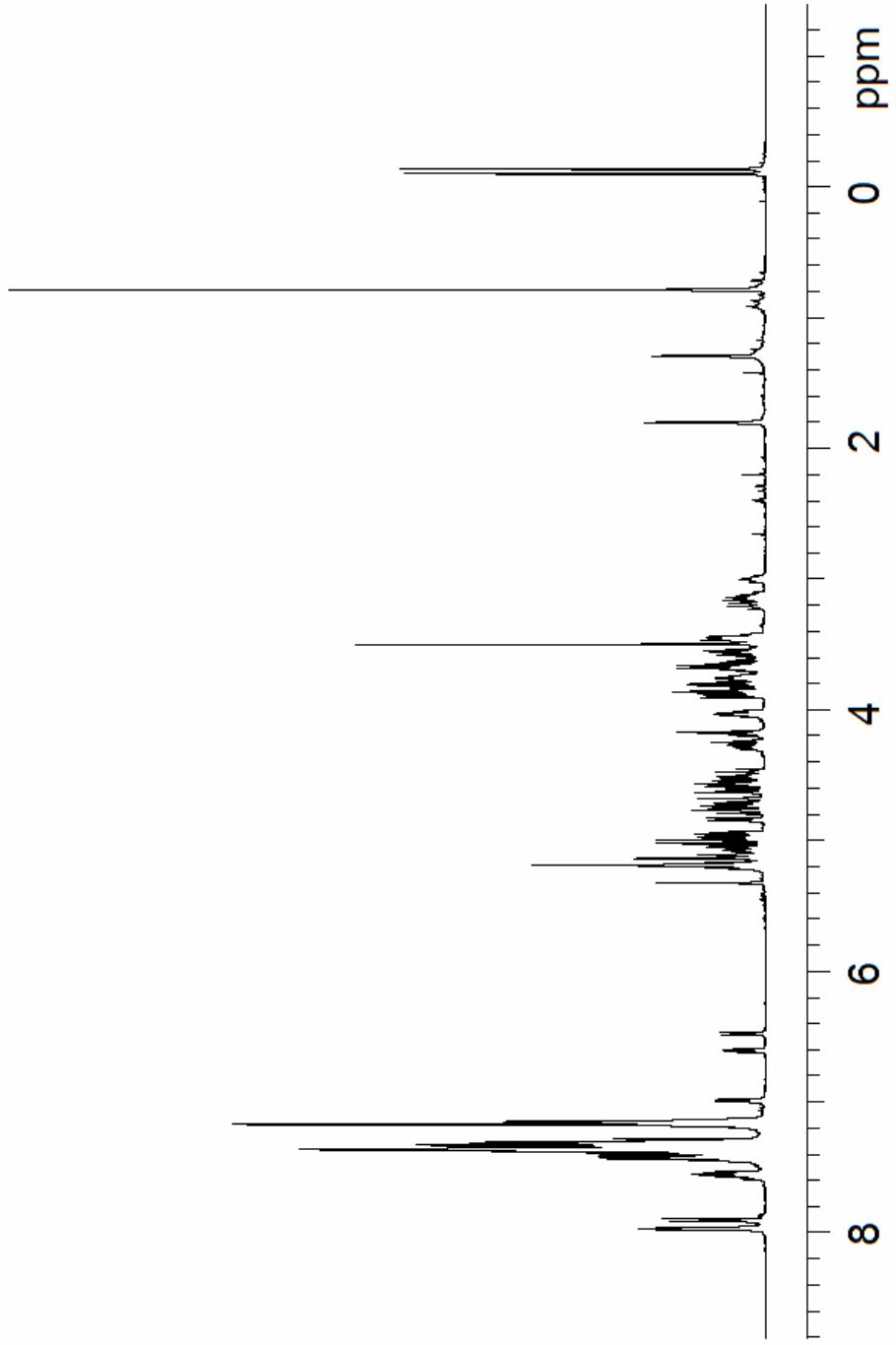

**Figure 3.41.** $^{13}$C-NMR of compound **26** (125 MHz, $CDCl_3$)

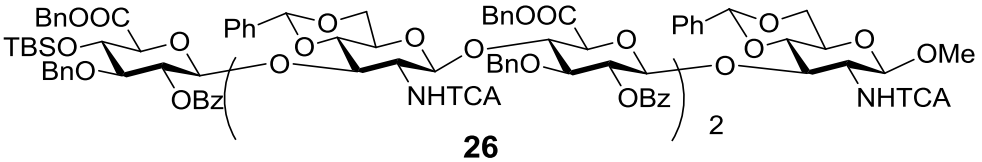


**26**

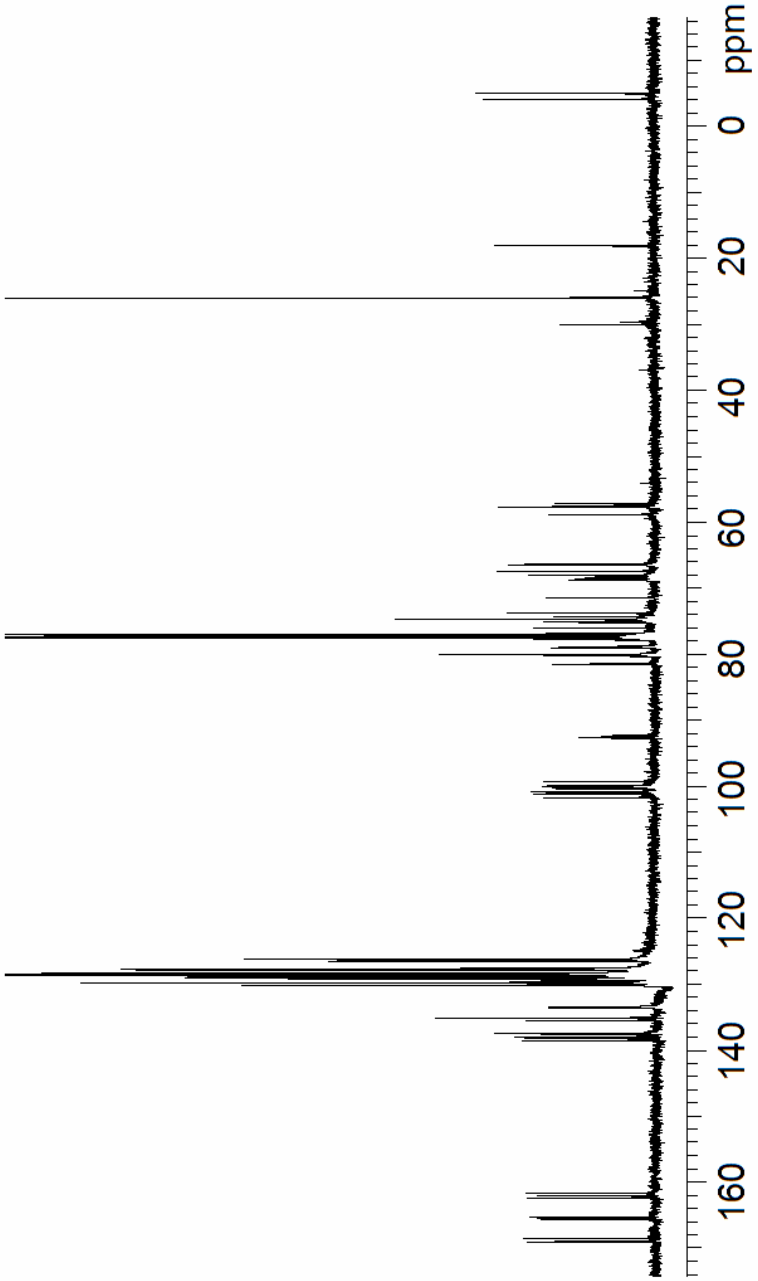

**Figure 3.42.** $^{1}H–^{1}H$ gCOSY of compound **26** (500 MHz, $CDCl_3$)

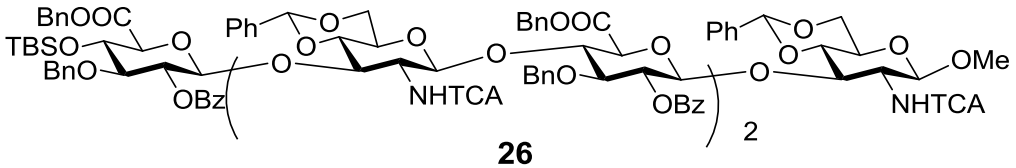


**26**

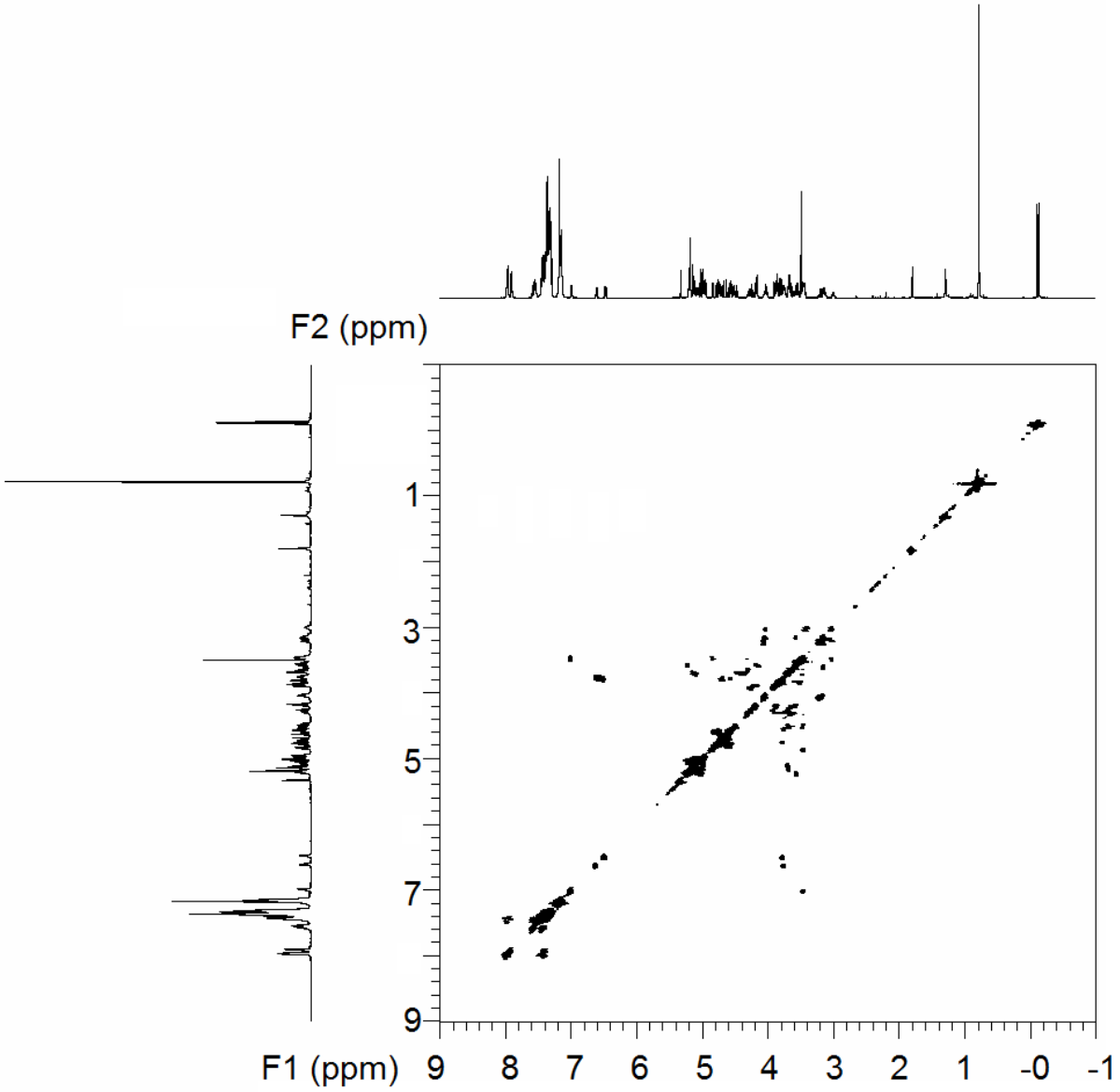

**Figure 3.43.** $^{1}H$–$^{13}C$ gHMQC of compound **26** (500 MHz, $CDCl_3$)

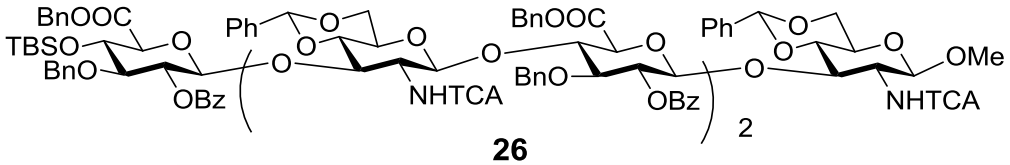


**26**

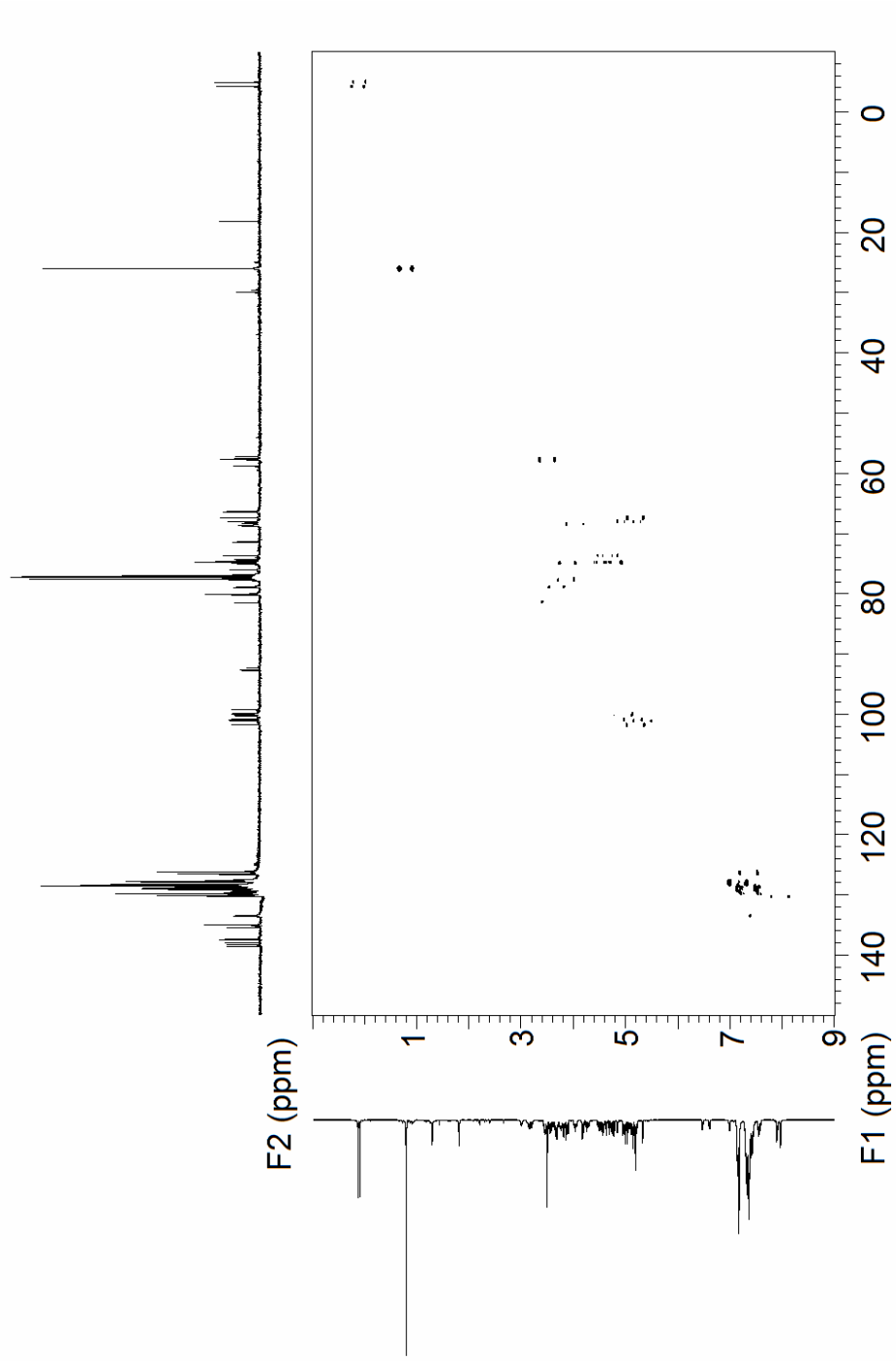

**Figure 3.44.** $^{1}H–^{13}C$ gHMQC (without $^{1}H$ decoupling) of compound **26** (500 MHz,$CDCl_3$)

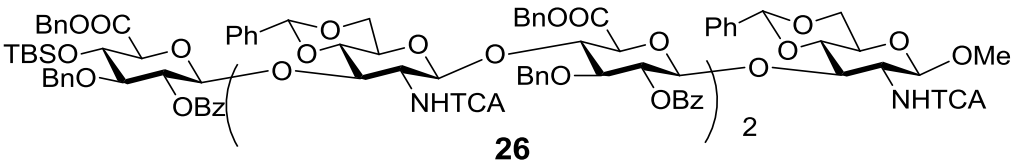


**26**

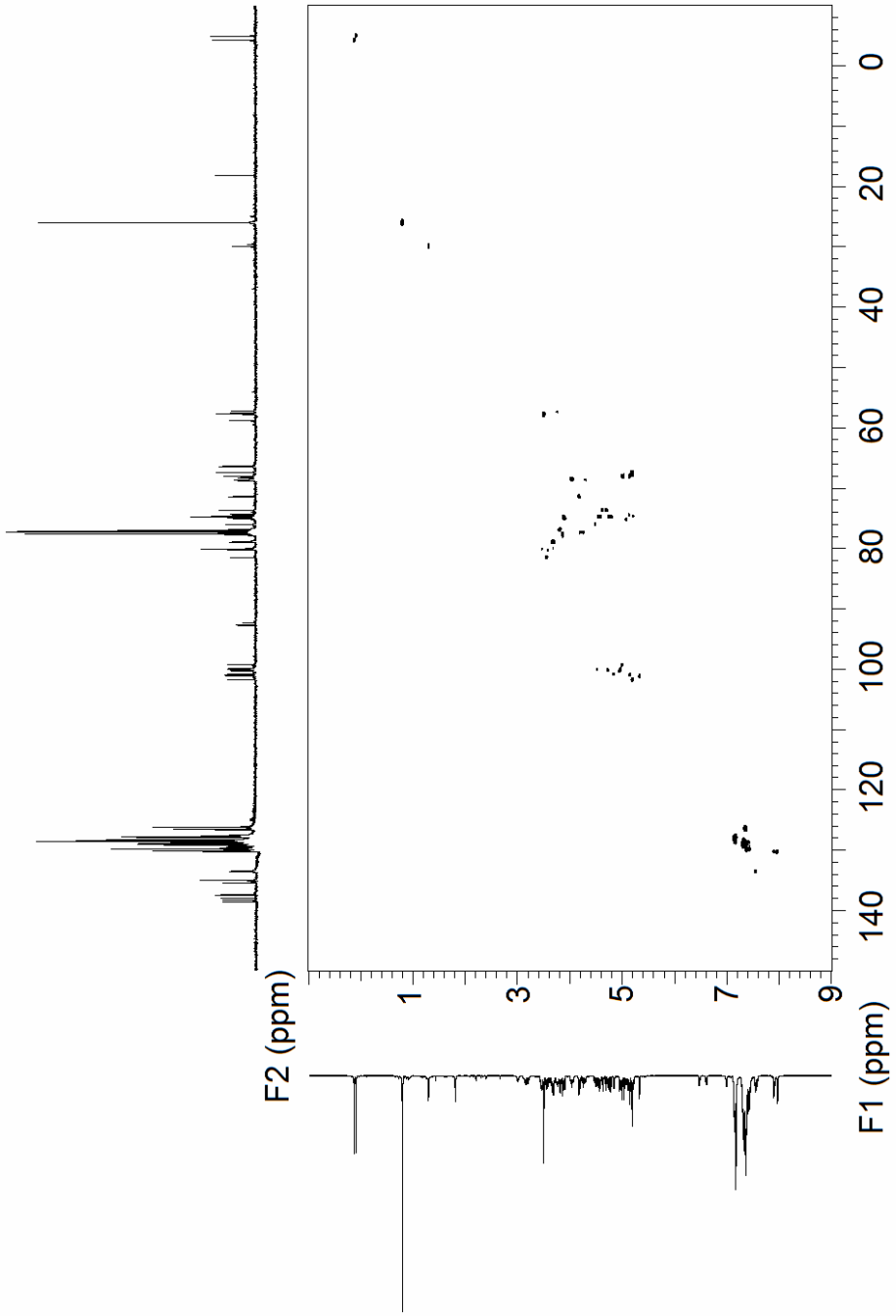

**Figure 3.45.** $^{1}H–^{13}C$ gHMBC of compound **26** (500 MHz, $CDCl_3$)

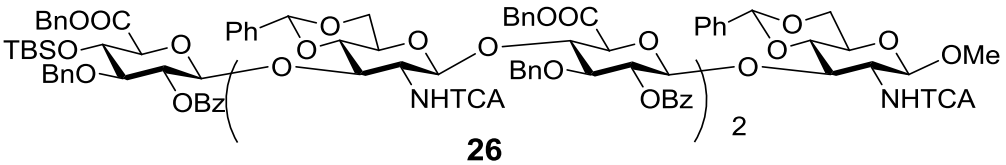


**26**

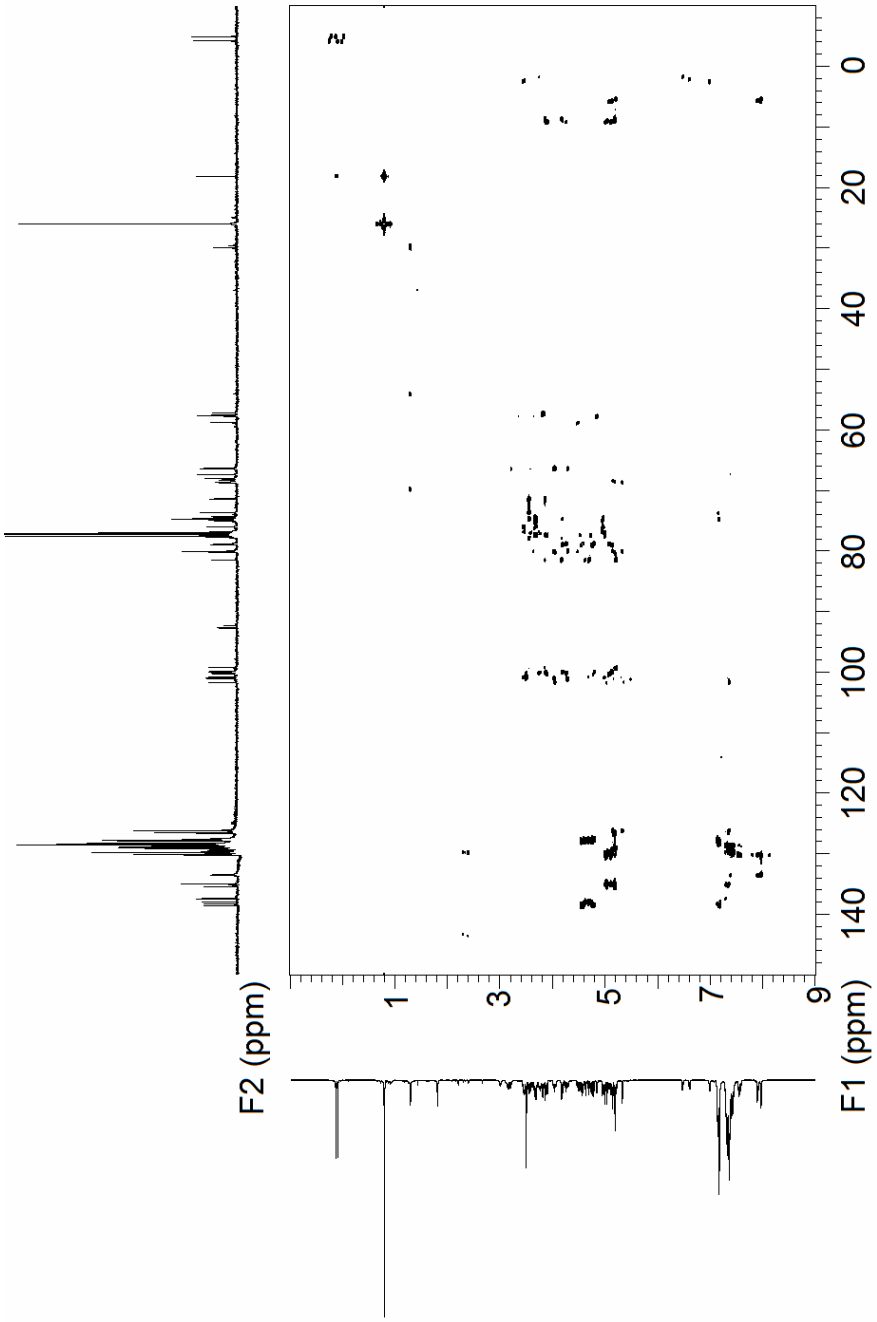

**Figure 3.46.** $^{1}$H-NMR of compound **27** (500 MHz, $CDCl_3$)

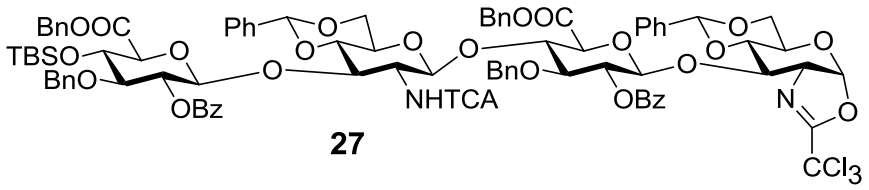


**27**

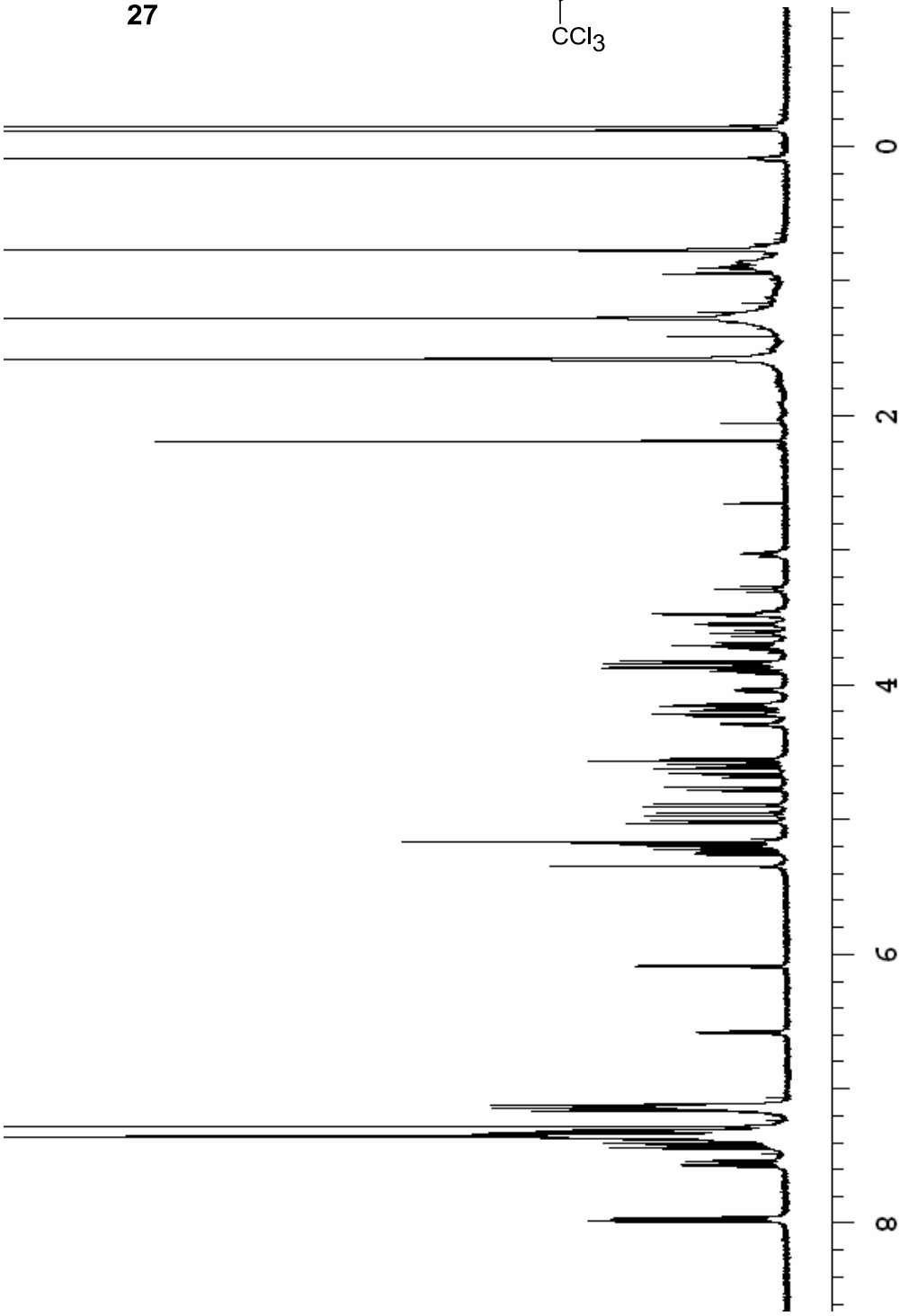

**Figure 3.47.** $^{13}$C-NMR of compound **27** (125 MHz, $CDCl_3$)

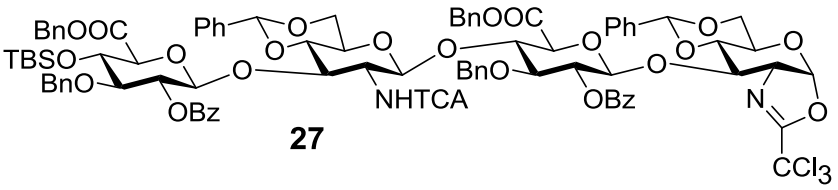


**27**

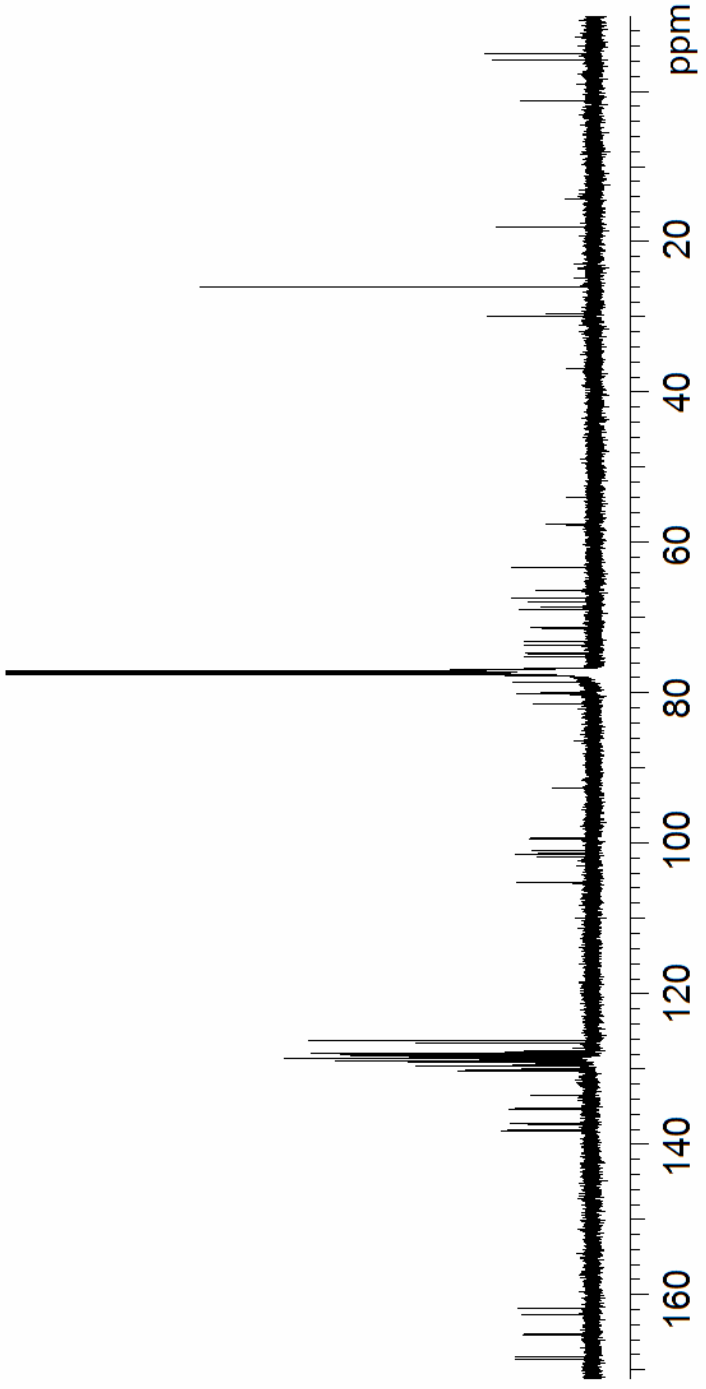

**Figure 3.48.** $^{1}H–^{1}H$ gCOSY of compound **27** (500 MHz, $CDCl_3$)

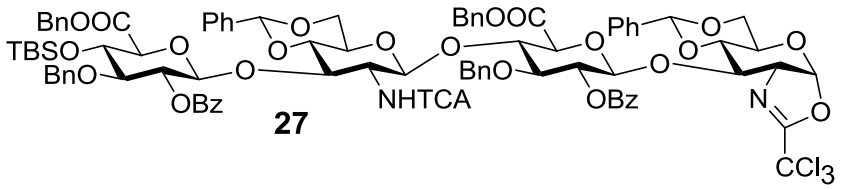


**27**

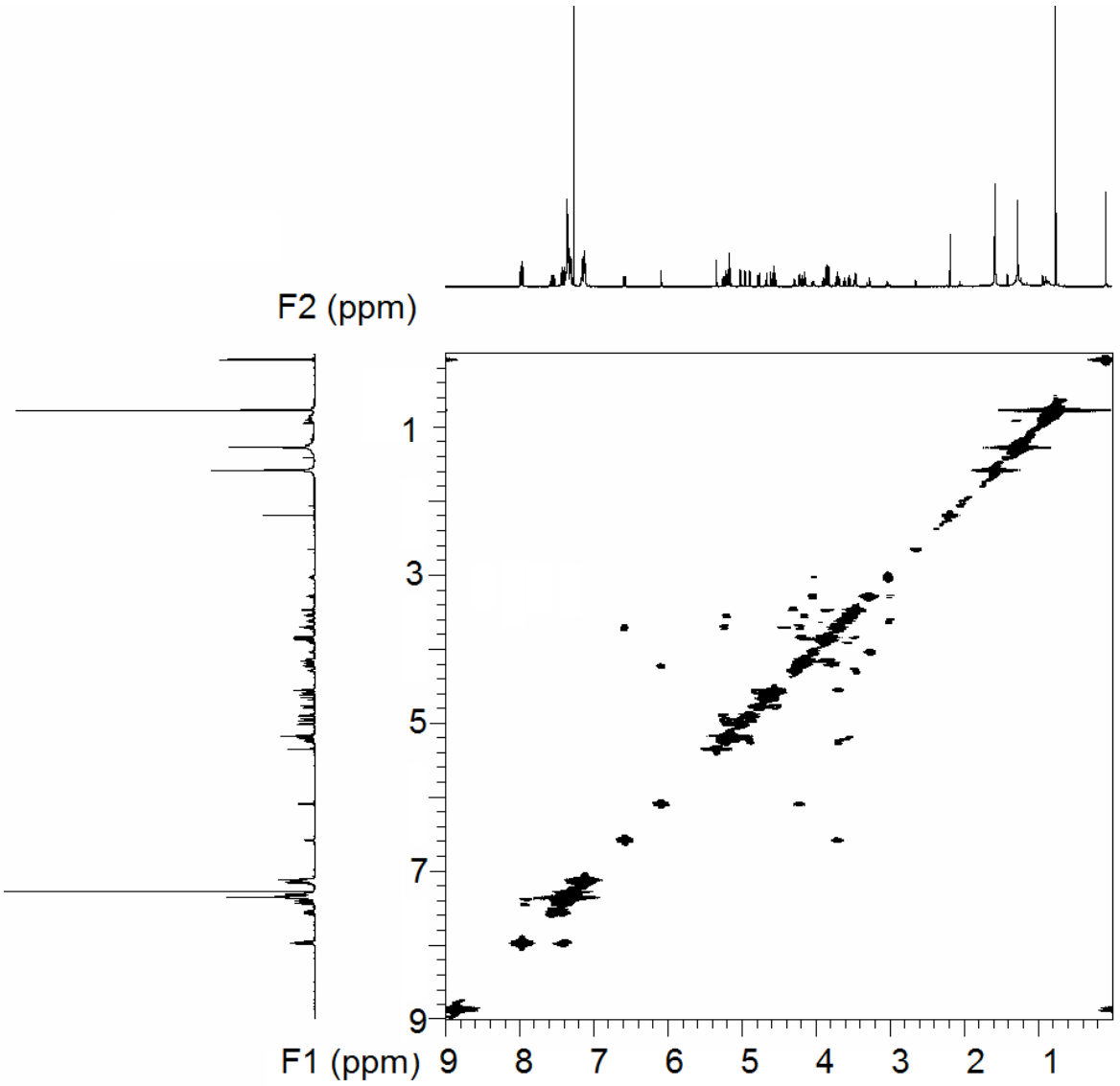

**Figure 3.49.** $^{1}H$–$^{13}C$ gHMQC of compound **27** (500 MHz, $CDCl_3$)

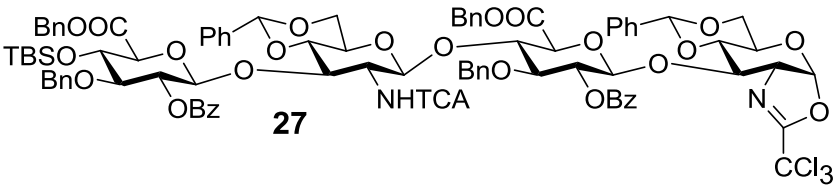


**27**

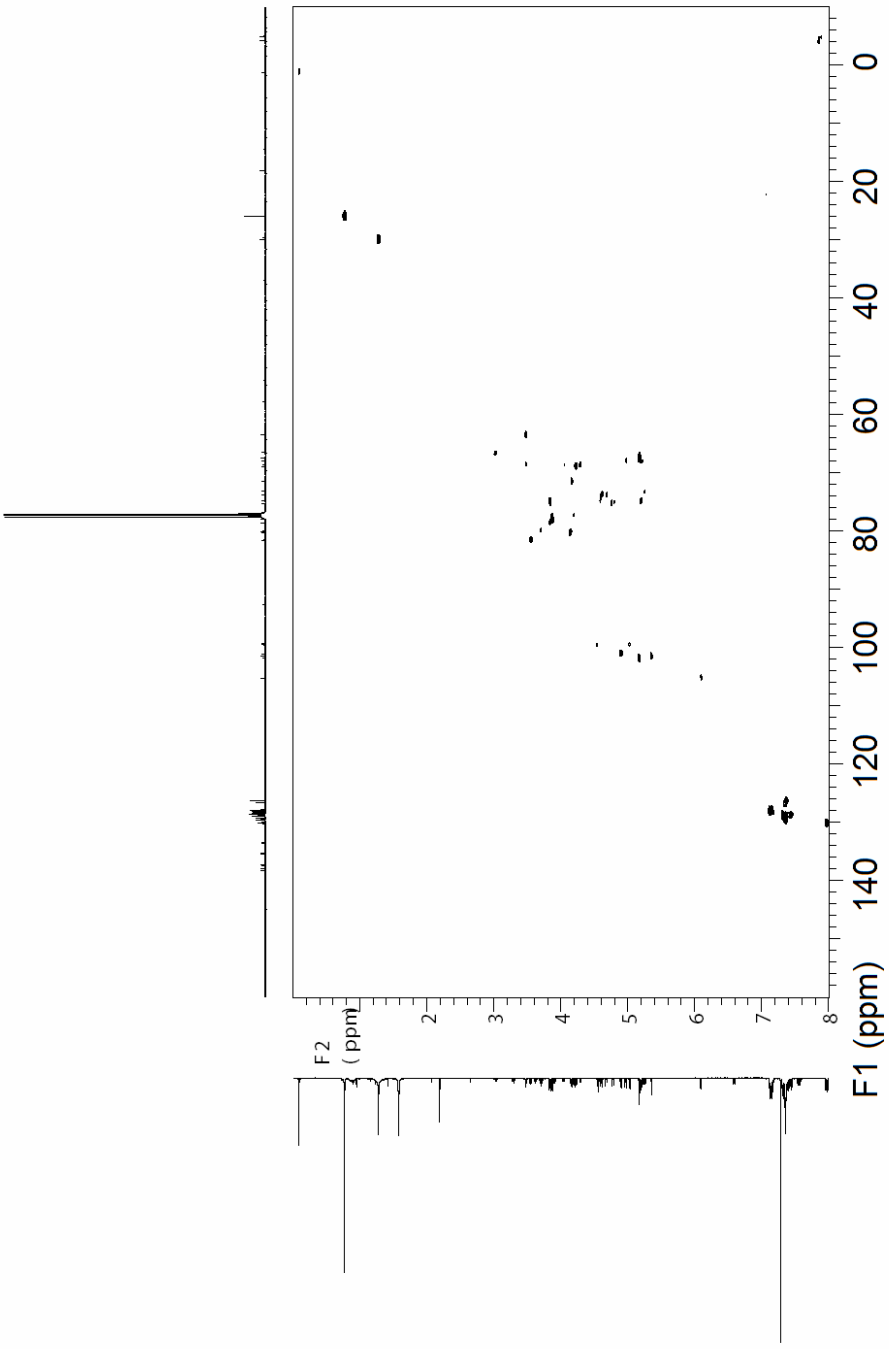

**Figure 3.50.** $^{1}$H-NMR of compound **28** (500 MHz, $CDCl_3$)

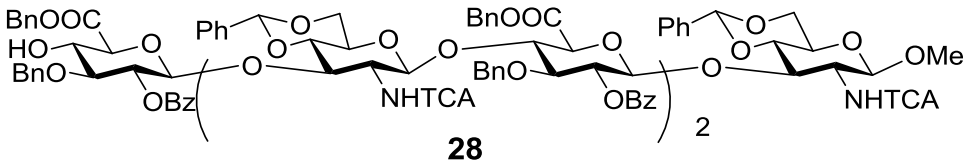


**28**

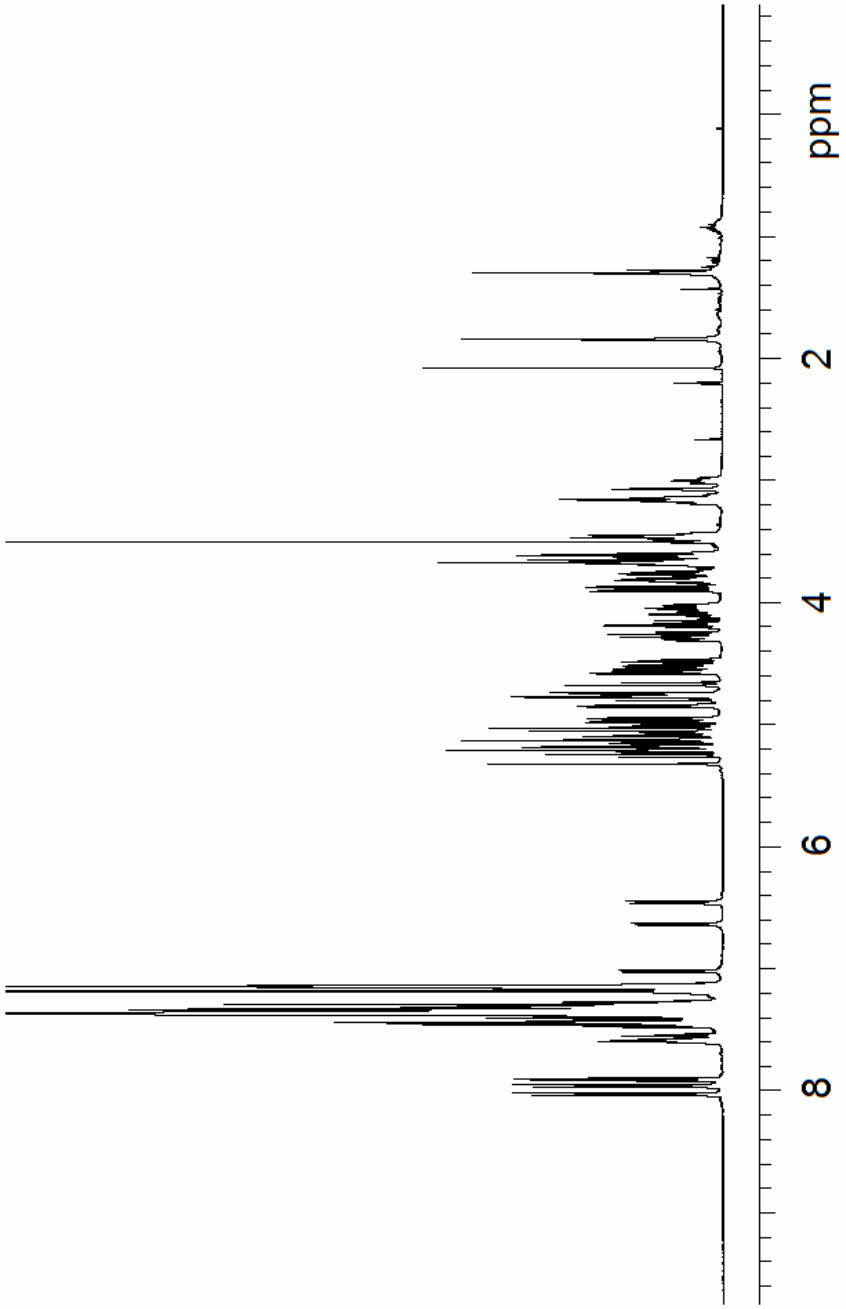

**Figure 3.51.** $^{13}$C-NMR of compound **28** (125 MHz, $CDCl_3$)

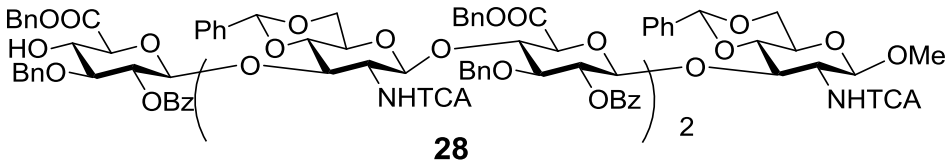


**28**

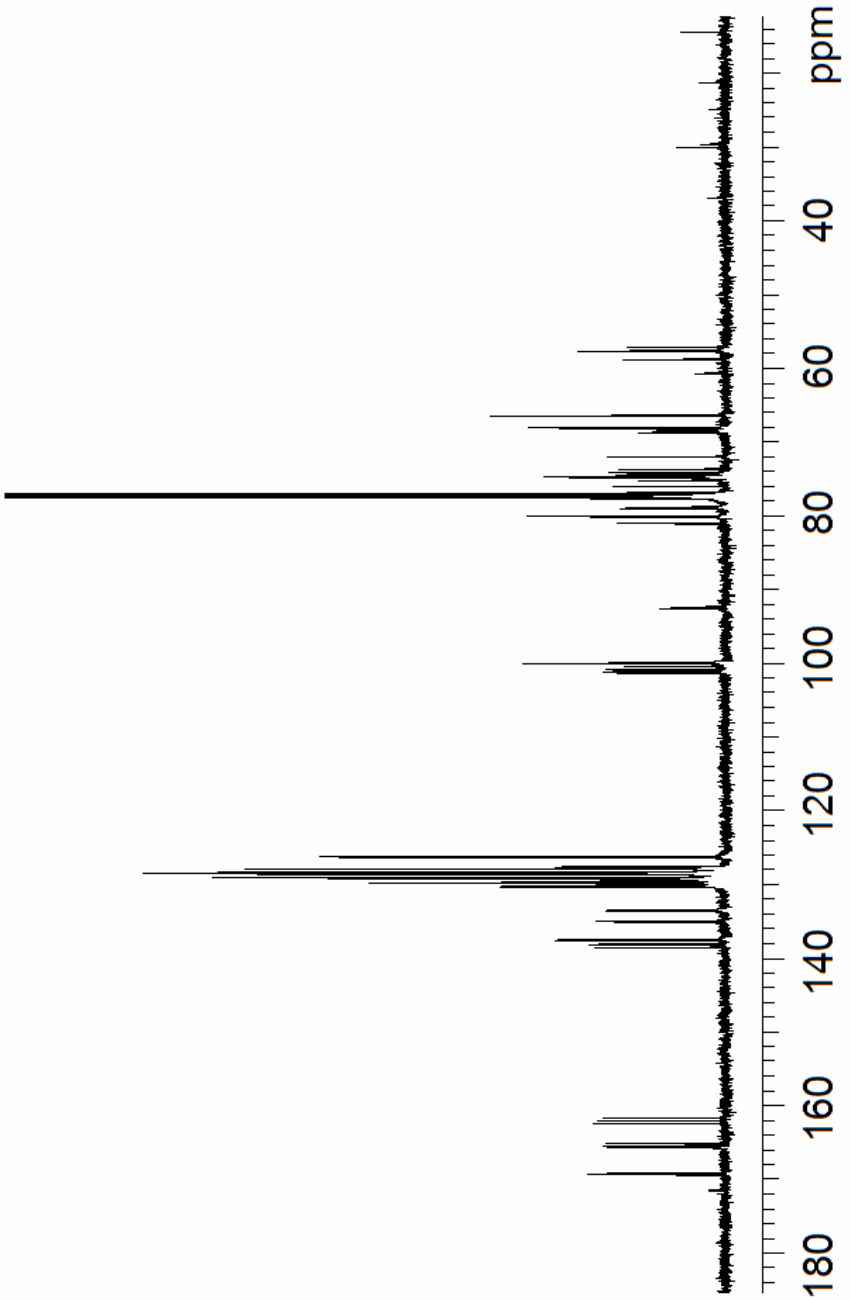

**Figure 3.52.** $^{1}H–^{1}H$ gCOSY of compound **28** (500 MHz, $CDCl_3$)

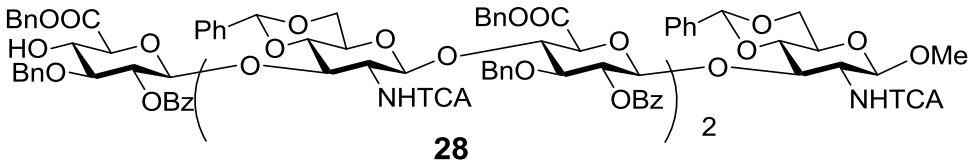


**28**

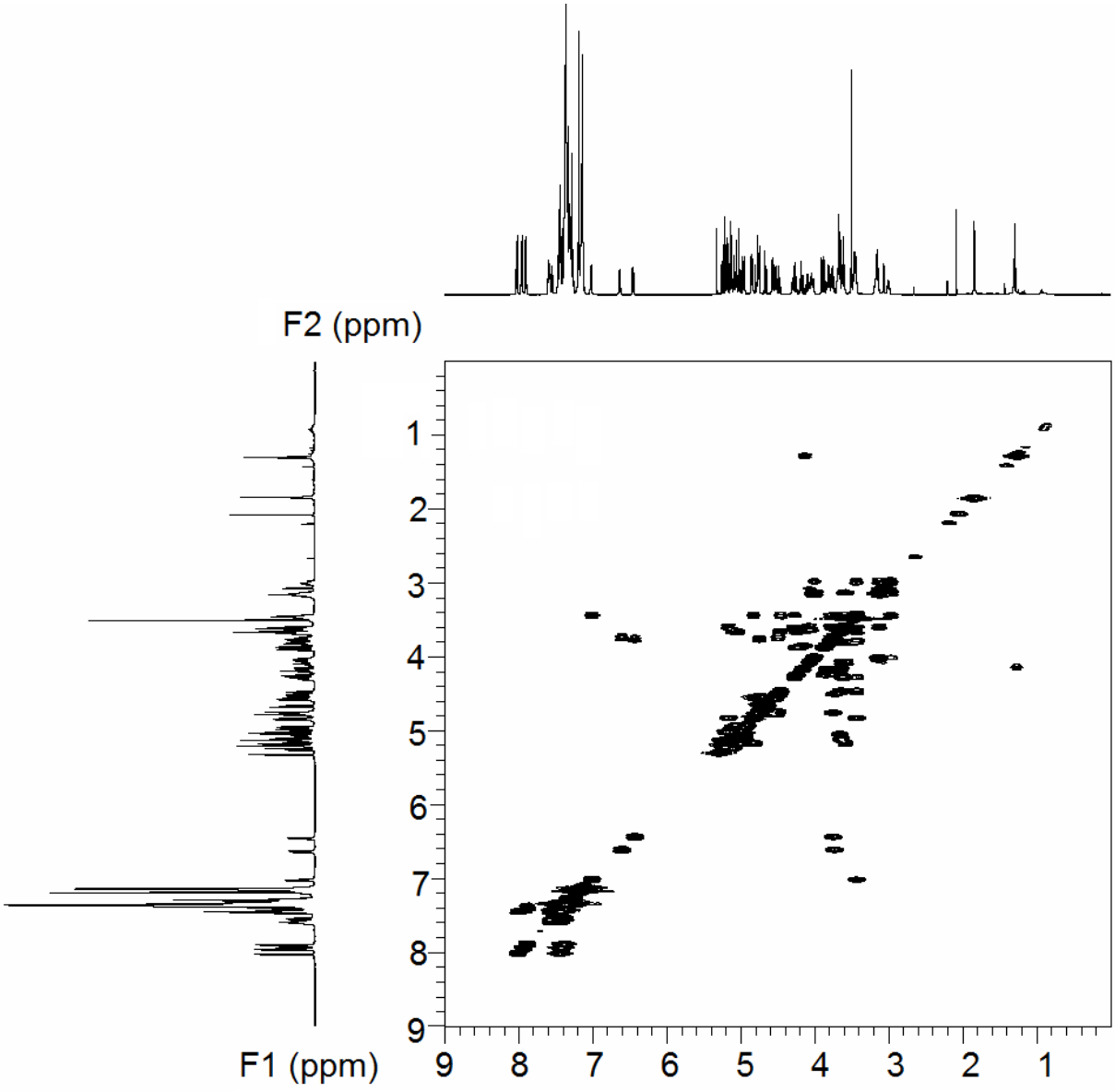

**Figure 3.53.** $^{1}H$–$^{13}C$ gHMQC of compound **28** (500 MHz, $CDCl_3$)

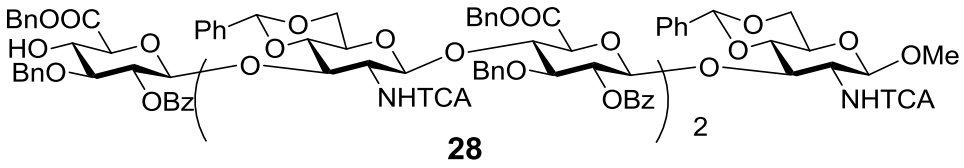


**28**

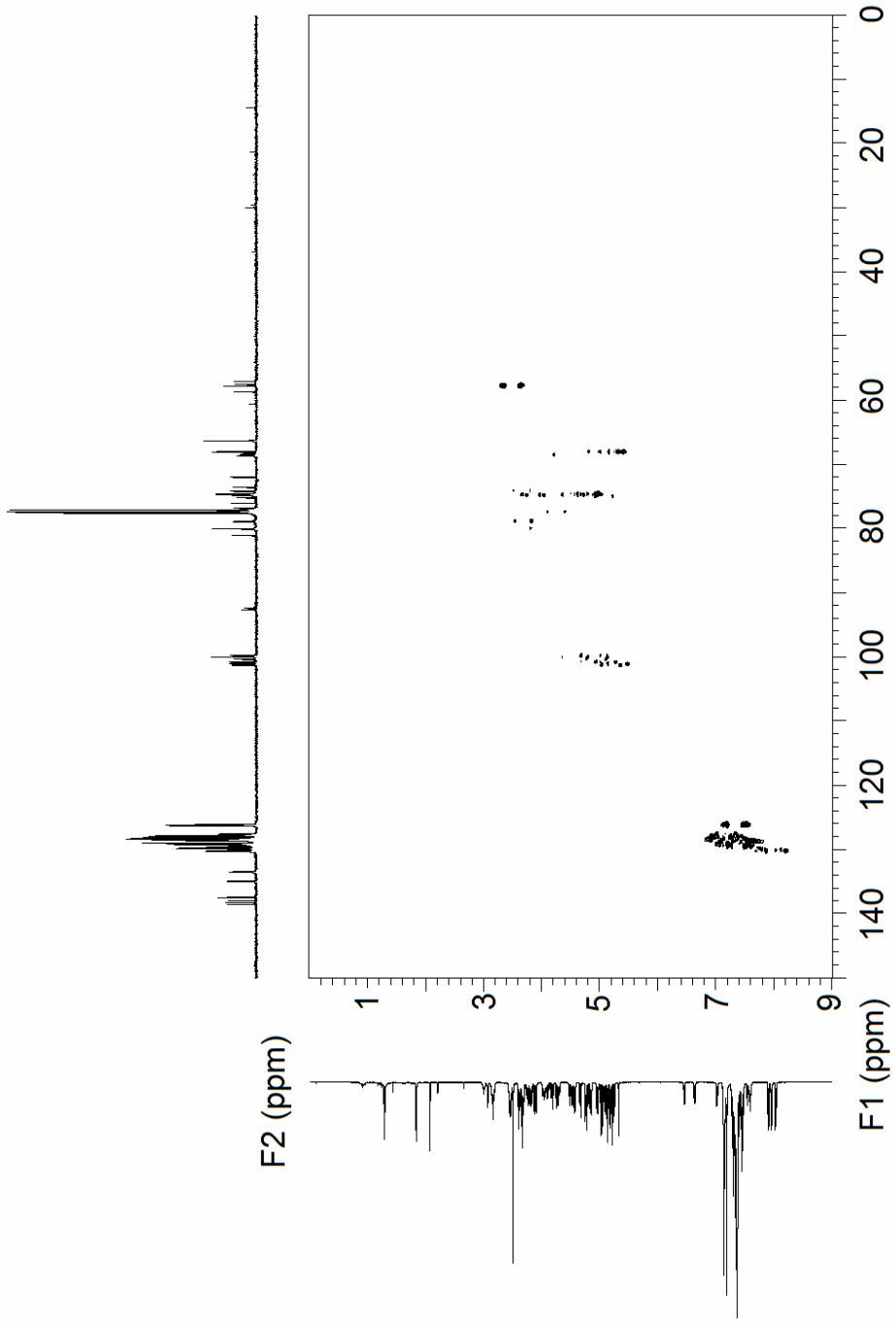

**Figure 3.54.** $^{1}H–^{13}C$ gHMQC (without $^{1}H$ decoupling) of compound **28** (500 MHz,$CDCl_3$)

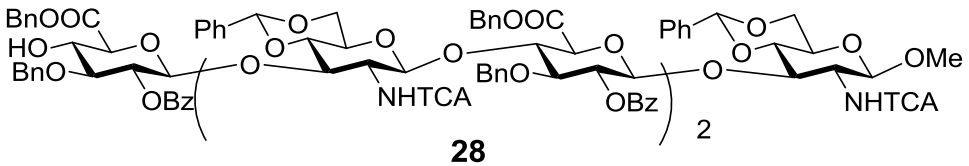


**28**

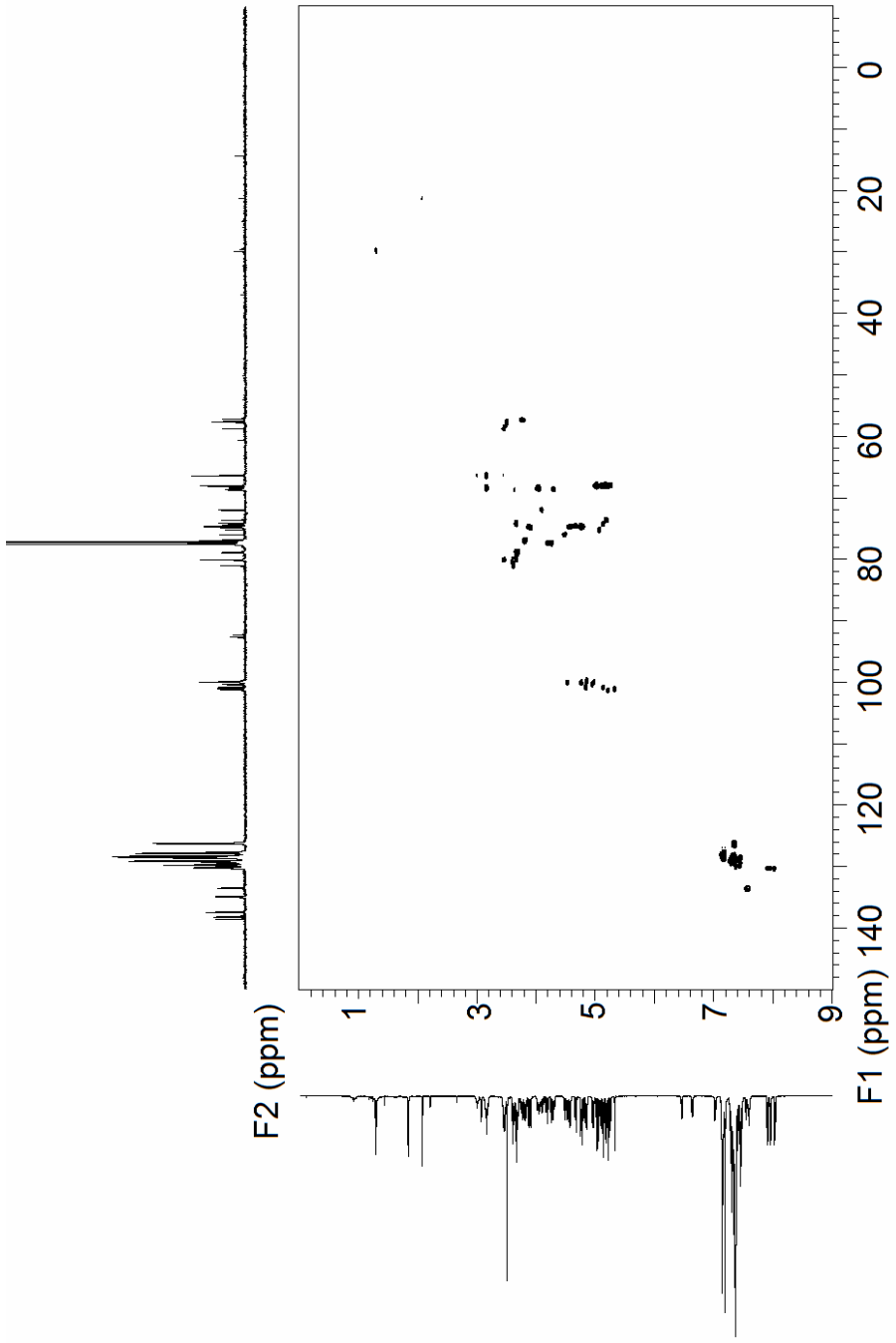

**Figure 3.55.** $^{1}H$–$^{13}C$ gHMBC of compound **28** (500 MHz, $CDCl_3$)

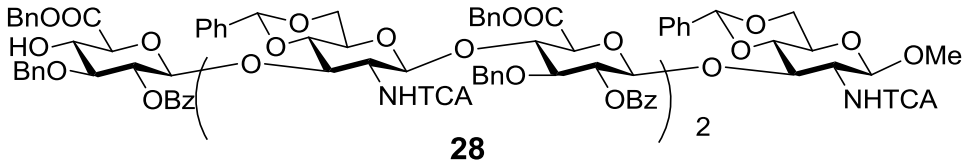


**28**

..

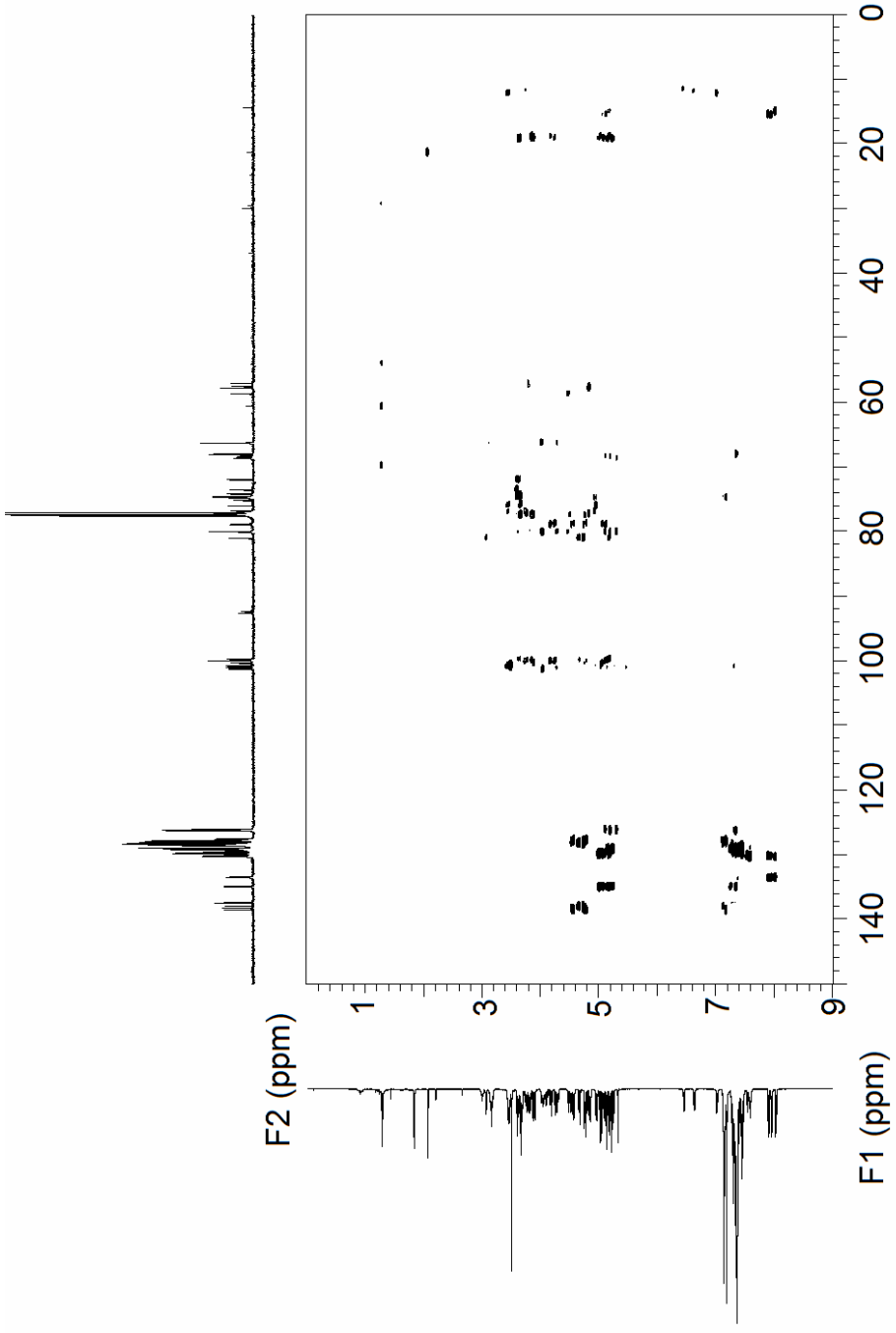

## References

## References


1. Aruffo, A., CD44: One ligand, two functions. *J Clin Invest* **1996,** *98*, 2191-2192.

2. DeGrendele, H. C.; Estess, P.; Picker, L. J.; Siegelman, M. H., CD44 and its ligand hyaluronate mediate rolling under physiologic flow: A novel lymphocyte-endothelial cell primary adhesion pathway. *J Exp Med* **1996,** *183*, 1119-1130.

3. Jalkanen, S.; Bargatze, R. F.; de los Toyos, J.; Butcher, E. C., CD44 and hyaluronan dependent rolling interactions of lymphocytes on tonsillar stroma. *J Cell Biol* **1987,** *105*, 983–990.

4. Jiang, D.; Liang, J.; Fan, J.; Yu, S.; Chen, S.; Luo, Y.; Prestwich, G. D.; Mascarenhas, M. M.; Garg, H. G.; Quinn, D. A.; Homer, R. J.; Goldstein, D. R.; Bucala, R.; Lee, P. J.; Medzhitov, R.; Noble, P. W., Regulation of lung injury and repair by toll-like teceptors and hyaluronan. *Nat Med* **2005,** *11*, 1173-1179.

5. Misra, S.; Ghatak, S.; Zoltan-Jones, A.; Toole, B. P., Regulation of multidrug resistance in cancer cells by hyaluronan. *J Biol Chem* **2003,** *278*, 25285-25288.

6. Ghatak, S.; Misra, S.; Toole, B. P., Hyaluronan oligosaccharides inhibit anchorage-independent growth of tumor cells by suppressing the phosphoinositide 3-kinase/Akt cell survival pathway. *J Biol Chem* **2002,** *277* (41), 38013-38020.

7. McKee, C. M.; Penno, M. B.; Cowman, M.; Bao, C.; Noble, P. W., Hyaluronan (HA) gragments induce chemokine gene expression in alveolar macrophages. *J Clin Invest* **1996,** *98*, 2403–2413.

8. Tammi, R.; MacCallum, D.; Hascall, V. C.; Pienimäki, J. P.; Hyttinen, M.; Tammi, M., Hyaluronan bound to CD44 on keratinocytes is displaced by hyaluronan decasaccharides and not hexasaccharides. *J Biol Chem* **1998,** *273*, 28878-28888.

9. Asari, A., Novel functions of hyaluronan oligosaccharides. *Glycoforum Hyaluronan Today* **2005**, http://www.glycoforum.gr.jp/science/hyaluronan/hyaluronanE.html.

10. Blatter, G.; Jacquinet, J.-C., The use of 2-deoxy-2-trichloroacetamido-D-glucopyranose derivatives in dyntheses of hyaluronic acid-related tetra-, hexa-, and octa-saccharides having a methyl $\beta$-D-glucopyranosiduronic acid at the reducing end. *Carbohydrate Res* **1996,** *288*, 109-125.

11. Huang, L.; Huang, X., Highly efficient syntheses of hyaluronic acid oligosaccharides. *Chem Eur J* **2007,** *13*, 529-540.

12. Zeng, Y.; Wang, Z.; Whitfield, D.; Huang, X., Installation of electron donating protective groups, a strategy for glycosylating unreactive thioglycosyl acceptors using the pre-activation based glycosylation method. *J Org Chem* **2008,** *73*, 7952-7962.

13. Wuts, P. G. M.; Greene, T. W., *Protective groups in organic synthesis*. 4th ed.; Wiley-Interscience: New York, 2006.

14. Hinklin, R. J.; Kiessling, L. L., *p*-Methoxybenzyl ether cleavage by polymer-supported sulfonamides. *Org Lett* **2002,** *4*, 1131-1133.

15. Sun, B.; Srinivasan, B.; Huang, X., Pre-activation based one-pot synthesis of an $\alpha$-(2,3)-sialylated core-fucosylated complex type bi-antennary *N*-glycan dodecasaccharide. *Chem Eur J* **2008,** *14*, 7072-7081.

16. Halkes, K. M.; Slaghek, T.; Hypponen, T. K.; Kruiskamp, P. H.; Ogawa, T.; Kamerling, J. P.; Vliegenthart, J. F. G., Synthesis of hyaluronic-acid-related oligosaccharides and analogues, as their 4-methoxyphenyl glycosides, having *N*-acetyl-$\beta$-D-glucosamine at the reducing end. *Carbohydrate Res* **1998,** *309*, 161-174.

17. Dinkelaar, J.; Gold, H.; Overkleeft, H. S.; Codee, J. D. C.; van der Marel, G. A., Synthesis of hyaluronic acid oligomers using chemoselective and one-pot strategies. *J Org Chem* **2009,** *74*, 4208-4216.

18. Huang, X.; Huang, L.; Wang, H.; Ye, X.-S., Iterative one-pot oligosaccharide synthesis. *Angew Chem Int Ed* **2004,** *43*, 5221-5224.

19. Crich, D.; Smith, M.; Yao, Q.; Picione, J., 2,4,6-Tri-*tert*-butylpyrimidine (TTBP): A cost effective, readily available alternative to the hindered base 2,6-Di-*tert*-butylpyridine and its 4-substituted derivatives in glycosylation and other reactions. *Synthesis* **2001**, 323-326.

20. Donohoe, T. J.; Logan, J. G.; Laffan, D. D. P., Trichloro-oxazolines as activated donors for aminosugar coupling. *Org Lett* **2003,** *5*, 4995-4998.

21. Sherman, A. A.; Yudina, O. N.; Mironov, Y. V.; Sukhova, E. V.; Shashkov, A. S.; Menshov, V. M.; Nifantiev, N. E., Study of glycosylation with *N*-trichloroacetyl-D-

glucosamine derivatives in the syntheses of the spacer-armed pentasaccharides sialyl lacto-*N*-neotetraose and sialyl lacto-*N*-tetraose, their fragments, and analogues. *Carbohydrate Res* **2001,** *336*, 13-46.

22. Dinkelaar, J.; Codee, J. D. C.; van den Bos, L. J.; Overkleeft, H. S.; van Boom, J. H.; van der Marel, G. A., Synthesis of hyaluronic acid oligomers using $Ph_2SO/Tf_2O$-mediated glycosylations. *J Org Chem* **2007,** *72*, 5737-5742.

# CHAPTER 4

## Design and Synthesis of $HA_5$ Analogues as Potential Inhibitors of CD44-HA Binding

### 4.1. Introduction

HA is a non-sulfated negatively charged linear polysaccharide, which is composed of 2,000-25,000 repeating units of disaccharide: [-D-glucuronic acid-*β*-1→3-*N*-acetyl-D-glucosamine-*β*-1→4-]. Tumor microenvironments contain different type of cells and ECM. HA and HA binding proteins are the major components of ECM[1]. CD44 is the primary receptor for HA. Multivalent HA-CD44 interactions induce direct and indirect interactions with RTKs including ErbB2 and EGFR, and non-receptor kinases of Src family or Ras family GTPases. Adaptor proteins such as Vav2, Grb2, and Gab-1 mediate the formation of the signaling complex and mediate the interaction of CD44 with upstream effectors such as RhoA, Rac1 and Ras, which eventually influence downstream MAPK and PI3K/Akt signaling pathways[2-4]. The above signaling pathways promote tumor cell invasiveness, proliferation, survival and MDR[5-6].

Multivalent HA-CD44 interactions are required for formation of constitutive signaling complexes. Replacement of the multivalent interactions with monovalent interactions by the treatment with sHA causes disassembly of constitutive signaling complexes and attenuated signaling pathway[2, 7-10]. These finally led to the inhibition of tumor cell proliferation and MDR.

Other than sHAs, the first reported CD44-HA inhibitors are **F-16438s** isolated from

fungus strain SANK 30502 by Takahashi's group in 2006. The $IC_{50}$ values were reported in the μM range[7-8]. A year later, the Takahashi's group reported another inhibitor, **F-19848A** from fungus strain SANK 20204, with $IC_{50}$ values in the μM range[9]. However none of those $IC_{50}$ values was compared with sHAs in the same inhibitory assay, and how those inhibitors bind CD44 was not characterized.

**Figure 4.1.** Inhibitors reported by Takahashi's group

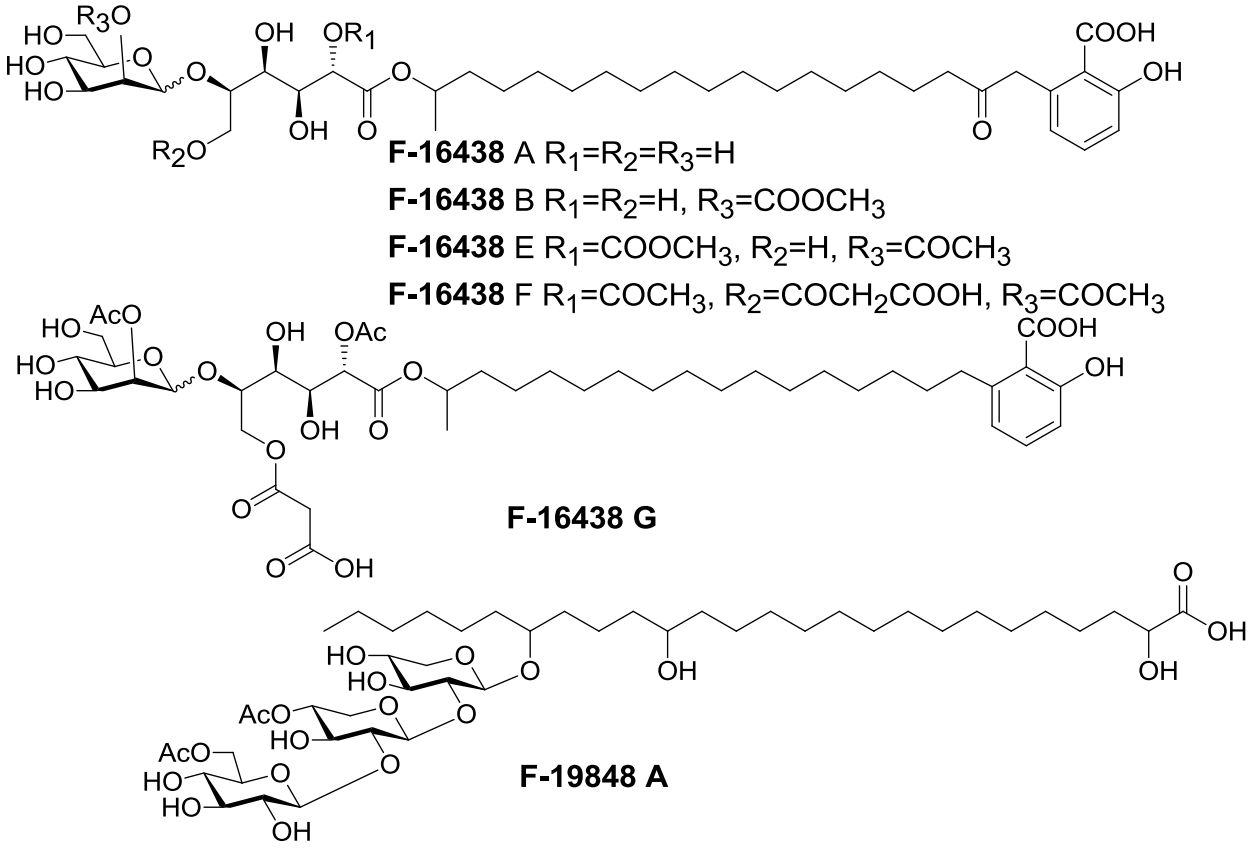


In 2007, Jackson's group reported the co-crystal structure of the CD44 hyaluronan binding domain and $HA_8$[10]. In the co-crystal structure, $HA_8$ binds to a shallow groove and the interactions are dominated by hydrogen bonds and hydrophobic interactions. The hydrophobic interactions are from sugar rings from GlcNAc4 to GlcUA7

and the methyl group in GlcNAc6. The H-bonds are from GlcUA5 to GlcNAc8 as summarized in **Figure 4.2**[10]. That $HA_{10}$ (Kd = 61 μM[10]) binds slightly stronger than $HA_8$ (Kd = 125 μM[10]) can not be explained by the co-crystal structure, as the terminal GlcUA1, GlcNAc2 and GlcUA3 do not show much interaction with the protein.

**Figure 4.2.** H-bonds in CD44-$HA_8$ co-crystal structure

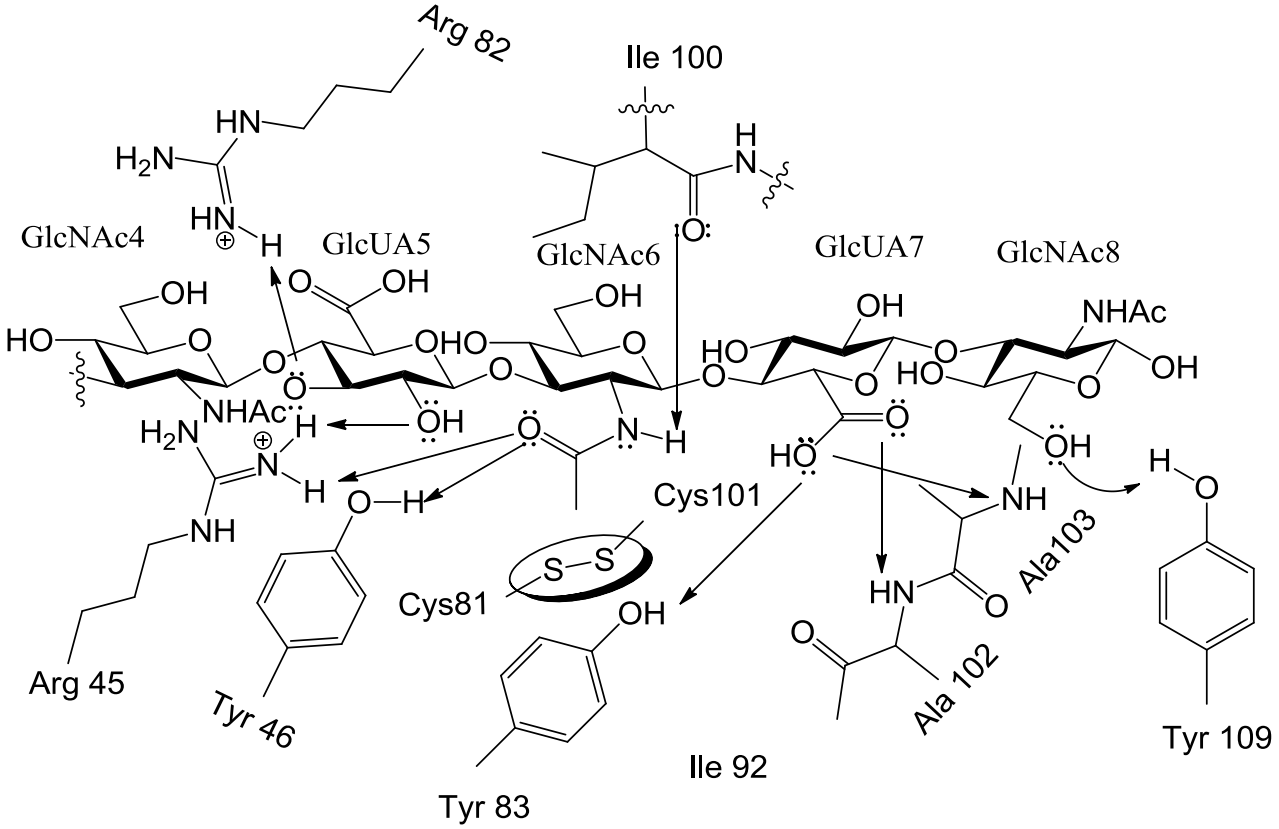


The other factor that may play a role is HA dynamics. The HA polymer has been characterized as stiffened worm-like coil in solution. The presence of intramolecular H-bonds in aqueous solution leads to stiffening of the HA polymer[11]. In the case of oligomers, conformations become more rigid as the chain length is increased due to the terminal rings being less constrained by having fewer intramolecular H-bonds. The more

dynamical nature generate a greater entropic penalty which might explain the affinity difference between $HA_{10}$ and $HA_8$[11-16].

Nilsson's group accomplished beautiful work on the discovery of Galectin-3 ligands **2** (Kd = 0.88 μM), which bound 76 times stronger than the native ligand **1** (Kd = 0.88 μM) (**Figure 4.3**)[17-18]. The co-crystal structure of Galectin-3 and analogue **2** showed that the affinity enhancement came from the arginine-arene interaction between Arg 144 and the aromatic group in analogue **2** (**Figure 4.4**)[18]. Based on this discovery, Nilsson and co-workers addressed the second arginine-arene interaction between Arg186 and another aromatic group (**Figure 4.3**), and found ligand **3** (Kd = 46 nM), which bound 1457 times stronger than ligand **1**[19]. Paulson and co-workers reported the a MAG ligand **5** (**Figure 4.5**), which bound 83 times stronger than ligand **4**[20]. Docking results suggested that the increased affinity is due to a stacking interaction of the *para*-fluorobenzyl moiety with Arg118. Inspired by their work, our goal was is to add extra functionality for approaching extra hydrophobic interaction with the hydrophobic pocket formed by tyrosine 46 (Tyr46), Tyr83, isoleucine 111 (Ile111), serine 114 (Ser114), threonine 116 (Thr116) and Tyr119 (shown orange in **Figure 4.6**).

**Figure 4.3.** Ligands of Galectin-3

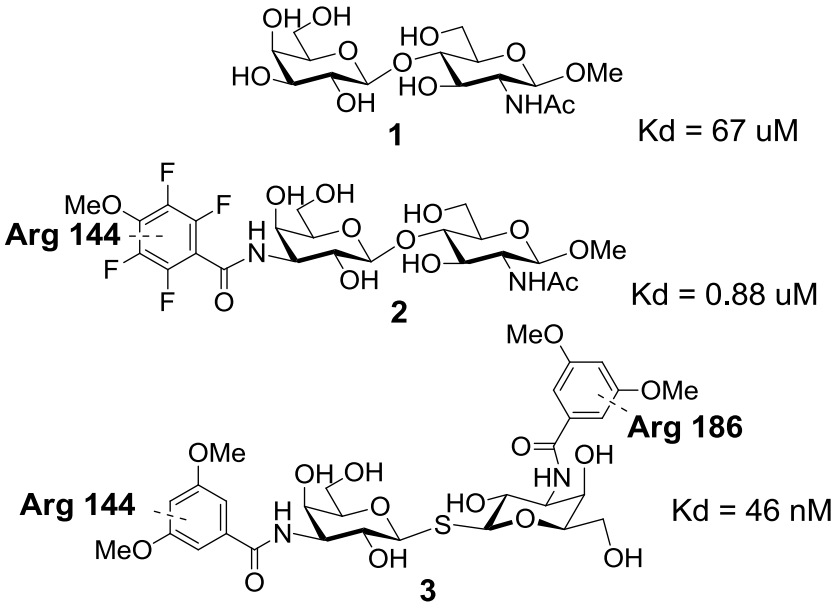


**Figure 4.4.** Co-crystal structure of galectin-3 and analogue **2**. Adapted with permission from Ref 18. **Copyright 2005 American Chemical Society**.

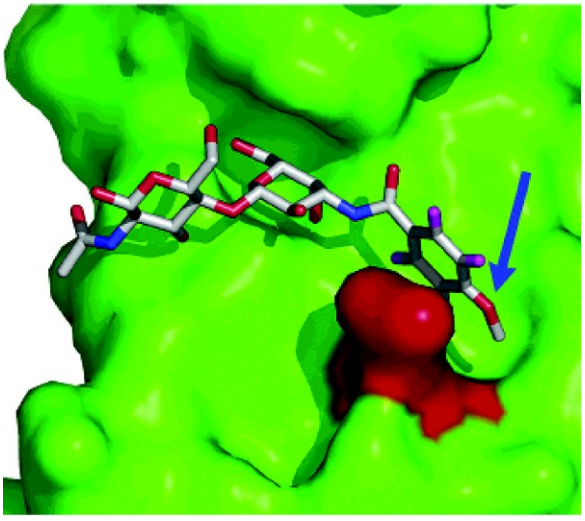

**Figure 4.5.** MAG Ligands

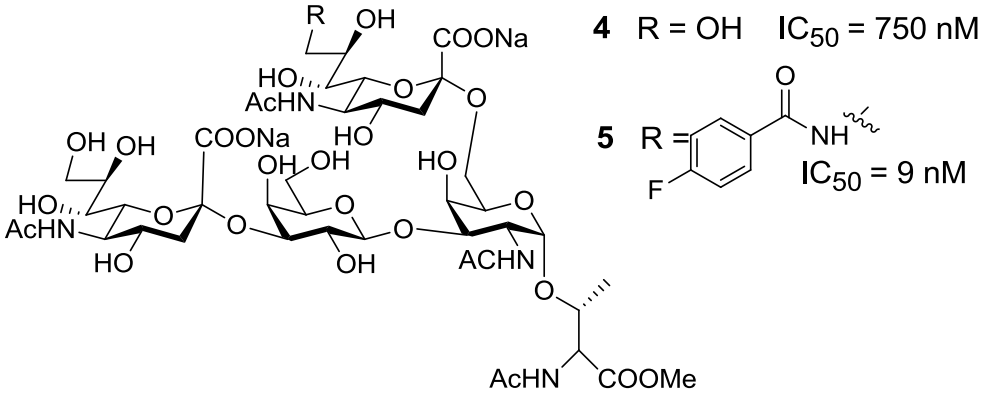


**Figure 4.6.** The hydrophobic pocket in CD44-$HA_8$ co-crystal structure

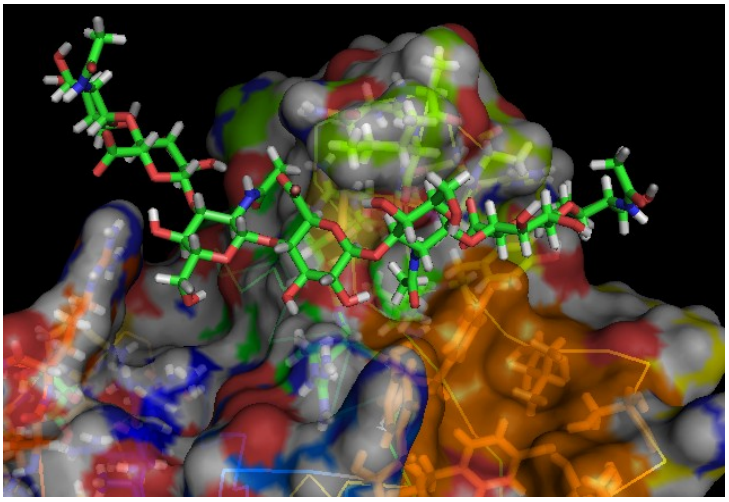

## 4.2. Results and Discussion

### 4.2.1. $HA_2$ Library

#### 4.2.1.1. The Design and Synthesis of $HA_2$ Library

We started with a $HA_2$ library which is synthetically more available than sHA analogues with more sugars. The docking result (**Figure 4.7**) showed that the linker might be too long for directing the aromatic groups into the hydrophobic pocket (colored

in red). Syntheses of the $HA_2$ library proceeded smoothly (**Scheme 4.1**). Coupling monosaccharide **6** and **7** yielded disaccharide **8** in 70% yield. PMB groups in compound **8** were removed by DDQ, and then the primary OH was oxidized to COOH. The benzoyl (Bz) and Phth groups were cleaved by $MeNH_2$, and the exposed OH groups were acetylated. Finally the COOH group was protected as a methyl ester to produce disaccharide **9**. Various hydrophobic functionalities were then conjugated to compound **9** by azide alkyne cycloaddition. After hydrolysis, the hyaluronan disaccharide ($HA_2$) library (Compounds **10** - **16**) was generated.

**Figure 4.7.** Docking results of $HA_2$ library

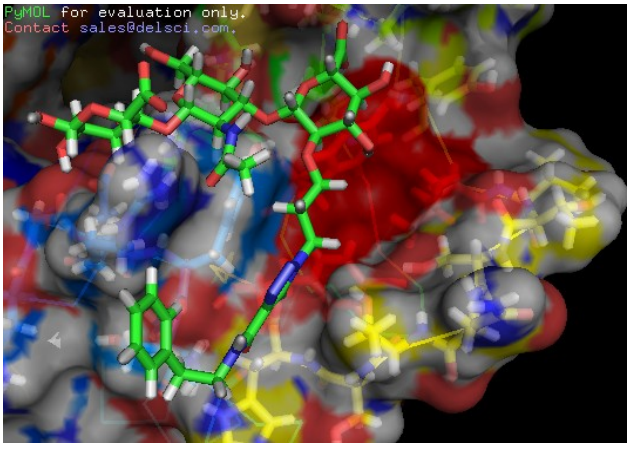

**Scheme 4.1.** The syntheses of $HA_2$ library

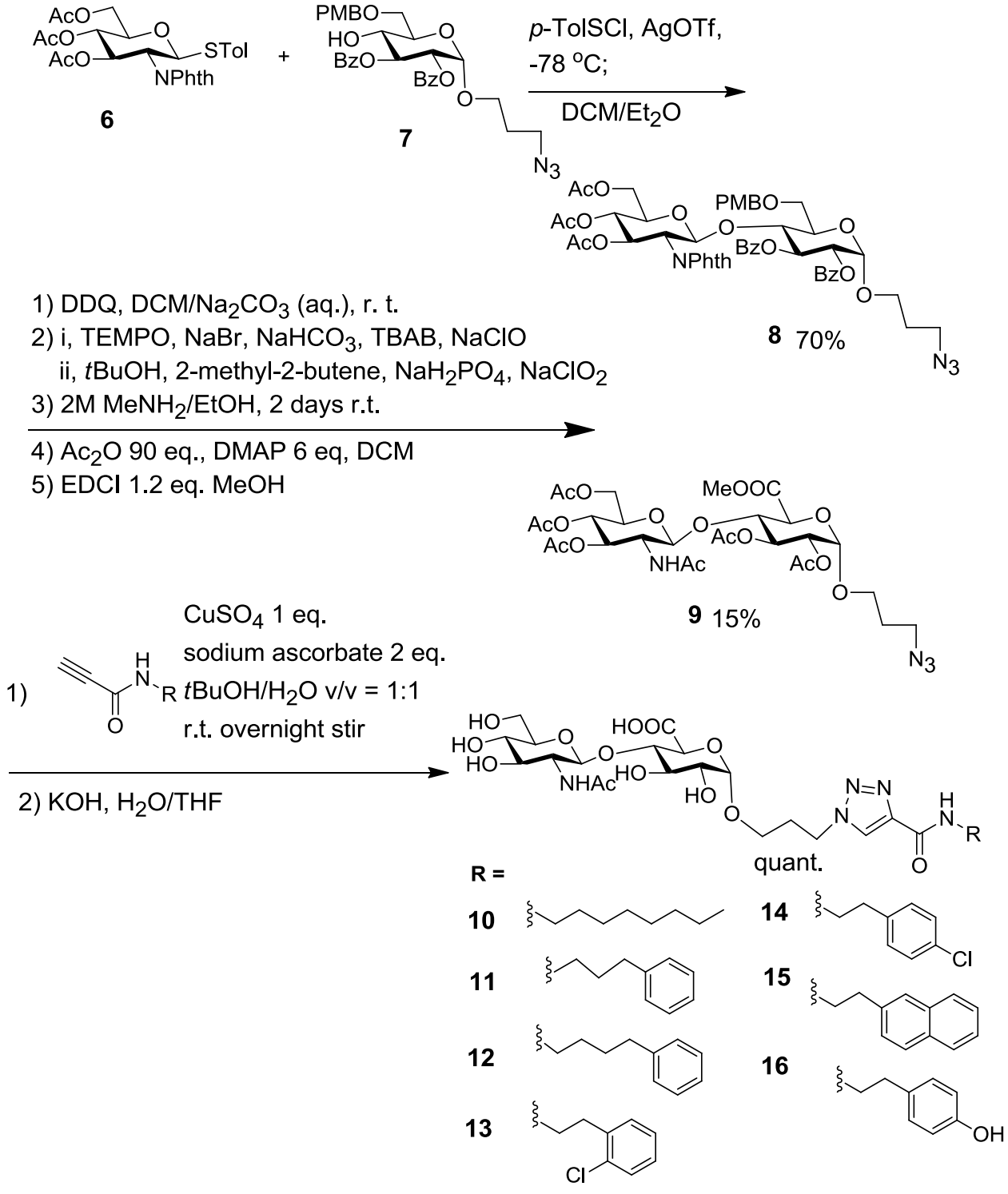


**4.2.1.2. The ELISA**

**Scheme 4.2.** Synthesis of Biotin-HA

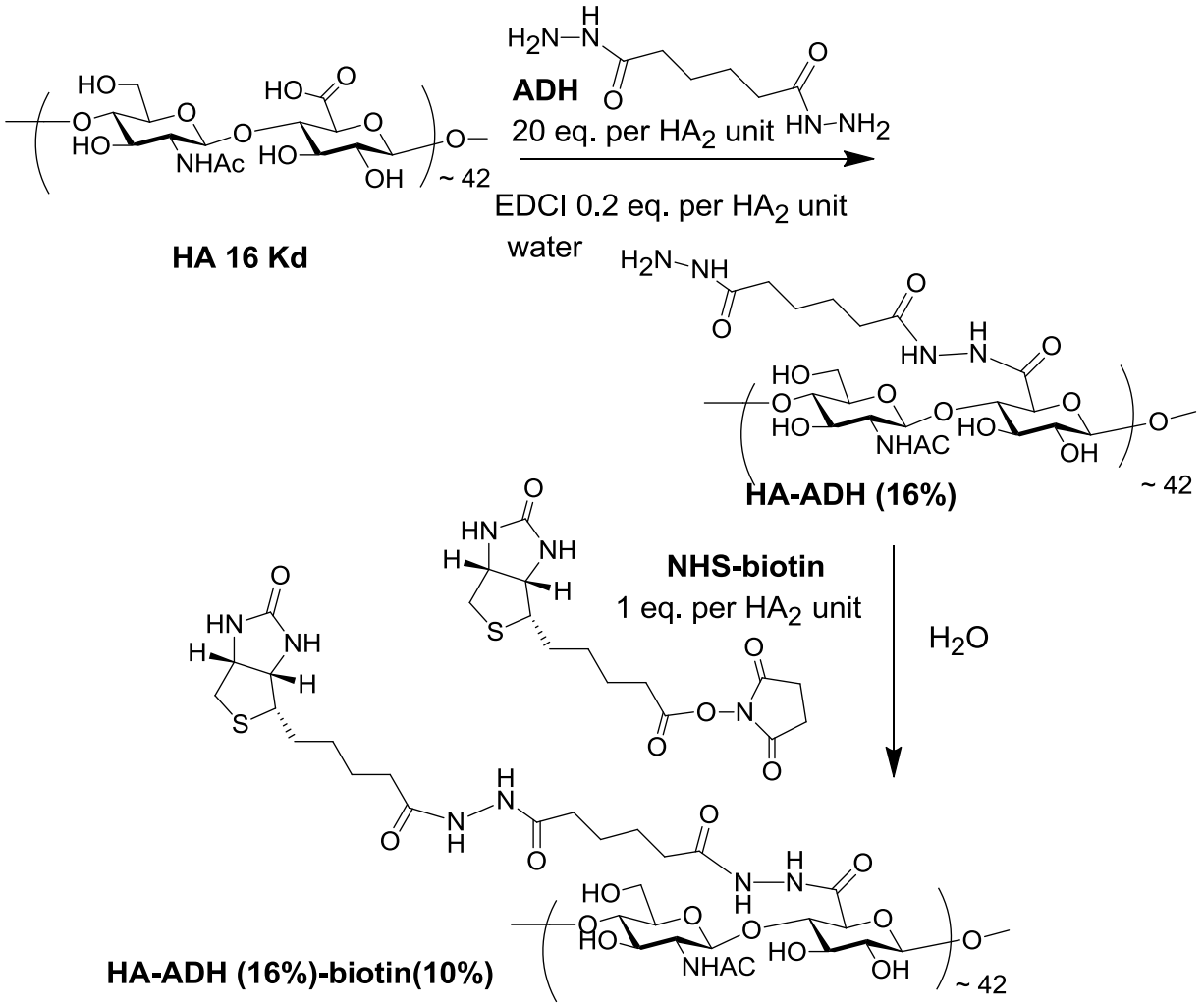


The design of a screening assay for lectin is challenging by their tendency to bind weakly to carbohydrate ligands. An inhibitory ELISA was established for studying the binding affinity of the analogues. First anti-IgG antibody coated 96-well plate was used to catch CD44/IgGFc chimera. Compared to direct coating of the plate with CD44, this xIgG–IgGFc/CD44 layout helps to fully expose the CD44 HA binding domain and reduce the amount of expensive CD44 used. The mixture of biotin-HA and sHA analogues were then added to the plate. Biotin-HA polymer with different percentages of biotin was

synthesized based on Prestwich's work[21]. HA with 10% biotin turned out to be the best for ELISA (**Scheme 4.2**). Too much biotin decreases the binding affinity between HA and CD44, while too little biotin reduces the binding affinity between biotin-HA and avidin-HRP. Finally, avidin conjugated horseradish peroxidase (avidin-HRP) was added to quantify the amount of biotin-HA attached to the CD44.

To test the efficiency of this ELISA method, the inhibitory potency of $HA_8$ was measured (**Figure 4.8**). Since $HA_8$ inhibits the binding between biotin-HA and CD44, when the $HA_8$ concentration increased, less biotin-HA binds to the CD44 coated plate, leading to decreased signal. The $IC_{50}$ of $HA_8$ by this inhibitory ELISA is 136.8 μM.

**Figure 4.8.** $HA_8$ inhibition curve

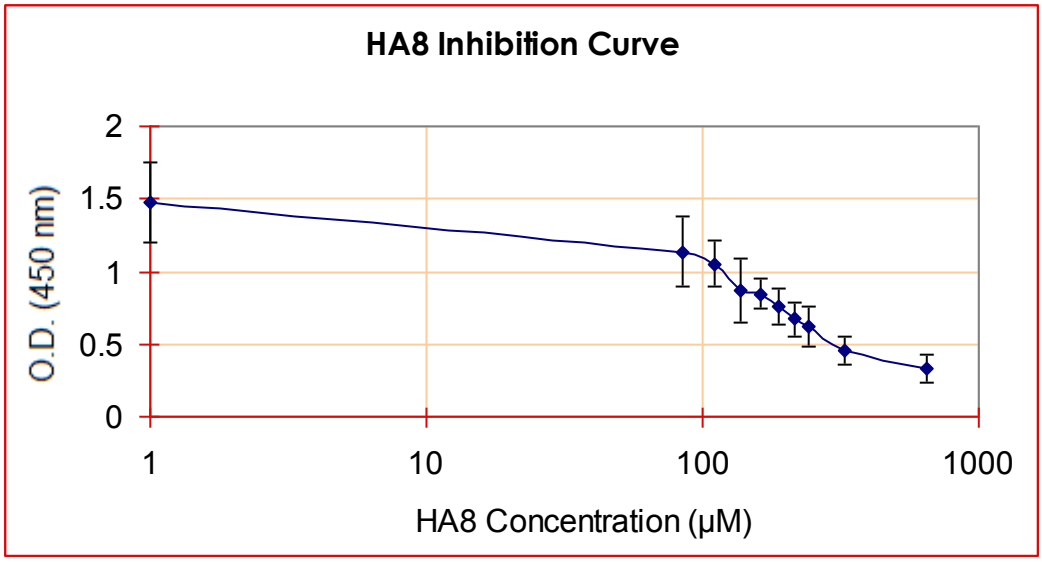


#### 4.2.1.3. Results and Discussion

The results of the inhibition ELISA for compounds **10** - **16** are shown in **Figure 4.9**. **Inhibitor NEG** was the group without HA inhibitor, which was used as minimum inhibition.

**HA 16 kDa** was the group with HA polymer 16 kDa 2.5 μg per well, which was used as maximum inhibition. **HA8 (25 μg)** was the group with 25 μg $HA_8$ per well. **HA4 (200 μg)** was the group with 200 μg $HA_4$ per well. All other groups were measured in the presence of 200 μg compounds **10** - **16** per well. Based on these results, 25 μg per well $HA_8$ and 200 μg per well $HA_4$ could inhibit HA-CD44 binding. However, 200 μg per well compounds **10** - **16** did not show any inhibition to HA-CD44 interaction.

An unexpected result is that compound **10** could obviously increase the signal. To confirm this result, an alternative ELISA method was used. First the plate was coated with HA (from rooster comb) 5μg/well in pH 9.3 buffer at $22^0$C overnight. Then the plate was blocked with 1% bovine serum albumin (BSA) in PBS for 90 min at $37^0$C. Next, the mixture of CD44 and inhibitor was added and the plate was incubated at $37^0$C for 45 min. Then MEM-85, a CD44 monoclonal antibody, 0.1 μg/well was added and the plate was incubated at $22^0$C for 1 hr. Next, anti-mouse IgG Fc-HRP (1x 2000 dilution), which bound MEM-85, was added and the plate was incubated at $22^0$C for 1 hr. Finally TMB solution was added and the plate was read at 450 nm. In this inhibitory ELISA, the wells with inhibitors, which reduce the binding between the HA coated plate and free CD44 protein, would show decreased signals. The inhibitory or enhancive ability of compound **10**, linker **1** and **2** (**Figure 4.11**) were evaluated by this ELISA method. The results are shown in **Figure 4.10**. **Inhibitor NEG** was the group without HA inhibitor, which was used as minimum inhibition. **HA 16 kDa (50 μg)** was the group with HA polymer 16 kDa 50 μg per well, which was used as maximum inhibition. Various amount (1.56 - 200 μg

per well ) of compound **10** were tested, but none of them show any inhibitory or enhancive effects. Various amount (1.5625 - 200 μg per well ) of **linker 1** or **linker 2**, which are parts of compound **10**, were tested as well. **Linker 1** showed moderate inhibitory effect at 100 μg per well, and **linker 2** showed moderate inhibitory effect at 200 μg per well.

In summary, the $HA_2$ library failed to show any inhibitory or enhancive effect on CD44-HA interaction. This result might be attributed to two reasons. Most interactions between sHA and CD44 were missing in $HA_2$ analogues, or our previous docking results indicated that the linker in the $HA_2$ library might be too long for directing the hydrophobic groups into CD44 hydrophobic pocket.

**Figure 4.9.** Inhibition ELISA of compounds **10** - **16**

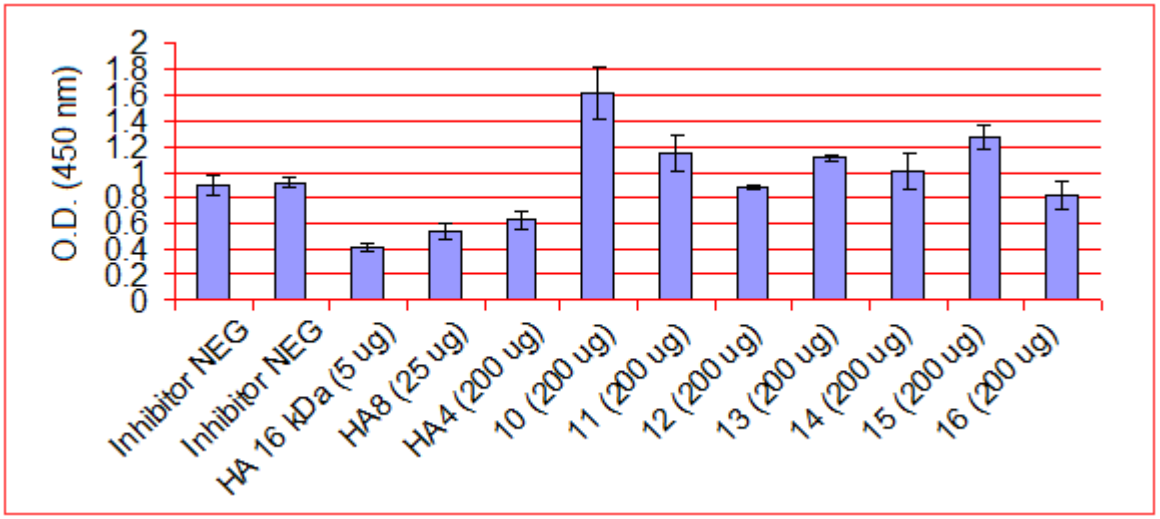

**Figure 4.10.** Alternative Inhibition ELISA of compound **10**, Linker **1** and **2**

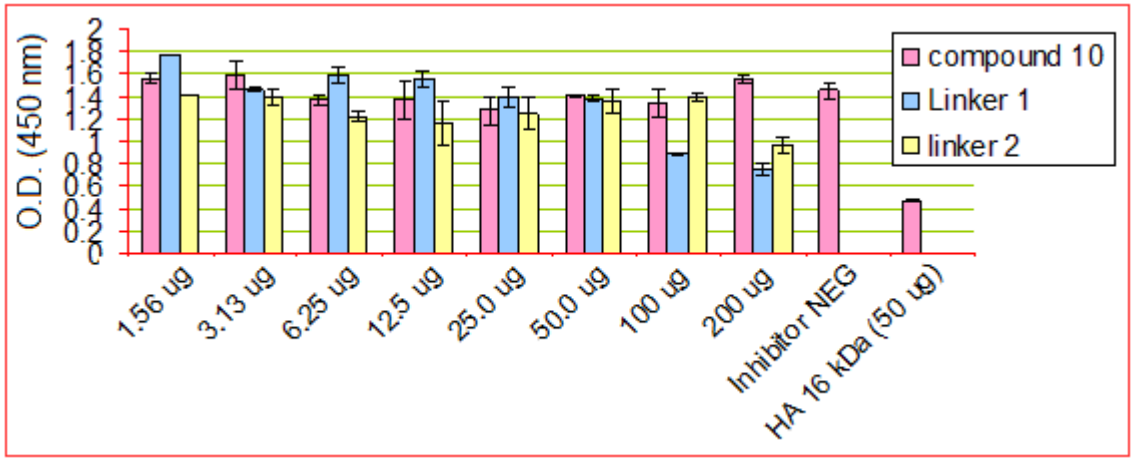


**Figure 4.11.** Compound **10**, Linker **1** and **2**

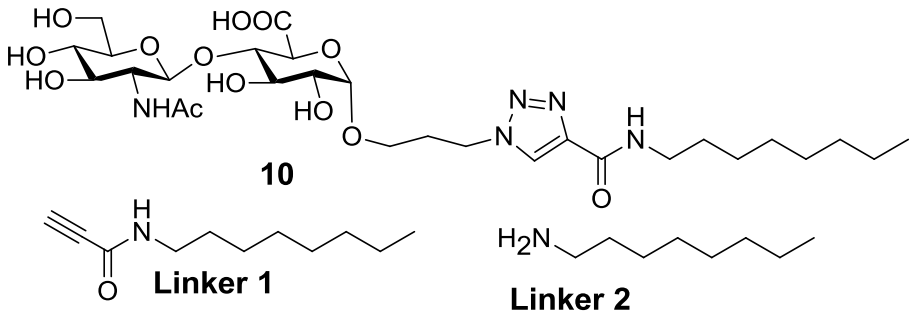


### 4.2.2. $HA_5$ Library

#### 4.2.2.1. The Design

Based on the results of $HA_2$ library. The design philosophy for the $HA_5$ library is to keep most functionality required to address CD44-$HA_8$ interactions, and add extra functionality to approach extra hydrophobic interaction with the hydrophobic pocket formed by Tyr46, Tyr83, Ile111, Ser114, Thr116 and Tyr119 (shown orange in **Figure 4.6**). $HA_5$ backbone GlcUA3 to GlcUA7 (**Figure 4.12**) was kept and the hydrophobic group was connected to an artificial 3-axial-amino group on GlcUA7. The analogues were

carefully evaluated by manually written into the co-crystal PDB file (2JCQ) by Pymol and Chemdraw 3D with the assumption that the conformation and interactions of $HA_5$ backbone remain exactly the same as it is in the CD44-$HA_8$ co-crystal structure. Visualization of the amide linked hydrophobic groups contacting protein hydrophobic pocket is shown in **Figure 4.13**.

**Figure 4.12.** $HA_5$ backbone

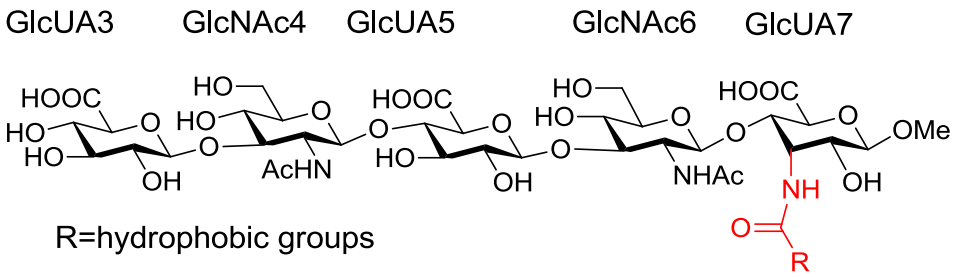


**Figure 4.13.** Visualization of the amide linked hydrophobic groups in CD44 HABD

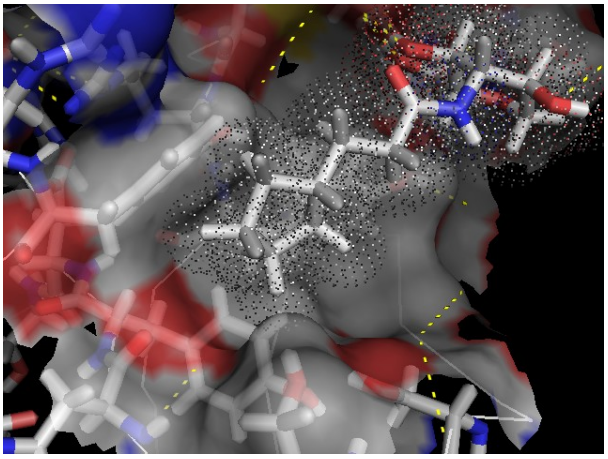

#### 4.2.2.2. The Syntheses

The most challenging part in this project is synthesis. With traditional synthetic methods which build up oligosaccharide from monosaccharide building blocks, it takes years to get one oligosaccharide synthesized. To simplify the synthesis of $HA_5$ library, a cutting edge route was chose. $HA_5$ **17** would be directly built up from $HA_4$ building blocks

**18**. Compound **18** would be acquired several steps from compound **20**. Compound **20** would be generated by enzymatic digestion of HA polymer **21** (**Scheme 4.3**).

**Scheme 4.3.** Retrosynthetic scheme of compound **17**

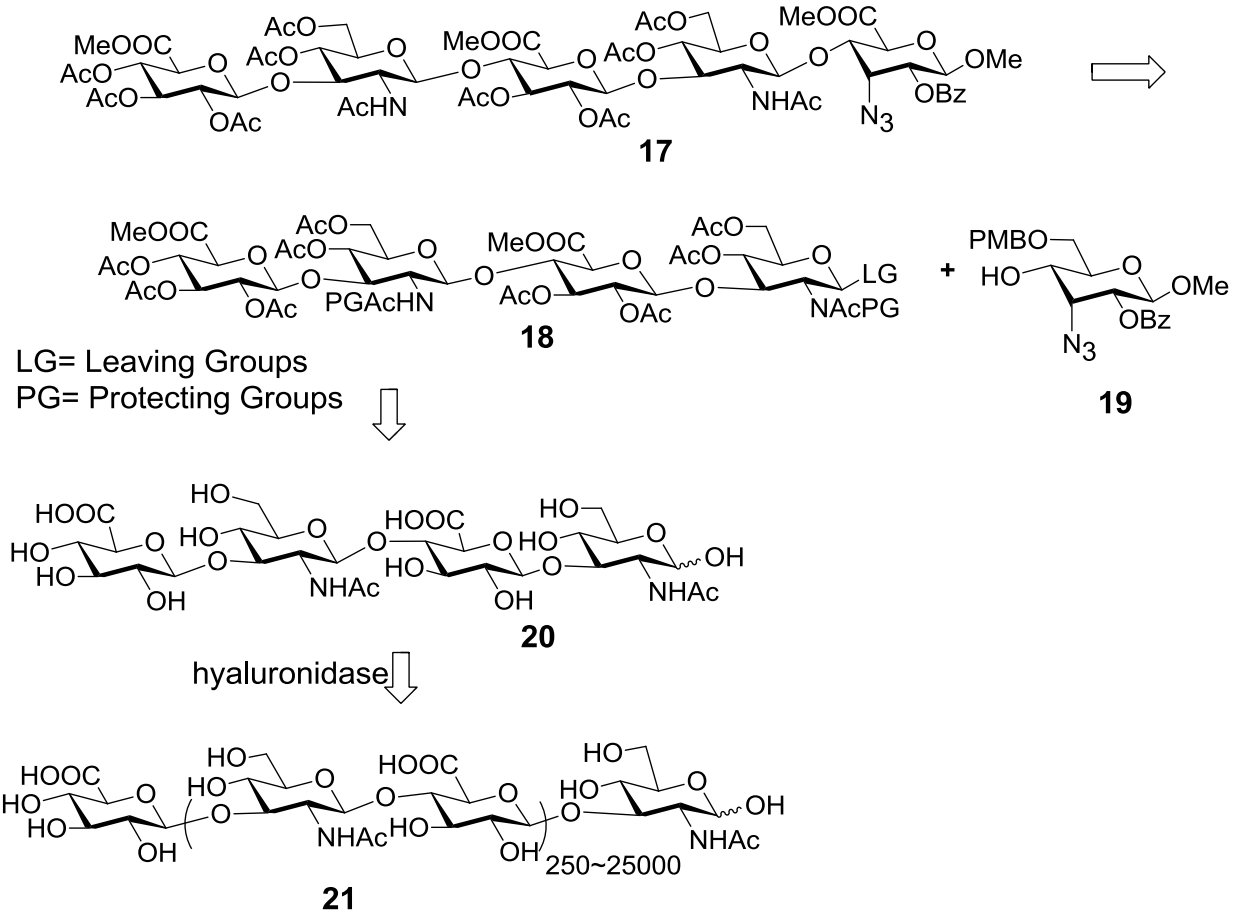


Based on the DeAngelis' and Asari's work[22-23], the enzymatic reaction from **21** to **20** was scaled up to 80 g (**Scheme 4.4**). Since only $HA_4$ not the longer oligomers is the target molecule, the reaction time was elongated up to 8 weeks to push the reaction to completion. Compound **20** was precipitated out of the reaction mixture by mixed solvent of $H_2O$/EtOH (v/v 1:9), while the acetate salt in the digestion buffers stay in the mother

liquor. Crude compound **20** was converted to its TBA form **22** with Dowex strong acidic resin TBA form for improving the solubility in DMF. Subsequential methylation and acetylation yielded compound **23**. Compound **23** was purified by silica gel column chromatography with DCM/EA/MeOH system, and the overall yield from crude **20** was 35%.

**Scheme 4.4.** Synthesis of compound **23**

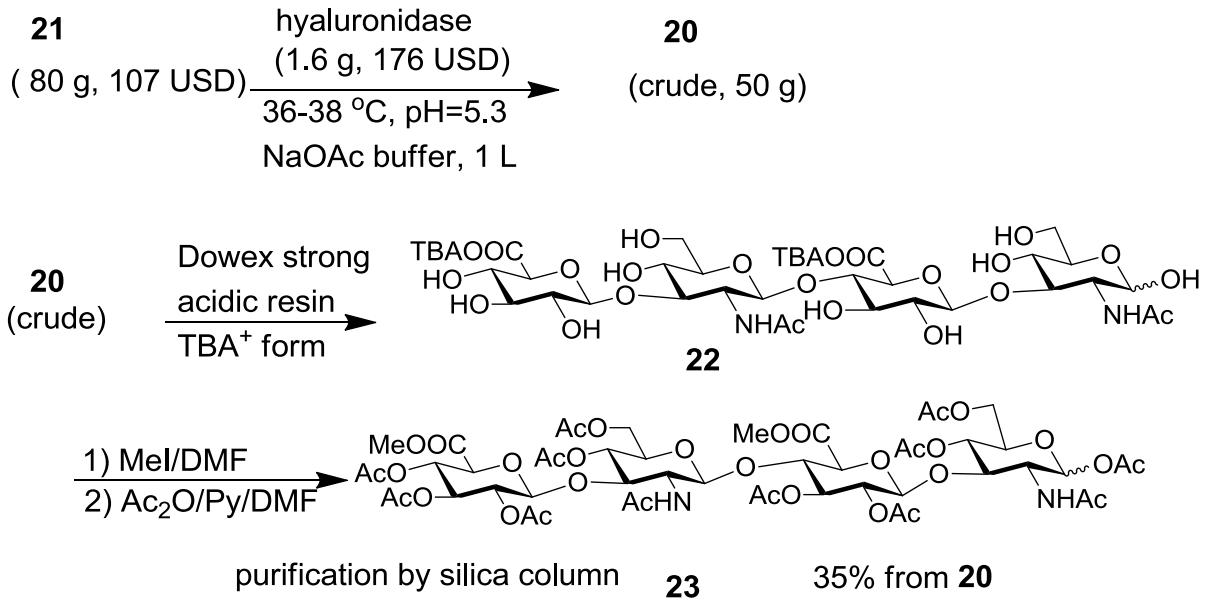


The synthesis toward pentasaccharide **27** with donor **25** was unsuccessful (**Scheme 4.5**). The anomeric OAc in tetrasaccharide **23** was converted to *α*-bromide, and then converted to *β*-STol in 47% yield for 2 steps (**Scheme 4.5a**). The NHAc groups in compound **24** were converted to $NAc_2$ in 65% yield. However, donor **25** was not be able to coupled to acceptor **26** with both AgOTf/*p*-TolSCl and AgOTf/DMTST promoting systems (**Scheme 4.5b**).

**Scheme 4.5.** Synthesis towards $HA_5$ with STol donor

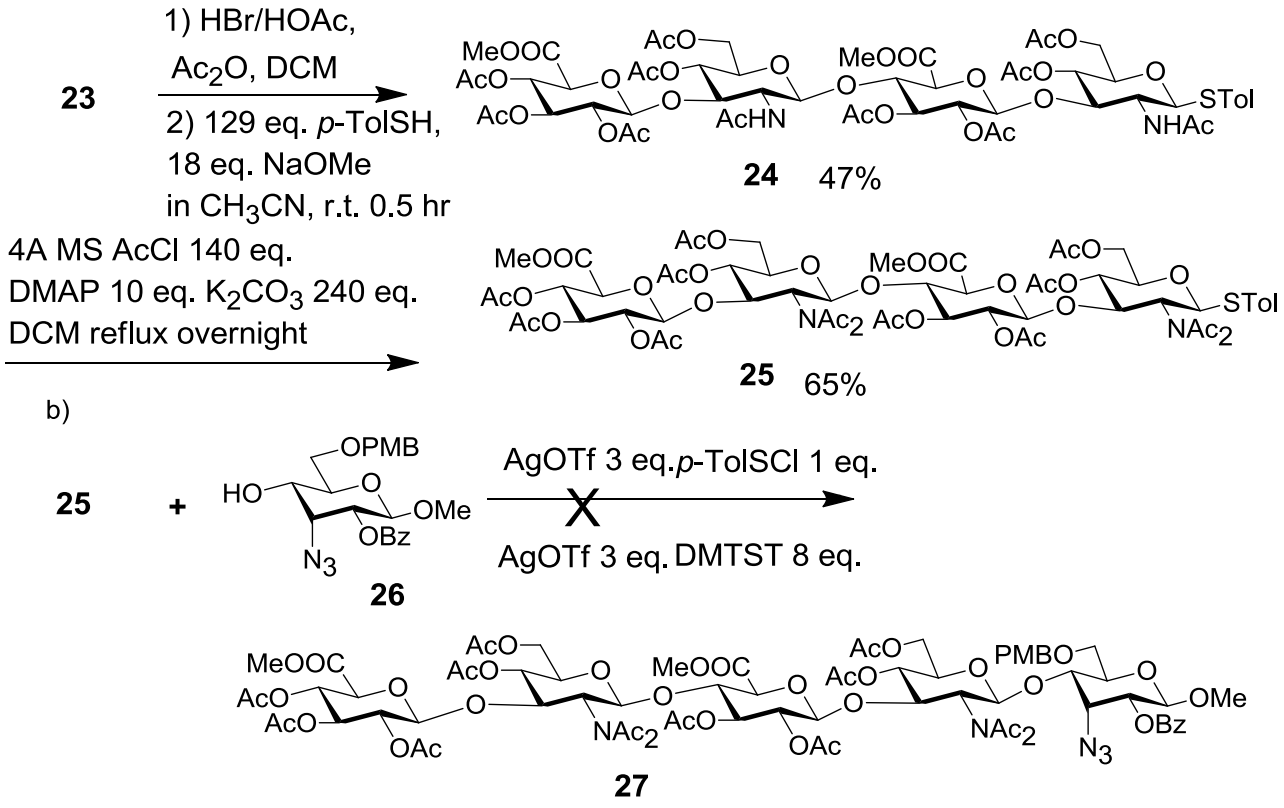


The syntheses on the glycosylation with Br donor failed as well. The coupling reaction between model donor **28** and acceptor **26** failed to produce disaccharide **29** (**Scheme 4.6a**). Donor **28** decomposed in the glycosylation condition. Model donor **30** quantitatively converted to oxzoline **31** in the glycosylation condition (**Scheme 4.6b**). Anomeric Cl donor **32** might be an alternative to Br donor. However, the transformation from **23** to **32** failed. Glycosidic bonds in compound **23** got cleaved in the strong acidic conditions used for the above transformation (**Scheme 4.6c**).

**Scheme 4.6.** Synthesis towards $HA_5$ with Br donor

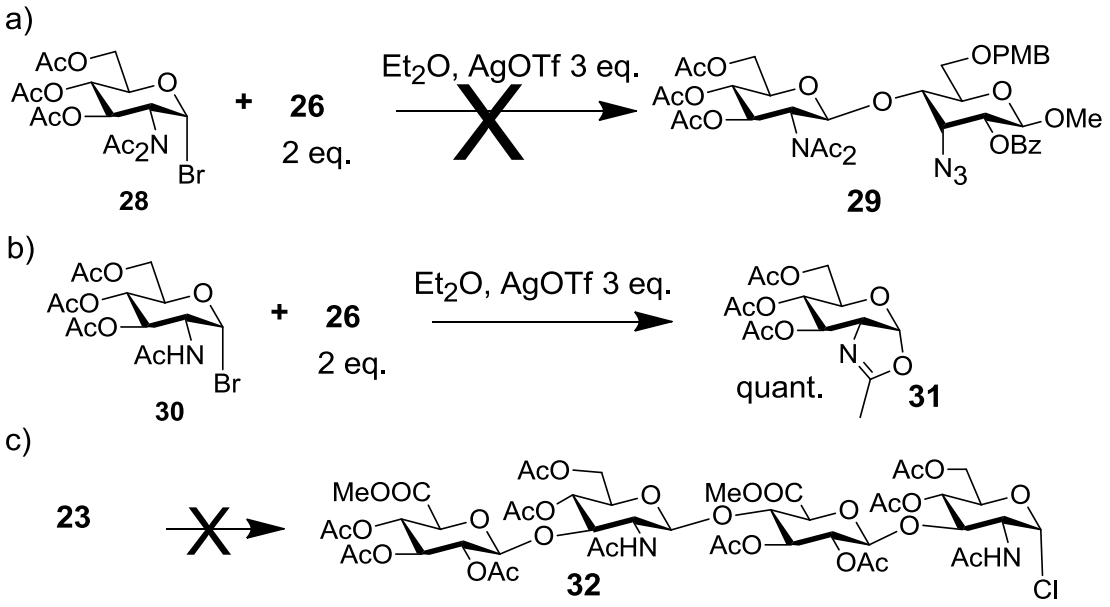


Trichloroacetimidate donor might be a good alternative to Br donor and STol donor. The NHAc groups in tetrasaccharide **23** was converted to $NAC_2$ groups to produce compound **33** (**Scheme 4.7a**). To get the trichloroacetimidate donor, the anomeric Ac group in compound **33** had to be removed to get **34**. However, $NH_4OAc$ 5 eq. was not able to cleave the anomeric Ac group in compound **33**. And there was no selectivity between the anomeric Ac and $NAc_2$ group in presence of 1.5 eq. $NH_2NH_2{\cdot}HOAc$ (**Scheme 4.7b**).

So far, all the attempts toward the construction of an *O*-linkage between a $HA_4$ and a glucose failed. The failure of coupling with STol donor **25** and Br donor **30** could be attributed to the highly disarmed nature of the donor. Not only the acetyl groups but also the $NAc_2$ groups next to the anomeric position contribute to its disarmed nature.

Alternatively an *S*-linkage could be used to mimic the *O*-linkage. Thioglycoside **35** could be generated from compound **36** and compound **37** (**Scheme 4.8a**).

**Scheme 4.7.** Synthesis towards $HA_5$ with trichloroacetimidate donor

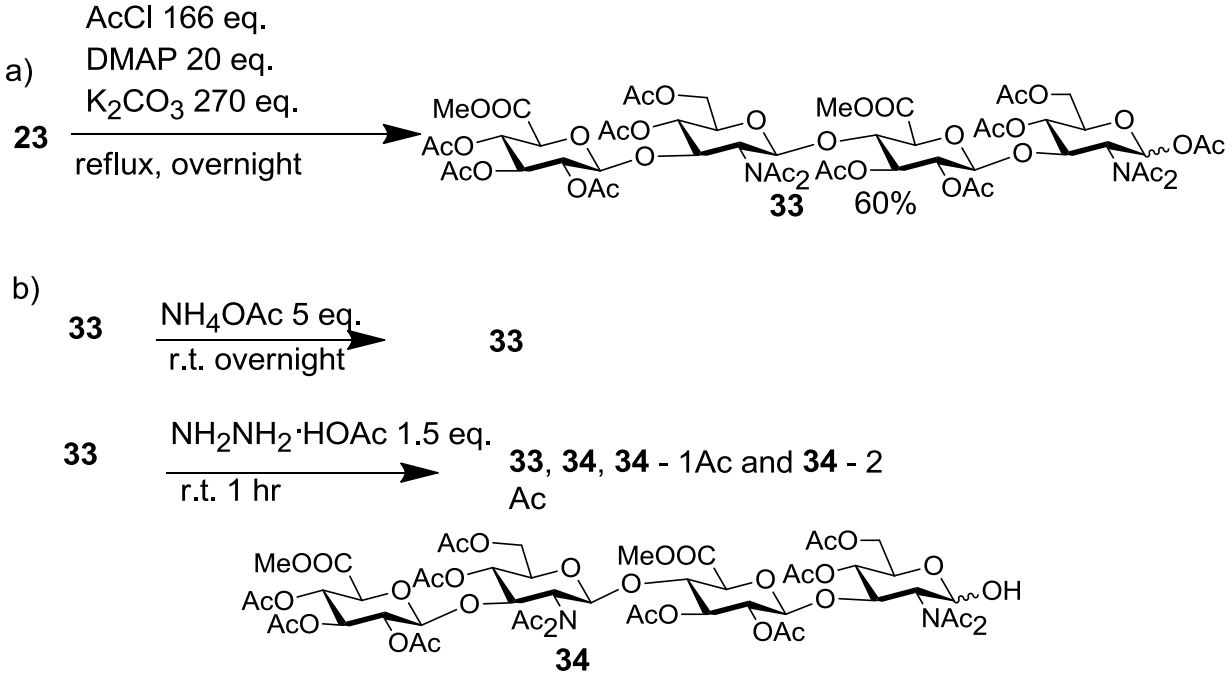


Compound **36** was generated in 3 steps from compound **23** in 30% overall yield (**Scheme 4.8b**). First, the anomeric OAc groups was converted the *α*-bromide in strong acidic condition, in which part of the glycosidic linkages got cleaved to generate trisaccharide and disaccharide side products. This was followed by conversion of *α*-bromide to *β*-SAc by a combination of tetrabutylammonium thioacetate (TBASAc) and thioacetic acid (HSAc). HSAc was used to adjust the acidity of the reaction mixture for minimizing the oxazoline formation. In the third step, in low temperature, 0.5 eq. NaOMe was used to selectively remove anomeric acetic group in quantitative yield to give compound **36**.

**Scheme 4.8.** Synthesis route towards $HA_5$ thioglycoside

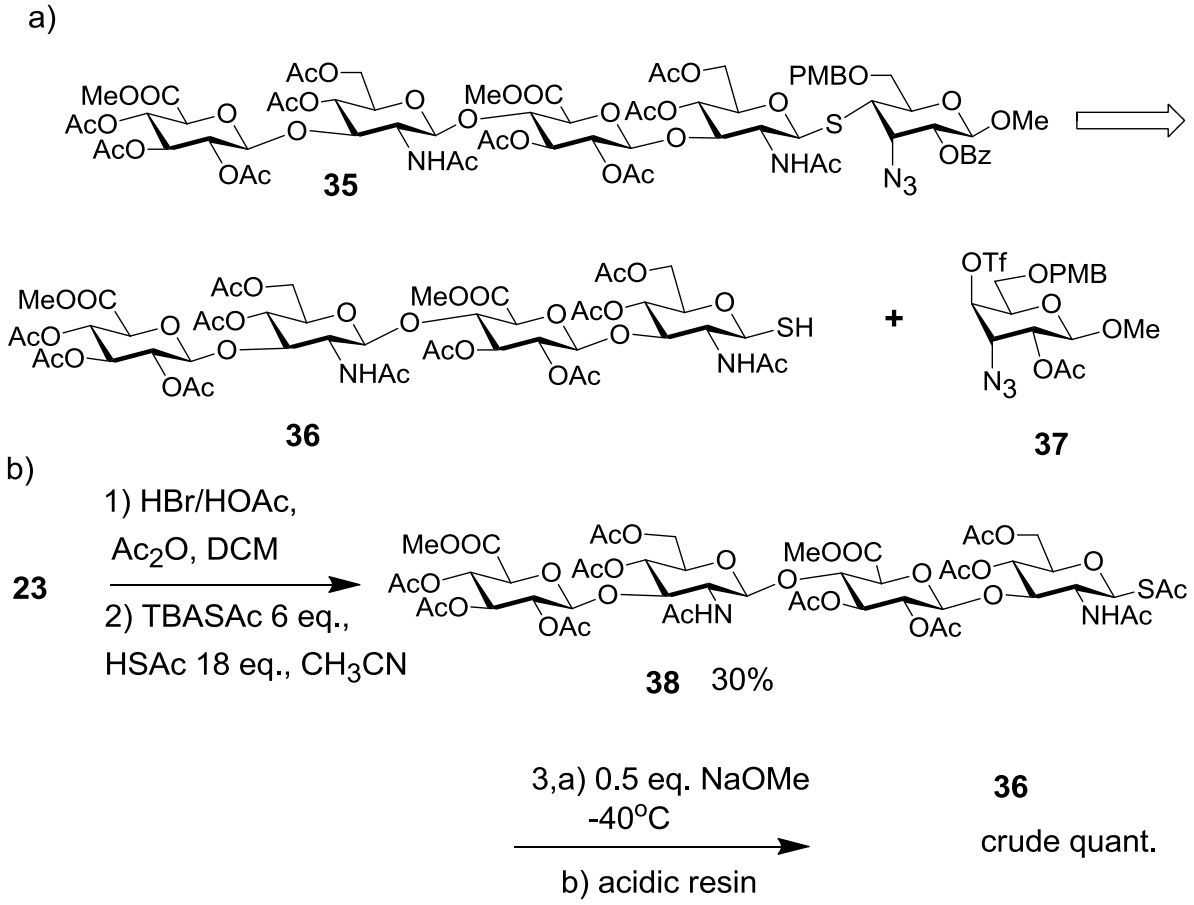


Glucosamine **39** was used as a model molecule of compound **36** (**Scheme 4.9a**). Coupling reaction between glucosamine **39** and galactose **37** failed to yield thioglycoside **44**. The azido group in galactose **37** was not stable in the presence of compound **39** and thioaziridine **40** was formed as the major product. As 3-axial-$NH_2$ was synthetically challenging, 3-axial-OH could be an alternative functionality to direct the hydrophobic groups into the hydrophobic pocket. However, coupling between compound **39** and galactose **41** did not work. The main side products were the disulfide **42** and elimination product **43** (**Scheme 4.9b**). Fortunately coupling between Glucosamine **39** and galactose **46** worked. After delevulinoylation, compound **47** was produced in 56% yield

for 2 steps. However, the conversion from compound **47** to compound **48** failed possibly due to the steric hindrance. Therefore, the attempt to acquire 3-axial-OH from compound **47** through 3-triflate compound **48** failed. (**Scheme 4.9c**)

**Scheme 4.9.** Synthesis toward $HA_2$ thioglycoside

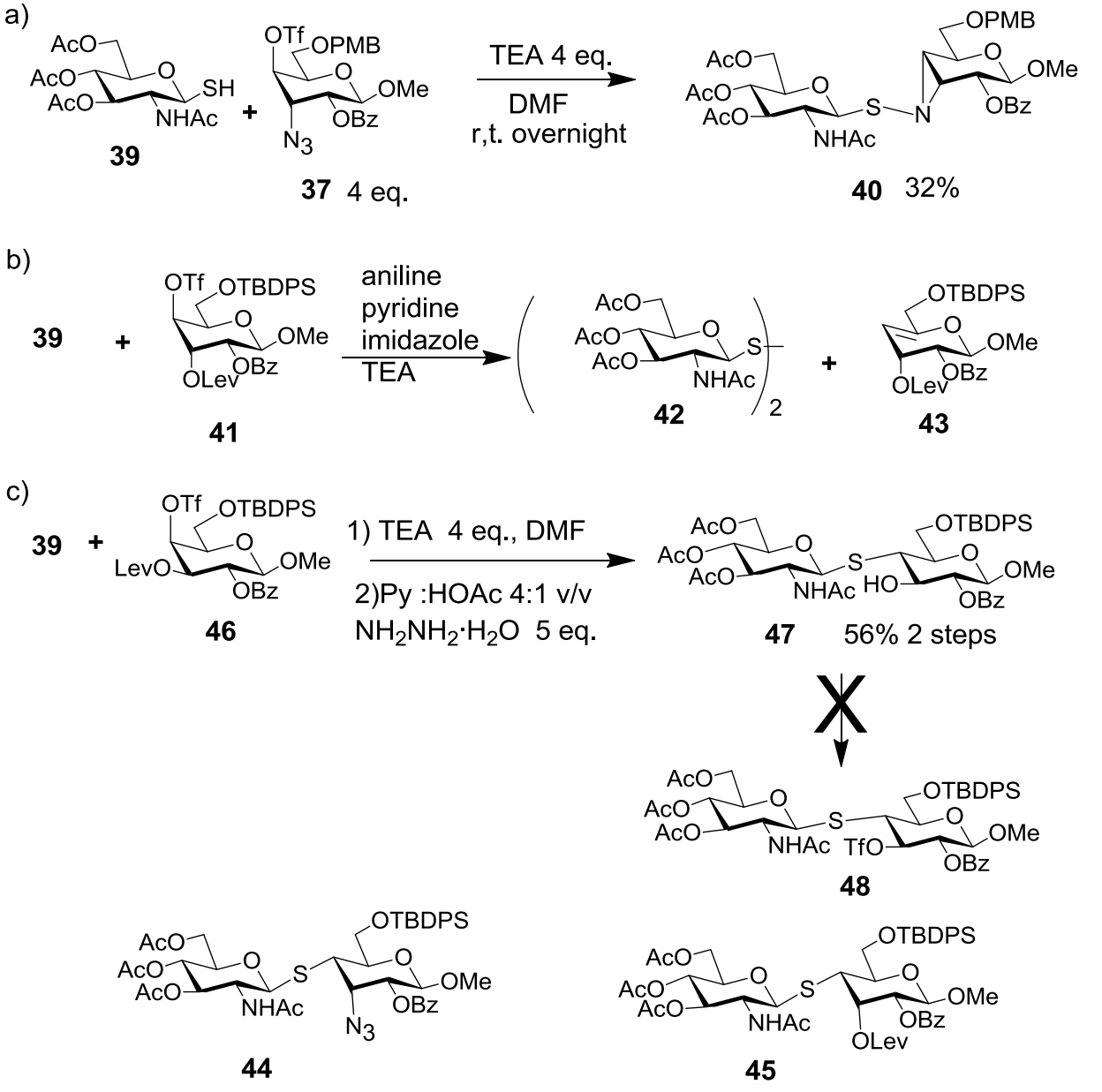


Due to difficulties in the syntheses of analogues with 3-axial-$NH_2$ or 3-axial-OH groups (**Figure 4.14a** library A), alternative functional groups, COOH or 3-equatorial-OH in

GlcUA7, could be used to direct the hydrophobic group into the pocket by simply rotating S-C4 bond (**Figure 4.14b** library B, **Figure 4.14c** library **C**). However, in those alternative libraries, the hydrogen bonds (H-bonds) from COOH in GlcUA7 would be missing, and the conformation after S-$C_4$ rotation might not be favored.

**Figure 4.14.** $HA_5$ analogues

**a) Library A**

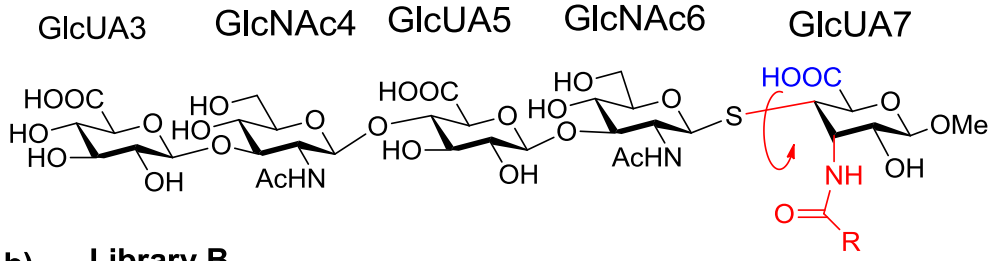


**b) Library B**

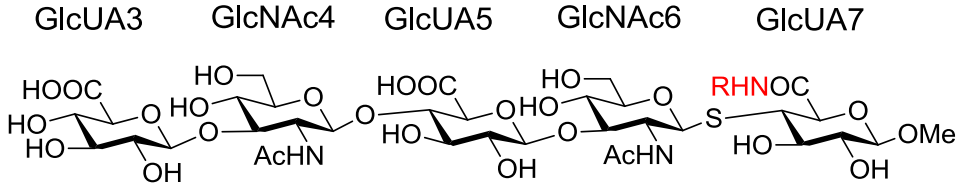


**c) Library C**

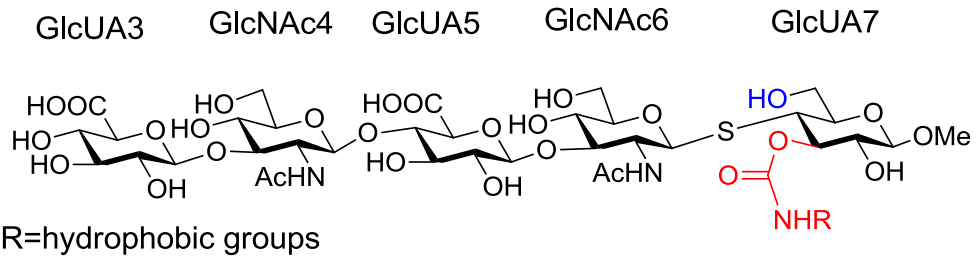


Five compounds **49** - **53** in library B (**Figure 4.15**) and six compounds **54** - **59** in library C (**Figure 4.16**) were selected to be synthesized by manually drawing the R groups into the co-crystal structure with Pymol and Chemdraw 3D. Results are shown in **Figure 4.17** - **4.19**. The compounds **49**, 53, 57 and **58** may have hydrophobic interaction

with the pocket. Compound **50** may have *π*-*π* stacking with the aromatic ring of Tyr46. Compounds **51** and **54** may have *π*-*π* stacking with the aromatic ring of Tyr83. Compounds **52**, **55** and **59** may have *π*-*π* stacking with the aromatic ring of Tyr83 and H-bond with side chain OH in S134. One benzene ring in compound **56** may have hydrophobic contact with the pocket and the other benzene ring may possess T-shaped *π*-*π* stacking with Tyr46 (blue). Compound **53** may have both hydrophobic interaction and H-bond with OH group in Thr116.

**Figure 4.15.** Library B

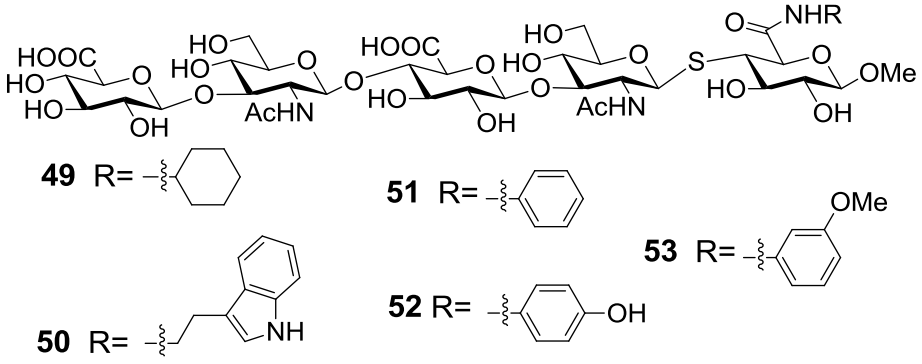


**Figure 4.16.** Library C

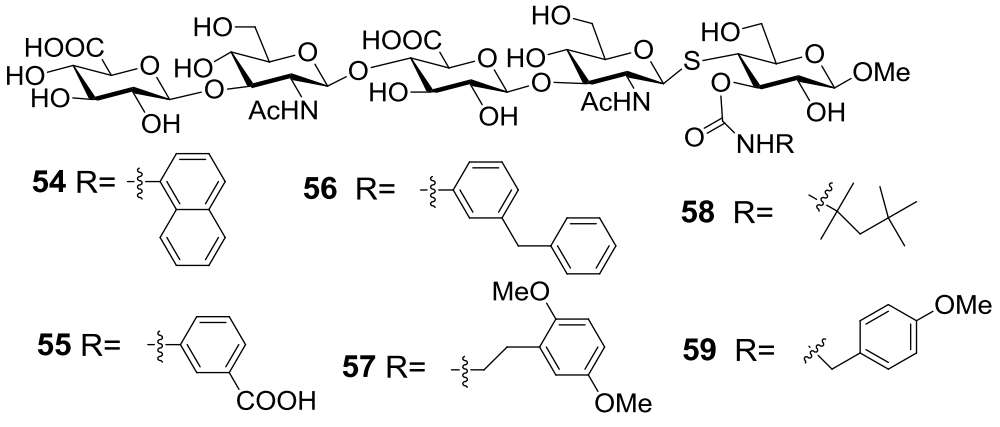

**Figure 4.17.** Visualizations of compounds **49** and **50** in CD44 HABD

Compound **49**

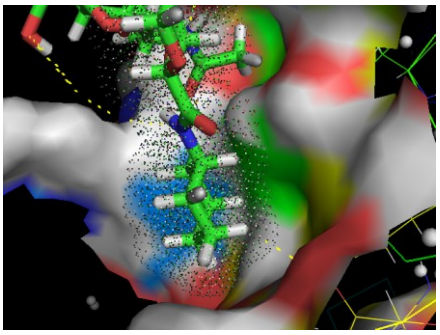

Compound **50**

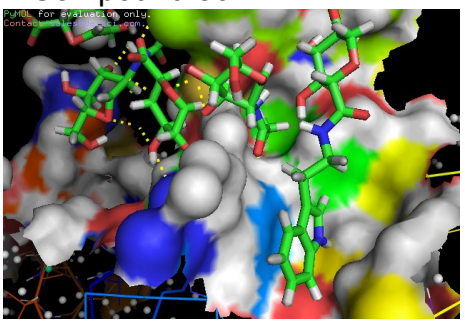

**Figure 4.18.** Visualizations of compounds **51** - **55** in CD44 HABD

Compound **51**

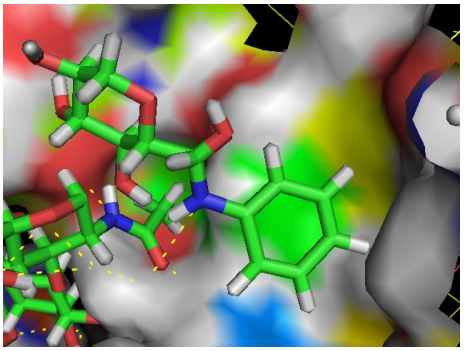

Compound **52**

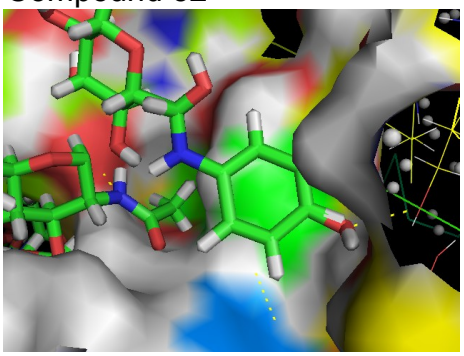

Compound **53**

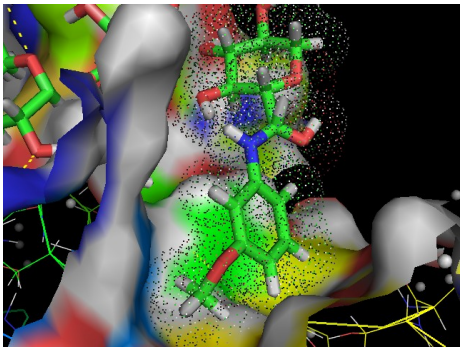

Compound **54**

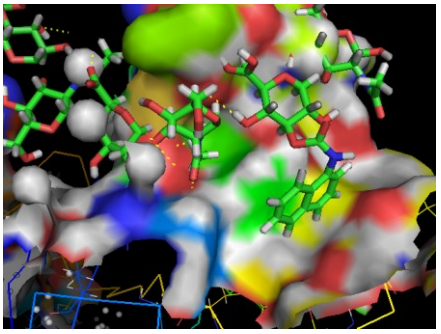

Compound **55**

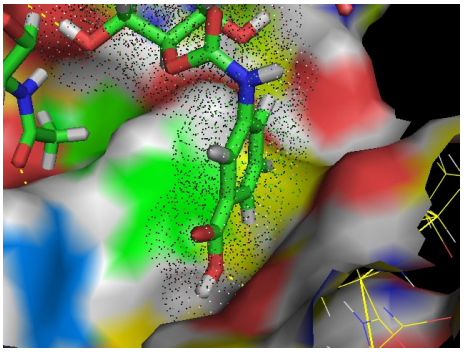

**Figure 4.19.** Visualizations of compounds **56** - **59** in CD44 HABD

Compound **56**

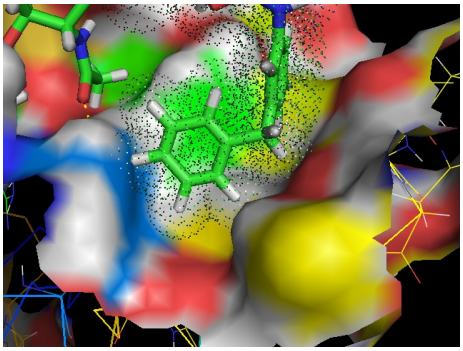

Compound **57**

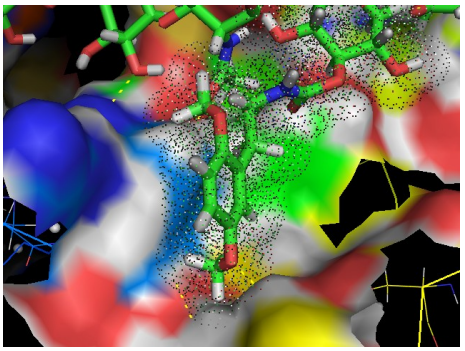

Compound **58**

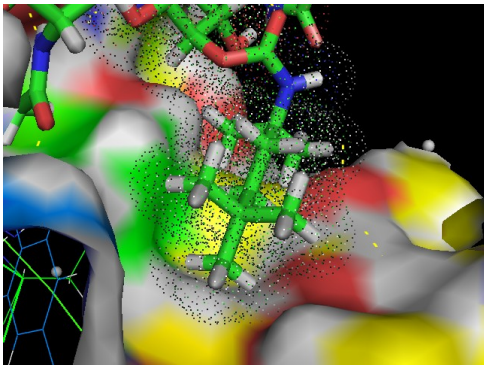

Compound **59**

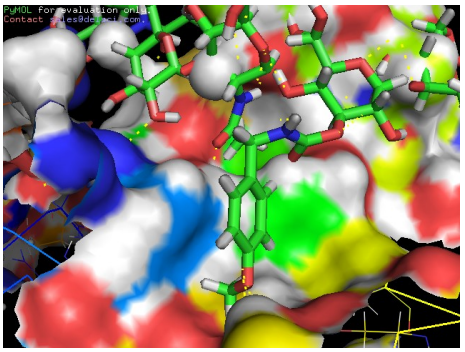

The synthesis of the compounds **49** - **59** proceeded smoothly as shown in **Scheme 4.10** and **Scheme 4.11**. Tetrasaccharide **36** was coupled with galactose **60** to generate pentasaccharide **61**. The TBDPS group in pentasaccharide **61** was removed to yield pentasaccharide **62**. The primary OH in pentasaccharide **62** was oxidized to COOH and coupled to the hydrophobic groups by amide linkage. Compounds **49** - **52** were yielded by one step deprotection (**Scheme 4.10**). Similarly, compound **36** was coupled with galactose **46** to yield pentasaccharide **63**. Compound **63** was converted to compound **64** in 3 steps. The 3-OH in compound **64** was conjugated to the hydrophobic groups though carbamate linkages. Compound **54** - **59** were yielded by one step deprotection (**Scheme 4.11**). The result of deprotection of compound **65** was different

**Scheme 4.10.** Synthesis of library B

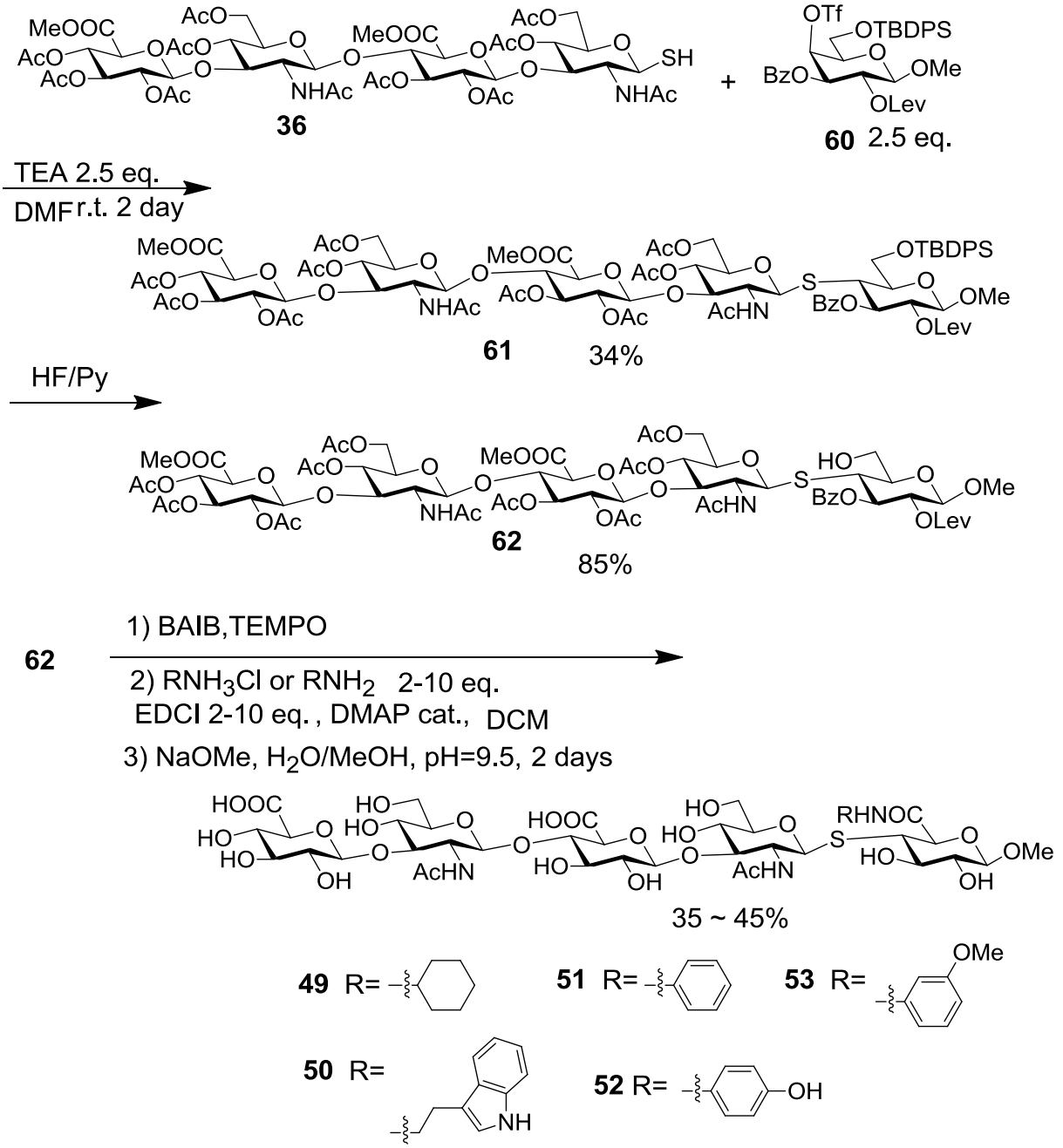


from other compounds in library C (**Scheme 4.12**). In exactly the same condition, part of 3-carbamate group migrated to the 2 position to generate compound **66**. The mixture of compounds **59** and **66**, which could not be separated by high performance liquid chromatography (HPLC), was used for ELISA screening.

**Scheme 4.11.** Synthesis of library C

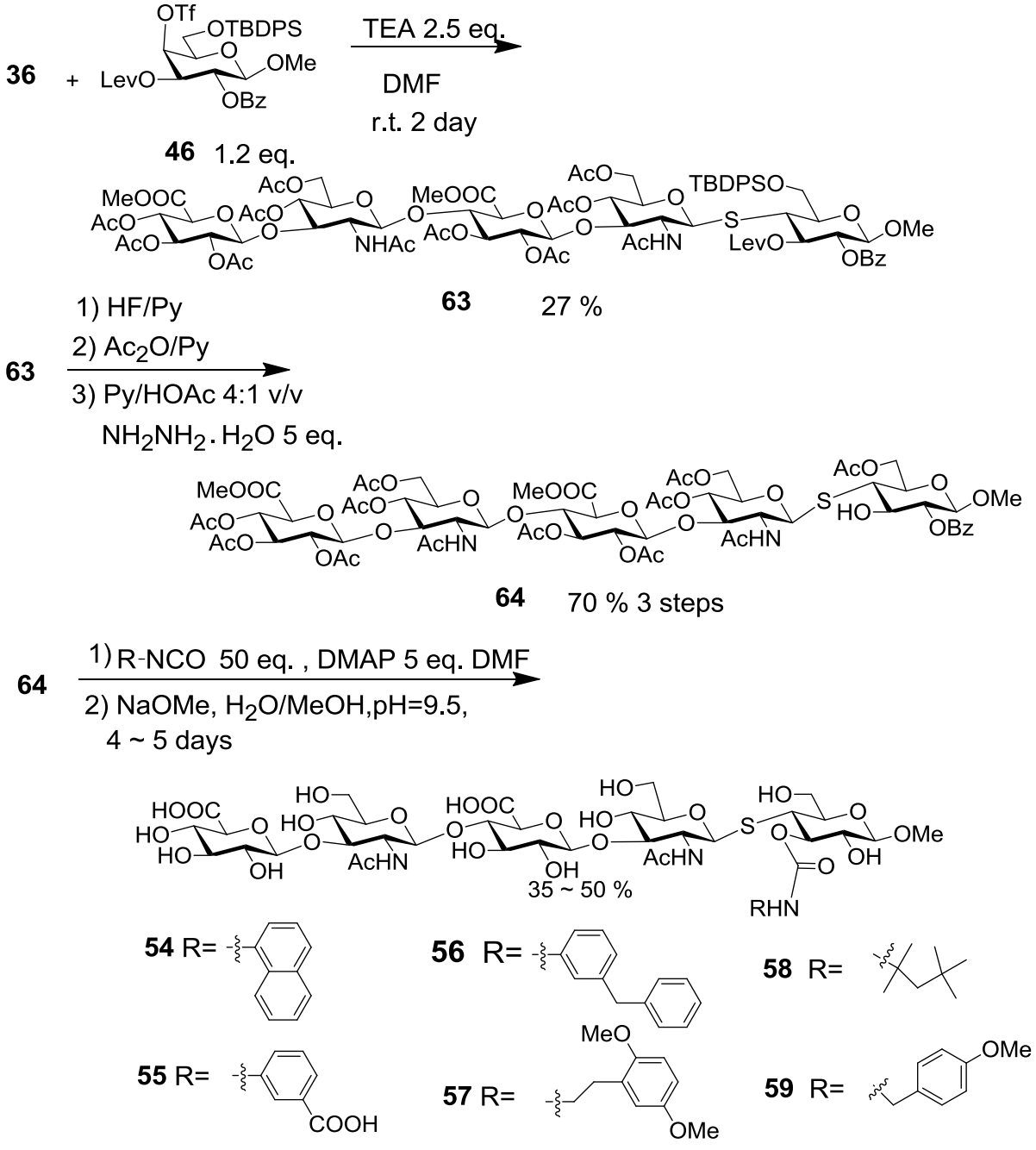


Compared to traditional synthesis in **chapter 3**, this synthetic strategy is more efficient in generating oligosaccharide libraries due to two main advantages. First, pentasaccharides were constructed directly from tetrasaccharide building blocks. Second, the very simple one step deprotection is much more convenient compared to

the complicated multiple step deprotections in **chapter3**.

**Scheme 4.12.** Deprotection of compound **65**

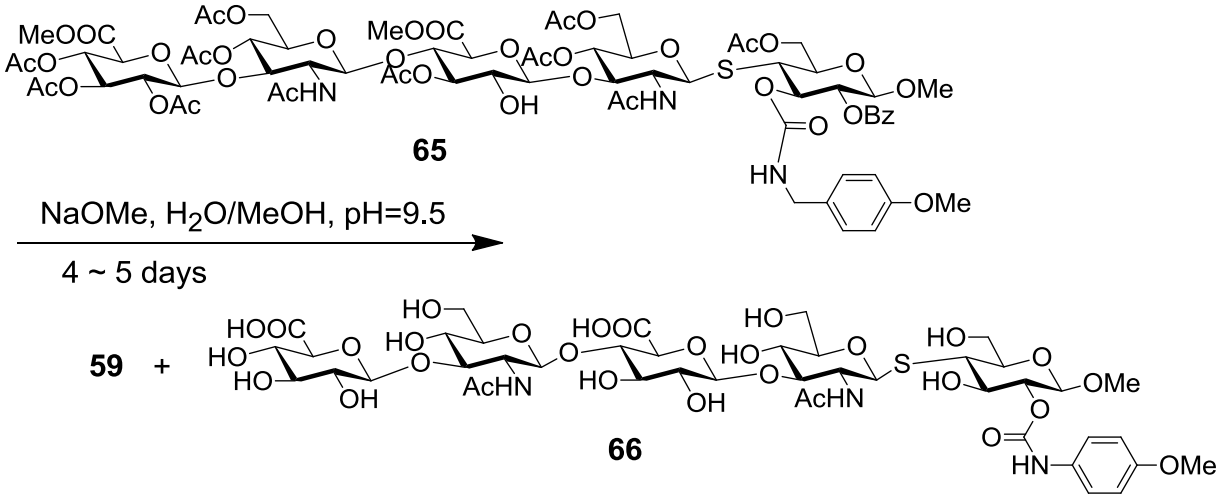


#### 4.2.2.3. Results and discussion

The inhibitory ELISA was used to study the binding between compounds **49** - **59** and CD44 (**Figure 4.20**). **CD44 NEG** was the groups without CD44, which was used as negative control. **Inhibitor NEG** was the group without HA inhibitor, which was used as minimum inhibition. **HA 16 kDa** was the group with HA polymer 16 kDa 2.5 μg per well, which was used as maximum inhibition. All other groups were measured in the presence of 235 μM of $HA_5$ analogues as potential inhibitors. Pentasaccharide 67 without hydrophobic functionality was used to compare with compounds **49** - **59**.

First, there was clear trend that **$HA_8$** bound stronger than **$HA_6$** and **$HA_6$** bound stronger than **$HA_4$**. Second, the binding affinity of **67** was similar to **$HA_4$**. Third, the binding affinities of compounds **49**, **50**, **51**, **52**, **53**, **54**, **55, 57**, **58** and **59** were about the same as **67**. Fourth, the binding affinity of compound **56** was comparable to **$HA_6$**.

Inhibition curve of compound 56, $HA_6$ and $HA_8$ was shown in **Figure 4.22**.

**Figure 4.20.** Inhibition ELISA of sHA and analogues

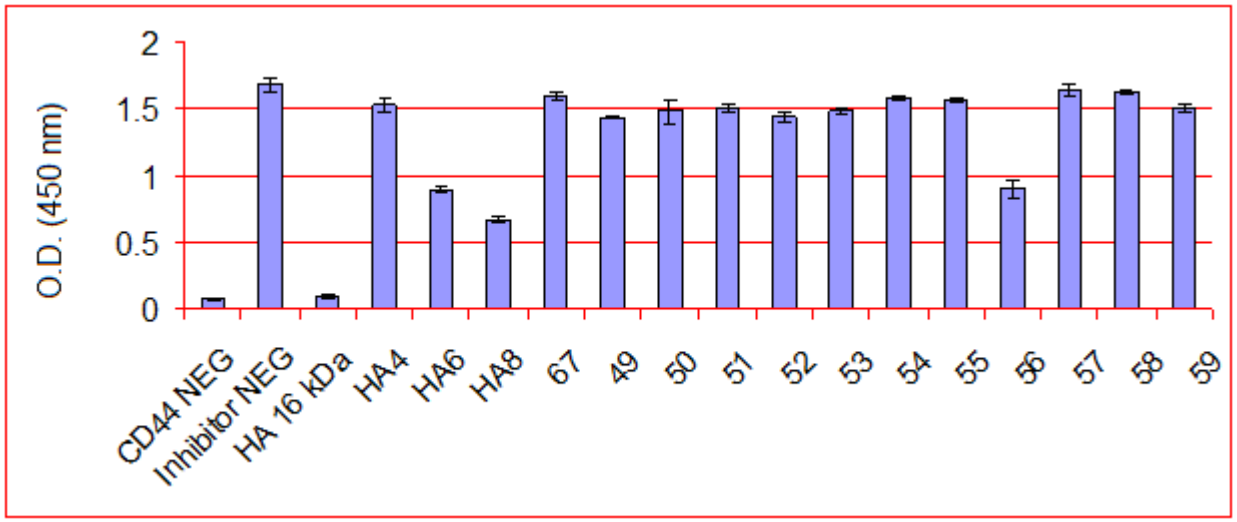


**Figure 4.21.** sHA and analogues

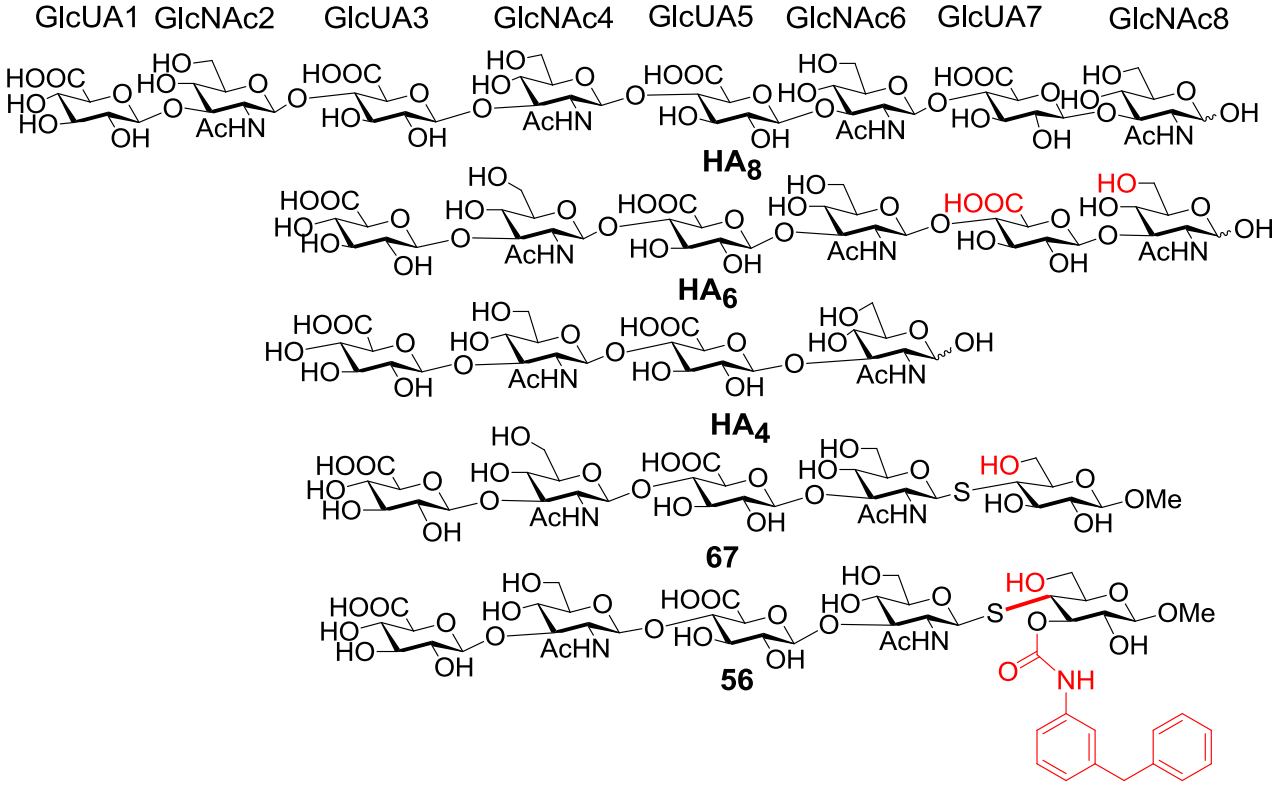


The difference in binding affinity between compound **67** and compound **56** indicated that aromatic group in compound **56** clearly contributes to the binding of

compound **56** to CD44. H-bonds in **$HA_6$** from COOH of GlcUA7 and the primary OH of GlcNA8 are missing in compound **56**, which may contribute to the loss of favored enthalpy in binding. Computer screening results (**Figure 4.17 - 4.19**) shown that all hydrophobic groups in compounds **49** - **59** have interactions with CD44, but only the binding affinity of compound **56** was comparable to **$HA_6$**. The explanation might be that interactions of the hydrophobic group in compounds **49**, **50**, **51**, **52**, **53**, **54**, **55, 57**, **58** and **59** to CD44 was not strong enough to overcome the loss of favored enthalpy caused by the loss of H-bond mentioned before. The special orientation of the two benzene rings in compound **56,** which might contribute to the T-shaped *π*-*π* stacking with Tyr46, might make compound **56** a better inhibitor than other $HA_5$ analogues. Following this result, beyond this thesis, analogues similar to compound **56** with subtle difference on the aromatic functionality could be synthesized to further enhance binding.

**Figure 4.22.** Inhibition curve of compound 56, $HA_6$ and $HA_8$

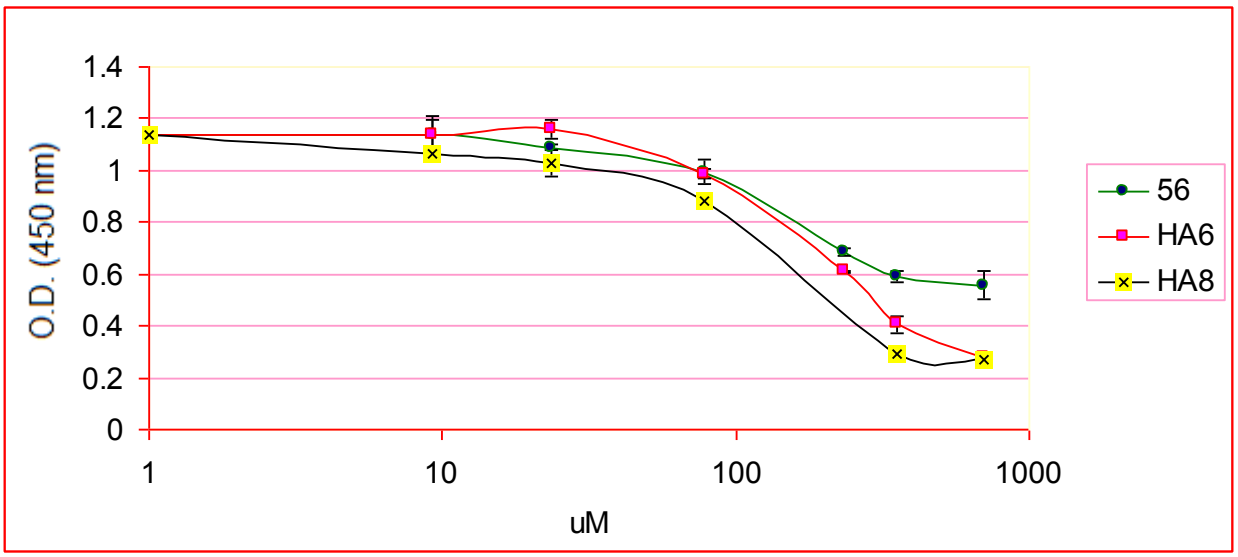

## 4.3. Conclusion

The purpose for this project is to design and synthesize analogues based on co-crystal structure of CD44 and $HA_8$. Due to synthetic difficulties, the initial design of library A was abolished. By rotating S-C4 bond, new analogues, library B and library C**,** were generated. 11 compounds in library B and library C were synthesized by a cutting edge method, and screened by inhibitory ELISA. Finally, it was found that the aromatic group in compound **56** contributes to the binding of compound **56** to CD44. And this interaction overcomes the loss of favored enthalpy caused by the loss of H-bonds from COOH of GluUA7 and primary OH of GlcNAc8. Although the binding affinity of **56** is only comparable to $HA_6$ and less than $HA_8$, this provides a new direction towards further design of novel HA inhibitors.

**4.4. Experimental Section:**

**1-[3-(O-(2-*N*-acetyl-2-deoxy-*β*-D-glucopyranosyl)-(1→4)-*α*-D-glucopyranosyl uronic acid-1-yl)-propyl]-1*H*-[1,2,3]-triazole-4-carboxylic acid octylamide (10):** The mixture of donor **6** (595 mg, 1.10 mmol), acceptor **7** (325 mg, 0.550 mmol, 0.5 eq.) and freshly activated MS-4Å (4 g) in a mixture solvent of DCM and MeCN (v/v 40:1, 20 ml) was stirred for 1 hr at -78 °C, followed by the addition of AgOTf (848 mg, 3.30 mmol, 3 eq.) in $Et_2O$ (10 ml). After 5 min, *p*-TolSCl (173 µl, 1.10 mmol, 1 eq.) was added via a syringe to activate the donor. The yellow color of the reaction disappears quickly and TLC analysis showed the donor was completely consumed. The reaction mixture was warmed to −10 °C under stirring in 2 hrs. TEA (0.5 ml) was then added and the mixture was diluted with DCM (100 ml) and filtered over celite. The celite was further washed with DCM until no organic compounds were observed in the filtrate by TLC. All DCM solutions were combined and washed twice with a saturated aqueous solution of $NaHCO_3$ (100 ml) and twice with $H_2O$ (100 ml). The organic layer was concentrated and the crude product was purified by silica gel chromatography to produce disaccharide **8** in 70% yield. Disaccharide **8** was subjected to deprotection of PMB and oxidation of alcohol to carboxylic acid following the general procedures on page 61. The yielding disaccharide (230 mg, 0.255 mmol) was dissolved in 2M $MeNH_2$ (14 ml). The reaction was stirred at r.t. for 2 days. The solvent was removed and the crude mixture was co-evaporated with toluene, then DMAP (188 mg, 1.53 mmol, 6 eq. ), $Ac_2O$ (0.200 ml, 23.0 mmol, 90 eq.) and DCM (16 ml) were added. The reaction mixture was stirred at r.t.

overnight, concentrated and co-evaporated with toluene. EDCI (158 mg, 0.826 mmol, 3 eq.) and anhydrous MeOH (3 ml) were added. The reaction mixture was stirred at r.t. overnight, concentrated, and purified by silica gel chromatography to yield compound **9** in 15% yield for 5 steps. Compound **9** (6 mg, 0.008 mmol), alkyne (7 mg, 0.04 mmol, 5 eq.), $CuSO_4$ (2 mg, 0.008 mmol, 1 eq.) and sodium ascorbate (3.2 mg, 0.016 mmol, 2 eq.) were dissolved in a mixture solvent of *t*BuOH and $H_2O$ (2 ml, v/v=1:1). The reaction mixture was stirred at r.t. overnight, concentrated, and purified by silica gel chromatography. The resulting disaccharide was dissolved in a mixture solvent of THF and $H_2O$ (2 ml, v/v=1:1) and KOH (41 µl 0.1M KOH in $H_2O$, 41 µmol, 1.5 eq.) was added. The reaction mixture was stirred at r.t. overnight, concentrated and purified by Sephadex G-15 size exclusion chromatography to produce compound **10** in quant. yield for 2 steps. $^1$H NMR (500 MHz, $D_2O$): δ = 0.74 (t, 3H, *J* = 7.0 Hz), 1.14-1.27 (m, 10H), 1.52 (t, 2H, *J* = 7.5 Hz), 1.92 (s, 3H, NHCO*CH*$_3$), 2.16-2.20 (m, 2H), 3.28-3.81 (m, 13H), 3.92 (d, 1H, *J* = 10.0 Hz 1H, H-5), 4.43 (d, 1 H, *J* = 9.0 Hz, H-1'), 4.52 (t, 2 H, *J* = 7.0 Hz), 4.78 (d, 1 H, *J* = 3.5 Hz, H-1), 8.32 (s, 1H, $CH_{arom}$); HRMS [M]: m/z: calcd for $C_{28}H_{47}N_5O_{13}$ 661.3170, found 661.3145.

**1-[3-(O-(2-*N*-acetyl-2-deoxy-*β*-D-glucopyranosyl)-(1→4)-*α*-D-glucopyranosyl uronic acid-1-yl)-propyl]-1*H*-[1,2,3]-triazole-4-carboxylic acid 3-phenylpropylamide (11).** Compound **11** was produced following the same procedure for the synthesis of compound **10**. $^1$H NMR (500 MHz, $D_2O$): δ = 1.92 (t, 2H, *J* = 7.0 Hz,), 1.98 (s, 3H,

NHCO*CH3*), 2.14-2.22 (m, 2H), 2.67 (t, 2H, *J* = 8.0 Hz), 3.31-3.77 (m, 15H), 3.82 (d, 1H, *J* = 12.5 Hz 1H, H-5), 4.43 (d, 1 H, *J* = 8.5 Hz, H-1'), 4.50-4.56 (m, 2 H), 4.76 (d, 1 H, *J* = 3.5 Hz, H-1), 7.10-7.25 (m, 5H, $CH_{arom}$), 8.27 (s, 1H, $CH_{arom}$); HRMS [M]: m/z: calcd for $C_{29}H_{41}N_5O_{13}$ 667.2701, found 667.2718.

**1-[3-(O-(2-*N*-acetyl-2-deoxy-*β*-D-glucopyranosyl)-(1→4)-*α*-D-glucopyranosyl uronic acid-1-yl)-propyl]-1*H*-[1,2,3]-triazole-4-carboxylic acid 4-phenylbutanyl amide (12).** Compound **12** was produced following the same procedure for the synthesis of compound **10**. $^1$H NMR (500 MHz, $D_2O$): 1.10 (t, 2H, *J* = 7.5 Hz), 1.52-1.56 (m, 4H), 1.93 (s, 3H, NHCO*CH3*), 2.18-2.25 (m, 2H), 2.54 (t, 2H, *J* = 7.5 Hz), 3.28-3.72 (m, 15H), 3.78 (d, 1H, *J* = 11.5 Hz 1H, H-5), 4.38 (d, 1 H, *J* = 8.5 Hz, H-1'), 4.46-4.49 (m, 2 H), 4.70 (m, 1 H, H-1), 7.09-7.22 (m, 5H, $CH_{arom}$), 8.26 (s, 1H, $CH_{arom}$); HRMS [M]: m/z: calcd for $C_{30}H_{43}N_5O_{13}$ 681.2857, found 681.2869.

**1-[3-(O-(2-*N*-acetyl-2-deoxy-*β*-D-glucopyranosyl)-(1→4)-*α*-D-glucopyranosyl uronic acid-1-yl)-propyl]-1*H*-[1,2,3]-triazole-4-carboxylic acid 2-(2-chlorophenyl) ethanylamide (13).** Compound **13** was produced following the same procedure for the synthesis of compound **10**. $^1$H NMR (500 MHz, $D_2O$): δ = 1.89 (s, 3H, NHCO*CH3*), 2.08-2.14 (m, 2H), 2.93 (t, 2H, *J* = 6.5 Hz), 3.26-3.70 (m, 15H), 3.76 (d, 1H, *J* = 11.5 Hz 1H, H-5), 4.35 (d, 1 H, *J* = 8.5 Hz, H-1'), 4.41-4.47 (m, 2H, NH), 4.58 (d, 1 H, *J* = 4.0 Hz, H-1), 7.07-7.26 (m, 4H, $CH_{arom}$), 8.17 (s, 1H, $CH_{arom}$); HRMS [M]: m/z: calcd for $C_{28}H_{38}ClN_5O_{13}$ 687.2155, found 687.2124.

**1-[3-(O-(2-*N*-acetyl-2-deoxy-*β*-D-glucopyranosyl)-(1→4)-*α*-D-glucopyranosyl**

**uronic acid-1-yl)-propyl]-1*H*-[1,2,3]-triazole-4-carboxylic acid 2-(4-chlorophenyl) ethanylamide (14).** Compound **14** was produced following the same procedure for the synthesis of compound **10**. $^1$H NMR (500 MHz, $D_2O$): δ = 1.89 (s, 3H, NHCO*CH*$_3$), 2.08-2.14 (m, 2H), 2.77 (t, 2H, *J* = 7.0 Hz), 3.27-3.69 (m, 15H), 3.75 (d, 1H, *J* = 11.0 Hz 1H, H-5), 4.35 (d, 1 H, *J* = 8.5 Hz, H-1'), 4.43-4.47 (m, 2H, NH), 4.81 (s, 1 H, H-1), 7.10-7.18 (m, 4H, $CH_{arom}$), 8.18 (s, 1H, $CH_{arom}$); HRMS [M]: m/z: calcd for $C_{28}H_{38}ClN_5O_{13}$ 687.2155, found 687.2201.

**1-[3-(O-(2-*N*-acetyl-2-deoxy-*β*-D-glucopyranosyl)-(1→4)-*α*-D-glucopyranosyl uronic acid-1-yl)-propyl]-1*H*-[1,2,3]-triazole-4-carboxylic acid 2-(naphthalen-2-yl) ethanylamide (15).** Compound **15** was produced following the same procedure for the synthesis of compound **10**. $^1$H NMR (500 MHz, $D_2O$): 1.93 (s, 3H, NHCO*CH*$_3$), 2.08-2.14 (m, 2H), 3.00 (t, 2H, *J* = 6.0 Hz), 3.27-3.74 (m, 15H), 3.79 (d, 1H, *J* = 12.5 Hz 1H, H-5), 4.40 (d, 1 H, *J* = 8.0 Hz, H-1'), 4.43-4.45 (m, 2H, NH), 4.61 (s, 1 H, H-1), 7.39-7.77 (m, 7H, $CH_{arom}$), 8.13 (s, 1H, $CH_{arom}$); HRMS [M]: m/z: calcd for $C_{32}H_{41}N_5O_{13}$ 703.2701, found 703.2674.

**1-[3-(O-(2-*N*-acetyl-2-deoxy-*β*-D-glucopyranosyl)-(1→4)-*α*-D-glucopyranosyl uronic acid-1-yl)-propyl]-1*H*-[1,2,3]-triazole-4-carboxylic acid 2-(4-hydroxyphenyl) ethanylamide (16).** Compound **16** was produced following the same procedure for the synthesis of compound **10**. $^1$H NMR (500 MHz, $D_2O$): δ = 1.90 (s, 3H, NHCO*CH*$_3$), 2.08-2.14 (m, 2H), 2.72 (t, 2H, *J* = 6.5 Hz), 3.28-3.78 (m, 16H), 4.36 (d, 1 H, *J* = 8.5 Hz,

H-1'), 4.48-4.45 (m, 2H), 6.67-7.05 (m, 7H, $CH_{arom}$), 8.20 (s, 1H, $CH_{arom}$);HRMS [M]: m/z: calcd for $C_{28}H_{39}N_5O_{14}$ 669.2494, found 669.2481.

**Preparation of HA-ADH-biotin:**

**1) HA-ADH:** HA (16 kDa, 100 mg, 0.260 mmol $HA_2$) was dissolved in $H_2O$ (25 ml). To this mixture was added adipic dihydrazide (ADH) (905 mg, 20 eq., 5.20 mmol), and 1-ethyl-3-(3-dimethyl-aminopropyl)carbodiimide hydrochloride (EDCI) (8.0 mg, 0.2 eq. 0.052 mmol). The pH of the reaction mixture was maintained at 4.75 by addition of 0.1 N HCl until no further rise in pH was observed. The pH of the reaction mixture was then raised to 7.0 by addition of 1 N NaOH. After dialysis and lyophilization, HA-ADH was yielded as a white solid with 16% ADH per $HA_2$ unit. In $^1$H-NMR spectra, the integrations of $CH_2$ groups (from ADH) and NHAc groups (from HA) were used to characterize the degree of substitution[21].

**2) NHS-biotin:** Biotin (100 mg, 0.4 mmol), *N*-hydroxysuccinimide (NHS) (47 mg, 1 eq., 0.4 mmol) and *N*, *N'*-Dicyclohexylcarbodiimide (DCC) (110 mg, 1.3 eq. 0.520 mmol) were dissolved in DMF (3 ml). The reaction mixture was sonicated for 10 hrs. The crude product was concentrated and precipitated out with $Et_2O$ (15 ml) for 3 times to yield a white solid 150 mg. This crude mixture was used for the synthesis of biotin-ADH-HA[24].

**3) HA-ADH-biotin:** HA-ADH (50 mg) and NHS-biotin (150 mg) were dissolved in $H_2O$ (10 ml). The reaction mixture was sonicated overnight. After dialysis and lyophilization, HA-ADH-biotin was yielded as a white solid with 16% ADH and 10% biotin

per $HA_2$ unit. In $^1$H-NMR spectra, the integrations of $CH_2$ groups (from ADH and biotin) and NHAc groups (from HA) were used to characterize the degree of substitution.

**Procedure for inhibitory ELISA**

Goat anti-human IgG (Fc) (3 μg in 100 μl phosphate buffered saline (PBS) per well) was added to the 96-well microtiter plate, and the plate was incubated in 4 °C overnight. The plate was washed with 0.5% PBS-Tween 20 (PBST) (200 μl per well) for 3 times. Then 5% BSA in PBS (200 μl per well) was added and the plate was incubated at 37 °C for 90 min. The plate was washed with 0.5% PBST (200 μl per well) for 3 times and PBS (200 μl per well) once. Then recombinant human CD44/Fc chimera (0.2 μg in 100 μl PBS per well) was added, and the plate was incubated at 37 °C for 45 min. The plate was washed with 0.05% PBST (200 μl per well) for 3 times and PBS (200 μl per well) once. Then HA-ADH-biotin (0.5 μg per well) was pre-mixed with sHA or analogues in 100 μl PBS and the mixtures were added. The plate was incubated at 22 °C for 2 hrs, then washed with 0.05% PBST (200 μl per well) for 3 times and PBS (200 μl per well) once. Avidin-HRP 1 x 2000 (100 μl per well) in 0.2% BSA-PBS was added, and the plate was incubated at 22 °C for 1 hr. The plate was washed with 0.05% PBST (200 μl per well) for 3 times. Fresh prepared 3,3′,5,5′-tetramethylbenzidine (TMB) solution (200 μl per well) was added. And the plate was kept in dark at 22 °C for 15 min. 0.5 M $H_2SO_4$ (50 μl per well) was added, and the plate was read at 450nm.

**Digestion of HA polymer:**

80 g HA (sodium salt, pure powder, food grade) was partially dissolved in 1L digestion buffer (0.15M NaCl, 0.1M NaOAc, pH was adjusted to 5.2 by AcOH). Bovine testicular hyaluronidase (200 mg, 400-1000 u/mg) was added. The reaction was stirred at 37 °C in an oil bath for 8 weeks. Hyaluronidase 75 mg was added every 3 days. The reaction was monitored by TLC with *t*-butanol (*t*BuOH)/$H_2O$/AcOH (1.5:1:1) and stained by 1, 3-dihydroxylnaphalene (0.2 g in 50 ml 5% $H_2SO_4$/ethanol (EtOH)). When the major product was $HA_4$, the reaction mixture was heated up to 100 °C. 900 ml $H_2O$ was removed by high vacuum rotary evaporator, and crude $HA_4$ 50 g was precipitated out by EtOH (900 ml), sodium acetate (NaOAc) was left in mother liquor, and the crude $HA_4$ was directly used for next step[21-22].

**Methyl *S*-(2-acetamido-3,4,6-tri-*O*-acetyl-2-deoxy-*β*-D-glucopyranoside) -(1→3)- 2-*O*-benzoyl-3,4-dideoxy-3,4-epimino-6-*O*-*p*-methoxybenzyl-*β*-D-allopyranoside (40): 39** (0.025 mmol, 9.0 mg) and **37** (0.0375 mmol, 1.5 eq., 21.0 mg ) were co-evaporated with toluene, and dissolved in anhydrous DMF (3 ml). TEA (1 mmol, 4 eq., 14 µl) was added at 0 °C and the reaction mixture was stirred at r.t. overnight. Then the crude mixture was concentrated and purified by silica gel chromatography with toluene/acetone system to yield **40** (32%). $^1$H NMR (500 MHz, $CDCl_3$): δ = 1.83 (s, 3H), 1.99 (s, 3H), 2.00 (s, 3H), 2.01 (s, 3H) (OCOC*H*$_3$ x3, NHCOC*H*$_3$), 2.54 (dd, 1H, *J* = 1.5 Hz, 7.5 Hz, H-4), 2.83 (dd, 1H, *J* = 4.0 Hz, 7.5 Hz, H-3), 3.31-3.35 (m, 1H, H-5), 3.45 (s, 3H, $C_6H_4OC$*H*$_3$), 3.58 (dd, 1H, *J* = 6.5 Hz, 10.0 Hz, H-6), 3.67 (dd, 1H, *J* = 5.0 Hz, 10.0

Hz, H-6), 3.80 (s, 3H, OC*H*$_3$ anomeric), 3.97-4.03 (m, 2H, H-6' x2), 4.07-4.13 (m, 2H, H-2', H-5), 4.52 (d, 1H, *J* = 7.0 Hz, C*H*$_2$PMP), 4.53 (d, 1H, *J* = 7.0 Hz, C*H*$_2$PMP), 4.53 (d, 1H, *J* = 9.5 Hz, H-1), 4.66 (d, 1H, *J* = 11.0 Hz, H-1'), 4.88 (t, 1H, *J* = 9.5 Hz, H-3'), 4.95-5.00 (m, 2H, H-2, H-4'), 5.55 (d, 1H, *J* = 9.5 Hz, NH'), 6.87-6.88 (m, 2H, $CH_{arom}$), 7.48-7.51 (m, 2H, $CH_{arom}$), 7.59-7.61 (m, 1H, $CH_{arom}$), 7.24-7.26 (m, 2H, $CH_{arom}$), 8.12-8.14 (m, 2H, $CH_{arom}$); $^{13}$C NMR (gHMQC decoupling, 500 MHz, $CDCl_3$): δ = 17.2 x 3, 19.2 (OCO*C*H$_3$ x3, NCO*C*H$_3$), 37.8 (C-3), 39.8 (C-4), 46.1 ($C_6H_4OCH_3$), 47.4 ($OCH_3$ anomeric), 51.8 (C-6'), 56.7 (C-2), 58.4 (C-6), 58.9 (C-4'), 60.8 (C-5), 61.0 (C-2'), 61.4 (C-3'), 63.2 (C-5'), 75.1 (C-1'), 82.8 (C-1), 113.9 x 2, 127.9 x 2, 128.7, 129.3 x 2, 129.8 x 2, (Carom x9); HRMS [M ]: m/z: calcd for $C_{36}H_{44}N_2O_{14}S$ 760.2513, found 760.2519.

**Acetyl *O*-(methyl 2,3,4-tri-*O*-acetyl- *β*-D-glucopyranosyluronate)-(1→3)-*O*-(2-acetamido-3,6-di-*O*-acetyl-2-deoxy-*β*-D-glucopyranosyl)-(1→4)-*O*-(methyl 2,3-di -*O*-acetyl-*β*-D-glucopyranosyluronate)-(1→3)-(2-acetamido-3,6-di-*O*-acetyl-2-deoxy - 1-thio- *β*-D-glucopyranoside (38):** Ion exchange resin (Dowex 50WX4 $Na^+$ form, 39 g) was washed with $H_2O$ (500 ml) for 3 times and stirred in 5% HCl (500 ml) at r.t. for 1 hr. The filtered resin was washed with $H_2O$ (500 ml) for 3 times. Tetrabutylammonium hydroxide (TBAOH) (40% wt. $H_2O$, 45 ml) was added to adjust the pH to 12. Then the filtered resin was washed with $H_2O$ (500 ml) for 3 times. TBA resin was stirred with crude **20** (15 g) in $H_2O$ (300 ml) for one day. The resin was filtered out and could be reused. $H_2O$ was removed and the $HA_4$-TBA (**22**) (17 g) was yielded as a white solid with 80%

TBA per $HA_2$. The degree of substitution was characterized by $^1$H-NMR. Compound **22** (17 g) was co-evaporated with toluene, and dissolved in anhydrous DMF (150 ml). MeI (30 ml) was added and the reaction mixture was stirred at 35 °C for 3 days. DMF was removed by high vacuum rotary evaporator, and the solid was dissolved in MeOH (300 ml). After filtration, the filtrate was collected and the crude HA methyl ester (15 g) was obtained as light yellow solid. Crude HA methyl ester (12 g) was co-evaporated with toluene, and dissolved in anhydrous DMF (25 ml), Py (25 ml) and $Ac_2O$ (40 ml). The reaction mixture was stirred at 40 °C for 2 days. The solvents were removed, and the crude product was dissolved in DCM (70 ml). The solution was poured into $Et_2O$ (250 ml) to precipitate the product. After filtration and purification by silica gel chromatography (DCM/MeOH), **23** (8.2 g) was yielded as α/β mixture (35% from crude **20**). Compound **23** (0.48 mmol, 590 mg) was co-evaporated with toluene and dissolved in DCM (3 ml). $Ac_2O$ (0.2 ml) was added and the reaction mixture was stirred at r.t. for 30 min. HBr (33% wt. in AcOH, 3 ml) was added at 0 °C dropwise and the reaction was stirred at r.t. for 6 hrs. The reaction was diluted with DCM (200 ml) and poured onto crushed ice in saturated NaCl (200 ml). The organic phase was separated and washed with saturated $NaHCO_3$ until the pH reached 7, which was then dried over $Na_2SO_4$, filtered, and concentrated. The resulting crude residue was co-evaporated with toluene, and dissolved in anhydrous MeCN (3 ml). The mixture of TBASAc (2.60 mmol, 5 eq., 777 mg) and HSAc (7.34 mmol, 15 eq., 525 µl) in anhydrous MeCN (1 ml) was added to the reaction mixture dropwise at 0 °C. The reaction was stirred at r.t. for 4.5 hrs. The crude mixture was concentrated and

purified with silica gel chromatography (DCM/MeOH) to yield **38** (370 mg, 30%). $^{1}$H NMR (500 MHz, $CDCl_3$): δ = 1.95 (s, 3H) x2, 1.96 (s, 3H) x2, 1.72 (s, 3H), 2.00 (s, 3H), 2.02, (s, 3H), 2.03 (s, 3H) x2, 2.33 (s, 3H, SCOC*H*$_3$), 3.05-3.10 (m, 1H, H-2''), 3.60-3.62 (m, 1H, H-5''), 3.67 (s, 3H, COO C*H*$_3$), 3.73-3.83 (m, 4H, H-5, COOC*H*$_3$), 3.93-4.00 (m, 4H, H-5''', H-5', H-3, H-6''), 4.02-4.09 (m, 3H, H-4', H-6, H-2), 4.13 (dd, 1H, *J* = 5.0 Hz, 12.5 Hz, H-6), 4.28 (dd, 1H, *J* = 4.5 Hz, 12.5 Hz, H-6''), 4.43 (t, 1H, *J* = 9.5 Hz, H-3'), 4.59 (d, 1H, *J* = 8.0 Hz, H-1'''), 4.75-4.80 (m, 3H, H-1'', H-1', H-2'), 4.4 (t, 1H, *J* = 9.5 Hz, H-2'''), 4.86 (t, 1H, *J* = 9.5 Hz, H-4''), 4.88 (t, 1H, *J* = 9.5 Hz, H-4), 5.03 (t, 1H, *J* = 8.5 Hz, H-3'), 5.08 (t, 1H, *J* = 9.5 Hz, H-4'''), 5.16 (d, 1H, *J* = 9.0 Hz, H-1), 5.17 (t, 1H, *J* = 9.5Hz, H-3'''), 6.22 (d, 1H, *J* = 6.5 Hz, NH''), 6.35 (d, 1H, *J* = 8.5 Hz, NH); $^{13}$C NMR (125 MHz, $CDCl_3$): δ = 20.3 x2, 20.4, 20.5 x3, 20.7 x2 (OCO*C*$H_3$ x9), 23.2, 23.5 (NCO*C*$H_3$ x2), 30.8 (SO*C*$H_3$), 52.6 (COO*C*$H_3$), 53.0 (COO*C*$H_3$), 57.5 (C-2''), 61.9 (C-6''), 62.2 (C-6), 68.1 (C-4''), 68.3 (C-4), 69.3 (C-4'''), 71.2 (C-2'), 71.5 (C-2'''), 71.6 (C-5''), 72.1 x2 (C-3', C-3'''), 72.1 x2 (C-5', C-5'''), 74.7 (C-4'), 75.8 (C-2), 76.2 (C-5), 76.8 (C-3''), 79.7 (C-3), 81.2 (C-1), 98.9 (C-1'), 100.6 (C-1''), 100.1 (C-1'''), 177.9, 167.8, 169.2, 169.3, 169.4, 169.7 x2, 170.0 x2, 170.1, 170.4 (O*C*O*C*$H_3$ x9, NH*C*O*C*$H_3$ x2, S*C*O*C*$H_3$, *C*OO*C*$H_3$ x2); HRMS $[M + Na]^+$: m/z: calcd for $C_{50}H_{68}N_2O_{32}SNa$ 1263.3374, found 1263.3434.

**Preparation of monosaccharide 35, 36, 37, 38, 15 and 23:**

**Scheme 4.13.** Preparation of monosaccharide 35, 36, 37, 38, 15 and 23

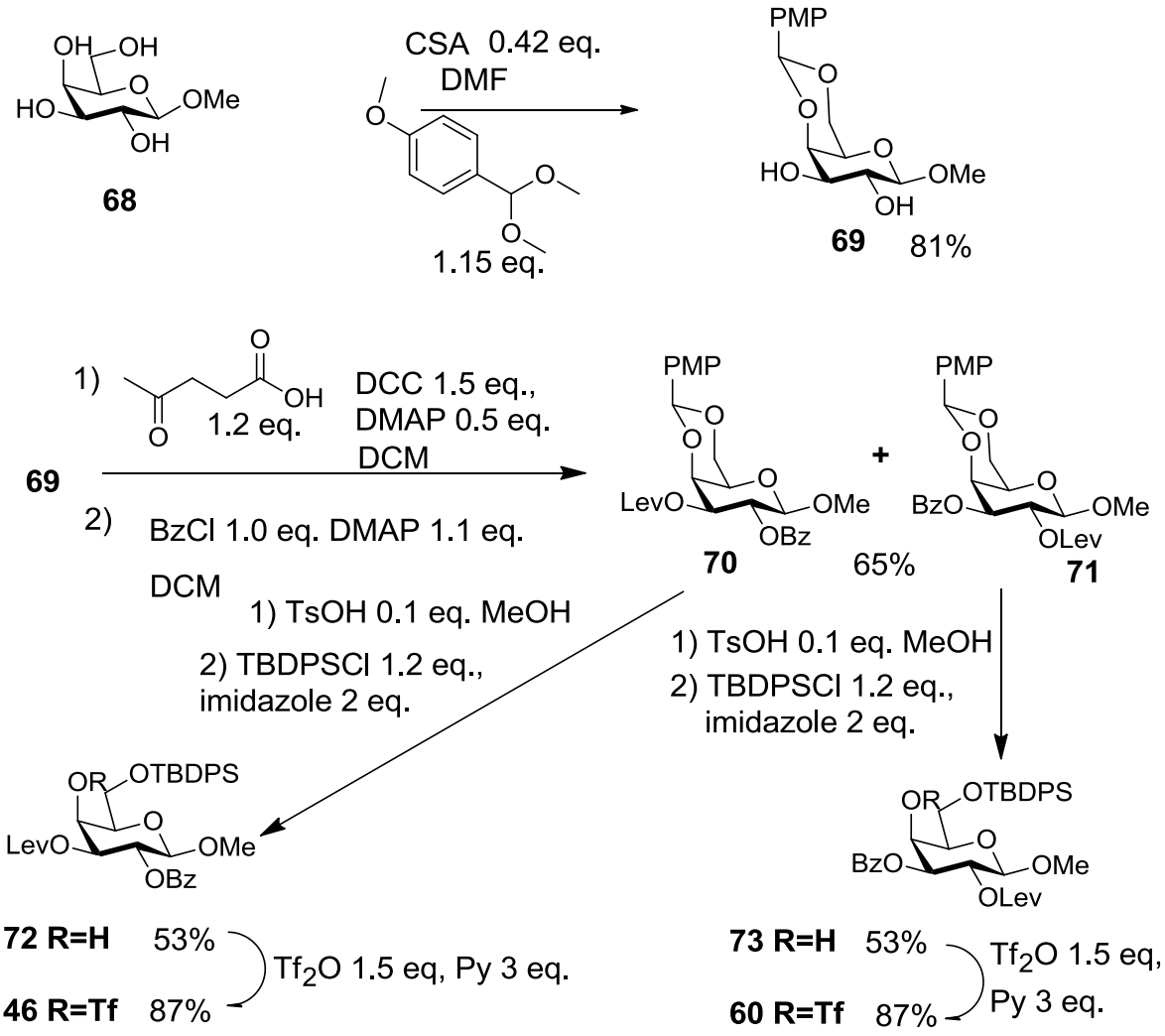


Methyl-*β*-D-galactoside **68** (7.7 mmol, 1.5 g) and CSA (3.2 mmol, 0.42 eq., 0.75 g) were co-evaporated with toluene and dissolved in anhydrous DMF (80 ml). Anisaldehyde dimethyl acetal (8.8 mmol, 1.15 eq, 1.5 ml) was added, and the reaction was stirred at 80 °C for 2 hrs. TEA (3.2 mmol, 0.42 eq., 0.45 ml) was added to adjust the pH to 7. The crude mixture was concentrated and purified by silica gel chromatography (toluene/acetone) to yield compound **69** (1.95 g, 81%). Compound **69** (17.4 mmol, 5.4 g)

and DCC (26.0 mmol, 1.5 eq., 5.57 g) were co-evaporated with toluene and dissolved in anhydrous DCM (260 ml). Levulinic acid (20.8 mmol, 1.2 eq., 2.10 ml) and DMAP (8.70mmol, 0.5 eq., 1.08 g) were added. The reaction mixture was stirred at r.t. overnight, and dilute with DCM (600 ml). The solid was removed by filtration. The crude product was concentrated and purified by silica gel chromatography (toluene/acetone) to yield the a mixture of 3-*O*-Lev and 2-*O*-Lev (1:1, 11.8 mmol. 4.85 g), which was co-evaporated with toluene and dissolved in anhydrous DCM (80 ml). Benzoyl chloride (BzCl) (14.2 mmol, 1.2 eq, 1.65 ml) and 4-dimethylaminopyridine (DMAP) (17.8 mmol, 1.5 eq., 2.17 g) were added to the reaction mixture. After 4 hrs, the reaction mixture was concentrated to yield a mixture of compound **70** and **71**. Compound **70** (5.65 mmol. 2.90 g) and **71** (5.65 mmol. 2.90 g) were separated by the combination of gel chromatography purification (toluene/acetone v/v 10:1) and crystallization (EA/Hexane, DCM/$Et_2O$). **70** (1.17 mmol. 0.600 g) was dissolved in MeOH (3ml), and *p*-toluenesulfonic acid (TsOH) (0.117 mmol, 0.1 eq., 22.0 mg) was added. The reaction mixture was stirred at r.t. for 2 hrs, and quenched with TEA (0.117 mmol, 0.1 eq., 11.4 µl). The crude mixture was concentrated and purified by silica gel chromatography (toluene/acetone) yielding a diol (330 mg, 0.84 mmol). The diol (330 mg, 0.84 mmol) was co-evaporated with toluene and dissolved in anhydrous DCM (5 ml). Imidazole (1.68 mmol, 2 eq.,113 mg) and *tert*-butyl diphenylchlorosilane (TBDPSCl) (0.870 mmol, 1.05 eq., 0.23 ml) were added, and the reaction mixture was stirred at r.t. overnight. The crude mixture was directly purified by silica gel chromatography (Hexane/EA/DCM) to yield **72** (0.390 g, 0.615 mmol).

Compound **73** was synthesized in 53% yield from **71** following the same procedures as **72**. Compound **72** (51 mg, 0.080 mmol) was dissolved in DCM (1.5 ml). Py (0.26 mmol, 7 eq, 15 µl) and $Tf_2O$ (0.12 mmol, 1.5 eq, 20 µl) were added sequentially at 0 °C. The reaction was stirred at r.t. for 1 hrs. The crude mixture was directly purified by silica gel chromatography (Hexane/EA/DCM) to produce compound **46** (45 mg, 0.07 mmol). Compound **66** was formed in 87% yield from compound **73** following the same procedure as compound **46**.

**Methyl 2-*O*-benzoyl-3-*O*-levulinyl-4, 6-*O*-*p*-methoxybenzylidene -*β*-D-glucopyranoside (70)**. $^1$H NMR (500 MHz, $CDCl_3$): δ = 1.88 (s, 3H $CH_2CH_2COCH_3$), 2.42-2.63 (m, 4H, $CH_2CH_2COCH_3$), 3.50 (s, 3H, $C_6H_4OCH_3$), 3.55 (t, 1H, *J* = 1.0 Hz, H-5), 3.79 (s, 3H, $OCH_3$ anomeric), 4.06 (dd, 1H, *J* = 1.0 Hz, 12.5 Hz, H-6'), 4.33 (dd, 1H, *J* = 1.0 Hz, 12.5 Hz, H-6), 4.36 (dd, 1H, *J* = 1.0 Hz, 3.5 Hz, H-4), 4.56 (d, 1H, *J* = 8.0 Hz, H-1), 5.15 (dd, 1H, *J* = 3.5 Hz, 10.5 Hz, H-3), 5.47 (s, 1H, CHPh), 5.62 (dd, 1H, *J* = 8.0 Hz, 10.5 Hz, H-2), 6.87-6.90 (m, 2H, $CH_{arom}$), 7.41-7.47 (m, 4H, $CH_{arom}$), 7.53-7.57 (m, 1H, $CH_{arom}$), 7.99-8.01 (m, 2H, $CH_{arom}$); $^{13}$C NMR (125 MHz, $CDCl_3$): δ = 28.2 ($CH_2CH_2COCH_3$), 29.4 ($CH_2CH_2COCH_3$), 37.8 ($CH_2CH_2COCH_3$), 55.3 ($OCH_3$ anomeric), 56.5 ($C_6H_4COCH_3$), 66.4 (C-5), 68.8 (C-6), 68.9 (C-2), 72.0 (C-3), 73.4 (C-4), 101.0 (CHPh), 101.9 (C-1), 113.5 x2, 127.8 x2, 128.4 x2, 129.2 x2, 129.7, 130.1, 133.1, 160.1 (Carom x12), 165.2, 172.1 (COPh, $OCOCH_2CH_2COCH_3$), 206.1 ($OCOCH_2CH_2COCH_3$); HRMS $[M + Na]^+$: m/z: calcd for $C_{27}H_{30}O_{10}Na$ 537.1737, found 537.1763.

**Methyl 2-*O*-benzoyl -6-*O*-*tert*-butyldiphenylsilyl-3-*O*-levulinyl -*β*-D-glucopyranoside (72)**. $^1$H NMR (500 MHz, $CDCl_3$): δ = 1.04 (s, 9H, $SiC(CH_3)_3$), 2.05 (s, 3H, $CH_2CH_2COC\mathit{H}_3$), 2.41-2.56 (m, 2H, $C\mathit{H}_2CH_2COCH_3$), 2.63-2.56 (m, 2H, $CH_2C\mathit{H}_2COCH_3$), 3.01 (d, 1H, *J* = 4.0 Hz, OH), 3.46 (s, 3H, $OCH_3$ anomeric), 3.65 (dt, 1H, *J* = 1.0 Hz, 5.5 Hz, H-5), 3.93 (dd, 1H, *J* = 5.5 Hz, 10.5 Hz, H-6), 3.99 (dd, 1H, *J* = 5.5 Hz, 10.5 Hz, H-6'), 4.29 (dd, 1H, *J* = 1.0 Hz, 4.0 Hz, H-4), 4.49 (d, 1H, *J* = 8.5 Hz, H-1), 5.06 (dd, 1H, *J* = 3.0 Hz, 10.5 Hz, H-3), 5.56 (dd, 1H, *J* = 8.5 Hz, 10.5 Hz, H-2), 7.36-7.45 (m, 8H, $CH_{arom}$), 7.53-7.57 (m, 1H, $CH_{arom}$), 7.70-7.71 (m, 4H, $CH_{arom}$), 8.00-8.01 (m, 2H $CH_{arom}$); $^{13}$C NMR (125 MHz, $CDCl_3$): δ = 19.2 ($Si\mathit{C}(CH_3)_3$), 26.7 ($SiC(\mathit{C}H_3)_3$), 28.3 ($CH_2\mathit{C}H_2COCH_3$), 29.6 ($\mathit{C}H_2CH_2COCH_3$), 38.1 ($CH_2CH_2CO\mathit{C}H_3$), 56.5 ($OCH_3$), 63.2 (C-6), 67.4 (C-4), 67.7 (C-2), 74.2 x2 (C-3, C-5), 102.1 (C-1), 127.8 x2, 127.8 x2, 128.4 x2, 129.8, 129.3 x3, 132.8, 133.0, 133.1 x2, 135.5 x3, 135.7 x3(Carom x18), 165.3, 172.0 (*C*OPh, O*C*O *C*$H_2CH_2COCH_3$), 207.2 ($CH_2CH_2\mathit{C}OCH_3$); HRMS $[M + Na]^+$ calcd for $C_{35}H_{42}O_9SiNa$ 657.2496, found 657.2514.

**Methyl 3-*O*-benzoyl-2-*O*-levulinyl-4, 6-*O*-*p*-methoxybenzylidene -*β*-D-glucopyranoside (71)**. $^1$H NMR (500 MHz, $CDCl_3$): δ = 2.02 (s, 3H $CH_2CH_2COC\mathit{H}_3$), 2.49-2.65 (m, 4H, $C\mathit{H}_2C\mathit{H}_2COCH_3$), 3.54 (s, 3H, $C_6H_4OC\mathit{H}_3$), 3.58 (d, 1H, *J* = 1.0 Hz, H-5), 3.77 (s, 3H, $OCH_3$ anomeric), 4.07 (dd, 1H, *J* = 2.1 Hz, 12.5 Hz, H-6'), 4.34 (dd, 1H, *J* = 1.5 Hz, 12.5 Hz, H-6), 4.50-4.52 (m, 1H, H-4), 4.51 (d, 1H, *J* = 8.0 Hz,H-1), 5.15 (dd, 1H, J = 3.5 Hz, 10.5 Hz, H-3), 5.45 (s, 1H, C*H*Ph), 5.57 (dd, 1H, *J* = 8.0 Hz, 10.5 Hz,

H-2), 6.83-6.84 (m, 2H, $CH_{arom}$), 7.38-7.55 (m, 5H, $CH_{arom}$), 7.99-8.01 (m, 2H, $CH_{arom}$); $^{13}C$ NMR (125 MHz, $CDCl_3$): δ = 28.0 ($CH_2\mathit{C}H_2COCH_3$), 29.7 ($CH_2CH_2CO\mathit{C}H_3$), 37.9 ($\mathit{C}H_2CH_2COCH_3$), 55.3 ($C_6H_4CO\mathit{C}H_3$), 56.6 ($OC\mathit{H_3}$ anomeric), 66.4 (C-5), 68.9 (C-6), 72.8 (C-3), 73.5 (C-4), 100.8 ($\mathit{C}$HPh), 101.7 (C-1), 113.4 x2, 127.6 x2, 127.8, 128.4 x2, 129.9, 130.0 x2, 133.4, 160.0 ($C_{arom}$ x12), 166.2, 171.6 ($\mathit{C}$OPh, $O\mathit{C}OCH_2CH_2COCH_3$), 205.9 ($CH_2CH_2\mathit{C}OCH_3$); HRMS $[M + Na]^+$ :m/z: calcd for $C_{27}H_{30}O_{10}$ Na 537.1737, found 537.1739

**Methyl 3-*O*-benzoyl -6-*O*-*tert*-butyldiphenylsilyl-2-*O*-levulinyl -*β*-D-glucopyranoside (73)**. $^1H$ NMR (500 MHz, $CDCl_3$): δ = 1.03 (s, 9H, $SiC(CH_3)_3$), 2.01 (s, 3H, $CH_2CH_2COC\mathit{H_3}$), 2.45-2.64 (m, 4H, $C\mathit{H_2}C\mathit{H_2}COCH_3$), 2.80 (d, 1H, *J* = 4.5 Hz, OH), 3.50 (s, 3H, $OCH_3$ anomeric), 3.64-3.66 (m, 1H, H-5), 3.92 (dd, 1H, *J* = 4.5 Hz, 10.5 Hz, H-6), 3.98 (dd, 1H, *J* = 6.0 Hz, 10.5 Hz, H-6'), 4.39 (t, 1H, *J* = 3.0 Hz, H-4), 4.43 (d, 1H, *J* = 8.0 Hz, H-1), 5.11 (dd, 1H, *J* = 3.0 Hz, 10.0 Hz, H-3), 5.49 (dd, 1H, *J* = 8.0 Hz, 10.0 Hz, H-2), 7.34-7.45 (m, 8H, $CH_{arom}$), 7.54-7.58 (m, 1H, $CH_{arom}$), 7.66-7.70 (m, 4H $CH_{arom}$), 8.02-8.04 (m, 4H $CH_{arom}$) ; $^{13}C$ NMR (125 MHz, $CDCl_3$): δ = 19.1 ($Si\mathit{C}(CH_3)_3$), 26.7 ($SiC(\mathit{C}H_3)_3$) 28.0 ($CH_2\mathit{C}H_2COCH_3$), 29.6 ($\mathit{C}H_2CH_2COCH_3$), 37.9 ($CH_2CH_2CO\mathit{C}H_3$), 56.6 ($OCH_3$), 63.4 (C-5), 68.0 (C-2), 69.3 (C-6), 73.8 (C-3), 74.4 (C-4), 102.0 (C-1), 127.8 x2, 127.8 x2, 128.5 x2, 129.4, 129.9 x2, 130.0 x2, 132.6, 132.8, 133.4, 135.5 x2, 135.6 x2 ($C_{arom}$ x18), 165.9, 171.6 ($\mathit{C}$OPh, $O\mathit{C}O\mathit{C}H_2CH_2COCH_3$), 205.9 ($CH_2CH_2\mathit{C}OCH_3$); HRMS $[M + Na]^+$ calcd for $C_{35}H_{42}O_9SiNa$ 657.2496, found 657.2474.

**Methyl *S*-(methyl 2,3,4-tri-*O*-acetyl- *β*-D- glucopyranosyluronate)-(1→3)-*O*-(2-acetamido-3,6-di-*O*-acetyl-2-deoxy-*β*-D-glucopyranosyl)-(1→4)-*O*-(methyl 2,3-di-*O*-acetyl-*β*-D-glucopyranosyluronate)-(1→3)-(2-acetamido-3,6-di-*O*-acetyl-2-deoxy- *β*-D-glucopyranosyl)-(1→4)-3-*O*-benzoyl-6-*O*-*tert*-butyldiphenylsilyl-2-*O*-levulinyl-*β*-D-glucopyranoside (61): 38** (0.04 mmol, 50 mg) was dissolved in MeOH (1 ml) and DCM (1 ml). NaOMe (1M in MeOH, 0.02 mmol, 0.5 eq.) was added in 5 portions at -40 °C. After the starting material was consumed, acidic resin (IR 120) was added to adjust the pH to 4.5. The crude **36** was concentrated, and co-evaporated with toluene. Crude **36** (0.04 mmol) and freshly prepared compound **60** (0.08 mmol, 2 eq.) were dissolved in anhydrous DMF (2 ml). TEA (0.12 mmol, 3 eq, 15 µl) was added at 0 °C, and the reaction mixture was stirred at r.t. for 2 days. The reaction mixture was concentrated and purified by silica gel chromatography (toluene/ acetone) to yield compound **61** in 34% yield. $^1$H NMR (500 MHz, $CDCl_3$): δ = 1.01 (s, 9H, SiC($CH_3$)$_3$), 1.51 (s, 3H, NHCOC$H_3$), 1.81 (s, 3H, OCOC$H_3$), 1.92 (s, 3H), 1.95 (s, 3H), 1.96 (s, 3H), 1.97 (s, 3H), 1.98 (s, 6H), 1.99 (s, 3H), 2.02 (s, 3H), 2.03 (s, 3H), 2.04 (s, 3H), 2.44-2.64 (m, 4H, $CH_2CH_2COCH_3$), 3.04-3.10 (m, 1H, H-2’’’), 3.31 (t, 1H, *J* = 11.0 Hz, H-4), 3.47 (s, 3H, $OCH_3$ anomeric), 3.58-3.69 (m, 2H, H-5’, H-5’’’), 3.69 (s, 3H, COOC$H_3$), 3.69-3.75 (m, 1H, H-5), 3.78-3.84 (m, 1H, H-3’), 3.84 (s, 3H, COOC$H_3$), 3.92-4.09 (m, 8H, H-6 x2, H-2’, H-6’, H-4’’, H-5’’, H-6’’’, H-5’’’’), 4.28 (dt, 2H, *J* = 4.5 Hz, 13.0 Hz, H-6’, H-6’’’), 4.36 (d, 1H, *J* = 8.5 Hz, H-1), 4.44 (t, 1H, *J* = 9.5 Hz, H-3’’’), 4.61 (d, 1H, *J* = 8.0 Hz, H-1’’’’), 4.63 (d, 1H, *J* = 8.0 Hz, H-1’’), 4.73-4.78 (m, 3H, H-4’, H-2’’’’, H-2’’), 4.80 (d, 1H, *J* = 8.0 Hz,

H-1’’’), 4.82 (d, 1H, *J* = 10.5 Hz, H-1’), 4.87 (t, 1H, *J* = 9.5 Hz, H-4’’’), 5.06 (t, 1H, *J* = 9.0 Hz, H-3’’’’), 5.10 (t, 1H, *J* = 9.0 Hz, H-4’’’’), 5.13 (t, 1H, *J* = 8.5 Hz, H-2), 5.18 (t, 1H, *J* = 9.0 Hz, H-3’’), 5.41 (dd, 1H, *J* = 9.0 Hz, 11.0 Hz, H-3), 5.50 (d, 1H, *J* = 10.0 Hz, NH’’’), 5.67 (d, 1H, *J* = 8.0 Hz, NH’), 7.33-7.48 (m, 8H, $CH_{arom}$), 7.58-7.61 (m, 1H, $CH_{arom}$), 7.69-7.73 (m, 4H, $CH_{arom}$), 7.97-8.05 (m, 2H, $CH_{arom}$); $^{13}C$ NMR (125 MHz, $CDCl_3$): δ = 19.3 ($C_q$, Si*C*$(CH_3)_3$), 20.4 x3, 20.5 x3, 20.6 x2, 20.7 (OCO*C*$H_3$ x9), 22.9, 23.5 (NHCO*C*$H_3$ x2), 26.8 (SiC(*C*$H_3)_3$), 27.9 ($CH_2$*C* $H_2COCH_3$), 29.4 ($CH_2C$ $H_2CO$*C*$H_3$), 37.9 (*C*$H_2CH_2COCH_3$), 45.2 (C-4), 52.7 (COO*C* $H_3$), 52.9 (C-5), 53.0 (COO*C*$H_3$), 56.3 (O*C*$H_3$ anomeric), 58.0 (C-2’’’), 61.9, 62.6 (C-6’, C-6’’’), 62.9 (C-6), 68.0 (C-4’’’), 68.8, 69.4, 70.9, 71.0, 71.8, 71.9, 72.0, 72.1 x 2, 72.3 x 2, 72.7, 74.5, 75.7, 75.7 (C-2, C-3, C-2’, C-4’, C-5’, C-2’’, C-3’’, C-4’’, C-5’’ C-5’’’, C-2’’’’, C-3’’’’, C-4’’’’, C-5’’’’), 76.2 (C-3’’’), 80.3 (C-3’), 81.5 (C-1’), 98.5 (C-1’’’), 99.9 (C-1’’’’), 101.1 (C-1’’), 101.2 (C-1), 127.5, 127.6, 127.7, 127.8, 128.6, 128.9, 129.6, 129.7, 130.1, 133.1, 133.4, 134.0, 135.5,135.6 x2, 135.7, 135.8 x2 ($C_{arom}$ x18),166.9, 167.5, 167.8,169.0, 169.2, 169.3 x2, 169.7, 169.9, 170.2 x2, 170.6, 170.6, 170.9, 171.4 (O*C*O$CH_3$ x9, NH*C*O$CH_3$ x2, *C*O$OCH_3$ x2, O*C*O$CH_2CH_2COCH_3$, *C*OPh), 205.9 (O$CO$*C*$H_2CH_2$*C*O$CH_3$); HRMS $[M + NH_4]^+$: m/z: calcd for $C_{83}H_{110}N_3O_{39}SSi$ 1832.6206, found 1832.6115.

**Methyl *S*-(methyl 2,3,4-tri-*O*-acetyl- *β*-D- glucopyranosyluronate)-(1→3)-*O*-(2-acetamido-3,6-di-*O*-acetyl-2-deoxy-*β*-D-glucopyranosyl)-(1→4)-*O*-(methyl 2,3-di -*O*-acetyl-*β*-D-glucopyranosyluronate)-(1→3)-(2-acetamido-3,6-di-*O*-acetyl-2-deoxy - *β*-D-glucopyranosyl)-(1→4)-2-*O*-benzoyl-6-*O*-*tert*-butyldiphenylsilyl-3-*O*-levulinyl**

**-*β*-D-glucopyranoside (63):** Crude **36** (0.04 mmol) and freshly prepared **46** (0.04 mmol, 1.25 eq.) were dissolved in anhydrous DMF (2 ml). TEA (0.12 mmol, 2.5 eq, 12.5 µl) was added at 0 °C, and the reaction mixture was stirred at r.t. for 2 days. The reaction mixture was concentrated and purified by silica gel chromatography (toluene/ acetone) to yield compound **63** in 27% yield. $^{1}$H NMR (500 MHz, $CDCl_3$): δ = 1.02 (s, 9H, SiC($CH_3$)$_3$), 1.95 (s, 3H), 1.96 (s, 9H), 1.98 (s, 9H), 2.00 (s, 3H), 2.03 (s, 3H), 2.04 (s, 3H), 2.06 (s, 3H), 2.20 (s, 3H), 2.29-2.34 (m, 1H, $CH_2CH_2COCH_3$), 2.51-2.56 (m, 1H, $CH_2CH_2COCH_3$), 2.66-2.86 (m, 2H, $CH_2CH_2COCH_3$), 2.96-3.01 (m, 1H, H-2'''), 3.33-3.46 (m, 4H, H-4, $OCH_3$ anomeric), 3.55 (t, 1H, *J* = 9.5 Hz, H-3'), 3.60-3.65 (m, 2H, H-5', H-5'''), 3.69 (s, 3H, $COOCH_3$), 3.72-3.87 (m, 7H, H-5, $COOCH_3$, H-6 x 2, H-5''), 3.91-4.00 (m, 3H, H-5'''', H-6', H-6'''), 4.01 (t, 1H, *J* = 9.5 Hz, H-4'') 4.14-4.25 (m, 2H, H-2', H-6'), 4.33 (dd, 1H, *J* = 5.0 Hz, 12.5 Hz, H-6'''), 4.45 (d, 1H, *J* = 8.0 Hz, H-1), 4.46 (d, 1H, *J* = 10.0 Hz, H-1'), 4.49 (t, 1H, *J* = 9.5 Hz, H-3'''), 4.59 (d, 1H, *J* = 8.0 Hz, H-1''''), 4.68 (d, 1H, *J* = 8.5 Hz, H-1''), 4.76 (dd, 1H, *J* = 8.0 Hz, 9.5 Hz, H-2''''), 4.80 (d, 1H, *J* = 8.5 Hz, H-1'''), 4.81 (dd, 1H, *J* = 8.5 Hz, 9.5 Hz, H-2''), 4.82 (t, 1H, *J* = 9.5 Hz, H-4'), 4.86 (t, 1H, *J* = 9.5 Hz, H-4'''), 5.06 (t, 1H, *J* = 9.5 Hz, H-3''), 5.10 (t, 1H, *J* = 9.5 Hz, H-4''''), 5.17 (dd, 1H, *J* = 8.0 Hz, 11.5 Hz, H-2), 5.18 (t, 1H, *J* = 9.5 Hz, H-3''''), 5.33 (dd, 1H, *J* = 10.0 Hz, 11.5 Hz, H-3), 5.62 (d, 1H, *J* = 7.0 Hz, NH'''), 6.89 (d, 1H, *J* = 10.0 Hz, NH'), 7.31-7.46 (m, 8H, $CH_{arom}$), 7.57-7.60 (m, 1H, $CH_{arom}$), 7.69-7.74 (m, 4H, $CH_{arom}$) 7.98-8.00 (m, 2H, $CH_{arom}$); $^{13}$C NMR (125 MHz, $CDCl_3$): δ = 19.3 ($C_q$, Si*C*($CH_3$)$_3$), 20.4

x2, 20.5 x2, 20.6 x2, 21.0 x3 (OCO*C*$H_3$ x9), 23.2, 23.5 (NHCO*C*$H_3$ x2), 26.8 (SiC(*C*$H_3$)$_3$), 27.7 ($CH_2$*C* $H_2$COCH$_3$), 29.7 ($CH_2$C $H_2$CO*C*H$_3$), 37.7 (*C*$H_2$$CH_2$COCH$_3$), 43.7 (C-4), 52.7 (COO*C* H$_3$), 53.0 (C-2'), 53.3 (COO*C*H$_3$), 56.3 (O*CH*$_3$ anomeric), 58.2 (C-2'''), 61.9 (C-6'''), 62.9 (C-6), 63.3 (C-6'), 67.9 (C-4'''), 68.5 (C-2''), 69.4 (C-4''''), 70.1 (C-3), 70.7 (C-4'), 72.0 (C-2''''), 72.1 (C-5'/ C-5'''), 72.3 (C-3''), 72.3 (C-5''''), 74.0 (C-2), 74.0 (C-3''''), 74.6 (C-5''), 75.8 (C-4''), 75.8 (C-5'/ C-5'''), 75.9 (C-3'''), 76.5 (C-5), 80.2 (C-3'), 80.6 (C-1'), 98.4 (C-1'''), 99.9 (C-1''''), 101.2 (C-1), 101.4 (C-1''), 127.5 x2, 127.7 x3, 128.5, 129.5, 129.6, 129.7, 129.8, 133.2, 133.3, 133.4, 135.6 x2, 135.8 x3 ($C_{arom}$ x18),164.5, 165.3, 166.9,167.5, 168.9, 169.2, 169.3, 169.7, 169.8, 169.9, 170.2, 170.3, 170.3, 170.6, 170.9, 172.7 (O*C*OCH$_3$ x9, NH*C*OCH$_3$ x2, *C*OOCH$_3$ x2, O*C*OCH$_2$CH$_2$COCH$_3$, *C*OPh), 209.6 (OCOCH$_2$CH$_2$*C*OCH$_3$); HRMS $[M + Na]^+$: m/z: calcd for $C_{83}H_{106}N_2O_{39}SSNai$ 1837.5760, found 1837.5684.

**Methyl *S*-(methyl 2,3,4-tri-*O*-acetyl- *β*-D- glucopyranosyluronate)-(1→3)-*O*-(2-acetamido-3,6-di-*O*-acetyl-2-deoxy-*β*-D-glucopyranosyl)-(1→4)-*O*-(methyl 2,3-di-*O*-acetyl-*β*-D-glucopyranosyluronate)-(1→3)-(2-acetamido-3,6-di-*O*-acetyl-2-deoxy-*β*-D-glucopyranosyl)-(1→4)-3-*O*-benzoyl-2-*O*-levulinyl-*β*-D-glucopyranoside (62):** **61** (60 mg, 0.033 mmol) was dissolved in Py (1.5 ml) in a plastic flask followed by the addition of 65–70% HF/Py solution (0.3 ml) at 0 °C. The solution was stirred for 4 hrs, diluted with DCM (15 ml) and washed with 10% aqueous $CuSO_4$ solution (15 ml). The aqueous phase was extracted with DCM (30 ml) twice and the combined organic layers

were washed with a saturated aqueous solution of $NaHCO_3$ to remove HF. The crude product was purified by silica gel chromatography to yield compound **62** in 85% yield. $^1$H NMR (500 MHz, $CDCl_3$): δ = 1.55 (s, 3H), 1.91 (s, 3H), 1.96 (s, 3H), 1.97 (s, 6H), 1.98 (s, 6H), 2.00 (s, 3H), 2.02 (s, 3H), 2.04 (s, 3H), 2.06 (s, 3H), 2.43-2.60 (m, 4H, $CH_2CH_2COCH_3$), 3.05-3.35 (m, 2H, H-4, H-2'), 3.50 (s, 3H, $OCH_3$ anomeric), 3.60-3.63 (m, 2H, H-5, H-5'''), 3.70 (s, 3H, $COOCH_3$), 3.70-3.74 (m, 1H, H-5), 3.84 (s, 3H, $COOCH_3$), 3.79-3.93 (m, 1H, H-3'''), 3.94-4.09 (m, 8H, H-6 x2, H-2''', H-5'''', H-4'', H-5'', H-6', H-6''' ), 4.18-4.31 (m, 2H, H-6', H-6''') 4.42 (d, 1H, *J* = 8.0 Hz, H-1), 4.44 (dd, 1H, *J* = 7.0 Hz, 10.5 Hz, H-3'), 4.61 (d, 1H, *J* = 7.5 Hz, H-1''''), 4.66 (d, 1H, *J* = 7.5 Hz, H-1''), 4.76 (dd, 1H, *J* = 7.5 Hz, 9.0 Hz, H-2''''), 4.78 (dd, 1H, *J* = 7.5 Hz, 9.0 Hz, H-2''), 4.79 (d, 1H, *J* = 8.0 Hz, H-1'''), 4.81 (t, 1H, *J* = 9.0 Hz, H-4'''), 4.87 (t, 1H, *J* = 10.0 Hz, H-4'), 4.89 (d, 1H, *J* = 10.5 Hz, H-1'), 5.06 (t, 1H, *J* = 9.0 Hz, H-3'''), 5.11 (t, 1H, *J* = 9.0 Hz, H-4''''), 5.11 (t, 1H, *J* = 10.0 Hz, H-2), 5.19 (t, 1H, *J* = 9.5 Hz, H-3''), 5.40 (dd, 1H, *J* = 9.0 Hz, 11.0 Hz, H-3), 5.70 (d, 1H, *J* = 8.5 Hz, NH'''), 5.76 (d, 1H, *J* = 7.5 Hz, NH'), 7.43-7.46 (m, 2H, $CH_{arom}$), 7.57-7.60 (m, 1H, $CH_{arom}$), 8.00-8.01 (m, 2H, $CH_{arom}$); $^{13}$C NMR (125 MHz, $CDCl_3$): δ = 20.4 x2, 20.5 x2, 20.6 x2, 20.7 x3 ($OCOCH_3$ x9), 22.9, 23.5 ($NHCOCH_3$ x2), 27.8 ($CH_2C$ $H_2COCH_3$), 29.7 ($CH_2C$ $H_2COCH_3$), 37.9 ($CH_2CH_2COCH_3$), 45.7 (C-4), 52.7 ($COOC$ $H_3$), 53.0 ($COOCH_3$), 57.0 ($OCH_3$ anomeric), 57.9 (C-2'), 61.9, 62.1 (C-6', C-6'''), 62.7 (C-6), 68.0 (C-4'), 68.7 (C-4'''), 69.4 (C-2), 71.0 x2 (C-3, C-2''''), 71.9 x2, 72.0 (C-2'', C-5', C-5'''), 72.1 (C-3''''), 72.3 x2, 72.6, (C-2''', C-3'', C-4''''), 74.5 (C-5''''), 75.7, 75.9 (C-4'', C-5''), 76.2 (C-5), 77.0 (C-3'), 79.

(C-3’’’), 81.6 (C-1’), 98.5 (C-1’’’), 99.9 (C-1’’’’), 101.1 (C-1’’), 101.6 (C-1), 128.2, 128.6, 128.8, 129.0, 130.0, 134.0 ($C_{arom}$ x6), 167.0, 167.2, 167.9, 169.0 169.3 x2, 169.6, 169.7, 170.1 x2, 170.2, 170.6 x2, 171.1, 171.4 (O*C*O$CH_3$ x9, NH*C*O$CH_3$ x2, *C*OO$CH_3$ x2, O*C*O$CH_2CH_2COCH_3$, *C*OPh), 205.9 (OCO$CH_2CH_2$*C*O$CH_3$); HRMS $[M + Na]^+$: m/z: calcd for $C_{67}H_{88}N_2O_{39}SNa$ 1599.4583, found 1599.4655.

**Methyl *S*-(methyl 2,3,4-tri-*O*-acetyl- *β*-D- glucopyranosyluronate)-(1→3)-*O*-(2-acetamido-3,6-di-*O*-acetyl-2-deoxy-*β*-D-glucopyranosyl)-(1→4)-*O*-(methyl 2,3-di -*O*-acetyl-*β*-D-glucopyranosyluronate)-(1→3)-(2-acetamido-3,6-di-*O*-acetyl-2-deoxy - *β*-D-glucopyranosyl)-(1→4)-6-*O*-acetyl-2-*O*-benzoyl-*β*-D-glucopyranoside (64):** The TBDPS group in **63** (0.017 mmol, 30 mg) was removed following the same procedure as the synthesis of **62**. Without column purification, the crude mixture was co-evaporated with toluene and dissolved in Py (0.7 ml) and $Ac_2O$ (0.7 ml). After 3 hrs at r.t., the solvent was removed. The reaction mixture was co-evaporated with toluene to remove trace amount of $Ac_2O$, and dissolved in AcOH (0.4 ml) and Py (1.6 ml). Hydrazine monohydrate (0.085 mmol, 5 eq., 4.3 µl) was added and the reaction mixture was stirred at r.t. overnight. Acetone (0.1 ml) was added, and reaction mixture was concentrated and purified by silica gel chromatography (DCM/ MeOH) to yield **64** (70% for 3 steps). $^1$H NMR (500 MHz, $CDCl_3$): δ = 1.91 (s, 3H), 1.94 (s, 3H), 1.98 (s, 3H) x2, 1.99 (s, 3H), 2,.00 (s, 3H), 2.01 (s, 3H) , 2.02 (s, 3H), 2.03 (s, 3H), 2.04 (s, 6H), 2.13 (s, 6H), 2.77 (t, 1H, *J* = 10.5 Hz, H-4), 2.92-2.18 (m, 1H, H-2’), 3.48 (s, 3H, $OCH_3$ anomeric),

3.55-3.62 (m, 3H, H-2’’’, H-5, H-5’’’), 3.69 (s, 3H, COOC*H*$_3$), 3.68-3.74 (m, 1H, H-5’’’), 3.80 (s, 3H, COOC*H*$_3$), 3.76-3.81 (m, 1H, H-3), 3.93-4.31 (m, 8H, H-5’’’’, H-5’’, H-4’’, H-6’ x2, H-6’’’ x2, H-3’’’), 4.46 (d, 1H, *J* = 8.0 Hz, H-1’), 4.46 (d, 1H, *J* = 8.0 Hz, H-1), 4.50-4.54 (m, 3H, H-6 x2, H-3’) 4.59 (d, 1H, *J* = 8.0 Hz, H-1’’’’), 4.65 (d, 1H, *J* = 8.0 Hz, H-1’’), 4.77 (d, 1H, *J* = 8.0 Hz, H-1’’’), 4.78 (dd, 1H, *J* = 8.0 Hz, 9.5 Hz, H-2’’’’), 4.78 (dd, 1H, *J* = 8.0 Hz, 9.5 Hz, H-2’’), 4.78 (t, 1H, *J* = 9.0 Hz, H-4’’’), 4.84 (t, 1H, *J* = 9.5 Hz, H-4’’’), 4.86 (t, 1H, *J* = 9.5 Hz, H-4’), 5.03 (t, 1H, *J* = 9.0 Hz, H-3’), 5.05 (t, 1H, *J* = 9.5 Hz, H-2), 5.01 (t, 1H, *J* = 9.5 Hz, H-4’’’’), 5.18 (t, 1H, *J* = 9.5 Hz, H-3’’’’), 5.87 (d, 1H, *J* = 8.5 Hz, NH’), 6.30-6.33 (m, 1H, NH’’’), 7.40-7.43 (m, 2H, $CH_{arom}$), 7.53-7.56 (m, 1H, $CH_{arom}$), 8.01-8.03 (m, 2H, $CH_{arom}$); $^{13}$C NMR (125 MHz, $CDCl_3$): δ = 20.4 x 3, 20.5, 20.6 x3, 20.7 x2, 21.0 (OCO*C*$H_3$ x10), 23.5 x2 (NHCO*C*$H_3$ x2), 50.5 (C-4), 52.7 (COO*C*$H_3$), 53.0 (COO*C*$H_3$), 56.9 ($OCH_3$ anomeric), 58.2 (C-2’), 61.9, 62.6 (C-6’, C-6’’’), 63.7 (C-6), 68.0 (C-4’), 68.1 (C-4’’’), 68.6 (C-2’’/ C-2’’’’), 69.4 (C-4’’’’), 71.4 (C-2’’/ C-2’’’’), 71.8, 71.9 ( C-5’, C-5), 72.1 (C-3’’’’), 72.3 x2 (C-2, C-5’’’’), 73.0 (C-2’’’), 74.5 x2 (C-3, C-4’’/ C-5’’), 74.8 (C-3), 75.4 (C-3’’’), 75.7 (C-4’’/ C-5’’), 75.9 (C-5’’’), 76.6 (C-3’, C-3’’’), 77.0 (C-1’), 98.4 (C-1’’’), 100.0 (C-1’’’’), 100.8 (C-1’’), 101.4 (C-1), 128.4 x2, 129.7, 129.9 x2, 133.3 ($C_{arom}$ x6), 166.1, 167.0, 167.9, 169.0 169.3 x3, 169.7, 170.2 x2, 170.6, 170.9, 171.2, 171.3, 171.4 (O*C*O$CH_3$ x9, NH*C*O$CH_3$ x2, *C*OO$CH_3$ x2, O*C*O$CH_2CH_2$CO$CH_3$, *C*OPh), 205.9 (OCO$CH_2CH_2$*C*O$CH_3$); HRMS [M + Na]$^+$: m/z: calcd for $C_{64}H_{84}N_2O_{38}S$ Na 1543.4320, found 1543.4391.

**Methyl *S*-(*β*-D-glucopyranosyluronic acid)-(1→3)-*O*-(2-*N*-acetyl-2-deoxy-*β*-D-glucopyranosyl)-(1→4)-*O*-(*β*-D-glucopyranosyluronic acid)-(1→3)-*O*-(2-*N*-acetyl-2-deoxy-*β*-D-glucopyranosyl)-(1→4)-*N*-cyclohexyl-*β*-D-glucopyranuronamide (49): 62** (0.0036 mmol, 5.7 mg) was dissolved in DCM (0.5 ml), *t*BuOH (0.5 ml) and $H_2O$ (0.25 ml). TEMPO (0.0036 mmol, 1 eq., 0.60 mg) and BAIB (0.0036 mmol, 1 eq., 3.0 mg) were added and reaction mixture was stirred at r.t. overnight. The crude mixture was concentrated and dissolved in DCM (1 ml). Cyclohexylamine (0.0043 mmol, 1.2 eq, 0.43 mg), EDCI (0.0054 mmol, 1.5 eq. 1.0 mg) and DMAP (0.001 mmol, 0.3 eq, 0.2 mg) were added. The reaction mixture was stirred at r.t. overnight and purified by silica gel chromatography. The product was dissolved in MeOH (0.3 ml) and $H_2O$ (0.3 ml). The pH was adjusted to 9.5 by 1 M NaOMe in MeOH, and reaction mixture was stirred at r.t. for 2 days. 1 M HCl was added to adjust the pH to 7 and the reaction mixture was concentrated and purified by Sephadex G-15 size exclusion chromatography to give the desired product **49** in 40% yield from **62** for three steps). $^1$H NMR (600 MHz, $D_2O$): δ = 1.20-1.38 (m, 6 H, *C*$H_2$ x3), 1.63-1.65 (m, 1 H, *C*H), 1.74-1.79 (m, 2 H, *C*$H_2$), 1.88-1.91 (m, 2 H, *C*$H_2$), 2.02 (s, 3H, NHCO*CH*$_3$), 2.05 (s, 3H, NHCO*CH*$_3$), 3.03 (t, 1H, *J* = 10.8 Hz, H-2'), 3.33-3.39 (m, 3H, H-2, H-2'', H-2''''), 3.51-3.69 (m, 12 H), 3.73-3.78 (m, 7 H), 3.86-3.89 (m, 1H, H-2'''), 3.92 (d, 1 H, *J* = 14.4 Hz, H-5, H-5'' or H-5''''), 3.94 (d, 1 H, *J* = 12.0 Hz, H-5, H-5'' or H-5''''), 3.97 (d, 1 H, *J* = 12.6 Hz, H-5, H-5'' or H-5''''), 4.08 (d, 1 H, *J* = 10.8 Hz, H-1'), 4.41 (d, 1 H, *J* = 7.8 Hz, H-1, H-1'' or H-1''''), 4.49 (d, 1 H, *J* = 8.4 Hz, H-1, H-1'' or H-1''''), 4.53 (d, 1 H, *J* = 8.4 Hz, H-1, H-1'' or H-1''''), 4.59 (d, 1 H, *J* = 8.4 Hz,

H-1’’’), 4.71 (d, 1 H, *J* = 10.8 Hz, NH’’’); HRMS [M]: m/z: calcd for $C_{41}H_{65}N_3O_{27}S$ 1063.3526, found 1063.3520.

**Methyl *S*-(*β*-D-glucopyranosyluronic acid)-(1→3)-*O*-(2-*N*-acetyl-2-deoxy-*β*-D-glucopyranosyl)-(1→4)-*O*-(*β*-D-glucopyranosyluronic acid)-(1→3)-*O*-(2-*N*-acetyl-2-deoxy-*β*-D-glucopyranosyl)-(1→4)-*N*-2-(1H-indol-3-yl)ethyl-*β*-D-glucopyranuronamide (50):** Compound **50** was synthesized in 45% from compound **62** following the procedure for the synthesis of compound **49**. $^1$H NMR (600 MHz, $D_2O$): δ = 1.84 (s, 3H, NHCO*CH*$_3$), 1.89 (s, 3H, NHCO*CH*$_3$), 2.76 (t, 1H, *J* = 10.8 Hz, H-2’), 2.85-2.89 (m, 1 H, *C*$H_2$), 2.91-2.93 (m, 1 H, *C*$H_2$), 3.13-3.24 (m, 3H, H-2, H-2’’, H-2’’’’), 3.34-3.65 (m, 19 H), 3.67-3.71 (m, 1H, H-2’’’), 3.71 (d, 1 H, *J* = 10.2 Hz, H-5, H-5’’ or H-5’’’’), 3.78 (d, 1 H, *J* = 12.6 Hz, H-5, H-5’’ or H-5’’’’), 3.78 (d, 1 H, *J* = 12.6 Hz, H-5, H-5’’ or H-5’’’’), 3.87 (d, 1 H, *J* = 10.8 Hz, H-1’), 4.18 (d, 1 H, *J* = 7.8 Hz, H-1, H-1’’ or H-1’’’’), 4.30 (d, 1 H, *J* = 8.4 Hz, H-1, H-1’’ or H-1’’’’), 4.32 (d, 1 H, *J* = 7.8 Hz, H-1, H-1’’ or H-1’’’’),4.38 (d, 1 H, *J* = 10.2 Hz, NH’’’), 4.43 (d, 1 H, *J* = 8.4 Hz, H-1’’’), 7.02-7.05 (m, 1H, $CH_{arom}$), 7.10-7.12 (m, 1H, $CH_{arom}$), 7.14 (s, 1H, $CH_{alkene}$), 7.36-7.38 (m, 1H, $CH_{arom}$), 7.57-7.59 (m, 1H, $CH_{arom}$); HRMS [M]: m/z: calcd for $C_{45}H_{64}N_4O_{27}S$ 1124.3479, found 1124.3564.

**Methyl *S*-(*β*-D-glucopyranosyluronic acid)-(1→3)-*O*-(2-*N*-acetyl-2-deoxy-*β*-D-glucopyranosyl)-(1→4)-*O*-(*β*-D-glucopyranosyluronic acid)-(1→3)-*O*-(2-*N*-acetyl-2-deoxy-*β*-D-glucopyranosyl)-(1→4)-*N*-phenyl-*β*-D-glucopyranuronamide (51):** compound **51** was synthesized in 40% from compound **62** following the procedure for the

synthesis of compound **49**. $^1$H NMR (600 MHz, $D_2O$): δ = 1.76 (s, 3H, NHCO*CH*$_3$), 2.05 (s, 3H, NHCO*CH*$_3$), 3.14 (t, 1H, *J* = 10.8 Hz, H-2'), 3.32-3.35 (m, 2H, H-2, H-2'' or H-2''''), 3.42-3.45 (m, 1H, H-2, H-2'' or H-2''''), 3.48-3.80 (m, 19 H), 3.80-3.86 (m, 1H, H-2'''), 3.88 (d, 1 H, *J* = 10.2 Hz, H-5, H-5'' or H-5''''), 3.93 (d, 1 H, *J* = 12.6 Hz, H-5, H-5'' or H-5''''), 3.93 (d, 1 H, *J* = 12.6 Hz, H-5, H-5'' or H-5''''), 4.26 (d, 1 H, *J* = 9.0 Hz, H-1'), 4.45 (d, 1 H, *J* = 7.0 Hz, H-1, H-1'' or H-1''''), 4.48 (d, 1 H, *J* = 7.8 Hz, H-1, H-1'' or H-1'''' ), 4.51 (d, 1 H, *J* = 7.8 Hz, H-1, H-1'' or H-1''''), 4.57 (d, 1 H, *J* = 9.0 Hz, H-1'''), 4.67 (d, 1 H, *J* = 9.6 Hz, NH'''), 7.32-7.34 (m, 1H, $CH_{arom}$), 7.49-7.51 (m, 1H, $CH_{arom}$), 7.58-7.59 (m, 2H, $CH_{arom}$); HRMS [M]: m/z: calcd for $C_{41}H_{59}N_3O_{27}S$ 1057.3057, found 1057.3108.

**Methyl *S*-(*β*-D-glucopyranosyluronic acid)-(1→3)-*O*-(2-*N*-acetyl-2-deoxy-*β*-D-glucopyranosyl)-(1→4)-*O*-(*β*-D-glucopyranosyluronic acid)-(1→3)-*O*-(2-*N*-acetyl-2-deoxy-*β*-D-glucopyranosyl)-(1→4)-*N*-4-hydroxyphenyl-*β*-D-glucopyranuronamide (52):** Compound **52** was synthesized in 35% from compound **62** following the procedure for the synthesis of compound **49**. $^1$H NMR (600 MHz, $D_2O$): δ = 1.93 (s, 3H, NHCO*CH*$_3$), 2.05 (s, 3H, NHCO*CH*$_3$), 3.11 (t, 1H, *J* = 10.8 Hz, H-2'), 3.34-3.48 (m, 3H, H-2, H-2'', H-2''''), 3.51-3.80 (m, 19 H), 3.84-3.88 (m, 1H, H-2'''), 3.88 (d, 1 H, *J* = 12.6 Hz, H-5, H-5'' or H-5''''), 3.93 (d, 1 H, *J* = 10.2 Hz, H-5, H-5'' or H-5''''), 3.94 (d, 1 H, *J* = 10.8 Hz, H-5, H-5'' or H-5''''), 4.19 (d, 1 H, *J* = 10.5 Hz, H-1'), 4.46 (d, 1 H, *J* = 7.8 Hz, H-1, H-1'' or H-1''''), 4.49 (d, 1 H, *J* = 8.4 Hz, H-1, H-1'' or H-1''''), 4.49 (d, 1 H, *J* = 8.4 Hz, H-1, H-1'' or H-1''''), 4.58 (d, 1 H, *J* = 8.4 Hz, H-1'''), 4.67 (d, 1 H, *J* = 10.8 Hz, NH'''),

6.64-6.65 (m, 2H, $CH_{arom}$), 7.23-7.24 (m, 2H, $CH_{arom}$); HRMS [M]: m/z: calcd for $C_{42}H_{61}N_3O_{28}S$ 1073.3006, found 1073.3060.

**Methyl *S*-(*β*-D-glucopyranosyluronic acid)-(1→3)-*O*-(2-*N*-acetyl-2-deoxy-*β*-D-glucopyranosyl)-(1→4)-*O*-(*β*-D-glucopyranosyluronic acid)-(1→3)-*O*-(2-*N*-acetyl-2-deoxy-*β*-D-glucopyranosyl)-(1→4)-*N*-3-methoxyphenyl-*β*-D-glucopyranuronamide (53):** Compound **53** was synthesized in 35% from compound **62** following the procedure for the synthesis of compound **49**. $^1$H NMR (600 MHz, $D_2O$): δ = 2.05 (s, 6H, NHCO*CH*$_3$ x2), 3.03 (t, 1H, *J* = 10.8 Hz), 3.32-3.36 (m, 2H), 3.50-3.61 (m, 11H), 3.70-3.97 (m, 16 H), 4.24 (d, 1 H, *J* = 10.8 Hz, H-1'), 4.44 (d, 1 H, *J* = 8.4 Hz, H-1, H-1'' or H-1''''), 4.48 (d, 1 H, *J* = 7.2 Hz, H-1, H-1'' or H-1''''), 4.51 (d, 1 H, *J* = 7.8 Hz, H-1, H-1'' or H-1''''), 4.57 (d, 1 H, *J* = 8.4 Hz, H-1'''), 4.66 (d, 1 H, *J* = 10.8 Hz, NH'''), 6.92-6.94 (m, 1H, $CH_{arom}$), 7.18-7.20 (m, 1H, $CH_{arom}$), 7.28-7.29 (m, 1H, $CH_{arom}$), 7.41-7.44 (m, 1H, $CH_{arom}$); HRMS [M]: m/z: calcd for $C_{42}H_{61}N_3O_{28}S$ 1087.3162, found 1087.3182.

**Methyl *S*-(*β*-D-glucopyranosyluronic acid)-(1→3)-*O*-(2-*N*-acetyl-2-deoxy-*β*-D-glucopyranosyl)-(1→4)-*O*-(*β*-D-glucopyranosyluronic acid)-(1→3)-*O*-(2-*N*-acetyl-2-deoxy-*β*-D-glucopyranosyl)-(1→4)-3-naphthalen-1-ylcarbamate-*β*-D-glucopyranoside (54):** Compound **64** (0.0035 mmol, 5.2 mg) was co-evaporated with toluene and dissolved in DCM (1 ml). Naphthalen-1-yl isocyanate (0.17 mmol, 50 eq., 25 µl) was added and the reaction mixture was stirred for 2 days. The crude mixture was purified by silica gel chromatography and dissolved in MeOH (0.3 ml) and $H_2O$ (0.3 ml). The pH was adjusted to 9.5 by 1 M NaOMe in MeOH and the reaction mixture was stirred at r.t. for 4

days. 1 M HCl was added to adjust the pH to 7 and the reaction mixture was concentrated and purified by Sephadex G-15 size exclusion chromatography to give the desired product compound **54** in 50% yield from **64** for 2 steps. $^1$H NMR (600 MHz, $D_2O$): δ = 2.05 (s, 6H, NHCO*CH*$_3$ x2), 3.32-3.37 (m, 3H, H-2, H-2'', H-2''''), 3.47-3.80 (m, 19 H), 3.84-3.94 (m, 7H, H-2''', H-2', H-5'', H-5'''', $C_6H_4OCH_3$), 4.20 (d, 1 H, *J* = 12.0 Hz, H-1'), 4.48 (d, 3 H, *J* = 7.8 Hz, H-1, H-1'', H-1''''), 4.57 (d, 1 H, *J* = 8.4 Hz, H-1'''), 7.60-7.70 (m, 4H, $CH_{arom}$), 7.93-7.41 (m, 1H, $CH_{arom}$), 8.03-8.04 (m, 1H, $CH_{arom}$), 8.16-8.17 (m, 1H, $CH_{arom}$); HRMS [M]: m/z: calcd for $C_{46}H_{63}N_3O_{28}S$ 1137.3319, found 1137.3282.

**Methyl *S*-(*β*-D-glucopyranosyluronic acid)-(1→3)-*O*-(2-*N*-acetyl-2-deoxy-*β*-D-glucopyranosyl)-(1→4)-*O*-(*β*-D-glucopyranosyluronic acid)-(1→3)-*O*-(2-*N*-acetyl-2-deoxy-*β*-D-glucopyranosyl)-(1→4)-3-(3-carboxyphenyl)carbamate-*β*-D-glucopyranoside (55):** Compound **55** was synthesized in 40% from **64** following the procedure for the synthesis of compound **54**. $^1$H NMR (600 MHz, $D_2O$): δ = 1.64 (s, 3H, NHCO*CH*$_3$ ), 2.06 (s, 3H, NHCO*CH*$_3$), 3.32-3.37 (m, 3H, H-2, H-2'', H-2''''), 3.47-3.80 (m, 19 H), 3.84-3.94 (m, 7H, H-2''', H-2', H-5'', H-5'''', $C_6H_4OCH_3$), 4.22 (d, 1 H, *J* = 10.8 Hz, H-1'), 4.48 (d, 1 H, *J* = 12.6 Hz, H-1, H-1'' or H-1''''), 4.49 (d, 1 H, *J* = 7.8 Hz, H-1, H-1'' or H-1''''), 4.52 (d, 1 H, *J* = 8.4 Hz, H-1, H-1'' or H-1''''), 4.58 (d, 1 H, *J* = 8.4 Hz, H-1'''), 4.85-4.86 (m, 1H), 5.02-5.08 (m, 1H), (NH' or NH'''), 7.46-8.11 (m, 4H, $CH_{arom}$); HRMS [M]: m/z: calcd for $C_{43}H_{61}N_3O_{30}S$ 1131.3061, found 1131.3084.

**Methyl *S*-(*β*-D-glucopyranosyluronic acid)-(1→3)-*O*-(2-*N*-acetyl-2-deoxy-*β*-D-glucopyranosyl)-(1→4)-*O*-(*β*-D-glucopyranosyluronic acid)-(1→3)-*O*-(2-*N*-acetyl-2-deoxy-*β*-D-glucopyranosyl)-(1→4)-3-(3-benzylphenyl)carbamate-*β*-D-glucopyranoside (56):** Compound **56** was synthesized in 45% yield from compound **64** following procedure for the synthesis of compound **54**. $^1$H NMR (600 MHz, $D_2O$): δ = 1.54 (s, 3H, NHCO*CH*$_3$), 2.05 (s, 3H, NHCO*CH*$_3$), 3.29-3.30 (m, 1H), 3.33-3.35 (m, 2H) 3.49-3.60 (m, 13 H), 3.74-4.02 (m, 15H), 4.20-4.22 (m, 1H, H-1'), 4.41-4.43 (m, 1H, H-1, H-1'' or H-1''''), 4.49 (d, 2H, *J* = 7.2 Hz, H-1, H-1'' or H-1''''), 4.59 (d, 1 H, *J* = 8.4 Hz, H-1'''), 5.00-5.01 (m, 1H, NH'/NH'''), 7.14-7.41 (m, 9H, $CH_{arom}$); HRMS [M]: m/z: calcd for $C_{49}H_{67}N_3O_{28}S$ 1177.3632, found 1177.3612.

**Methyl *S*-(*β*-D-glucopyranosyluronic acid)-(1→3)-*O*-(2-*N*-acetyl-2-deoxy-*β*-D-glucopyranosyl)-(1→4)-*O*-(*β*-D-glucopyranosyluronic acid)-(1→3)-*O*-(2-*N*-acetyl-2-deoxy-*β*-D-glucopyranosyl)-(1→4)-3-2,5-dimethoxyphenethylcarbamate-*β*-D-glucopyranoside (57):** Compound **57** was synthesized in 35% from compound **64** following procedure for the synthesis of compound **54**. $^1$H NMR (600 MHz, $D_2O$): δ = 1.97 (s, 3H, NHCO*CH*$_3$), 2.05 (s, 3H, NHCO*CH*$_3$), 2.66-2.95 (m, 4H, $CH_2CH_2$), 3.34-3.61 (m, 16H), 3.72-3.89 (m, 19H), 3.94 (d, 1H, *J* = 11.4 Hz, H-1'), 4.15 (d, 1H, *J* = 11.4 Hz NH'/NH'''), 4.20 (d, 1H, *J* = 10.8 Hz, NH'/NH'''), 4.49 (d, 1H, *J* = 7.8 Hz, H-1, H-1'' or H-1''''), 4.50 (d, 2 H, *J* = 7.2 Hz, H-1, H-1'' or H-1''''), 4.59 (d, 1 H, *J* = 7.8 Hz, H-1'''), 6.86-6.92 (m, 2H, $CH_{arom}$), 7.01-7.05 (m, 1H, $CH_{arom}$); HRMS [M]: m/z: calcd for $C_{46}H_{69}N_3O_{30}S$ 1175.3687, found 1175.3688.

**Methyl *S*-(*β*-D-glucopyranosyluronic acid)-(1→3)-*O*-(2-*N*-acetyl-2-deoxy-*β*-D-glucopyranosyl)-(1→4)-*O*-(*β*-D-glucopyranosyluronic acid)-(1→3)-*O*-(2-*N*-acetyl-2-deoxy-*β*-D-glucopyranosyl)-(1→4)-3-2,3,3-trimethylbutan-2-ylcarbamate-*β*-D-glucopyranoside (58):** Compound **58** was synthesized in 20% from compound **64** following the procedure for the synthesis of compound **54**. $^1$H NMR (600 MHz, $D_2O$): δ = 0.56 (s, 3H, $CH_3$), 0.86 (s, 6H, $CH_3$), 1.20 (s, 6H, $CH_3$), 1.87 (s, 6H, NHCO*CH*$_3$), 3.18-3.79 (m, 33H), 4.20-4.27 (m, 2H, NH), 4.31-4.43 (m, 5H, H-1, H-1, H-1'', H-1''' and H-1''''); HRMS [M]: m/z: calcd for $C_{44}H_{73}N_3O_{28}S$ 1123.4101, found 1123.4058.

**Methyl *S*-(*β*-D-glucopyranosyluronic acid)-(1→3)-*O*-(2-*N*-acetyl-2-deoxy-*β*-D-glucopyranosyl)-(1→4)-*O*-(*β*-D-glucopyranosyluronic acid)-(1→3)-*O*-(2-*N*-acetyl-2-deoxy-*β*-D-glucopyranosyl)-(1→4)-3- (4-methoxyphenyl)methanylcarbamate-*β*-D-glucopyranoside (59):** Compound **59** was synthesized in 50% (as a mixture of compound **59** and **61**) from compound **64** following the procedure for the synthesis of compound **54.** For the deprotection step, side product **61** was generated by 3-carbamate group migration. The mixture of compound **59** and **61** could not be separated by HPLC. HRMS [M]: m/z: calcd for $C_{65}H_{73}N_3O_{29}S$ 1131.3424, found 1131.3374.

**Methyl *S*-(*β*-D-glucopyranosyluronic acid)-(1→3)-*O*-(2-*N*-acetyl-2-deoxy-*β*-D-glucopyranosyl)-(1→4)-*O*-(*β*-D-glucopyranosyluronic acid)-(1→3)-*O*-(2-*N*-acetyl-2-deoxy-*β*-D-glucopyranosyl)-(1→4)-*β*-D-glucopyranoside (67):** Compound **64** was dissolved in MeOH (0.3 ml) and $H_2O$ (0.3 ml), and the pH was adjusted to 9.5 by 1 M NaOMe in MeOH. The reaction mixture was stirred at r.t. for 2 days. 1 M HCl was added

to adjust the pH to 7 and the reaction mixture was concentrated and purified by Sephadex G-15 size exclusion chromatography to give the desired product **67** in 70% yield from compound **64**. $^{1}$H NMR (600 MHz, $D_2O$): δ = 2.05 (s, 3H, NHCO*CH*$_3$), 2.06 (s, 3H, NHCO*CH*$_3$), 2.85 (t, 1H, *J* = 11.4 Hz), 3.29-3.40 (m, 3H), 3.51-3.95 (m, 27H), 4.10 (d, 1H, *J* = 12.0 Hz, H-1'), 4.37 (d, 1H, *J* = 7.8 Hz 1H, H-1, H-1'' or H-1''''), 4.49 (d, 1 H, *J* = 7.8 Hz, H-1, H-1'' or H-1'''') 4.52 (d, 1 H, *J* = 7.8 Hz, H-1, H-1'' or H-1''''), 4.59 (d, 1 H, *J* = 7.8 Hz, H-1'''); HRMS [M]: m/z: calcd for $C_{35}H_{56}N_2O_{27}S$ 968.2791, found 928.2816.

Appendix B

**NMR Spectra**

**Figure 4.23.** $^{1}$H-NMR of compound **10** (500 MHz, $CDCl_3$)

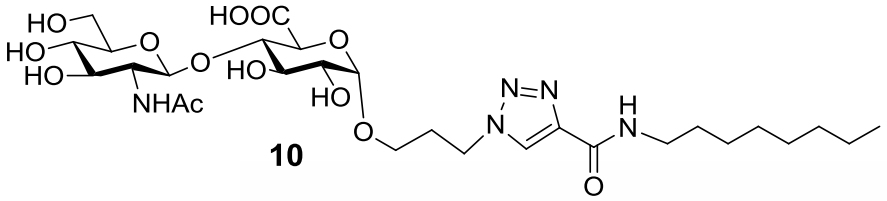


**10**

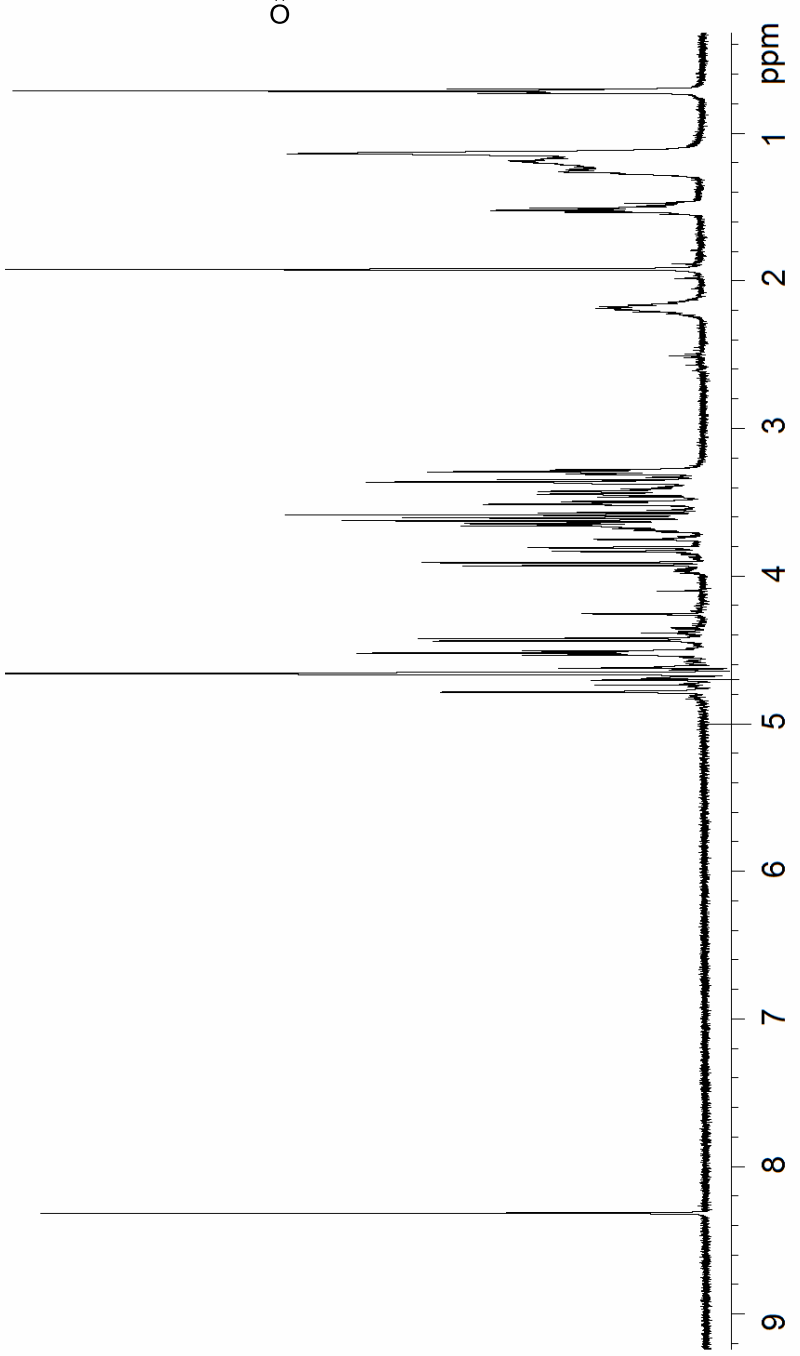

**Figure 4.24.** $^{1}$H-NMR of compound **11** (500 MHz, $CDCl_3$)

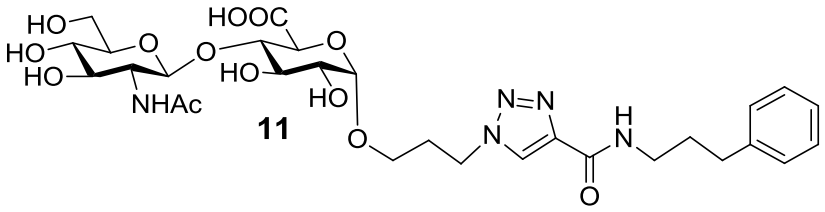


**11**

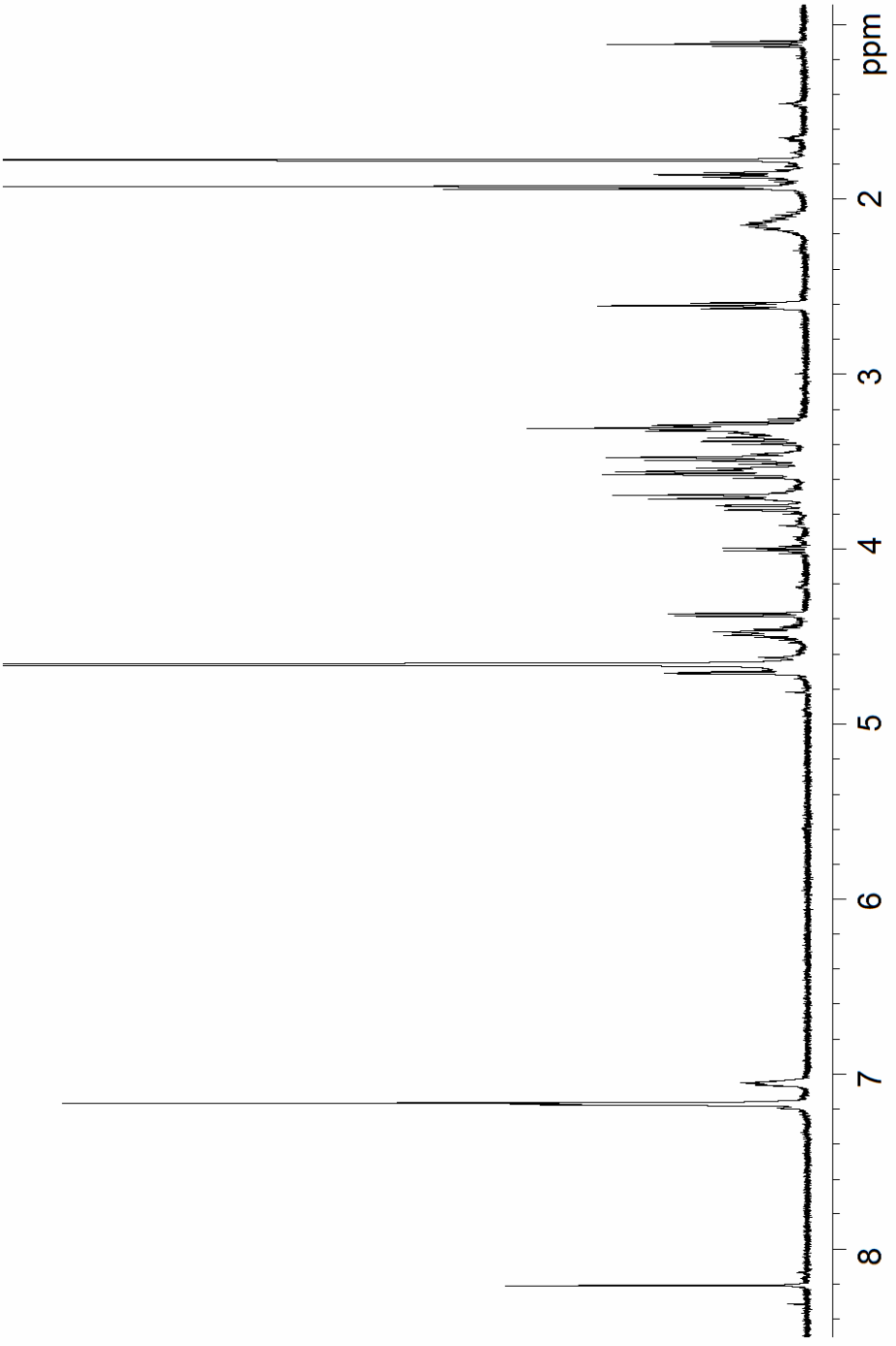

**Figure 4.25.** $^{1}$H-NMR of compound **12** (500 MHz, $CDCl_3$)

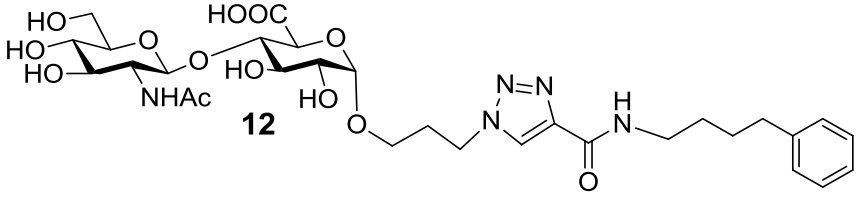


**12**

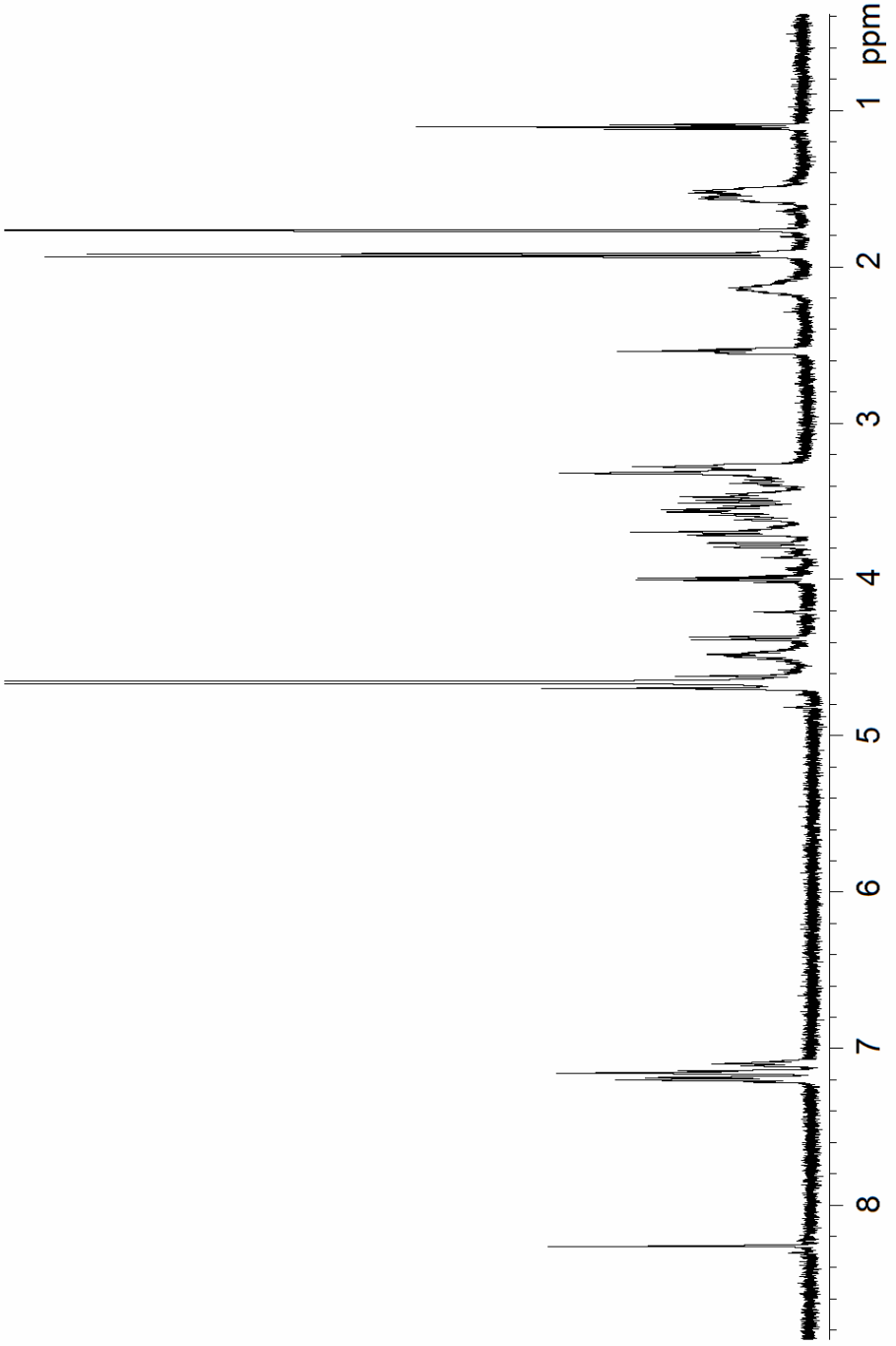

**Figure 4.26.** $^{1}$H-NMR of compound **13** (500 MHz, $CDCl_3$)

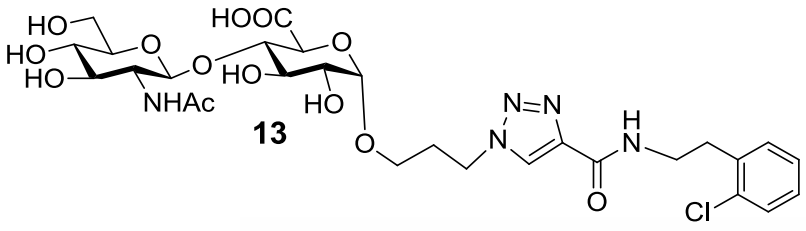


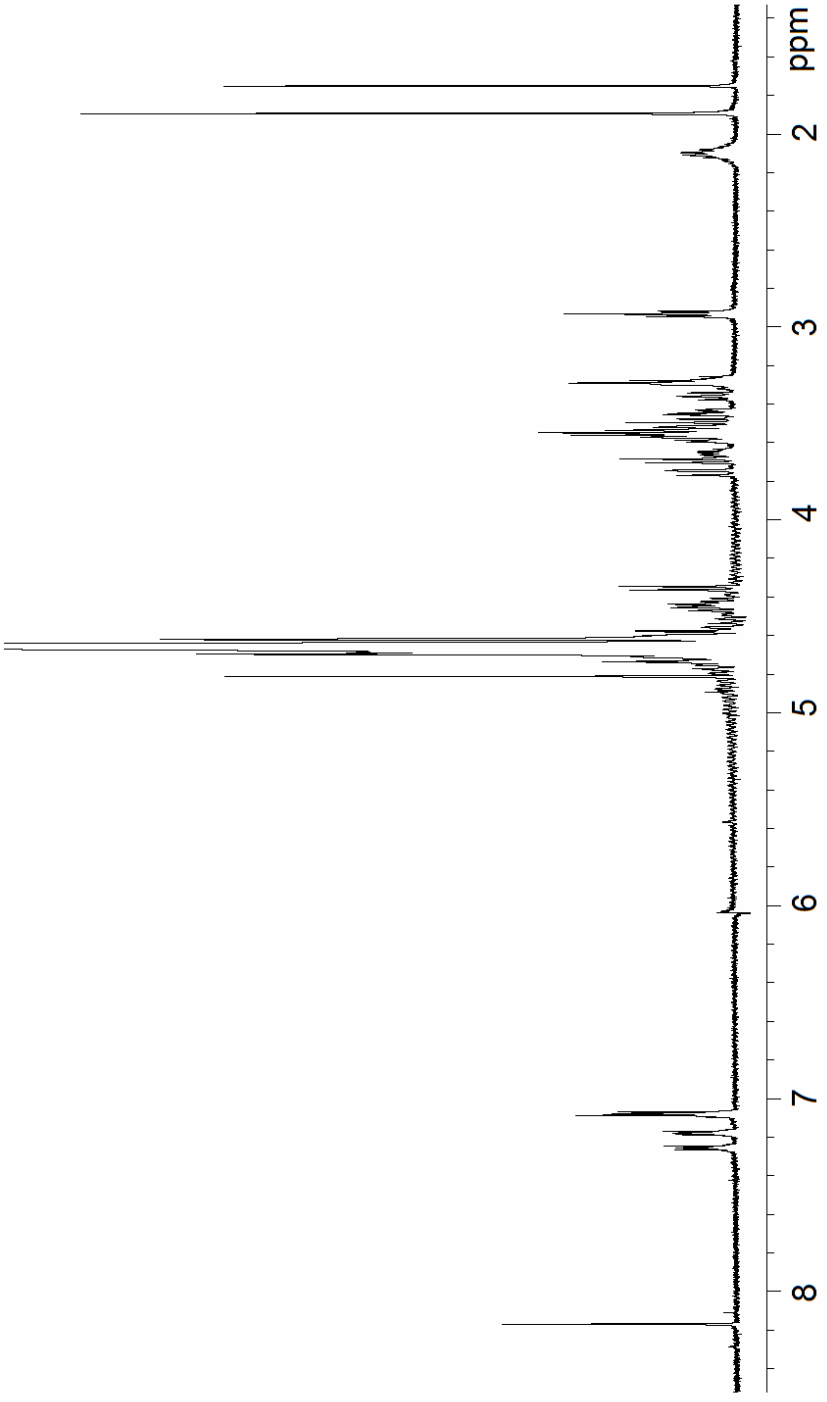

**Figure 4.27.** $^{1}$H-NMR of compound **14** (500 MHz, $CDCl_3$)

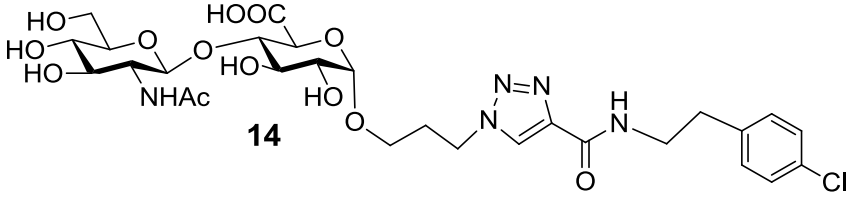


**14**

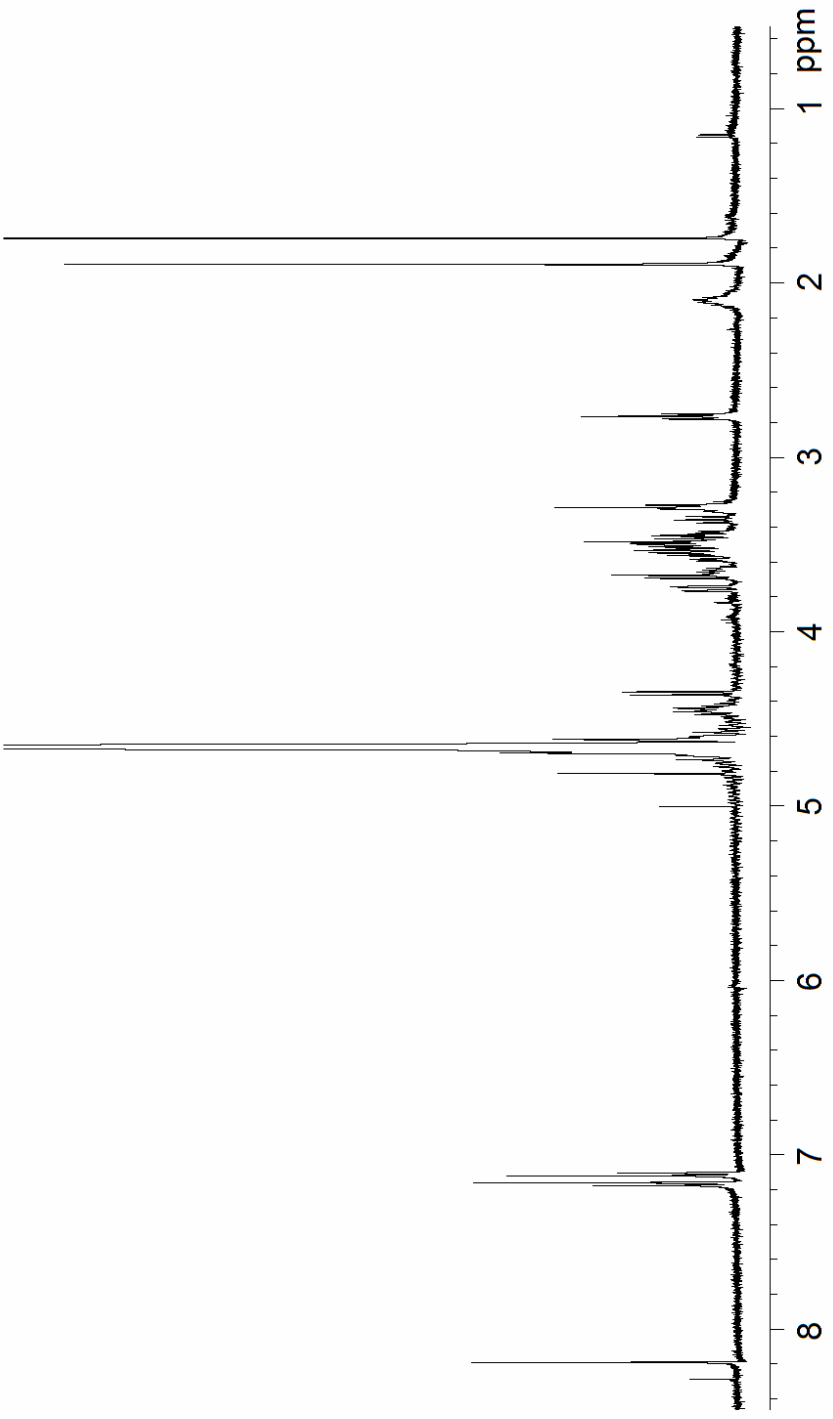

**Figure 4.28.** $^{1}$H-NMR of compound **15** (500 MHz, $CDCl_3$)

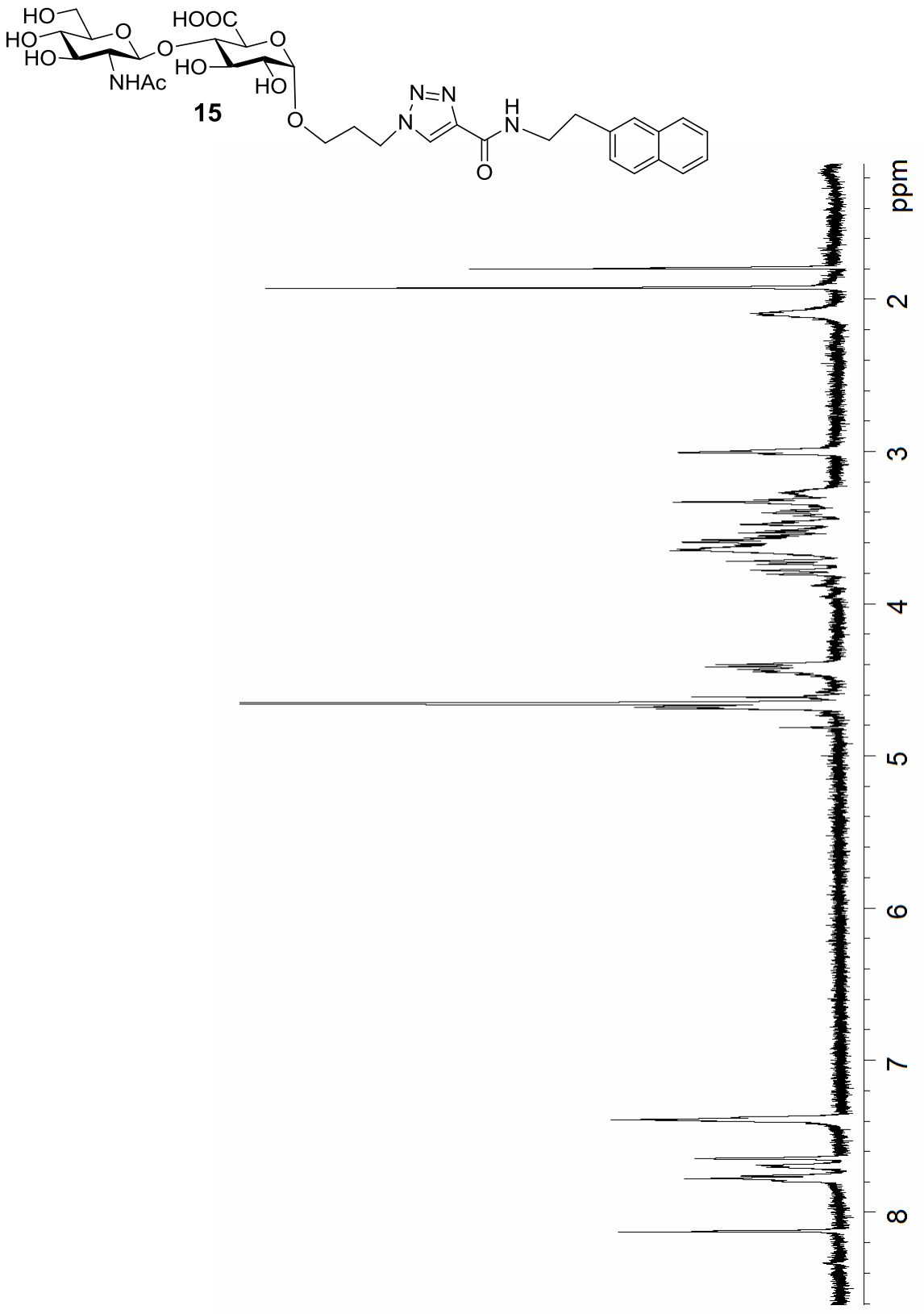

**Figure 4.29.** $^{1}$H-NMR of compound **16** (500 MHz, $CDCl_3$)

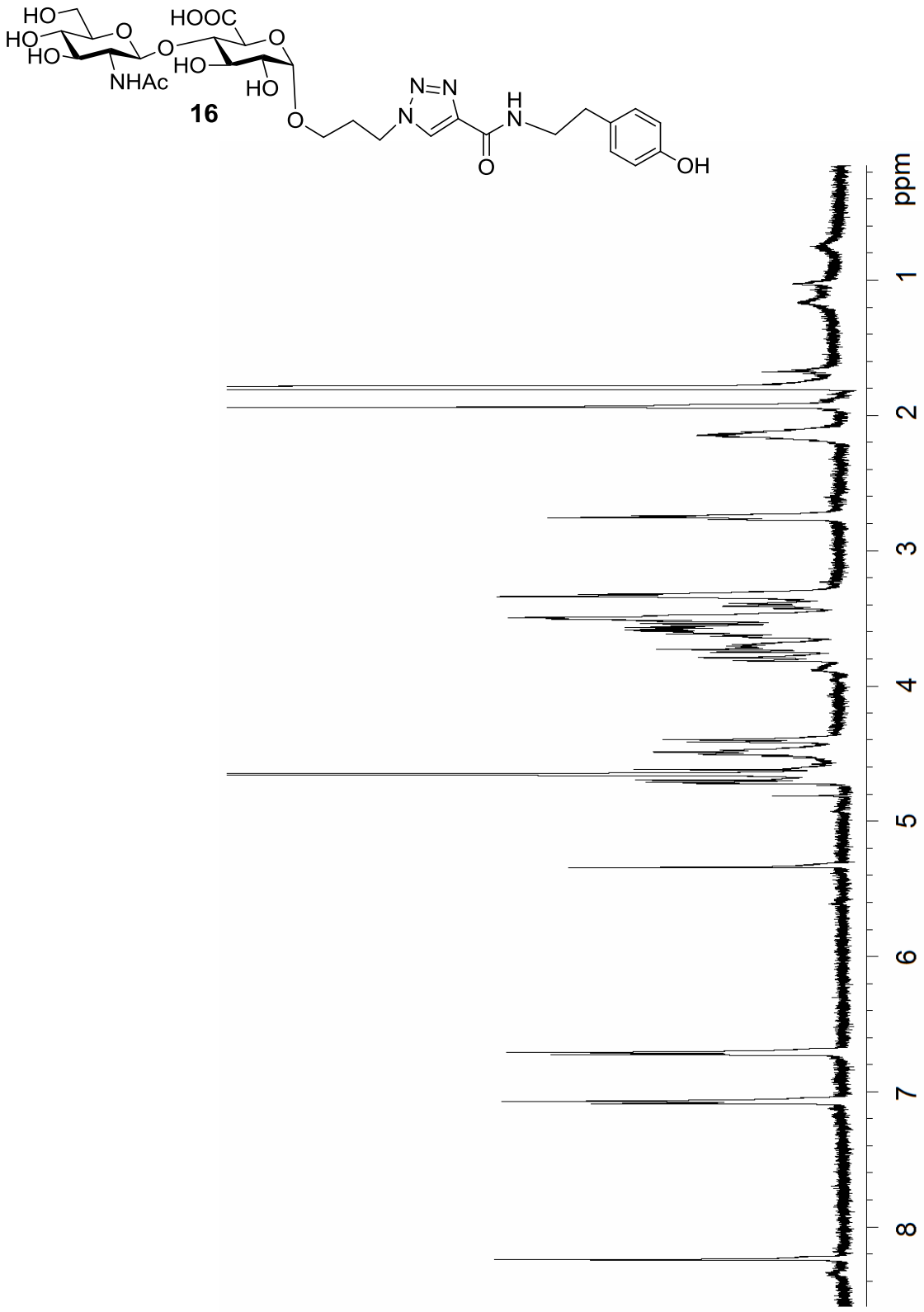

**Figure 4.30.** $^{1}$H-NMR of compound **38** (500 MHz, $CDCl_3$)

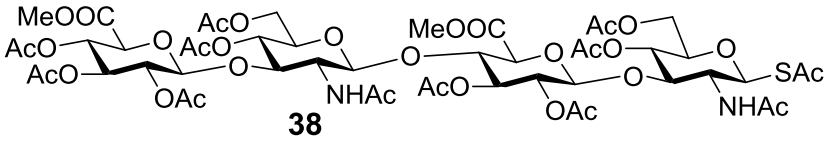


**38**

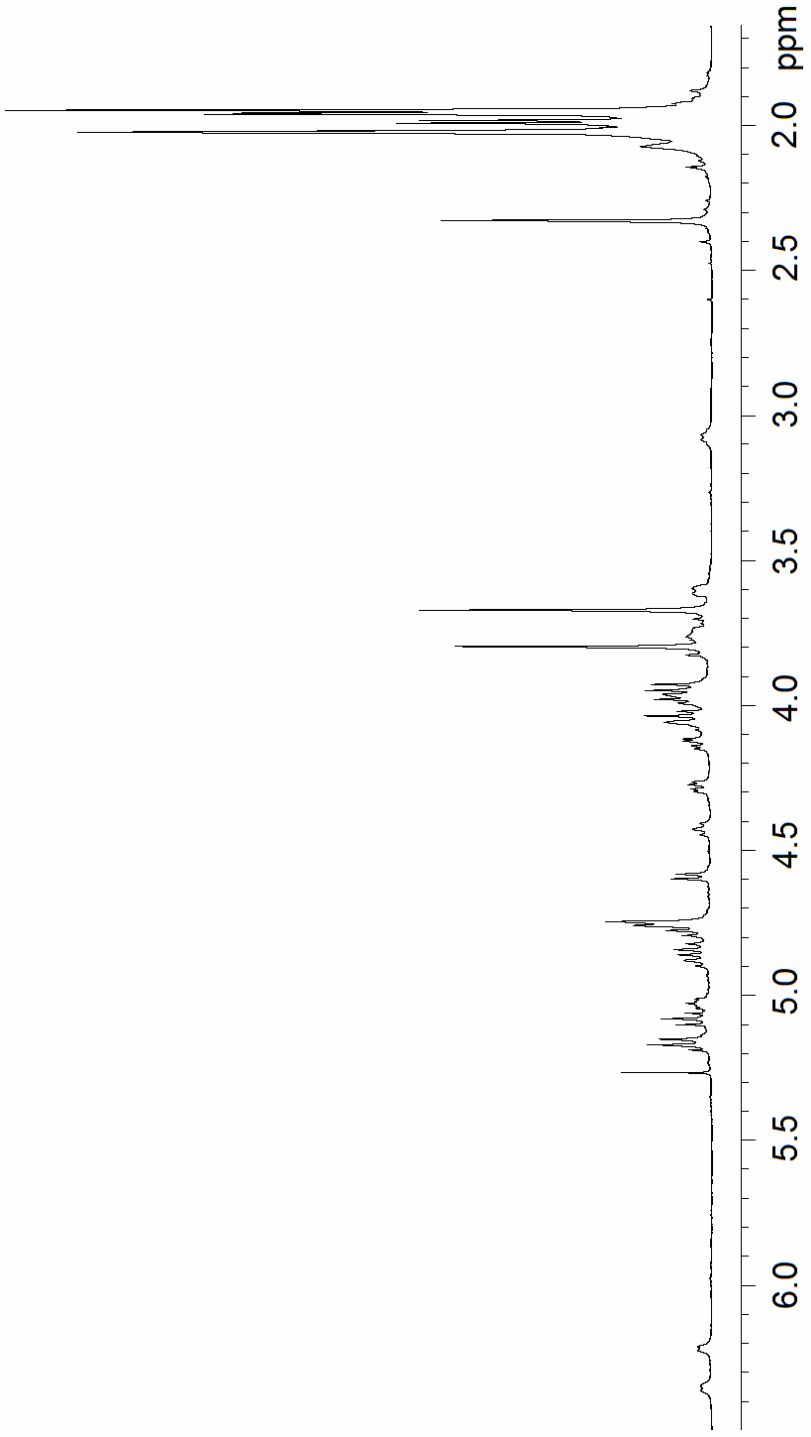

**Figure 4.31.** $^{13}$C-NMR of compound **38** (125 MHz $CDCl_3$)

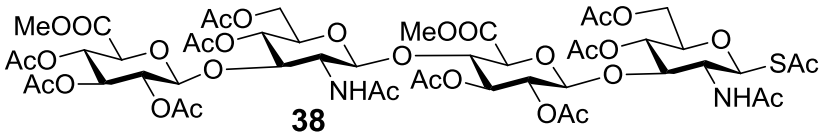


**38**

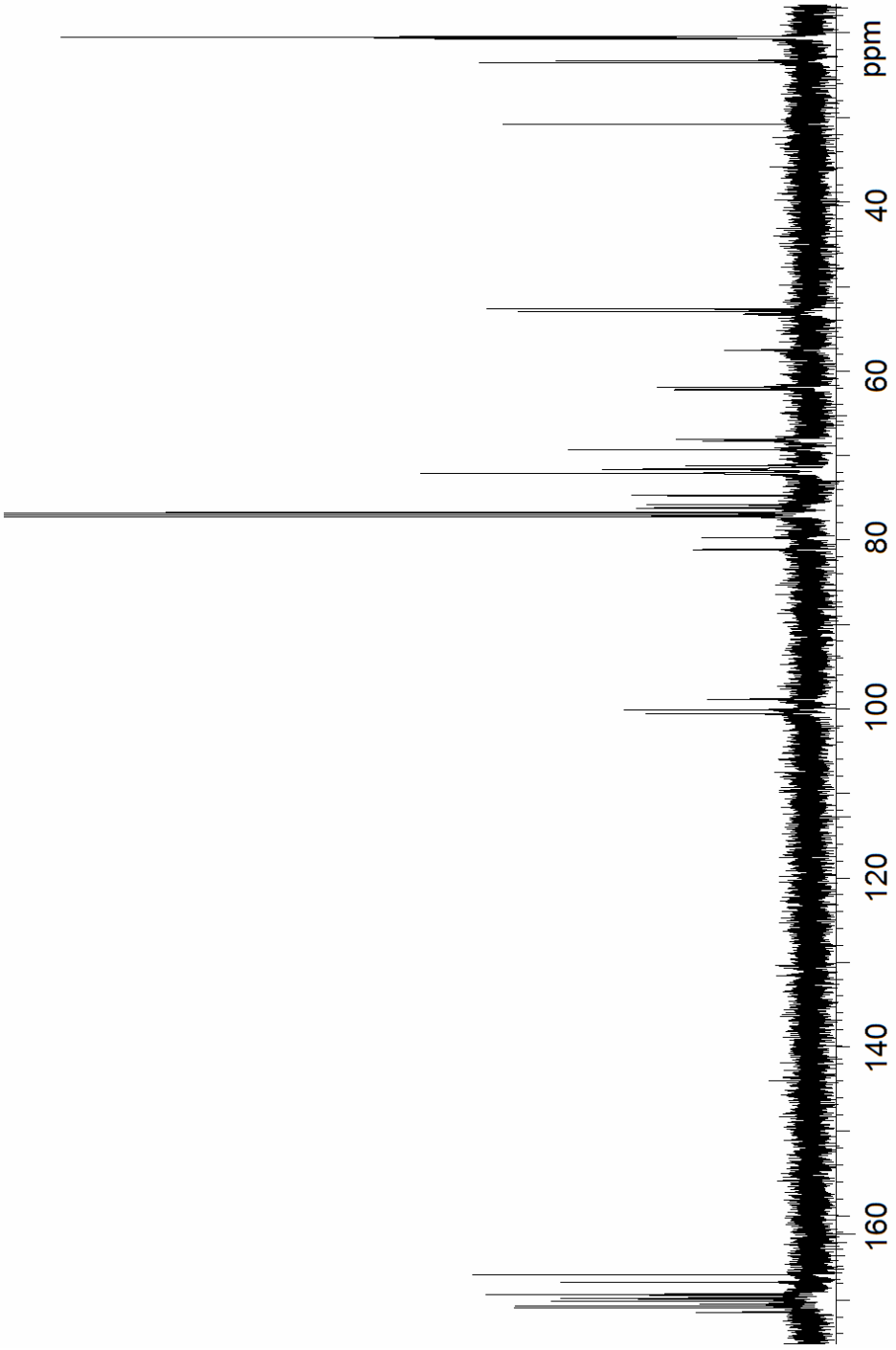

**Figure 4.32.** $^{1}H–^{1}H$ gCOSY of compound **38** (500 MHz, $CDCl_3$)

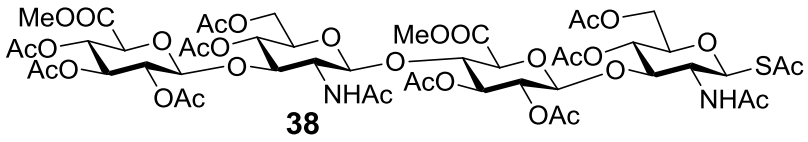


**38**

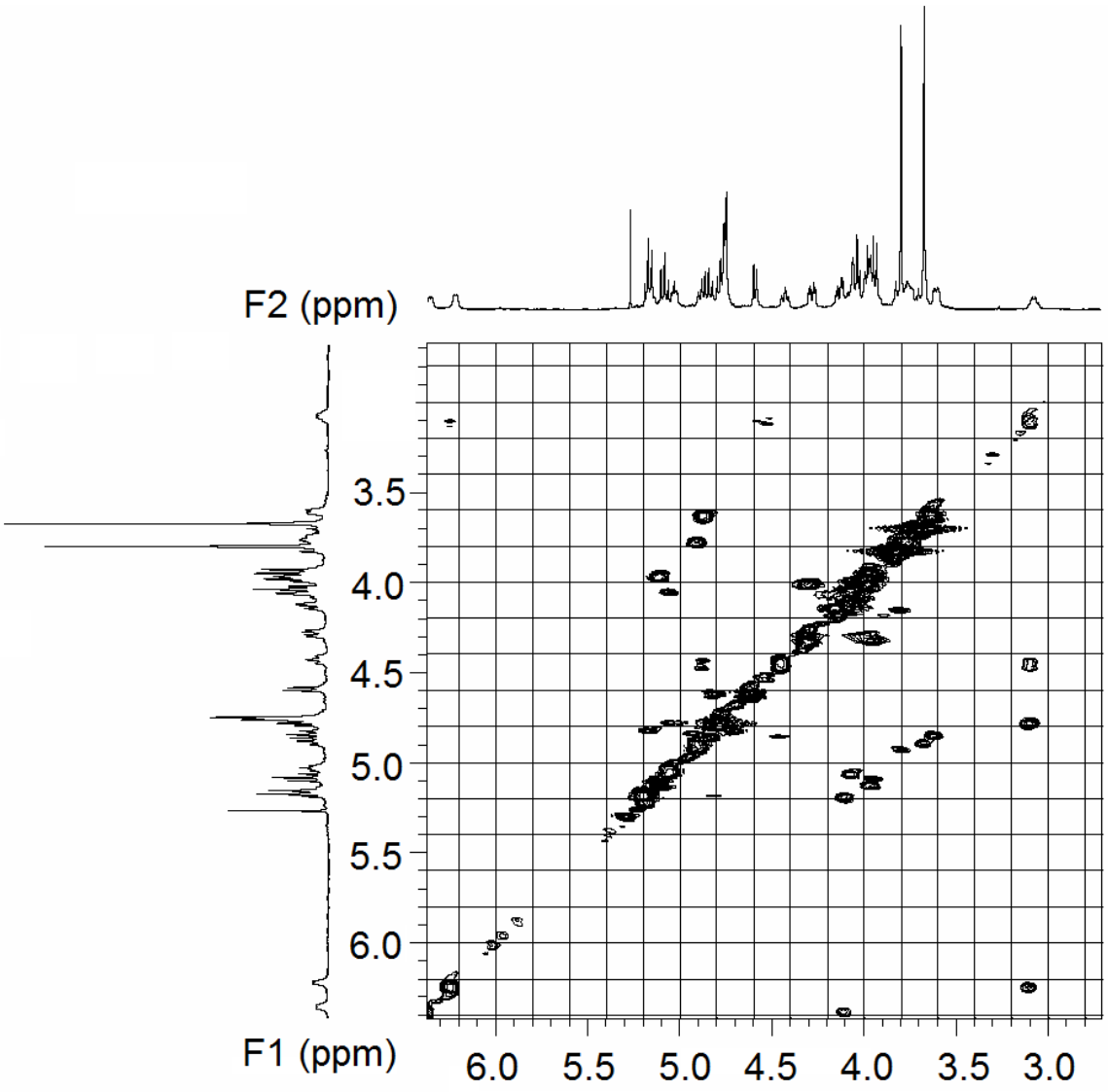

**Figure 4.33.** $^{1}H–^{13}C$ gHMQC of compound **38** (500 MHz, $CDCl_3$)

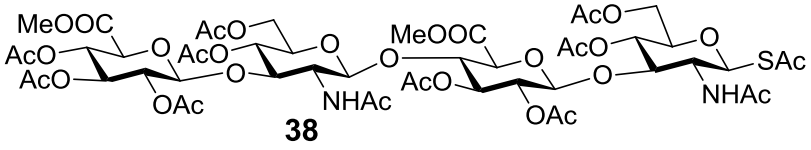


**38**

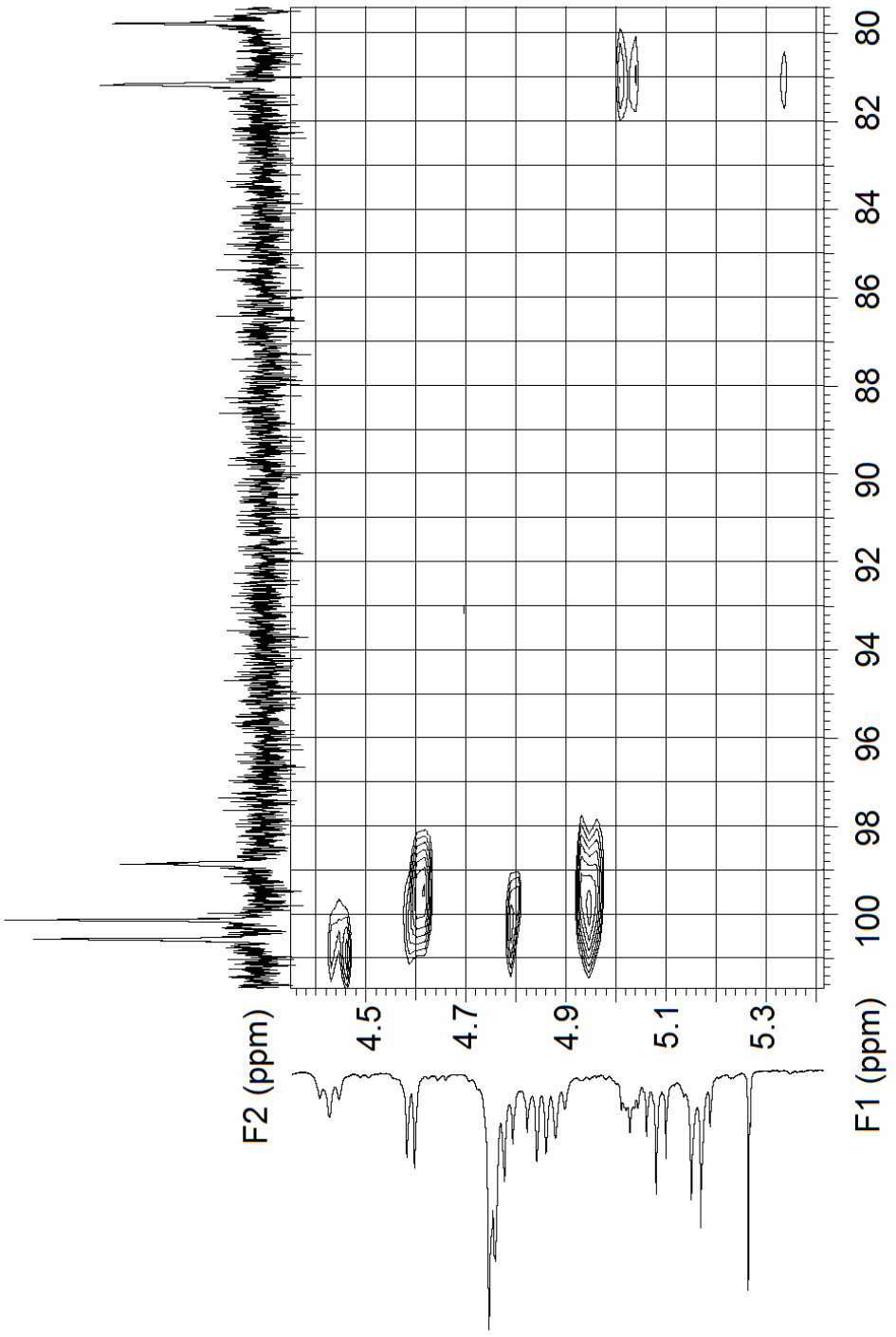

**Figure 4.34.** $^{1}H–^{13}C$ gHMQC (without $^{1}H$ decoupling) of compound **38** (500 MHz,$CDCl_3$)

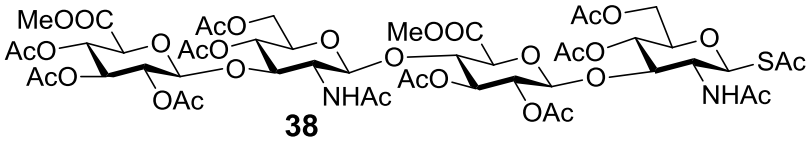


**38**

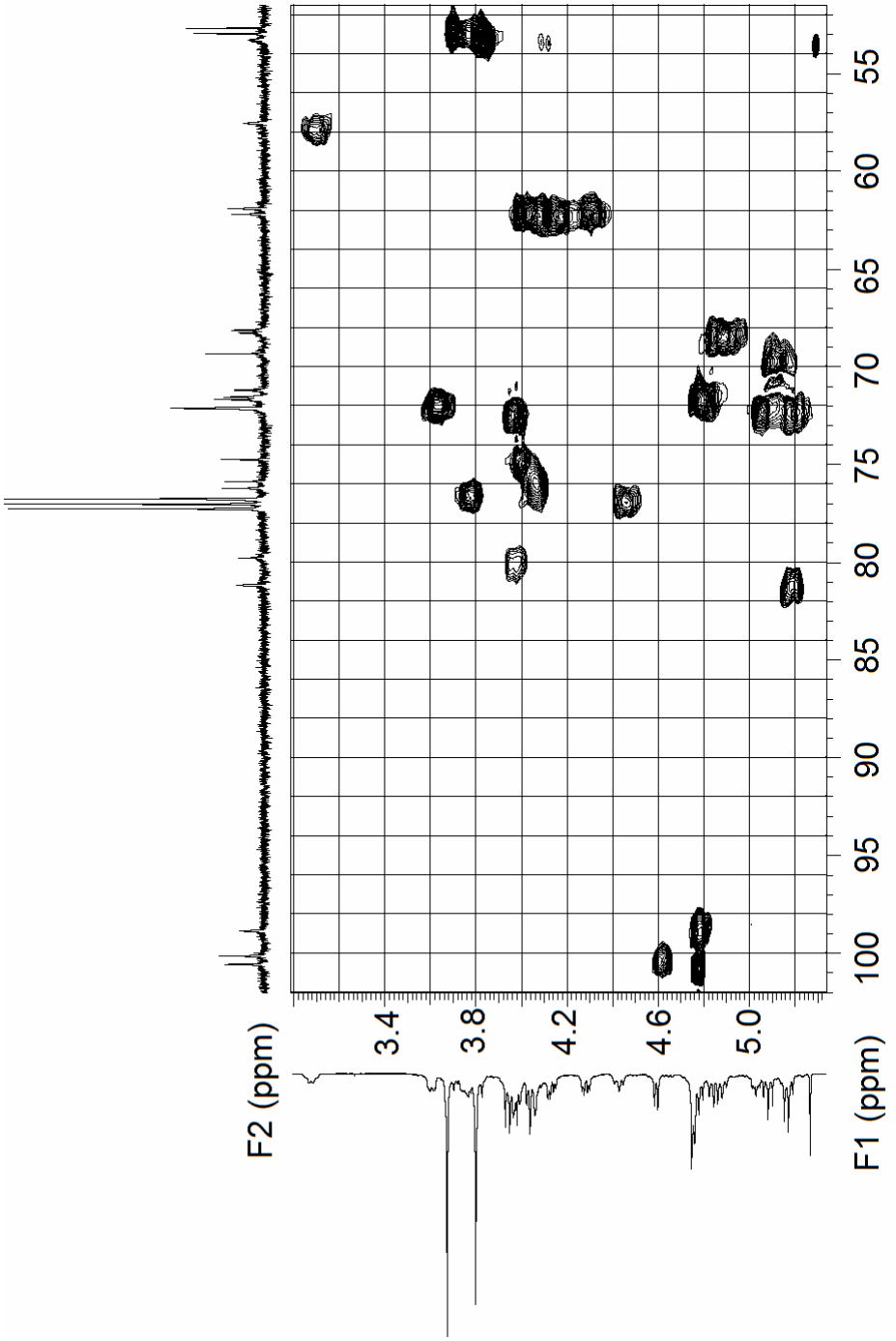

**Figure 4.35.** $^{1}H–^{13}C$ gHMBC of compound **38** (500 MHz, $CDCl_3$)

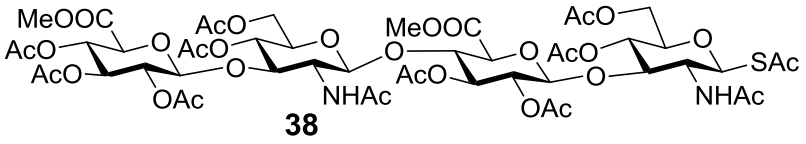


**38**

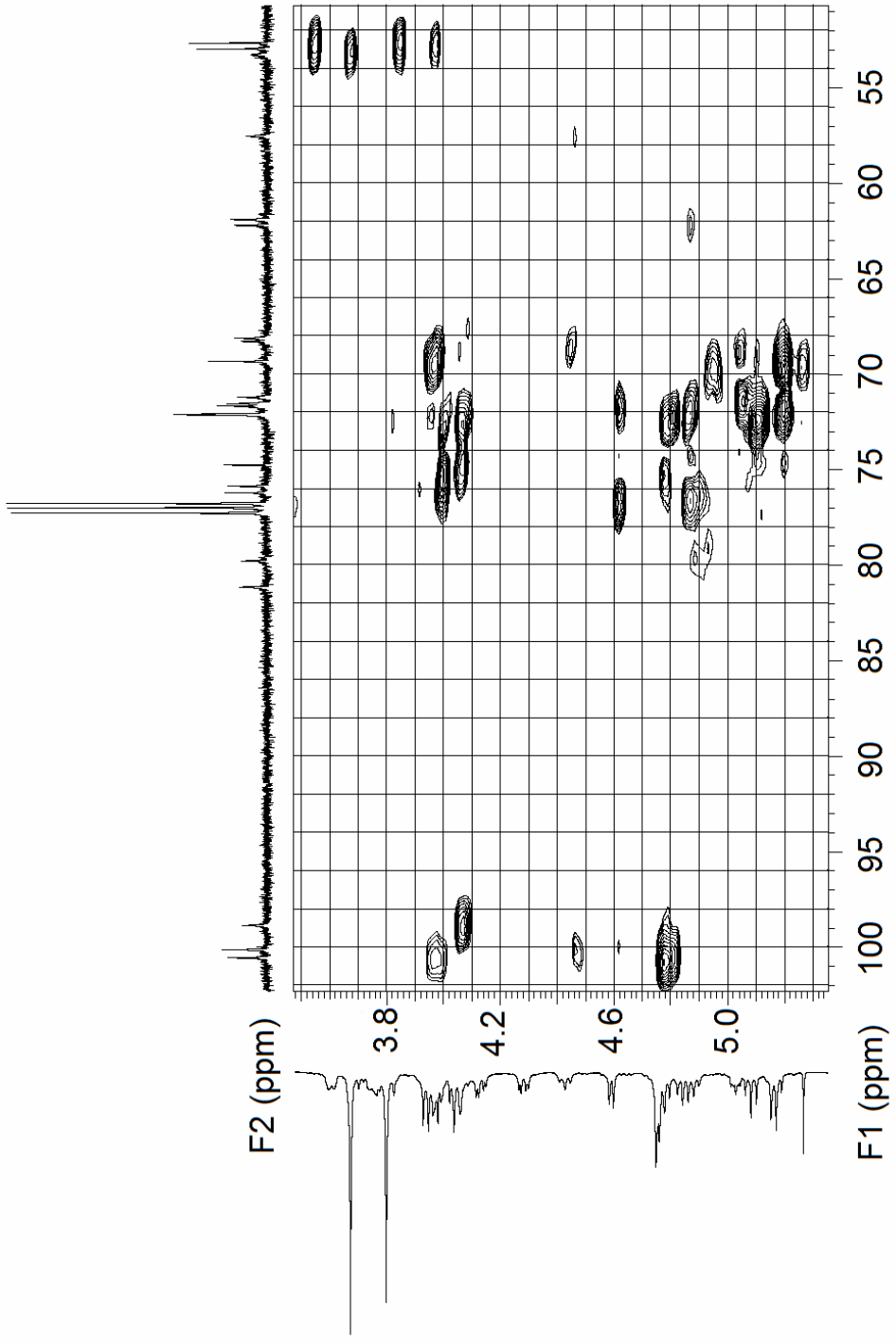

**Figure 4.36.** $^{1}$H-NMR of compound **40** (500 MHz, $CDCl_3$

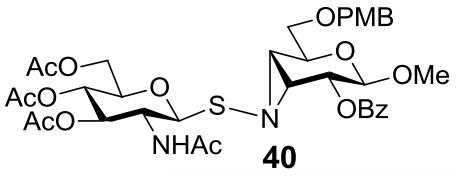


**40**

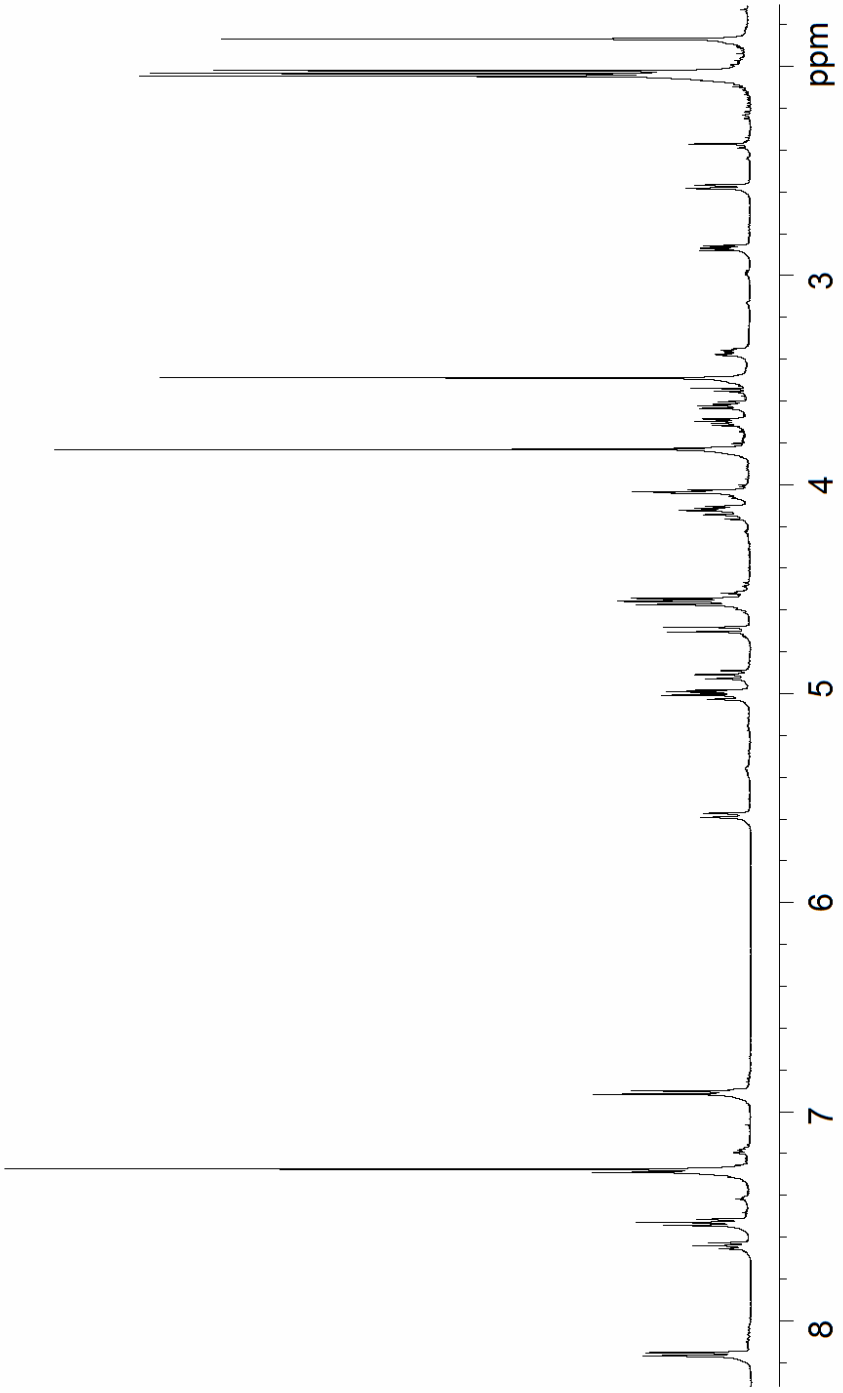

**Figure 4.37.** $^{1}H–^{1}H$ gCOSY of compound **40**(500 MHz, $CDCl_3$)

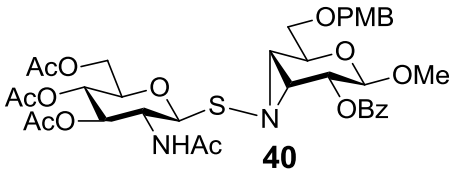


**40**

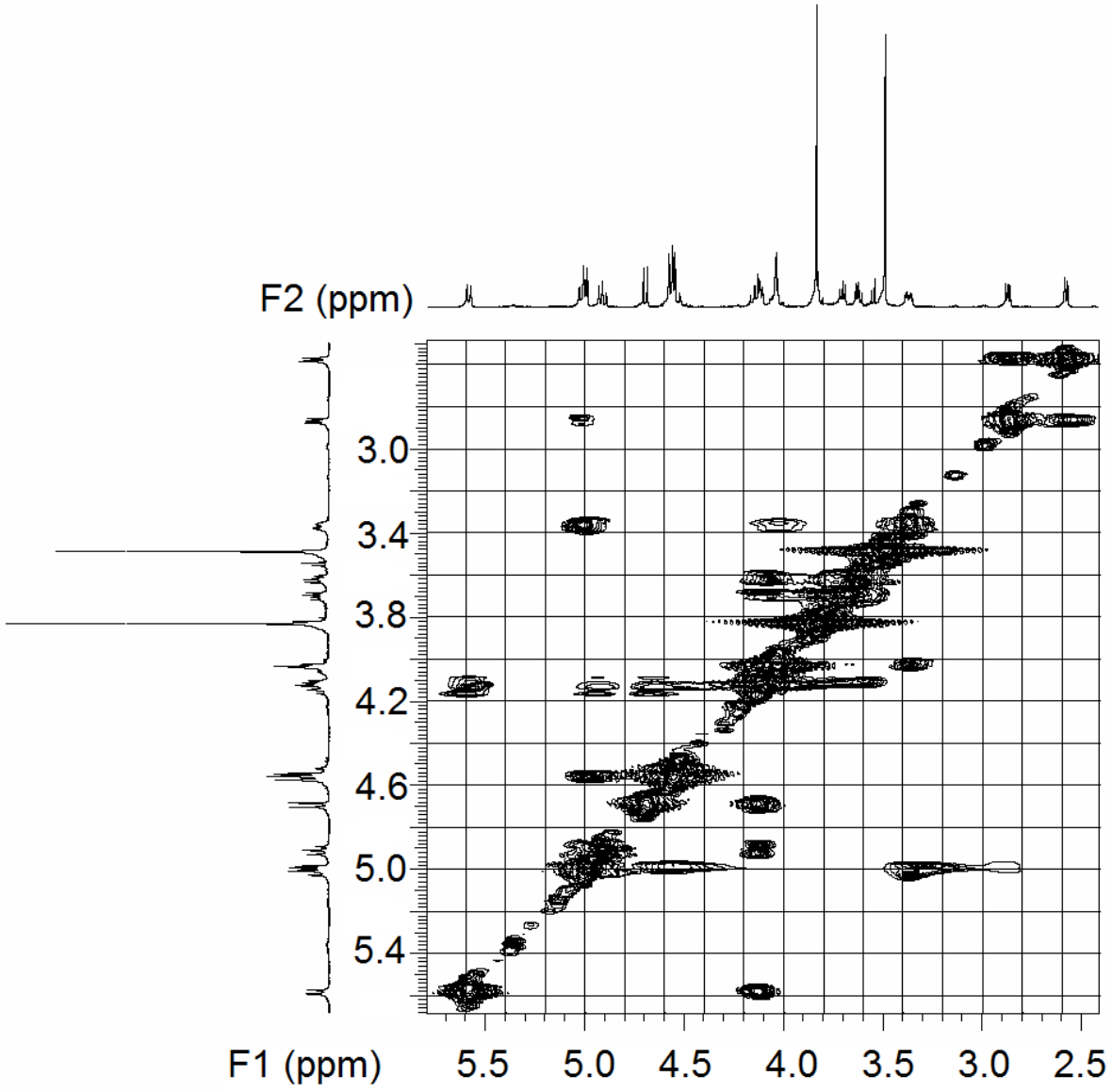

**Figure 4.38.** $^{1}H–^{13}C$ gHMQC (without $^{1}H$ decoupling) of compound **40** (500 MHz,$CDCl_3$)

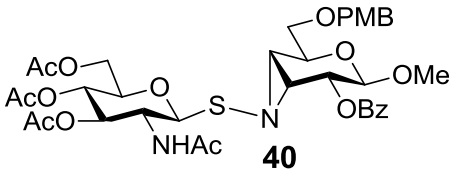


**40**

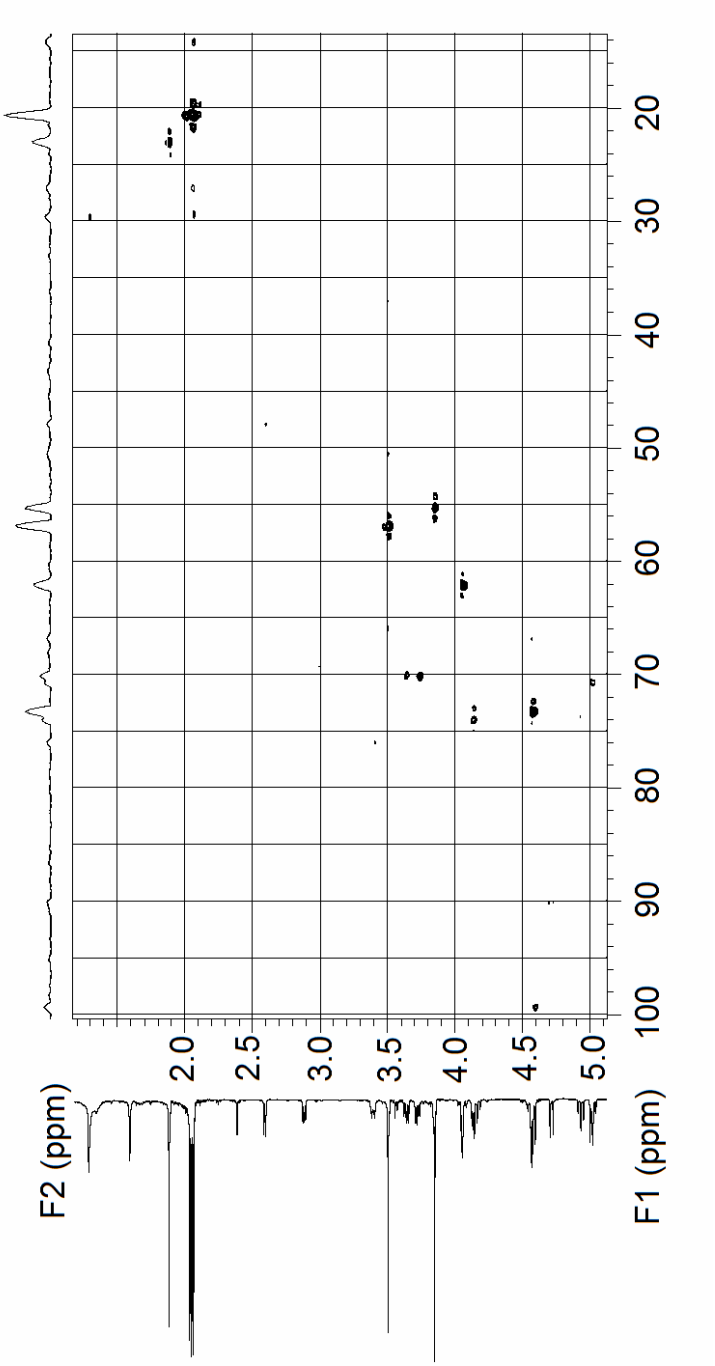

**Figure 4.39.** $^{1}H–^{13}C$ gHMBC of compound **40** (500 MHz, $CDCl_3$)

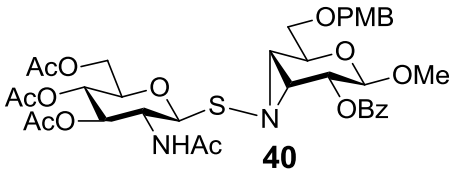


**40**

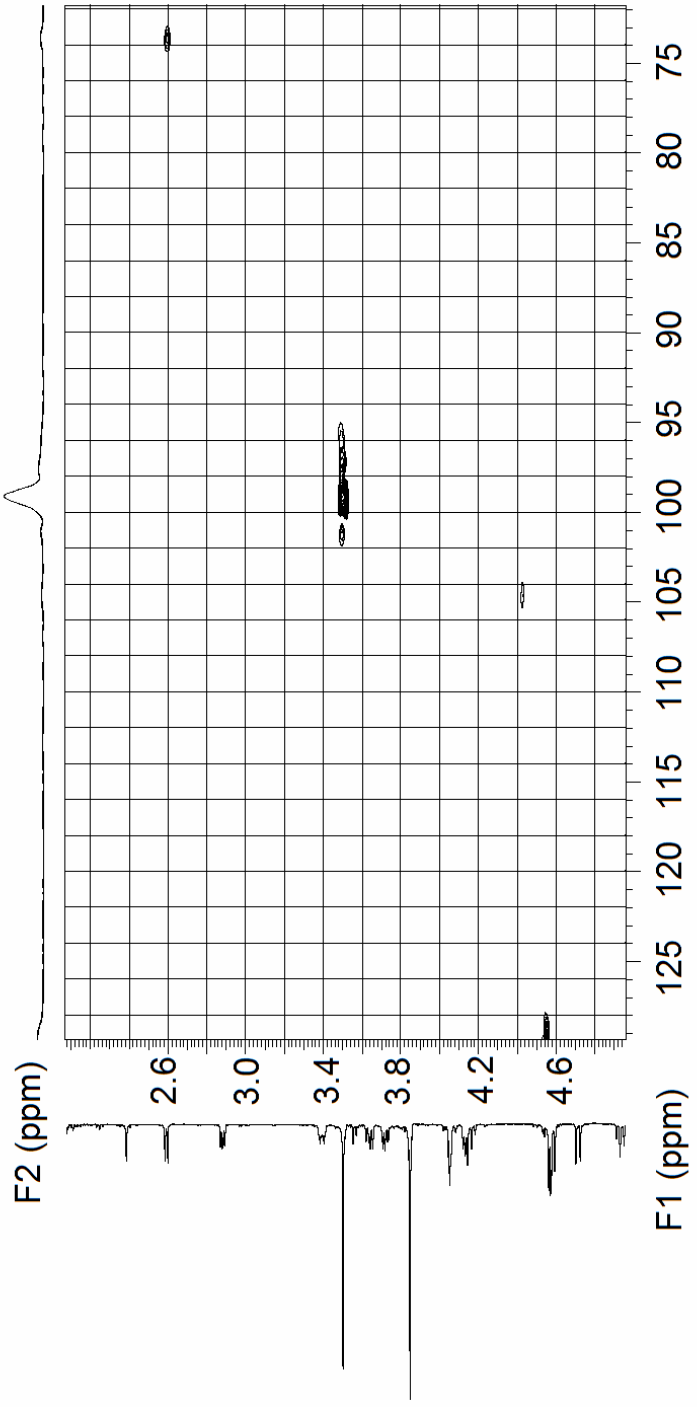

**Figure 4.40.** $^{1}$H-NMR of compound **72** (500 MHz, $CDCl_3$)

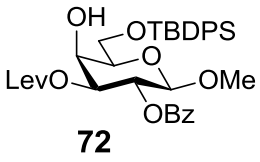


**72**

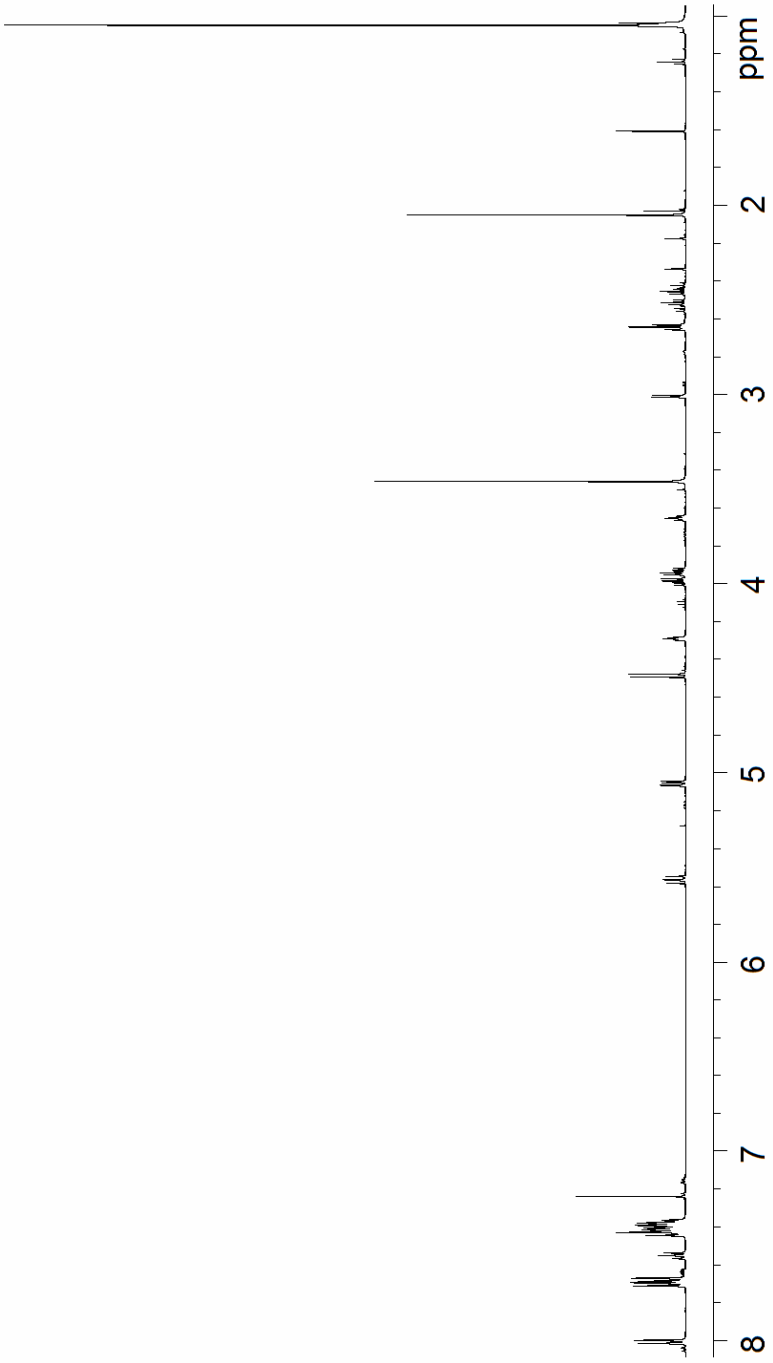

**Figure 4.41.** $^{13}$C-NMR of compound **72** (125 MHz, $CDCl_3$)

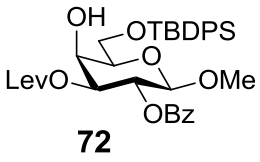


**72**

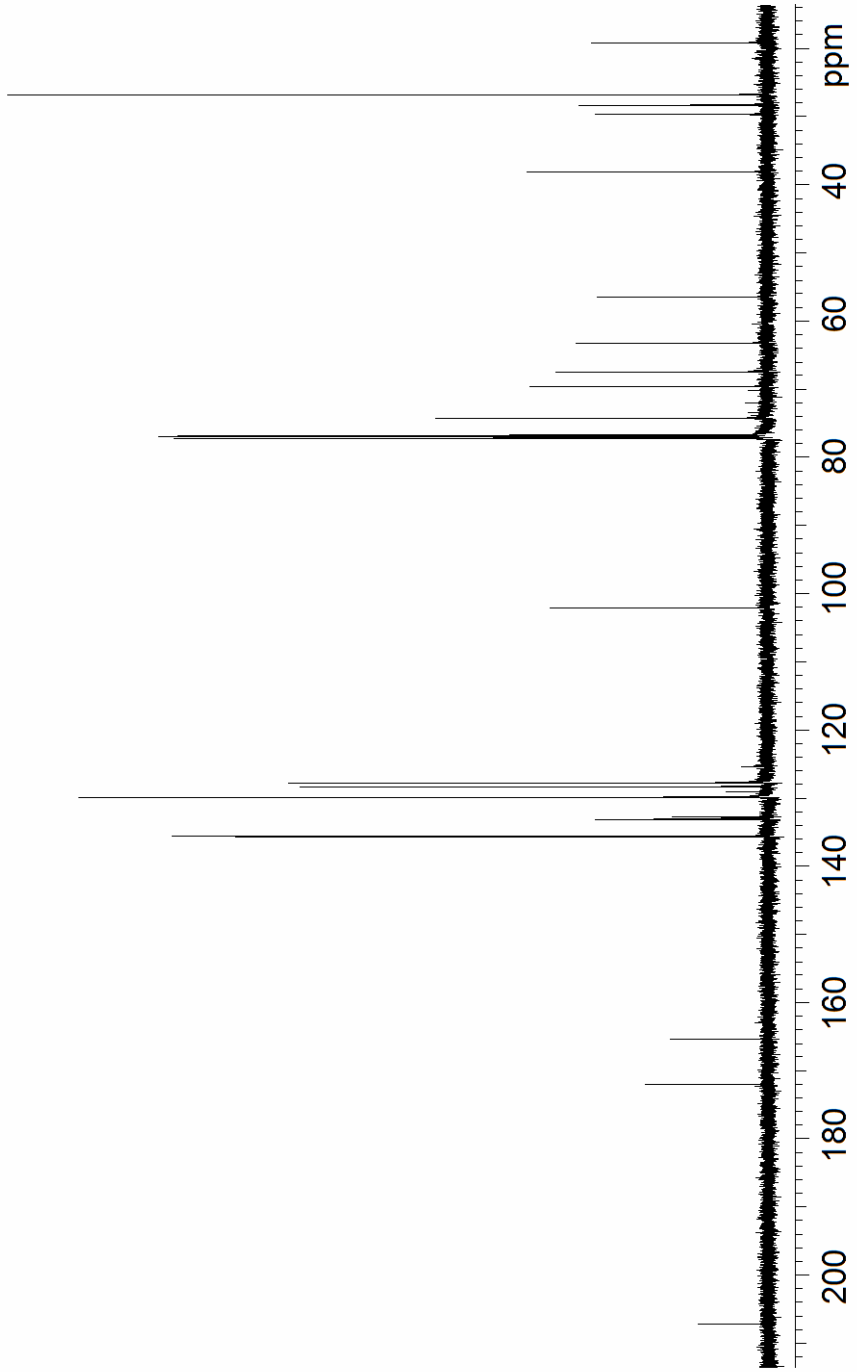

**Figure 4.42.** $^{1}H–^{1}H$ gCOSY of compound **72** (500 MHz, $CDCl_3$)

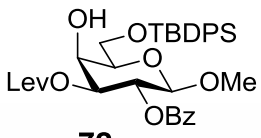


**72**

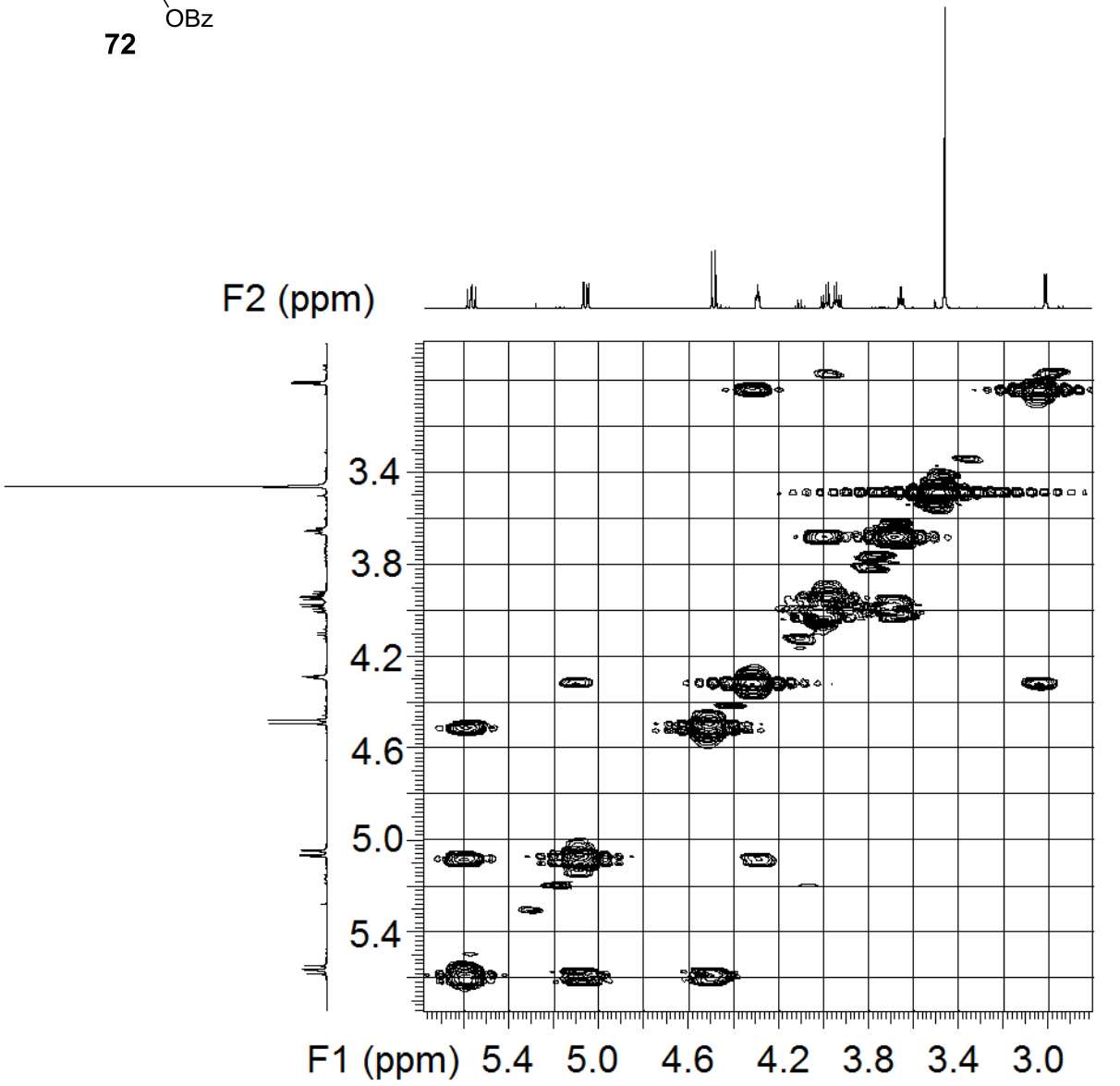

**Figure 4.43.** $^{1}H–^{13}C$ gHMQC (without $^{1}H$ decoupling) of compound **72** (500 MHz,$CDCl_3$)

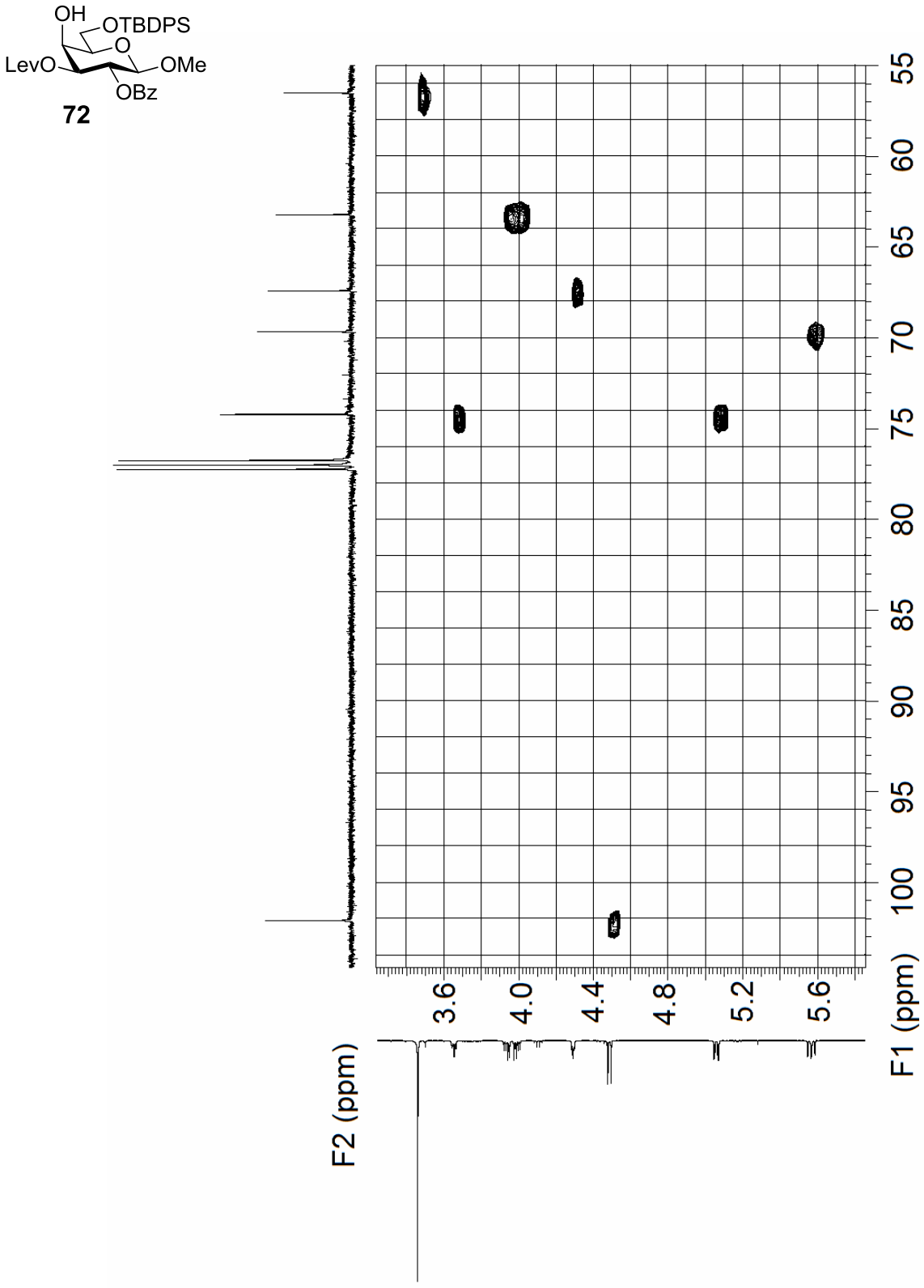

**Figure 4.44.** $^{1}$H-NMR of compound **73** (500 MHz, $CDCl_3$)

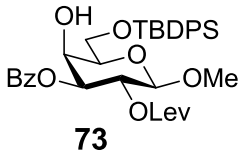


**73**

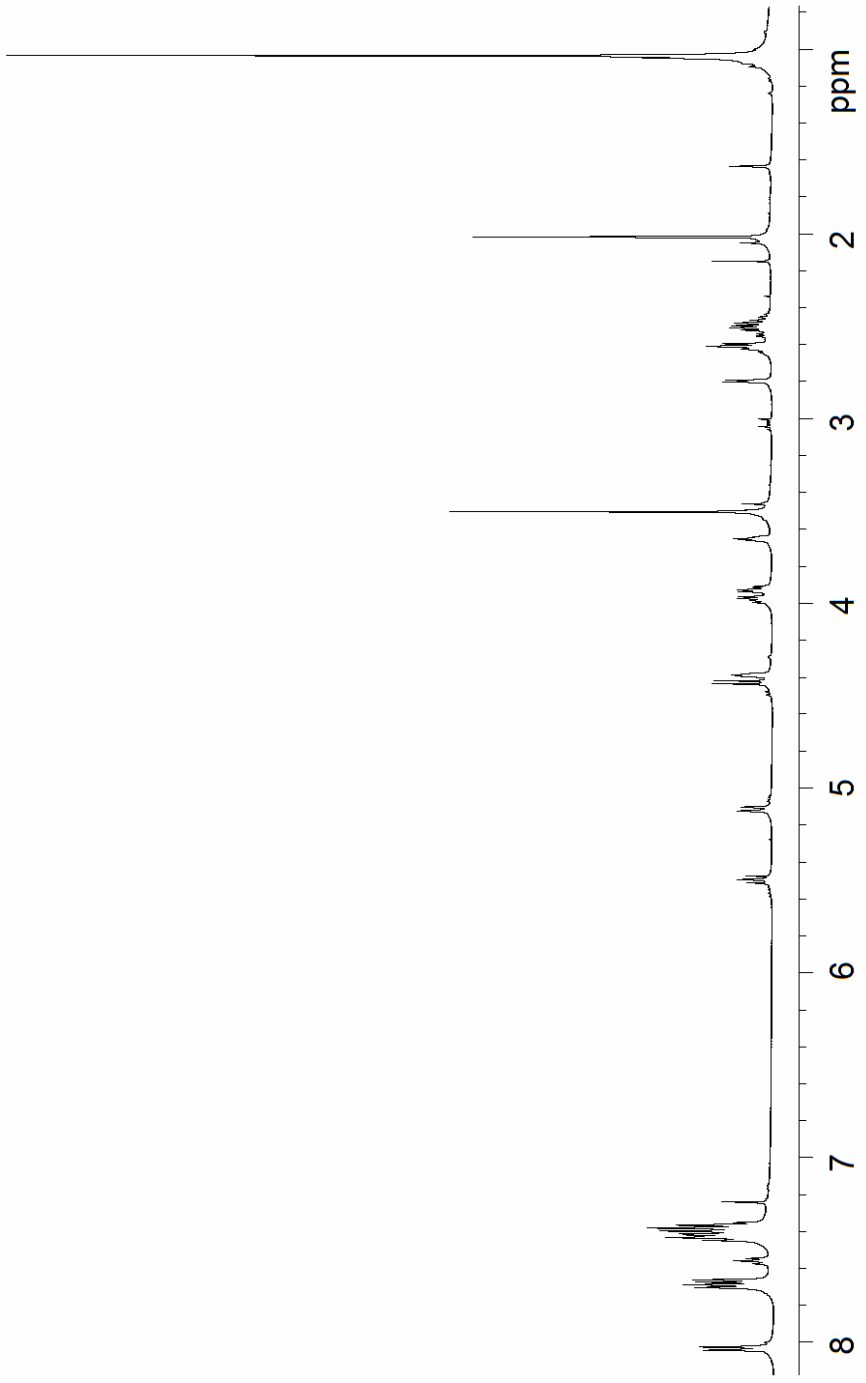

**Figure 4.45.** $^{13}$C-NMR of compound **73** (125 MHz, $CDCl_3$)

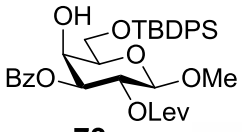


**73**

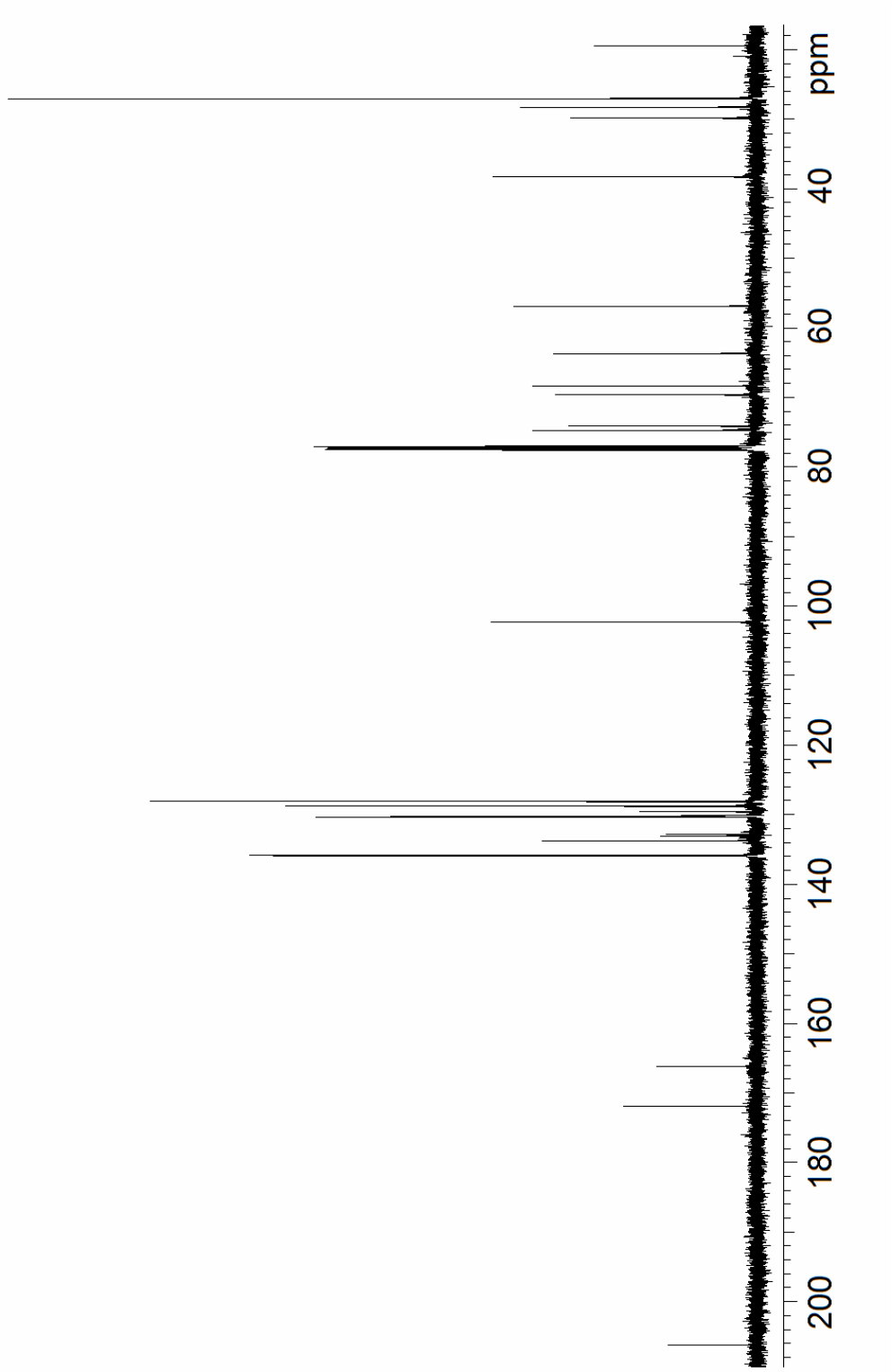

**Figure 4.46.** $^{1}H–^{1}H$ gCOSY of compound **73** (500 MHz, $CDCl_3$)

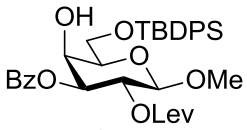


**73**

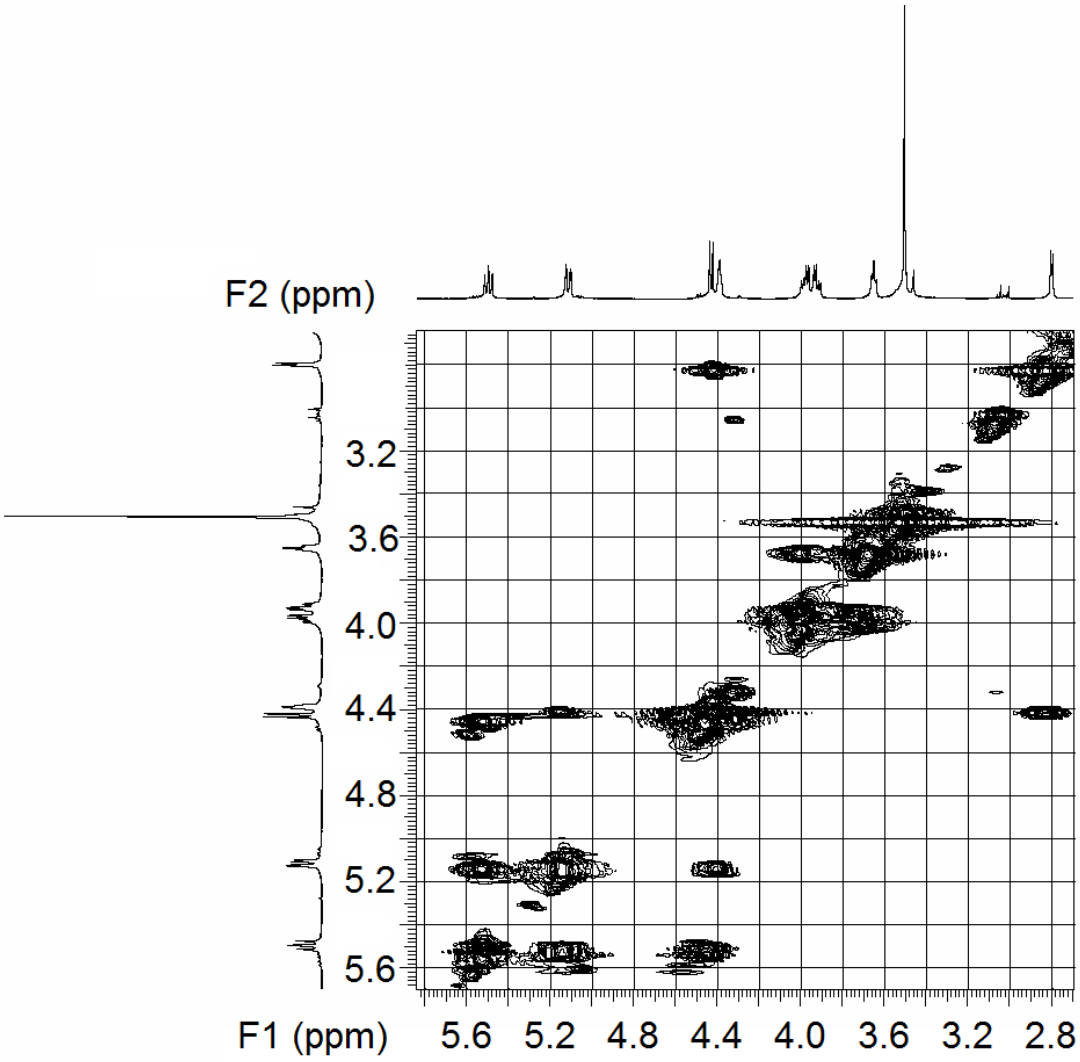

**Figure 4.47.** $^{1}H–^{13}C$ gHMQC (without $^{1}H$ decoupling) of compound **73** (500 MHz,$CDCl_3$)

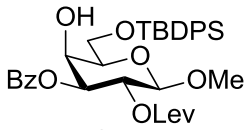


**73**

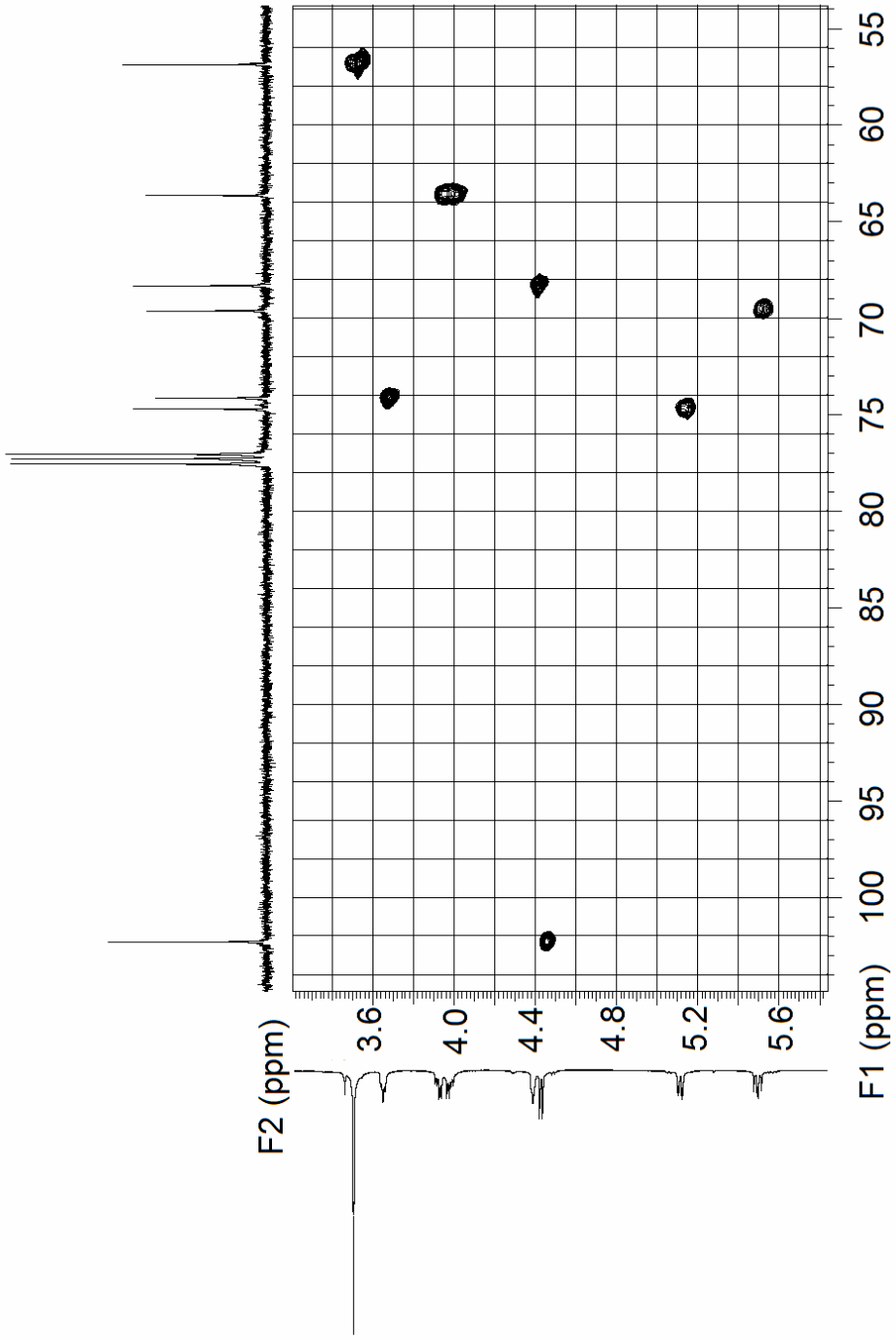

**Figure 4.48.** $^{1}$H-NMR of compound **61** (500 MHz, $CDCl_3$)

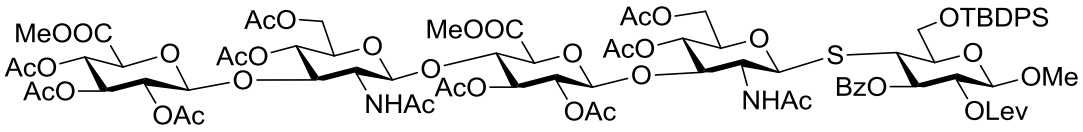


**61**

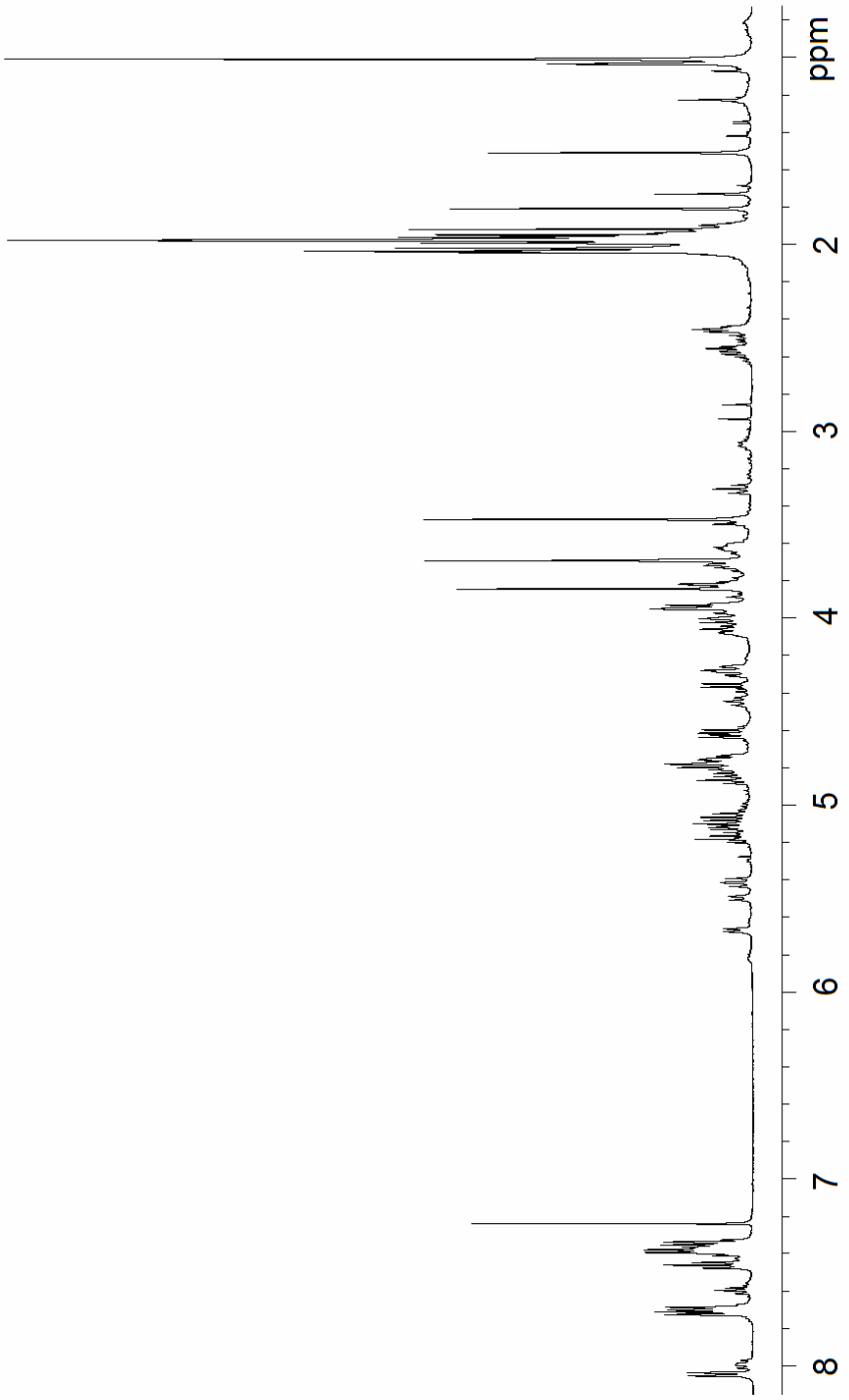

**Figure 4.49.** $^{13}$C-NMR of compound **61** (125 MHz, $CDCl_3$)

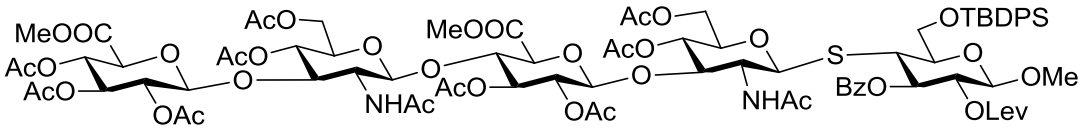


**61**

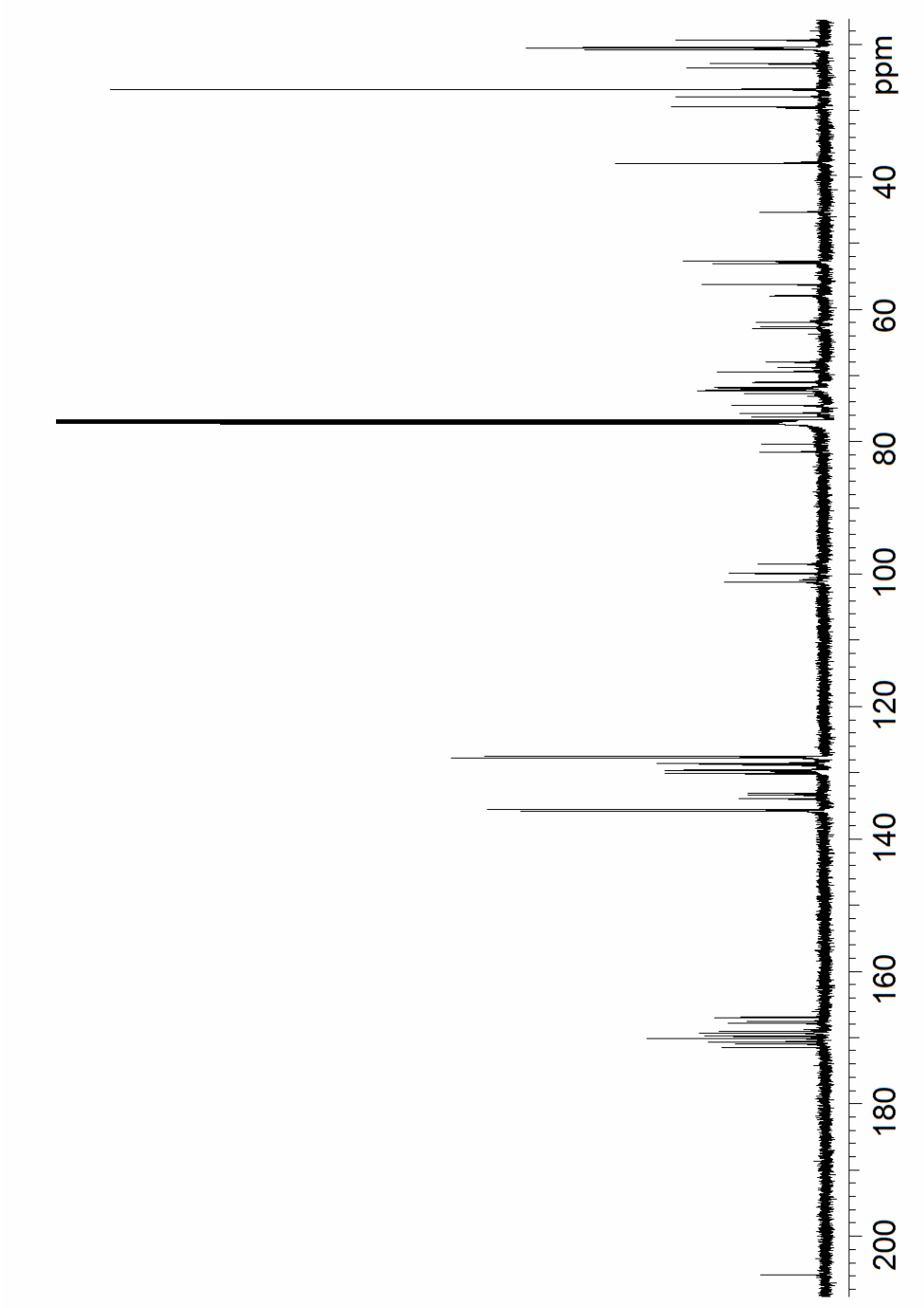

**Figure 4.50.** $^{1}H–^{1}H$ gCOSY of compound **61** (500 MHz, $CDCl_3$)

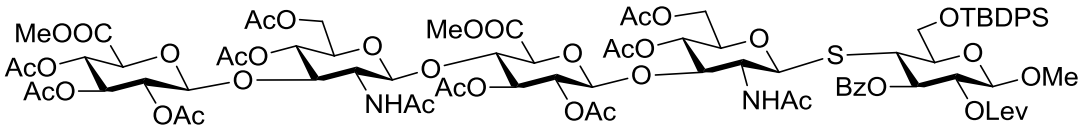


**61**

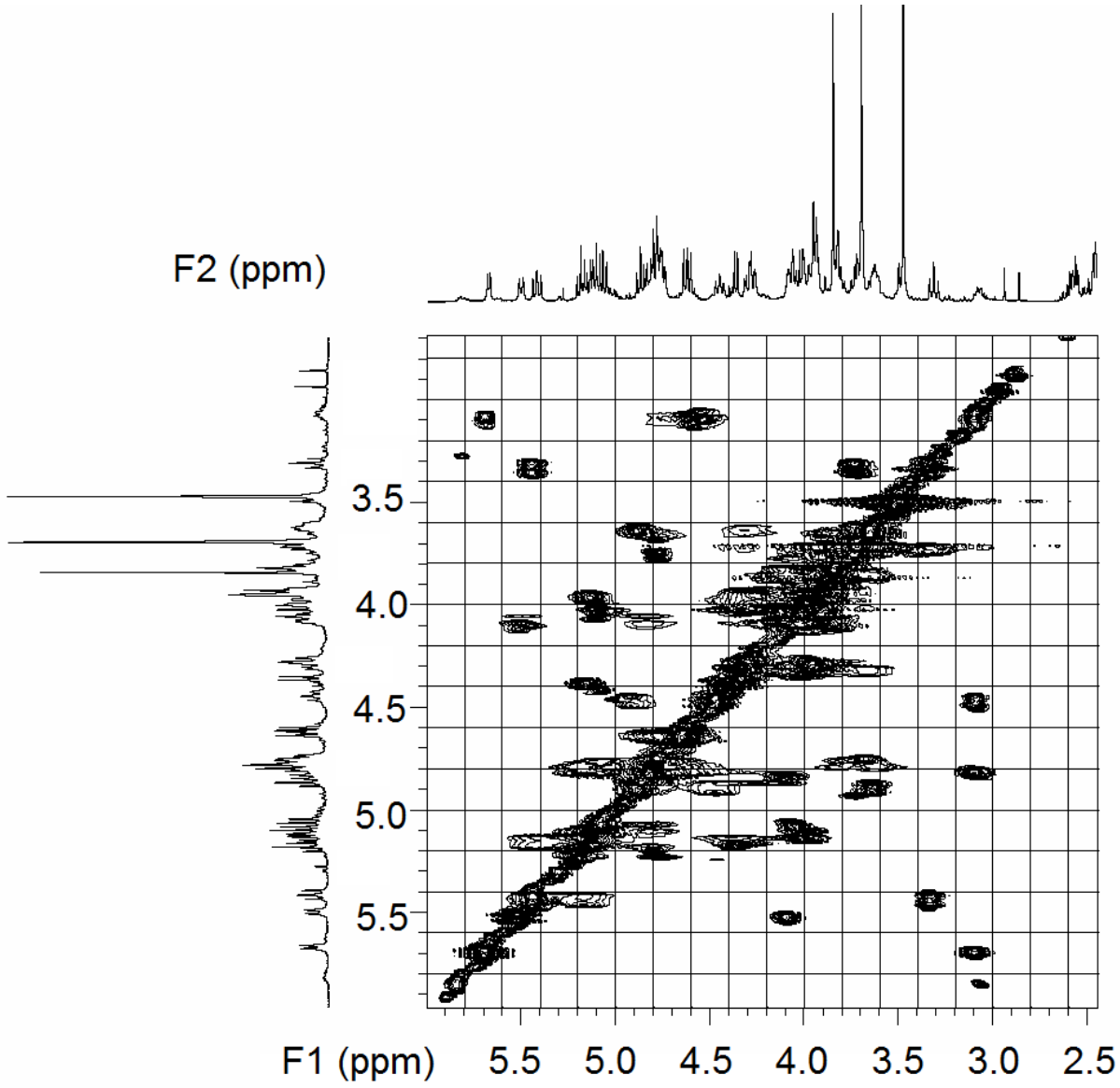

**Figure 4.51.** $^{1}H–^{13}C$ gHMQC of compound **61** (500 MHz, $CDCl_3$)

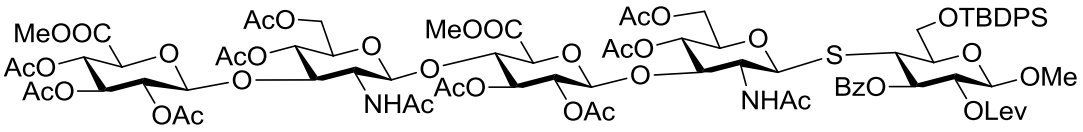


**61**

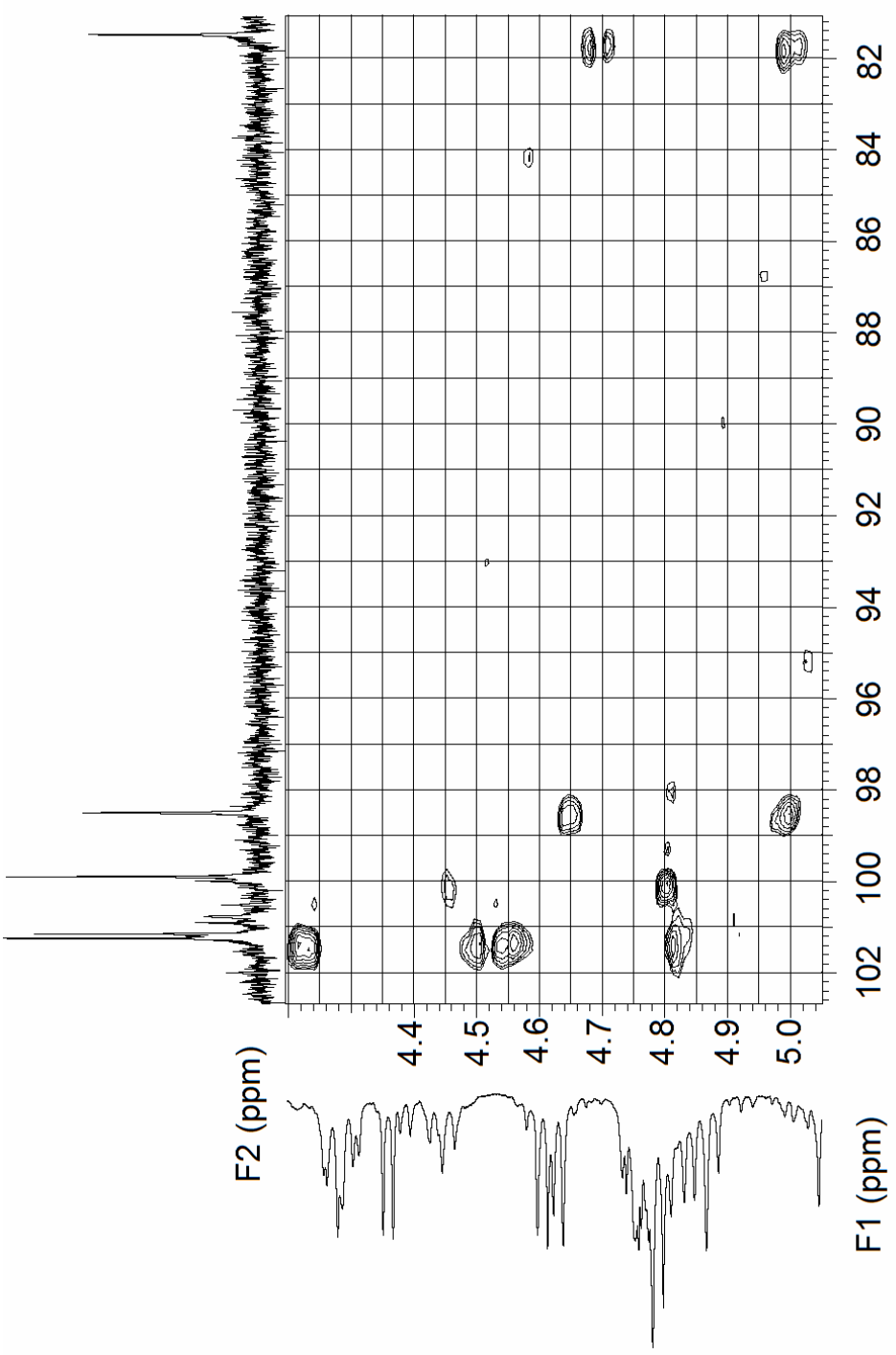

**Figure 4.52.** $^{1}H–^{13}C$ gHMQC (without $^{1}H$ decoupling) of compound **61** (500 MHz,$CDCl_3$)

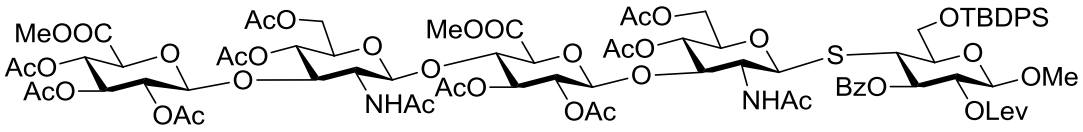


**61**

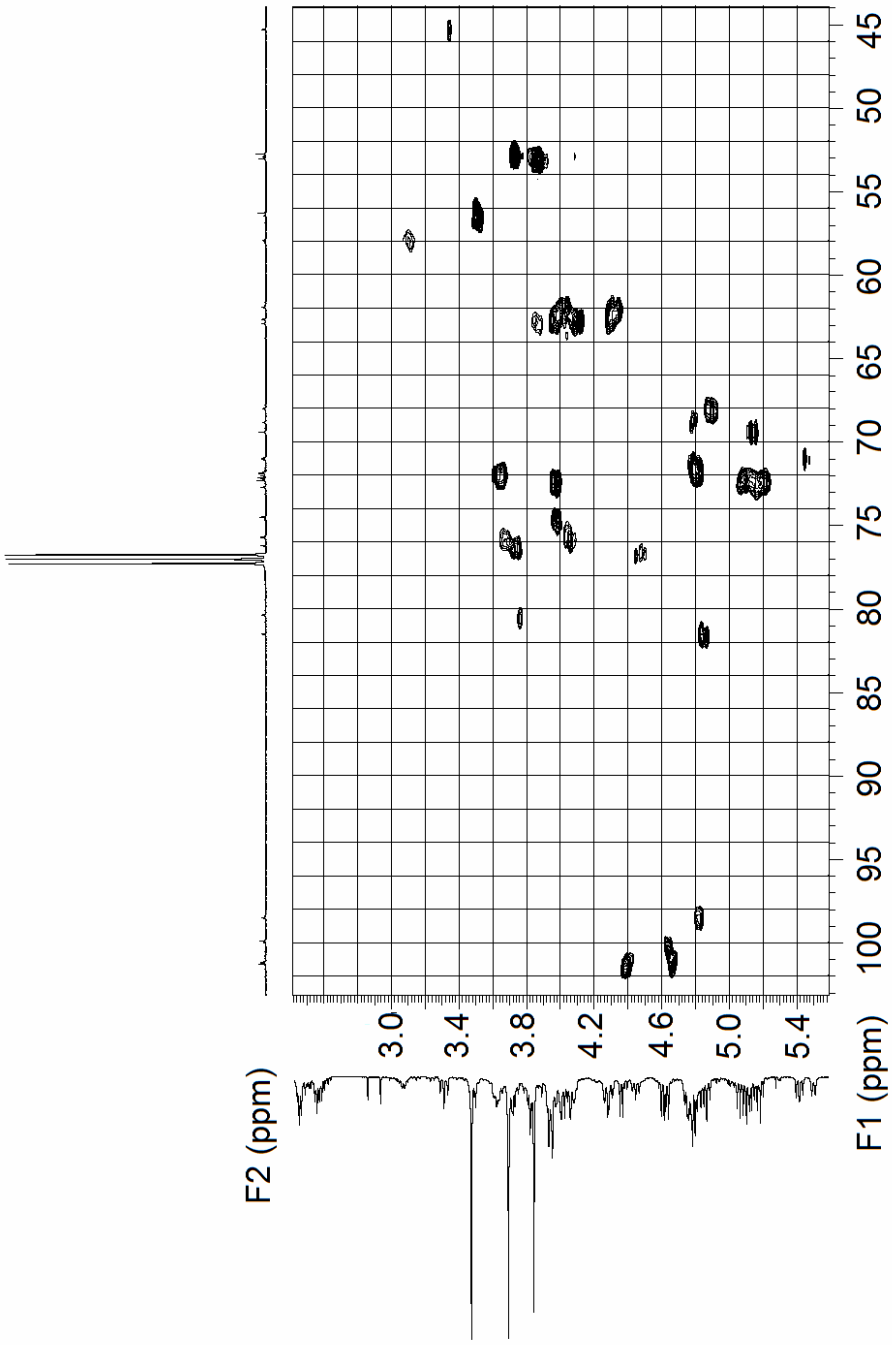

**Figure 4.53.** $^{1}H–^{13}C$ gHMBC of compound **61** (500 MHz, $CDCl_3$)

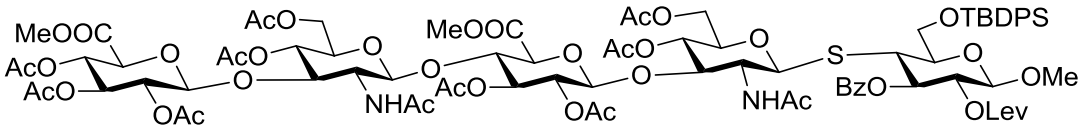


**61**

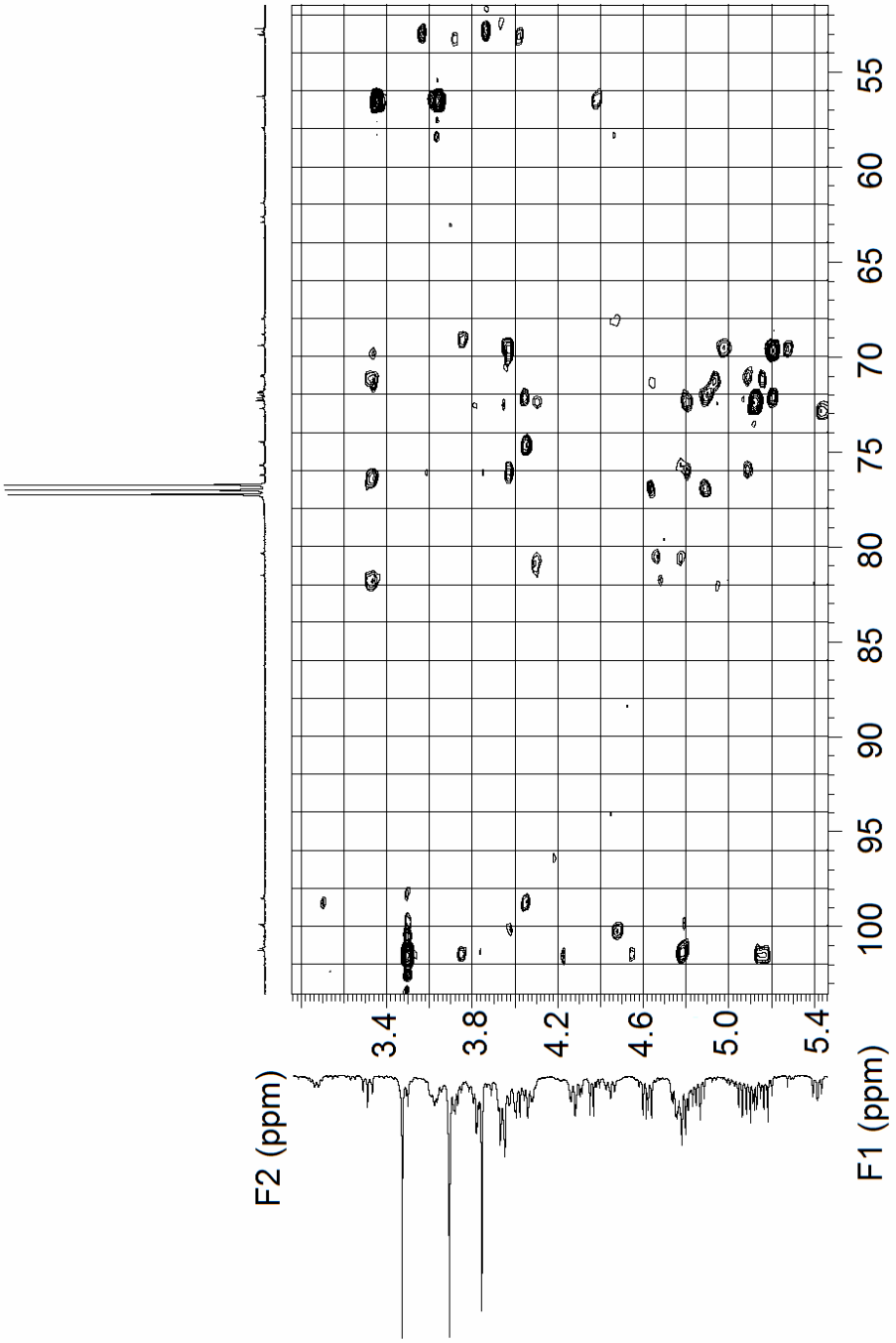

**Figure 4.54.** $^{1}$H-NMR of compound **62** (500 MHz, $CDCl_3$)

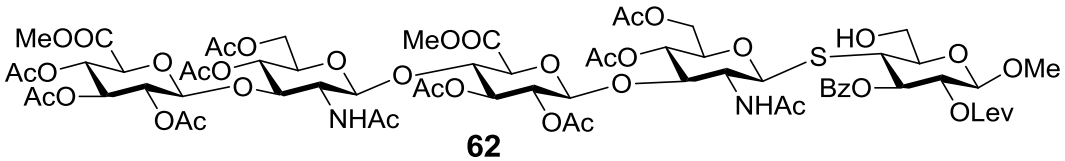


**62**

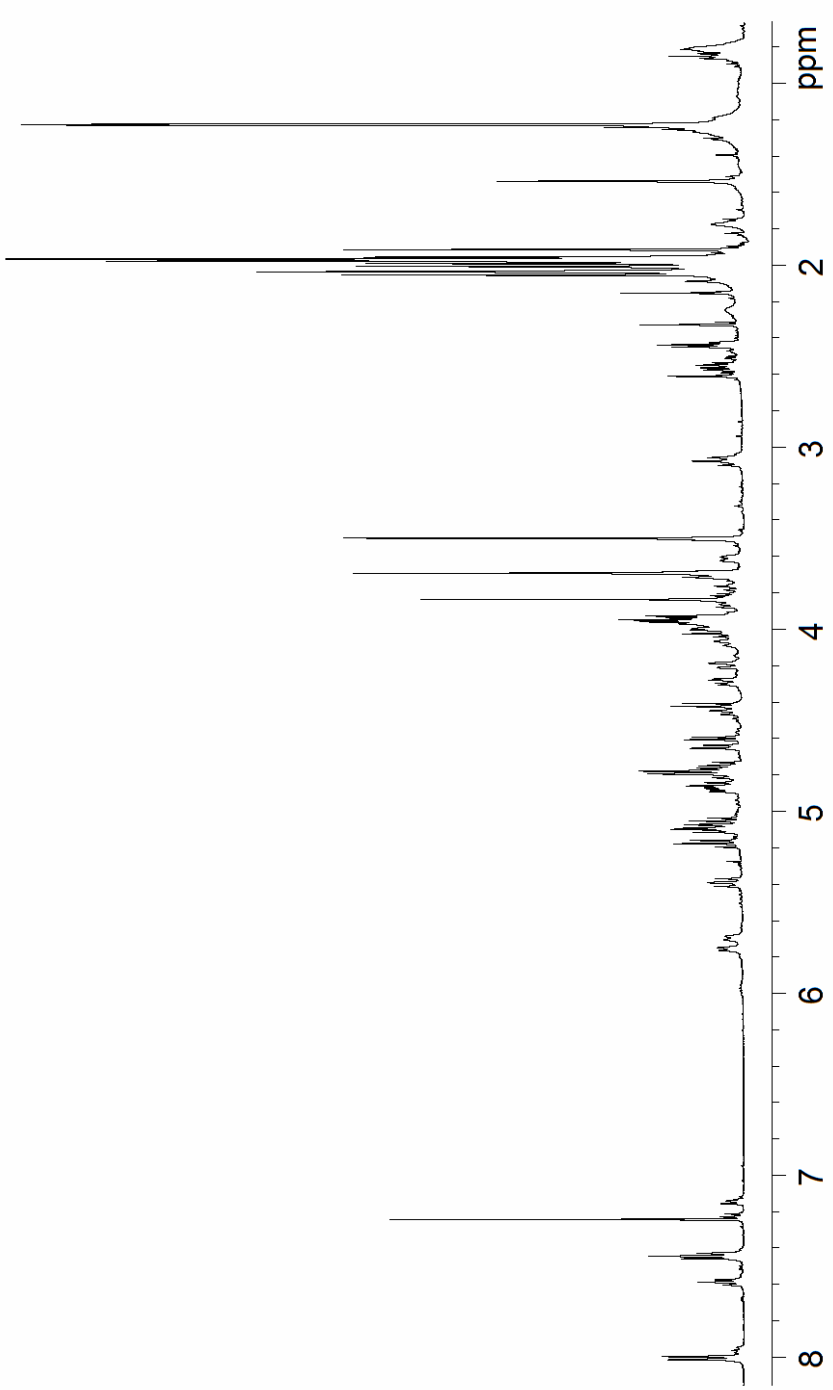

**Figure 4.55.** $^{13}$C-NMR of compound **62** (125 MHz, $CDCl_3$)

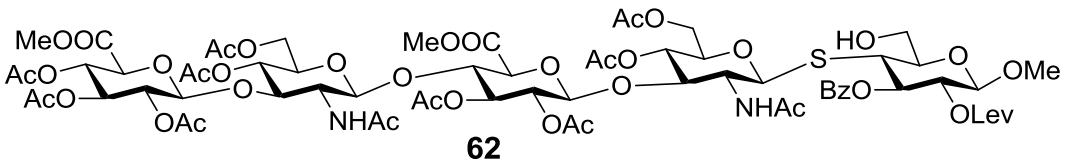


**62**

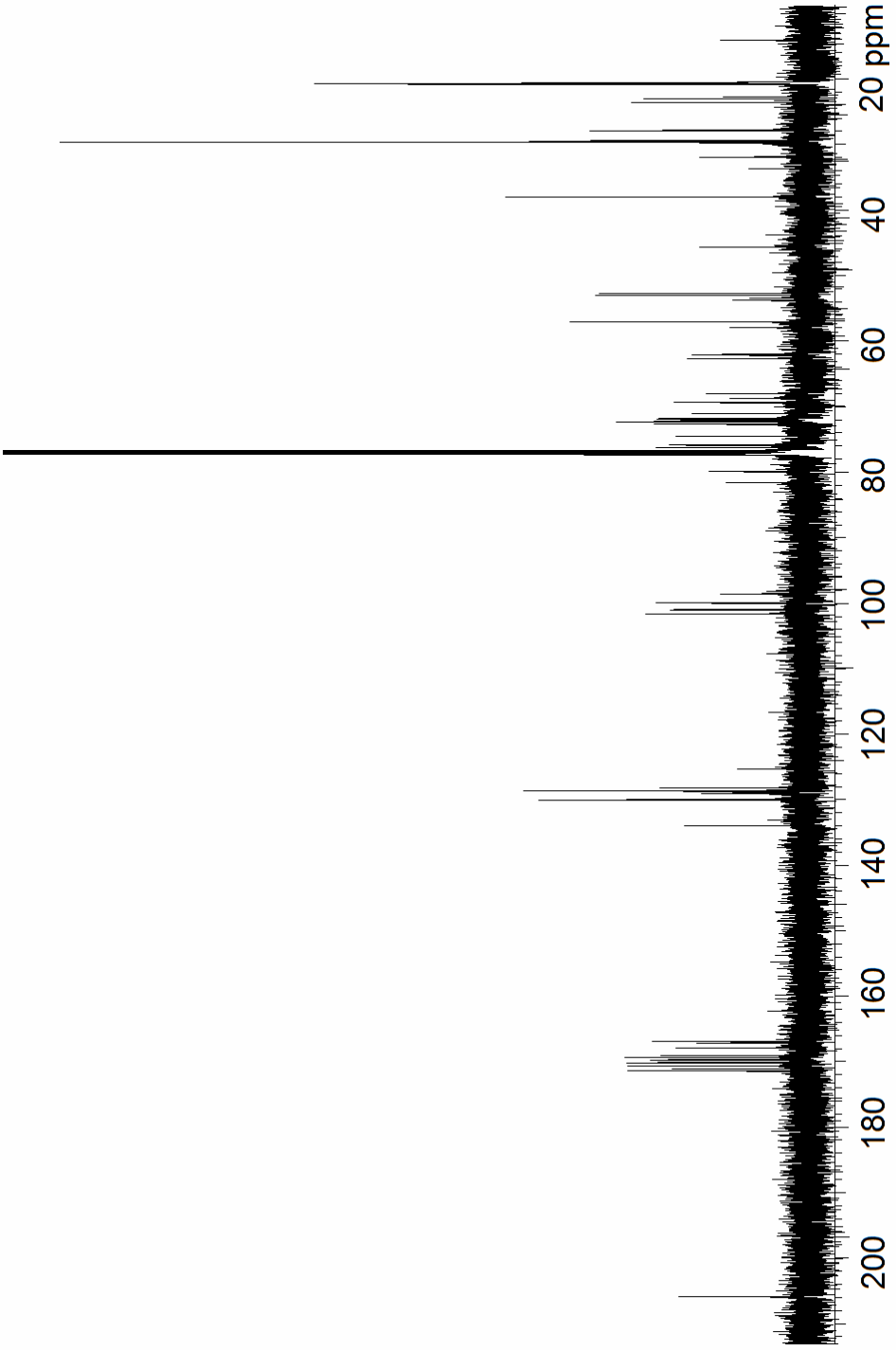

**Figure 4.56.** $^{1}H–^{1}H$ gCOSY of compound **62** (500 MHz, $CDCl_3$)

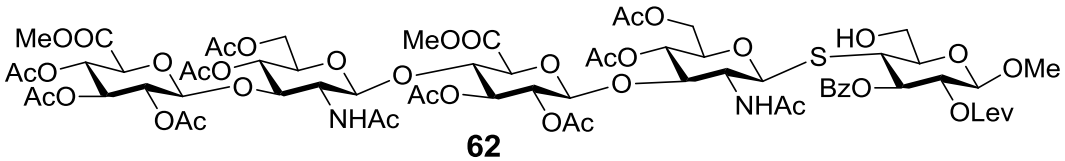


**62**

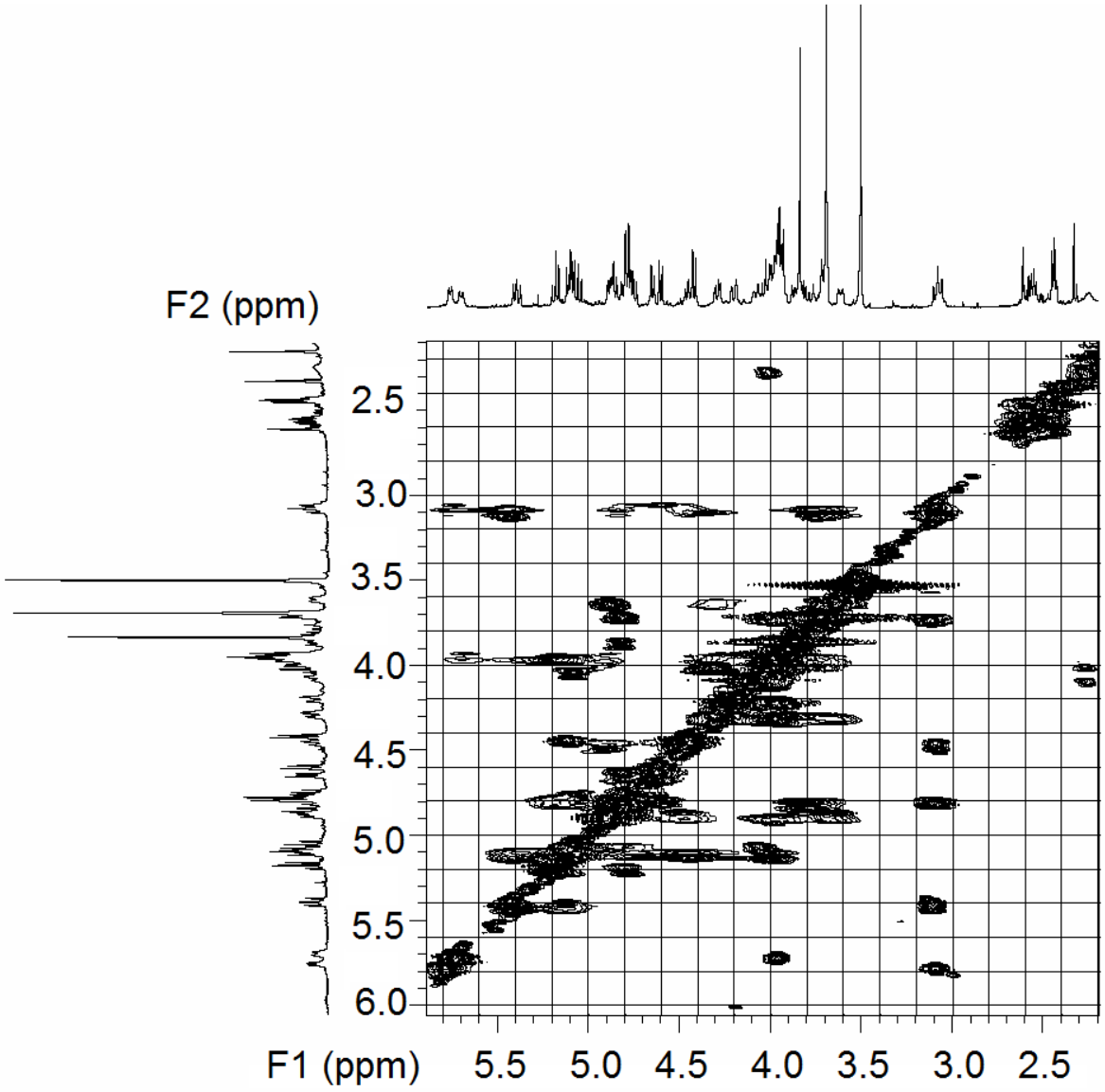

**Figure 4.57.** $^{1}H–^{13}C$ gHMQC (without $^{1}H$ decoupling) of compound **62** (500 MHz,$CDCl_3$)

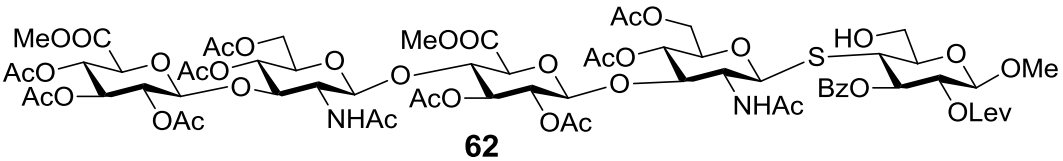


**62**

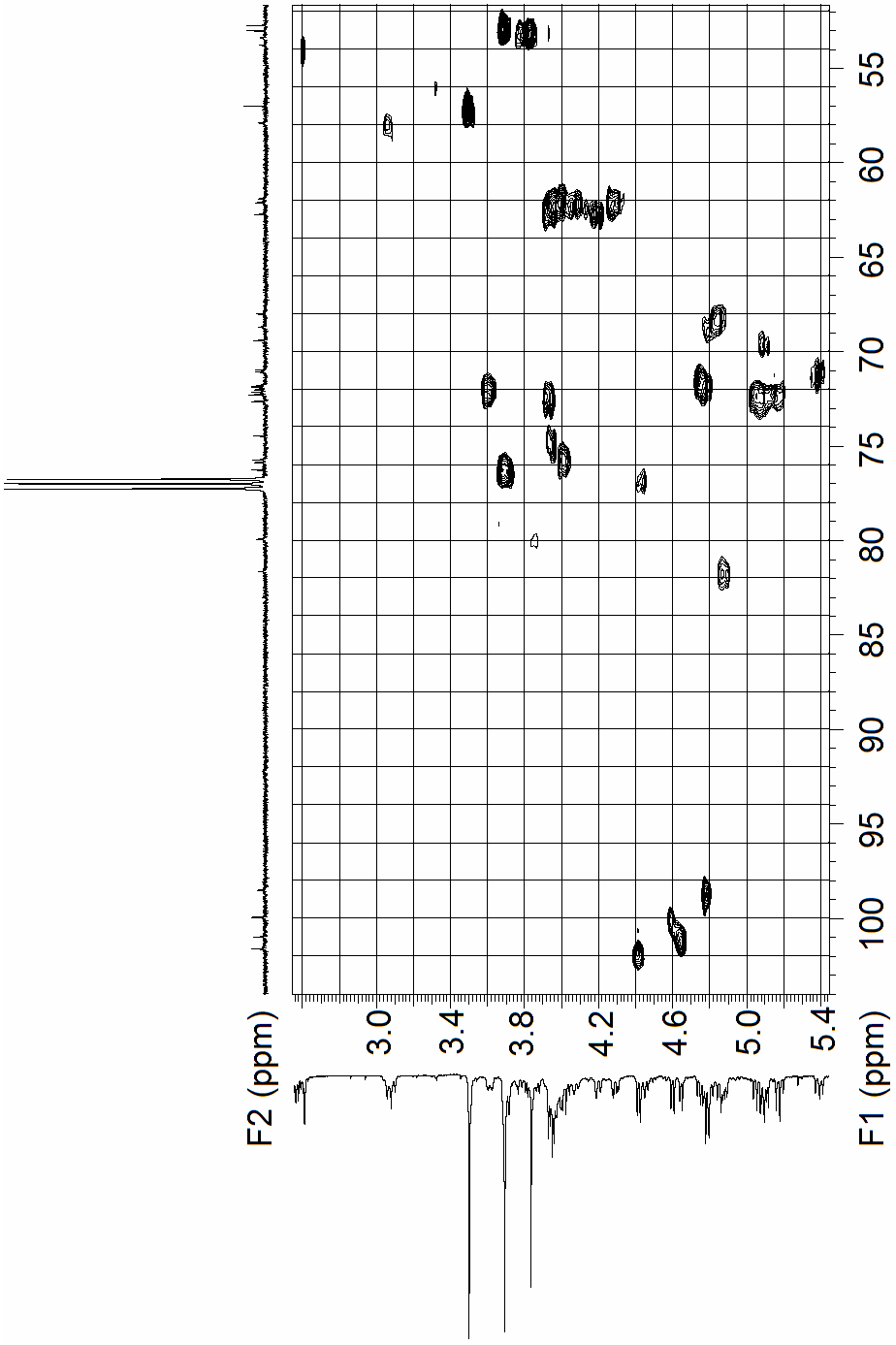

**Figure 4.58.** $^{1}H–^{13}C$ gHMBC of compound **62** (500 MHz, $CDCl_3$)

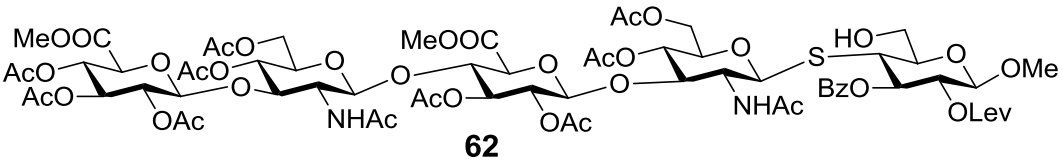


**62**

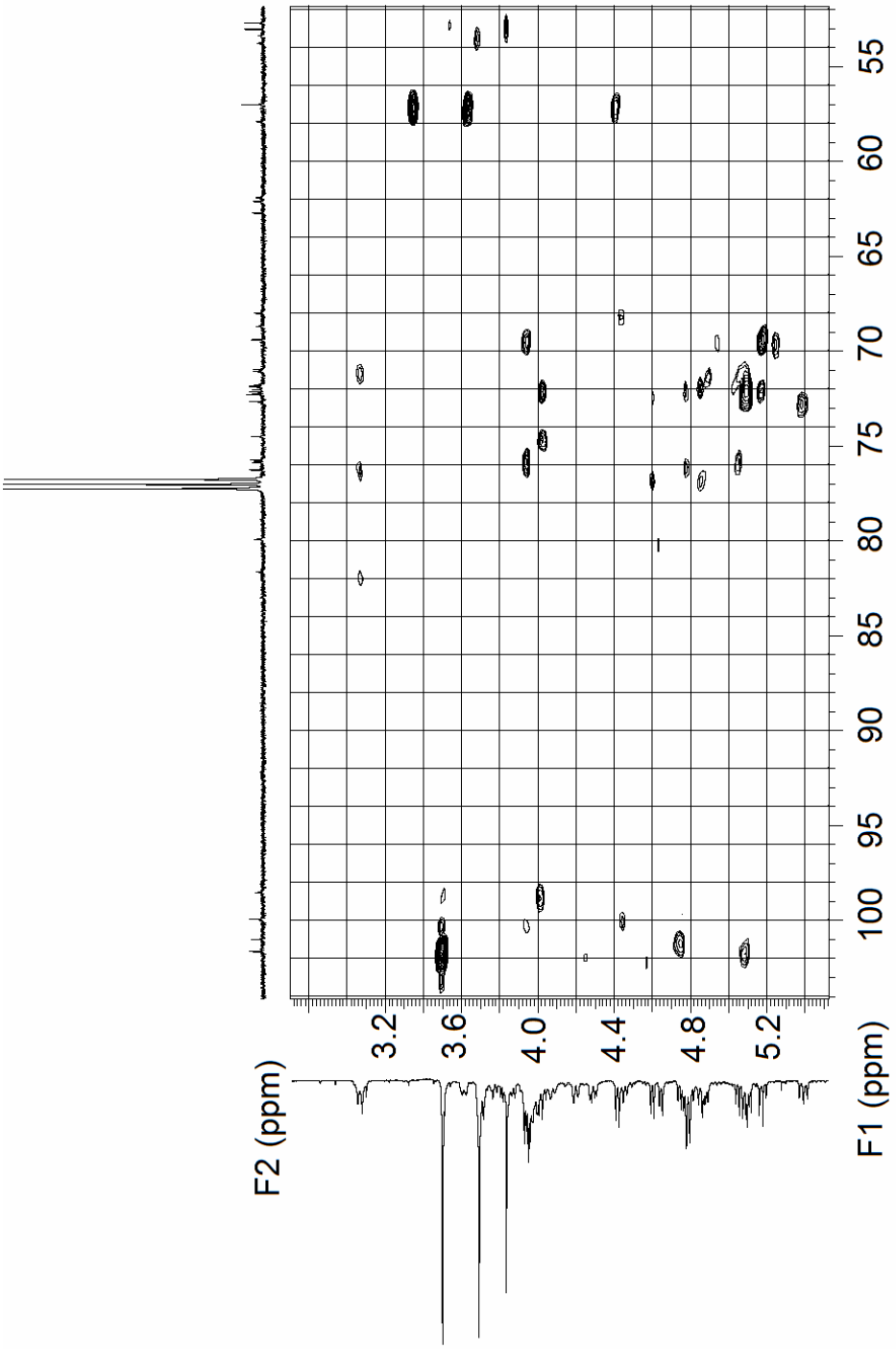

**Figure 4.59.** $^{1}$H-NMR of compound **63** (500 MHz, $CDCl_3$)

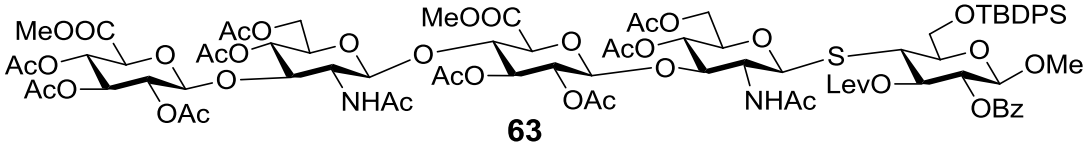


**63**

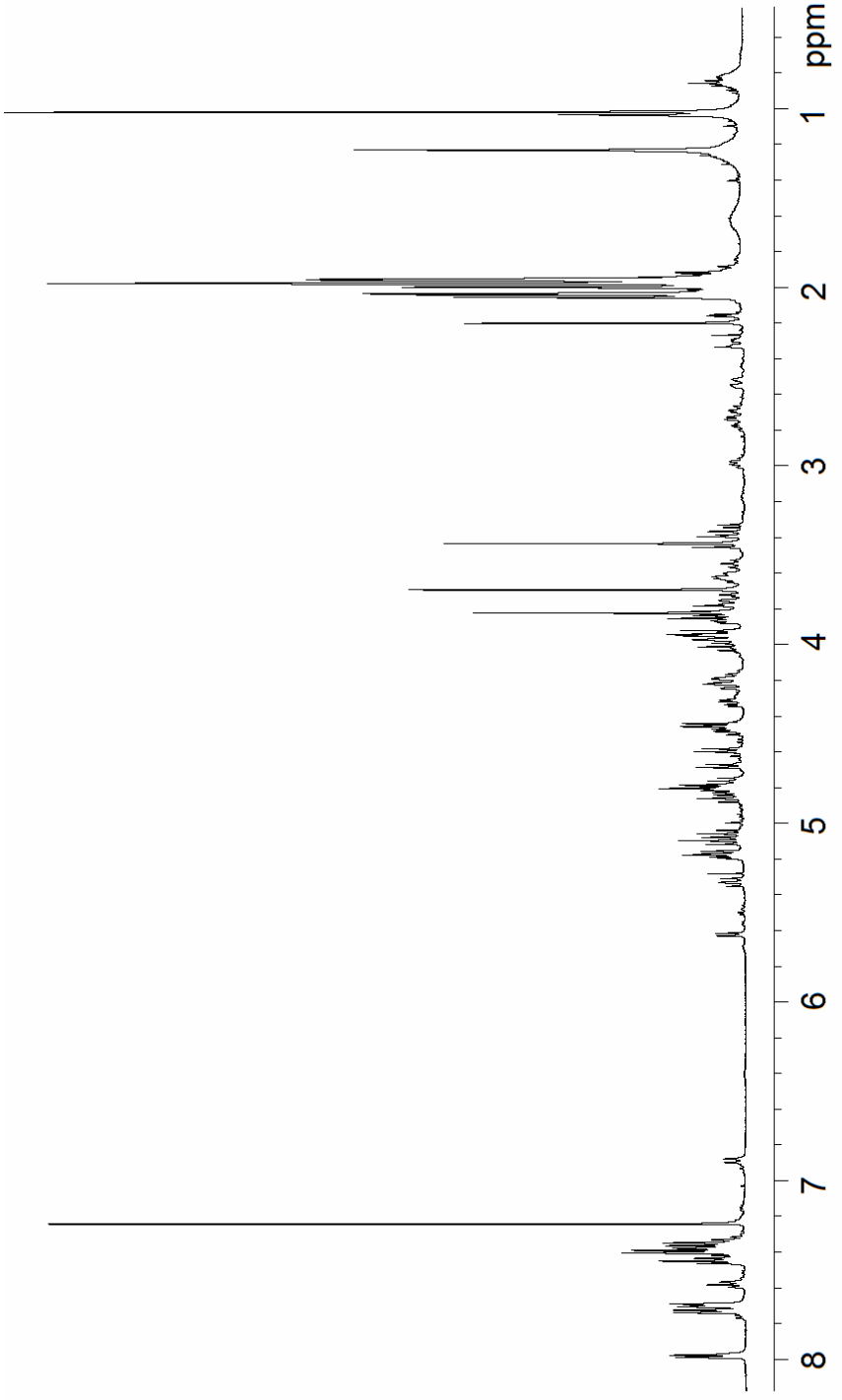

**Figure 4.60.** $^{13}$C-NMR of compound **63** (125 MHz, $CDCl_3$)

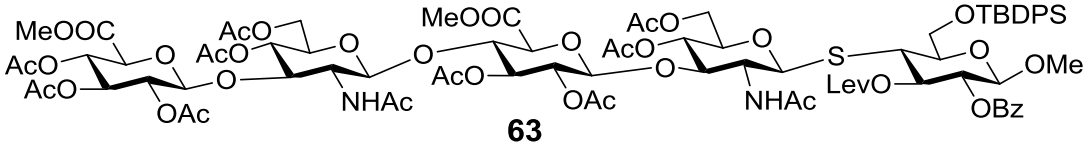


**63**

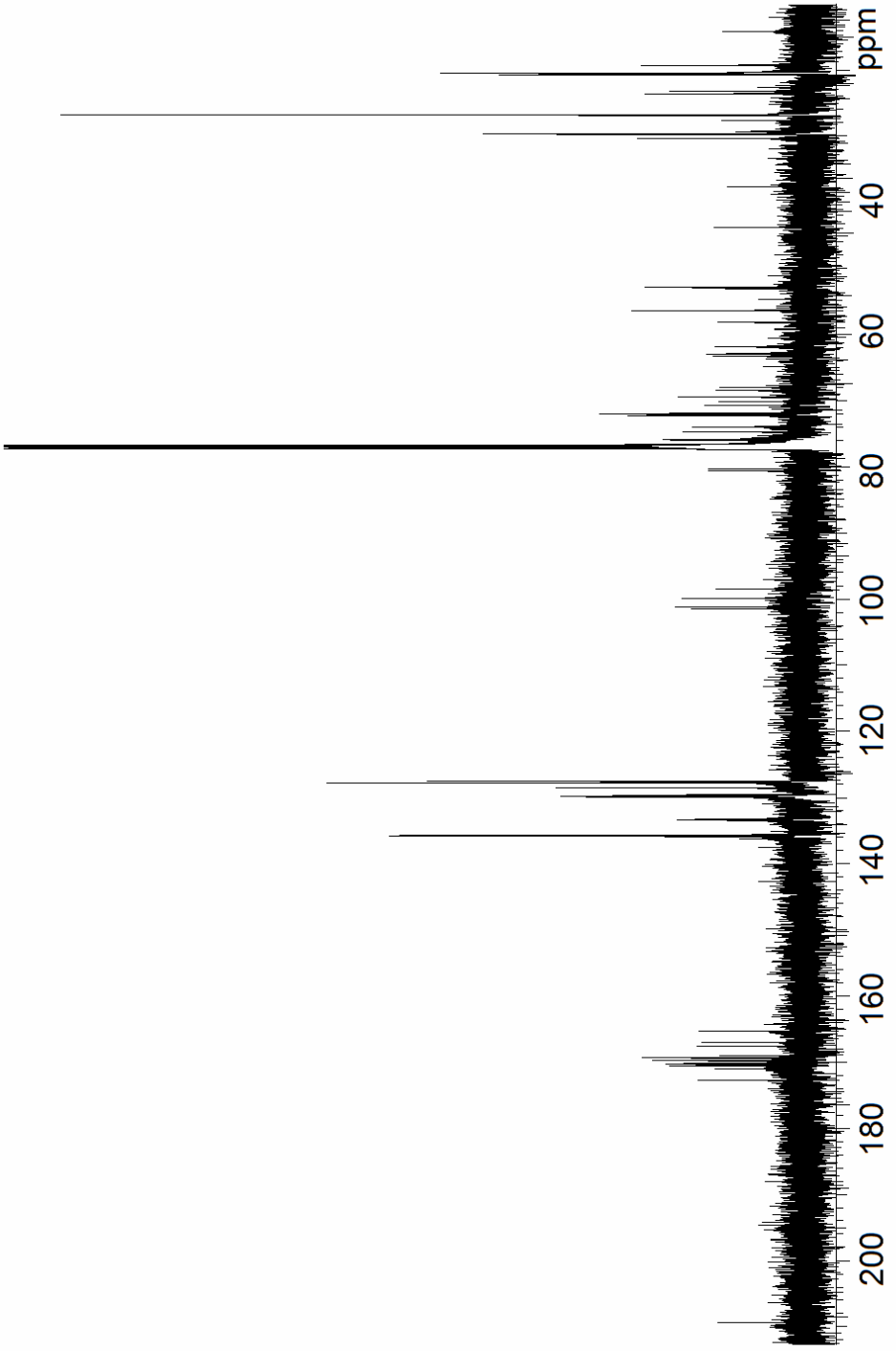

**Figure 4.61.** $^{1}H–^{1}H$ gCOSY of compound **63** (500 MHz, $CDCl_3$)

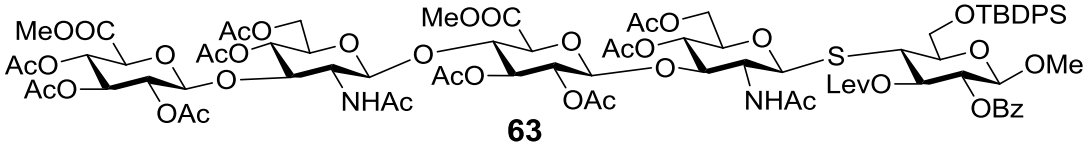


**63**

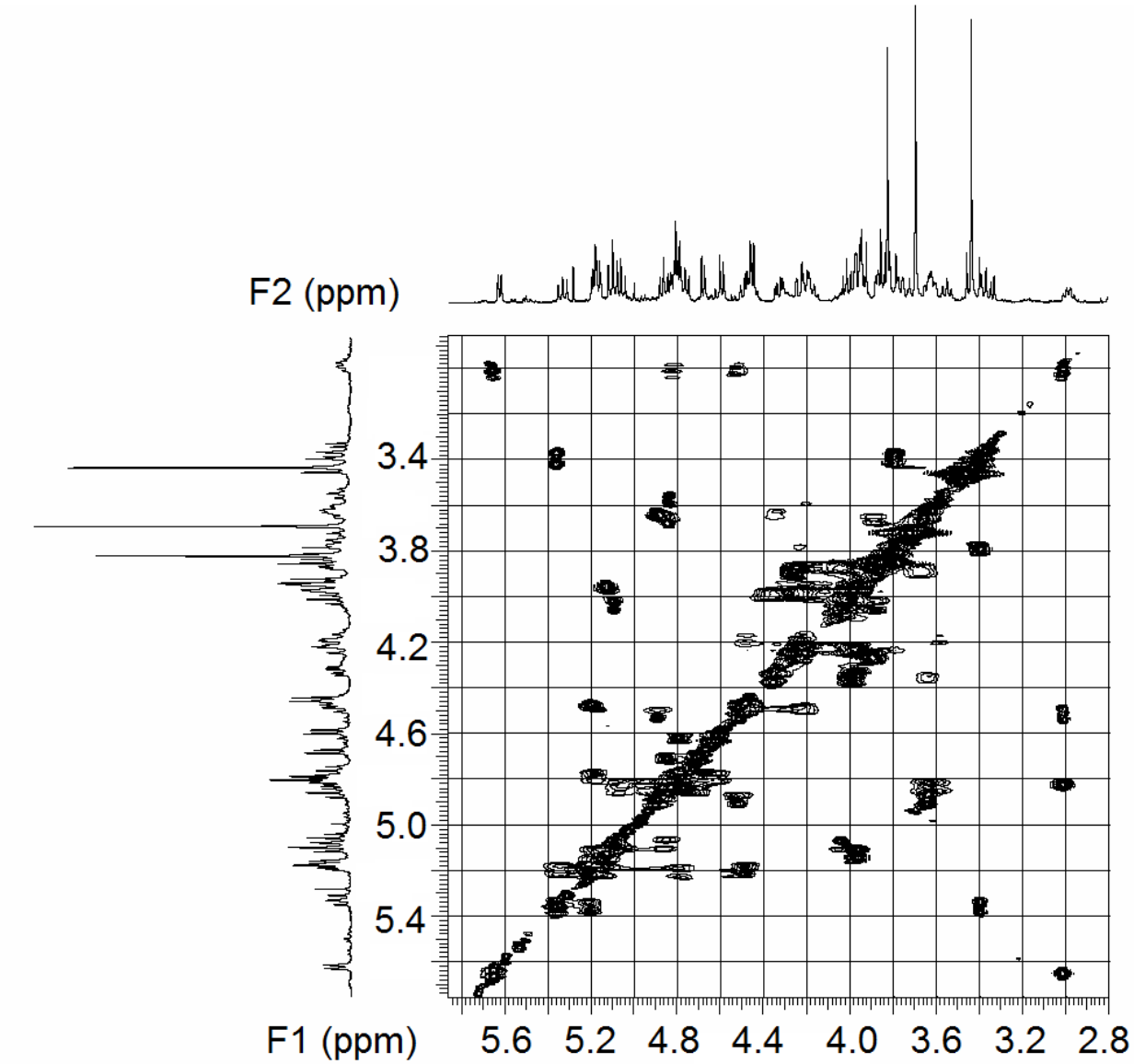

**Figure 4.62.** $^{1}H$–$^{13}C$ gHMQC of compound **63** (500 MHz, $CDCl_3$)

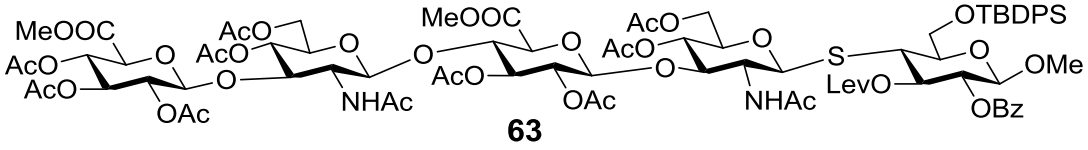


**63**

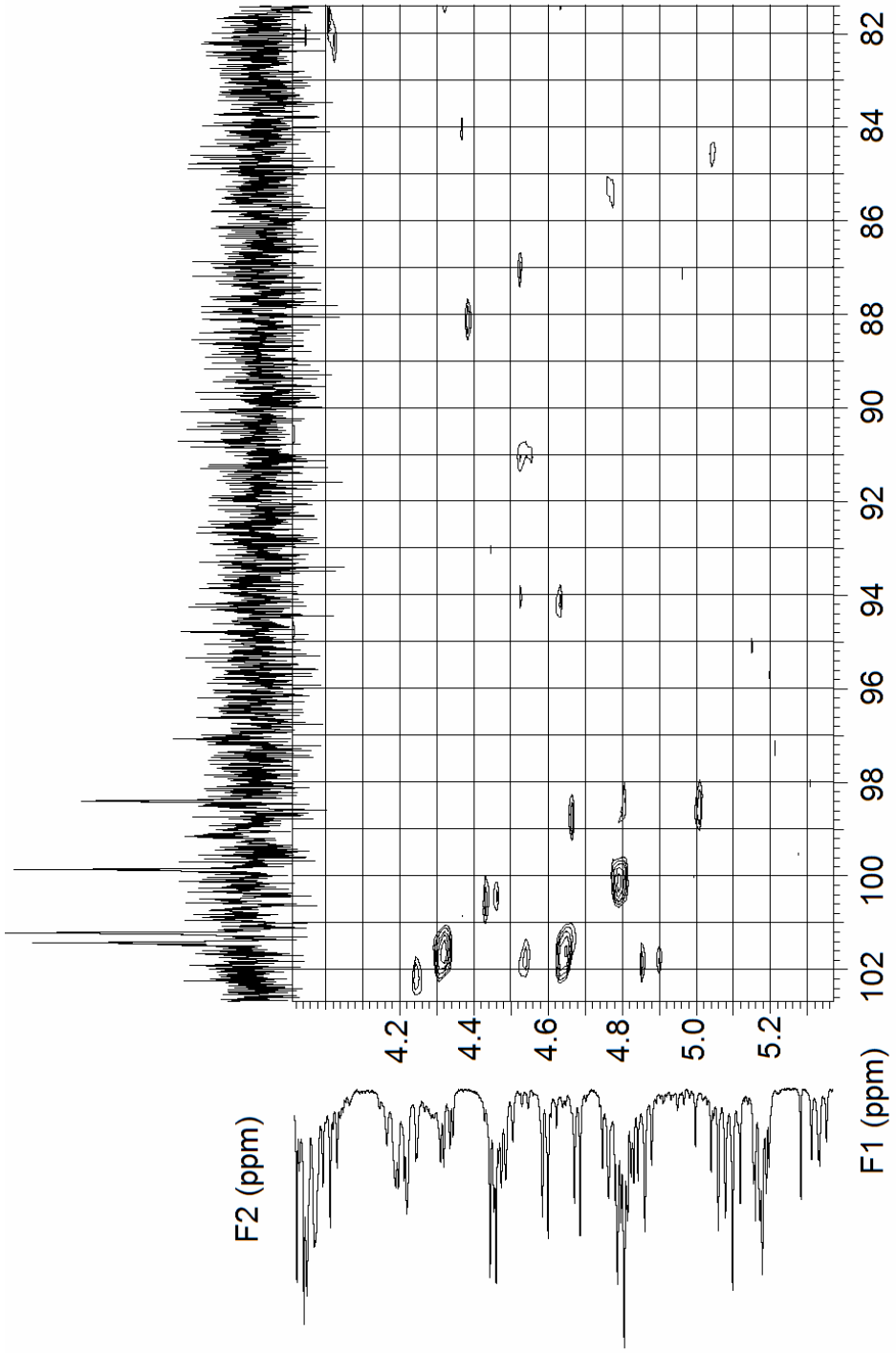

**Figure 4.63.** $^{1}H–^{13}C$ gHMQC (without $^{1}H$ decoupling) of compound **63** (500 MHz,$CDCl_3$)

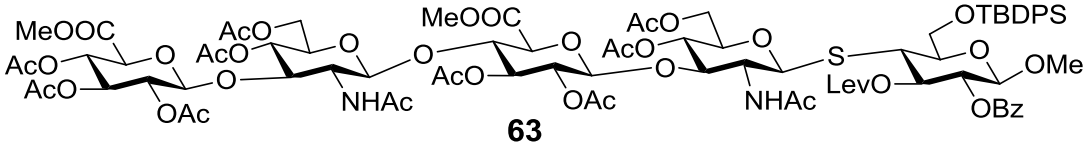


**63**

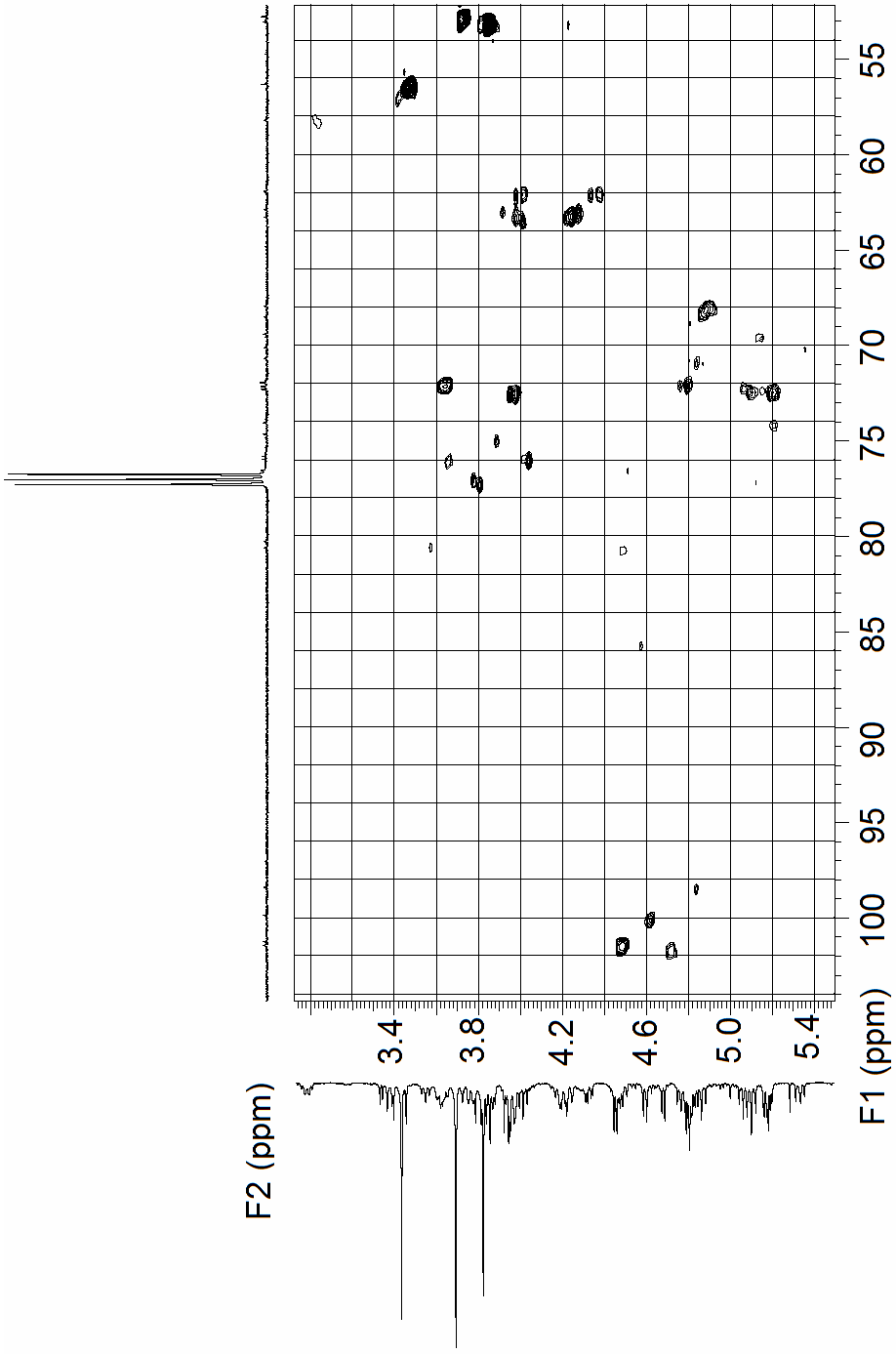

**Figure 4.64.** $^{1}$H-NMR of compound **64** (500 MHz, $CDCl_3$)

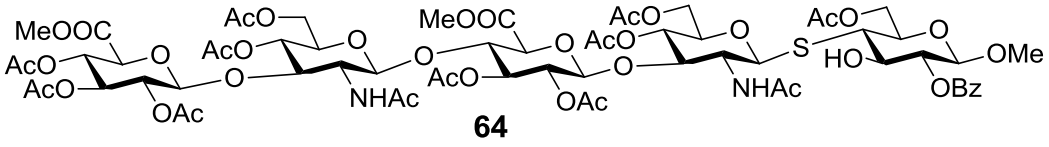


**64**

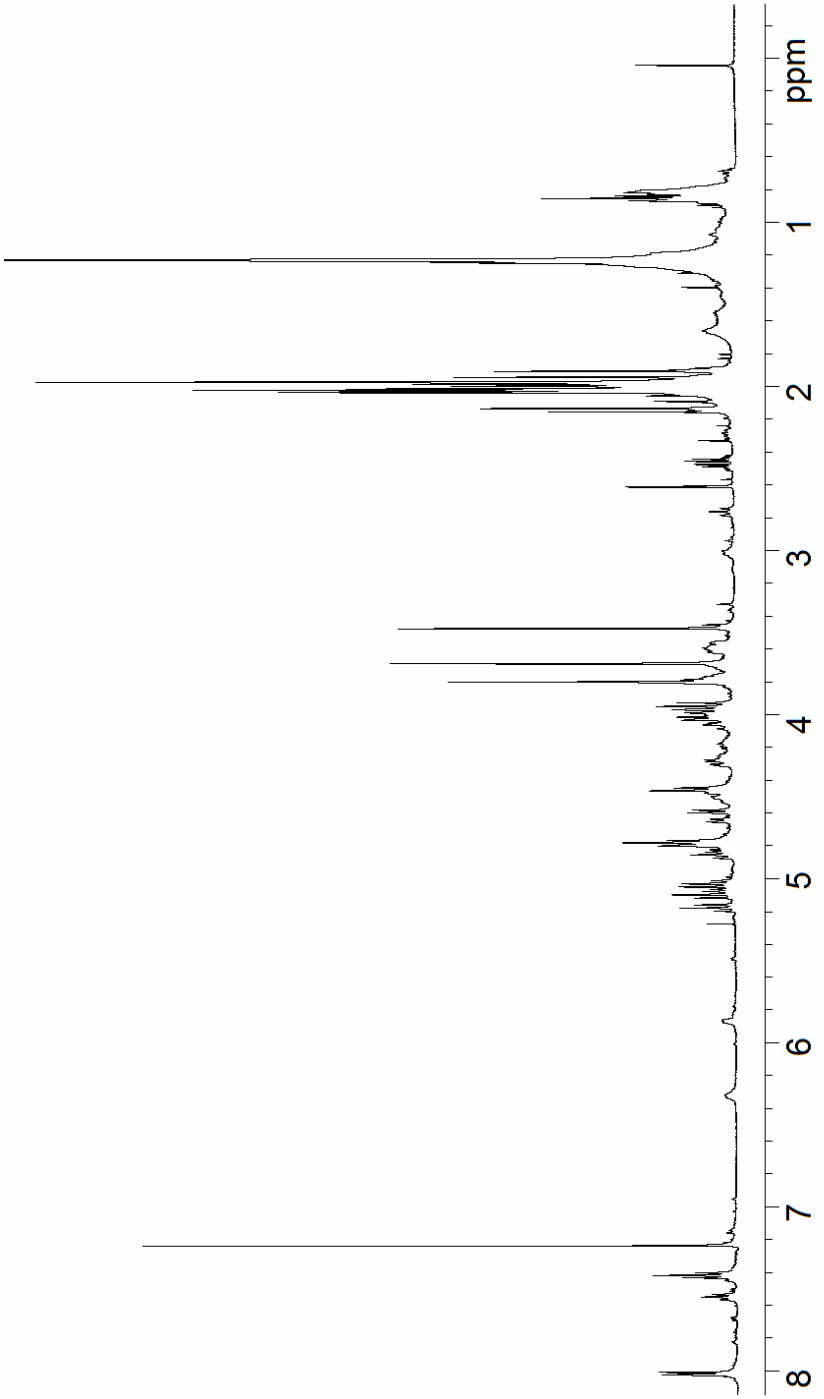

**Figure 4.65.** $^{13}$C-NMR of compound **64** (125 MHz, $CDCl_3$)

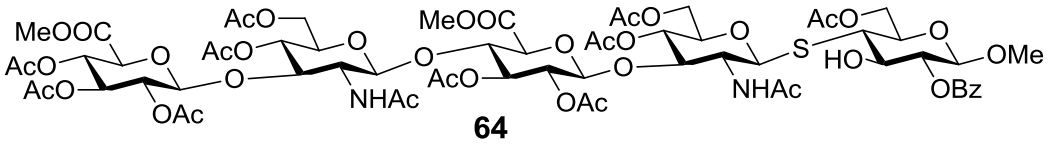


**64**

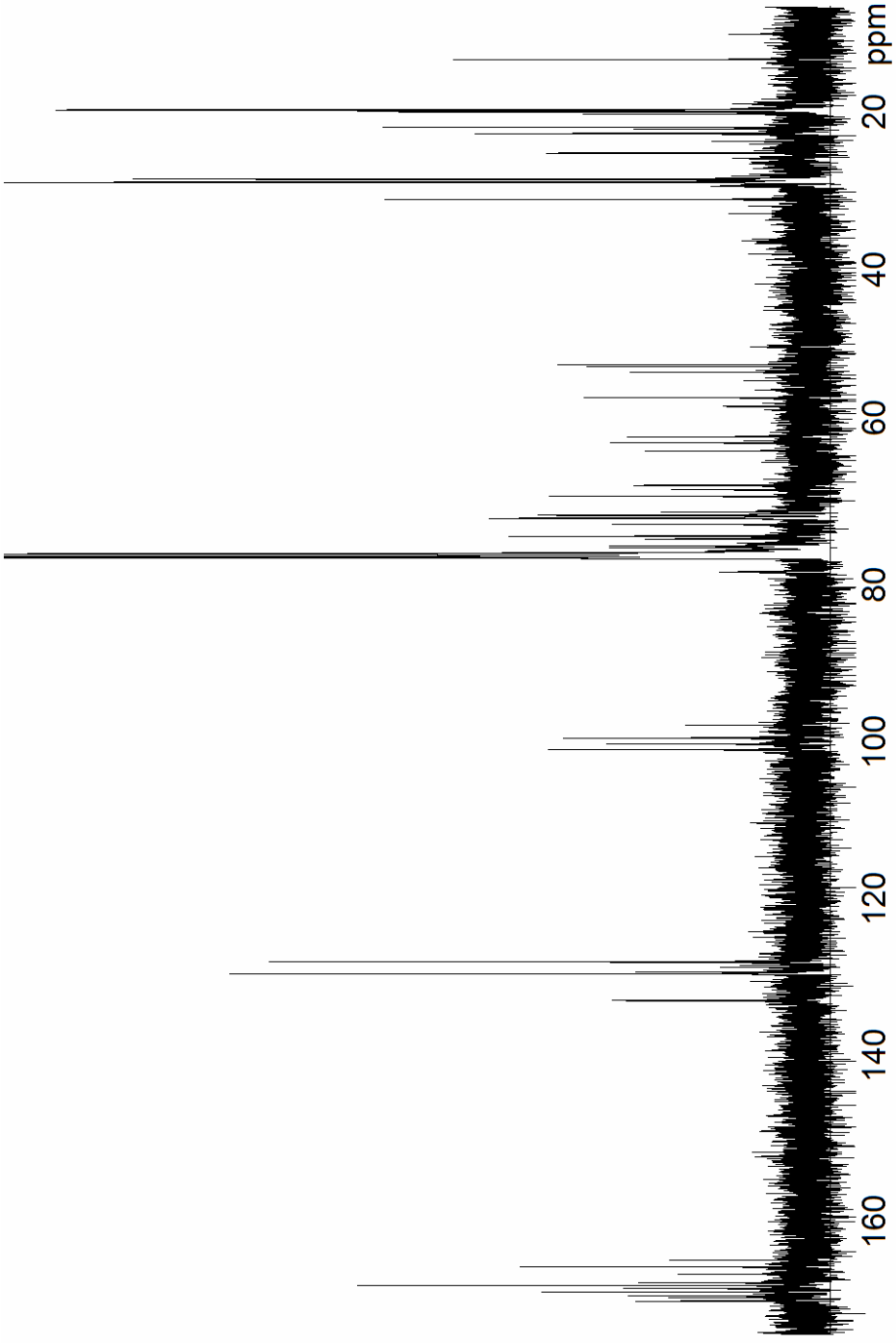

**Figure 4.66.** $^{1}H–^{1}H$ gCOSY of compound **64** (500 MHz, $CDCl_3$)

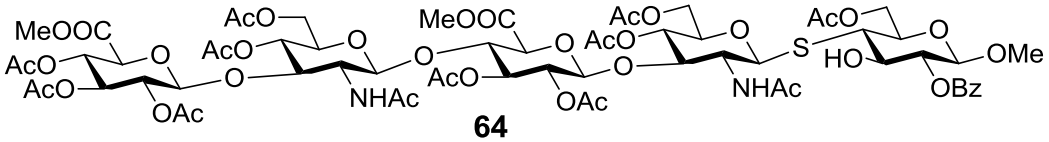


**64**

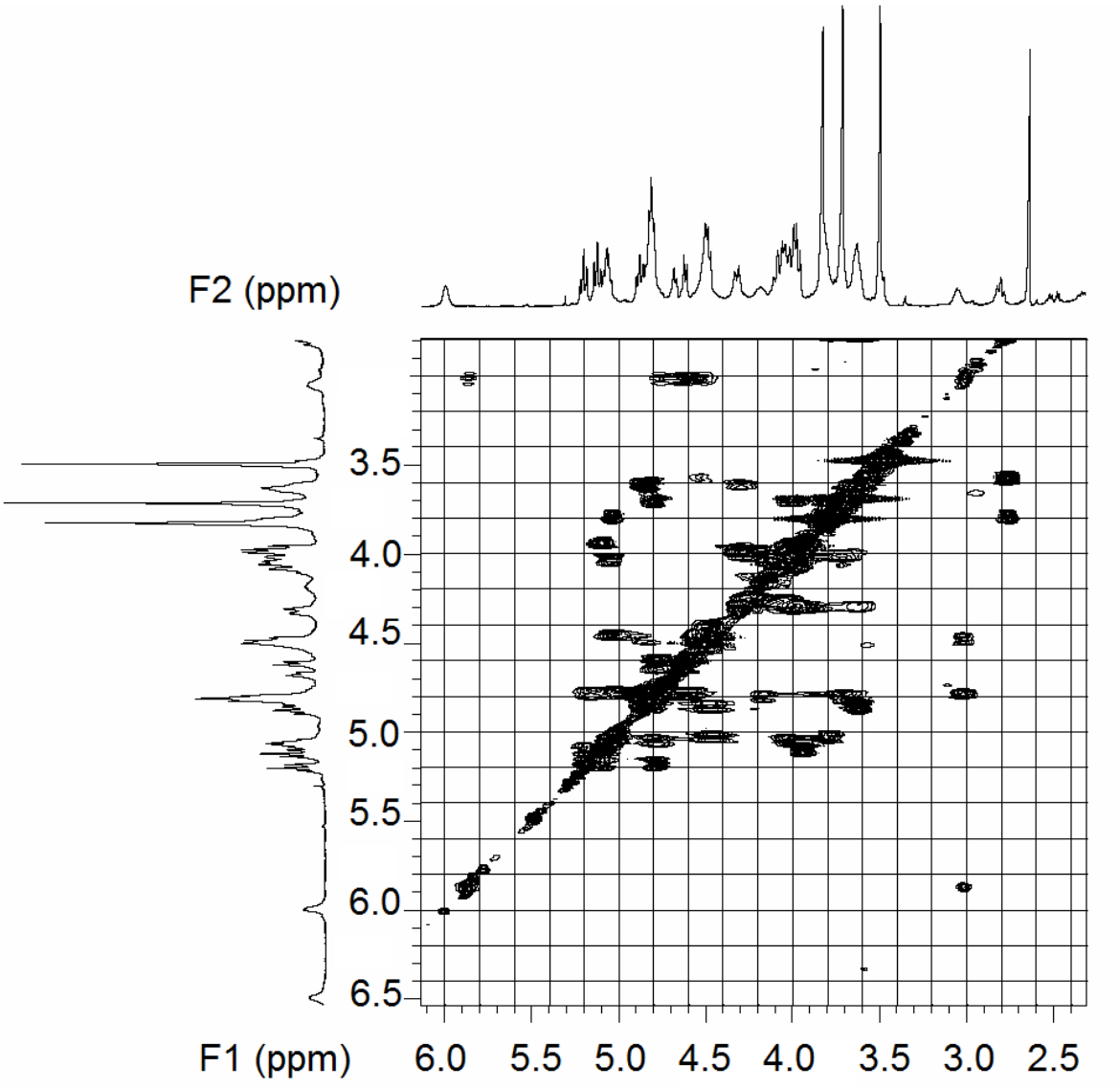

**Figure 4.67.** $^{1}H–^{13}C$ gHMQC (without $^{1}H$ decoupling) of compound **64** (500 MHz,$CDCl_3$)

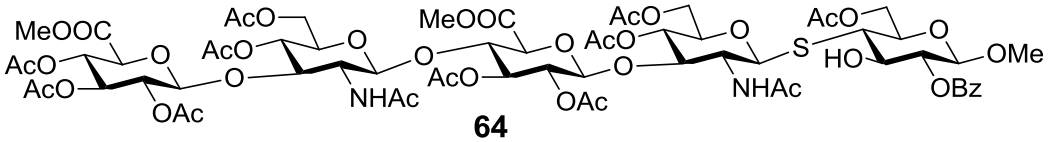


**64**

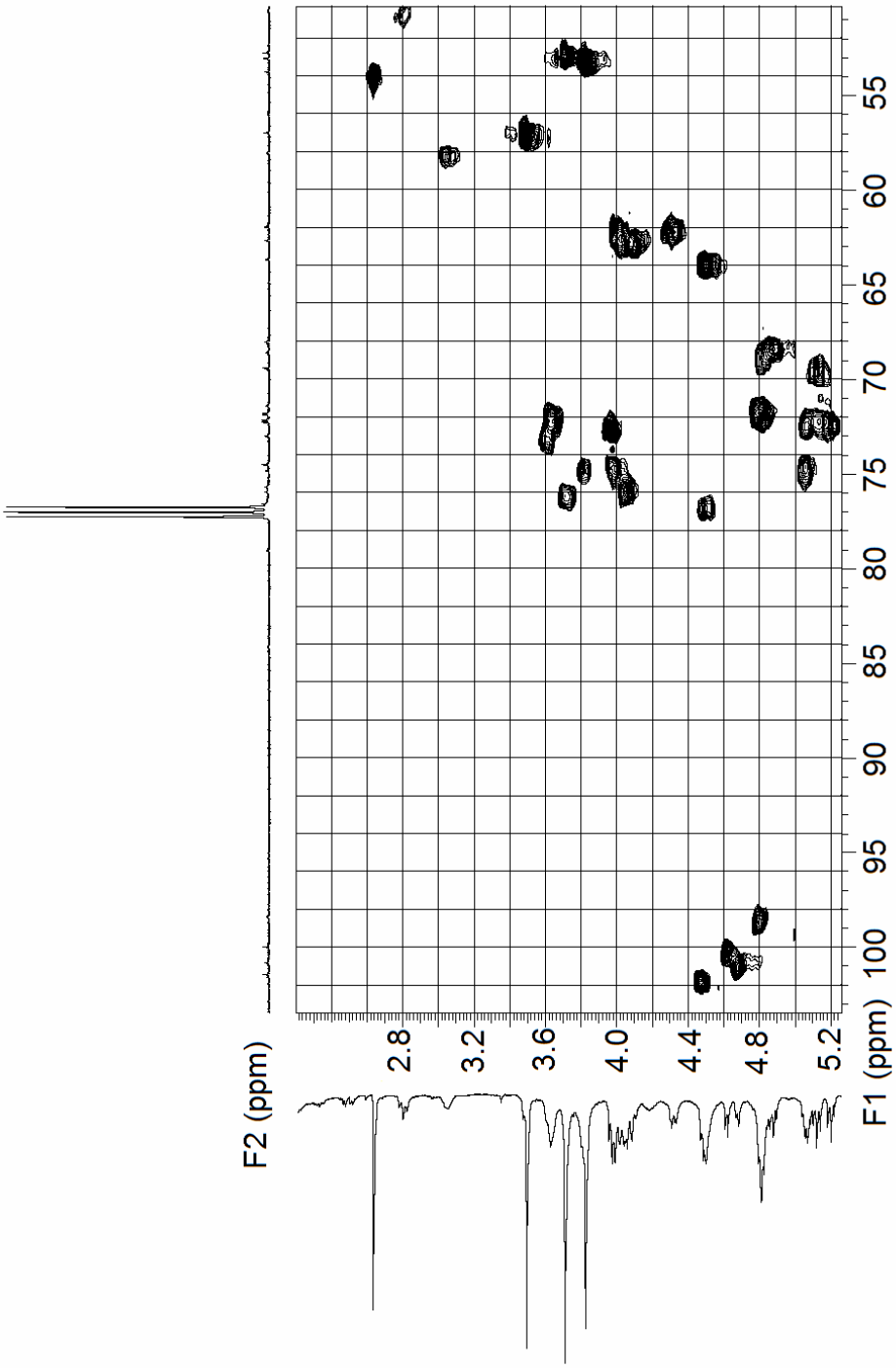

**Figure 4.68.** $^{1}$H-NMR of compound **49** (600 MHz, $D_2O$)

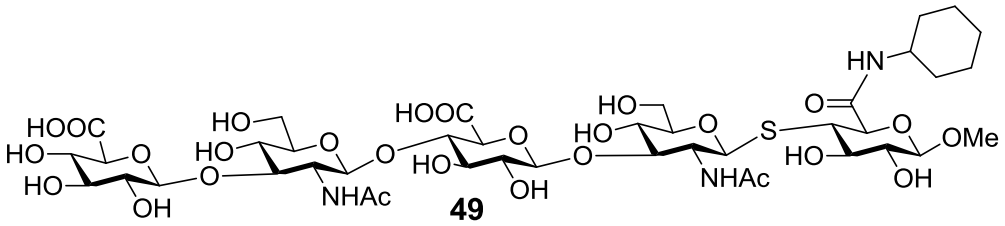


**49**

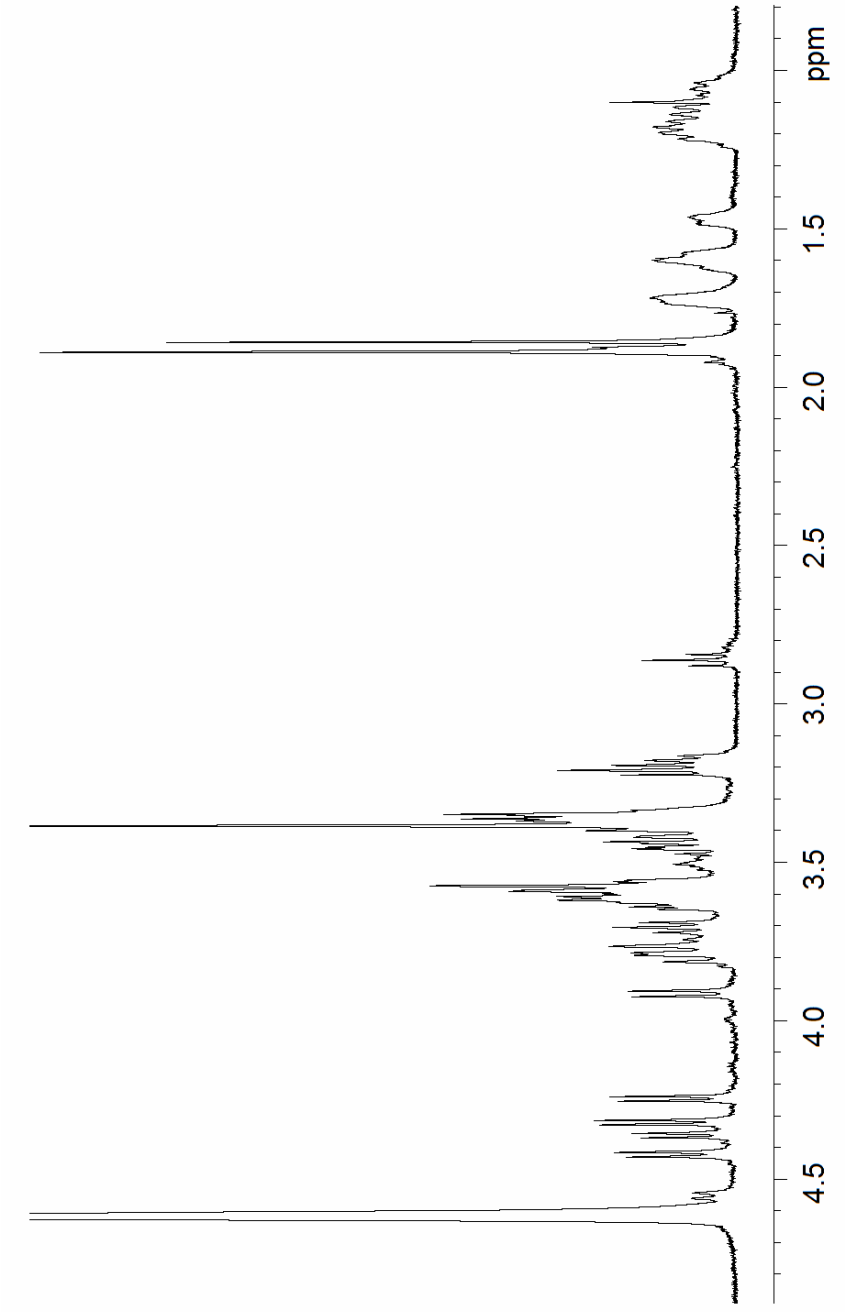

**Figure 4.69.** $^{1}H–^{1}H$ gCOSY of compound **49** (600 MHz, $D_2O$)

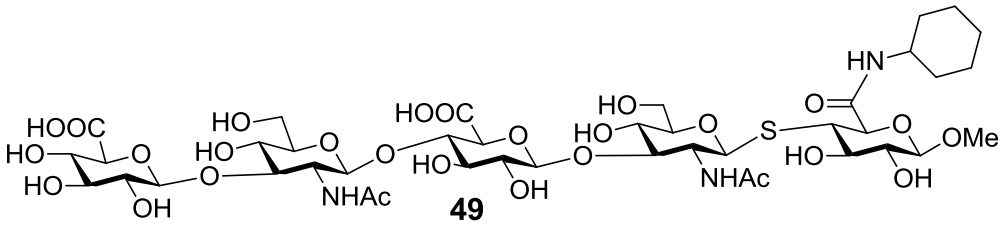


**49**

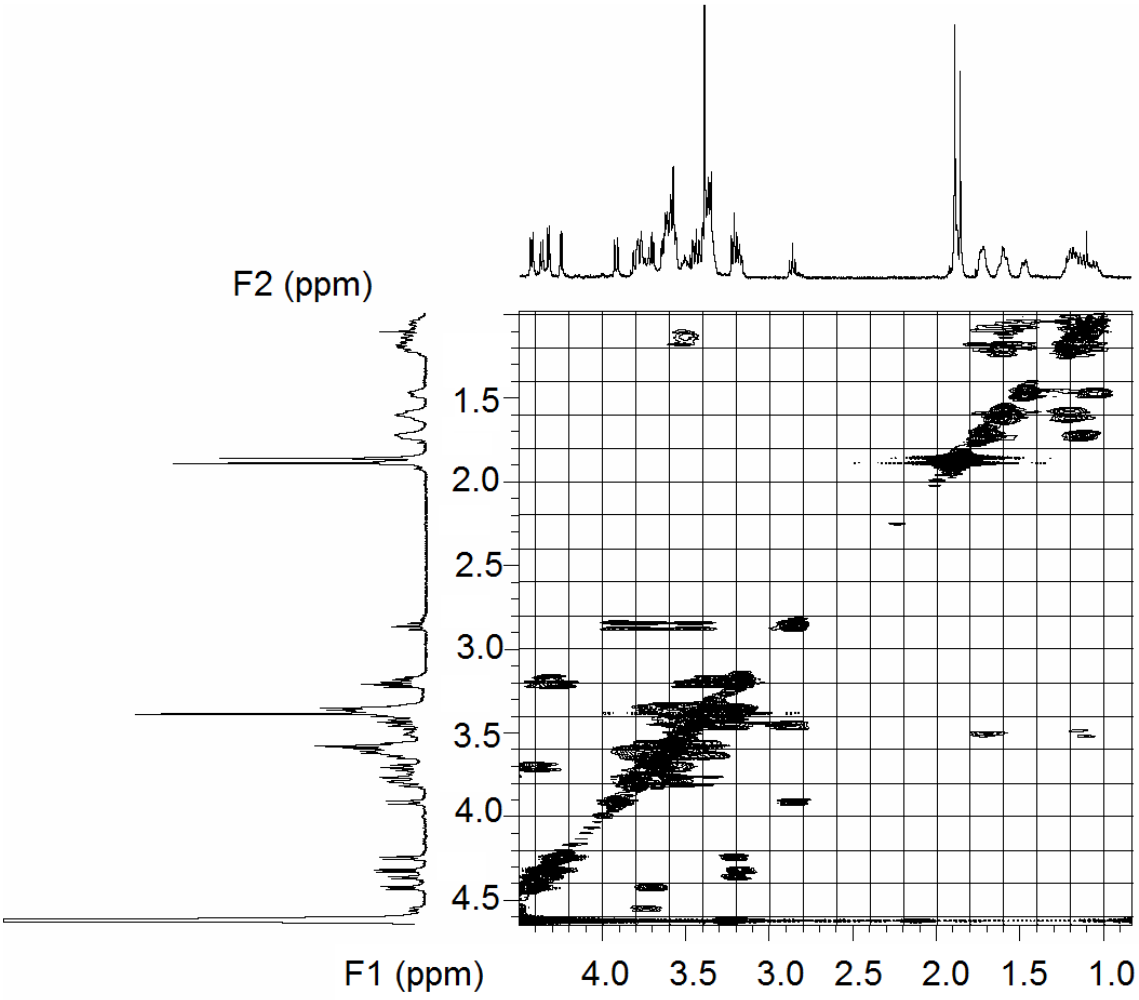

**Figure 4.70.** $^{1}$H-NMR of compound **50** (600 MHz, $D_2O$)

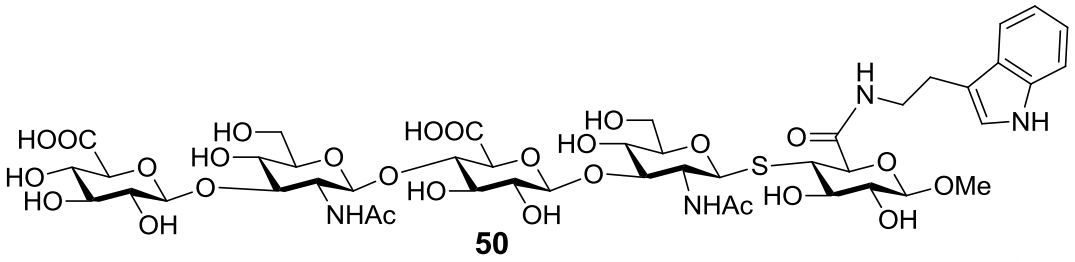


**50**

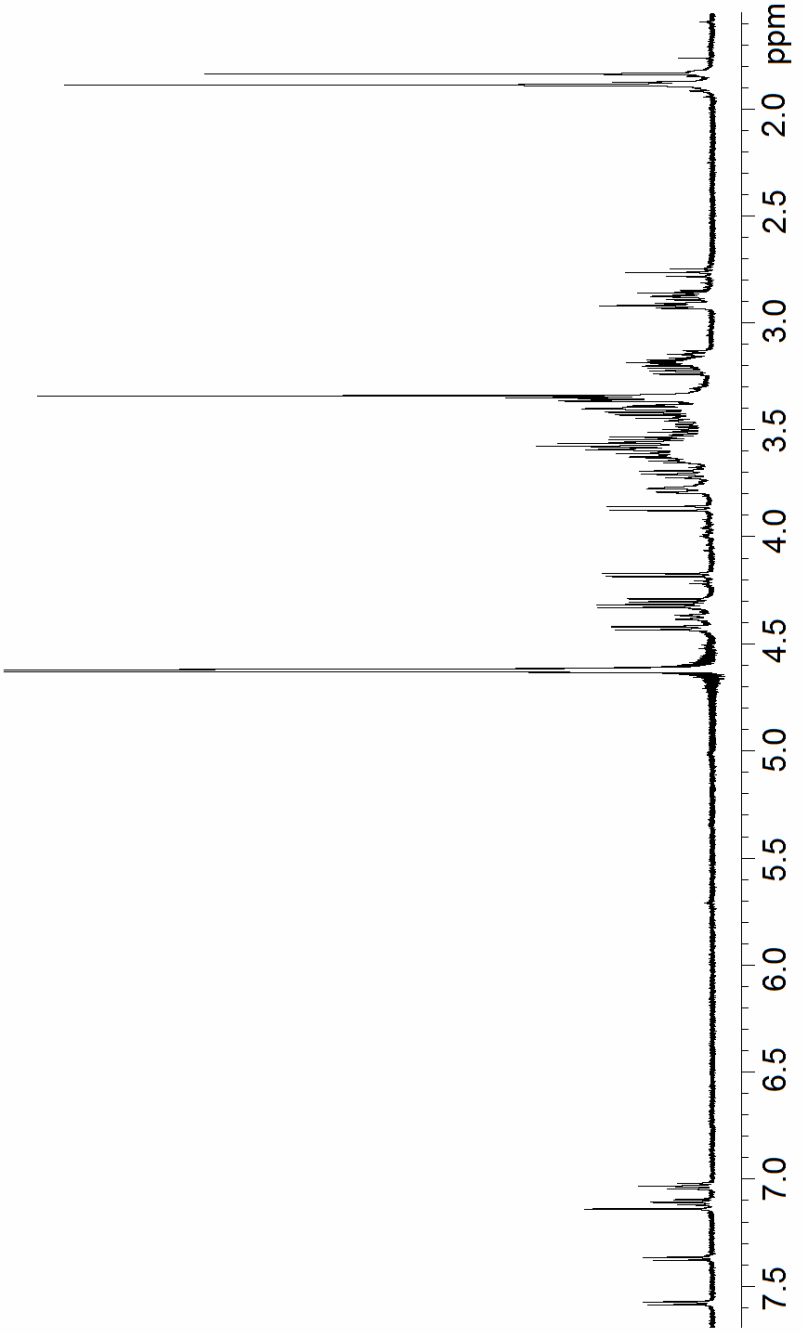

**Figure 4.71.** $^{1}H–^{1}H$ gCOSY of compound **50** (600 MHz, $D_2O$)

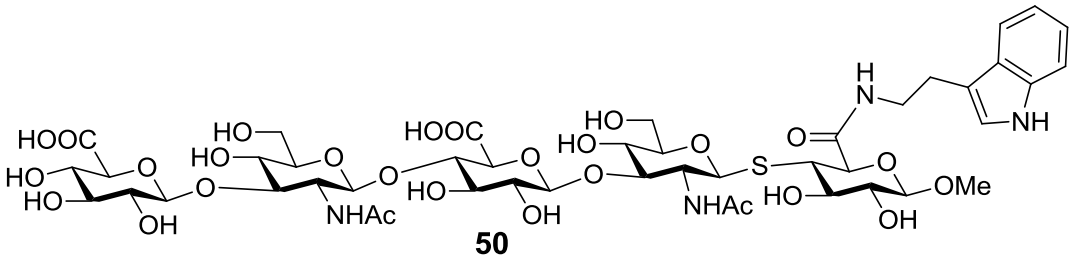


**50**

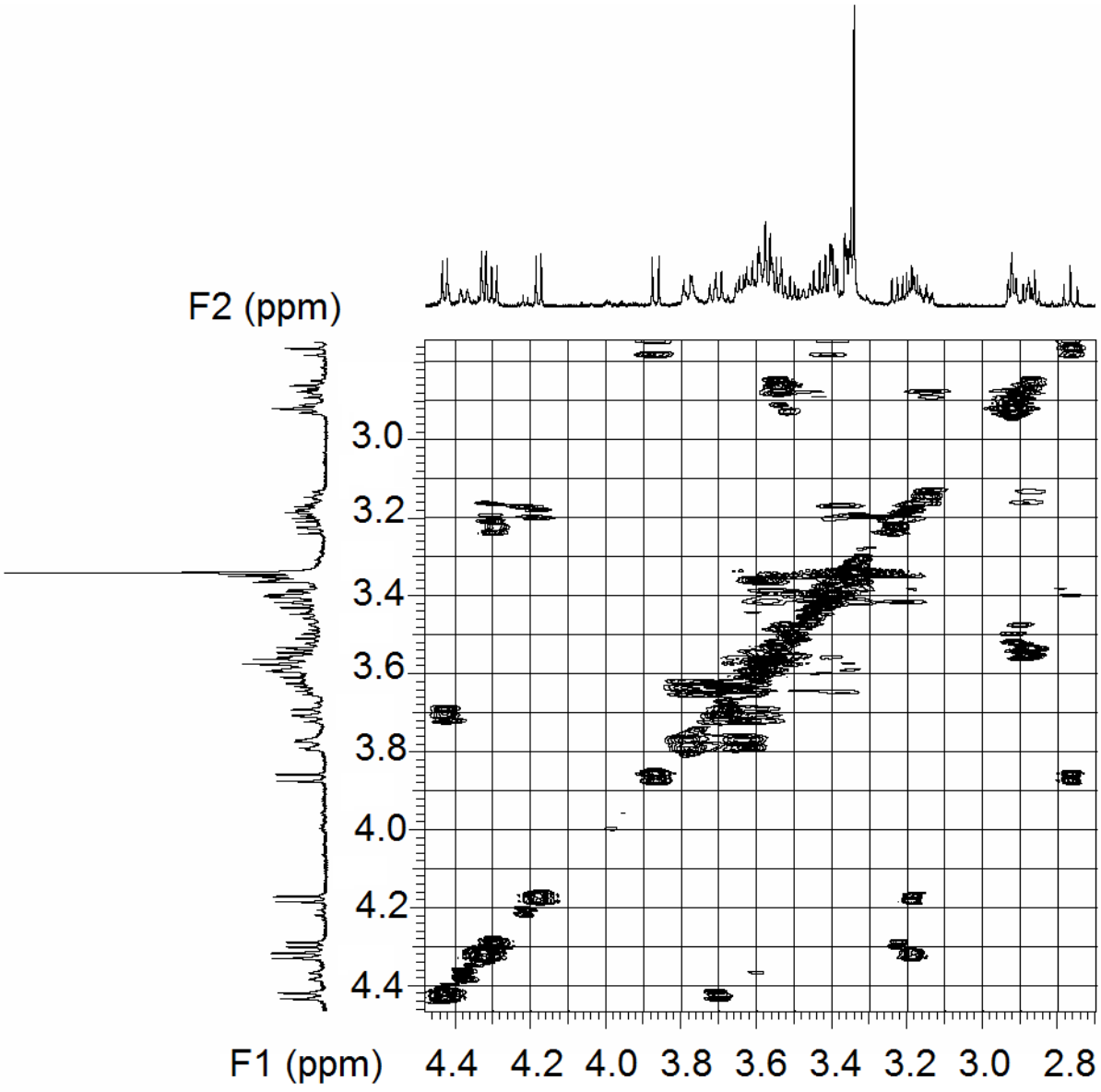

**Figure 4.72.** $^{1}$H-NMR of compound **51**(600 MHz, $D_2O$)

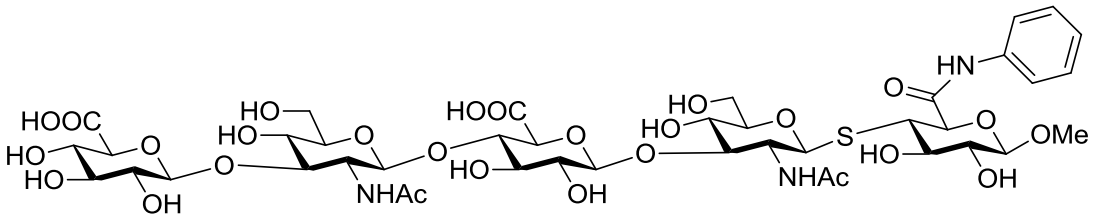


**51**

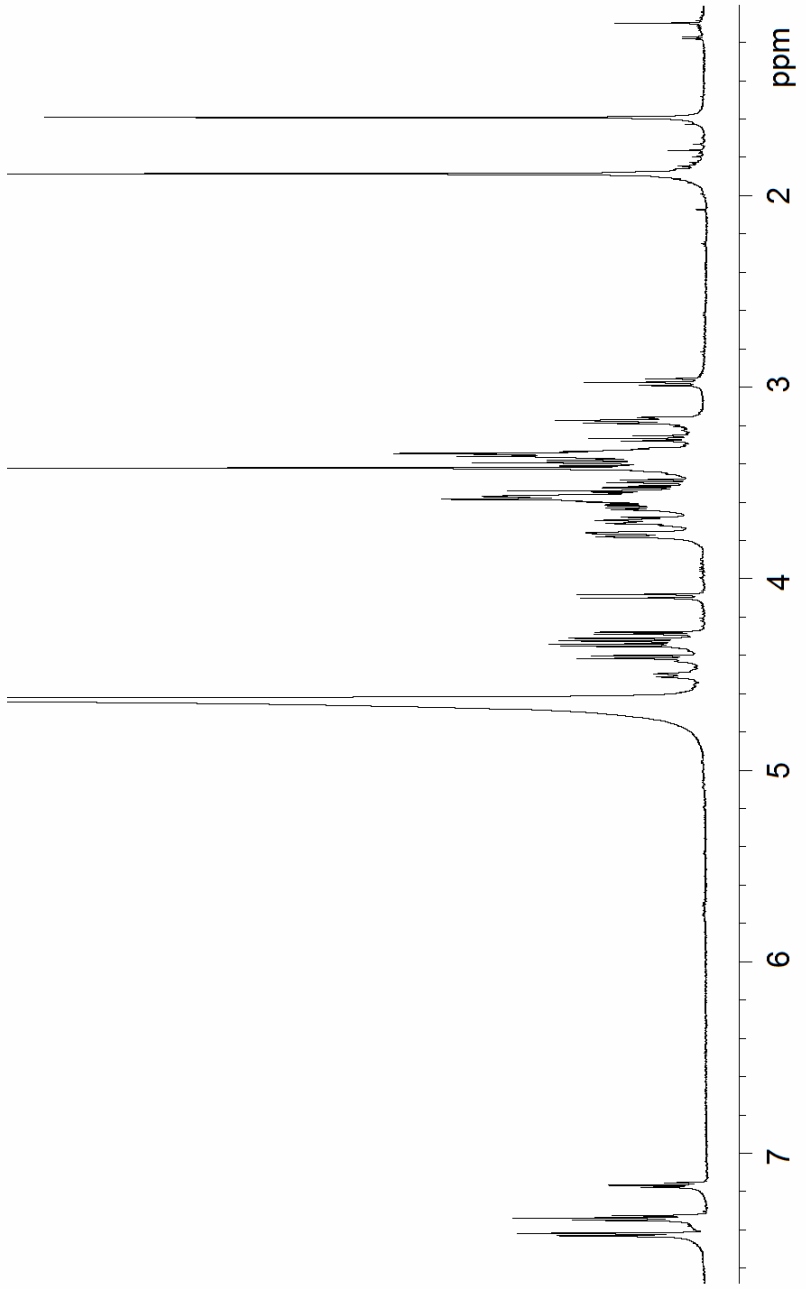

**Figure 4.73.** $^{1}H$–$^{1}H$ gCOSY of compound **51** (600 MHz, $D_2O$)

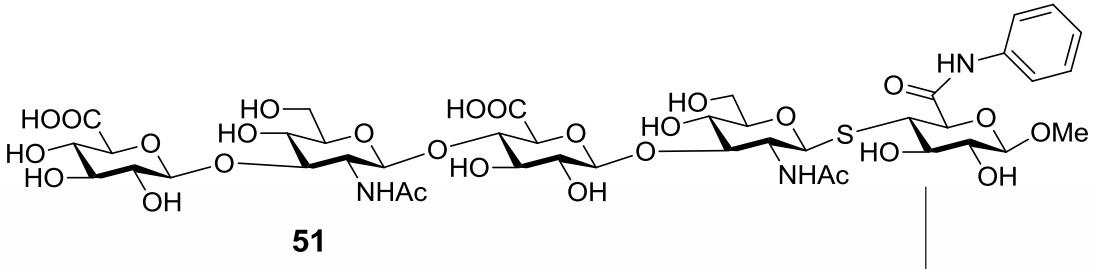


**51**

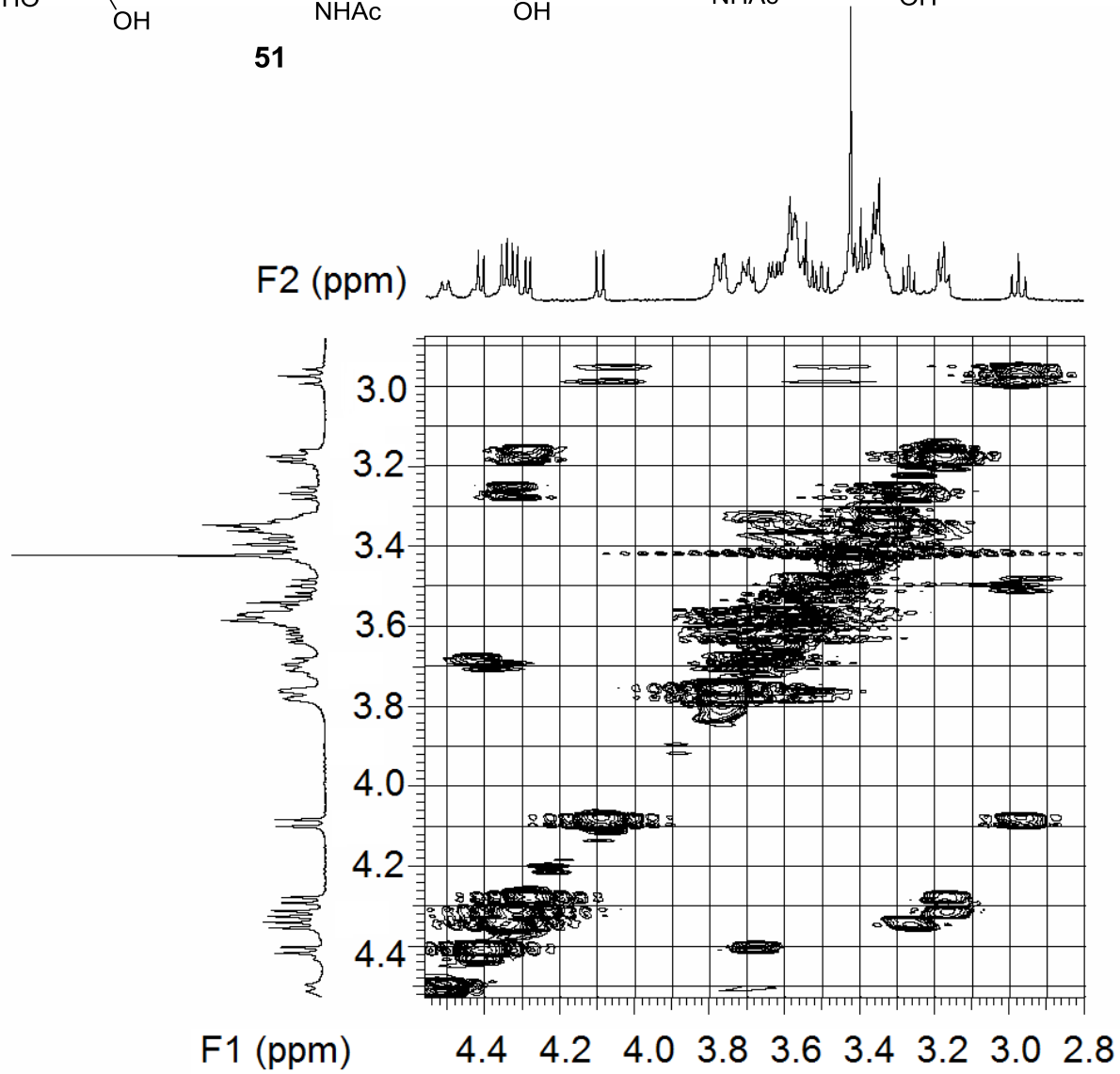

**Figure 4.74.** $^{1}$H-NMR of compound **52** (600 MHz, $D_2O$)

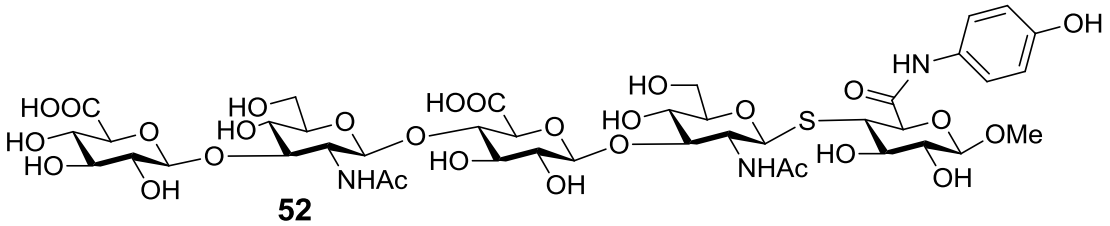


**52**

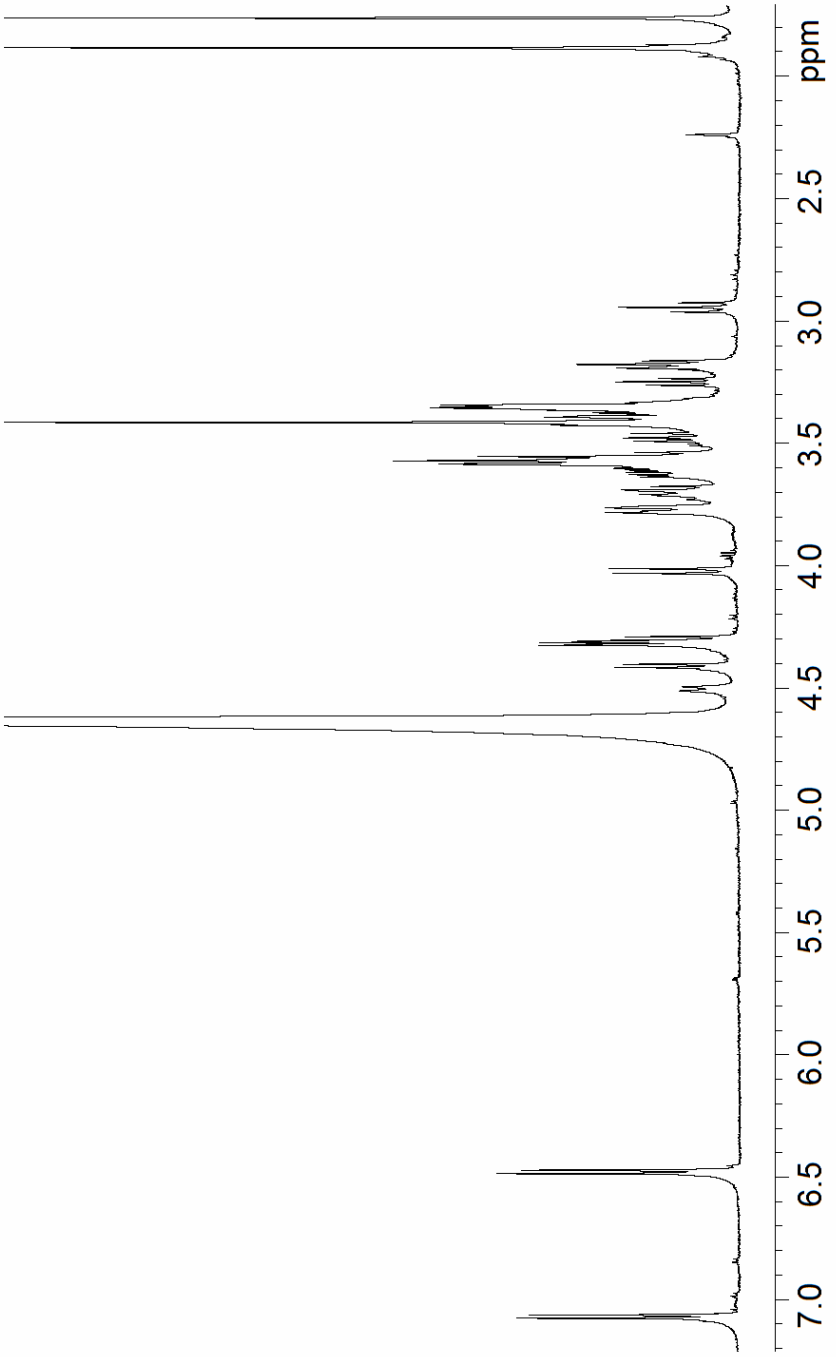

**Figure 4.75.** $^{1}H$–$^{1}H$ gCOSY of compound **52** (600 MHz, $D_2O$)

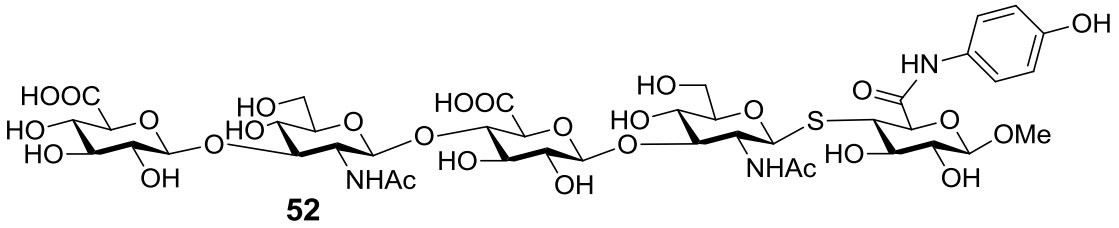


**52**

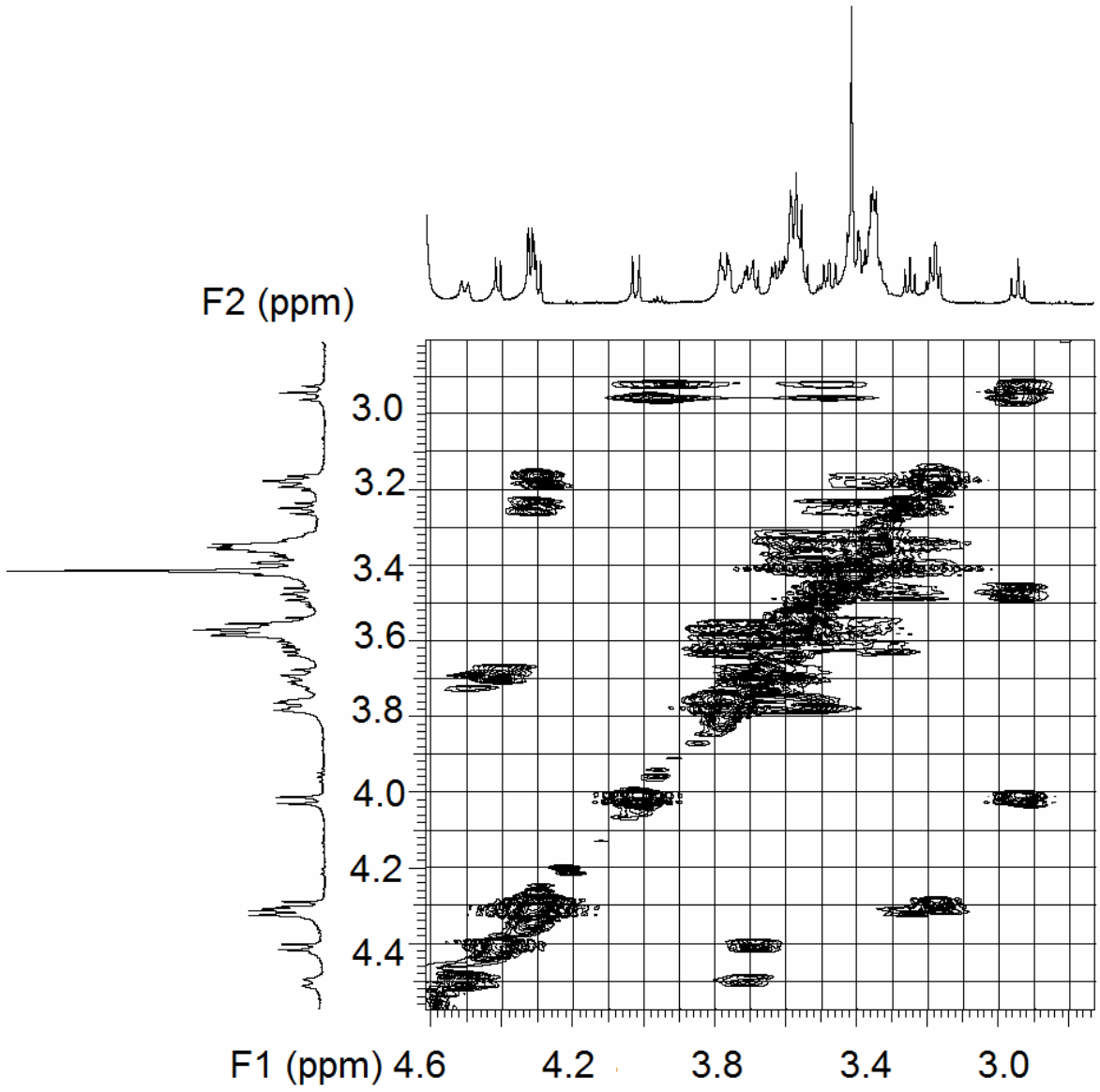

**Figure 4.76.** $^{1}$H-NMR of compound **53** (600 MHz, $D_2O$)

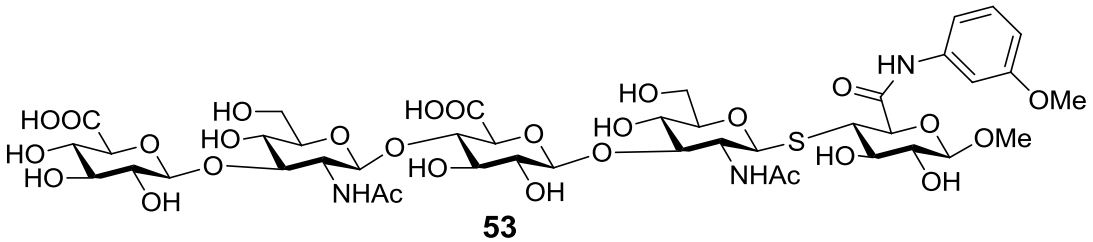


**53**

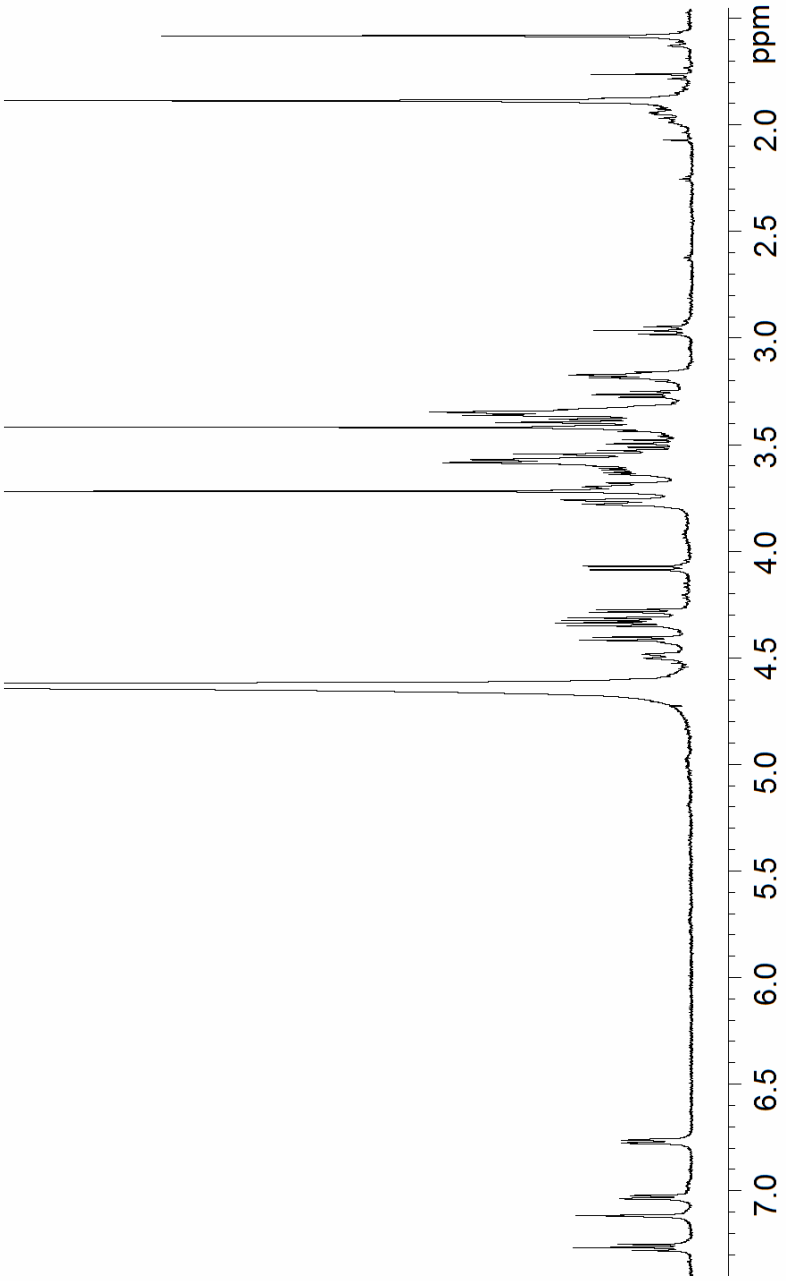

**Figure 4.77.** $^{1}H–^{1}H$ gCOSY of compound **53** (600 MHz, $D_2O$)

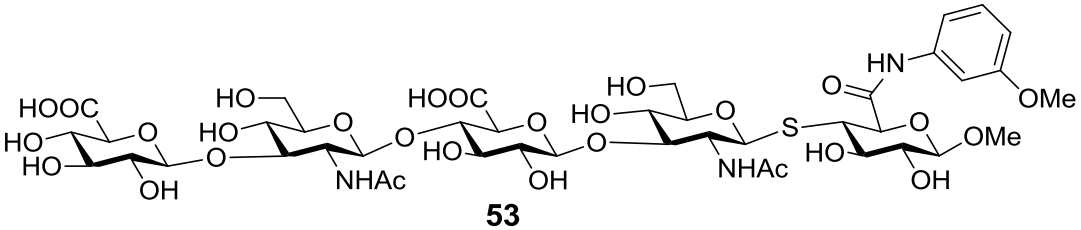


**53**

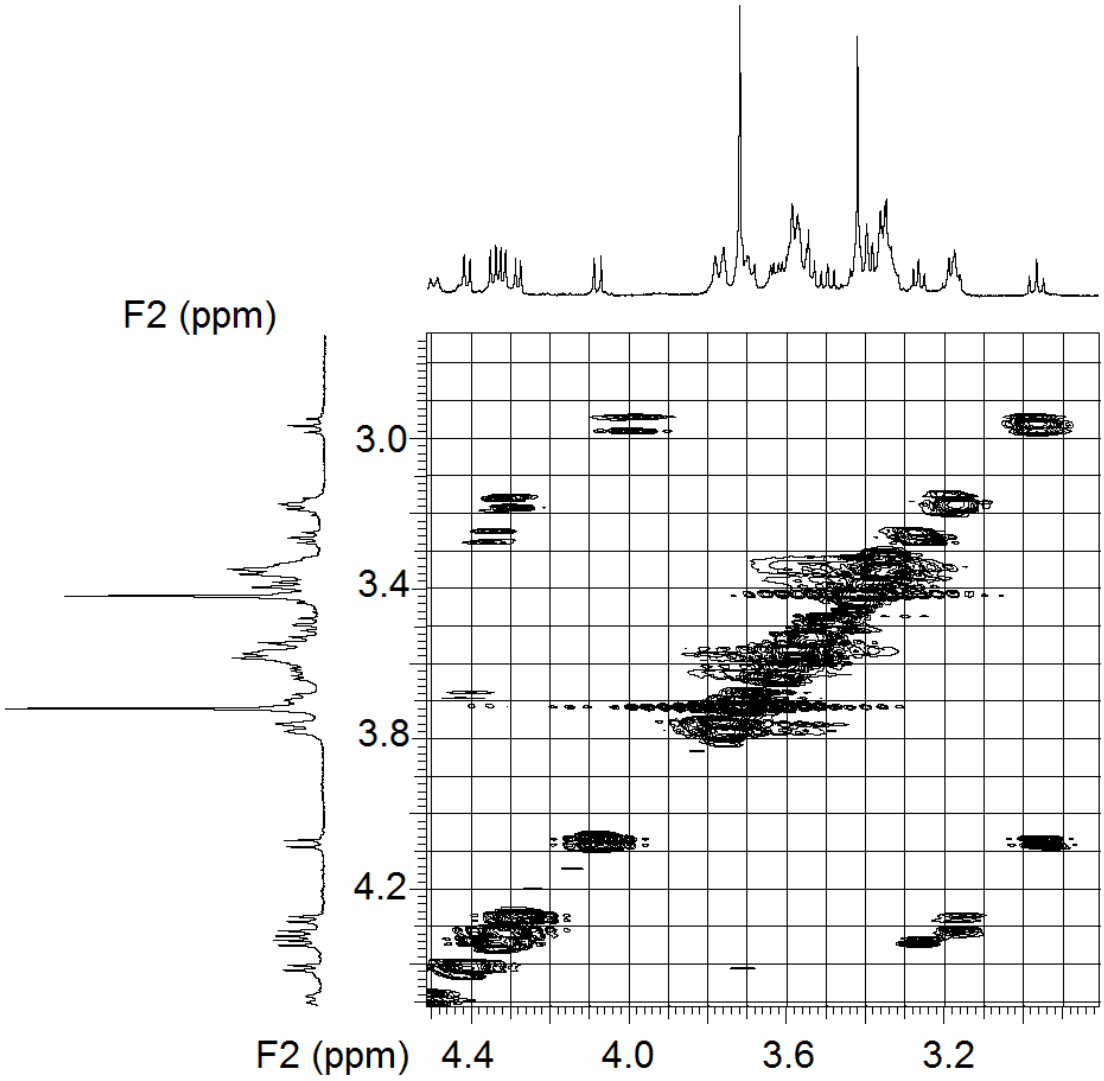

**Figure 4.78.** $^{1}$H-NMR of compound **54** (600 MHz, $D_2O$)

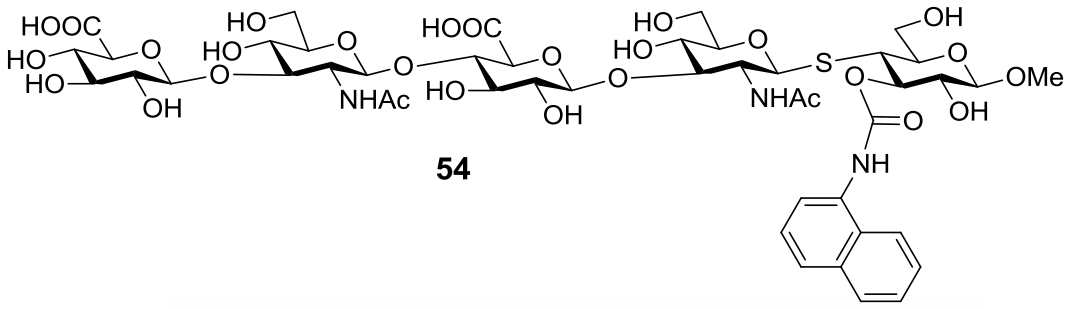


**54**

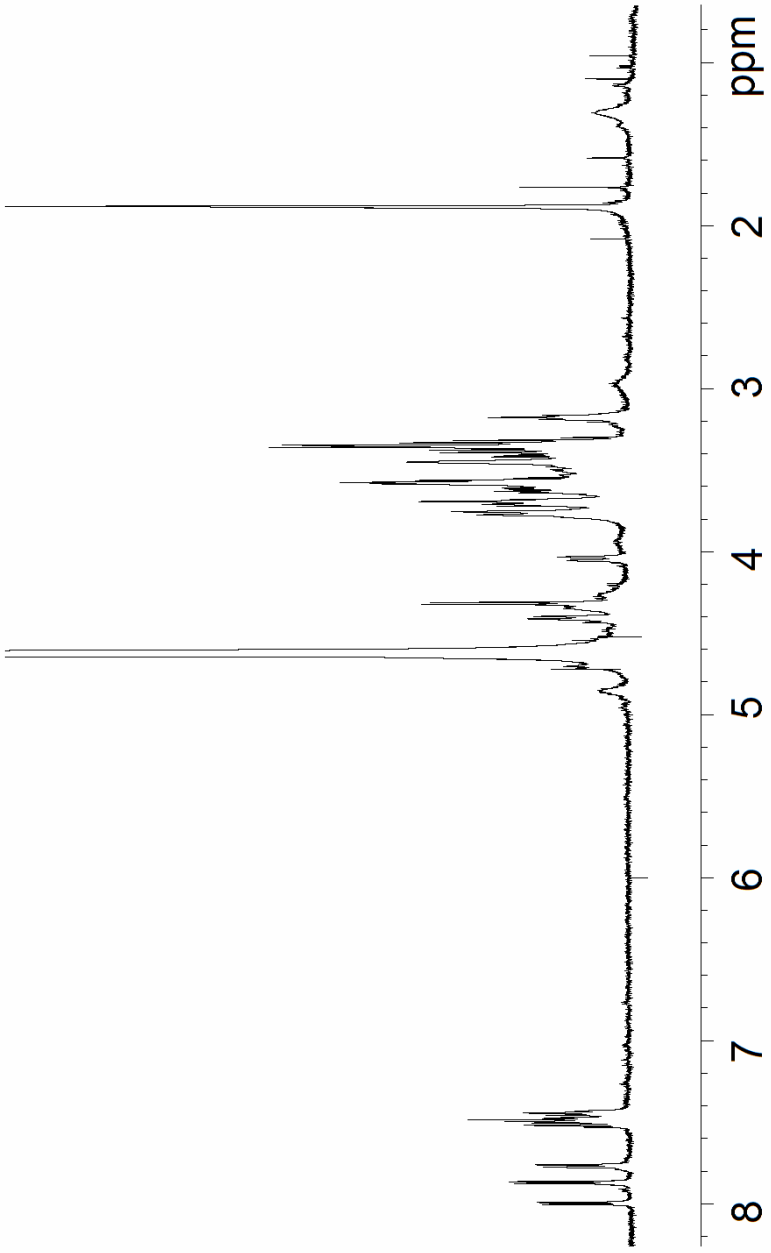

**Figure 4.79.** $^{1}H–^{1}H$ gCOSY of compound **54** (600 MHz, $D_2O$)

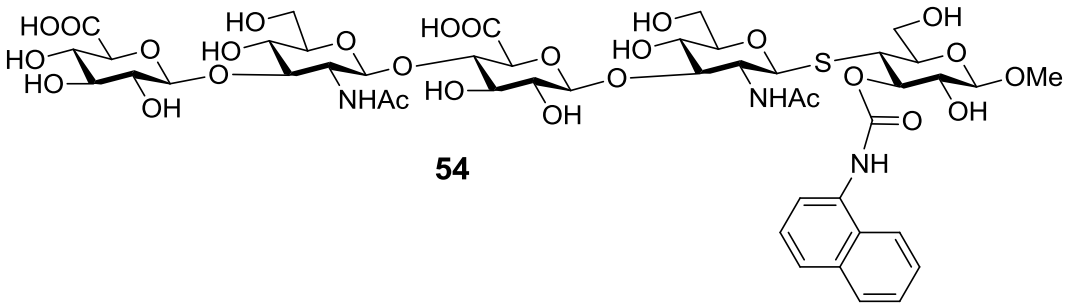


**54**

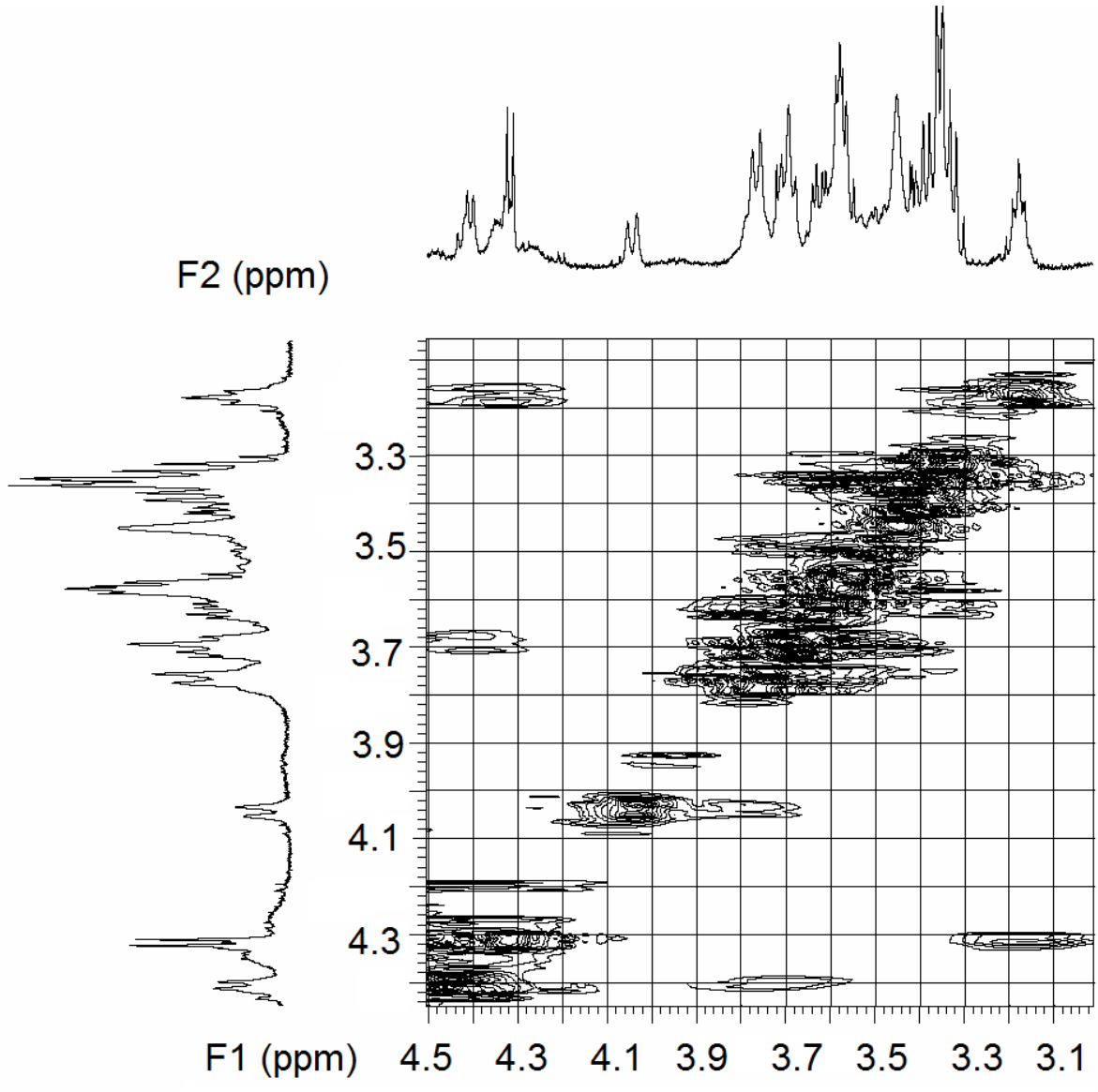

**Figure 4.80.** $^{1}$H-NMR of compound **55** (600 MHz, $D_2O$)

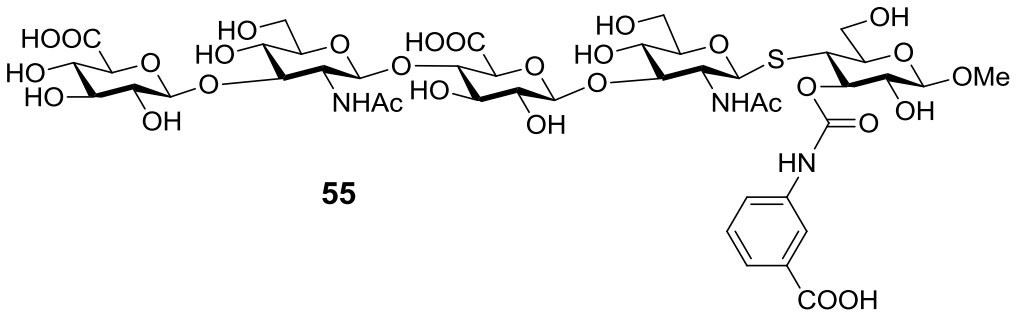


**55**

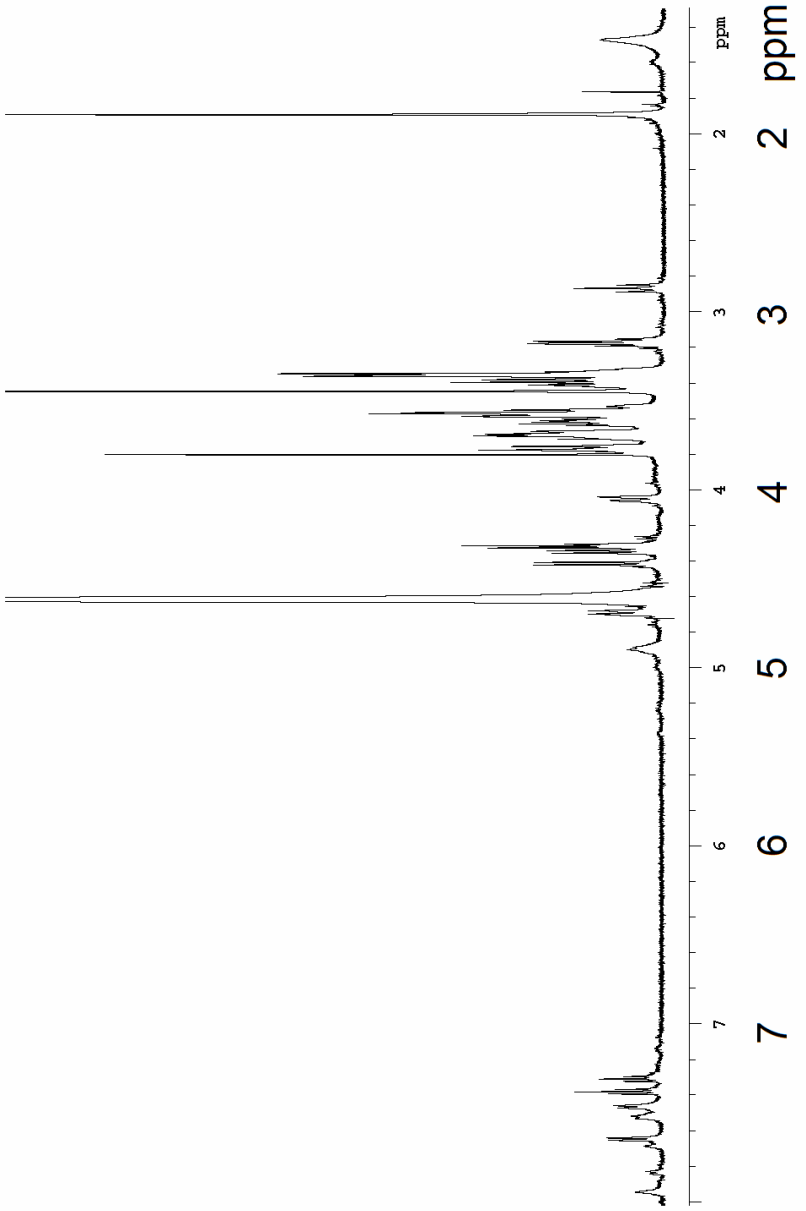

**Figure 4.81.** $^{1}H–^{1}H$ gCOSY of compound **55** (600 MHz, $D_2O$)

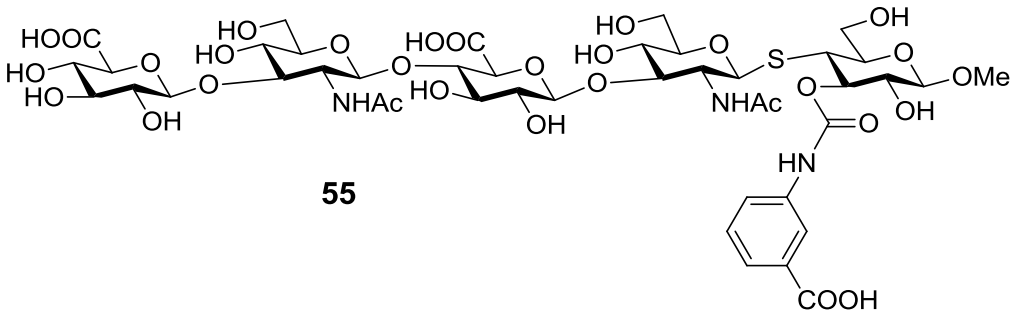


**55**

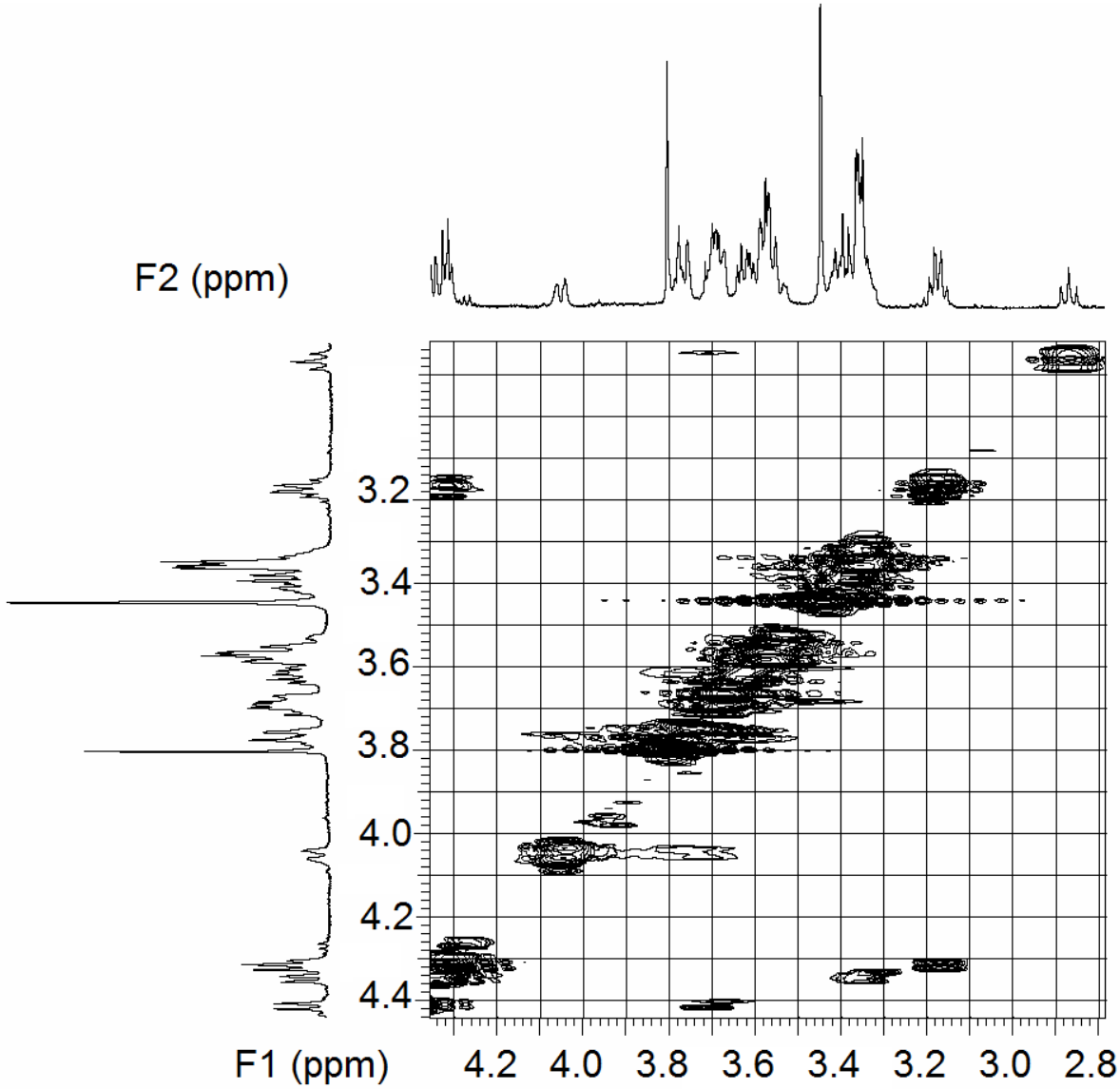

**Figure 4.82.** $^{1}$H-NMR of compound **56** (600 MHz, $D_2O$)

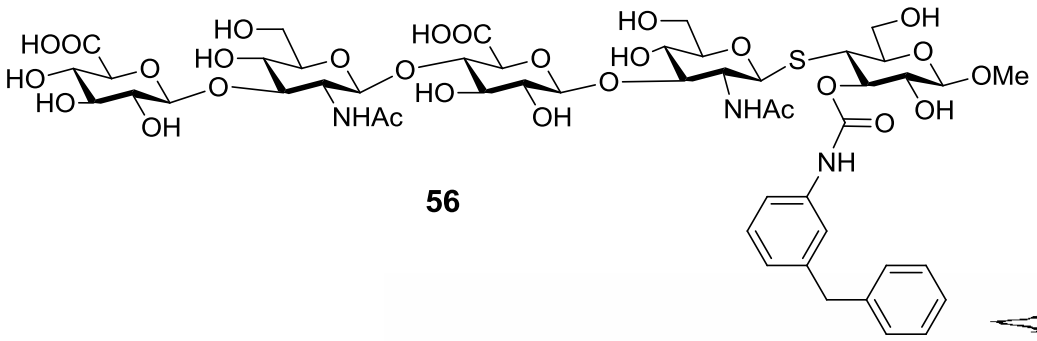


**56**

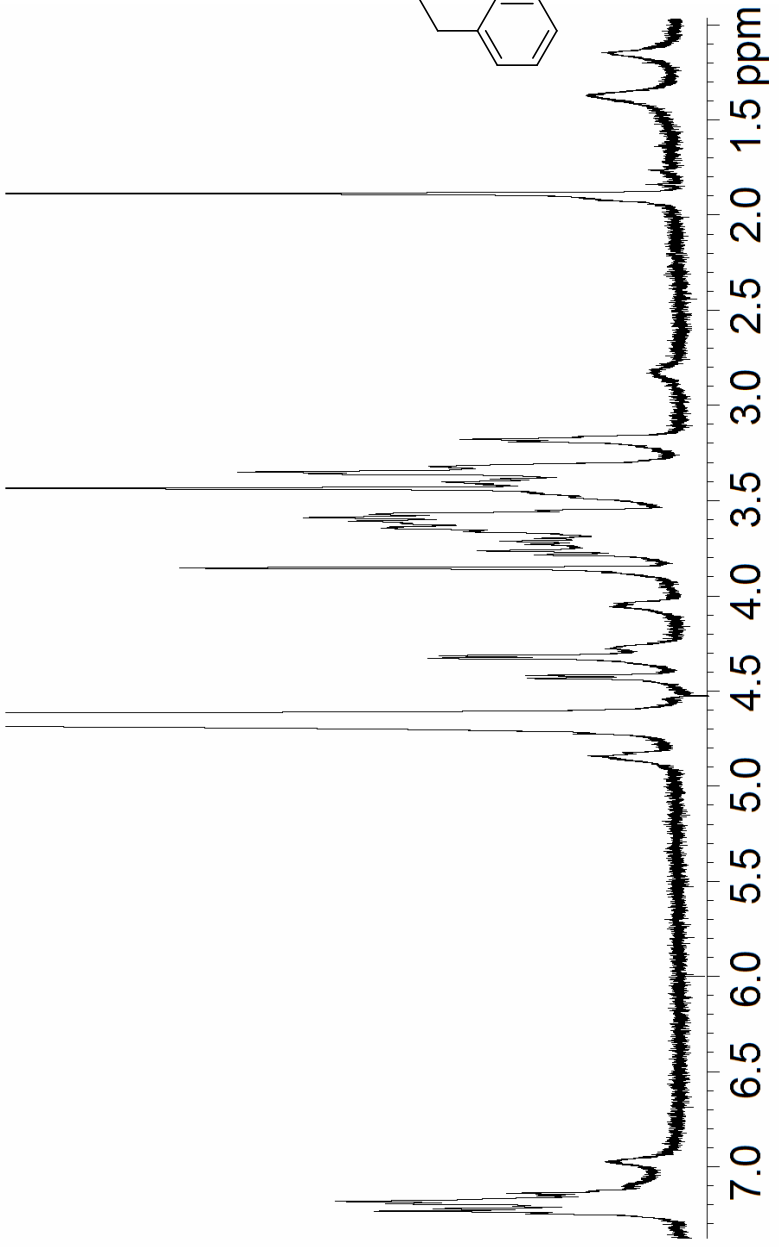

**Figure 4.83.** $^{1}H–^{1}H$ gCOSY of compound **56** (600 MHz, $D_2O$)

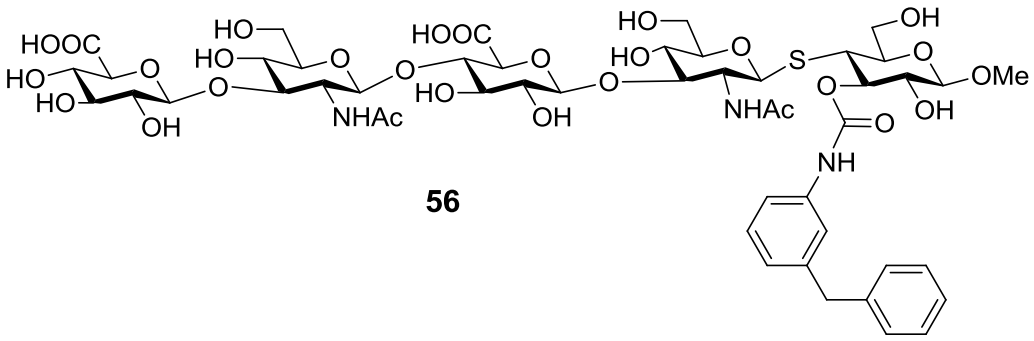


**56**

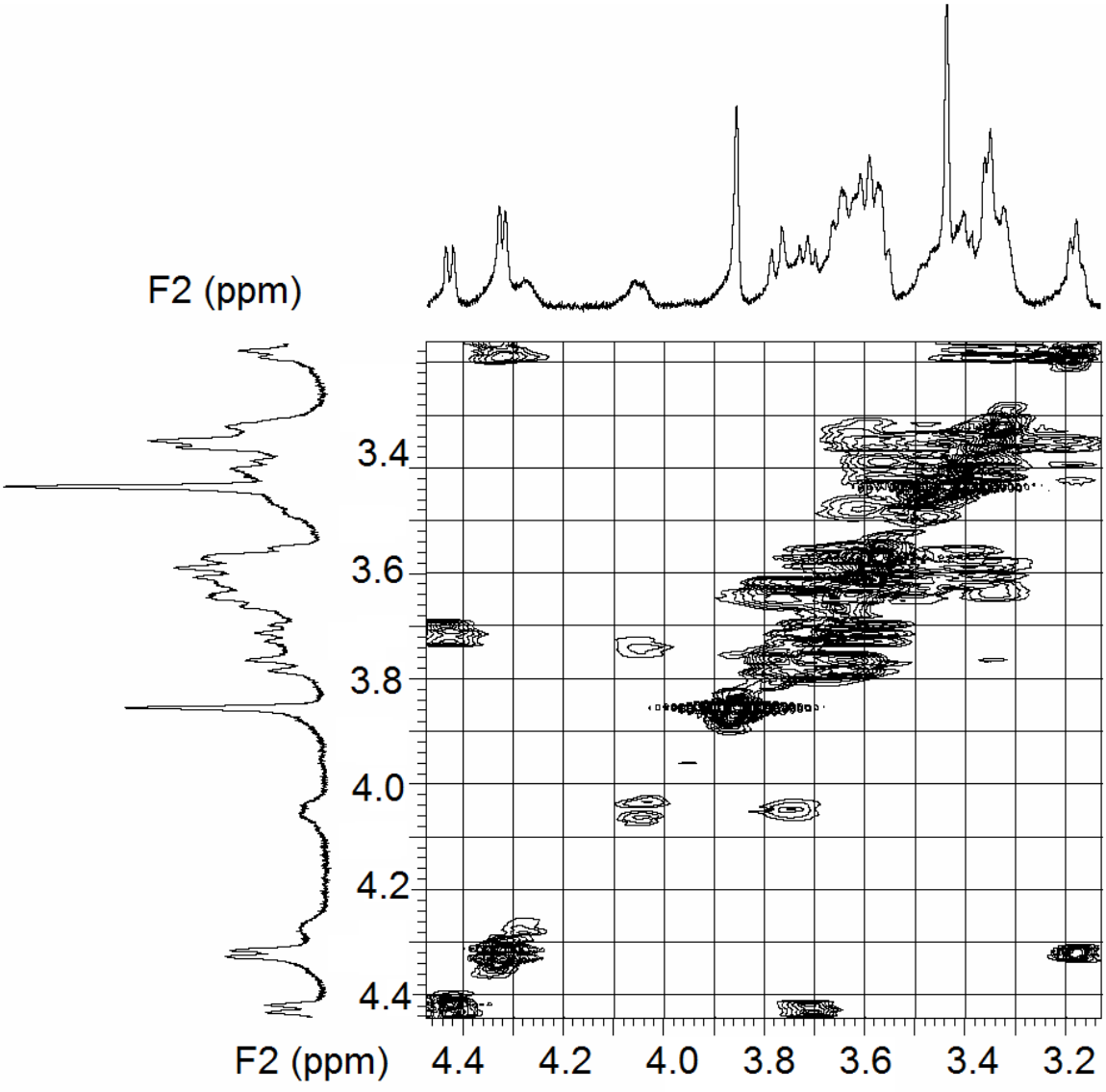

**Figure 4.84.** $^{1}$H-NMR of compound **57** (600 MHz, $D_2O$)

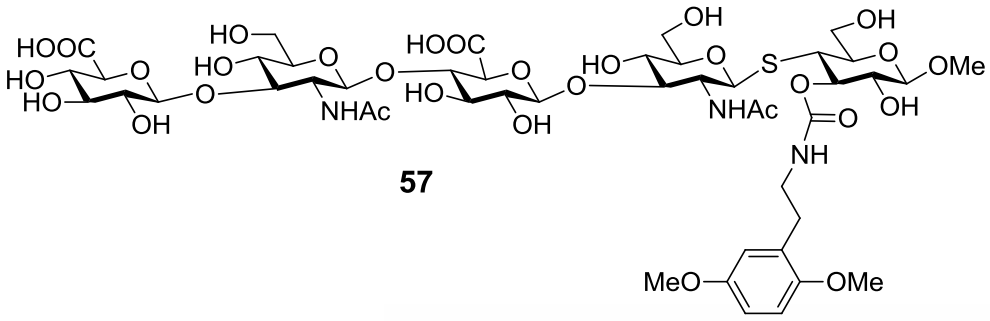


**57**

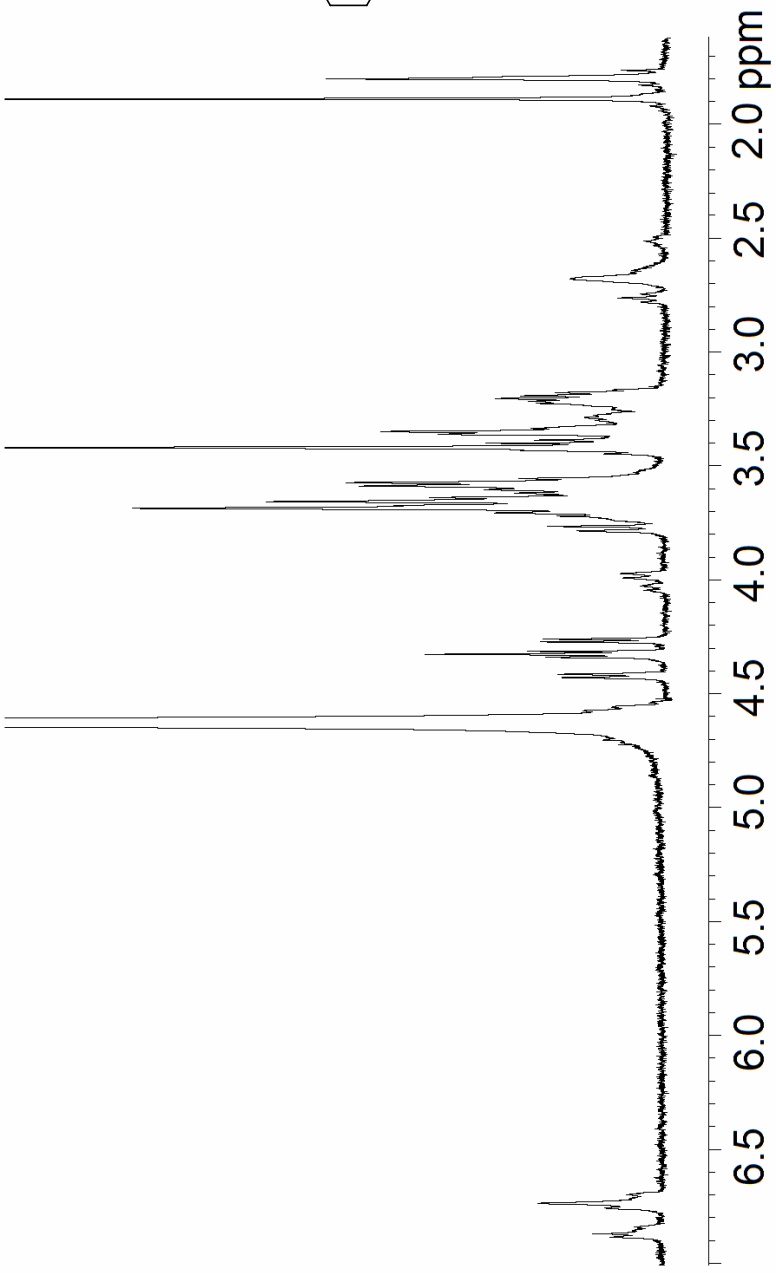

**Figure 4.85** $^{1}H–^{1}H$ gCOSY of compound **57** (600 MHz, $D_2O$)

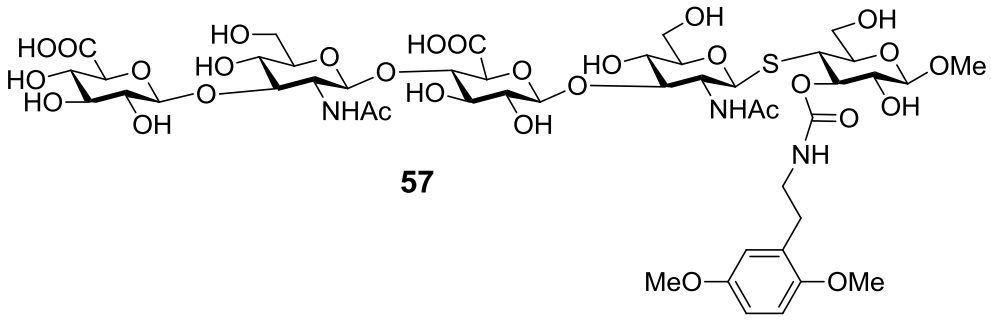


**57**

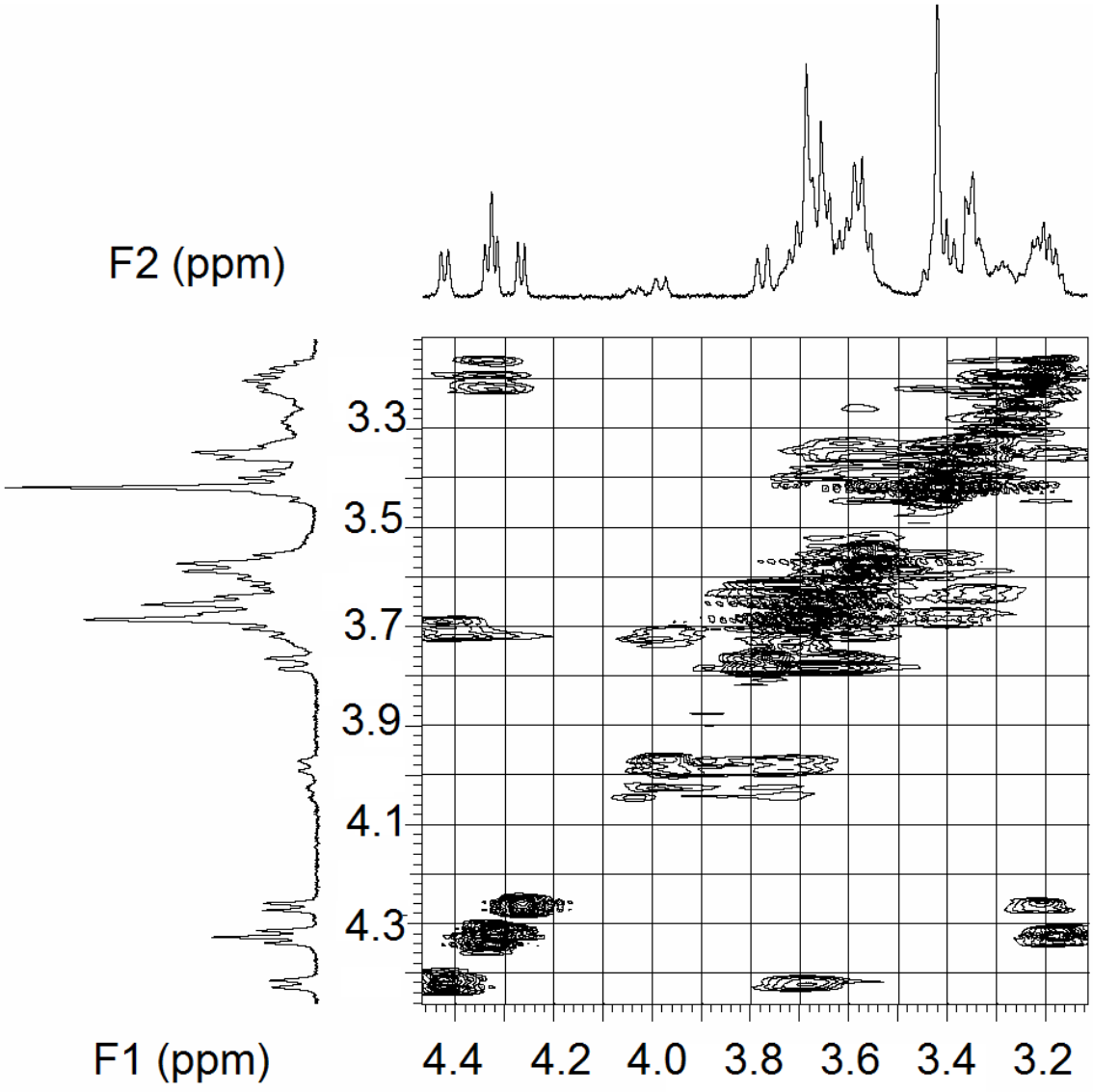

**Figure 4.86.** $^{1}$H-NMR of compound **58** (600 MHz, $D_2O$)

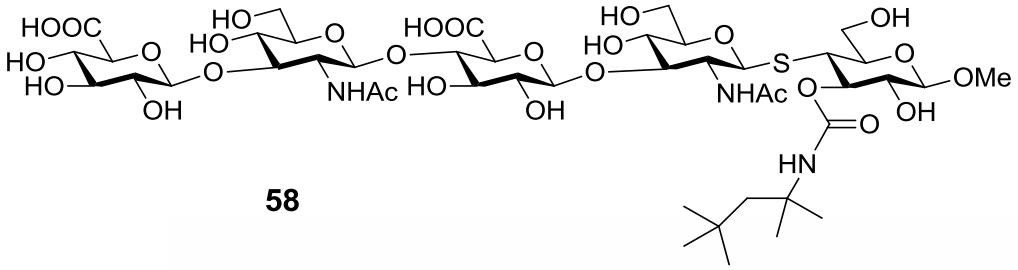


**58**

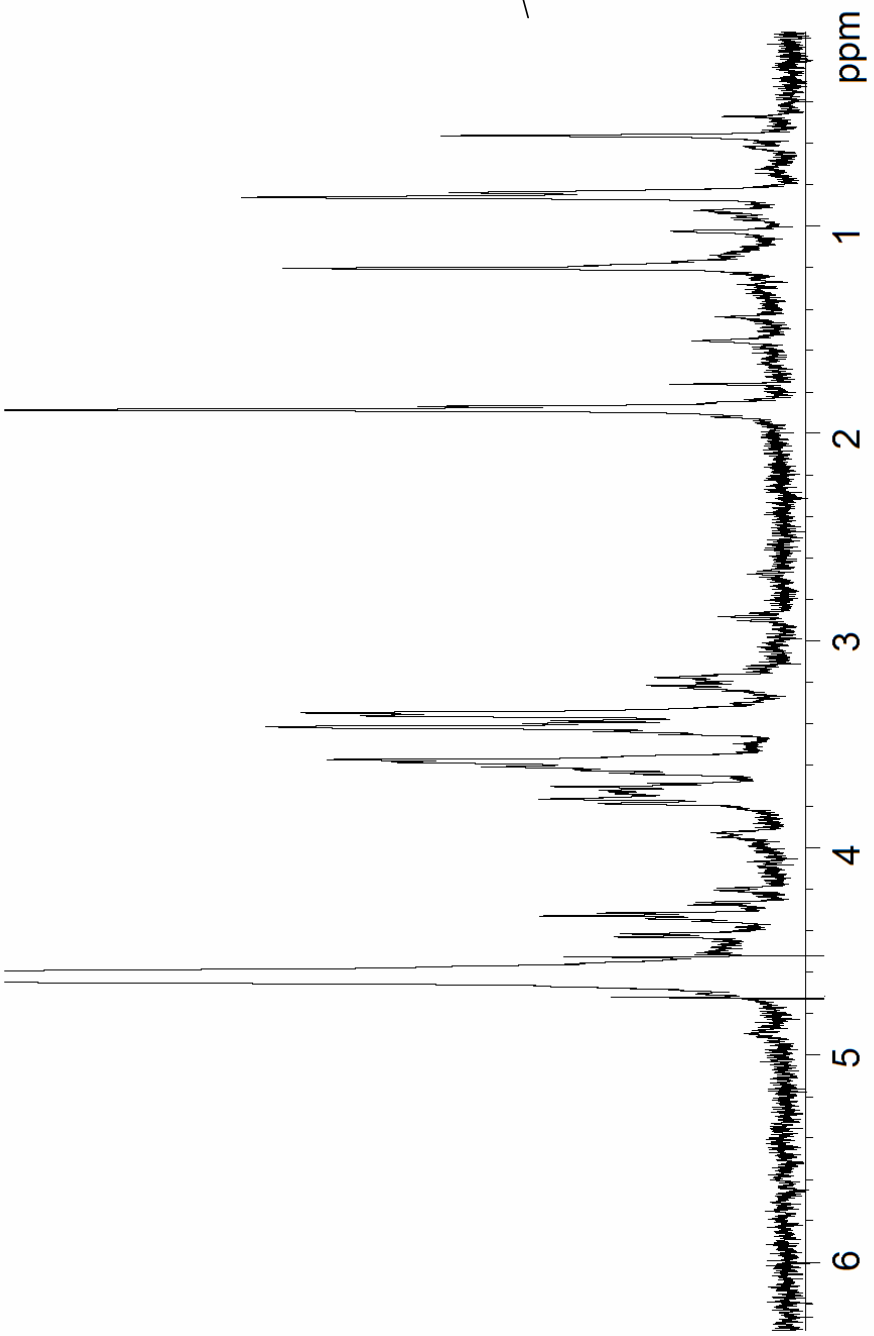

**Figure 4.87.** $^{1}$H-NMR of compound **58** (600 MHz, $D_2O$)

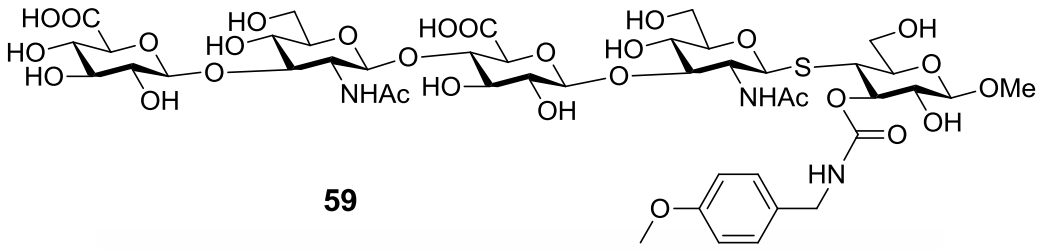


**59**

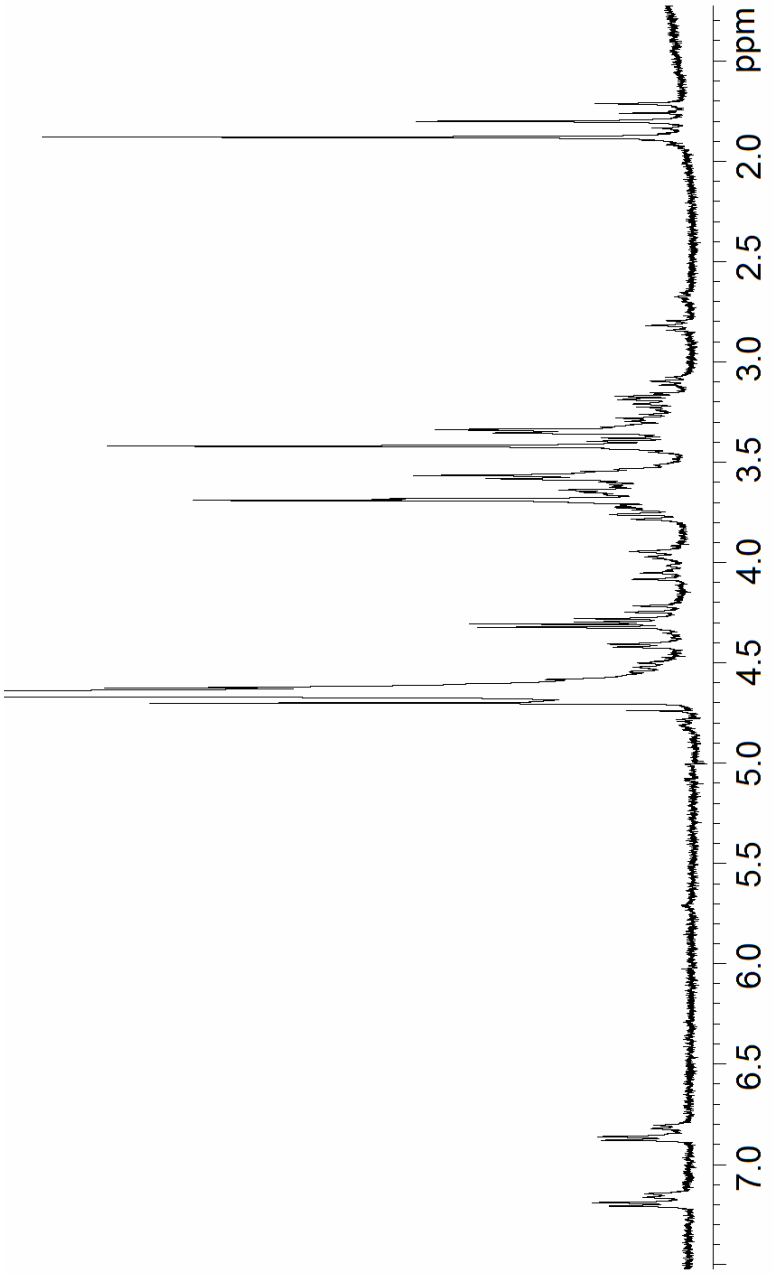

**Figure 4.88.** $^{1}$H-NMR of compound **67** (600 MHz, $D_2O$)

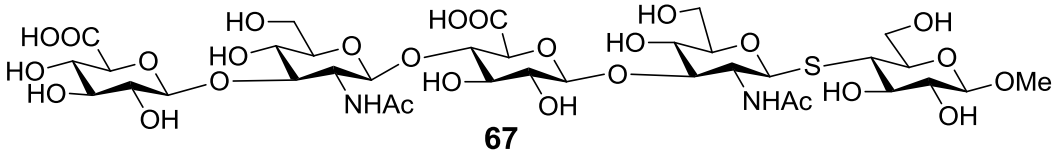


**67**

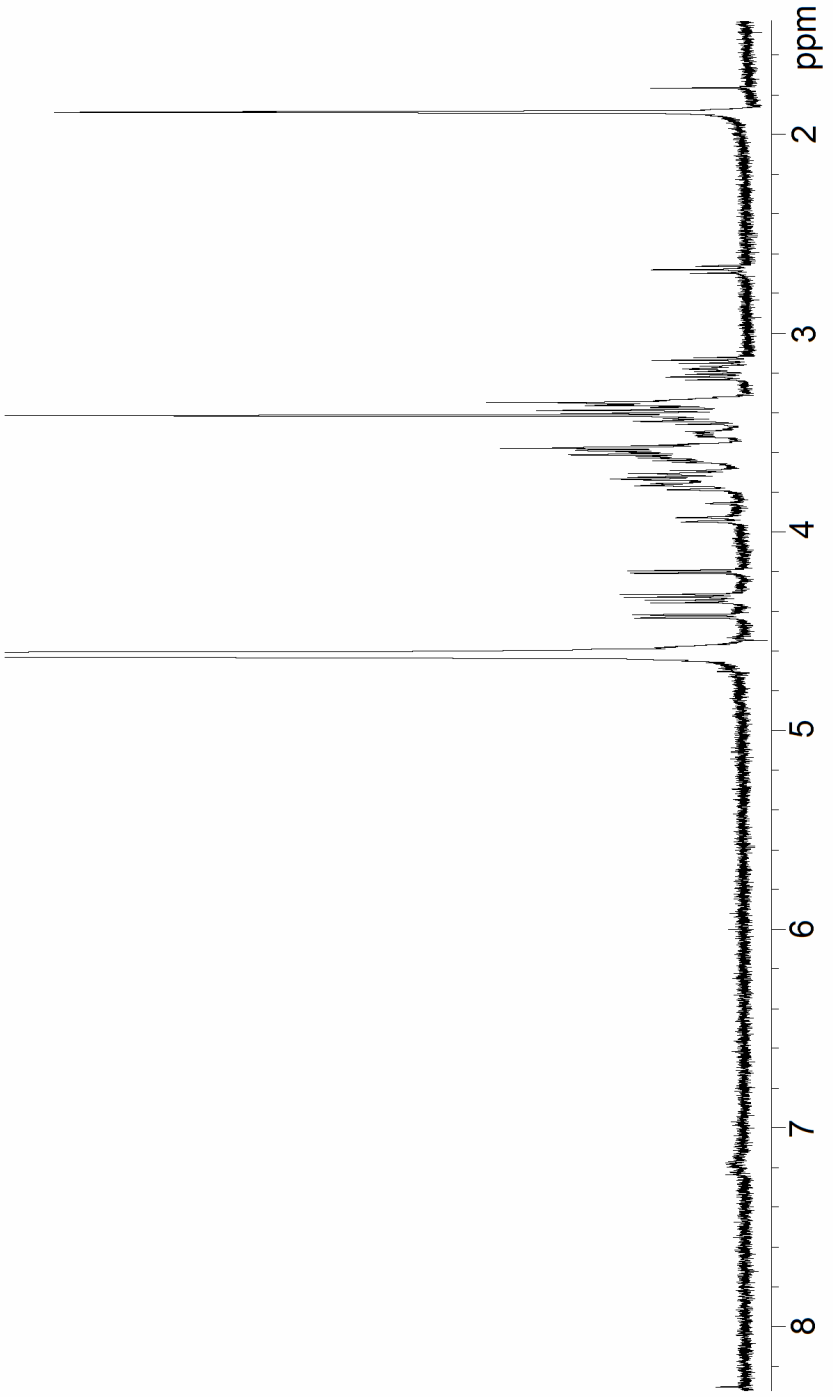

## References

## References


1. Toole, B. P., Hyaluronan: From extracellular glue to pericellular cue. *Nat Rev Cancer* **2004,** *4* (7), 528-539.

2. Toole, B. P.; Ghatak, S.; Misra, S., Hyaluronan oligosaccharides as a potential anticancer therapeutic. *Curr Pharm Biotechnol* **2008,** *9* (4), 249-252.

3. Bourguignon, L. Y. W., Hyaluronan-mediated CD44 activation of RhoGTPase signaling and cytoskeleton function promotes tumor progression. *Semin Cancer Biol* **2008,** *18* (4), 251-259.

4. Turley, E. A.; Noble, P. W.; Bourguignon, L. Y. W., Signaling properties of hyaluronan receptors. *J Biol Chem* **2002,** *277* (7), 4589-4592.

5. Toole, B. P., Hyaluronan-CD44 interactions in cancer: Paradoxes and possibilities. *Clin Cancer Res* **2009,** *15* (24), 7462-7468.

6. Toole, B. P.; Slomiany, M. G., Hyaluronan, CD44 and emmprin: Partners in cancer cell chemoresistance. *Drug Resist Updates* **2008,** *11* (3), 110-121.

7. Harada, H.; Nakata, T.; Hirota-takahata, Y.; Tanaka, I.; Nakajima, M.; Takahashi, M., F-16438s, novel binding inhibitors of CD44 and hyaluronic acid. *J Antibiot* **2006,** *59* (12), 770-776.

8. Hirota-takahata, Y.; Harada, H.; Tanaka, I.; Nakata, T.; Nakajima, M.; Takahashi, M., F-16438s, novel binding inhibitors of CD44 and hyaluronic acid. *J Antibiot* **2006,** *59* (12), 777-784.

9. Hirota-Takahata, Y.; Harada, H.; Tanaka, I.; Nakata, T.; Nakajima, M.; Takahashi, M., F-19848 A, a novel Inhibitor of hyaluronic acid binding to cellular receptor CD44. *J Antibiot* **2007,** *60* (10), 633-639.

10. Banerji, S.; Wright, A. J.; Noble, M.; Mahoney, D. J.; Campbell, I. D.; Day, A. J.; Jackson, D. G., Structures of the Cd44-hyaluronan complex provide insight into a fundamental carbohydrate-protein interaction. *Nat Struct Mol Biol* **2007,** *14* (3), 234-239.

11. Cleland, R. L., Viscometry and sedimentation equilibrium of partially hydrolyzed hyaluronate: Comparison with theoretical models of wormlike chains. *Biopolymers* **1984,** *23* (4), 647-666.

12. Scott, J. E.; Heatley, F.; Hull, W. E., Secondary structure of hyaluronate in solution. A proton NMR investigation at 300 and 500 MHz in dimethyl sulfoxide solution. *Biochem J* **1984,** *220*, 197-205.

13. Almond, A.; Brass, A.; Sheehan, J. K., Dynamic exchange between stabilized conformations predicted for hyaluronan tetrasaccharides: Comparison of molecular dynamics simulations with available NMR data. *Glycobiology* **1998,** *8* (10), 973-980.

14. Guss, J. M.; Hukins, D. W. L.; Smith, P. J. C.; Winter, W. T.; Arnott, S.; Moorhouse, R.; Rees, D. A., Hyaluronic acid: Molecular conformations and interactions in two sodium salts. *J Mol Biol* **1975,** *95*, 359-384.

15. Almond, A.; Brass, A.; Sheehan, J. K., Oligosaccharides as model systems for understanding water−biopolymer interaction: Hydrated dynamics of a hyaluronan decamer. *J of Phys Chem B* **2000,** *104* (23), 5634-5640.

16. Blundell, C. D.; DeAngelis, P. L.; Day, A. J.; Almond, A., Use of $^{15}$N-NMR to resolve molecular details in isotopically-enriched carbohydrates: Sequence-specific observations in hyaluronan oligomers up to decasaccharides. *Glycobiology* **2004,** *14* (11), 999-1009.

17. Sörme, P.; Qian, Y.; Nyholm, P.-G.; Leffler, H.; Nilsson, U. J., Low micromolar inhibitors of galectin-3 based on 3'-derivatization of *N*-acetyllactosamine. *ChemBioChem* **2002,** *3* (2-3), 183-189.

18. Sörme, P.; Arnoux, P.; Kahl-Knutsson, B.; Leffler, H.; Rini, J. M.; Nilsson, U. J., Structural and thermodynamic studies on cation−$\pi$ interactions in lectin−ligand complexes: High-affinity galectin-3 inhibitors through fine-tuning of an arginine−arene interaction. *J Am Chem Soc* **2005,** *127* (6), 1737-1743.

19. Cumpstey, I.; Salomonsson, E.; Sundin, A.; Leffler, H.; Nilsson, U. J., Double affinity amplification of galectin–ligand interactions through arginine–arene interactions: synthetic, thermodynamic, and computational studies with aromatic diamido thiodigalactosides. *Chem Eur J* **2008,** *14* (14), 4233-4245.

20. Zeng, Y.; Rademacher, C.; Nycholat, C. M.; Futakawa, S.; Lemme, K.; Ernst, B.; Paulson, J. C., High affinity sialoside ligands of myelin associated glycoprotein. *Bioorg Medi Chem Lett* **2011,** *21* (17), 5045-5049.

21. Pouyani, T.; Prestwich, G. D., Biotinylated hyaluronic acid: A new tool for probing hyaluronate-receptor interactions. *Bioconjugate Chem* **1994,** *5*, 370-372.

22. Tawada, A.; Masa, T.; Oonuki, Y.; Watanabe, A.; Matsuzaki, Y.; Asari, A., Large-scale preparation, purification, and characterization of hyaluronan oligosaccharides from 4-mers to 52-mers. *Glycobiology* **2002,** *12*, 421-426.

23. Mahoney, D. J.; Aplin, R. T.; Calabro, A.; Hascall, V. C.; Day, A. J., Novel methods for the preparation and characterization of hyaluronan oligosaccharides of defined length. *Glycobiology* **2001,** *11*, 1025-1033.

24. Susumu, K.; Mei, B. C.; Mattoussi, H., Multifunctional ligands based on dihydrolipoic acid and polyethylene glycol to promote biocompatibility of quantum dots. *Nat Protocols* **2009,** *4* (3), 424-436.